VOL.
4
58/59

THE INTERNATIONAL JOURNAL OF

Applied Radiation and Isotopes

Volume 4 1958/9

Editorial Board

P. C. AEBERSOLD
Washington

A. H. W. ATEN, Jr.
Amsterdam

M. BRUCER
Oak Ridge

G. D. CALKINS
Columbus

J. COURSAGET
Saclay

V. E. KONDRATIEV
Moscow

M. MAGAT
Paris

B. MANOWITZ
New York

J. L. PUTMAN
Harwell

H. SELIGMAN
Harwell

Editorial Advisory Board

Austria
B. Karlik, Vienna

Argentina
E. E. Galloni, Buenos Aires

Belgium
Z. M. Bacq, Liége
P. C. Capron, Louvain

France
L. Bugnard, Paris
C. H. Fisher, Saclay
B. Goldschmidt, Paris
M. Haissinsky, Paris

Germany
H. Langendorff, Freiburg
M. Maier-Leibnitz, Munich
F. Strassmann, Mainz
F. Weygand, Berlin

Israel
I. Dostrovsky, Rehovoth

Italy
G. Bolla, Milan
E. B. Chain, Rome
A. Perussia, Milan
G. Trabacchi, Rome

Japan
Masao Tsuzuki, Tokio

Portugal
H. de Carvalho, Lisbon

Scandinavia
G. C. de Hevesy, Stockholm

Switzerland
H. H. Staub, Zürich

U.N.E.S.C.O.
P. Auger, Paris

United Kingdom and Commonwealth
J. S. Anderson, Victoria
R. H. Betts, Chalk River, Ontario
A. Charlesby, Shrivenham
Sir John Cockcroft, Harwell
V. R. Khanolkar, Bombay
Sir Hans Krebs, Oxford
C. P. LeBlond, Montreal
A. S. McFarlane, London
Sir E. Rock Carling, London
J. W. T. Spinks, Saskatoon

U.S.A.
J. C. Bugher, New York
V. Conquest, Chicago
G. Dean, New York
R. D. Evans, Cambridge
M. Harris, Spokane, Wash.
W. B. Mann, Washington
H. F. Mark, New York
H. R. Nelson, Columbus, Ohio
S. Warren, Boston

U.S.S.R.
N. A. Bach, Moscow
G. M. Frank, Moscow
G. V. Kurdiumov, Moscow

Pergamon Press New York • London • Paris • Los Angeles

VOL
4
1958/

CONTENTS OF VOLUME 4

NUMBERS 1/2

D. E. HULL: The total-count technique: a new principle in flow measurement 1
H. NESMEYANOV: The use of radioactive isotopes for determining saturated vapour pressure . . 16
J. GOLDEN, P. R. LANCASTER and G. W. ROWE: An examination of lubrication with soap, using radioactive sodium stearate 30
V. B. MILLER, M. B. NIEMAN and S. P. SOLODOVNIKOV: Application of the light intermittency method to investigations on isotopic exchange reactions in gas and liquid phase 36
P. LEVEQUE, P. MARTINELLI et S. MAY: Quelques exemples d'applications à l'analyse chimique du spectromètre-γ à scintillations 41
D. GIBBONS: The determination of gold in biological materials by neutron activation analysis . . 45
RAYMOND G. ROSE: The influence of ionizing radiations on the penetration of sodium into the central nervous system 50
D. J. MEWISSEN: Le critère de mortalité et sa quantité d'information dans l'experimentation radiobiologique 58
M. L. BEAUMARIAGE: Essais de prevention et traitement du mal des rayons chez le poussin . . 69
R. WORRALL and A. CHARLESBY: Effect of additives on the radiation induced polymerization of *iso*butene 84
JEROME WEISS: A survey of chemical dosimetric systems 89
J. TROCKER, C. FISHER et A. RAGGENBASS: Contribution à l'étude de préparation des sources de coesium^{137} 96
Technical Notes:
FAZLE HOSAIN: Use of RIHSA in differentiating ascites due to nephritis and cirrhosis . . . 108
A. IA. MARGULIS and A. V. KHRUSTALEV: On the spatial distribution of the gamma-ray dose from a plane source 109
P. C. RAJAM, M. E. WIRGAU and U. M. TSAO: All-glass apparatus for microsynthesis of radioactive solids 111
G. L. LOCHER: Micro counter tubes for beta-gamma measurements 112
B. GRIMELAND: Absolute counting of β-particles by means of a plastic scintillator 116
D. V. COHN, W. E. CARTER and R. ANDERSON: An automatic sample changer for well-type scintillation counters 118
N. S. KORSHUNOV and M. V. KHATSKEVICH: A remotely operating flowmeter 121
Book Reviews 124

NUMBERS 3/4

C. T. RAY and G. E. BURCH: Rates of transfer of Rb^{86}, K^{42}, K^{39}, Cl^{36}, Cl^{35}, Na^{22}, and Na^{23} across a blister surface on the forearm of normal man and patients with chronic congestive heart failure . . 129
ARTHUR R. SCHULERT, EDWIN A. PEETS, DANIEL LASZLO, HERTA SPENCER, MARTIN CHARLES and JOSEPH SAMACHSON: Comparative metabolism of strontium and calcium in man 144
MERRILL A. BENDER and MONTE BLAU: A versatile, high-contrast photoscanner for the localization of human tumors with radioisotopes 154
FREDERIC LUDWIG: Le rôle de la phagocytose reticuloendotheliale dans l'organisme multicellulaire irradié—I. L'étude de l'àction à distance des radiotoxines au moyen de techniques de parabiose . . 162
J. R. LUICK, D. T. TORELL and W. SIRI: A method for the determination of water intake of grazing sheep 169
W. GEBAUHR und J. MARTIN: Ermittlung von Spurenverunreinigungen im Reinstphosphor durch Aktivierungsanalyse 173
E. E. VAINSTEIN and YU. I. BELYAEV: Use of radioactive isotopes in studying the spatial distribution of elements in direct current arc plasma during spectrochemical determination of impurities in uranium 179
B. LIONEL FUNT and ARLENE HETHERINGTON: The influence of chain length on the luminescent output of plastic scintillators 189

VOL. 4 58/59

A. R. Ronzio: Metal loaded scintillator solutions 196
V. A. Nikashina, A. Kh. Breger, M. M. Senyavin and A. V. Gordievsky: Stability to radiation of the cation exchange resins 201
C. H. Carlson, L. Singer, D. H. Service and W. D. Armstrong: Preparation of carrier free radiofluoride with a new estimate of the half-life of F^{18} 210
H. J. M. Bowen: The determination of copper and zinc in biological material by activation analysis . 214
T. E. Banks, R. Tupper, E. M. A. White and A. Wormall: Micro-determination of zinc in blood and other tissues by neutron activation analysis 221
David L. Joftes: Radio-iodine counting in unanesthetized mice 227
P. J. Campion: The standardization of radioisotopes by the beta-gamma coincidence method using high efficiency detectors 232
Y. Le Gallic et M. Thenard: Mesure absolue des émetteurs β de faible énergie et de faible activité spécifique 249
S. M. Makin: Porosity detection in magnesium alloys using paraffin containing Pd^{109} 253
C. G. Clayton: Leak detection in an underground gasification system 256
Technical Notes:
R. C. Axtmann and LeConte Cathey: Liquid scintillators containing metallic ions 261
M. C. Anta and M. L. Roda Santos: The irradiation of indigocarmine with α-particles and X-rays . 261
Gerald A. Edwards, Cecile H. Edwards and Evelyn L. Gadsden: An inexpensive metabolism apparatus for collecting CO_2, excreta and blood from small experimental animals 264
D. G. Arnott and H. R. Knight: An apparatus for the intracavity administration of radioactive colloidal gold 266
R. Dutta-Choudhuri and H. Roy: Effects of ionizing radiations on tissue mast cells 268
A. I. Osipov *et al.*: The use of radioactive isotopes in the study of the kinetics of scrap melting and slag formation in a scrap ore process 270
Book Reviews 273
Forthcoming Papers 274

VOL.
4
1958/5

AUTHOR INDEX

Alekseev, V. I. 270
Anderson, R. 118
Anta, M. C. 261
Armstrong, W. D. 210
Arnott, D. G. 266
Axtmann, R. C. 261
Banks, T. E. 221
Beaumariage, M. L. 69
Belyaev, Yu. I. 179
Bender, M. A. 154
Blau, M. 154
Bowen, H. J. M. 214
Breger, A. Kh. 201
Bul'skii, M. T. 270
Burch, G. E. 129
Campion, P. J. 232
Carlson, C. H. 210
Carter, W. E. 118
Cathey, LeC. 261
Charles, M. 144
Charlesby, A. 84
Clayton, C. G. 256
Cohn, D. V. 118
Dutta-Choudhuri, R. 268
Edwards, C. H. 264
Edwards, G. A. 264
Fisher, C. 196
Funt, B. L. 189
Gadsden, E. L. 264
Gebauhr, W. 173
Gibbons, D. 45
Golden, J. 30
Goldshtein, L. G. 270
Gordievsky, A. V. 201
Grimeland, B. 116
Hetherington, A. 189
Hosain, F. 108
Hull, D. E. 1
Joftes, D. L. 227
Khatskevich, M. V. 121
Khrustalev, A. V. 109
Knight, H. R. 266
Korshunov, N. S. 121
Lancaster, P. R. 30
Laszlo, D. 144
Le Gallic, Y. 249
Leveque, P. 41
Locher, G. L. 112
Ludwig, F. 162
Luick, J. R. 169
Makin, S. M. 253
Margulis, A. Ia. 109
Martin, J. 173
Martinelli, P. 41
May, S. 41
Mewissen, D. J. 58
Miller, V. B. 36
Nesmeyanov, H. 16
Nieman, M. B. 36
Nikashina, V. A. 201
Ofengenden, A. M. 270
Osipov, A. I. 270
Peets, E. A. 144
Raggenbass, A. 96
Rajam, P. C. 111
Ray, C. T. 129
Ronzio, A. R. 196
Rose, R. G. 50
Rowe, G. W. 30
Roy, H. 268
Samachson, J. 144
Santos, M. L. Roda 261
Sazonov, M. L. 270
Schulert, A. R. 144
Senyavin, M. M. 201
Service, D. H. 210
Shvartsman, L. A. 270
Singer, L. 210
Siri, W. 169
Skrebtsov, A. M. 270
Solodovnikov, S. P. 36
Spencer, H. 144
Surov, V. F. 270
Sviridenko, F. F. 270
Telesov, S. A. 270
Thenard, M. 249
Torell, D. T. 169
Trocker, J. 96
Tsao, U. M. 111
Tupper, R. 221
Vainstein, E. E. 179
Weiss, J. 89
White, E. M. A. 221
Wirgau, M. E. 111
Wormall, A. 221
Worrall, R. 84

International Journal of Applied Radiation and Isotopes, 1958, Vol. 4, pp. 1–15. Pergamon Press Ltd., London

The Total-Count Technique: A New Principle in Flow Measurement

D. E. HULL
California Research Corporation, Richmond, California

(*Received* 30 *December* 1957)

This paper describes a new principle for measuring flow in all kinds of streams. A known quantity of radiotracer A is mixed in the flowing stream. A counter fixed in or near the stream, some distance downstream, registers a total of N counts from the tracer while it passes. The flow rate Q is given by the relation

$$Q = \frac{AF}{N}$$

The constant factor F is determined by laboratory calibration of the counter.

This simple formula is a completely general expression for the absolute flow rate of liquids and gases in any kind and size of conduit. It applies without modification over an extremely wide range.

The total count above and below the junction of confluent streams measures the flow at each point. The total count in a divergent stream, no matter what fraction of the tracered stream it carries, depends only on the flow of the whole stream.

These principles are applied to measure flow of water and oil in pipes in operating industrial plants. Also, water flow is measured in open channels and natural streams. Other applications of the total-count method are to the measurement of leaks in condensers and heat exchangers, and of entrainment in distillation columns.

LA METHODE DES IMPULSIONS TOTALES: UN NOUVEAU PRINCIPE POUR MESURER UN COURANT COULANT

Cet article décrit un nouveau principe pour mesurer des courants coulants de toutes sortes. Une quantité connue d'un traceur radio-actif A est mélangée dans un courant coulant. Un compteur fixé dans le courant ou dans son voisinage à quelque distance aval régistre un nombre total N d'impulsions du traceur pendant son passage. La vitesse du courant Q est donnée par l'équation

$$Q = \frac{AF}{N}$$

Le facteur constant F est déterminé par calibrage du compteur au laboratoire.

Cette simple formule représente une expression très générale de la vitesse absolue du courant des liquides et des gaz en toutes sortes et dimensions de conduits. Elle est applicable sans modification dans une portée très étendue.

Le nombre total des impulsions en amont et en aval de la jonction de deux courants confluents mesure le courant à chaque point. Mais le nombre total des impulsions dans un courant divergent partiel, quelconque soit la fraction qu'il représente du courant total contenant le traceur, dépend seulement de l'écoulement du courant total.

Ces principes sont employés pour mesurer l'écoulement d'eau et d'huile dans les conduits des installations industrielles en fonctionnement. De même, on mesure l'écoulement de l'eau dans des canaux ouverts ou dans les rivières naturelles. D'autres applications de la méthode des impulsions totales sont les mesures d'échappements dans les condensateurs et les échangeurs de chaleur et de l'entrainement dans les colonnes de distillation.

VOL. 4 8/59

МЕТОДИКА ПОЛНОГО ОТСЧЕТА: НОВЫЙ ПРИНЦИП ИЗМЕРЕНИЯ ТЕЧЕНИЯ

В данной статье описывается новый принцип измерения течения любых потоков. Определенное количество радиоактивного изотопа A подмешивается к потоку. Счетчик, установленный в потоке, или вблизи него, вниз по течению, регистрирует полное число N импульсов проходящего мимо него изотопа. Скорость течения Q дается уравнением

$$Q = \frac{AF}{N}$$

Постоянную прибора F определяют лабораторной калибровкой счетчика.

Эта простая формула является совершенно общим выражением для абсолютной скорости течения жидкостей и газов в канале любого вида и размера. Она применима без изменений в очень широких пределах.

Полный отсчет выше и ниже места слияния потоков позволяет измерять течение в каждой точке. Полный отсчет в расходящемся потоке зависит только от течения всего потока, независимо от того, какую часть меченого потока он захватывает.

По этому принципу измеряется течение воды и нефти в трубах при работе промышленных установок, а также течение воды в открытых каналах и в естественных потоках. Другим применением метода полного отсчета является измерение утечки в конденсорах и теплообменниках, а также увлечения жидкости в перегонных колонках.

DIE GESAMTIMPULSZAHLMETHODE: EIN NEUES PRINZIP FUER STROEMUNGSMESSUNGEN:

Dieser Artikel beschreibt ein neues Prinzip fuer Stroemungsmessungen in Stroemen aller Art. Eine bekannte Menge eines Radioisotopen A wird dem fliessenden Strom beigemischt. Ein Zaehler der im Strom oder in seiner Naehe in einiger Entfernung stromab angebracht ist, registriert eine Gesamtzahl N der Impulse des Isotopen waehrend seines Vorbeifliessens. Die Fliessgeschwindigkeit Q ist gegeben durch die Beziehung

$$Q = \frac{AF}{N}$$

Der konstante Faktor F wird bestimmt durch Eichung des Zaehlers im Laboratorium.

Diese einfache Formel ist ein voellig allgemeiner Ausdruck fuer die absolute Stroemungsgeschwindigkeit von Fluessigkeiten and Gasen in Leitungen aller Art und Groesse. Sie gilt unveraendert fuer ein ausserordentlich weites Gebiet.

Die Gesamtimpulszahl oberhalb und unterhalb der Vereinigung zusammenfliessender Stroeme misst die Stroemung an jedem Punkte. Aber die Gesamtimpulszahl in einem sich verzweigenden Strom, ohne Ruecksicht darauf welchen Bruchteil des isotophaltigen Stromes die Abzweizung fuehrt, ist lediglich abhaengig von der Stroemung des Gesamtstroms.

Diese Grundsaetze werden benuetzt um die Stroemung von Wasser und Oel in den Roehren von in Betrieb befindlichen industriellen Anlagen zu messen. Ebseno wird die Stroemung von Wasser in offenen Kanaelen und natuerlichen Flusslaeufen gemessen. Weitere Anwendungen des Prinzips der Gesamtimpulszahlmethode sind Messungen von Leckagen in Kuehlern oder Kondensatoren und Waermeaustauschern, und des uebergeschleppten Materials in Destillationskolonnen.

VOL. 4 1958/5

The measurement of flow rates is a fundamental problem in many fields of engineering. Diligent theoretical and experimental attacks on the problem during the past half century have yielded a variety of approximate solutions. Each of these has its particular field of successful application. No single method is yet applicable to the whole range of flow rates which it falls to the engineer to measure.

The devices commonly used in industry to measure flow in pipes suffer from a number of theoretical and practical shortcomings. A Pitot tube measures linear velocity at the tip of the tube. To get a volume rate requires either a traverse of the stream with the

Pitot tube or use of an empirical formula relating average flow to flow at the center. Orifice plate flow meters not only depend on a formula with a wide range of empirical coefficients but, when orifices erode or build up scale, their accuracy is impaired. Approximate formulas are used to relate the pressure drop to flow rate in pipes, through an empirical friction factor that depends on the nature of the pipe wall. Displacement meters give precise results on clean liquids if carefully maintained and frequently calibrated, but they are costly and not suitable for large flow rates. Water flow over a weir can be measured with a semi-empirical formula at rates not too far from that for which the weir is designed; but, at abnormally low or high rates, the formula breaks down.

This paper describes a new principle for measuring flow in all kinds of streams over a wide range of flow rates. It is based on the counting of radioactive radiations and is called the total-count principle. Briefly, the method is this: A measured quantity of radiotracer is mixed in a flowing stream. A counter is fixed in or near the stream some distance below the starting point, and it registers counts from the tracer while it passes. The relation between the total number of counts N, the quantity of tracer A, and the flow rate Q is given simply by the formula

$$Q = \frac{AF}{N} \qquad (1)$$

The calibration factor F is characteristic of the isotope, the counter, and the geometrical relation between the counter and the stream.

TOTAL-COUNT PRINCIPLE

An observation made while analyzing radioactive measurements in a long petroleum pipeline[1] led to the discovery of the total-count principle. We had made a pulsed injection of tracer into a pipeline at Rangely, Colorado, and observed its passage with Geiger counters at several stations along the line toward Salt Lake City, Utah. At first the tracer passed quickly in a sharp peak with a high maximum counting rate. At each successive station, the peak was flattened, having a smaller maximum and being spread out more along the stream (see Fig. 1). It appeared that the decrease in peak height was just compensated by the increase in breadth so that the area under the curve was constant. The area under the curve represented simply the total count in excess of background during passage of the tracer.

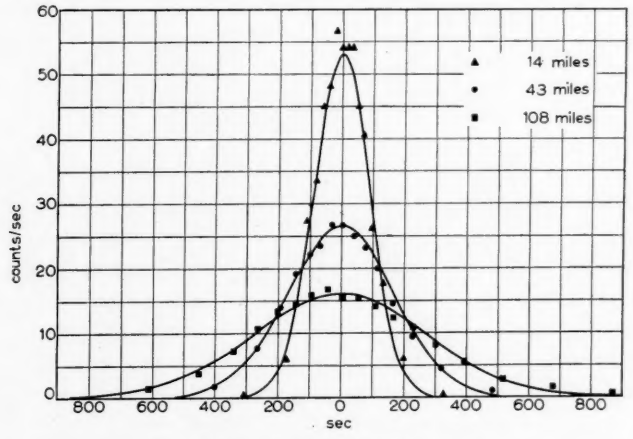

FIG. 1. Spreading of radioactive tracer wave

Reflecting on this observation, I realized that the number of counts recorded must be independent of the distribution of the tracer along the stream. If the tracer is mixed homogeneously across the pipe, a radioactive atom passing the counter station has a certain chance p of emitting a gamma ray which will discharge the counter. This chance is not affected by the presence or absence of neighboring radioactive atoms. If A atoms are in the tracer pulse, the number of counts observed is simply $A\,p$, regardless of the distribution of the A atoms along the stream.

In the tests made in the Rangely pipeline, constant velocity was maintained. The constancy of total counts must depend upon this condition. If the rate of flow of a tracer atom past the counter is changed, the chance of its tripping the counter is affected. The chance p is the product of three factors, λ, t, and G, where λ is the usual disintegration constant of the radioelement, t is the time the atom spends in the region of the counter, and G is the average product of geometrical and sensitivity factors for detecting disintegrations that occur in this region. If the flow rate increases, the time t in the vicinity of the counter decreases, and the number of counts decreases in proportion. So the total count is inversely proportional to the flow rate.

Relative rates could be measured by the relation

$$Q_1/Q_2 = N_2/N_1 \tag{2}$$

for a constant quantity of tracer. More generally, the amount of tracer used in different tests varies; and, of course, the number of counts is proportional to the number of tracer atoms used. To allow for this variable, we may rewrite our proportion

$$Q_1/Q_2 = A_1N_2/A_2N_1 \tag{3}$$

or simply

$$Q = F\,A/N \tag{1}$$

If the constant factor F could be determined, we would have, not just a relative, but an absolute method of measuring flow rates. It is, in fact, possible to determine F in the following way. A piece of pipe similar to the one used in the flow measurements, several inches longer than the counter tube, is filled with a solution of the tracer at a known concentration (Fig. 2). The counter is affixed to the tube in the same geometrical configuration as in the field test, and the counting rate R is measured.

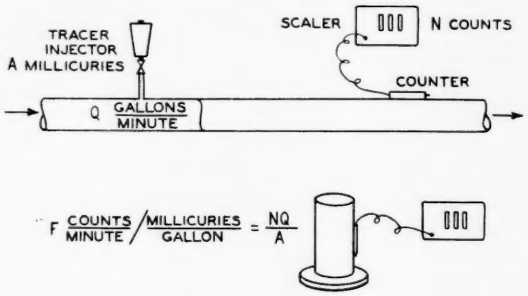

FIG. 2. Flow rate by total count

The rate is, of course, proportional to the concentration C, and a counting factor F' is calculated

$$F' = \frac{R \text{ counts/min}}{C\ \mu\text{c/gal}} \tag{4}$$

Note that the units of this factor can be rearranged, thus

$$F' \frac{\text{counts}}{\mu\text{c}} \cdot \frac{\text{gal}}{\text{min}}$$

and that, dimensionally, F' is the same as F in equation (1).

$$F \frac{\text{counts}}{\mu\text{c}} \cdot \frac{\text{gal}}{\text{min}} \times \frac{A\mu\text{c}}{N \text{ counts}} = Q \frac{\text{gal}}{\text{min}} \tag{5}$$

Is it in fact the same F? The following analysis shows that it is.

Let N be the total number of counts and R be the instantaneous counting rate, both corrected for background. Then, integrated over the time required for the tracer to pass,

$$N = \int R\,dt \tag{6}$$

Now R is proportional to the continually varying concentration, C, of the tracer. The proportionality constant is the factor, F'.

$$R = F'C \tag{7}$$

Substituting,

$$N = F'\int C\,dt \tag{8}$$

VOL. 4 1958/5

Let Q be the volume flow rate, which is kept constant. Then, dq, the increment of volume passing during the interval dt, is

$$dq = Q\,dt \tag{9}$$

Again substituting,

$$N = \frac{F'}{Q}\int C\,dq \tag{10}$$

But the integral of radioisotope concentration over the total volume is simply the total quantity, A, of radiotracer.

$$\int C\,dq = A \tag{11}$$

Hence,

$$N = \frac{F'A}{Q} \tag{12}$$

and, solving for flow rate,

$$Q = \frac{F'A}{N} \tag{13}$$

This shows that the counting sensitivity factor F', determined in a static measurement, is the same as the F in equation (1), which relates counts to flow rates.

GENERAL PRINCIPLE

The radiotracer total-count principle is a special case of a more general integral-measurement principle. It is more obvious than other cases and will probably find wider application because the integral of counting rate is derived from the data in a simple way, owing to the nature of the measurement. However, in theory, the continuously measured value of any property that is proportional to the concentration of a foreign substance introduced into a stream can be integrated while the stream containing the added substance is passing the measuring instrument; this integral is analogous in every way to the N of equation (1). The sensitivity of the instrument is determined at a known concentration of the substance to be added; this gives a calibration factor analogous to F.

Flow rate by total-count method

An opportunity to make a practical test of the method came with a problem of measuring condenser water rates in a petroleum refinery. Cesium[134] chloride was used as a water-soluble tracer, diluted in 1 pint of 1% sodium chloride solution. It was measured by counting its gamma rays with a Geiger counter in a standard position.[2]

In the field, the tracer solution was poured into a "Sparklet" bottle, which is designed for preparing "carbonated water" with CO_2 cartridges (Fig. 3). A special cap, equipped with a valved exit tube and a pressure gage, was put on the metal bottle and screwed down tight. With the valve shut, the bottle was inverted and attached to the pipe through a connection from which

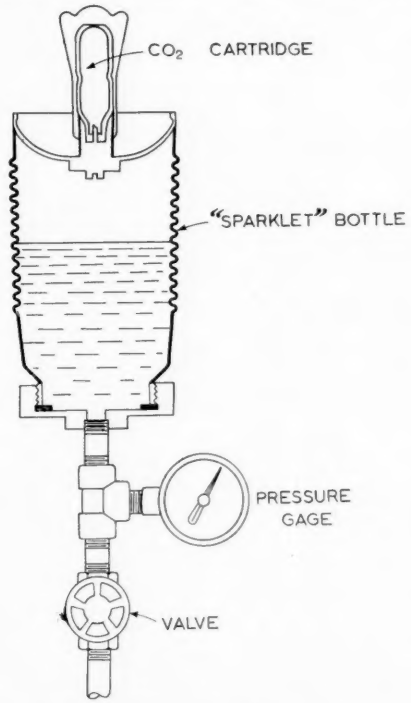

FIG. 3. Pressurised injector for liquid tracer

a pressure gage was disconnected. Then a CO_2 cartridge was screwed down on the hollow needle which admits the gas into the bottom of the inverted bottle. At the appropriate time, the tracer was forced

into the pipeline by opening the valve on the bottle.

The tracer was counted in the pipeline with counter tubes attached to the pipe downstream. We chose a convenient location where a 3 ft straight section of pipe was available with known size, wall thickness, and lining. The precision of the measurement was increased by connecting four 1 × 12 in. tubes in parallel. A portable, battery-operated scale-of-eight scaler was connected to the tubes. After a few minutes' counting to compute the background rate, we noted the time and the scaler reading. Then we injected the tracer by opening the valve carefully, observing the pressure drop on the gage in order to avoid too rapid an injection. (A counting rate higher than about 100 counts/sec would jam the scaler.) After a sudden drop to the line pressure showed that the tracer bottle was empty,

TABLE 1. Pipe calibration factors
Cesium[134] with 1 × 12 in. GM tube

Pipe diameter (in.)	counts/min / μc/gal
3	116
4	205
6	264
8	315
14	482

we watched the scaler until it returned to background. The time and scaler reading were again noted. Then a final background count was taken. Ideally, this should check the initial background.

For determining the calibration factor, F, for the 8 in. pipe, a section of similar pipe about 2 ft long was closed at one end. It was filled with a solution containing 42·3 μc/gal of cesium[134] in 1% sodium chloride. A 1 × 12 in. Geiger tube was taped to the outside of the pipe midway between the two ends, and the counting rate was measured to 0·5 per cent standard deviation. Several of the pipe sizes commonly used in refinery water systems were calibrated in this manner. A list of some pipes thus calibrated, with the corresponding F values, is given in Table 1.

The experimental data taken in a typical measurement of condenser flow rate are shown in Table 2. A weighted average of the initial and final backgrounds was used to compute the background correction to be subtracted from the gross count recorded during passage of the tracer. From the net count, the activity of the tracer measured by counting in the laboratory, and the pipe factor from Table 1 multiplied by the number of tubes, the flow rate was calculated with equation (1).

TABLE 2. Flow rate by total-count method

Pipe size		8 in.
Initial background		6960/16 = 435 counts/min
Final background		4024/9 = 447 counts/min
Gross counts		6176 counts/3 min
Background		1320 = 3 × 440
Net count	N	4856 counts
Activity of tracer	A	4240 μc
Calibration factor	F	315 × 4 = 1260
Flow rate	Q	1100 gal/min
Standard deviation		±25

The meter on the feed line to this condenser showed a reading of 510 gal/min, but it was believed unreliable because of corrosion by HF in the line. Calculations based on the heat supplied to the feed preheaters had pointed to a flow rate of about 1100 gal/min. The radioactive test confirmed the doubt about the meter and corroborated the heat balance figure.

TABLE 3. Flow rates in 8 in. pipe

Test no.	1A	1B	2A	2B
Tracer activity, μc	926	1038	992	979
Net total counts	924	1050	1310	1256
Flow rate, gal/min	1260	1240	950	980
Standard deviation	±80	±60	±50	±50

Table 3 shows the internal consistency of the method in two pairs of duplicate tests.

Check with two-point method

In a later test, it was possible to check the total-count method more directly against

VOL 4 1958/

an independent measurement. This was also a radioactive method, in which the time of transit between detectors at two points is measured with a pulsed injection of radioactive liquid.[3] The linear flow rate is multiplied by the cross-section of the pipe to get the volume flow rate. This test was made on a line supplying cooling water to a section of the refinery. Two Geiger tubes were mounted on the 12 in. pipe, 132·2 ft apart, and connected together into a rate meter with a recorder attached. At a point several hundred feet farther downstream, four tubes were taped to a 6 in. pipe and connected to a scaler. The tracer was injected as quickly as possible in order to produce sharp peaks on the rate meter. The same tracer pulse, passing subsequently through the total-count setup, was used to get the flow rate by this method. The results of the test are tabulated in Table 4.

TABLE 4. Check between total-count and two-point methods

	Test 1	Test 2
Two-point method		
Time between peaks	0·626 min	0·535 min
Displacement	$\frac{\pi}{4}\frac{(11{\cdot}38)^2 \times 132{\cdot}2 \times 12}{231} = 699$ gal	
Flow rate	1120 ± 35 gal/min	1310 ± 40 gal/min
Total-count method		
Tracer injected	2660 μc	2280 μc
Net total count	2380	1980
Flow rate	1180 ± 70 gal/min	1210 ± 70 gal/min

The two-point method has not been studied thoroughly, but it is based on a simple geometric principle and is quite acceptable for an intercomparison. The concordant results demonstrate the fundamental soundness of the total-count principle.

Accuracy of total-count technique

The total-count flow method has an intrinsic accuracy limited to about 1 per cent by the number of counts easily obtained and by the reproducibility of Geiger counters. A relative accuracy of 2–5 per cent was obtained in the tests described above.

Sources of error which can affect the relative values obtained in successive tests are:

(1) Statistical error of counting. This is determined chiefly by the number of counts, which in turn is determined by the quantity of tracer used. It is usually in the range of 1 to 3 per cent. Background errors are normally less than this.

(2) Differences in mounting the tubes on the pipe from test to test and from the laboratory calibration test. The count rate is reduced if the tubes are not tight against the pipe. A 1/16 in. gap causes an error of about 3 per cent.

(3) Slack fill or foaming in the pipe. These must be avoided in accurate work.

(4) Retention of tracer in the pint bottle, the injector, and its connections to the line. The magnitude of this error was estimated by counting the empty containers after the test. On the average, the tracer injected was about 1 per cent less than the amount measured. The activity left in the valve and nipple to the line was not over a few tenths of 1 per cent.

The cumulative resultant of all these sources of error is shown as the standard deviation in the calculated flow rate in Tables 3 and 4.

In addition to these, there are sources of absolute error in several assumptions implicit in using pipe factors measured in the laboratory on field tests. These assumptions are:

(1) The sensitivity of each of the counter tubes is equal to that of the tube used for calibration. Experience with 1 × 12 in.

Geiger tubes shows that they have the same absolute sensitivity within 1 or 2 per cent.

(2) The contribution to the counting rate from solution more than 6 in. beyond the ends of the counter tubes is negligible. We have found this to be correct within 0·5 per cent.

(3) No corrosion or deposits have affected the wall thickness of the pipe in the field. This is probably the largest source of error in this method; we have encountered errors as much as 10 per cent in old pipes, which were probably due to this effect.

Confluent streams

In confluent streams, a single injection of tracer may be counted in passage at different points to measure the flow rate, not only

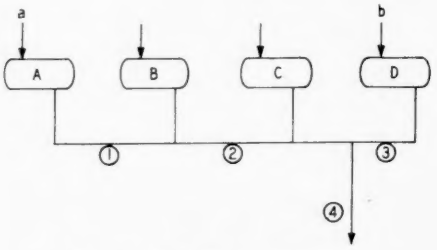

FIG. 4. Flow rates in condensers

at the starting point, but also after it is augmented by tributary streams. Such situations are not uncommon in industrial cooling units. An example of such a problem was the individual water rates in a bank of four condensers. Both the feed and discharge of these condensers went through manifolds with short connections. The path of the discharge is shown in the diagram (Fig. 4). Since the effluent from the discharge manifold is between condensers C and D, at least two injections of tracer were required to measure all the flow rates. We selected two points for injection and took measurements as follows:

1. At *a*, with counters at positions 1 and 2.
2. At *b*, with counters at positions 3 and 4.

All the pipe was 14 in. so only a single calibration was necessary. Since the flow rates at positions 1, 2, 3, and 4 were expected to be roughly in the ratio 1:2:1:4, we used more counters at the points of faster flow to equalize the number of counts. The results of these tests, shown in Table 5, further validate the principle set out in equation (2), that the total count is inversely proportional to the flow rate.

TABLE 5. Simultaneous measurement of confluent rates

Injection point	Position	No. of counters	Tracer, (μc)	Counts	Flow rate, (gal/min)
a	1	2	3020	2530	1150
	2	4		1584	3680
b	3	1	5520	1866	1430
	4	4		1540	6940
		Individual flow rates			
	Condenser A				1150
		B			2530
		C			1830
		D			1430

Divergent streams

When a tracered stream is divided into separate streams, application of the total-count principle leads to an unexpected result. Intuitively, one might expect that a fractional number of counts would appear in the divergent stream, depending on the fraction of the stream it carried. However, let us use equation (1) to calculate this number. Assume that the divergent stream carries the fraction x of the total flow. The flow rate through it will be xQ, and the amount of tracer carried through it will be xA. Hence, the number of counts observed at a standard position on the pipe will be

$$N = \frac{xA\,F}{xQ} = \frac{AF}{Q} \qquad (14)$$

That is to say, the number of counts observed on a portion of the stream in the branch is independent of the branching ratio. It is the same number of counts that would be recorded if the whole stream went through the branch, and this is true no matter how large or how small x is. Thus, the fraction x need not be known. However, it must remain constant during a test.

This principle was checked experimentally

VOL. 4 1958/5

in the measurements already referred to in Table 4. Only a fraction of the total flow was through the 6 in. pipe on which the total counts were measured. It was about 25 per cent in the first test and 60 per cent in the second. In spite of this circumstance, the flow rates indicated by the total-count method on these widely varying fractions were those for the total flow and checked well with the results of the two-point method.

This result leads immediately to many interesting possibilities. A situation in which the main flow is in an inaccessible pipe, or one for which the calibration is not known, presents no hindrance to measurement if a branch stream flows in a pipe which is accessible and which has been calibrated. An even more useful technique is to attach a short length of calibrated pipe and draw off through it a small sampling stream. In its simplest form this could be merely a bucket with a counter dipping into the liquid.

The method permits a closer approach to the intrinsic accuracy of the total-count method than any other because the counting geometry is not merely similar to the laboratory calibration setup but is identical with it. This eliminates a source of error which is often the largest in the field. Also, the counting sensitivity with the tube inside the stream is much higher than with the tube outside the pipe. Thus, the statistical accuracy obtainable with a given amount of tracer is better with the counter inside the sampling stream.*

This application is illustrated by measurements made on a circulating solvent stream used for dissolving gases in one part of the cycle which are stripped in another. The measurement was requested to check the calibration of flow meters in the line. Because of the circulation, it was necessary to finish the measurement of the tail on the tracer wave before the leading edge of the wave came around the second time.

To obtain high counting sensitivity, four 1 by 12 in. tubes were mounted together in a bundle in a snugly fitting plastic pipe. This was set in a sample bucket in which the liquid stream entered at the bottom and overflowed through a drain above the top of the tubes. The bucket held 3·5 gal in the cylindrical annulus. It was calibrated with a solution of triphenylstibine containing antimony^{124}. The factor was 11,440 counts/min per μc/gal. The background with clean solvent in the bucket was 6·6 counts/sec.

This counting bucket was connected to the stream to be measured, and a sampling stream of about 1·6 gal/min was turned into it. Then the tracer was injected and the count observed. The count had scarcely returned to background, after about 11 min, when it began to rise again in response to the second passage of the tracer. After about an hour, the tracer was uniformly distributed throughout the system, with an average count rate in the bucket of 23·2 counts/sec. In the meantime, an alternate pump had been put onstream, and another tracer test was made. To demonstrate the independence of the total count from sampling rate, the flow through the bucket was doubled. The pertinent data from these tests are given in Table 6. For comparison with the results from the new technique, flow rates were measured simultaneously with four counters strapped to the pipe. These are also listed in the table. Also, the meter readings for the two tests are shown.

TABLE 6. Flow rates by sampling bucket method

	Test 1	Test 2
Sample rate (gal/min)	1·6	3·4
Sb^{124} injected (mc)	0·462	0·492
Net total counts	15,460	20,740
Flow rate (gal/min)	342 ± 4	272 ± 3
By counters on pipe	303 ± 13	248 ± 6
Flow meter readings	245	226

The errors shown are based on counting statistics. The ratio of the rate measured by the two tracer methods is constant within the counting error, but there is a systematic

* A question as to the possible effect of non-uniform flow through the counting bucket is considered in Appendix I.

error between the two methods. The error is probably in the pipe calibration factor, making the counter–on–pipe results low by about 10 per cent. The meter readings were low, as had been suspected.

Open streams

Nothing in the principle of the total-count method requires that the flowing stream be confined in a pipe. All that is necessary is that a radiation detector be exposed to the tracered stream in a geometrical configuration which can be duplicated in a laboratory calibration. An open stream may have a very irregular contour; but if the counter can be suspended in it a foot or more away from the sides and bottom, the necessary condition is met. Gamma-rays from parts of the stream farther away will not reach the counter in sufficient numbers to contribute to the counting rate.

It was shown in the foregoing that not all the stream need be observed to get a correct total count. Any small portion of it is a sufficient sample, and we can choose to take that sample in the middle or anywhere else in the stream. According to the theory, the linear velocity of the sample stream relative to the rest of the stream makes no difference. As long as the isotope is well mixed in the stream and the sample is representative of the whole stream, we can choose to measure it in a slow-moving pool or in a swift current.

This technique was first used in the field in the measurement of a water effluent stream from a large refinery. This was chiefly salt water which had been used for cooling various refinery units. It was all combined in a settling tank to separate hydrocarbons which collected in the water from miscellaneous sources. The water from this separator flowed out through a 5×9 ft enclosed concrete channel, 150 ft long, into an open canal.

For this test, a bundle of four 12 in. Geiger tubes was mounted in a 3 ft plastic pipe. This floated vertically in water with the tubes about 10 in. under the surface. This detector was calibrated for the test in a 175 gal tank of cesium^{134} chloride solution. The counting sensitivity was

$$16{,}000 \frac{\text{counts/min}}{\mu\text{c/gal}}$$

The tank was 35 in. in diameter, so the thickness of solution surrounding the counters was about 16·5 in. This is about five times the thickness for half-absorption of the cesium gamma rays; hence, the calibration factor found should be within 3 per cent of that in an infinite medium.

We made three tests, placing the counter in three different positions in the stream.

(1) In midstream, in a strong, turbulent current.

(2) About 2 ft from the west side of the channel, where the counter swung around in an ellipse alternately in a strong current and in relatively quiet water near the edge.

(3) About 2 ft from the east side of the stream in a region of very strong turbulence where the backwater from a tributary stream merged with the main stream.

TABLE 7. Flow rates in open channel

Position	Tracer (mc)	Counts	Flow rate (gal/min)
1	7·33	7000	16,700 ± 200
2	1·81	1670	17,300 ± 600
3	1·39	910	24,400 ± 1200

The results are shown in Table 7.

The check in values at the first two points is well within the statistical accuracy of the measurement. This leads to two conclusions:

(1) The tracer was thoroughly mixed in the stream.

(2) The same values being found in quiet and in swift water supports the theoretical prediction that eddy currents do not affect the measurement (see Appendix II).

The third measurement was made in a portion of the stream where the tracered water was diluted with untracered water from the side stream. Consequently, the count was low and the calculated flow rate too high. This points to a warning that

the method is valid only for completely mixed streams. Farther downstream, where the diluting water would be thoroughly mixed with the whole stream, a uniformly lower count would be expected, corresponding to the higher flow rate.

The first test was made on a stream with so little hydrostatic head that no conventional metering device could be used. Later, an opportunity came to measure a stream that was equipped with a calibrated hook gage set over a horizontal weir. The check between the total-count method and the hook gage was quite satisfactory. A cesium^{134} tracer charge of 4·83 mc gave 5723 counts, corresponding to a flow of 19·4 million gal/day. The hook gage indicated a flow of 19·3.

Natural streams

The total-count method can also be applied to measure flow in creeks and rivers. It is necessary only to mix the tracer thoroughly across the stream. This was demonstrated on a stream flowing down the west slope of Mt. Tamalpais in Marin County, California, directly into the Pacific Ocean.

The counter bundle was floated in the stream, suspended from an overhanging branch of a tree. After a background count, 2·59 millicuries of cesium^{134} was poured into a narrow cascade 120 ft upstream. Activity first arrived at the counter 70 sec later, but it took 45 min for it all to pass. The total count corresponded to a flow of 380 ft^3/min. Another test was made with a fresh batch of tracer a mile downstream, just above the confluence of a tributary. A flow of 400 ft^3/min was found. A third test, four miles farther down, showed 1340 ft^3/min.

The first two values were essentially duplicate tests because no tributary joined the stream between the test points. The third was consistent with the confluence with a somewhat larger stream and one or two smaller branches. Also, the results were consistent with rough estimates of the cross-section and linear velocity at each of the test stations.

A striking result of the test was the extensive longitudinal mixing. It took 10 sec to pour the tracer in; the initial concentration of cesium was

$$\frac{2590\ \mu c}{380\ \text{ft}^3/\text{min} \times 7{\cdot}48\ \text{gal/ft}^3 \times 10/60\ \text{min} \times 3785\ \text{cm}^3/\text{gal}} = 1{\cdot}4 \times 10^{-3}\ \mu c/\text{cm}^3$$

Downstream 120 ft the maximum counting rate was 3160 counts/min. Hence the cesium concentration was

$$\frac{3160\ \text{counts/min}}{16{,}000\ \text{counts/min} \cdot \text{gal}/\mu c \times 3785\ \text{cm}^3/\text{gal}} = 5 \times 10^{-5}\ \mu c/\text{cm}^3$$

A mile downstream, the maximum counting rate from this tracer batch was 32 counts/min showing a concentration of 5×10^{-7} $\mu c/cm^3$. Thus, in 120 ft the tracer was diluted by a factor of 30, in a mile by 3000.

These observations have two important consequences to the practicality of this method. First, it will be possible to measure streams at relatively close-spaced stations. Because of the rapid dilution, one test will not interfere with another one a few miles downstream. Second, it is very simple to meet radiological safety standards. The AEC limit for cesium^{137} in drinking water for continuous non-occupational exposure is $1{\cdot}5 \times 10^{-4}$ $\mu c/cm^3$. The above-cited figures are well below this, even at the point of measurement. It is easy to regulate the rate of pouring to keep even the initial concentration below the tolerance level.

Leak rates

The total-count principle has been applied to other problems. We have used it to measure quantitatively the size of leaks from one liquid stream into another through heat exchangers and condensers. In this problem, we know the flow; and we want to determine the quantity of tracer diverted to the cross-stream from the stream in which it is injected. For this purpose, equation (1) is rewritten

$$A = NQ/F \qquad (15)$$

Counters are exposed to both streams, and the total count from a charge of tracer is measured on each. The ratio between the tracer in the cross-stream and that in the primary stream is

$$A_2/A_1 = N_2Q_2F_1/N_1Q_1F_2 \qquad (16)$$

For this application, the quantity of tracer injected does not have to be accurately known. If, as is often true, the two pipes are the same size, $F_1 = F_2$, and the equation becomes simply

$$A_2/A_1 = N_2Q_2/N_1Q_1 \qquad (17)$$

The fraction of the liquid leaking out of the primary stream is given by the ratio of the A's. In heat exchangers sometimes the primary stream returns as the secondary stream after passing through a process vessel, and even the flow rates cancel out, leaving

$$A_2/A_1 = N_2/N_1 \qquad (18)$$

An example of the use of this technique was the leakage of cooling water from a condenser into a gasoline condensate line. A solution of 2·3 mc of cesium[134] chloride was injected into the cooling water line, flowing at 75 gal/min. Water leaking into the gasoline stream from this and other lines was collected in a settler and drawn off through a 12 in. pipe at a rate of 1·4 gal/min. A net total count of 300 ± 85 was observed from a Geiger tube on the pipe. The 12 in. pipe had not been calibrated, but we estimated a factor of 480 for it. Thus, the activity leaking into the product stream was

$$\frac{300 \times 1{\cdot}4}{480} = 0{\cdot}9\ \mu c$$

only 0·04 per cent of the 2300 μc in the cooling water line. Thus, only 0·03 gal/min of the water in the gasoline line came from this source. Other sources of leakage were responsible for the major part of it.

When the leak is calculated to be as small as it was in this case, this question often arises: Did the excess count, 300 in this case, really represent a leak into the line on which the counter was placed, or was it caused by radiation from the pipe carrying the main charge of tracer, shining across the space between the pipes? In this case, the alternative was excluded by an estimate of its maximum possible magnitude. The cooling water passed the counter in a 3 in. pipe 10 ft away. The counting factor for a long pipe in this configuration was calculated from the geometrical factors to be about

$$6{\cdot}7\ \frac{\text{counts}}{\text{min}} \Big/ \frac{\mu c}{\text{gal}}.$$

Hence, the number of counts expected from unobstructed "shine" at this distance was

$$\frac{2300 \times 6{\cdot}7}{75} = 200.$$

This number must be reduced by absorption in the 12 in. water pipe and three $\frac{3}{8}$ in. pipe walls; also, a thick concrete slab blocked the view of the 3 in. pipe upstream from the point of closest approach. From these factors, we estimated an attenuation of roughly 64, leaving only about three net counts that could be attributed to "shine." Hence, the leak was real.

Entrainment in distillation

Another example of this type of application is to the problem of entrainment in distillation processes. Tar must be excluded from refined petroleum products to a very high degree because it contains nonvolatile metals and coke which would leave deposits in engines and burners. The only mechanism by which these can enter the distillate is by mechanical entrainment. A nonvolatile tracer compound can be used to measure the extent of entrainment with high sensitivity.

Data obtained from the injection of 10 mc of cobalt[60] naphthenate into a lubricating oil still, illustrate this type of problem. The distillate was removed at several different points on the column. The condensate lines from two take-off points were logged with Geiger counts several hundred feet downstream. A counter was also attached to the asphalt line to count the main charge of tracer. The pipes were all the same size, permitting the use of equation (17) for the

VOL. 4 1958/5

numerical comparisons. The results are shown in Table 8.

Gas velocities

The total count principle can be applied also to the measurement of gas velocities. We are working on applications of this kind to various problems. First field tests suggest that this may have a field of usefulness as wide as the liquid flow measurement.

TABLE 8. Entrainment in lubricating oil distillation

Product line	Flow rate, (bbl/hr)	Tubes	Counts	Entrained (%)
Asphalt bottoms	311	1	62,300	—
"Lube G" overhead	33	4	490 ± 78	0·021 ± 0·003
"Lube F" overhead	64	4	158 ± 45	0·013 ± 0·003

ADVANTAGES AND LIMITATIONS OF TOTAL-COUNT METHOD

The total-count method has several inherent advantages over conventional flow-gaging methods. The simplicity of the total-count principle is in striking contrast to the complex formulas of hydrodynamics. The flow rate comes out directly in absolute units. The total-count formula is completely general. It applies as well to a leaking faucet as to a plunging cataract. No equipment need be installed inside the piping; no dams or weirs need be built in streams. Without interrupting the flow of the stream, easily portable equipment is attached to the pipe or floated in the creek. This means the flow can be measured in systems where no meters exist, or existing meters can be checked and calibrated against this absolute flow gage.

The most important limitation on the total-count method stems from its discontinuous nature. A shot of radioactivity gives a result valid at that moment. Although it could be adapted to routine periodic tests in a place where other methods could not be used, its discrete output does not lend itself naturally to continuous recording.

In some instances, the adding of radioactivity to the stream will be considered objectionable. This limitation should not be found unduly severe, however. The concentrations needed for good counting rates are usually close to or less than drinking water standards; and the variety of short-lived isotopes available will usually make it possible to avoid this hindrance.

A word should be said about the superiority of the total-count method over the radioactive dilution method for gaging flow rates. In this older method, a uniform solution of radioisotope is metered at a steady known rate into the stream. The concentration downstream is monitored until it reaches a steady value. The ratio between this value and the concentration in the metering bottle is also the ratio between the metered rate and the flow in the stream. In practice, it is found difficult to hold the injection rate steady. Also, it takes too much isotope to reach a steady concentration in any but the smallest streams. The total-count method is more efficient both in amount of isotope and in equipment required.

Acknowledgements—I am indebted to many persons for assistance in the measurements described in this paper: to Messrs. A. L. PURVIS and G. H. KEIRNS for their collaboration in the first experimental demonstration of the method; to Mr. M. MACOMBER for data relating to the accuracy of the method; to Mr. J. B. MCMASTER for the leak test data; and to my close friend and colleague, Dr. B. A. FRIES, for his constant patience in listening to and criticizing the details of the theory, and for his counsel on this paper.

The total-count method is the subject of patent applications in several countries by the California Research Corporation.[4]

REFERENCES

1. Hull D. E. and Kent J. W. *Industr. Engng. Chem.* **44,** 2745 (1952).
2. Hull D. E. and Keirns G. H. *Nucleonics* **14,** No. 8, 95 (1956).
3. Metcalf G. H. *U.S. Pat.* 2631242 (1953).
4. U.S. Patents 2826699 and 2826700 (now granted).

APPENDIX I

Effect of nonuniform flow through counting bucket

The nonsymmetric construction of the counting bucket raised a question about the effect of non-uniform flow through it on the total count. The sample stream entered at one side of the bottom of the bucket below the counter bundle. It overflowed through a hole at the top of the opposite side. Quite possibly the linear velocity is different up different sides of the bucket. Does this cause an error in the total count?

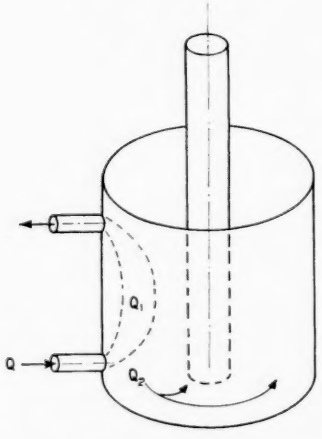

Fig. 5. Effect of channel in counting bucket

To analyse this problem, imagine a channel between the inlet and the overflow bounded by imaginary walls (Fig. 5). Suppose the fraction x of the total flow through the bucket follows this channel, and the fraction $1 - x$ flows through the rest of the bucket.

Now the calibration factor that would be found for the channel—that is, the counting rate with the channel alone filled with a tracer solution at a concentration of 1 μc/gal—would be aF, where F is the factor found when the whole bucket is filled with tracer. Likewise, the factor for the rest of the bucket is $(1 - a)F$.

With this imaginary division of the flow, the total count will be the sum of the counts from the two paths.

$$N = N_1 + N_2 \tag{1}$$

$$= \frac{A_1F_1}{Q_1} + \frac{A_2F_2}{Q_2} \tag{2}$$

$$N = \frac{xA\,aF}{xQ} + \frac{(1 - x)\,A(1 - a)F}{(1 - x)Q} \tag{3}$$

$$= \frac{A}{Q}aF + \frac{A}{Q}(1 - a)F \tag{4}$$

$$= \frac{A}{Q}F$$

Now any flow pattern through the counting bucket could be analyzed into a number of channels, and the separate counts from these channels could be represented as a series by terms like those in equation (3). There would be a series $a_1, a_2, \ldots a_n$ with a sum equal to unity and another series $x_1, x_2, \ldots x_n$ also with a sum of unity. Regardless of the individual values of the a's and x's, the sum of the terms will always be AF/Q. Hence, the conclusion is that a non-uniform flow of any pattern whatever through the counting bucket will give the same total count as a perfectly uniform flow.*

APPENDIX II

Effect of eddy current on total count

A special problem arises in the measurement of irregular streams. Eddy currents may cause recirculation of part of the tracered stream, bringing the same radioactive atoms past the counter more than once. Will this give an erroneous count? The following analysis shows that it will not.

Consider a model of the eddy current like that

* *Note added in proof:* This prediction was confirmed experimentally in a series of tests with the sampling bucket. Baffles were introduced at the top and bottom of the bucket to force the flow (1) to the outside of the bucket, and (2) along the axial counter bundle. The total counts thus observed, with tracer quantity and flow rate unchanged, are compared with the counts (3) with the flow unhindered, and (4) calculated from $N = AF/Q$.

(1) Channeled outside 24,000. (2) Channeled inside 23,900. (3) Not channeled 24,000. (4) Calculated 23,800.

VOL. 4 1958/5

shown in Fig. 6, in which a small pipe loop is attached to a large pipe. The main flow is in the direction ABCD in the large pipe, but a part of the stream is carried back through the small pipe from

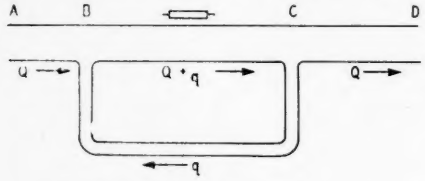

FIG. 6. Effect of eddy current

C to B. The primary current entering at A is Q. This is augmented by the eddy current q between B and C. Suppose a counter is exposed to this part of the stream between B and C. A tracer in the stream will, on its first passage, be accelerated at B and will give less than a normal count, namely,

$$N_1 = \frac{AF}{Q+q} \tag{1}$$

At C, however, the fraction

$$\frac{q}{Q+q}$$

of the tracer will be caught in the eddy current and will come past the counter again. The second time, it will give

$$N_2 = \frac{q}{(Q+q)} \cdot \frac{AF}{(Q+q)} \tag{2}$$

counts. Similarly, on a third passage, there will be

$$N_3 = \left(\frac{q}{Q+q}\right)^2 \frac{AF}{Q+q} \tag{3}$$

counts, etc. The total count will finally be the sum of the infinite series

$$\left[1 + \frac{q}{Q+q} + \left(\frac{q}{Q+q}\right)^2 + \ldots\right] \frac{AF}{Q+q} \tag{4}$$

The sum of the series terms is

$$\frac{1}{1-q/(Q+q)} = \frac{Q+q}{Q} \tag{5}$$

Hence, the total count

$$N = N_1 + N_2 + N_3 + \ldots$$

$$N = \frac{Q+q}{Q} \cdot \frac{AF}{Q+q} = \frac{AF}{Q} \tag{6}$$

the same as if no eddy current existed.

Note that, in this analysis, it is not necessary to assume that the eddy mixes with the whole stream. The large pipe may represent only a sample of the previously mixed stream, and the argument is still valid.

International Journal of Applied Radiation and Isotopes, 1958, Vol. 4, pp. 16–29. Pergamon Press Ltd., London

The Use of Radioactive Isotopes for Determining Saturated Vapour Pressure

H. NESMEYANOV*

A brief survey is given of methods, techniques and experimental arrangements for measuring vapour pressure using radioactive isotopes. Determination of the vapour pressure by a static method from a direct measurement of the radioactivity of the vapour with a counter, from the activity determined by a photographic method or by radio-chemical methods, is described. Papers concerned with the measurement of the vapour pressure by the boiling point and the jet-method are discussed. The variations in Langmuir's method depending on the evaporation of material from a filament and from a crucible are analysed. The vapour pressure of liquid metals and liquid alloy components is calculated from the activity of the condensate. A variation of the method is described in which the vapour pressure is determined from the radioactivity of part of the condensate. The integral and differential variations (integral with collection of all the vapour and differential with collection only of part of the vapour phase) of Knudsen's method are discussed, together with results of vapour pressure measurements of elements and alloy components by radiometric analysis of the condensate. The last section describes measurements of vapour pressure by the isotope exchange method.

A table is given showing the comparative sensitivity of the different methods of measuring vapour pressure.

VOL
4
1958/

L'EMPLOI DES ISOTOPES RADIOACTIFS POUR DÉTERMINER LA TENSION DE VAPEUR SATURÉE

On présente une revue brève des méthodes, des techniques et des arrangements expérimentaux pour la mesure de la tension de vapeur en utilisant les isotopes radioactifs. On décrit la mesure de la tension de vapeur par une méthode statique en mesurant directement la radioactivité de la vapeur avec un compteur, ou en mesurant l'activité ou par une méthode photographique ou par des méthodes radio-chimiques. On discute des communications portant sur la mesure de la tension de vapeur par les méthodes de point d'ébullition et de jet. Les variations dans la méthode de Langmuir qui dépendent de l'évaporation du matériel d'un filament et d'un creuset sont analysées. La tension de vapeur des métaux liquides et des composants des alliages liquides se calcule de l'activité du condensé. On décrit une variation de la méthode où la tension de vapeur se détermine de la radioactivité d'une partie du condensé. Les variations intégrales et différentielles (intégrales, recueillant toute la vapeur et différentielles, recueillant une partie seulement de la phase vapeur) de la méthode de Knudsen sont discutées, ainsi que les résultats de mesures de la tension de vapeur d'éléments et de composants d'alliages par le dosage radiométrique du condensé. La dernière section décrit la mesure de la tension de vapeur par la méthode d'échange isotopique.

On présente un tableau indiquant la sensibilité rélative des différentes méthodes de mesurer la tension de vapeur.

ИСПОЛЬЗОВАНИЕ РАДИОАКТИВНЫХ ИЗОТОПОВ ДЛЯ ОПРЕДЕЛЕНИЯ ДАВЛЕНИЯ НАСЫЩЕННОГО ПАРА

Дается краткий обзор методов и схем аппаратуры для измерения давления пара с помощью радиоактивных изотопов. Описывается определение давлений пара статическим методом по непосредственному измерению радиоактивности пара счетчиком

* Translated by L. C. Ronson from *Atomnaya Energiya* (1957) **3,** No. 9, 227.

или по определению активности радиографическим методом и химическим путем. Приводятся работы по измерению давления пара, выполненные методом точки кипения и методом струи. На примере двух работ рассматривается метод Лангмюра в варианте испарения вещества с нити и испарения из тигля. Давление пара жидких металлов и компонентов жидких сплавов вычисляется из активности конденсата. Описывается вариант метода, в котором давление пара определяется по радиоактивности части конденсата. Излагаются интегральный (с собиранием всего пара) и дифференциальный (с собиранием лишь части паровой фазы) варианты метода Кнудсена и результаты измерения давления пара элементов и компонентов сплавов с радиометрическим анализом конденсата. В последнем разделе описываются измерения давления пара методом изотопного обмена.

Приводится таблица сравнительной чувствительности различных методов измерения давления пара.

DIE VERWENDUNG VON RADIO-ISOTOPEN ZUR BESTIMMUNG VON GESÄTTIGTEM DAMPFDRUCK

Ein kurzer Überblick über Methoden und experimentelle Anordnung zur Messung von Dampfdrucken mittels Radio-Isotopen wird gegeben. Es wird die Dampfdruckbestimmung mittels statistischer Methode durch Direktmessung der Aktivität des Dampfes durch Zähler, Aktivitätsbestimmungen mittels photographischer Methode oder durch radiochemische Methoden beschrieben. Ein Bericht über Arbeiten über Dampfdruckbestimmungen bei Siedetemperatur und nach der Jet-Methode wird gegeben. Veränderlichkeiten in Langmuir's Methode in Abhängigkeit von der Verdampfung von einem Heizfaden und einem Tiegel werden analysiert. Der Dampfdruck von flüssigen Metallen und flüssigen Legierungskomponenten wird aus der Aktivität der Kondensate errechnet. Eine Abänderung der Methode wird beschrieben, in welcher der Dampfdruck aus der Aktivität eines Teiles des Kondensates bestimmt wird. Variationen von Knudsen's Methode (integral: Sammlung des gesamten Dampfes, differentiell: Sammlung nur eines Teiles der Dampfphase) werden besprochen und mit den Ergebnissen der Dampfdruckmessungen von Elementen und Liegerungskomponenten mittels radiometrischer Analyse der Kondensate verglichen. Der letzte Abschnitt beschreibt Dampfdruckmessungen mit Hilfe der Isotopen-Austauschmethode. Eine Tabelle zeigt den Vergleich der Empfindlichkeit der verschiedenen Dampfdruckmessmethoden.

VOL. 4 58/59

The pressure of saturated vapour must be known in order to calculate the thermodynamic functions of a material. The most accurate values of the thermodynamic functions can be obtained from the relation between vapour pressure and temperature over a wide range of temperatures, and especially in the region of low vapour pressures. At normal temperatures, the vapour pressures of solid materials, in particular metals and their alloys, are measured in small fractions of a mm of mercury.

Various methods can be employed to measure saturated vapour pressure: the static method, the boiling point method, the dynamic method (inert gas stream), Langmuir's method (evaporation with open surface), Knudsen's diffusion method, and the isotope exchange method. The greatest errors in any of these methods arise in measuring the temperature, and also from the use of insufficiently pure materials. To increase the accuracy or sensitivity of the measurements, radioactive isotopes are used. In this case, the accuracy of the results is also dependent upon the accuracy of the activity measurement. It is important that the isotope used should be radiochemically pure; high chemical purity of the material used for the measurement is less important.

1. STATIC METHOD

The static method has two main variations. In the first, a direct measurement is made of the pressure of vapour in a given volume which is in equilibrium with the condensed phase, using a mercury, ionization, quartz or some other type of manometer.

This method was first applied[1] using P^{32} to determine the vapour pressure of solid

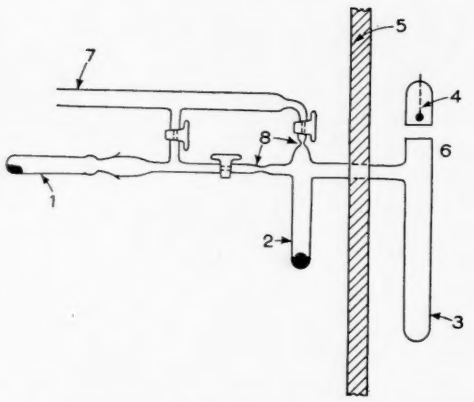

FIG. 1. Apparatus of DAINTON and KIMBERLEY[1] for measuring the vapour pressure of phosphorus.
1 = red phosphorus, 2 = white phosphorus, 3 = test tube 4 = counter, 5 = screen, 6 = small window, 7 = vacuum connection, 8 = constriction for sealing.

white phosphorus (Fig. 1), and phosphorus pentoxide[2] and the vapour pressure of liquid zinc[3] labelled with Zn^{65} (Fig. 2).

To measure the vapour pressure, the material under investigation is placed in a closed constant-temperature chamber which has previously been highly evacuated. The pressure is found from the radioactivity of the vapour measured by means of a counter. It is thus easy to measure the variation of activity as a function of temperature with high accuracy, and to determine the heat of evaporation in the measured temperature interval. To convert to absolute vapour pressure, it is necessary to know the vapour pressure at one of the temperatures[1] or to determine the relation between activity and the number of molecules by applying corrections for the geometrical factor and for the absorption of the radiation.[2] This last procedure is extremely complicated, and it is therefore useful to calibrate the equipment with material of known activity containing the isotope in question.

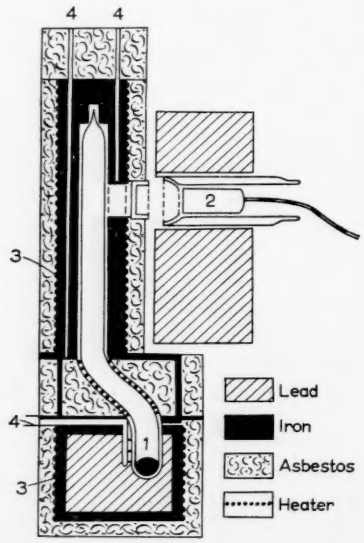

FIG. 2. Apparatus of GROATTO and RICCOBONI[3] for measuring vapour pressures.
1 = evacuated glass or quartz tube containing material under investigation, 2 = counter, 3 = heated block, 4 = thermocouple leads.
Squares, top to bottom: lead, iron, asbestos, heater.

An original variation on the static method was developed[4] for determining the vapour pressure of polonium. It is suitable for measuring the vapour pressure of other α-emitters. Polonium was placed in a cylinder attached to a spherical glass vessel which was evacuated. The polonium vapour filled the sphere until the equilibrium pressure was reached. The quantity of polonium in the sphere was found from the number of α-particles ν, incident per 1 cm^2 of internal sphere surface. These particles were recorded by a photographic emulsion, the number of tracks being measured under a microscope. The calculation was based on the expression

$$P = \frac{3kT}{\lambda t r}\nu, \qquad (1)$$

where k is Boltzmann's constant, T the absolute temperature, t the exposure time, λ the decay constant, and r the radius of the sphere. To take into account the variation of activity with time, a correction for decay $(1 - e^{-\lambda t})$ was included in the denominator.

With this method and an exposure time of thirty days, it was possible to measure exceedingly small vapour pressures. The vapour pressure of polonium at room temperature was found to be 5×10^{-15} mm Hg. On the other hand, if the equilibrium condensed phase is absent, erroneous results

VOL
4
1958/5

can be obtained. Moreover, the assumption that the vapour consists of polonium atoms is doubtful.

In a second version of the method,[5] the number of molecules in a known volume at a given temperature is determined. The radioactive material to be studied (Fig. 3) is placed in a glass vessel 1, 2 which is then evacuated, sealed off, and placed in a constant-temperature furnace. After sufficient time for equilibrium between the condensed phase and the vapour to be established, the vessel is separated in a furnace into two parts at the constriction, 3. The upper part of the vessel 1 is then opened and washed with a solvent containing the carrier. From the activity of the resultant solution the quantity of radioactive material is obtained. Knowing the volume of the vessel, the amount of the material and its molecular weight, it is then easy to determine the saturated vapour pressure from Clapeyron's equation.

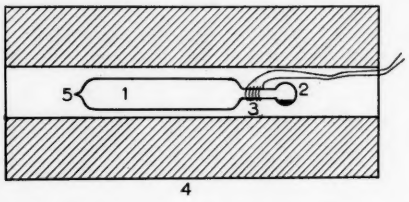

FIG. 3. Schematic diagram of the apparatus used by NESMEYANOV and IOFA[5] for measuring vapour pressure by a static method.
1, 2 = glass or quartz tube containing material, 3 = separating region, 4 = furnace, 5 = vacuum system sealing-off tip.

This method can give accurate results, but it is tedious and, moreover, the maximum temperature cannot exceed the melting point of quartz. This limitation also applies to the first variation of the static method.

2. BOILING POINT METHOD

A liquid boils when the external pressure is equal to its saturated vapour pressure. This phenomenon is widely used for determining the vapour pressure of materials and metals which boil readily at fairly low pressures. The material under investigation is placed in a vessel in which a given pressure (measured by a manometer) is maintained. The temperature is then increased to the boiling point; this is determined by different methods, which are the main source of error. This method was used[6] for determining the vapour pressure of zinc. Zinc containing Zn^{65} was placed in the lower part (Fig. 4) of a bent quartz tube 2 terminating in a U-shaped condenser 11. The end of the tube containing the molten zinc was placed in an electrically heated copper block. The remaining part of the tube up to the condenser was surrounded by a spiral heater and thermally insulated to prevent condensation of the vapours at the tube walls. At the middle of the horizontal part of the tube a space 9 was provided to which heating could be connected at any given moment. The vertical and horizontal sections of the tube were separated by a partition with an opening in it, 7. The tube was connected at the ground joint 10 to the vacuum system and argon reservoir. The system was evacuated, outgassed and filled with argon to a definite pressure. The metal in the tube was then rapidly heated to a temperature 10–15° below the boiling point. Further heating was carried out at a rate of 0·3° per min; heat to the middle part of the tube was

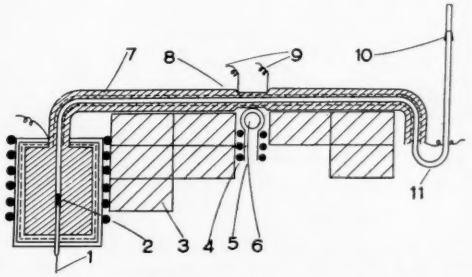

FIG. 4. Apparatus of SMIRNOV and DETKOV[6] for determining vapour pressure by the boiling point method.
1 = thermocouple, 2 = metal in quartz tube, 3 = lead block, 4 = cooler, 5 = counter screen, 6 = counter, 7 = partition with orifice, 8 = region of vapour condensation, 9 = arrangement for connecting heater in condensation area, 10 = ground joint to vacuum connection. 11 = region of condensation of vapour.

then cut off and the radioactivity of the condensate forming on the walls was measured with a counter 6 at given intervals. The variation of activity as a function of time shows a discontinuity at the boiling point. It was shown theoretically and experimentally[7] that, with a diaphragm and aperture providing an obstruction to the vapour stream, the position of the boiling point can be clearly defined; there is an upper limit to the value of the aperture at which the discontinuity becomes sharp and its character is dependent upon the velocity near the boiling point. The authors obtained satisfactory results over a wide range of temperatures.

3. DYNAMIC METHOD (JET METHOD)

A jet of a gas, inert relative to the material, is passed over the said material which is heated to a definite temperature and carries the vapour along. The rate of vapour removal depends on the rate of flow of the gas. The experimental results for different velocities when extrapolated to zero velocity permit calculation of the saturated vapour pressure from the formula

$$P = P_1 \frac{n}{n + n_1} \qquad (2)$$

where P is the vapour pressure of the material studied, P_1 the total pressure of the inert gas and of the vapour, n the quantity of molecules of the material carried out by n_1 molecules of the inert gas.

The quantity of material evaporating is determined from the loss of weight of the material or from the quantity of condensate. In the latter case it is possible to use radioactive indicators to good effect. This method was used[8] recently for determining the partial vapour pressure of a solution of bromine in carbon tetrachloride using Br^{82}. A jet of air was passed over the bromine solution. The gas mixture was then passed through a vessel containing a counter and then into a condenser. The quantity of condensate was determined from measurements of radioactivity, the external pressure and the volume of the gas mixture passing through.

4. LANGMUIR'S METHOD (EVAPORATION FROM A FREE SURFACE)

The amount of material evaporated per unit time from a square cm of free specimen surface in a vacuum, is determined by a relation due to Langmuir

$$G = \alpha P \sqrt{\left(\frac{M}{2\pi RT}\right)} \qquad (3)$$

where G is the rate of evaporation in g/cm² sec, P the vapour pressure in dyne/cm², M the molecular weight, R the gas constant in erg/°, T the absolute temperature, α a dimensionless evaporation coefficient determining the fraction of surface from which evaporation in fact occurs. Although this coefficient is assumed equal to unity in the great majority of cases, such an assumption may introduce serious errors into calculations.

The quantity of material evaporated can be determined from the weight of the condensate obtained by comparing its activity with the specific activity of the original material containing the radioactive isotope.

This method was used[9] to find the vapour pressure of strontium oxide employing Sr^{89} applied to a platinum filament. The filament was heated in a vacuum by an electric current. The temperature of the strontium oxide on the filament was measured with an optical pyrometer. The strontium oxide vapour condensed on the glass walls of the vessel containing the filament and was washed off with hydrochloric acid. The strontium content in the solution was determined by potentiometric titration, by weighing and from the radioactivity.

This apparatus was rather crude since it was necessary in each case to break the glass vessel after exposure. In addition, the surface-area of the evaporating material was inaccurately measured. An improved

VOL. 4 1958/5

apparatus was used[5] for determining the vapour pressure of solid cadmium and zinc (Fig. 5) containing Cd^{113}* and Zn^{65} respectively. The metal was electroplated on to a silver-coated porcelain tube. This tube was then slipped over an iron or molybdenum wire 2 acting as a heater and connected to molybdenum electrodes 3, sealed into the ground joint. A glass bell-jar with cooling jacket 8 was fitted over the ground joint and then evacuated. The temperature was

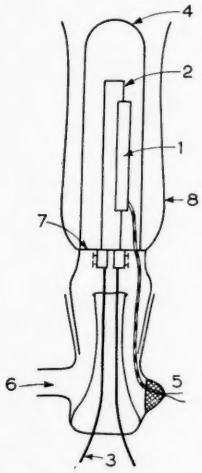

FIG. 5. Apparatus of NESMEYANOV, PRISELKOV and CHERNOROTOV[5] for measuring the vapour pressure of solid zinc and cadmium by the Langmuir method.
1 = silvered porcelain tube carrying layer of investigated material, 2 = iron or molybdenum wire, 3 = molybdenum electrodes, 4 = condensation bell-jar, 5 = thermocouple, 6 = to vacuum, 7 = mica plate, 8 = cooling jacket.

measured with a thermocouple 5 the hot junction of which was attached to a hollow in the porcelain tube at the metal surface. Errors arising in the temperature measurement due to heat conduction along the thermocouple leads must be taken into account. Frequently, one of the most important sources of error with Langmuir's method is the temperature difference between the bulk of the metal and its surface. At the end of this experiment, the condensate was washed off the glass bell jar and the quantity of metal determined from the activity of the solution.

In the last few years, another version of Langmuir's method has been widely employed. A ring from the investigated material is heated in a vacuum by high frequency currents. A large quantity of metal is needed for the experiment, but radioactive indicators can be used, for instance, by depositing them on the ring or cylinder from another inert material.

Langmuir's method was also applied to determine the vapour pressure of liquid silver[10] and the partial vapour pressures of the components of alloys of silver with lead, and of iron with phosphorus,[11] silicon, sulphur[12] and chromium[13] using respectively Ag^{110}, P^{32}, S^{35}, Fe^{59} and Cr^{51}. Evaporation took place from the open surface of the metal in the crucible. The crucible was attached to the base of a glass vessel, the upper part of which formed a glass bell-jar (Fig. 6). The base of the instrument and the bell-jar 2 were connected by a ground joint 7. The equipment was connected to a vacuum system 9. The metal in the crucible was heated by an induction coil 3 and the temperature was measured by a thermocouple 8 introduced from below into the crucible base. The quantity of material evaporated was determined from the activity of the condensate. As in the other versions of Langmuir's method described above, inaccuracy occurs in the determination of the exposure time unless devices are used to isolate the condenser from the vapours during the heating of the crucible to the required temperature, and during its cooling: an additional inaccuracy arises from the tendency of the metal surface to assume a spherical shape under the effect of the high-frequency currents.

Reference must be made to one investigation[14] in which evaporation took place in a vacuum from the free surface of a disc of solid metal and the condensate was collected on a target disc of a different metal situated parallel to the first and some distance from it. By applying to the case of evaporation from a flat surface a law postulating the independence of the distribution of the molecular current on the nature of the evaporated material, the authors derived a

relation determining the fraction of the molecular stream incident on the target

$$k = \frac{1}{2l^2}\left[r^2 + \sqrt{(h^2 + l^2 + r^2)^2 - 4l^2r^2} + \sqrt{(h^2 + l^2)^2}\right] \quad (4)$$

where l is the specimen radius, r the target radius, and h the specimen-target distance.

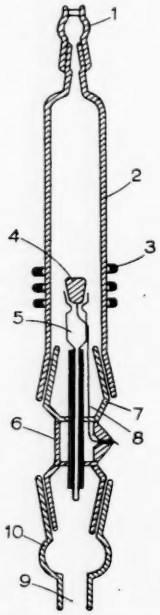

FIG. 6. Apparatus of LYUBIMOV and GRANOVSKAYA[10] for determining the vapour pressure of liquid metals by the Langmuir method.
1 = ground joint with quartz window, 2 = condenser, 3 = high frequency induction furnace, 4 = crucible containing metal, 5,7 = crucible support, 6 = intermediate ground joint, 8 = thermocouple, 9 = to vacuum system, 10 = ground joint.

The value of k can be obtained experimentally from the ratio of the quantity of material condensing on the target to the weight loss of the specimen. A check showed good agreement between experimental and calculated k values.

The vapour pressure of cobalt containing Co^{60} and iron containing Fe^{59} was determined from the expression

$$P = \frac{I}{\beta_0 k S t}\sqrt{\left(\frac{2\pi RT}{M}\right)} \quad (5)$$

where t is the exposure time in seconds, S the specimen area in cm², β_0 the activity of 1 g of the initial metal, I the measured activity of the condensate.

In calculations using this expression it was assumed that the coefficient of evaporation

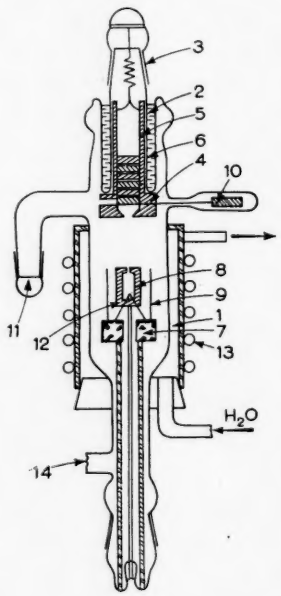

FIG. 7. Apparatus for determining vapour pressure by the differential diffusion method.
1 = cooling jacket, 2 = Dewar vessel with liquid nitrogen, 3 = ground joint, 4 = collimator, 5 = target casette, 6 = targets, 7 = effusion chamber mounting, 8 = effusion chamber, 9 = screen, 10 = push rod, 11 = target store, 12 = thermocouple, 13 = high frequency induction heater, 14 = to vacuum system.

is unity and that all the vapour is condensed at the target. Several targets arranged as shown in Fig. 7 were placed in the apparatus. By this means a number of measurements could be obtained without breaking the vacuum.

One defect in this method is that the induction heating of the metal surface is probably non-uniform.

VOL. 4 1958/5

5. KNUDSEN'S EFFUSION METHOD (ESCAPE OF VAPOUR THROUGH A SMALL APERTURE INTO VACUUM)

This method is based on Knudsen's equation for the quantity of vapour passing by effusion* through an ideally small aperture (infinitely thin wall) into a vacuum:

$$g = At\,(P - P_1)\sqrt{\left(\frac{M}{2\pi RT}\right)} \qquad (6)$$

where $P - P_1$ is the vapour pressure difference between the two sides of the aperture in dyne/cm², A the area of the effusion orifice in cm², t the effusion time in sec, R the gas constant in ergs.

The experiment is so arranged that in the volume on one side of the orifice there is a saturated vapour pressure, and on the other side a vacuum $P_1 = 0$. Effusion occurs through an aperture in a cylindrical chamber. Both the orifice and the chamber have a resistance to the vapour stream depending on the ratio of their diameters and heights. The resistance of the effusion chamber is small as a rule and can be neglected. The resistance of the orifice is represented by a Clausing coefficient K, the ratio between the number of molecules passing through the effusion orifice to the number of molecules incident at the orifice. The vapour pressure, taking into account the factor K, is given by the expression

$$P = \frac{g}{KAt}\sqrt{\left(\frac{2\pi RT}{M}\right)} \qquad (7)$$

In principle the method should give accurate results when there is molecular streaming through the effusion orifice i.e. when the dimensions of the orifice are smaller than the mean free path of the molecules, (in practice when the pressure is below 10^{-1} mm Hg) with an equilibrium pressure in the diffusion chamber. The value of K, A and t can be determined with great accuracy. The most important errors arise in the measurement of temperature. The value of M for vapours is very difficult to determine since existing methods give no constant values; thus in most cases M is assumed equal to the weight of an unassociated molecule. The material of the effusion chamber must not react with the vapour and the condensation of the material on the collector must be complete.

Two variations of the effusion method are used. The first, the integral method, is based on the determination of the total quantity of material passing through the effusion orifice during a time t. This can be found either from the loss in weight of the material in the effusion chamber, or from the amount of condensate. In the latter case the use of radioactive indicators considerably improves the sensitivity of the method.

The second, differential, method has been developed in the last few years[15,16] and has been widely used since. Its sensitivity is appreciably less than that of the integral method since only a proportion of the effusion current is collected.

The equipment used by the various workers is not fundamentally different although that used by HALL[21] is novel in construction. The basic scheme used by most workers is shown in Fig. 7. A small central portion of the molecular beam selected by the collimator 4 is condensed on the flat metal targets 6 cooled by liquid nitrogen 2. The discs are changed without breaking the vacuum by means of a push rod 10. In most investigations an induction coil 13 is used for high frequency heating, the coil being outside the glass vessel. At the end of a series of exposures the instrument is dismantled and the activity of the discs measured with a counter. Expression (7) is used to calculate the vapour pressure with the addition of a factor to take into account the fraction of the molecular beam passing through the collimator

$$\frac{D^2 + 4h^2}{D^2} \qquad (8)$$

where D is the diameter of the collimator aperture, and h the distance between the effusion orifice and the collimator. Insufficient accuracy of alignment may introduce

* Flow of gas through a small aperture.

considerable errors.[14] In addition, for β-emitters the weights of condensates on the target must be kept similar from one experiment to the next.

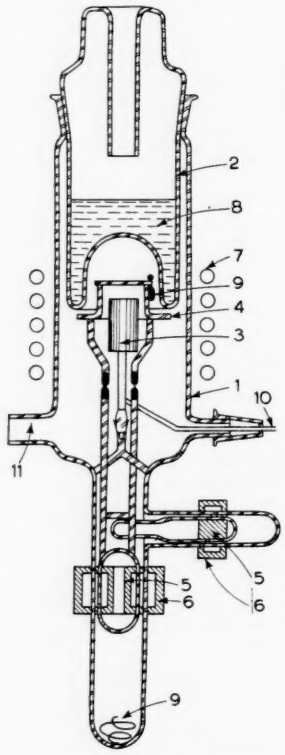

FIG. 8. Apparatus of PRISELKOV and NESMEYANOV[30] for determining vapour pressure by the integral diffusion method.
1 = body, 2 = condensation bell jar, 3 = effusion chamber, 4 = top screening, 5 = armature, 6 = electromagnets, 7 = inductor, 8 = liquid air, 9 = spring, 10 = thermocouple, 11 = to vacuum system.

The method has been used to measure:

(1) The vapour pressure of americium[18] which was calculated according to Raoult's law from the vapour pressure above the powdered solid solution of americium in plutonium; the result agrees well with later direct determinations.[19]

(2) The vapour pressure of uranium[20] which was found from the fission product activity produced by irradiating the uranium on the target in a nuclear reactor.

(3) The vapour pressure of gold (Au^{198}) in solid solutions of gold and copper.[17]

(4) The vapour pressure of trivalent plutonium and americium halides,[21,22] plutonium dioxide,[23] uranium dioxide[24] beryllium oxide (Be^{7}),[25] calcium (Ca^{45}),[26] silver (Ag^{110}),[17] iron (Fe^{59}),[27] cobalt (Co^{60}),[28] and alloys of silver (Ag^{110}) and gold.[29]

In one investigation of the vapour pressure of silver[5] by the differential method it was shown that the inaccuracies mentioned above can be aggravated by the high frequency field perturbing the molecular beam.

The integral diffusion method was developed first using high frequency heating (determination of vapour pressure of solid

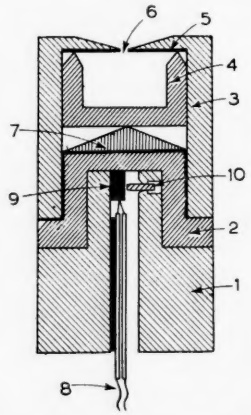

FIG. 9. Effusion chamber apparatus of PRISELKOV and NESMEYANOV (Fig. 8).
1 = base, 2 = bottom liner, 3 = lower cover, 4 = insert, 5 = diaphragm, 6 = diaphragm aperture, 7 = cone, 8 = thermocouple, 9 = hot junction, 10 = clamping screw.

calcium (Ca^{45}) and strontium (Sr^{89})[30]—Figs. 8 and 9) and then for normal heating[31] (determination of the vapour pressure of Sb^{126}—solid antimony).

In all the experiments the vapour was condensed on a collector, then washed off and the activity of the solution determined with a counter. The devices 4, 5 and 6 (Fig. 8) by which the molecular beam could be cut off during the time the chamber was being heated to the required temperature and during its cooling, considerably increased

VOL 4 1958/

the accuracy of the measurements and the fact that the whole condensate can be collected is a marked advantage of this apparatus compared to that used in the differential version. The method was used for measurements of the vapour pressure of solid zinc and cadmium (Zn^{65}, Cd^{113*})[32] arsenic (As^{76}), copper, silver and gold (Cu^{64}, Ag^{110}, Au^{198}).[33]

Investigations of the vapour pressures of the components of metallic alloys and of mixed salt crystals are of great interest. Alloys investigated are Sb–Zn As–Zn As–Cd and Zn–Cd, comprising eutectics and chemical compounds.

The investigations have shown that there are two types of alloys forming chemical compounds. In the first type, the vapour pressure is different for each component. During evaporation the compounds ZnSb, Zn_3Sb_2 dissociate at the alloy surface, and it behaves similarly to a solid solution. The vapour pressure of zinc over the whole range of concentration is proportional to its molecular fraction in the alloy, whilst the vapour pressure of antimony in all the alloys is similar to the vapour pressure of pure antimony. Obviously the surface layer of crystalline materials may behave quite differently from the bulk of the material; during evaporation in the surface layer of the system antimony–zinc dissociation of the compounds of zinc and antimony takes place with a rapid distillation of the more volatile zinc and as a result the surface is enriched in antimony. On the other hand, alloys of the second type (chemical compounds of zinc and cadmium with arsenic) do not dissociate during evaporation, and the vapour pressures of each of the components are similar. The heat of dissociation of these compounds is higher than the heat of evaporation, and lower in the case of antimony and zinc.

The vapour pressure of the eutectic alloys[34] (Zn–Cd, KCl–NaCl) is equal to the vapour pressure of the pure components.

Investigation of the vapour pressure of the components of solid solutions of metals[33] and chlorides of potassium and aluminium[35] showed the suitability of the method for studying the thermodynamics of solid solutions. Diagrams plotting the vapour pressure against composition for the systems Au–Ag and Au–Cu show variations from Raoult's law. The complex nature of the curves on the diagrams for the system KCl–RbCl indicates a change of binding in the crystal lattice. The results obey the Gibbs-Duhem equation and agree with values obtained by other authors and other methods.

The integral diffusion method has also been used for an investigation[36] of the vapour pressures of solid solutions using Zn^{65}. Completely satisfactory results were obtained.

6. ISOTOPE EXCHANGE METHOD

This method[37,38] is based on the measurement of the molecular exchange velocity via the gas phase between two specimens of the material having the same chemical but different isotopic composition. The following exchange cases are possible:

(a) specimens placed close to one another,
(b) specimens situated in the same plane,
(c) specimens separated by a diaphragm with a small orifice.

The absolute rate of exchange at a given temperature is determined by the rate of evaporation and the rate of diffusion of the molecules towards the centre of the specimen. The relations between the rate of evaporation, the coefficient of diffusion and time are determined from the solution of the diffusion equation with boundary conditions appropriate to an evaporation process. This solution can only be given in the form of an equation containing the Gaussian probability integral[37,39,40] from which a simplified expression can be obtained by expanding the probability function in series.[38]

For specimens situated in the same plane the final equation can be written in the form:

$$I = \frac{\alpha K G b S_2}{c^2}\left(v^2 - \frac{4}{3}\cdot\frac{v^3}{\sqrt{\pi}} + \frac{1}{2}v^4 - \frac{8}{15}\cdot\frac{v^5}{\sqrt{\pi}} + \cdots\right). \qquad (9)$$

where $v = c\sqrt{t} = (\alpha KG/\rho) \cdot \sqrt{(t/D)}$; $b = \beta_0 S_1/(S_1 + S_2)$; I is the activity of the originally inactive specimen in disintegrations/sec, α the dimensionless evaporation coefficient, K a dimensionless Clausing coefficient, G the rate of evaporation in g/cm²/sec, ρ the density in g/cm³, β_0 the specific activity of the initial radioactive specimen in disintegrations/sec/g, S_1 the area of the radioactive specimen in cm², S_2 the area of the inactive specimen in cm², t the exchange time in sec, D the diffusion coefficient in cm²/sec.

In practice, the measurements were carried out over a time interval such that the first two terms of the equation are sufficient. When the specimen surfaces are in one plane the rate of transfer increases and expression (9) assumes a form in which for specimens of the same area G is replaced by $2G$. If the exchange time is small, then all terms of the series expansion beyond the first can be neglected and the expression assumes a form giving a linear relationship between activity and time. If the surface area of the radioactive specimen is much smaller than that of the inactive one and their surfaces are facing, a different solution can be used[41] in which the linear portion of the activity–time relation is larger.

The solution of the exchange problem without series expansion for the case of specimens the surfaces of which are facing one another, is ultimately reduced to the following expressions:[38]

$$A = \sqrt{\frac{t'}{\pi}} + \tfrac{1}{4} e^{A t'} \left[1 + \Phi\left(2\sqrt{t'}\right)\right] - \tfrac{1}{4} \quad (10)$$

and

$$I = \frac{\beta_0 \rho S_2}{h} \left\{ h \sqrt{\left(\frac{Dt}{\pi}\right)} + \tfrac{1}{4} \exp\left(4h^2 Dt\right) \times \left[1 - \Phi(2h\sqrt{Dt})\right] - \tfrac{1}{4} \right\} \quad (11)$$

where A is a dimensionless function of t', characterizing the accumulation of the radioactive isotope, $t' = h^2 Dt$; $h = G\alpha K/\rho D$; and Φ is the probability integral.

A graphical method has to be used to determine the rate of evaporation from expressions (10) and (11). The theoretical curve A against t' is first plotted with a double-logarithm and the experimental data used to find the relation log I against log t. Superimposition of the second curve on the first leads to the value t', h and D.

The isotope exchange method allows the simultaneous determination of rate of evaporation and of diffusion coefficient by measuring the variation of activity of the previously inactive specimen as a function of time at a constant temperature. Since the position of the specimens does not vary with time, the method can be applied to measure the partial vapour pressures of the components of alloys. The main difficulty of this method is the need to determine the evaporation coefficient α.

When the specimens are separated by a space having a large resistance to the vapour stream[42] or by a diaphragm with a small aperture[38,39] then in each compartment containing the specimens saturated vapour will be formed. From experiments at different temperatures it was possible to obtain the heat of evaporation from the variation of log I. In order to find the absolute value of the rate of evaporation the exchange need not be carried out through a diaphragm with aperture area S. It is sufficient to use for the calculation equation (9) by substituting $2GS/S_2$ for $S_1 G/(S_1 + S_2)$. In this substitution the increase of activity takes place linearly over a fairly long period of time.

Figures 10 and 11 show schematically the arrangements and chambers used for measuring the rate of evaporation and the coefficient of diffusion by the isotope exchange method.[43] The metal exchange chamber, with a screen separating the specimens during the heating of the chamber to the required temperature, was placed in an evacuated beryl or quartz chamber. The chamber was heated by a high frequency inductor or a miniature resistance furnace placed inside the vacuum chamber. The plates were exposed for a definite time at a constant temperature. The radioactivity of the previously inactive specimen and the specific activity of the initial specimen were measured.

VOL.
4
1958/5

Rates of evaporation of solid silver[38] using Ag^{110} and solid bismuth[43] (almost to 4×10^{-11} mm Hg) using Bi^{210} have been measured. In a similar apparatus but with a diaphragm having a calibrated aperture, measurements were made of the rate of evaporation of zinc (Zn^{65}) and cadmium (Cd^{113*}).[44] The results were in good agreement with data given in the literature obtained by other methods.

In investigations of the rate of evaporation of silver (Ag^{110}) from alloys with gold[31] tin and lead[45] a simplified method was used.

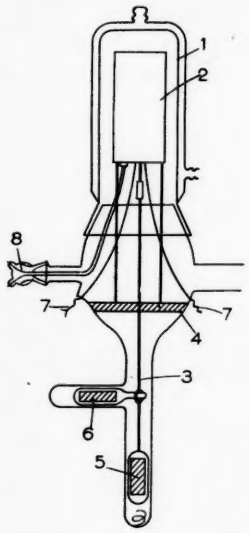

FIG. 10. Apparatus of NESMEYANOV and others[43] for measuring saturated vapour pressure by the isotope exchange method.
1 = removable cooling jacket, 2 = furnace with exchange chamber, 3 = screen holder, 4 = furnace support, 5, 6 = armatures, 7 = molybdenum electrodes, 8 = thermocouple.

Metallic discs (inactive and radioactive) of equal surface area were placed one on top of the other separated by an air space by means of mica rings. Such packs were put into the evacuated furnace for a given period after which the activity of the previously inactive specimen was determined.

A more complex technique was used[41] in determining the rate of evaporation of iron from iron–chromium alloys using Fe^{59}. The metal specimens were placed in ten corundum

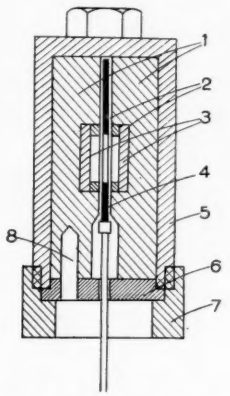

FIG. 11. Exchange chamber in NESMEYANOV's apparatus.
1 = insert, 2 = support rings, 3 = specimens, 4 = screen, 5 = case of chamber, 6 = lid, 7 = threaded base, 8 = recess for thermocouple.

trays 7 (Fig. 12), with a small radioactive specimen 9 in the hollow and a large inactive specimen 8 on the edge of the tray above it. Alloys of different composition were placed in each tray. These trays were fastened in a set which was placed inside the molybdenum resistance furnace 6, under an evacuated bell-jar. The plates were exposed for a definite period of time and then the activity

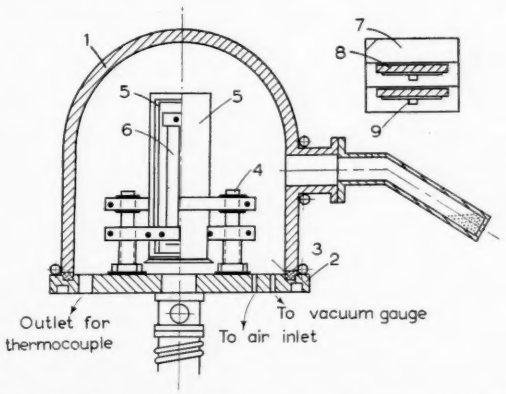

FIG. 12. Apparatus of IVANOV and MATVEEVA[46] for determining the vapour pressure by the isotope exchange method
1 = copper bell jar, 2 = steel plate, 3 = plastic seal, 4 = watercooled electrodes, 5 = molybdenum screen, 6 = molybdenum heater, 7 = corundum crucibles, 8 = inactive specimen (target), 9 = radioactive specimen. Script: (left) = thermocouple bush, (right) = vacuum gauge to air valve.

of the previously inactive specimens was measured. The evaporation rate and vapour pressure were obtained from the activity.

In all the above, it has been assumed that all isotopes have the same value of saturated vapour pressure. This is, however, only approximately so and in all calculations it is necessary to multiply the vapour pressure by the coefficient

$$f = \sqrt{\frac{M_i}{M_e}} \qquad (12)$$

where M_i is the molecular (atomic) weight of the single isotopic molecule and M_e the molecular weight of the molecules consisting of a natural mixture of isotopes.

Data giving the sensitivity of the methods for measuring vapour pressure at a 10 per cent counting efficiency for a specimen with an activity of 1 curie are listed in Table 1.

TABLE 1

Methods	Pressure (mm Hg)
LANGMUIR	10^{-12}
KNUDSEN (integral)	10^{-9}
KNUDSEN (differential)	10^{-7}
Isotope exchange	10^{-12}
NESMEYANOV, IOFA (static)	10^{-7}

The employment of radio isotopes holds out special promise for measurement of the saturated vapour pressures of metals and their alloys.

REFERENCES

1. DAINTON F. S. and KIMBERLEY H. M., *Trans. Faraday Soc.* **46,** 912 (1950).
2. ROSEN F. D. and DAVIS W., *Rev. Sci. Instrum.* **24,** 349 (1953).
3. GROATTO U. and RICCOBONI L., *Chim. Industr.* **37,** 538 (1955).
4. AUSLANDER J. S. and GEORGESCU I. I., *Int. Conf. on Peaceful Uses of Atomic Energy, Geneva,* 1955 Paper 1090.
5. NESMEYANOV A. N., Measurement of vapour pressure of solid materials in binary alloys. *Collected Papers, All Soviet Conference on the Use of Radioactive and Stable Isotopes,* Vol. 2, *Metallurgy and Metallography.* Academy of Sciences, Moscow. In press.
6. SMIRNOV M. V. and DETKOV S. N., *Dokl. Akad. Nauk. SSSR,* **98,** 777 (1954).
7. DETKOV S. N., *Zh. fiz. khim.* **31,** 83 (1957).
8. BARTHEL C. and DODE M., *Bull. Soc. Chim. Fr.* 1312 (1954).
9. MOORE G. E., ALLISON H. W. and STRUTHERS I. D., *J. Chem. Phys.* **18,** 1572 (1950).
10. LYUBIMOV A. P. and GRANOVSKAYA A. A., *Zh. fiz. khim.* **27,** 10 (1953).
11. LYUBIMOV A. P. and GRANOVSKAYA A. A., *Zh. fiz. khim.* **27,** 1437 (1953).
12. GRANOVSKAYA A. A. and LYUBIMOV A. P., *Metallurgical Applications of Radioactive Isotopes* p. 66 Gostekhizdat (1955).
13. LYUBIMOV A. P. and GRANOVSKAYA A. A., *Metallurgical Applications of Radioactive Isotopes* p. 95 Gostekhizdat (1955).
14. MATVEEVA M. P., POPOV I. A. and IVANOV L. I., Quotation from Kyikov I. S. and Popov I. A., *Metallurgical Application of Radioactive Isotopes* p.127 Gostekhizdat (1956).
15. CARNIGLIA S. C. and CUNNINGHAM B. B., *J. Amer. Chem. Soc.* **77,** 1502 (1955).
16. TOMLIN D. H., *Proc. Phys. Soc.* B **67,** 787 (1954).
17. SCHADEL H. M. and BIRCHENALL C. E., *J. Metals* **188,** 1134 (1950).
18. PHIPPS T. E., SEARS G. W., SEIFERT R. L. and SIMPSON O. C., *Int. Conf. on Peaceful Uses of Atomic Energy, Geneva,* 1955 Paper 375.
19. ERWAY N. D. and SIMPSON O. C., *J. Chem. Phys.* **18,** 953 (1950).
20. RAUH E. G. and THORN R. J., *J. Chem. Phys.* **22,** 1414 (1954).
21. HALL L. D., *J. Chem. Soc.* **73,** 757 (1951).
22. PHIPPS T. E., SEARS G. W., SEIFERT R. L. and SIMPSON O. C., *J. Chem. Phys.* **18,** 713 (1950).
23. CARNIGLIA S. C. and CUNNINGHAM B. B., *J. Amer. Chem. Soc.* **77,** 1451 (1955).
24. ACKERMAN R. J., ANL–5482 (1955).
25. PHIPPS T. E., SEARS G. W. and SIMPSON O. C., *J. Chem. Phys.* **18,** 724 (1950).
26. ERWAY N. D. and SEIFERT L. K., *J. Electrochem. Soc.* **98,** 83 (1951).
27. KORNEV YU. V., *Dokl. Akad. Nauk SSSR* **93,** 467 (1953).
28. KORNEV YU. V. and GOLYBKIN V. N., *Dokl. Akad. Nauk SSSR* **99,** 565 (1954).
29. KORNEV YU. V. and VAINTAIKIN E. Z., *Zh. fiz. khim.* **30,** 1540 (1956).
30. PRISELKOV YU. A. and NESMEYANOV A. N., *Dokl. Akad. Nauk SSSR* **95,** 1207 (1954).
31. NESMEYANOV A. N. and IOFA B. Z., *Dokl. Akad. Nauk SSSR* **98,** 993 (1954).

VOL.
4
1958/5

32. Nesmeyanov A. N., Iofa B. Z., Strel'nikov A. A and Firsov V. G., *Zh. fiz. khim.* **30,** 1250 (1956).
33. Nesmeyanov A. N., Smakhtin L. A. and Lebedev V. I., *Dokl. Akad. Nauk SSSR* **112,** 700 (1957).
34. Nesmeyanov A. N. and Sazonov L. A., *Zh. nauk. khim.* **2,** 946 (1957).
35. Nesmeyanov A. N. and Sazonov L. A., *Zh. nauk. khim* **2,** 1183 (1957).
36. McKinley I. D. and Vanu I. E., *J. Chem. Phys.* **22,** 1120 (1954).
37. Nesmeyanov A. N., Lozgachev V. I. and Lebedev N. F., *Dokl. Akad. Nauk SSSR* **102,** 307 (1955).
38. Nesmayanov A. N., Lebedev N. F., Lozgachev V. I. and Chudinov E. G., *Moscow Conference on the Peaceful Uses of Atomic Energy*, 1955 p. 79. Academy of Sciences (1955).
39. Zhukhovitskii A. A., *Moscow Conference on the Peaceful Uses of Atomic Energy*, 1955 p. 101. Academy of Sciences (1955).
40. Zhukhovitskii A. A., Yanitskaya M. E. and Kryukov S. M., *Zh. fiz. khim.* **29,** 1338 (1955).
41. Ivanov L. I., Kulikov I. S. and Matveeva M. P. *Izv. Akad. Nauk. SSSR, otd. tekh. nauk* No. 8 (1955).
42. Zhukhovitskii A. A., Yanitskaya M. E., Kryukov S. M. and Galitsin A. G., *Dokl. Akad. Nauk SSSR* **102,** 127 (1955).
43. Nesmeyanov A. N., Iofa B. Z. and Karasev B., *Dokl. Akad. Nauk SSSR* **112,** 882 (1957).
44. Nesmeyanov A. N. and Il'icheva I. M., *Zh. fiz. khim.* In press.
45. Zhukhovitskii A. A. and Yanitskaya M. E., *Dokl. Akad. Nauk. SSSR.* In press.
46. Ivanov L. I. and Matveeva M. P., *A New Apparatus and a Method for Measuring the Vapour Pressure of a Metal* II–57–17/4. Thermal Power Research Institute, U.S.S.R. State Technological Centre and U.S.S.R. Academy of Sciences (1957).

OL.
4
8/59

International Journal of Applied Radiation and Isotopes, 1958, Vol. 4, pp. 30–35. Pergamon Press Ltd., London

An Examination of Lubrication with Soap, using Radioactive Sodium Stearate

J. GOLDEN, P. R. LANCASTER and G. R. ROWE
Tube Investments Research Laboratories, Hinxton Hall, Saffron Walden, Essex

(*Received* 3 *February* 1958; *in revised form* 24 *February* 1958)

This paper describes an experimental study of the behaviour of a soap coating on rectangular mild steel bars drawn slowly under plane strain conditions between hard cylindrical dies. Loads up to 5 tons were applied to reduce the cross-section of the bars by 5–30 per cent in one pass. Purified sodium stearate was neutron-activated and was used as the lubricant. It is found that although the drawing conditions are designed to discourage hydrodynamic lubrication, films of soap over 1000 Å thick can pass between the dies and the specimens.

The soap film thickness decreases steadily as the percentage reduction of area of the specimen is increased and eventually at about 30 per cent reaches a value of 600 Å, comparable with the maximum height of the surface asperities. At this stage the smooth surface of the specimen can be seen to be damaged and "pick-up" is found to occur.

The use of radioactive sodium stearate has proved to be an especially sensitive method for estimating soap throughout. Less than one complete monolayer could be detected with reasonable accuracy.

VOL.
4
1958/5

UN EXAMEN DE LA LUBRIFICATION AU SAVON, UTILISANT LE STÉARATE DE SODIUM RADIOACTIF

Cette communication décrit une étude expérimentale sur le comportement d'un enduit de savon sur des barres rectangulaires d'acier doux tirées lentement, sous des conditions de déformation plane, entre des coussinets durs cylindriques. Des charges de jusqu'à 5 tonnes servaient à réduire la section transversale des barres par 5–30 pour cent à une passe. Du stéarate de sodium purifié fut employé, après activation aux neutrons, comme lubrifiant. On a trouvé que, bien que les circonstances du tirage soient arrangées pour décourager la lubrification hydrodynamique, des pellicules de savon dépassant 1000 Å d'épaisseur peuvent passer entre les coussinets et les échantillons.

L'épaisseur de la pellicule savoneuse diminue régulièrement avec la diminution pour cent la section de l'échantillon et enfin, à environ 30 pour cent, atteint une valeur de 600 Å, comparable à la hauteur maximum des aspérités de la surface. A ce point une détérioration se fait voir sur la surface lisse de l'échantillon et il se trouve du "cueillage."

L'emploi du stéarate de sodium radioactif s'est montré une méthode particulièrement sensible pour le dosage du savon. L'observation est possible à une précision raisonnable de moins d'une couche monomoléculaire entière.

ИСПЫТАНИЕ МЫЛЬНОЙ СМАЗКИ, В КОТОРОЙ ИСПОЛЬЗУЕТСЯ РАДИОАКТИВНЫЙ СТЕАРИНОВОКИСЛЫЙ НАТРИЙ

В данной статье описываются экспериментальные исследования поведения мыльной пленки на прямоугольных стержнях из мягкой стали при медленной протяжке между твердыми цилиндрическими валиками. Для уменьшения поперечного сечения стержней на от 5 до 30% за один проход применялась нагрузка до 5 тонн. В качестве смазки был применен очищенный стеариновокислый натрий, активированный нейтронами.

Найдено, что хотя условия протяжки не благоприятствуют гидродинамической смазке, между прокатываемым образцом и валиками может удерживаться мыльная пленка толщиной свыше 1000 ангстрем.

С возрастанием процента уменьшения площади образца толщина пленки непрерывно уменьшается, достигая при 30%-ном уменьшении сечения примерно 600 ангстрем, т.е. величины вполне сравнимой с максимальной вышиной шероховатостей поверхности. На этой стадии происходят повреждения гладкой поверхности образца и наблюдаются "задиры".

Применение радиоактивного стеариновокислого натрия оказалось исключительно чувствительным методом определения мыльной пленки. Толщина меньше одного полного монослоя могла быть определена с достаточной точностью.

EINE UNTERSUCHUNG VON SEIFE ALS GLEITMITTEL VON RADIOAKTIVEM NATRIUM-STEARAT

Dieser Bericht beschreibt experimentelle Untersuchungen des Verhaltens eines Seifenüberzuges auf rechtwinkelige Weichsthalbarren, welche langsam bei ebener Beanspruchung über zylindrische Blöcke gezogen werden. Belastungen biszu 5 t wurden verwendet um denquerschnitt der Barren bei einem Durchgang um 5–30% zu verringer. Neutronen-aktiviertes, gereinigtes Natrium-Stearat wurde als Gleitmittel verwendet. Es zeigte sich das, obwohl die Ziehbedingungen so gestaltet waren um hydrodynamische Schmierung möglichst zu verhindern, einen mehr als 1000 Å dicker Seifenfilm zwischen den Blöcken und der Probe passieren kann. Die Seifenfilmdicke nimmt stetig ab, je mehr die Fläche der Probe verringert wird und erreicht bei etwa 30% der ursprünglichen Flächengrösse ihren Wert von 600 Å welcher vergleichbar ist mit der maximalen Höhe der Oberflächenrauhheit. In deisem Stadium sieht man wie die glatte Oberfläche der Probe zerstört wird und wie ein "pick-up" stattfindet.

Die Verwendung von Radio-Natrium-Stearat hat sich als besonders empfindliche Methode zur Bestimmung der gesamten Seifenmenge erwiessen. Weniger als eine komplette monomolekulare Schicht konnte mit vernünftiger Genauigkeit nachgewiesen werden.

OL.
4
8/59

INTRODUCTION

Extensive studies of frictional behaviour under laboratory conditions have been made elsewhere using light loads and low speeds. On the other hand much work has been done under practical industrial conditions where accurate control of conditions is difficult.

The present experiments were designed to reproduce the heavy loads encountered in industrial tube-drawing, but with a laboratory equipment in which the conditions can be carefully controlled. Sodium stearate was neutron-activated to produce Na^{24}. This makes it possible to assess accurately the small quantities of lubricant which pass through the rubbing interface and so to assess the effectiveness of lubrication under increasingly severe conditions.

EXPERIMENTAL

(1) *Drawing apparatus and force measurements*

The whole apparatus is contained in a vacuum tank to allow atmosphere control, particularly control of humidity, but in these experiments the normal atmosphere was admitted all the time. The essential working parts are shown diagrammatically in Fig. 1.

A rectangular metal bar specimen S, usually $\frac{1}{2} \times \frac{1}{2} \times 10$ in., is drawn longitudinally between two hard steel cylindrical dies D_1 and D_2 by a rigid carriage moved steadily at low speed (5 in/min) by a 20 ton motor-driven hydraulic ram. These conditions were chosen to reduce hydrodynamic contributions to the lubrication. The die D_1 is rigidly attached to the wall of the containing vacuum tank and the lateral

force on the specimen is applied by a separate ram carrying the second die.

The thrusts on the rams are measured by recording the oil pressures in the ram cylinders, corrections being made for the ram friction at various pressures. This introduces some error, and it is proposed in future experiments to rely upon strain gauges attached to the lateral ram head and to the specimen shackle.

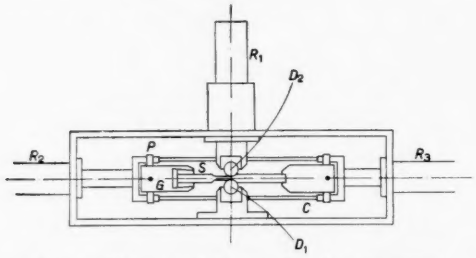

FIG. 1. Diagram of the bar-drawing apparatus. The die D_1 is fixed to the case of the friction machine. D_2 is another die housed at the end of a hydraulically operated ram R_1. The specimen is secured at the left-hand end in the wedge grips of the shackle G, which is free to rotate about the axis of pin P. The specimen is drawn under approximately plane-strain conditions, by application of a force to the rigid carriage C from the ram R_3.

A specimen was installed in the apparatus so that it was horizontal and close to the static die. A symmetrical pair of cylindrical indentations was then made by applying pressure to the ram carrying the die D_2. When an appropriate reduction of area had been reached, as indicated by a dial gauge, the hydraulic valve was closed. The lateral ram was then started and the specimen commenced to draw steadily. As the drawing began the indicated load on the dies fell to about one half, since the interfacial pressure between specimen and die was then taken only on the forward face of the die. This load is of course the valid one for friction measurement and was recorded.

It was found that after only a short distance (about 1 cm) both drawing load on the travelling ram and die load on the cylindrical dies became steady and constant.

(2) *Activation and application of soap*

Seven grams of purified sodium stearate were sealed off in a silica ampoule and irradiated for two days in a flux of 10^{12} neutrons/cm^2/sec. This irradiation produces 89 per cent of the equilibrium activity of Na^{24} which has a half-life of 15·0 hr. Since the equilibrium activity is 380 mc/g of sodium the activity produced will be 25 mc/g of sodium stearate.

This level of activity proved to be very convenient for counting but could easily be reduced for future experiments and still yield results of adequate accuracy. Four hours after the end of irradiation the ampoule was opened and the radioactive sodium stearate was dissolved in warm water to make a 14% solution. Less than 10 ml of this solution was found to be adequate for the experiments reported here.

The specimens used for these experiments were 0·15 per cent carbon steel. They were finished by machining and hand grinding on abrasive paper, down to 15 μ grit-size under water. The warm soap solution (at 65°C) was applied to one face of the bar specimen by means of a glass rod. An inactive solution of the same concentration was applied to the opposite face. The specimens were then stored for about 20 hr in free air at about 19°C with a relative humidity between 60 and 70 per cent.

(3) *Assessment and standardization of soap throughput*

The counting assembly. After the bar had been drawn, a 6 cm length was cut out of the drawn section which was of constant width but of varying thickness depending on the reduction. A standard commercial scintillation counting assembly was used. (see Fig. 2). The aluminium can which provides a light-tight enclosure for the phototube plus scintillator also provides a suitable flat face against which to place the bar specimens. It was decided that a demountable arrangement would be best so that thorough decontamination of the counter would be simple. Although the specimens vary in thickness the technique presents the radioactive face at the same distance from the can. Two lines were

VOL 4 1958/

drawn across the circular face of the can slightly more than $\frac{1}{2}$ in. apart so that a bar specimen could easily be centrally aligned. To prevent direct contact with the can small pieces of aluminium 0·25 mm thick were placed at each end between the bar and the can. A suitable length of Sellotape was then used to fix the bar to the can. The scintillation head could now be placed in the lead well and counting begun.

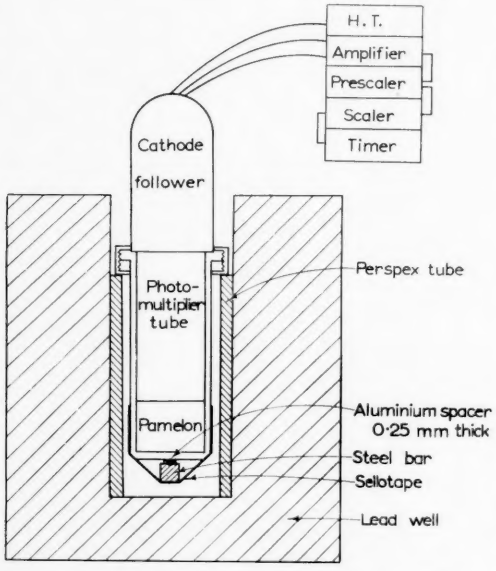

FIG. 2. A diagram of the scintillation counter assembly.

After removal of a bar the end of the can was stripped of Sellotape and washed with water. It was observed that there was negligible rise in background rate. The piece of plastic scintillator (Pamelon) was 3·8 cm in diameter and 3 cm long. The distance from the radioactive face of the specimen to the scintillator was 1·25 cm.

Sodium-24 emits β-particles of maximum energy 1·39 meV and γ-rays of energy 1·37 and 2·76 meV. Since the face of the aluminium can has a thickness of about 220 mg/cm^2 only about 2 per cent of the β-activity is detected. This reduces the efficiency somewhat but has the advantage of making the results less susceptible to self-absorption difficulties. Calibration of the counting system gave:

2170 counts/min/μg of soap

The activation level of the soap used was 25×10^{-3} μc/μg of soap. Hence the overall efficiency is approximately 4 per cent. This efficiency can be increased by at least a factor of 2 using a sodium iodide crystal as detector. For the work described this increase was unnecessary.

To obtain accurate results specimens were coated with radioactive soap on only one side. It is, however, possible to assess specimens with opposite faces bearing radioactive soap if the radiation absorption characteristics are known.

Standardization. A length of clean steel bar was shown to make no contribution to the counting rate. Lengths of bar $6 \times 1{\cdot}25 \times 1{\cdot}25$ cm were prepared as standards by placing an aliquot of the standard soap solution (66 mg in 250 ml) on one face and evaporating off the water. Twelve standardizations were made with different samples at different times, throughout the experiments. The mean result was 2170 ± 110 counts/min/μg of soap. An autoradiograph showed that a specimen which was visibly fairly uniform, possessed local concentrations. The counting geometry is such that non-uniformity of distribution on the bar will create errors. The bar-drawing machine produces specimens with fairly even spread of soap, so that comparison between specimens is more accurate than the absolute calibration.

Autoradiographs. Autoradiographs were taken of bar specimens by placing the active faces in contact with X-ray film (Ilford Industrial C) in a light-tight box. Exposures of approximately one hour were necessary the day after commencement of the experiments.

Protection. All work involving the handling of more than a few μg of radioactive soap was carried out behind walls of lead 2 in. thick. The main bulk of the soap solution not being used for coating specimens was stored away from the laboratory in which the bar specimens were drawn. Each coated specimen carried only relatively slight

activity and the massive walls of the bar-drawing machine reduced the radiation considerably. Specimens were transferred with the aid of a specially made long-handled tool. Coating of specimens was carried out over a bench sink with Formica surrounds. No experimenters received more than one third of a tolerance dose during the week.

A decay curve was followed for four days using a thin end window Geiger counter and a value of 15·0 $\pm$ 0·2 hr was obtained for the half-life. After further counting no contaminating long-lived activity which might have created an ingestion risk was found. The source used gave 27 $\times$ 10^3 counts/min, 30 hr after the stearate left the pile. After nine days this had decayed to less than 2 counts/min and was indistinguishable from background.

RESULTS AND DISCUSSION

The reduction quoted is a measured reduction of thickness of the specimen. Actually the drawing conditions are such that the strain is very nearly plane; that is, the lateral flow of metal is negligible.

The sodium stearate which had been radioactivated left the pile at 6 a.m. on a Monday morning and counting was performed from the middle of that day until Friday midday. Counts were taken for a sufficient time to yield a result with standard deviation less than one per cent. Since the counting rates were conveniently high only a few minutes were necessary for each specimen.

The background was negligibly small (ca. 50 counts/min) compared with the counting rates of the specimens, so that highly accurate background estimation was unnecessary. Before mounting a specimen the sides adjacent to the active face were cleaned of any small amounts of radioactive soap. A few checks on the reproducibility of the specimen-mounting arrangement were carried out. Complete demounting and reassembly in opposite orientation gave results lying within $\pm$2 per cent of the mean.

TABLE 1. Throughput of soap

Specimen	Counts/min 10^{-3}	Surface area of specimen (cm²)	Percentage reduction of bar thickness
56	303	7·55	4
57	269	7·62	9
58	148	7·69	20
59	124	8·00	23
60	102	7·81	30

The surface area of the specimens was measured and the weight of soap on unit area calculated using the above calibration (2170 counts/min/μg). Assuming the density of the soap to be 1 and the soap film to be uniform its thickness was estimated (Fig. 3).

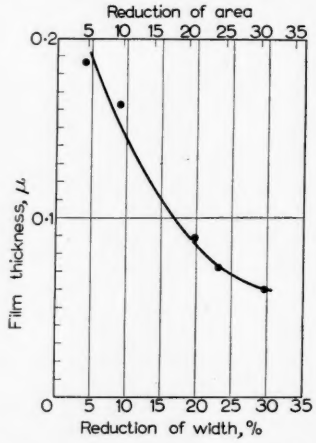

FIG. 3. The variation of soap throughput with bar reduction.

These results do not allow for any water which may be retained in the dried soap, but this is known to be very small (less than 2 per cent).

The thickness of the soap film decreases steadily as the severity of the draw is increased. The average roughness of the surface, measured as the average departure from a mean-area datum line, is about 0·08 μ in the freshly prepared conditions. It is interesting to notice that the measured mean thickness of the soap film after a 30 per cent reduction draw is shown by Fig. 3 to be about 0·06 μ.

Fig. 4 shows the profile of the specimen to be reasonably regular before and after the draw. We may thus say, roughly, that the soap film after the 30 per cent draw is just about adequate to keep the asperities of the bar from contact with the die. Photographs of the drawn specimens show that for reductions below 30 per cent the drawn surface is unmarred but after a draw of 35 per cent considerable scoring of the bar is visible and there is appreciable "pick-up" or transfer of specimen metal to the die. This aspect will be more fully examined in later experiments. For reductions below 30 per cent the coefficient of friction was found to be nearly constant, independent of reduction, at about $\mu = 0{\cdot}15$. The autoradiographs showed a decrease in intensity with increasing drawing severity which supports the counting results. It was observed that after the heavier draws the soap film was almost uniform, but that local pockets still remained after the light draws. This means that the assumption of uniform soap film thickness for the lighter draws is less valid and the curve shown in Fig. 3 should be less steep. Nevertheless, it appears that films of soap over 1000 Å thick can pass between die and specimen, even when very heavy loads are imposed.

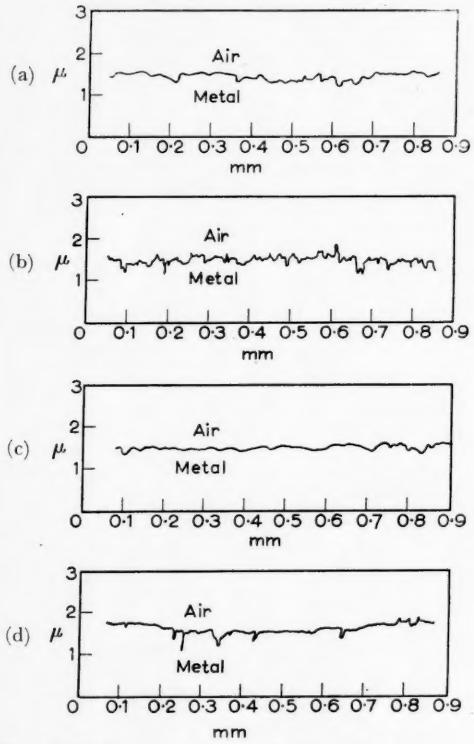

FIG. 4. Profilometer records of the surfaces before and after a 30% draw.
(a) longitudinal before drawing.
(b) transverse before drawing.
(c) longitudinal after drawing.
(d) transverse after drawing.

The use of radioactivated sodium stearate has proved to be an especially sensitive method for estimating soap films on drawn specimens of metal. The thinnest film actually measured during these experiments was 600 Å. This gave 102 $\times$ 10^3 counts/min. Since the background count was 50 counts/min, less than one complete monolayer could be detected with reasonable accuracy.

Acknowledgements—We thank the Chairman of Tube Investments Limited for permission to publish these results. We also thank Mrs. B. J. FRANCIS and Mr. D. J. C. STEARN for their assistance.

International Journal of Applied Radiation and Isotopes, 1958, Vol. 4, pp. 36–40. Pergamon Press Ltd. London

Application of the Light Intermittency Method to Investigations on Isotopic Exchange Reactions in Gas and Liquid Phase

V. B. MILLER, M. B. NEIMAN and S. P. SOLODOVNIKOV

(*Received* 12 *March* 1958)

Radioisotopic exchange reactions have not been so far investigated in detail by the light intermittency method. It is shown that this method can be used for reactions not only with quadratic but also with linear chain termination involved. Both termination processes were observed in isotopic exchange between CH_2I_2 and I_2^{131}.

The new technique is based on separation of alkyl iodides from active iodine by adsorbing the latter on an active silver layer.

APPLICATION DE LA MÉTHODE À LUMIÈRE INTERMETTANTE À LA RECHERCHE DES RÉACTIONS D'ÉCHANGE ISOTOPIQUE EN PHASE GAZEUSE ET EN PHASE LIQUIDE

La méthode à illumination intermittente n'a pas été employée jusqu'ici pour l'étude détaillée des réactions à échange radioisotopiques. Il se montre que cette méthode peut servir pour des réactions qui entraînent une fin de chaîne, non seulement quadratique, mais aussi linéaire. Tous deux procédés de terminaison se montrèrent dans l'échange isotopique entre CH_2I_2 et I_2^{131}.

La nouvelle technique dépend de la séparation des iodures alcoyls de l'iode actif en adsorbant celui-ci sur une couche d'argent actif.

ПРИМЕНЕНИЕ МЕТОДА ПРЕРЫВИСТОГО ОСВЕЩЕНИЯ ДЛЯ ИЗУЧЕНИЯ РЕАКЦИЙ ИЗОТОПНОГО ОБМЕНА В ГАЗОВОЙ И ЖИДКОЙ ФАЗЕ

Реакции изотопного обмена до сих пор не исследовались достаточно подробно методом прерывистого освещения. Показано, что этот метод может быть применен не только при квадратичном но и при линейном обрыве. Оба процесса обрыва исследовались при изотопном обмене между CH_2I_2 и I_2^{131}.

Новая методика основана на отделении алкилиодидов от радиоактивного иода путем поглощения последнего активным слоем серебра.

UNTERSUCHUNGEN VON ISOTOPEN IONENAUSTAUSCHREAKTIONEN IN GASFÖRMIGER UND FLÜSSIGER PHASE MIT HILFE DER INTERMITTIERENDEN-LICHT-METHODE

Radioisotope Ionenaustauschreaktionen wurden bisher noch nicht im Detail mit der intermittierenden-Licht-Methode untersucht. Es wird gezeigt, dass diese Methode nicht nur für quadratischen, sondern auch bei linearem Kettencharakter verwendet werden kann. Beide Prozessarten werden beim Isotopenaustausch zwischen CH_2J_2 und J_2^{131} beobachtet.

Die neue Methode basiert auf einer Trennung des Alkyliodids von aktivem Jod durch Adsorption des letzteren an einer aktiven Silberschicht.

VOL
4
1958/

Isotopic exchange reactions often serve as pilot reactions in investigations on the mechanism of substitution processes.[1,2]

Photosensitized isotopic exchange reactions of haloid alkyles RX with halogene molecules X_2 can be considered as an example of this type of reaction

$$X_2 + h\nu \xrightarrow{\rho Ia} X + X$$

$$RX^* + X \xrightarrow{k_1} XX^* + R$$

$$R + X_2 \xrightarrow{k_2} RX + X$$

$$RX^* + X \xrightarrow{k_3} RX + X^*$$

$$X + X \xrightarrow{k_4} X_2$$

To determine k_1, k_2 and k_3 it is necessary to know the quadratic termination constant k_4. This can be achieved by means of the light intermittency method.

This method permits determination of the constants for recombination reactions from measurements of lifetimes of radicals τ and of the energy of absorbed light ρIa.[4]

The theory of the method implies that lifetimes of radicals are connected with the time of the light flash λ and with parameter m according to

$$\tau = \frac{\lambda}{m} \tag{1}$$

Parameter m can be estimated from comparison of experimental and theoretical results. On the other hand

$$\tau = \frac{R_{st}}{W_{term}} \tag{2}$$

where R_{st} is the steady concentration of radicals, and W_{term} the rate of chain termination.

In case of a fully quadratic termination

$$R_{st} = \sqrt{\frac{(\rho Ia)}{K_4}} \tag{3}$$

and

$$W_{term} = K_{term} R_{st}^2 \tag{4}$$

Hence

$$\tau = \frac{1}{\sqrt{(K_4 \rho Ia)}} \tag{5}$$

The lifetimes of chain centres can be obtained by measuring the reaction rate as a function of the speed of light intermittency. Evaluation of the quadratic termination constant requires further measurements of the absorbed light energy (ρIa).

The constants for chain termination in reactions $CH_2\dot{I}_2 + I_2$ and $CH\dot{I}_3 + I_2$ have also been determined by the intermittent illumination technique. The reactions were studied both in gas and liquid phase.

EXPERIMENTAL

Traced alkyl iodide obtained by exchange between RI and NaI^{131} was used in investigating the isotopic exchange reaction of RI with I_2. An ampoule containing a mixture of RI and NaI^{131} was heated for several hours in a water bath at a temperature of 100°C. Alkyl iodide was then separated from the water solution of NaI, freed from I_2 by sodium sulfite, washed by water, dried by dehydrated sodium sulfate and distilled in vacuum.

The apparatus shown in Fig. 1 was used for the experiments on kinetics of isotopic exchange between $CH_2\dot{I}_2$ and I_2 in the gas phase. A glass reaction vessel (1) with plane parallel glasses was placed into an air thermostat (4) with a stove (19). The temperature inside the thermostat was maintained constant (± 1°C) by means of a thermoregulator. The air was mixed by a ventilation valve (18). Iodine crystals were contained in a trap (3) inserted into a Dewar vacuum flask (23) filled with snow or with water of a determined temperature. Oxygen was removed from methylene iodide in the trap by repeated freezing and pumping.

All the stop-cocks that were subject to contact with iodine vapours were lubricated with clean phosphoric acid and a viscous high-temperature lubricant. The upper part

* Radioactive isotope.

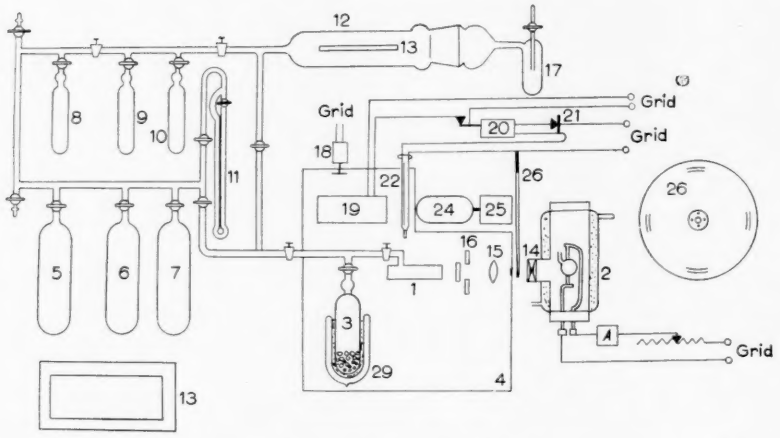

FIG. 1. Set-up of the apparatus for investigating isotopic exchange reactions in the gas phase by the method of intermittent illumination.
1—reaction vessel; 2—mercury lamp with cylinder; 3—trap with iodine; 4—air thermostat; 5, 6, 7—gas cylinders; 8—trap with methylene iodide; 9, 10—traps; 11—mercury manometer; 12—separation tube; 13—silver covered plate; 14—condenser; 15—lens; 16—light filters; 17—trap; 18—ventilation valve; 19—stove; 20—relay; 21—rectifier; 22—contact thermometer; 23—Dewar vacuum flask; 24—electric motor; 25—reductor; 26—disc with sectors.

VOL. 4 1958/5

of the stop-cock was lubricated by the viscous lubricant and the lower part, adjoining the valve opening, by phosphoric acid. Under these conditions absorption of iodine by the lubricant was negligible.

The reaction mixture was irradiated by light from a mercury lamp (2) mounted in a metal cylinder which was cooled by water to ensure steady working conditions of the lamp.

The optics consisted of a condenser (14), a lens (15) giving a parallel light beam, and light filters (16).

Intermittent illumination was obtained through discs (26) from which sectors have been cut, spaced so as to provide a light to dark ratio of 1 : 3. The discs were driven by an electric motor connected to them via a reductor (25). The latter ensured rotation decrease ratios of 1 : 10, 1 : 100, 1 : 1000.

Thus using discs with a different number of sectors and changing the speed of rotation we could also change the time of the light flash from 1 to 10^{-4} sec.

A method for separating chemical substances

After the experiment had been carried out the components of the mixture were separated by adsorption of iodine on a glass covered by a silver layer (13). The silver covered glass was placed into a tube (12) with a trap connected to it through a ground-glass joint (17). By cooling the trap with liquid nitrogen the mixture could be let from the reaction vessel into the tube (12) where iodine was adsorbed on silver. Adsorption of I_2 was checked by means of active iodine (I^{131}) admitted into the reaction vessel, where iodine was deposited on the plate. Repeated measurements of the deposit have confirmed that iodine was fully separated from the gas mixture. Special experiments have shown that there was no exchange between AgI on the plate and CH_2I_2 in the gas phase under experimental conditions used.

After separating the reaction components the trap (17) was removed, the plate taken out and its activity measured by a counter.

A slightly different technique used in experiments for determining the lifetimes of iodine atoms in solution will be described later.

The reaction mixture was irradiated in a

vessel placed in a water thermostat. Iodine was separated by extraction of I_2 with Na_2SO_3. Iodine atoms formed in the water layer were deposited by titration with a solution of $AgNO_3$ in the presence of eosine. The deposit activity was measured by a counter.

The light source intensity was determined by means of a thermopile calibrated with Heffner's lamp.

EXPERIMENTAL RESULTS

1. *Gas phase exchange between* $CH_2\overset{*}{I}_2$ *and* I_2

Exchange between $CH_2\overset{*}{I}_2$ and I_2 was studied both in the dark and under illumination. In both cases the exchange reaction proceeded at a pressure of iodine 0·2 mm and of methylene iodide 1 mm, and at a temperature of 30°C. The reaction vessel volume was 82 cm² (cross-section 3·4 cm, length 9 cm).

Preliminary experiments have shown that exchange in the dark was negligibly slow. Concentrations of methylene iodide and iodine were such that absorption of light and the chemical reaction rate could be estimated by absorption of methylene iodide in the near ultra-violet region. Absorption spectra of methylene iodide and iodine, obtained with a spectrophotometer, are shown in Fig. 2.

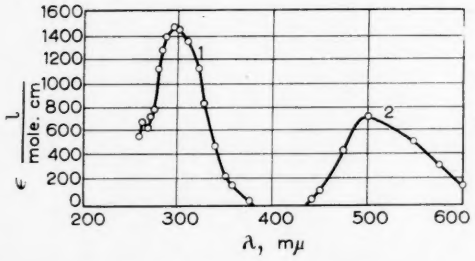

FIG. 2. Plot for absorption of CH_2I_2 (curve 1) and I_2 (curve 2).
λ—wavelength in mμ, ε—extinction coefficient in l/cm mole.

The lifetimes of radicals were obtained by the intermittent light technique. Exchange did not exceed 10 per cent, which shows that the ratio of reaction rates under intermittent and steady illumination was equal to the concentration ratio of the radicals.

To avoid termination at the wall the runs were carried out in the presence of an inert solvent, namely nitrogen ($P_{N_2} = 60$ mm). The dependence of W_0/W_{st} on λ can be seen from Fig. 3, where W_0 is the reaction rate under intermittent and W_{st} under steady

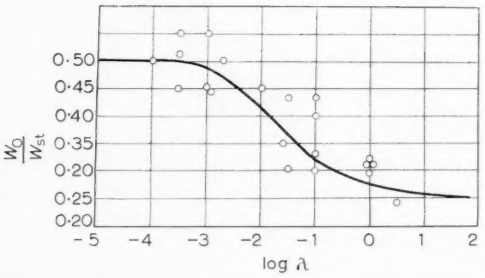

FIG. 3. Dependence of W_0/W_{st} on λ in reaction $CH_2\overset{*}{I}_2 + I_2$.
W_0—rate of exchange under intermittent illumination W_{st}—rate of exchange under steady illumination λ—time of light flash in sec. $P_{CH_2I_2}$—1 mm; P_{I_2}—0·2 mm; $T = 30°C$; P_{N_2}—60 mm Hg.

illumination. The change of W_0/W_{st} from 0·5 to 0·25 indicates a purely quadratic mechanism of termination in agreement with the method's theory. The mean lifetime of τ radicals

$$\tau = \frac{(R_{st})}{K_4(R_{st})^2} = \frac{1}{K_4(R_{st})} = \frac{1}{\sqrt{(K_4\rho Ia)}} = \frac{\lambda}{m} \quad (6)$$

was calculated using the theoretical plot for (R_0/R_{st}) (R_0 being the radical concentration under intermittent illumination) and the experimental plot for W_0/W_{st}.

λ was measured experimentally and m was obtained from the theoretical plot by means of the $R_0/R_{st} = W_0/W_{st}$ ratio.

It follows from Fig. 3 that $\tau = 2 \times 10^{-2}$ sec.

* Radioactive isotope.

The constant for $CH_2I + I$ recombination appeared to be 3×10^{-12} cm³/sec.

2. *Reactions* $CH\overset{*}{I}_3 + I_2$ *and* $CH_2\overset{*}{I}_2 + I_2$ *in* cyclo*hexane solution*

The concentration of $CH\overset{*}{I}_3$ in our experiments was 0·00026 mole/l., 0·025 mole/l. for $CH_2\overset{*}{I}_2$ and 0·0025 mole/l. for I_2. In the runs carried out to determine the lifetimes of radicals the degree of conversion was as small as in the gas phase reaction.

The solutions were illuminated with visible light absorbed only by I_2 molecules, iodine atoms being formed by reaction

$$I_2 + h\nu = 2I$$

Experimental evidence on the lifetimes of I atoms in reactions involving $CH\overset{*}{I}_3$ and $CH_2\overset{*}{I}_2$ is given in Fig. 4.

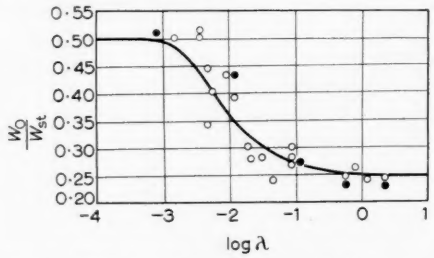

Fig. 4. Plot for the lifetime of iodine atoms in a *cyclo*hexane solution.

$T = 24°C$ $[I_2] = 0·0025$ mole/l.

Circles—$[CH\overset{*}{I}_3] = 0·00026$ mole/l.

Dots—$[CH_2\overset{*}{I}_2] = 0·025$ mole/l.

In accordance with equation (5) the lifetimes of I atoms depend on the concentration of I_2 but are not connected with the concentration of alkyl iodide taking part in the reaction. As can be seen from the figure, experimental points for two haloid alkyl reactions fall on one curve, within the experimental error. The mean lifetime in this case will be of the order of 2×10^{-3} sec and the recombination constant for iodine atoms 2×10^{-11} cm³/sec.

It would be of interest to note that at low concentrations (0·00025 mole/l.) and when the solvent is saturated with oxygen the plot for the dependence of W_0/W_{st} on λ will greatly differ from that for high concentrations of I_2. This can be seen from Fig. 5.

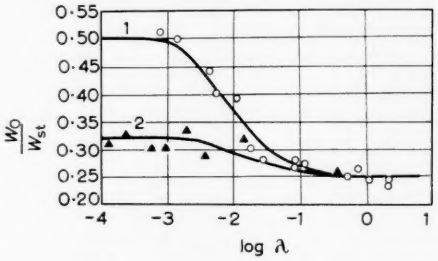

Fig. 5. Influence of oxygen on the isotopic exchange rate between $CH\overset{*}{I}_3$ and I_2.

Curve 1—$CH\overset{*}{I}_3 + I_2$

O—$[CH\overset{*}{I}_3] = 0·00026$ mole/l.; $[I_2] = 0·0025$ mole/l.

Curve 2—$CH\overset{*}{I}_3 + I_2 + O_2$

Δ—$[CHI_3] = 0·00033$ mole/l.; $[I_2] = 0·00025$ mole/l.; $[O_2] = 0·0001$ mole/l.

With increase of the rotation speed the reaction rate increased twofold in case of high concentrations (curve 1) and only by a factor of 1·28 at low concentrations (curve 2). These experimental results prove that in the presence of oxygen, linear termination occurs together with quadratic termination by reaction

$$I + I = I_2$$

Such a termination may obviously take place on collisions of chain centres with oxygen molecules. The nature of these centres was not determined.

REFERENCES

1. Sibbett D. I. and Noyes R. M., *J. Amer. Chem. Soc.* **75,** 761 (1953).
2. Neiman M. B., Miller V. B. and Shapovalov Ju. M., *Voprosy khimicheskoy kinetiki, katalyza i reaktzionnoy sposobnosty* (Edited by the USSR Acad. of Sc.), p. 22 (1955).
3. Noyes R. M. and Zimmerman I., *J. Chem. Phys.* **18,** 656 (1950).
4. Melville H. W. and Burnett G. M., *Investigation of rates and mechanisms of reactions.* p. 133. Interscience Publishers, New York–London (1953).

* Radioactive isotope.

VOL. 4 1958/5

International Journal of Applied Radiation and Isotopes, 1958, Vol. 4, pp. 41–44. Pergamon Press Ltd., London

Quelques Exemples d'Applications à l'Analyse Chimique du Spectromètre-γ à Scintillations

P. LEVEQUE, P. MARTINELLI et S. MAY
Centre d'Etudes Nucléaires de Saclay—Section des Applications des Radioéléments

VOL.
4
8/59

Bien que beaucoup de travaux aient déjà traité de l'application de radioélément en chimie analytique quantitative, il nous paraît intéressant de présenter quelques méthodes qui ne sont que peu employées encore et qui permettent de résoudre certains problèmes difficilement solubles par les procédés plus courants.

Il s'agit en particulier de l'utilisation dans des buts analytiques de la spectrométrie du rayonnement et de l'application en analyse quantitative de la fluorescence-X excitée au moyen des rayons-β.

A FEW EXAMPLES OF THE APPLICATION OF THE SCINTILLATION γ-SPECTROMETER TO CHEMICAL ANALYSIS

Although there has already been much work in the field of the application of radioelements to quantitative analytical chemistry, it seems to us worth while to present a few methods which as yet are but little used and which allow of the handling of certain problems that are soluble only with difficulty by more usual procedures.

We are concerned particularly with the use of radiation spectrometry for analytical purposes and the application of X-fluorescence excited by β-rays to quantitative analysis.

НЕКОТОРЫЕ ПРИМЕРЫ ПРИМЕНЕНИЯ СЦИНТИЛЛЯЦИОННОГО γ-СПЕКТРОМЕТРА В АНАЛИТИЧЕСКОЙ ХИМИИ

Хотя большое число работ было уже посвящено применению радиоактивных элементов в количественной аналитической химии, однако нам кажется интересным изложить некоторые, пока еще мало применявшиеся методы, позволяющие решать проблемы, неразрешимые с помощью более общепринятой методики.

В частности, имеется в виду применение радиоспектрометрии для целей анализа вообще и для количественного анализа X-флуоресценции, вызванной β-облучением.

EINIGE BEISPIELE DER ANWENDUNG VON γ-SZINTILLATIONS-SPEKTROMETERN FÜR CHEMISCHE ANALYSEN.

Obwohl auf dem Gebiete der Anwendung von Radioelementen in der quantitiven Analyse bereits viel Arbeit geleistet wurde, scheint es uns doch wertvoll über einige, zur Zeit wenig gebräuchliche Methoden zu berichten, welche die Behandlung bestimmter, mit den üblichen Mitteln schwer lösbarer Probleme erlauben.

Es handelt sich dabei besonder um die Verwendung der Strahlungs-spektrometrie und um die Anwendung der durch Beta-Strahlung hervorgerufene Röntgenfluoreszenz in der quantitativen Analyse.

APPLICATIONS DE LA SPECTROMETRIE γ APPAREILLAGE

Nous avons utilisé un spectromètre-γ qui se composait de:

(1) Une tête de détection comprenant un cristal creux d'iodure de sodium (activé au thallium) de dimensions extérieures 1,75 × 2 in. La profondeur du canal central est de 1,5 in. et le diamètre 0,75 in. Ce détecteur est associé à un photomultiplicateur.

(2) Un amplificateur linéaire

(3) Un sélecteur à un canal de largeur variable jusqu'à 1,5 V

(4) Un intégrateur

(5) Un millivoltmètre enregistreur.

Dosage du cobalt en présence de fer

Les radioisotopes de ces éléments, produits par réaction (n, γ) à la pile, sont: cobalt 60 émetteur γ de 1,17 et 1.33 MeV et fer 59 émetteur γ de 1,1 et 1,3 MeV.

On s'aperçoit que les énergies-γ de ces éléments sont très voisines et à priori l'identification du radiocobalt en présence de radiofer n'est pas possible par spectrométrie-γ. Cependant en examinant les schémas de désintégration, on constate que les 2γ du radiofer sont en parallèle, alors que ceux du radiocobalt sont en cascade.

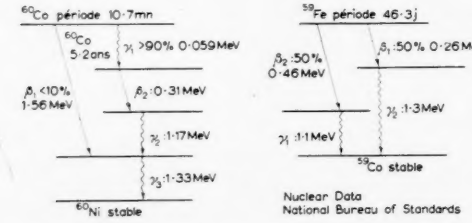

En plaçant le radiocobalt à l'intérieur du puits du cristal creux nous avons observé une énergie-γ de 2,5 MeV. Cette énergie-γ provient de la somme des énergies $\gamma_2 + \gamma_3$. Dans les mêmes conditions, le radiofer 59 ne donne pas ce phénomène.

Il est donc possible, de cette manière, de caractériser le cobalt 60 en présence de fer 59, ou d'identifier séparément l'un de ces deux radioéléments d'une manière certaine.

Nous avons utilisé cette méthode pour un dosage de cobalt dans un échantillon de fer. Pratiquement, l'échantillon liquide à analyser est placé dans un petit tube à essais pouvant entrer dans la cavité du puits du cristal creux d'iodure de sodium.

On fait le spectre-γ de cet échantillon et si l'on observe une raie d'énergie de 2,5 MeV, on compare son intensité à celle

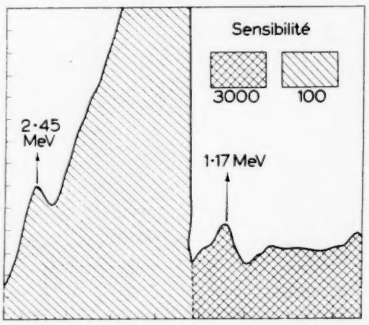

FIG. 1. Source de cobalt^{60} dans le puits du cristal

d'un étalon de radiocobalt 60. Il est facile ensuite de déterminer la proportion de cobalt dans l'échantillon à analyser.

Si l'on considère un rendement moyen pour chaque pic photoélectrique du cobalt 60 de 5 pour cent, la probabilité de coincidence du γ de 1,17 MeV et du γ de 1,33 MeV sera

$$5 \cdot 10^{-2} \times 5 \cdot 10^{-2} = 25 \cdot 10^{-4}$$

pour le pic de 2,5 MeV.

Le rapport de la hauteur du pic photoélectrique de 1,17 MeV à celle du pic de 2,5 MeV devrait donc être:

$$\frac{5 \cdot 10^{-2}}{25 \cdot 10^{-4}} = 20$$

La Fig. 1 nous montre qu'il en est ainsi expérimentalement:

hauteur du pic de 1,17 MeV: 5,3 cm × 30 (pour sensibilité 100)

hauteur du pic de 2,5 MeV: 7,4 cm (sensibilité 100)

$$\frac{\text{pic 1,17 MeV}}{\text{pic 2,5 MeV}} = \frac{159 \text{ cm}}{7{,}4} = 21{,}5$$

VOL 4 1958/

Dosage du tantale dans le niobium

La détermination du tantale dans le niobium n'est pas un problème aisé pour l'expérimentateur. Les deux éléments ont en effet des propriétés très voisines. Les méthodes classiques d'analyse sont peu précises, même les colorimétries, car de nombreux ions gênent; les séparations sont très délicates.

Par radioactivation le problème devient plus aisé. En effet, si l'on met un échantillon de niobium (dont on veut déterminer la teneur en tantale) à activer une nuit à la pile, on n'obtient en ce qui concerne le radioniobium que l'isotope 94 de période 6,6 min dont le schéma de désintégration est le suivant:

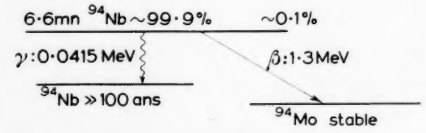

Le tantale dans les mêmes conditions donne deux isotopes: le tantale 182 de période 16,4 min (section efficace relative 0,034 barn) β:0,2 MeV, γ:0,18 MeV) et le tantale 182 de période 117 jours. Ce dernier a une section efficace relative de 21 barns. Il donne par désintégration des β^- de 0,53 MeV et des γ d'énergies variables dont les plus intenses sont 0.157–0,165–0,222–1,13–1,22 et 1,24 MeV.

On pouvait donc penser qu'il serait possible de doser par spectrométrie-γ le tantale dans le niobium, par discrimination d'énergie. Le dosage du tantale avait déjà été fait par d'autres méthodes radioactives.[1,2]

Le dosage proprement dit a été fait par les hauteurs relatives des pics d'énergie correspondant à 1,22 MeV (Fig. 2), d'une part dans l'échantillon de niobium, d'autre part dans un étalon de tantale qui a été irradié à la pile dans les mêmes conditions que l'échantillon à analyser.

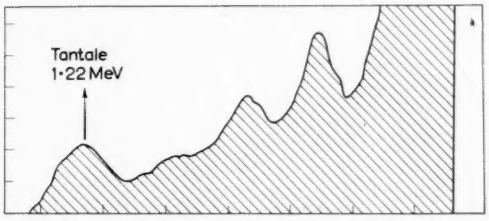

FIG. 2. Spectre de l'échantillon de niobium après irradiation

On s'est basé sur un des pics des basses énergies du tantale pour vérifier les résultats trouvés avec les pics les plus énergétiques.

Nous avons pu doser ainsi 0,8 pour cent de tantale dans un échantillon de niobium de 15 mg, par l'importance de la hauteur des pics d'une part et d'autre part par comptage direct des impulsions avec discrimination d'énergie.

Le radiotantale 182, de période 117 jours, sera donc facilement décelable et dosable par spectrométrie-γ, chaque fois qu'il sera dans une substance à vie courte, ou ayant des énergies-γ <1 MeV.

ANALYSE QUANTITATIVE BASEE SUR LA FLUORESCENCE-X EXCITEE AU MOYEN DE RAYONS-β: METHODE DE MESURES DES EPAISSEURS DE DEPOTS METALLIQUES

Cette méthode non destructive est basée sur la mesure de l'intensité des raies-X de fluorescence, excitées au moyen de rayons-β. Nous l'avons appliquée en particulier à la mesure des épaisseurs de dépots or sur cuivre, ainsi qu'au dosage du tungstène dans l'acier et des solutions de plomb dans l'eau.

Principe

On sait que les électrons perdent leur énergie dans la matière suivant divers processus et en particulier par émission d'un rayonnement électromagnétique. C'est le principe le plus couramment utilisé pour produire des rayons-X. Le rayonnement ainsi émis est constitué d'un fond continu

dû au freinage des électrons dans le champ électrique des noyaux, auquel se superposent les raies-X caractéristiques de l'élément irradié. Son énergie maximum est égale à celle des électrons incidents.

On peut également exciter les raies-X de fluorescence par irradiation au moyen de rayons-X dont l'énergie est au moins supérieure à celle des raies considérées. De nombreuses méthodes d'analyse sont actuellement basées sur ce principe.

La méthode décrite ici consiste à utiliser un isotope radioactif émetteur-β^- pur. Le faisceau de rayons-β^- est dirigé sur le revêtement métallique, l'alliage, la solution ou la poudre à analyser. Le rayonnement-X diffusé en arrière est détecté au moyen d'un compteur à scintillations et analysé par un sélecteur à un canal. L'intensité de la raie-X (K) donne une mesure de l'importance de l'élément correspondant.

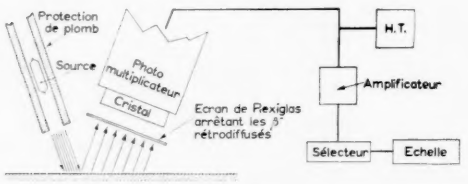

FIG. 3.

Les essais ont été effectués à l'aide du strontium 90 (+ yttrium 90), produit de fission de l'uranium 235 dont la période est de 25 ans, émetteur-β de 2,18 et 0,53 MeV.

Le détecteur est, dans ce cas particulier, un photomultiplicateur équipé d'un cristal mince d'iodure de sodium (épaisseur 1,5 mm, diamètre 30 mm). Le cristal mince permet de compter avec un faible rendement les rayons-X durs qui sont créés dans l'échantillon et diffusés dans le compteur, et dont les effets Compton dans le cristal viennent créer sous les pics photoélectriques un bruit de fond gênant.

Par l'emploi d'un cristal mince, on améliore le contraste obtenu au cours de deux mesures, et par conséquent la précision.

Précision des mesures

Dans le dosage du tungstène dans les aciers, il est possible d'apprécier des teneurs en tungstène voisines de 1 pour cent avec une erreur relative de 4 pour cent.

L'analyse de la teneur en platine des alliages platine–rhodium, basée sur la mesure des raies-X (K) dues au platine, se fait avec une erreur relative de 10 pour cent.

Le plomb, en solution aqueuse, de concentration variant de 1 à 10% peut être dosé par cette méthode, ainsi que le baryum jusqu'à 1% (erreur relative: dans le dosage du plomb: 6%, dans le dosage du baryum: 5%).

CONCLUSION

Ces quelques exemples d'utilisation du spectromètre-γ dans l'analyse chimique montrant l'intérêt de cette méthode qui possède sur l'analyse classique l'avantage d'être rapide et dans la plupart des cas non destructive. Elle permet le dosage de traces d'éléments indécelables par d'autres méthodes et possède encore le grand intérêt de pouvoir se faire sur une très faible masse de matière et de se répéter plusieurs fois consécutives sur le même échantillon, si les périodes des radioéléments formés ne sont pas trop longues.

Remerciements—Nous tenons à remercier Mme S. DECOUR et M. H. GOENVEC pour leur collaboration technique dans l'élaboration du présent travail.

BIBLIOGRAPHIE

1. KOHN *Dokl. Akad Nauk SSSR* 236 (1953).

2. BEYDON J. et FISHER C., *Analyt. Chim. Acta* 538 (1953).

International Journal of Applied Radiation and Isotopes, 1958, Vol. 4, pp. 45–49. Pergamon Press Ltd., London

The Determination of Gold in Biological Materials by Neutron Activation Analysis

D. GIBBONS
Isotope Division, Atomic Energy Research Establishment, Harwell

(*Received* 19 *February* 1958; *in revised form* 11 *March* 1958)

The determination of gold in biological materials by neutron irradiation followed by radiochemical purification of the resulting radioactive gold is described. As little as 10^{-10} g of gold can be determined with an accuracy of about 2 per cent. A simplified and more rapid method is also described for use where an accuracy of 5–10 per cent is sufficient.

LE DOSAGE DE L'OR DANS LES MATÉRIAUX BIOLOGIQUES PAR L'ANALYSE À ACTIVATION NEUTRONIQUE

On décrit le dosage de l'or dans les matières biologiques au moyen de l'irradiation à neutrons suive de la purification radiochimique de l'or radioactif ainsi obtenu. Il est possible de mesurer aussi peu que 10^{-10} g d'or, une précision d'environ 2 pour cent. On décrit aussi une méthode plus simple et plus rapide qui peut servir lorsqu'une précision de 5 à 10 pour cent suffira.

ОПРЕДЕЛЕНИЕ СОДЕРЖАНИЯ ЗОЛОТА В БИОЛОГИЧЕСКИХ ОБЪЕКТАХ ПО МЕТОДУ НЕЙТРОННОГО АКТИВАЦИОННОГО АНАЛИЗА

Описано определение содержания золота в биологических объектах путем облучения нейтронами и последующей радиохимической очистки образованного при этом радиоактивного золота. Чувствительность метода 10^{-10} грамм золота, при точности около 2%. Описан также более простой и быстрый метод, пригодный для тех случаев, когда можно удовлетвориться точностью в 5–10%.

GOLDBESTIMMUNG IN BIOLOGISCHEM MATERIL MITTELS NEUTRONENAKTIVIERUNGSANALYSE

Die Goldbestimmung in biologischem Material durch Neutronenbestrahlung mit darauffolgender radiochemischer Abtrennung des Radio-Goldes wird beschrieben. Mengen bis herab auf 10^{-10} g Gold können mit einer Genauigkeit von etwa 2% bestimmt werden. Es wird auch eine schnellere vereinfachte Methode angegeben, welche Werte von 5–10% Genauigkeit liefert.

INTRODUCTION

The determination of gold in biological materials has not hitherto often been required and consequently few methods have been published. However, with the widespread therapeutic use of radioactive colloidal gold (Au^{198}), a sensitive method is needed for determining the gold content of biological materials such as human liver and pleural fluids after the decay of the Au^{198} activity.

Such sensitive methods as are available are generally based on the colorimetric determination of the gold, after removal of the organic matter, with *o*-dianisidine[1] or *p*-dimethylamino-benzalrhodanine,[2] giving a detection sensitivity of 5·0 and 0·5 μg respectively. Spectrographic[3] and polarographic[4] methods have also been described, but these tend to be rather tedious and to sacrifice accuracy for sensitivity.

In 1948, Tobias and Dunn[5] determined the distribution of gold in the various tissues of a mouse and also in the red and white

blood cells and plasma of human blood by neutron activation analysis. Their method, however, involved treatment of the sample before irradiation and the use of an inadequate radiochemical purification procedure. More recently, MÜLLER[6] has determined the gold content of various tissues, but the method was slow since the induced activity to be attributed to the gold was found by resolution of the complex decay curve of the whole specimen.

Several methods have been published for the determination of gold in inorganic materials by activation analysis[7,8,9,10] which offer the advantages of high sensitivity (5×10^{-12} g)[11] and specificity, and eliminate corrections for reagent blanks. Recently, VINCENT and SMALES[12] determined gold in igneous rocks and the rigorous radiochemical procedure which they employed has been made the basis of one of the methods to be described.

PREPARATION OF SAMPLES

The principles of neutron activation analysis[13,14,15] are now well established and will not be elaborated here. The following precautions were taken in preparing samples and standards for irradiation.

In biological samples, the amount of gold likely to be present is usually so small that its dispersion is sufficient to eliminate any neutron self-absorption errors, and the neutron absorption cross-sections of the major constituents of biological materials are so small that shielding effects are negligible. The samples received the minimum possible treatment before irradiation so as to avoid possible contamination. The surface layers of new samples were removed with a silica knife and the samples were weighed and sealed in polythene bags.

The high neutron cross-section of gold can lead to difficulties in the preparation of standards. Neutrons are heavily absorbed in gold, resulting in a reduction of the effective flux, even in quite thin foil. A solution of gold chloride, sealed in a silica ampoule, was therefore used. After irradiation, the ampoule was washed out with inactive gold solution to ensure that all the standard was removed. The concentration and volume of the standard gold solution were adjusted to give approximately the same amount of gold as that expected in the sample, dispersed over a similar volume.

DEVELOPMENT OF THE METHODS

Several authors have used γ-scintillation spectrometers in neutron activation analysis.[16,17,18] Samples and standards are irradiated with neutrons in the usual way but, after little or no chemical separation, the required activity is measured with a scintillation counter in terms of selected γ-rays. The counting rate for γ-rays of a selected energy is obtained from an automatic plot of counting rate against energy by measuring the area under the appropriate photoelectric peak. This is the nuclear radiation analogue of light spectroscopy; the energy of the γ-ray characterizes the radioisotope and the area under the peak is a measure of the amount of the isotope present in the sample.

Attempts were made to determine the gold content of a sample of liver by γ-spectrometry in this way, without chemical separation. It was found impossible to distinguish the 0·41 MeV Au^{198} peak from the background due to Na^{24} and other γ-emitting impurities (Fig. 1). Gold, however, can be separated from the majority of elements present by ion exchange. KRAUS and NELSON[19] claimed that 99·9 per cent of the gold content of 10 ml of a $1{\cdot}4 \times 10^{-3}$ M solution of Au^{III} in 1 M HCl could be removed by 100 mg of an anion exchange resin (Dowex 1) in 5 min. This effect was confirmed for Deacidite FF (an equivalent to Dowex 1) using a small quantity of Au^{198} as tracer.

The irradiated liver samples were dissolved in aqua regia and evaporated to dryness to

VOL. 4 1958/5

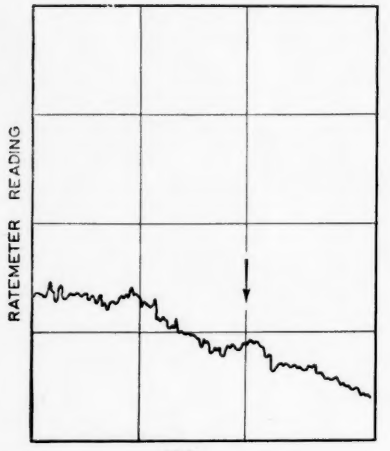

Fig. 1.

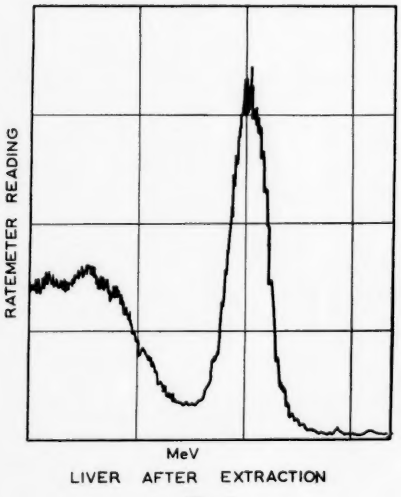

Fig. 2.

destroy the organic matter, dissolved in 10 ml 1 M HCl and stirred with 100 mg of Deacidite FF for 5 min. The resin was collected, washed with 1 M HCl and dried. The γ-spectrum of this sample is shown in Fig. 2 where the γ-activity of other elements can be seen to be virtually eliminated. The gold standard was treated similarly, and even here a measure of purification—from impurities present in the original gold—was observed (Figs. 3a and b). Comparative activities were obtained from Figs. 2 and 3b to determine the gold content of the original sample. Whilst this method is quite rapid, it is not chemically specific for gold, although the results obtained were sufficiently accurate for the particular determination in question. It was felt that a more accurate and reliable method should be developed, so the method of VINCENT and SMALES,[12] for the determination of gold in igneous rocks, was adapted for use on biological materials.

Chemical procedure (full method)

Samples of the biological materials, weighing about 1 g, were irradiated for a suitable period in a neutron flux of 10^{12} neutrons/cm^2/sec or more and then left for 24 hr to allow the short-lived activities to decay.

The sample was transferred to a 250 ml beaker and 30 mg of gold were added as chloride in 10 ml of solution, followed by 2 ml 100 vol. H_2O_2, 5 ml conc. H_2SO_4, 5 ml conc. HNO_3 and 2 ml 70% $HClO_4$. The beaker was covered and the mixture heated gently until the initial oxidation subsided, and was then heated more strongly until white fumes appeared. 20 ml aqua regia were added to complete the destruction of the organic matter, the solution evaporated almost to dryness, and the residue taken up in a mixture of 1 ml conc. HCl and 20 ml water.

Holdback carriers consisting of 10 mg NaCl and 10 mg ammonium phosphate were added, followed by a slight excess of magnesium powder over that required to precipitate the gold. After boiling to expel hydrogen, the mixture was cooled, centrifuged, the supernatant liquid decanted and the residue washed twice with 10 ml hot water. The residue was dissolved in a few drops aqua regia, evaporated nearly to dryness and warmed with 15 ml 10% HCl until a clear solution was obtained.

The gold was extracted from the solution in a separating funnel with 30 ml ethyl acetate and after separating the layers, the organic phase was washed twice with 20 ml 10% HCl. The ethyl acetate solution was evaporated to dryness, the residue dissolved in a few drops aqua regia and the solution was diluted with 10 ml water and acidified with 2 ml conc. HCl. The solution was heated almost to boiling and gold was precipitated by the addition of 0·5 g hydroquinone. The precipitate was centrifuged, washed twice with 10 ml hot water, redissolved in a few drops aqua regia and the reduction with hydroquinone repeated twice more. The precipitate was washed twice with 10 ml water, twice with 10 ml ethanol, slurried on to a weighed counting tray and dried to constant weight.

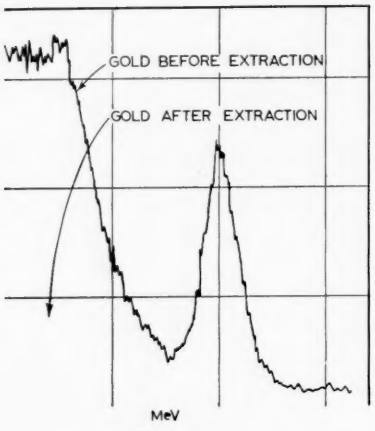

Fig. 3 (a)

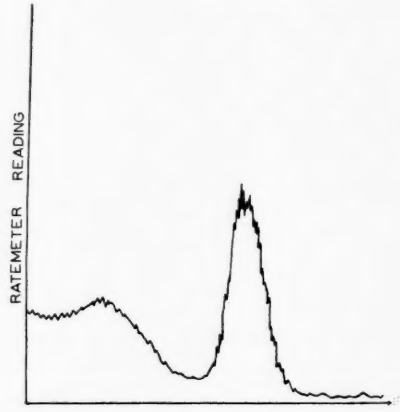

Fig. 3 (b)

The ampoule containing the irradiated standard gold solution was opened, filled with gold carrier solution and allowed to stand in a water bath for at least 10 min. The solution was transferred to a centrifuge tube with the remainder of the 10 ml gold carrier solution, 2 ml conc. HCl were added and the gold was precipitated with hydroquinone as above.

The activities of the two precipitates were determined by counting under an endwindow Geiger counter until 10^5 counts had been registered, provided that this could be achieved in a reasonable time. The counts were made under identical geometry conditions and, if the counts differed by more than a factor of two, the analysis was repeated if sufficient sample was available.

Rapid method

The full method gives very satisfactory results with a reproducibility of about 2 per cent, but takes several hours to complete. When time is limited and/or when an accuracy of 5–10 per cent is adequate, the following procedure is recommended.

The sample was dissolved in the mixed acids and gold was precipitated with magnesium powder as above. The precipitate was washed with hot water, dissolved in a few drops aqua regia and the solution diluted with 10 ml water and 10 ml mixed holdback carriers. 2 ml conc. HCl were added, the solution was heated almost to boiling and gold was precipitated by the addition of 0·5 g hydroquinone. The precipitate was washed, dried and weighed as before.

The gold activity was determined by plotting a γ-energy spectrum and measuring the area under the peak at 0·41 MeV by means of a planimeter, taking the extrapolated Compton response as the base line. If there was little or no γ-background in this region, the activity was determined by using a scaler to register the number of pulses in the channel at that point, or simply by measuring the linear height of the peak on the trace.

Since the γ-energies are, to some extent, characteristic of the different radioisotopes, the measurement

Table 1. Results of analysing samples for gold

Sample	Gold Added (ppm)	Ion exchange (ppm)	Full method (ppm)	Rapid method (ppm)
Liver sample from live patient	—	1·5	—	—
Liver sample from autopsy (healthy)	—	—	24·1 23·5	22·5 24·5
Liver sample from autopsy (Cancerous)	—	—	1·32 1·28	1·35 1·25
Pleural fluid (dehydrated)	—	—	0·78 0·76	0·85 0·75
Animal liver	1·00 1·00	— —	1·02 0·99	1·04 0·94
	0·10 0·10	— —	0·102 0·098	0·11 0·095
	0·010 0·010	— —	0·010 0·0098	0·010 0·009
	None	—	$<10^{-4}$	

VOL. 4 1958/5

of activity in this way acts as a purification step and the determination is therefore simplified.

Proof of radiochemical purity

In the full method, the purity of the separated gold was established by plotting β-particle absorption curves, decay curves and γ-energy spectra (when sufficient activity was available). The graphs obtained for the samples were compared with those obtained for the standards and with theoretical values of half-life and β- and γ-energies. In the rapid method, the fact that a γ-peak was taken as a measure of the activity was regarded as sufficient proof of purity, but this was confirmed by following the radioactive decay of the peak.

RESULTS

These two new procedures were tested and compared by analysing samples of contaminated liver and pleural fluid and also samples of animal liver to which known amounts of gold had been added. Small measured volumes of dilute gold solutions were injected, by means of a micrometer operated hypodermic syringe, into liver samples which had been partially dried to form a hard outer skin. Analysis of liver samples (to which no gold had been added) by the full method showed that the normal gold content was less than 10^{-4} ppm. The results obtained by the two methods of analysis are compared in Table 1.

Acknowledgements—Thanks are due to Dr. G. B. Cook for his advice and encouragement at all stages of this work, to Dr. R. A. Allen for determining the γ-ray spectra of Figs. 1–3, and to the Royal Cancer Hospital and Mount Vernon Hospital for samples.

REFERENCES

1. Block W. D. and Buchanan O. H. *J. Biol. Chem.* **136,** 379 (1940).
2. Merejkovsky B. K. *Bull. Soc. Chim. Biol., Paris* **15,** 1336 (1933).
3. Hermann J. *Coll. Czech. Chem. Comm.*, **6,** 37 (1934).
4. Jones A. G. BR-146.
5. Tobias C. A. and Dunn R. W. *Science* **109,** 109 (1949).
6. Müller J. H. Unesco/NS/RIC/205 *Paris Conference* (1957).
7. Hummel R. W. *Analyst* **82,** 483 (1957).
8. Smales A. A. *Geochim. Cosmoch. Acta* **8,** 300 (1955).
9. Goldberg E. D. and Brown H. *Analyt. Chem.* **22,** 308 (1950).
10. Goldberg E., Uchiyama A. and Brown H. *Geochim. Cosmoch. Acta* **2,** 1 (1951).
11. Jenkins E. N. and Smales A. A. *Quart. Rev., London* **10,** 83 (1956).
12. Vincent E. A. and Smales A. A. *Geochim. Cosmoch. Acta* **9,** 154 (1956).
13. Boyd G. E. *Analyt. Chem.* **21,** 335 (1949).
14. Smales A. A. *Ann. Repts. on Progr. Chem.* (*Chem. Soc.* London) **46,** 285 (1949).
15. Smales A. A. *Proc. Intern. Conf. Peaceful Uses Atomic Energy*, **15,** 73 (1956).
16. Salmon L. AERE C/M 206.
17. Peirson D. H. and Iredale P. Unesco/NS/RIC /53, *Paris Conference* (1957).
18. Connally R. E. *Analyt. Chem.* **28,** 1847 (1956).
19. Kraus K. A. and Nelson F. *J. Amer. Chem. Soc.* **76,** 984 (1954).

International Journal of Applied Radiation and Isotopes, 1958, Vol. 4, pp. 50–57. Pergamon Press Ltd., London

The Influence of Ionizing Radiations on the Penetration of Sodium into the Central Nervous System*

RAYMOND G. ROSE
The University of Texas M.D. Anderson Hospital and Tumor Institute, and
The University of Texas Postgraduate School of Medicine, Houston, Texas

(*Received* 28 *January* 1958)

High doses of irradiation are required to produce definite morphological changes in the central nervous system. The present experiment was conducted to see if functional derangements occur after comparatively small amounts of ionizing radiations.

Tracer studies with intravenously injected radioactive sodium were performed on rabbits to determine the rate and degree of sodium penetration into the cerebro-spinal fluid and brain. Other groups of rabbits were given large doses of Na^{24} or 100 to 1500 r of total body X-irradiation (followed by tracer doses of Na^{24} at varying intervals) to study the possible effects of such irradiation.

The data obtained showed an accelerated penetration of sodium into the CNS under these conditions, as well as an apparent increase in radio-sodium content in the CNS when compared with the control group. Histological changes were minimal at the highest dosage levels employed.

The significance and possible applications of these findings are discussed.

L'INFLUENCE DES RADIATIONS IONISANTES SUR LA PÉNÉTRATION DU SODIUM DANS LE SYSTÈME NERVEUX CENTRAL

Pour donner des changements morphologiques définis dans le système nerveux central, il faut de fortes doses d'irradiation. L'expérience ici décrite avait pour but de voir si des dérangements fonctionnels suivent des quantités assez petites de rayonnements ionisants.

Des études à indicateurs avec du sodium radioactif injecté dans les veines ont été faites sur des lapins afin d'observer la vitesse et le degré de pénétration du sodium dans le fluide cérébro-spinal et dans la cervelle. Des autres groupes de lapins ont reçu de grandes doses de Na^{24} ou bien entre 100 et 1500 r de rayons X au corps entier (suivi de doses indicatives de Na^{24} à des entre-temps variés) pour étudier les effets possibles de telle irradiation.

Les chiffres ainsi obtenus indiquèrent une pénétration accélérée de sodium dans le CNS sous ces conditions, ainsi qu'une augmentation apparente du taux de radio-sodium dans le CNS en comparison avec les contrôles. Les changements histologiques furent minimes aux plus grands des niveaux de dosage employés.

On discute l'importance et les applications possibles de ces découvertes.

ВЛИЯНИЕ ИОНИЗИРУЮЩЕГО ИЗЛУЕНИЯ НА ПРОНИКНОВЕНИЕ НАТРИЯ В ЦЕНТРАЛЬНУЮ НЕРВНУЮ СИСТЕМУ

Для того, чтобы вызвать органические морфологические изменения центральной нервной системы требуются высокие дозы облучения. Настоящий опыт был проделан с целью убедиться в том, что функциональные расстройства вызываются сравнительно небольшими дозами ионизирующего излучения.

Скорость и степень проникания натрия введенного внутривенно в спинно-мозговую

* From the Cancer Research Institute of the New England Deaconess Hospital and the Department of Pathology, Harvard Medical School, Boston, Mass. This work was performed under U.S. Atomic Energy Commission Contracts AT(30-1)-901 with the New England Deaconess Hospital and AT(30-1)-609 with the Harvard Medical School.

VOL
4
1958/

жидкость и мозг были исследованы на кроликах, с помощью метода меченых атомов. Другим группам кролков вводились большие дозы Ia^{24} или же их облучали Х-лучами от 100 до 1500 р (с последующим введением Ia^{24} через различные промежутки времени) и исследовались возможные эффекты такого облучения.

Полученные данные указывают на повышенное проникновение натрия в центральную нервную систему при этих условиях, так же как и на заметное увелчение содержания Ia^{24} в ЦНС облученных кроликов, по сравнению с контрольной группой. Гистологические изменения были минимальными при самых высоких дозах облучения.

Обсуждаются значение и возможность использования полученных данных.

DER EINFLUSS VON IONISIERENDER STRAHLUNG AUF DAS EINDRINGEN VON NATRIUM IN DAS ZENTRALNERVENSYSTEM

Um endgültige morphologische Aenderungen im Zentralnervensystem hervorzurufen sind hohe Bestrahlungsdosen erforderlich. Die vorliegenden Versuche sollten zeigen ob funktionelle Veränderungen bereits nach vergleichsweise kleinen Mengen von ionisierender Strahlung auftreten.

An Kaninchen wurden Spurenuntersuchungen mit intravenös injiziertem radioaktivem Natrium angestellt, um Menge und Grad des Eindringens von Na in die cerebro-spinale Flüssigkeit und das Gehirn festzustellen. Andere Kaninchen bekamen grosse Dosen von Na^{24} oder Ganzkörper-Röntgenbestrahlung von 100 bis 1500 r (gefolgt von Spurendosen von Na^{24} in verschiedenen Zeitabständen) um die möglichen Effekte solcher Bestrahlung zu studieren. Die dabei erhaltenen Daten zeigten sowohl ein beschleunigtes Eindringen von Na in das Zentralnerven system unter diesen Bedingungen, als auch ein merkliches Anwachsen des Gehaltes an radio aktivem Na im Zentralnervensystem im Vergleich zu den Kontrolltieren. Histologische Veränderungen waren selbst bei den höchsten angewendeten Dosen minimal.

Die Signifikanz und mögliche Anwendungen dieser Resultate werden diskutiert.

VOL. 4 58/59

THE availability of artificial radioactive isotopes has considerably enlarged our knowledge of the mechanics of cerebrospinal fluid formation and circulation. SWEET and his co-workers[1,2] have determined that electrolytes enter the CSF via the choroid plexus of the lateral ventricles, but electrolyte-free heavy water probably enters the CSF chiefly in the region of the cisterns. Other studies have indicated that some CSF is formed in the lumbar spaces.[3] Radioactive substances have also provided objective means of investigating the so-called blood–brain barrier and the influence it has on the penetration of organic and inorganic substances into the central nervous system under physiological conditions.

Within a relatively short time following injection, Na^{24} is uniformly dispersed throughout all body tissues and fluids in proportion to their stable sodium content, with the exception of the brain and sciatic nerve. This equilibrium is attained in about 10 min in rats,[4] 1 hr in dogs[5] and rabbits,[6] and 3 hr in man.[7]

MANERY and BALE[6] determined the brain concentration of Na^{24} to be 30 per cent of the stable sodium concentration at 1 hr after injection into the rabbit and 80 per cent at 3 hr. A similar slow penetration of P^{32} into the CNS was also found. They concluded that "certain barriers may be imposed between the blood and the extracellular phase of tissues and that the position of a substance as intra- or extra-cellular is not the sole determining factor." GREENBERG[5] using radioactive K, Na, Br, Rb, Sr, PO_4 and I, concluded that the delay in penetration into the CNS is selective and varies greatly for the different ions, with a progressive decrease in permeability in the order listed above. He found no maximum for Na in the CSF concentration curve. In his experiments, employing continuous open drainage of the cisterna magna of dogs, the ratio of Na^{24} concentration in the CSF vs. plasma was 60 per cent 1 hr following injection, 80 per cent at 2 hr and 110 per cent at 21 hr.

WANG[8] determined that the CSF vs.

plasma Na^{24} ratio in dogs was 50 per cent at 95 $\pm$ 6 min. The range of variation in the time to reach this value was from 45–118 min in his test animals.

The existence of this cephalo-hemic barrier has been verified morphologically. The pia and arachnoid are seen to follow the vessels into the brain, extending all the way along the veins and venules to the capillaries but not so far along the arterioles. The processes of the astrocytes form another lining as they attach either to the pial layer or directly to the capillary endothelium where there is no lepto-meningeal investment. "The pia arachnoid glia membrane not only bounds the perivascular spaces but also the subarachnoid spaces so that substances successfully permeating the CSF must still traverse this membrane in order to reach brain tissue. Thus all materials entering the brain must first penetrate the glial membrane, epithelial in origin and possessing the specific properties of epithelial tissues, namely a relative impermeability to negatively charged ions. Cations (Na, K) traverse the cerebral capillaries even more slowly than do anions (Cl, Br)".[9]

The integrity of the blood–brain barrier can be broken down under various pathological conditions, in a generalized or local fashion, notably with inflammatory lesions of the CNS, trauma, neoplasms, etc. There is morphological evidence of such a breakdown following massive doses of X-irradiation (3000 r or more). The brain parenchyma itself is relatively resistant to X-irradiation. Such changes as are found are chiefly those secondary to effects on the vascular endothelium. The initial response with such massive doses, usually apparent within 72 hr, is swelling or necrosis of the vascular endothelium, with the formation of a hyaline thrombosis within most vessels of capillary size. Loss or narrowing of the lumen occurs as a result of the fibrous changes in the vessel wall.[10]

Clemente and Holst, by means of trypan blue, studied changes in the blood–brain barrier in monkeys after irradiation.[11] No alterations were found after single doses of 1500 r. They state "if permeability changes in the blood–brain barrier were present, they were too slight to permit staining of the brain trypan blue." With irradiation doses of 4500–6000 r, staining of certain areas of the brain (hypothalamus and medulla) was consistently seen and was correlated with areas of astrocyte degeneration. Similar, but slight changes were seen after 2000 and 3000 r.

The present experiment was undertaken in an attempt to determine whether the blood–brain barrier was affected by doses of irradiation smaller than those required to produce morphological signs of irradiation damage. The method selected was the determination of the rate of entry of Na^{24} into the CSF and brain at set intervals after injection of the radioactive substance. Three series of experiments were performed: One group of animals was given tracer doses of Na^{24} in order to establish normal values for the rate of appearance in the CSF and brain; a second group was given a dose of Na^{24} large enough to exert a radiation effect; a third group received total body roentgen irradiation prior to receiving a tracer dose of Na^{24}.

Materials and methods

Radioactive sodium (Na^{24}) was prepared as isotonic saline with a pH of 7·7 and injected into the marginal ear vein of albino rabbits weighing 3·5 $\pm$ 1 kg. At either 6 or 24 hr intervals following injection, simultaneous cisternal and cardiac punctures were performed under nembutal anesthesia. (6, 12, 24, and 30 hr intervals were tested in a pilot study.) The animal was then sacrificed by pithing, the brain exposed and 1 mm slices taken from the superior surface of each cerebral hemisphere. These slices were weighed in the fresh state (approx. 250 mg), then desiccated and incinerated. Carefully measured samples of CSF and plasma were desiccated and counted under similar geometric conditions, for 2–5 min under an end-window Geiger–Mueller counter.

Animals in group one received tracer doses of Na^{24}, averaging 60 μc/kg. Group two received an average dose of 400 μc Na^{24}/kg. Group three received tracer doses of Na^{24}

VOL 4 1958/

following total body X-irradiation of 100 r, 500 r or 1500 r at 220 kV, Ma 10 inherent filtration equal to 3 mm of aluminum, without external filtration. The injection of Na^{24} was made immediately following the X-irradiation, except that half the animals receiving 1500 r were injected 24 hr following X-irradiation.

RESULTS

As a basis for comparison with the results obtained in these experiments, the stable sodium content of brain, CSF and plasma as determined by chemical analysis are as follows:

Plasma— 315–350 mg/100 cm³
(Aver. 330 mg. or 140 mEq./l.)
CSF— 300–380 mg/100 cm³
(90–120% of plasma Na)
Cerebrum—117·5 mg/100 cm³ (or 51·1 mEq./100 kg)
(37% of plasma Na)

TABLE 1. Control group receiving approx. 60 μc of Na^{24} per kg intravenously

Animal no.	Per cent of plasma activity in	
	Brain	CSF
6 hr sampling		
12	—	84·7
14	—	70·5
15	23·0	76·0
16	25·5	83·0
18	29·7	76·4
19	35·2	90·3
25	27·4	—
26	39·1	76·9
27	40·7	88·3
28	35·6	100·0
12 hr sampling		
14	—	109·0
12	—	118·0
24 hr sampling		
12	45·2	—
14	37·2	—
13	33·3	—
17	33·1	116·0
20	51·1	—
21	53·4	123·5
22	47·0	123·0
24	40·0	129·0
29	37·7	125·3
30	48·1	120·0
31	47·7	134·5
32	51·0	127·3

TABLE 2. Group receiving approx. 400 μc of Na^{24} per kg body weight

Animal no.	Per cent of plasma activity in	
	Brain	CSF
6 hr sampling		
2	47·2	—
3	46·3	77·6
7	—	124·8
8	—	123·8
33	50·4	110·0
35	35·5	89·5
36	33·5	83·7
43	33·9	91·0
51	38·0	65·4
12 hr sampling		
8	—	155·6
24 hr sampling		
4	63·5	—
1	45·6	90·7
5	45·0	—
8	54·8	99·2
11	50·6	152·2
34	47·5	138·0
44	49·7	135·4
52	52·8	124·0
30 hr sampling		
9	63·4	121·8
10	61·0	118·2

The data obtained in the control series using tracer doses of Na^{24} confirm the findings of earlier workers that sodium penetrates slowly into the nervous system. In the controls equilibrium was usually reached in the CSF (taken as approximately 120 per cent of plasma sodium) by 24 hr, although there was considerable individual (biological) variation among the test animals. Equilibrium in the brain appeared to be reached more slowly, by 30 hr. The CSF radiosodium concentration at 6 hr averaged 83 per cent of the

TABLE 3. Na^{24} concentration in brain and CSF (% plasma activity)

Brain	6 *hr interval*		24 *hr interval*	
	60 μc/kg	400 μc/kg	60 μc/kg	400 μc/kg
No. Animals	8	7	12	8
Average Na^{24} concentration	32·0	40·6	43·7	51·3
Range	(23·0–40·7)	(33·5–50·4)	(33·1–53·4)	(45·0–63·5)
CSF				
No. Animals	9	8	8	6
Average Na^{24} concentration	82·9	96·1	124·8	123·3
Range	(70·5–100·0)	(65·4–124·8)	(116·0–134·5)	(90·7–152·2)

concentration in the plasma, and 125 per cent at 24 hr. The Na^{24} concentration in the brain averaged 32 per cent that of the plasma at 6 hr and 43·7 per cent at 24 hr. (Tables 1, 3.)

In the group of animals where large doses of Na^{24} were administered, the results suggested that a more rapid equilibrium was being reached than with tracer doses. The radiosodium concentration in the CSF averaged 96 per cent of the plasma concentration at 6 hr and 123 per cent at 24 hr. In the brain it was 40·6 per cent at 6 hr and 51·3 per cent at 24 hr. (Tables 2, 3.)

In the group of animals receiving total body irradiation and tracer doses of radiosodium, those receiving 500 and 1500 r show values equivalent to those found in the animals receiving the large doses of radiosodium. Animals given 100 r total body irradiation showed values intermediate between the control group and the more heavily irradiated groups. (Table 4; summarized in Tables 5 and 6.)

A group receiving 1500 r 24 hr prior to injection of the radiosodium appeared to have higher concentration in the 24 hr specimens than those injected immediately after the 1500 r dose, suggesting increased permeability during the second day post-irradiation rather than during the first 24 hr.

The percentage of radioactivity in the brain and CSF as compared to plasma radioactivity is summarized in Table 7 for the control group and for the irradiated

TABLE 4. Percentage radioactivity in brain and CSF compared to radioactivity of plasma in animals exposed to total body irradiation

Animal no.	Irradiation dose (r)	Per cent of plasma activity in	
		Brain	CSF
6 *hr interval*			
53	100	34·9	—
54	100	33·3	102·0
55	100	39·2	150·0
57	500	37·8	88·7
58	500	36·4	80·5
60	500	44·3	95·3
61	1500	40·4	—
63	1500	33·5	91·0
66	1500	36·0	—
67	1500	44·7	115·5
24 *hr interval*			
68	100	47·5	—
69	100	42·3	—
70	100	53·3	143·7
71	500	49·0	127·0
73	500	49·9	190·0
74	500	51·6	118·0
76	1500	52·3	—
77	1500	60·0	162·2
79	1500	44·6	125·5
81	1500	52·0	146·0
82	1500	50·0	105·5

VOL 4 1958/

TABLE 5. Na^{24} concentration in brain after total body X-irradiation (% plasma activity)

Brain	6 *hr interval*			24 *hr interval*		
	100 r	500 r	1500 r	100 r	500 r	1500 r
No. Animals	3	3	4	3	3	5
Average Na^{24} concentration	35·8	39·2	38·7	47·7	50·2	51·8
Range	(33·3–39·2)	(36·4–44·3)	(33·5–44·7)	(42·3–53·3)	(49·0–51·6)	(44·6–60·0)

TABLE 6. Na^{24} concentration in CSF after total body X-irradiation (% plasma activity)

CSF	6 *hr interval*			24 *hr interval*		
	100 r	500 r	1500 r	100 r	500 r	1500 r
No. Animals	2	3	2	1	3	4
Average Na^{24} concentration	126·0	88·2	103·3	143·7	144·8	134·8
Range	(102·0–150·0)	(80·5–95·3)	(91·0–115·5)		(118·0–190·0)	(105·5–162·2)

TABLE 7. Na^{24} concentration (Summary)

Brain	Controls	Irradiated
6 hr	(8) 32·0	(14) 39·8
24 hr	(12) 43·7	(16) 51·3
CSF		
6 hr	(9) 82·9	(13) 95·4
24 hr	(8) 124·8	(13) 131·8

TABLE 8. Statistical analysis of data

I. *Effect of time*			
	Brain Na^{24} conc.	6 hr vs. 24 hr	C.R. = 3·8
	CSF Na^{24} conc.	6 hr vs. 24 hr	5·55
II. *Effect of size of dose of* Na^{24}			
	Brain Na^{24} conc.	60 μc vs. 400 μc	6 hr 2·4
			24 hr 2·2
			6 hr 2·37
	CSF Na^{24} conc.		24 hr 0·178
III. *Effect of X-radiation* (500 + 1500 r)			(1500 r only)
	Brain Na^{24} conc. irrad.	6 hr 2·41	1·76
		24 hr 1·91	2·52
	CSF Na^{24} conc.	6 hr 2·57	2·16
		24 hr 1·33	1·05

groups (400 μc of Na^{24} per kilogram or 500 and 1500 r total body X-irradiation). This is represented graphically in Figs. 1 and 2.

Statistical analysis of the increased Na^{24} content in the brain and CSF of these irradiated groups over that of the control group, indicates these differences to have a significance of 2 sigma or better. (Table 8.)

Histological examination of brain tissue disclosed no obvious microscopic evidence of irradiation effect on this tissue at these time intervals of 6–48 hr post-irradiation.

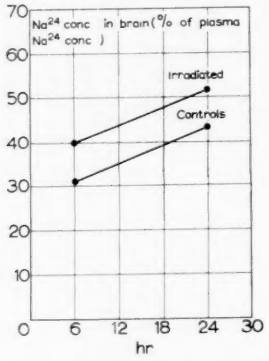

FIG. 1.

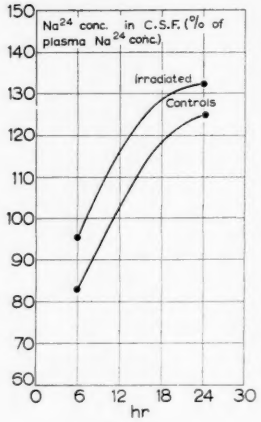

FIG. 2.

DISCUSSION

It would appear from the present data, therefore, that levels of irradiation considerably lower than those needed to produce histological evidence of injury or permeation of vital staining dyes, do effect alterations in the blood–brain barrier, leading to a more rapid passage of electrolyte into the central nervous system. This appears to be a primary result of irradiation on the blood–brain barrier with a breakdown in its selective permeability. The effect observed is not an artefact due to possible fall in plasma sodium (which was the unit of reference) since plasma sodium levels are known to rise after acute irradiation and thus would tend, if anything, to mask the effect observed here; nor is dehydration a significant factor.[12] After acute total body irradiation there is found to be no significant change in sodium space or total body water.[13]

It is interesting to speculate whether this increased electrolyte content of the brain following irradiation bears any relation to the symptoms of acute radiation sickness. This could be studied further, for example, by shielding the head while irradiating the animals and comparing the penetration rate of Na^{24} under these conditions with that in animals receiving total body irradiation or irradiation to the head alone. An extension of the study to determine the interval after irradiation at which increased permeability is maximal would be of value. Experiments using radio-iodinated serum albumin, tagged or stable chemotherapeutic drugs having a limited rate of entry into the CNS, etc., would appear to be a useful study with possible clinical significance.

SUMMARY

High doses of irradiation are required to produce definite morphological changes in the central nervous system. The present experiment was conducted to see if functional derangements occur after comparatively small amounts of ionizing radiations.

VOL. 4 1958/5

Tracer studies with intravenously injected radioactive sodium were performed on rabbits to determine the rate and degree of sodium penetration into the cerebro-spinal fluid and brain. Other groups of rabbits were given large doses of Na^{24} or 100 to 1500 r of total body X-irradiation (followed by tracer doses of Na^{24} at varying intervals) to study the possible effects of such irradiation.

The data obtained showed an accelerated penetration of sodium into the CNS under these conditions, as well as an apparent increase in radio-sodium content in the CNS when compared with the control group. Histological changes were minimal at the highest dosage levels employed.

The significance and possible applications of these findings are discussed.

Acknowledgements—The author would like to express his appreciation to DR. SHIELDS WARREN, Director of the New England Deaconess Cancer Research Institute, for his advice and encouragement during the course of these studies.

REFERENCES

1. SWEET W. H., SELVERSTONE B., SOLOMON A. and BAKAY L. *J. Clin. Invest.* **28,** 814 (1949).
2. SWEET W. H., SELVERSTONE B., SOLOWAY S. D. and STETTEN D. JR. *Surgical Forum* **1,** 376 (1950).
3. LINDER F., EICHLER O., and SCHMEISER K. *Lang. Arch. Dtsch. Z. Chir.* **276,** 286 (1951).
4. GREENBERG D. M., CAMPBELL W. W., and MURAYAMA M. *J. Biol. Chem.* **136,** 35 (1950).
5. GREENBERG D. M., AIRD R. B., BOELTER M. D. D., CAMPBELL W. W., COHN W. E., and, MURAYAMA M. D. *Amer. J. Physiol.* **140,** 47 (1943).
6. MANERY J. F. and BALE W. F. *Amer. J. Physiol.* **132,** 215 (1941).
7. KALTREIDER N. L., MENEELY G. R., ALLEN J. R., and BALE W. F. *J. Exp. Med.* **74,** 569 (1941).
8. WANG J. *J. Gen. Physiol.* **31,** 259 (1948).
9. HIMWICK H. E. *Brain metabolism and cerebral disorders* p. 118 Williams and Wilkins Co. Baltimore (1951).
10. DYKE C. G. and DAVIDOFF L. N. *Roentgen treatment of diseases of the nervous system* p. 18. Lea and Febiger Philadelphia. (1942).
11. CLEMENTE C. D. and HOLST E. A. *A. M. A. Arch. Neurol. Psychiat.* **71,** 66 (1954).
12. BENNETT C. R., BENNETT V. C. and HOWLAND J. W. *Fed. Proc.* **8,** 350 (1949).
13. SOBERMAN R. J., KEATING R. P. and MAXWELL R. D. *Amer. J. Physiol.* **164,** 450 (1951).

International Journal of Applied Radiation and Isotopes, 1958, Vol. 4, pp. 58–68. Pergamon Press Ltd., London

Le Critère de Mortalité et sa Quantité d'Information dans l'Experimentation Radiobiologique

D. J. MEWISSEN

Institut Interuniversitaire des Sciences Nucléaires, Université de Liège, Belgique

(*Received* 8 *November* 1957)

La mortalité après irradiation est une réponse quantale obéissant à une certaine loi de distribution de fréquence.

L'analyse des probits est la méthode statistique de choix pour obtenir le maximum d'information de la réponse quantale de mortalité. Il faut y avoir recours chaque fois qu'une estimation numérique précise est désirable.

La méthode de la dose létale pour tous les témoins possède des indications limitées mais a l'avantage de la simplicité et de l'économie.

A défaut de l'analyse par les probits, on peut utiliser la méthode du rapport des fréquences. La quantité d'information obtenue est maxima quand les proportions de mortalité (ou de survie) s'observent entre les limites un tiers—deux tiers, donc aux environs de la dose médiane effective.

Dans les expériences de "screening" le test sequentiel de mortalité fournit une réponse rapide avec un minimum d'animaux.

THE CRITERION OF MORTALITY AND ITS YIELD OF INFORMATION IN EXPERIMENTAL RADIOBIOLOGY

Mortality is a quantal response with a definite frequency distribution. Probit analysis is the appropriate method providing a maximum amount of information from the lethal quantal response. It should be used whenever a numerical assessment is required.

The method using a 100 per cent lethal dose for controls is of limited value. However it is simple and economical.

A frequency ratio method may be used instead of probit analysis. Mortality (or survival) proportions provide a maximum amount of information, within one third—and two third—limits, that is, in the vicinity of the median effective dose.

In screening experiments, the sequential test of mortality yields early data with the fewest possible animals.

КРИТЕРИЙ СМЕРТНОСТИ И ЕГО ЗНАЧЕНИЕ В ЭКСПЕРИМЕНТАЛЬНОЙ РАДИОБИОЛОГИИ

Смертность после облучения представляет количественную реакцию, подчиняющуюся определенному закону распределения.

Пробит-анализ это статистический метод, дающий наиболее полную информацию относительно смертности, как количественной реакции. Этот метод следует применять во всех тех случаях, когда желательна точная оценка результатов.

Метод определения летальной дозы имеет ограниченные возможности, однако характеризуется такими достоинствами как простота и экономичность.

VOL.
4
1958/5

Вместо пробит-анализа можно использовать метод исследования относительных частот распределения. При этом получаемая информация наиболее полна в тех случаях, когда относительная смертность (или выживаемость) ограничена значениями в пределах одной—двух третей, что приблизительно соответствует средне-летальной дозе.

В опытах с экранированием определение динамики смертности обеспечивает быстрое получение результатов с минимальным количеством животных.

DAS KRITERIUM DER STERBLICHKEIT UND DER BETRAG AN INFORMATIONEN IN DER EXPERIMENTELLEN RADIOBIOLOGIE

Die Sterblichkeit nach Bestrahlung ist ein quantisierter Effekt mit einer bestimmten Häufigkeitsverteilung. Probitanalyse ist die statistische Methode der Wahl, um bei quantisierter Sterblichkeit einen maximalen Betrag an Informationen zu gewähren. Sie sollte immer dann verwendet werden, wenn eine numerische Auswertung erforderlich ist.

Die Methode, welche 100% Lethaldosis für alle Kontrolltiere verwendet, ist nur zum Teil wertvoll. Sie ist jedoch einfach und sparsam.

An Stelle der Probitanalyse kann auch die Methode der Häufigkeitsverhältnisse verwendet werden. Hier erhält man ein Maximum an Informationen, wenn das Sterblichkeitsverhältnis (bzw. dass der Überlebensfälle) zwischen den Grenzen $\frac{1}{3}$–$\frac{2}{3}$ liegt, das heisst in der Nähe der 50% wirksamen Dosis.

Bei "Screening-Versuchen" führt die Wald'sche Seriensterblichkeitsanalyse sher rasch zu Ergebnissen und erfordert nur ein Minimum an Versuchstieren.

VOL. 4 8/59

INTRODUCTION

La mortalité est un critère fréquemment utilisé pour obtenir chez des organismes vivants irradiés, une mesure de la lésion radiologique. De nombreux travaux ont été publiés qui consistent essentiellement à étudier la mortalité observée, par exemple, parmi des groupes de souris, dans des conditions expérimentales déterminées.

La faveur dont jouit cette méthode s'explique sans peine. D'une part, l'estimation de la grandeur du dommage causé aux êtres vivants par les radiations est un problème fondamental de la radiobiologie. D'autre part, une manifestation de ce dommage, aisément observable chez les mammifères, est le raccourcissement de la vie moyenne et éventuellement la mort, dépendant notamment de la dose de radiations absorbées. L'intérêt du critère de mortalité parait universellement reconnu. Par contre, sa signification et son interprétation varient considérablement selon les auteurs, à cause de la diversité des schémas d'expérimentation. C'est pourquoi, il nous parait intéressant de revoir certaines acquisitions récentes de la statistique à propos du phénomène létal.

On sait depuis longtemps que la lésion radiologique est une fonction croissante de la dose administrée. Des travaux récents semblent indiquer que cette fonction est linéaire[1,2,3] mais la question est controversée.[4,5] Cette lésion est qualitativement et quantitativement influencée par de nombreux facteurs, les uns affectent le stimulus (radiations), les autres le récepteur (animal irradié). Dans quelle mesure et sous quelles conditions la mortalité est-elle un critère digne de foi pour l'estimation de la grandeur de la lésion radiologique?

RÉPONSE QUANTITATIVE ET RÉPONSE QUANTALE

Examinons comment la méthode est généralement appliquée en pratique. Dans certains cas, les facteurs de variations affectant le récepteur sont raisonnablement maintenus constants (race, sexe, âge, poids etc.). On étudie alors une caractéristique du stimulus en estimant la grandeur de la lésion résultante, au moyen de la mortalité.

Par exemple, on observe l'effet létal respectif de deux radiations de qualité différente sur des souris de race pure, en vue d'une estimation de leur efficacité biologique relative.

Dans d'autres cas, on peut inversément modifier les facteurs affectant le récepteur, en maintenant autant que possible le stimulus qualitativement et quantitativement constant. Ce procédé s'est avéré fructueux pour mettre en évidence chez des souris ou des rats, par exemple, l'action protectrice contre les radiations de certaines substances administrées avant l'irradiation.[6,7]

Remarquons que ces modalités méthodologiques ne sont que des cas particuliers de l'épreuve biologique (biological assay) prise dans son sens le plus large, c'est à dire selon la définition de Finney[8]: la mesure de la puissance d'un stimulus quelconque, physique, chimique ou biologique, physiologique ou psychologique, au moyen des réactions qu'il produit dans la matière vivante. Dans l'expérimentation dont il est question dans cet exposé, les réactions produites conduisent à la mort, utilisée comme critère de mesure.

L'expérimentateur a le choix entre deux procédés:

(1) Il peut observer la *survie*. Il s'agit de la mesure du temps requis pour la production d'un effet spécifié au lieu de la mesure de la grandeur d'un effet produit. La réponse est donc *quantitative* avec un sens restrictif car elle dépend d'un effet lui-même non quantitatif (la mort). Elle diffère essentiellement d'une réponse quantitative *vraie* dont la radiobiologie offre cependant de nombreuses applications. La variation de volume du thymus, celle du poids corporel de souris irradiées, en sont des exemples connus.

(2) Il peut enregistrer la *mortalité* après un laps de temps conventionnel, 30 jours par exemple. La mort est ici le critère adopté. Il s'agit d'un effet tout-ou-rien: c'est une réponse *quantale*.

Des réponses quantales autres que la mort sont aussi observées en radiobiologie: la germination d'une spore, l'éclosion d'un oeuf, la formation d'un embryon. Nous envisagerons ici certains problèmes statistiques posés par l'expérimentation utilisant la mort comme réponse quantale.

VARIABILITÉ DE LA RÉPONSE BIOLOGIQUE

Une caractéristique du matériel biologique est la variabilité de sa réponse à un stimulus déterminé, quels que soient les moyens mis en oeuvre pour conserver à ce stimulus, au cours d'essais répétés, des caractères qualitatifs et quantitatifs constants. Par exemple, une dose de rayons-X, voisine de la dose létale de 50 pour cent après 30 jours (D. L. 50/30 jours), délivrée à des lots de 25 souris de race pure, peut donner parfois une mortalité de 84 pour cent, parfois de 28 pour cent.[9] Divers auteurs ont insisté sur ce point important, notamment pour les expériences de protection de mammifères contre les radiations.[10,11] Ceci est en effet à l'antipode des garanties qui sont exigées d'un résultat expérimental digne de foi. Ces garanties sont doubles: d'une part, une précision définie par une erreur relative prédéterminée; d'autre part, la reproductibilité au cours d'essais successifs.

Cette variabilité de la réponse n'est pas l'apanage exclusif de l'épreuve biologique. On l'observe également dans les méthodes physiques, mais à un moindre degré et sous une forme plus simple. Le contraste entre méthodes physiques et biologiques a été excellemment mis en évidence par D. J. FINNEY.[8]

Imaginons le problème expérimental que voici: étant donnés deux projectiles, des billes en plomb de poids différents, on demande de déterminer le rapport de leur masse.

La méthode physique consiste à équilibrer sur une balance successivement chacun des deux projectiles par des masses marquées et à faire le rapport des valeurs observées. Bien que l'expérience prouve que plusieurs mesures répétées successivement sur le même projectile donneraient des résultats légèrement différents, nous pouvons, par le choix

VOL
4
1958/

judicieux de la balance, atteindre une précision prédéterminée. La reproductibilité des résultats sera observée dans les limites de l'erreur assignée. C'est pourquoi, une seule pesée suffira généralement à fournir une réponse satisfaisante.

Imaginons à présent que nous désirions estimer le même rapport de masse des projectiles par une méthode biologique. Nous pourrions, par exemple, laisser choir d'une même hauteur choisie, les billes de plomb sur la tête de rats vivants et enregistrer la mortalité observée dans deux groupes de rats, chacun des groupes étant "traité" par un des deux projectiles. La hauteur de chute—identique pour les deux séries—est choisie de telle manière qu'on observe dans l'une et l'autre un certain pourcentage de morts. Il est évident que la réponse quantale (tout-ou-rien) observée sera d'une grande variabilité. Elle est conditionnée par de nombreux facteurs dépendant tant du stimulus que du récepteur. Pour ce qui concerne le premier, la forme, le volume et l'élasticité du projectile sont certainement déterminants.

Supposons qu'ils soient rendus semblables pour les deux billes de plomb. Pour le récepteur, interviennent des facteurs plus nombreux encore: l'âge du rat, le poids, la race, le sexe peut-être, etc. Un moyen d'augmenter l'efficacité de la méthode est de standardiser les récepteurs d'une part, d'accroître leur nombre d'autre part, pour compenser les petites variations individuelles qui échappent à la standardisation. Nous pouvons alors peut-être observer une succession de morts et de vivants différente pour chacun des projectiles expérimentés.

Il est concevable que le rapport de mortalité dans les deux séries respectives fournisse une estimation du rapport des masses cherché. De toute évidence, seules de très longues séries peuvent éventuellement donner une réponse acceptable.

Envisageons le cas particulier où dans une série tous les rats sont morts—ou bien restent vivants. Cette série est impropre à l'estimation du rapport des masses. Elle n'apporte aucune valeur expérimentale, ni par elle-même, ni par comparaison avec une autre, pour l'estimation du rapport cherché. Nous reviendrons sur ce point important au sujet de l'expérimentation dite à dose létale pour les témoins.

Il existe cependant un schéma d'élaboration susceptible de fournir plus d'information. C'est d'expérimenter chaque projectile donné sur plusieurs groupes de rats. Pour chaque groupe la hauteur de chute choisie est identique mais elle varie de groupe à groupe. On peut ainsi rechercher pour l'une et l'autre bille de plomb quelle est la hauteur de chute qui occasionne un certain pourcentage de mortalité, par exemple 50 pour cent. Dès lors, la masse des projectiles peut s'exprimer en unités de hauteur de chute et le rapport des hauteurs correspondant à une même mortalité fournit une estimation meilleure du rapport des masses cherché. On a essentiellement transformé le critère d'estimation et un nouveau paramètre convenablement choisi est substitué à la mortalité. Nous envisagerons une transformation semblable en exposant l'analyse par les probits.

Ces considérations montrent l'intérêt de la statistique aussi bien pour *l'élaboration* de l'expérience que pour l'interprétation des observations dans l'expérimentation biologique utilisant une réponse quantale. Bien qu'à première vue plus maniables, les résultats d'expérimentation à réponse quantitative, posent également des problèmes statistiques importants mais ils sortent du cadre que nous nous sommes assignés ici.

LA TOLÉRANCE ET SA DISTRIBUTION DE FRÉQUENCE

Examinons de plus près certaines modalités des réponses quantales. Nous supposons qu'il s'agit de souris de race pure, choisies au hasard dans une population homogène, d'âge et de poids similaires, logées et nourries de manière standardisée. De telles souris sont fréquemment utilisées dans l'expérimentation biologique: c'est ce qui a motivé notre choix. Néanmoins les considérations développées sont aussi valables pour un autre matériel biologique présentant une réponse quantale sous l'effet d'un stimulus différent.

VOL. 4 58/59

Si une dose convenablement choisie de rayons-X est délivrée par irradiation totale à un groupe déterminé de souris et que la mortalité est observée après un laps de temps conventionnel, (ordinairement 30 jours) un certain nombre de souris meurent, d'autres pas. L'expérience montre que la proportion des individus exhibant la réponse caractéristique varie avec la dose administrée. En fait elle croit avec celle-ci selon une loi dite sigmoïdienne bien connue. Cette loi se vérifie expérimentalement sur de grandes populations de souris. Dans le cas pratique d'une population limitée on observe les caractéristiques suivantes. Il existe une dose pour laquelle aucune mortalité ne se produit: c'est la *dose-seuil*. Des doses croissantes déterminent une mortalité croissante avec une fréquence d'autant plus constante que la population est grande. Enfin une dose dite *létale* tue pratiquement tous les animaux. Ce phénomène est l'expression d'une *tolérance*, variable d'individu à individu, vis à vis de l'irradiation totale par rayons-X.

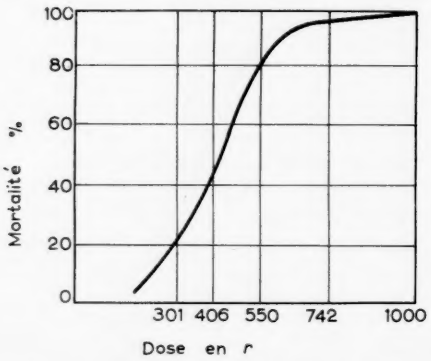

FIG. 1. Courbe sigmoïde de mortalité en fonction de la dose. Cette courbe représente aussi la fonction cumulative de distribution de la tolérance.

La tolérance est donc une variable présentant une certaine distribution de fréquence dans une population de souris. La tolérance aux rayons-X peut aussi être définie comme la dose spécifique et individuelle qui tue une souris prise au hasard et son unité de mesure est l'unité de radiation absorbée. Nous n'avons malheureusement aucun moyen de la mesurer directement.

Détermination indirecte de la tolérance

Remarquons d'abord que la tolérance est une variable aléatoire, c'est à dire une quantité qui peut prendre n'importe quelle valeur entre des limites spécifiées avec une fréquence relative de probabilité spécifiée. Par définition, une variable X est dite aléatoire si pour une valeur spécifique D, une probabilité définie existe que X prendra une valeur moindre que D.[12]

Dans une série de N souris, nous admettons que la tolérance varie d'individu à individu et prend N valeurs différentes. Une probabilité définie peut être attribuée à l'occurence chez une souris prise au hasard d'une tolérance plus petite que toute valeur D donnée. Cette probabilité est égalé à N_D/N, où N_D est le nombre de souris dans la série dont la tolérance est inférieure à D. Nous appelons P la proportion des souris d'une population infinie, dont la tolérance est inférieure à une valeur D.

En application de ceci, nous obtiendrons une estimation p de P en observant la mortalité dans un groupe limité de N souris soumises à une irradiation de D roentgens. La valeur de p se rapprochera d'autant plus de P que N est plus grand.

Si nous expérimentons une série de doses, chacune sur un groupe limité de souris, nous observerons pour chaque dose une proportion p de morts. Chaque valeur de p est une estimée du P correspondant, c'est à dire de la proportion dans une population dont le groupe expérimenté est un échantillon. C'est à partir de ces valeurs que les paramètres de distribution de la tolérance dans une population peuvent être calculés. De l'analyse précédente, il ressort en effet qu'une observation unique de la réponse quantale d'un groupe limité de souris irradiées ne peut prétendre à donner une valeur expérimentale digne de foi. Le problème est ramené à étudier la distribution de fréquence d'une tolérance, par conséquent à estimer les paramètres qui la définissent.

Considérons à nouveau une population infinie de souris. Soit $F(D)$ la probabilité pour que X prenne une valeur moindre que D. Donc $F(D)$ est une fonction de D et signifie tout simplement que pour une

VOL
4
1958/

valeur choisie D, $F(D)$ prend une valeur unique.

On appelle $F(D)$ la fonction cumulative de distribution de X. Il résulte que P est la fonction cumulative de distribution de la tolérance dans une population infinie de souris. La courbe représentative est présentée dans la Fig. 1, c'est la courbe sigmoïde bien connue de mortalité en fonction de la

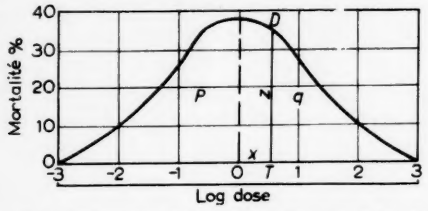

FIG. 2. Courbe cumulative de distribution de la tolérance après normalisation en portant en abcisse le logarithme de la dose.

dose. Elle indique également la proportion d'individus dont les tolérances sont plus petites qu'une valeur donnée.

L'expérience a montré qu'une telle distribution de tolérance est asymétrique si la dose est mesurée en abcisse sur une échelle décimale. On peut la "normaliser" autrement dit, la rendre symétrique par une transformation métamétrique de l'abcisse en échelle logarithmique (Fig. 2). Cette transformation présente de nombreux avantages au point de vue de l'analyse statistique. On démontre en effet qu'en différentiant la fonction cumulative de distribution d'une variable aléatoire on obtient sa fonction de densité de probabilité. Une des plus importantes de ces fonctions est la fonction de densité de probabilité *normale* dont la variable aléatoire est dite normalement distribuée. Cette fonction est symétrique par rapport à sa moyenne et sa courbe représentative est la courbe normale définie par la loi mathématique de Laplace-Gauss. Une distribution normale est complètement décrite par deux paramètres: la moyenne et l'écart-type.

La normalisation de la distribution de tolérance sur une échelle logarithmique des doses se justifie donc par la simplification qu'elle introduit dans l'analyse statistique. Elle ne préjuge pas de l'exactitude ou de la fausseté d'hypothèses postulant une relation logarithmique entre la dose de radiations reçues par la matière vivante et la grandeur de la lésion provoquée.

LA DOSE MÉDIANE EFFECTIVE

Avec un souci légitime de simplicité et d'économie, on a souvent tenté de définir un paramètre unique susceptible de caractériser la réponse quantale de mortalité, indépendamment de sa distribution sigmoïdienne de fréquence. L'examen de la littérature révèle que deux paramètres de ce type ont surtout retenu l'attention de différents expérimentateurs, en vue de la mesure de l'efficacité biologique des radiations en fonction d'une mortalité observée. Les uns se réfèrent à la *dose efficace minima* (ou dose létale minima ou dose-seuil) et entendent par là la dose immédiatement inférieure à celle qui tue le premier animal du groupe, c'est à dire celui dont la tolérance est la plus petite. D'autres préfèrent la *dose efficace maxima* (ou dose létale minima 100 pour cent) qui est la dose tuant à coup sûr tous les individus. Ces concepts se heurtent à de sérieuses difficultés sur le plan théorique et pratique. A cause de la forme sigmoidïenne de la fonction de tolérance pour une population infinie, il est malaisé d'évaluer numériquement l'un ou l'autre de ces paramètres pour des populations finies. Cette estimation dépend largement de la grandeur de l'échantillon de population utilisé. La présence, même dans un groupe sélectionné de souris, d'un animal dont la tolérance est anormalement basse—ou élevée—peut sérieusement fausser l'estimation numérique. Le choix de la dose efficace maxima recèle un autre écueil. La distribution de fréquence de la tolérance présentant une asymétrie droite, cette dose est relativement élevée par rapport à la tendance centrale. Après normalisation de cette distribution, la progression des doses est un effet logarithmique.

Il faut donc administrer une dose importante de radiations à un groupe de souris contrôlés si la certitude *absolue* est requise,

dans tous les cas répétés, de tuer à coup sûr tous les individus. Aussi n'est-il pas exceptionnel qu'une souris du groupe survive à une dose réputée 100 pour cent létale. Ceci met bien en lumière l'inconvénient majeur de ce critère: il tient à *un individu*.

Pour ce motif, nous préférons la dose létale moyenne (D.L. 50) ou dans un champ d'application plus large la *dose médiane effective*. C'est celle qui détermine la réponse quantale caractéristique chez la moitié des individus. Si le critère observé est la mortalité, elle tue 50 pour cent d'une population après un laps de temps conventionnel. Du point de vue statistique, elle présente l'avantage de s'identifier avec la tolérance moyenne μ. Or celle-ci est un des deux paramètres définissant une distribution de fréquence de la tolérance normalisée grâce à la transformation métamétrique de la dose. L'autre paramètre est la variance σ^2 qui mesure sa dispersion. La méthode des probits permet de calculer facilement l'un et l'autre. On voit sans peine les avantages que présente la caractérisation de l'efficacité du stimulus radiations par la distribution de la réponse quantale au moyen des deux paramètres: tolérance moyenne et variance. Si pour des raisons d'économie, l'expérimentateur opte pour le calcul d'un seul paramètre, la D.L. 50 ou dose médiane effective présente des avantages appréciables à condition que certaines précautions soient prises. L'objection que plusieurs auteurs font à la D.L. 50 réside dans la réelle difficulté de son estimation à partir d'un échantillon limité d'une population de souris. Sur la courbe sigmoïde de la tolérance, le point représentatif de la dose médiane se trouve au point d'inflexion, c'est à dire, à l'endroit où la pente est la plus abrupte. Par conséquent, un déplacement minime de la dose résulte en une variation beaucoup plus grande de l'effet létal.

Il faut donc s'entourer de strictes garanties physiques, requises pour la précision de la dose de radiations délivrée. Il est possible d'obtenir ces garanties dans l'expérimentation pratique par l'observance de règles bien définies.[13] Dans ces conditions, la reproductibilité de l'effet létal est très satisfaisante même sur des groupes limités de souris.

L'estimation de la dose médiane effective par la méthode des probits

Nous exposons succintement les principes généraux de la méthode des probits. Pour plus de détails, nous renvoyons le lecteur aux ouvrages spécialisés.[8,14]

L'analyse des probits est une méthode statistique pratique d'estimation des paramètres μ et σ^2 de la distribution de tolérance. Elle consiste essentiellement à transformer le pourcentage de mortalité observée en une valeur calculée appelée probit. Il existe des tables détaillées donnant la valeur du probit pour divers pourcentages. Cette transformation a pour résultat de rendre linéaire la courbe sigmoïde normalisée de mortalité, ce qui simplifie considérablement le traitement mathématique.

En pratique, on détermine le probit expérimental à partir de la mortalité observée dans plusieurs groupes de souris soumises à des doses d'irradiation croissantes selon une progression logarithmique, et distribués de part et d'autre de la D.L. 50 présumée. On calcule ensuite l'équation de la *droite de régression pondérée* des probits par une méthode dite de vraisemblance maxima. La pondération consiste à donner un poids différent aux divers points expérimentaux selon leur position plus ou moins proche de la tolérance moyenne calculée et en fonction du nombre d'animaux qui ont servi à leur estimation. Au moyen de l'équation de régression, la dose médiane effective est calculée, ainsi que ses limites fiduciaires à un seuil de probabilité convenablement choisi, généralement au seuil de 5 pour cent. Autrement dit, on obtient deux valeurs limites (de part et d'autre de l'estimée de la dose médiane effective) entre lesquelles la valeur vraie, rapportée à une population infinie de souris, à 95 chances sur 100 de se trouver.

Pour fixer les idées, supposons qu'on désire mettre en évidence l'effet protecteur d'un composé chimique contre le rayonnement-X. On calcule la dose médiane effective et ses limites fiduciaires pour des souris contrôles et pour des souris traitées par le protecteur présumé. On détermine ensuite si les doses médianes effectives respectives diffèrent entr' elles d'une manière significative. La méthode

VOL.
4
1958/5

est, dans ses principes, analogue à celle–hypothétique–qui a été imaginée pour mesurer le rapport de masse des billes en plomb. Dans les deux cas, la réponse quantale est transformée en un paramètre nouveau qui sert ensuite à estimer la relation cherchée entre deux grandeurs. Dans un cas, ce paramètre pourrait s'appeler la "hauteur de chute médiane effective", dans l'autre cas, c'est la dose de radiations médiane effective.

LA QUANTITÉ D'INFORMATION DE LA RÉPONSE QUANTALE

L'expérimentation quantale utilisant l' analyse des probits nécessite un nombre d'animaux relativement élevé et une longue étude statistique. Nous avons signalé l'existence dans la littérature d'autres méthodes utilisant une réponse quantale de mortalité sous une forme simplifiée. L'une des plus intéressantes est la *méthode dite de dose létale pour tous des témoins* ou dose létale minimum 100 pour cent. Elle a été intensément utilisée—et avec succès—dans les recherches sur la radioprotection chimique des mammifères.[11] Une certaine dose de rayons-X est délivrée par irradiation totale à un groupe de souris ou de rats témoins, telle qu'aucun survivant ne subsiste après un laps de temps conventionnel, 30 jours par exemple. La même dose est administrée à un groupe d'animaux issus d'une même population homogène mais soumis à un traitement spécifié: par exemple, une injection intrapéritonéale de cystamine immédiatement avant l'irradiation ou une injection intraveineuse d'une suspension de cellules médullaires homologues après l'irradiation. Dans l'un et l'autre cas, on observe, après 30 jours, une survie définie dans les groupes d'animaux traités. Ainsi sont mises en évidence l'action protectrice de la cystamine ou l'action thérapeutique de la moelle osseuse homologue.

Le procédé expérimental est simple, économique et ne requiert pas d'analyse statistique. Quelle est sa signification et quel degré de confiance peut lui être imparti?

Remarquons tout d'abord que cette méthode est un cas particulier de *l'épreuve biologique par rapport de fréquence.*[15] Celle-ci consiste à utiliser entre deux groupes d'animaux un certain rapport de fréquence observé pour obtenir une mesure d'une variable aléatoire différemment distribuée dans les deux groupes. Ainsi dans la méthode de dose létale minimum 100 pour cent appliquée aux problèmes de radioprotection, on observe une certaine proportion de mortalité dans le groupe protégé en opposition avec la proportion 100 pour cent du groupe contrôle, dans le but de mesurer la différence de tolérance vis à vis d'une irradiation totale, entre les deux groupes.

Etudions le problème statistique sous son aspect théorique. On se trouve en présence de deux échantillons de populations (contrôle et protégée) présentant chacune une certaine distribution de tolérance aux rayons-X. La courbe de la Fig. 3 représente la distribution normale de tolérance D dans l'un quelconque des deux groupes. En ordonnée est porté le nombre de souris exhibant une tolérance inférieure à toute dose D donnée. Le logarithme de la dose est porté en abcisse. Supposons qu'on observe une proportion p de morts. La droite DT divise l'aire d'intégration en dessous de la courbe en deux portions, l'une représente la proportion p de morts et l'autre la proportion q de survivants ($q = 1 - p$). La hauteur de l'ordonnée DT est représentée par z, et x mesure la distance de D à l'axe central au point 0 pris comme origine. Les valeurs de x sont positives à droite de 0 et négatives à gauche. Quand x varie de $-\infty$ à $+\infty$, la proportion de morts s'élève de 0 à 1. Dans le cas de la tolérance aux rayons-X, nous savons que x varie proportionnellement au logarithme de la dose D.

Il ressort de la Fig. 3 que si x s'accroit d'une quantité infinétésimale dx, l'accroissement correspondant de p est zdx. D'où l'on tire

$$\frac{dp}{dx} = z$$

On démontre que la quantité d'information

par rapport à x est donné par l'équation

$$I_x = I_p \left(\frac{dp}{dx}\right)^2, \quad I_x = x\frac{nz^2}{pq}$$

où n est le nombre d'animaux utilisés.[15]

Bien que $1/pq$ passe par un minimum quand $p = q$ (c'est à dire pour 50 pour cent de mortalité), la quantité d'information est maxima en ce point (à cause du carré de z

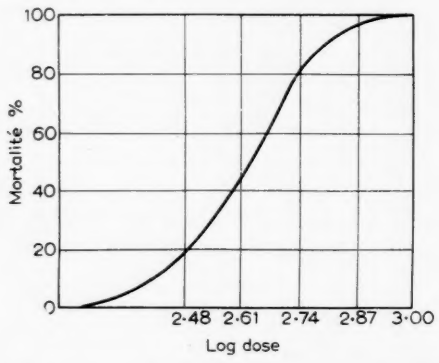

FIG. 3. Courbe de densité de la tolérance en fonction du logarithme de la dose. Cette courbe est normale et son aire d'intégration est égale à 1. ($p + q = 1$.)

qui passe par un maximum). Par conséquent pour un *test unique:*

(1) On obtient la précision la plus haute pour un nombre quelconque d'animaux en ajustant la valeur métamétrique de la dose (logarithme) approximativement au point de mortalité 50 pour cent.

(2) La précision diminue au fur et à mesure qu'on s'écarte de ce point.

(3) En pratique, la quantité d'information est maxima et ne varie guère entre les proportions de mortalité 1/3 et 2/3.

Reprenons l'analyse de la méthode de dose minimum létale 100 pour cent appliqué à la mise en évidence d'un radioprotecteur. Son fondement statistique est le suivant. On émet l'hypothèse que le groupe de souris contrôles et le groupe de souris, traitées par un composé chimique présumé radioprotecteur, pourraient être deux échantillons d'une même population de souris, équivalents, par conséquent, sous le rapport de la tolérance aux rayons-X. C'est ce qu'on appelle *l'hypothèse statistique nulle.* Si l'expérience ne la verifie pas, c'est à dire s'il existe une proportion plus grande de survivants parmi les animaux traités, l'hypothèse nulle est rejetée et le composé testé est déclaré radioprotecteur.

(1) Cas où l'effet protecteur est relativement grand, dans le cas par exemple où le facteur de réduction de dose est de l'ordre de grandeur de celui de la cystamine (1,5 à 2).

En observant un rapport de fréquence entre le groupe contrôle et le groupe protégé, on passe successivement d'une zone où la quantité d'information est petite (dans le groupe contrôle, p tend vers 1, q tend vers 0) à une zone où la quantité d'information est beaucoup plus grande (p et q tendent vers 0,5 dans le groupe protégé).

La probabilité pour qu'une erreur statistique de première espèce se produise varie dans chaque cas mais reste faible. On appelle erreur de première espèce le rejet d'une hypothèse nulle quand en fait elle est vraie. Par conséquent, le risque pratique est minime de déclarer radioprotecteur un composé chimique qui ne l'est pas.

(2) Cas où l'effet protecteur est relativement faible. On reste dans la zône où la quantité d'information est petite (dans le groupe contrôle, p tend vers 1, q tend vers 0; dans le groupe faiblement protégé, p est légèrement plus petit que dans le groupe contrôle). La probabilité pour qu'une erreur de seconde espèce se produise doit être prise en sérieuse considération. On appelle erreur de seconde espèce celle qui consiste à accepter l'hypothèse nulle quand en fait elle est fausse. Par conséquent, il existe un risque non négligeable de déclarer non efficace un composé chimique testé alors qu'en fait il est radioprotecteur.

Ceci illustre les limites de la méthode. Selon une observation très générale, elle perd en précision ce qu'elle gagne en simplicité. Elle reste indiquée chaque fois qu'on veut procéder rapidement et économiquement, à condition que l'effet escompté à mettre en évidence soit relativement grand. Elle risque de laisser passer inaperçu un effet réel mais relativement petit.

VOL. 4 1958/5

LE TEST SÉQUENTIEL

La méthode de dose minimum létale 100 pour cent n'est donc pas appropriée à la mise en évidence de petits effets modificateurs de la tolérance. Des résultats satisfaisants peuvent cependant être obtenus au moyen d'une *épreuve par rapport de fréquence* à condition que les mortalités enregistrées ne soient pas trop éloignées de celle qu'on obtient avec la dose médiane effective (D.L. 50).

L'expérience doit si possible être élaborée de telle manière que la dose utilisée entraine dans le groupe contrôle et dans le groupe protégé, une mortalité respective comprise entre les limites de 1/3 à 2/3.

On obtient ainsi le maximum possible d'information pour le nombre d'animaux dont on dispose. En effet, la pente de la courbe sigmoïde de la tolérance passe par un maximum au niveau de la D.L. 50. Un effet de réduction de dose, par exemple, même petit, entraine dans cette région une diminution de mortalité relativement plus importante qu'en n'importe quel autre endroit de la courbe. Pratiquement, on observera 30 jours après irradiation, les proportions de mortalité respectivement dans le groupe de souris contrôles et dans le groupe de souris traitées par un radio-protecteur présumé. Chacun de ces groupes étant un échantillon aléatoire, on peut calculer les limites de confiance des proportions observées rapportées à une population de souris. On calculera ensuite le degré de signification be la différence entre les proportions observées. On admet généralement que 0,05 est un seuil de probabilité satisfaisant.

Pour l'atteindre, il faut parfois disposer de groupes de souris relativement nombreux. C'est pourquoi cette méthode peut être trop onéreuse, notamment dans les expériences de "screening". Supposons qu'on désire apprécier le pouvoir radioprotecteur éventuel d'une série de composés chimiques. Le problème est alors de déterminer rapidement si, oui ou non, telle substance est radioprotectrice. Dans ce cas le test séquentiel est le procédé de choix.

L'analyse séquentielle est une méthode d'induction statistique récemment développée par WALD.[12] Son originalité est de ne pas fixer à l'avance le nombre d'observations requises pour fournir une réponse significative. La décision de poursuivre ou de terminer le test séquentiel dépend à tout moment des observations déjà faites. Cette réponse est obtenue avec un minimum d'animaux. En pratique, on peut procéder comme suit.

On irradie simultanément un groupe de cinq animaux contrôles et un groupe de cinq animaux traités par le radio-protecteur présumé. La dose délivré est calculée de telle sorte que l'irradiation entraine la mort des individus contrôles après un délai relativement court (de 6 à 12 jours par exemple). On note la mortalité dans le groupe traité au moment où trois des individus contrôles sont morts. Un calcul statistique rapide[16] donne ensuite une réponse affirmative, négative ou douteuse. Dans l'une des deux premières éventualités, le test est terminé, dans la dernière, deux nouveaux groupes sont irradiés et le cycle recommence jusqu'à ce qu'une réponse nette soit obtenue. Trois cycles y suffisent généralement. Ce test réclame en moyenne moins d'animaux que ceux précédemment décrits. Son efficience est vraiment remarquable.

L'homogénéité de la réponse quantale

Divers travaux récents semblent démontrer que la réponse quantale dans une population de souris irradiées n'est pas homogène,[17,18,19] c'est à dire qu'elle dépend de deux ou plusieurs composantes statistiques exerçant une action conjointe indépendante.[20,21]

Ceci n'a rien d'étonnant étant donné la complexité des mécanismes qui président à la mort par radiation chez les mammifères. Une de ces composantes pourrait être liée au sexe.[19] Le mécanisme de la réponse quantale de mortalité varie selon la dose administrée. Si la radioprotection chimique se traduit par un effet réducteur de dose, on risque, en comparant un groupe contrôle et un groupe protégé de souris, d'établir un rapport entre des phénomènes essentiellement

hétérogènes. Les effets de cette hétérogénéité sont minimum au centre de distribution de la tolérance, c'est à dire au voisinage de la dose médiane effective.[22] Cet élément mérite considération dans certains schémas d'expérimentation.

BIBLIOGRAPHIE

1. Blair H. A., *University of Rochester Report* UR 1206, p. 37 (1952).
2. Blair H. A., *University of Rochester Report* UR 312, p. 22. (1954).
3. Mewissen D. J., Comar, C L., Trum B. F. et Rust J. H., *Rad. Res.* **6,** 450 (1957).
4. Sacher Q. A., *Radiology* **67,** 240 (1956).
5. Yockey H. P., *Rad. Res.* **5,** 146, (1956).
6. Bacq Z. M. et Herve A., *Bull. Acad. Med. Belg.* **17,** 13 (1952).
7. Betz H. et Fruhling L., *C. R. Soc. Biol., Paris* **144,** 1013 (1950).
8. Finney D. J., *Probit Analysis. A Statistical Treatment of the Sigmoïd Response Curve.* (2nd Ed.) pp. 318. Cambridge University Press (1952).
9. Chapman W. H., Sipe C. R., Eltzholtz D. C., Cronkite E. P., et Chambers F. W. *Radiology* **55,** 865 (1950).
10. Bonnet-Maury P. et Patti F., *J. Radiol. Electrol.* **31,** 286 (1950).
11. Bacq Z. M. et Alexander P., *Principes de Radiobiologie.* Masson, Liège (1955).
12. Wald A., *Sequential Analysis* (3rd Ed.) John Wiley, New York (1952).
13. Ellinger F., Morgan J. E. et Cook E. B., *Radiology* **64,** 210 (1955).
14. Fisher R. A. et Yates F., *Statistical Tables.* Oliver and Boyd, Edinburgh (1957).
15. Fisher R. A., *The Design of Experiments.* Oliver and Boyd, Edinburgh (1953).
16. Kimball A. W., Burnett W. T. Jr., et Doherty D. G., *Rad. Res.* **7,** 1 (1957).
17. Betz E. H., *Contribution à l'Étude du Syndrome Endocrinien provoqué par l'Irradiation Totale de l'Organisme*, Georges Thone, Liège (1955).
18. Maisin J., Maldague P., Dunjic A. et Maisin H., *J. Belge Radiol.* **40,** 341 (1957).
19. Koch R., Catsch A. et Langendorff H., *Dtsch. Med. Wschr.* **82,** 1069 (1957).
20. Catsch A., *Advances in Radiobiology.* Proceedings of the fifth international Conference in Radiobiology, Stockholm (1956). Oliver and Boyd, Edinburgh (1957).
21. Mewissen D. J., *Acta Radiol.* **48,** 141 (1957).
22. Mewissen D. J., *Radiation Res.* **6,** 85 (1957).

VOL
4
1958/

International Journal of Applied Radiation and Isotopes, 1958, Vol. 4, pp. 69–83. Pergamon Press Ltd., London

Essais de Prevention et Traitement du Mal des Rayons chez le Poussin

M. L. BEAUMARIAGE

Laboratoire de Pathologie et de Thérapeutique générales et Laboratoire de Recherches pour la Protection des Populations civiles, Université de Liège

(*Received* 25 *October* 1957)

VOL. 4 58/59

Des poussins de race Rhode Island, âgés de 19 à 21 jours, sont exposés aux rayons-X. S'ils reçoivent une dose totale de 2000 r (débit: 100 r/min), la majorité des décès survient au cours des 48 premières heures. Il existe deux phases de létalité, l'une précoce, l'autre tardive.

Parmi des radioprotecteurs très efficaces chez la souris et le rat (cystéamine, cystamine, cystéine, tryptamine, diéthyldithiocarbamate de sodium, acide éthylènediaminotétraacétique, cyanure de sodium), seuls, le diéthyldithiocarbamate de sodium et la tryptamine sont faiblement actifs chez le poussin; le premier agit sur les deux phases de létalité, le second ne réduit que la mortalité tardivé. Il est peu probable qu'ils agissent par anoxie.

Les troubles fonctionnels et métaboliques qui suivent l'irradiation sont graves et précoces chez le gallinacé (collapsus circulatoire, libération d'histamine, hyperkaliémie). La déplétion préalable des stocks d'histamine tissulaire par la peptone et le 48/80 réduit le nombre de décès précoces sans modifier la mortalité tardive. Le Néoantergan est le seul parmi les antihistaminiques étudiés qui ait une action radioprotectrice. Celle-ci est appréciable au cours des deux phases de létalité. Injecté à titre curatif, il devient inefficace. Les traitements visant respectivement à corriger l'hyperkaliémie, à pallier un éventuel déficit cortico-surrénalien ou à lutter contre l'infection, sont restés sans résultats.

EXPERIMENTS IN THE PREVENTION AND TREATMENT OF RADIATION SICKNESS IN CHICKS

Rhode Island chicks aged 19 to 21 days are exposed to X-rays. If they receive a total dose of 2000 r (at a rate of 100 r/min), most of the deaths occur within the first 48 hours. There are two phases of lethality, one rapid and the other delayed.

Among radio-protective substances which are very effective in the mouse and rat (cysteamine, cystamine, cysteine, tryptamine, sodium diethyldithiocarbamate, ethylenediaminotetracetic acid, sodium cyanide) only sodium diethyldithiocarbamate and tryptamine are feebly active in the chick; the former affects both lethality phases, the latter reduces only the delayed mortality. It is unlikely that they act by anoxia.

The functional and metabolic disturbances resulting from irradiation are serious and appear promptly in fowls (circulatory breakdown, liberation of histamine, hyperkaliemia). Preliminary depletion of histamine reserves in the tissues by means of peptone and 48/80 reduces the number of early deaths without altering the delayed mortality rate. Of the anti-histamines studied, Neoantergan alone has a radioprotective action. This is appreciable in both lethality phases. When administered with curative intent, it becomes ineffective. Treatments aiming at correcting hyperkaliemia, palliating a subsequent cortico-surrenal deficiency or fighting infection have been without result.

ОПЫТЫ ПО ПРЕДУПРЕЖДЕНИЮ И ЛЕЧЕНИЮ ЛУЧЕВОЙ БОЛЕЗНИ У ЦЫПЛЯТ

Цыплята породы Род Айленд в возрасте от 19 до 21 дня подвергались действию рентгеновских лучей. Доза тотального облучения составляла 2000 р при мощности дозы 100/р мин. Смерть наступала чаще всего в течение первых 48 часов. Наблюдались два пика смертности—один ранний, другой поздний.

Из числа веществ, обладающих выраженным защитным действием для мышей и крыс (цистеамин, цистамин, цистеин, триптамин, диэтилдитиокарбамат натрия, этилендиаминтетрауксусная кислота, цианистый натрий), только диэтилдитиокарбамат натрия и триптамин имеют слабо выраженное защитное действие по отношению к цыплятам; первый влияет на оба пика смертности, второй не снижает позднего пика. Мало вероятно, что эффективность этих веществ обусловлена аноксией.

Функциональные и обменные нарушения, вызванные облучением, сильно выражены и рано проявляются у кур (циркуляторные коллапсы, высвобождение гистамина, гиперкалиемия). Предварительное истощение запасов тканевого гистамина с помощью пептона и 48/80 снижает количество ранних смертей, не оказывая воздействия на поздний пик смертности. Неоантерган является единственным из исследованных антигистаминных веществ, которое оказывает защитное действие. Оно проявляется в отношении обоих пиков смертности. При введении после облучения неоантерган оказывается неэффективным. Терапевтические меры, предпринятые для снижения гиперкалиемии, для выравнивания предполагаемой кортико-надпочечниковой недостаточности или для борьбы с инфекцией остаются безрезультатными.

VERSUCHE ÜBER PROPHYLAXE UND THERAPIE BEI STRAHLENKRANKHEIT DES KÜCKEN.

19 bis 21 Tage alte Rhode Island-Kücken werden röntgenbestrahlt. Bei 2000 r Gesamtdosis (Dosisrate: 100 r/min) tritt der Tod in der Mehrzahl der Fälle bereits innerhalb der ersten 48 Stunden ein. Es treten 2 Lethalitäsphasen auf, eine vorzeitige und eine verzögerte. Von den bei Maus und Ratte äusserst wirksamen Radioschutzmitteln (Cysteamin, Ciystamin, Cstein, Tryptamin, Natrium-Diäthyldithiocarbonat, Äthylendiamin-Tetraessigsäure, Natrium-Cyanid) sind vor allem Natrium-Diäthyldithiocarbaminat und Tryptamin bei jungen Hühnern von einer gewissen schwachen Wirksamkeit. Das erstgenannte wirkt sich auf beide Lethalitäsphasen aus, während das letztere nur die Zhal der verzögert lethalen Fälle herabsetzt. Dass es sich dabei um Anoxie handelt, ist wenig wahrscheinlich.

Funktions- und Stoffwechselstörungen (Kollaps, Histaminausschwemmung, Hyperkaliämie) als Folge von Bestrahlung sind bei Hühnern schwerwiegend und treten frühzeitig auf. Eine vorhergehende Entleerung der Vorräte an Gewebshistaminen durch Pepton und "48/80" verringert die Zahl der frühzeitigen Todesfälle, ohne jedoch die verzögerte Mortalität zu beeinflussen. Von den untersuchten Antihistaminen ist Neoantergan das einzige, dem eine Wirkung als Radioschutzmittel zukommt. Sie macht sich während beider Lethalphasen bemerkbar. Diese Wirksamkeit verschwindet jedoch, wenn Neoantergan zu Heilzwecken injiziert wird. Behandlungsversuche in der Richtung Korrektion der Hyperkaliämie, der Kompensation einer eventuellen Störung der Nebenniere, oder einer Bekämpfung bleiben ohne Resultat.

VOL 4 1958/

INTRODUCTION

Les oiseaux présentent une réactivité particulière vis-à-vis des radiations ionisantes. Ils sont plus radiorésistants que les mammifères[1] et leur sensibilité varie fortement en fonction de l'intensité du rayonnement (débit/min). En général, le débit est un facteur de moindre importance chez le mammifère.[21]

Selon Jacquez et Karnofsky,[14] Stearner et ses collaborateurs,[21,22] 50 à 90 pour cent des poussins de race Leghorn blanche, irradiés avec une dose totale de 1000 r et une intensité élevée (43 r/min), succombent en état de collapsus cardiovasculaire au cours des 24 à 48 heures qui suivent l'atteinte par les rayons-X (*phase de létalité précoce*).[27] La défaillance circulatoire aggrave ou crée les lésions rénales fréquemment observées à l'examen nécropsique.[23] Les survivants, ainsi que la plupart des poussins qui ont reçu la même dose totale de roentgens, mais avec un débit de 6 r/min,[21]

se comportent comme des mammifères et meurent au cours des deux semaines qui succèdent à l'irradiation (*phase de létalité tardive*). Une dose de rayons-X administrée avec une intensité élevée n'entraîne aucun décès précoce si l'on a soin de répartir la dose totale en fractions séparées par des intervalles de repos suffisamment longs.[22]

Les manifestations qui précèdent le décès précoce du poussin irradié (l'hypotension et l'atteinte rénale exceptées) s'observent aussi chez le coq adulte soumis aux rayons-X;[28] elles existent aussi chez le canard.[21] Toutefois, le pigeon irradié avec des rayons γ ne présente qu'exceptionnellement des manifestations pathologiques précoces.[26]

Chez l'oiseau, quelques essais de radioprotection au moyen d'agents physiques (écrans de plomb)[24] ont été tentés avec un succès variable. Parmi les agents pharmacodynamiques, l'adrénaline et l'hypoxie améliorent considérablement le pourcentage de survie des poussins (phases précoce et tardive).[25]

Le but de notre travail est de rechercher systématiquement:

(1) Si les poussins de race Rhode Island, irradiés avec une dose 100 pour cent létale, peuvent être protégés contre l'action des rayons-X par des substances considérées comme radioprotectrices chez la souris et le rat.

(2) Si des traitements visant à prévenir ou à corriger les troubles humoraux (histaminolibération), métaboliques (hyperkaliémie) ou endocriniens (insuffisance surrénalienne aiguë) déclenchés par l'irradiation, sont susceptibles d'accroître les chances de survie de l'oiseau irradié.

(3) Si une thérapeutique antiinfectieuse peut être également efficace dans ces circonstances.

TECHNIQUES

1. Animaux et irradiation

Nous avons utilisé plus de 1500 poussins de race Rhode Island, âgés de 19 à 21 jours, d'un poids moyen de 115 g. Les oiseaux sont répartis en lots variant de 5 à 50. Chaque expérience comporte 4 lots: un premier rassemble des animaux intacts. Le second lot est irradié, sauf indication contraire, avec une dose de 2000 r au débit de 100 r/min. Le troisième rend compte de la toxicité des substances dont on recherche l'éventuelle action radioprotectrice. Le quatrième, irradié avec une dose de 2000 r, reçoit les substances étudiées; en général, leur administration précède l'irradiation.

Les animaux sont introduits dans une boîte en carton (divisée en douze loges individuelles) et irradiés au moyen d'un appareil de radiothérapie Siemens Stabilivolt. Constantes physiques de l'irradiation: 200 kV, 15 mA, filtre: 3 mm Al, distance focale: 65 cm, débit: 100 r/min, champ: 33 × 24 cm; l'ampérage est de 8 mA au débit de 50 r/min.

Les poussins sont ensuite maintenus dans une chambre climatisée pendant un mois; leur régime alimentaire est constant.

L'autopsie des animaux est réalisée immédiatement après le décès. Dans quelques cas, nous avons prélevé des fragments d'organes pour examen histologique après fixation au liquide de Bouin, inclusion en paraffine et coloration à l'hémalun-éosine.

2. Substances étudiées et modalités de traitements

Elles seront énumérées au fur et à mesure de notre exposé. Les substances sont injectées, sauf indication contraire, par voie intrapéritonéale en solution aqueuse dans un volume de 0,5 ml par 100 g de poids du corps. Les solutions injectées sont au préalable rendues rigoureusement isotoniques par l'adjonction de NaCl.

3. Méthode d'appréciation des résultats

La signification statistique des mortalités précoce et tardive après irradiation est appréciée au moyen des tests d'indépendance et du calcul du

$$\chi^2 = \frac{(ad - bc)^2(a + b + c + d)}{(a + b)(c + d)(a + c)(b + d)}$$

dans laquelle a et b sont les valeurs témoins,

TABLEAU 1. Mortalité des poussins irradiés avec 2000 r de R.X. (200 kV, débit 100 r/min) après traitement par divers radioprotecteurs chez le Rongeur

Traitements Posologie (mg/100 g de poids du corps)	Nombre de poussins avant R.X.	Létalité après 30 jours		Symptomatologie après R.X.
		Nombre de décès	P*	
Aucun	136	127		adynamie dyspnée cyanose
NaCl 4,5	10	10	$0,3 < P < 0,5$ augm.	identique
Cystéamine-base 6	20	20	$0,2 < P < 0,3$ augm.	aggravée
10	25	21	$0,1 < P < 0,2$ dim.	aggravée
Cystamine-2 HCl 14,6	16	16	$0,2 < P < 0,3$ augm.	aggravée
Cystéine-HCl 30,6	25	22	$0,3 < P < 0,5$ dim.	aggravée
Tryptamine-HCL 3,5	30	24	$0,02 < P < 0,05$* dim.	identique
9,5	30	25	$0,05 < P < 0,1$ dim.	aggravée
Titriplex III 17	20	18	$0,5 < P < 0,7$ dim.	aggravée
34	15	14	$0,99 < P$ dim.	aggravée
Cyanure 0,5	18	16	$0,90 < P < 0,95$ dim.	aggravée

* Sont considérées comme statistiquement significatives les valeurs de $P < 0,05$.
La létalité précoce est du même ordre de grandeur dans tous les groupes.
Les doses reprises ci-dessus (à l'exception de la cystéamine 6 mg, de la tryptamine 3,5 mg et du titriplex III 34 mg) sont les doses qui manifestent un effet protecteur chez le rat ou la souris.

c et *d* les valeurs expérimentales. Dans notre cas, le degré de liberté *n* est égal à 1. Nous considérons comme statistiquement valable toute valeur de $P < 0,05$.[11]

N'ayant pas constaté de différence significative dans la survie des poussins appartenant aux différents groupes témoins irradiés, nous prenons comme base de référence la courbe de survie dressée en considérant l'ensemble des 136 poussins irradiés témoins. Ce nombre est pris comme chiffre de comparaison dans les tableaux d'analyse statistique des résultats de nos essais de radioprotection (Tableau 6 exclusivement).

RESULTATS

A. Sensibilité des Poussins de Race Rhode Island aux Rayons-X

Une dose de 750 r, 100 pour cent létale au 15me jour chez le jeune rat du même âge, n'entraîne chez le poussin qu'une mortalité très faible, toujours tardive et inconstante (Figs. 1 et 2).

Nous n'observons aucun décès après administration d'une dose de 500 r. A partir de 1000 r, les courbes de survie montrent de façon plus ou moins nette deux phases de mortalité: une *phase précoce* qui dure 48 heures, *une phase tardive* du 3me au 30me jour.

La mortalité au 30me jour s'accroît en

fonction de la dose totale administrée; elle atteint presque les 100 pour cent après 2000 r, que le débit atteigne 50 ou 100 r/min.

La mortalité précoce, plus élevée avec le

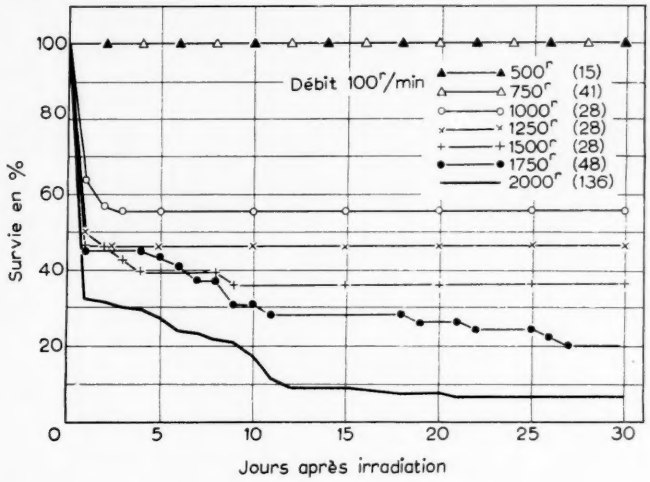

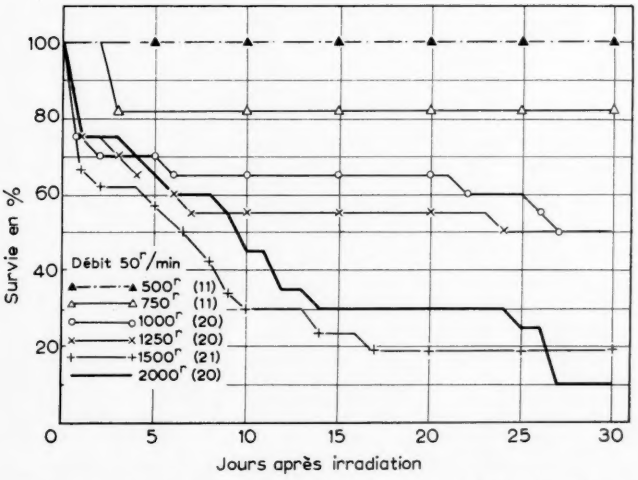

FIGS. 1, 2. Survie des poussins de race Rhode Island, irradiés avec des rayons-X, en fonction de la dose totale et de l'intensité (débit) utilisées.

débit de 100 r/min, augmente en fonction de la dose totale administrée. Si le débit est de 50 r/min, elle est relativement constante dans tous les groupes, tandis que la mortalité tardive s'accroît avec la durée de l'irradiation.

Nous n'avons pas constaté de variation dans la radiosensibilité en fonction du poids, du sexe ou de la saison; nos expériences ont été faites aussi bien en hiver qu'en été.

La gravité des signes cliniques et la précocité des décès atteignent leur maximum chez les poussins irradiés avec de fortes doses et l'intensité la plus élevée (100 r/min). La majorité des décès s'observe alors de 1 à 5 heures après l'irradiation; les décès deviennent rares après la douzième heure.

Le comportement des poussins est normal après une dose de 500 r. La symptomatologie,

discrète après 750 r, devient plus sévère au fur et à mesure que la dose totale administrée s'accroît. Les poussins exposés à une dose de 2000 r sous un débit de 100 r/min présentent, 45 à 60 minutes après l'irradiation, des troubles traduisant un état de collapsus circulatoire profond: adynamie, dyspnée, cyanose, tachycardie, réduction du sang circulant, hémoconcentration,* hypothermie. La mort de l'animal s'accompagne de convulsions généralisées, 15 à 30 minutes après l'apparition des premiers symptômes.

Le lendemain de l'irradiation, les animaux survivants restent prostrés, anorexiques, le plumage terne et hérissé, les ailes pendantes. Des lésions oedémateuses et hémorragiques apparaissent fréquemment à la face antérieure des pattes, plus rarement au niveau de l'extrémité céphalique (conjonctives, naissance du bec et muqueuse buccale). Les hémorragies sont très apparentes si le débit est de 100 r/min.

L'autopsie révèle des lésions vasculaires (congestion mésentérique, oedème, hémorragies viscérales et cutanées diffuses), des foyers de nécrose dans divers organes (tubes contournés et droits des reins, épithélium bronchique, cellules hépatiques et des canalicules biliaires, muqueuse glandulaire des différents segments intestinaux). Les uretères sont bourrés d'urate et, parfois, on constate la présence de sérosité jaunâtre dans la cavité péritonéale et le péricarde.

Les jours suivants, les animaux sont cachectiques. Les muqueuses et les organes sont pâles. Les lésions purpuriques des pattes, des muqueuses buccale et intestinale s'ulcèrent, les poumons présentent des foyers d'hépatisation, le volume de la rate diminue. Des formations arrondies, de volume variable, d'un blanc mastic, non enkystées, s'observent au niveau du foie, des poumons et du muscle cardiaque. L'examen histologique d'un de ces nodules hépatiques révèle la présence d'un gros foyer nécrotique, non systématisé, avec atteinte profonde des canalicules biliaires. Des dépôts d'urate peuvent s'observer au niveau du péricarde, du péritoine, et s'accumuler dans les uretères; ces manifestations indiquent habituellement, chez l'oiseau, l'existence d'une néphrite subaiguë. Nous avons aussi relevé quelques cas d'ascite, peu abondante, avec coloration légèrement ictérique du péritoine, des sacs aériques, des intestins et des reins. Jamais, nous ne constatons l'existence d'un syndrome hémorragipare tardif analogue à celui que présentent les mammifères irradiés.

B. Effet des Radioprotecteurs actifs chez les Mammifères

De nombreuses substances appartenant à des familles chimiques, qui n'ont à première vue aucun lien de parenté, protègent la souris et le rat contre les effets létaux des rayons-X. Leur action est considérée comme générale, puisqu'elle s'exerce aussi bien sur des organismes et des tissus vivants que sur des systèmes physicochimiques.[1]

Nous avons utilisé les meilleurs parmi les radioprotecteurs chimiques actifs chez les mammifères.[1] Ils sont dilués extemporanément et injectés 1 à 5 minutes avant l'irradiation (2000 r, 100 r/min) aux doses indiquées dans les Tableaux 1 et 2.

1. Substances soufrées: cystéamine et cystamine (Labaz), cystéine (Hoffman–La Roche)

La cystéamine-base (10 mg/100 g) neutralisée entraîne, chez le poussin normal, l'apparition d'adynamie et d'un peu de cyanose autour du bec sans autre manifestation respiratoire. Cette symptomatologie est plus accentuée après l'injection de bichlorhydrate de cystamine à quantité de soufre équivalente (14,6 mg/100 g). Trente pour cent des poussins décèdent. Le chlorhydrate de cystéine (30,6 mg/100 g) n'entraîne aucune manifestation toxique.

Comme le NaCl à 0,9%, les cystéamine, cystamine et cystéine sont dénuées de pouvoir protecteur (Tableau 1). Les manifestations pathologiques qu'entraîne l'irradiation chez les animaux traités, sont graves et

* A ce moment, on ne retire par ponction intracardiaque qu'un très petit volume de sang (0,2 à 0,5 ml) dont la teneur en éléments cellulaires est fortement augmentée (le volume plasmatique est réduit au 1/3 du volume sanguin total).

VOL. 4 1958/5

précoces; les décès surviennent plus tôt. La cystamine provoque la mort de tous les animaux injectés dans les 12 heures qui suivent l'irradiation. Les lésions anatomo-pathologiques sont semblables à celles des témoins irradiés.

mg/100 g. La récupération est parfaite dans tous les cas.

Le diéthyldithiocarbamate de sodium possède un pouvoir protecteur certain qui varie d'après la quantité injectée (Fig. 3). Administre-t-on 30 mg/100 g, le nombre des

TABLEAU 2. Mortalité des poussins irradiés avec 2000 r de R.X. (200 kV, 100 r/min) après injection intrapéritonéale de doses variables de diéthyldithiocarbamate de Na avant l'irradiation

Doses de diéthyl-dithiocarbamate (mg/100 g)	Nombre de poussins irradiés	Effet létal précoce		Effet létal tardif	
		Nombre de décès	*P*	Nombre de décès	*P*
Témoins non injectés	136	93		34	
20	20	14	$0{,}80 < P < 0{,}90$ augm.	3	$0{,}10 < P < 0{,}20$ dim.
30	30	13	$P < 0{,}01$* dim.	4	$P < 0{,}01$* dim.
40	30	18	$0{,}30 < P < 0{,}50$ dim.	6	$0{,}02 < P < 0{,}05$* dim.
60	30	25	$0{,}10 < P < 0{,}20$ augm.	3	$0{,}30 < P < 0{,}50$ dim.

* Ces valeurs sont statistiquement significatives ($P < 0{,}05$).

2. Tryptamine (Hoffman–La Roche)

Les manifestations toxiques (dyspnée, polypnée, prostration, défécation) sont faibles après l'injection de 3,5 mg/100 g; une dose de 9,5 mg/100 g entraîne le décès de 20 pour cent des poussins normaux. A l'autopsie, dilatation de l'oreillette droite et congestion mésentérique.

Quelle que soit la dose injectée, la tryptamine ne modifie pas le nombre des décès précoces, ni la symptomatologie qui suit l'irradiation. L'effet protecteur de 3,5 mg/100 g est très faible, mais statistiquement significatif si l'on considère la mortalité tardive, après 30 jours (Tableau 1). Une dose de 9,5 mg/100 g aggrave la symptomatologie présentée par le poussin irradié.

3. Agents de chélation

(*a*) *Diéthyldithiocarbamate de sodium (Merck)*. L'injection de 30 à 40 mg/100 g entraîne une polypnée intense et de la cyanose durant 1 à 2 heures. Les manifestations sont plus marquées et plus durables à la dose de 60 décès post-irradiation (précoces et tardifs) est réduit de manière significative. Avec 40 mg/100 g, l'effet radioprotecteur n'est significatif que pour la phase tardive (Tableau 2). L'injection de 60 mg/100 g aggrave l'effet létal précoce des rayons-X.

(*b*) *Acide ethylènediaminotétraacétique (Titriplex III Merck)*. Cette substance ne paraît pas toxique aux doses de 17 ou 34 mg/100 g chez le poussin normal; elle est dépourvue de propriété radioprotectrice (Tableau 1).

4. Cyanure de sodium (Merck)

Trente secondes après l'injection de cyanure de sodium, les poussins montrent des symptômes d'intoxication profonde. Tous sont adynamiques, certains d'entre eux respirent avec peine, d'autres présentent des épisodes de convulsions généralisées et meurent 2 à 3 minutes après l'injection. Les poussins survivant à l'intoxication aiguë par le cyanure ont par la suite un comportement tout à fait normal.

Le Tableau 1 montre que le cyanure n'est

pas radioprotecteur. Son effet toxique propre s'ajoute à l'action létale des rayons-X.

C. Action radioprotectrice des Histamino-Liberateurs et du Neoantergan chez le Poussin

Chez le mammifère, les rayons-X provoquent une libération importante de l'histamine tissulaire.[1,5,9,15,18] Celle-ci ne jouerait cependant qu'un rôle très secondaire dans le déterminisme du mal des rayons chez le mammifère.[1,18]

Lea[16] a supposé que chez le poussin irradié avec un débit élevé, certaines substances toxiques seraient produites, et que leur accumulation déterminerait la mort précoce de l'oiseau.

Nous avons supposé que l'une de ces substances pourrait bien être l'histamine; cette hypothèse est compatible avec l'état de collapsus cardio-vasculaire profond observé dans les heures qui suivent l'exposition aux rayons-X.[27]

1. Libération de l'histamine tissulaire par les rayons-X

Des lambeaux de peau de la région thoraco-abdominale, les poumons et un segment de la partie haute du jéjunum sont prélevés, chez des poussins normaux ou traités par histamino-libérateurs, après saignée de l'animal à la carotide et, chez des poussins irradiés, immédiatement après le décès. Leur histamine est extraite selon la méthode de Douglas, Feldberg, Paton et Schachter.[10] La teneur en histamine est estimée en comparant, chez le chat atropiné (1 mg/kg), l'intensité de la dépression artérielle qu'ils provoquent, aux effets tensionnels de quantités connues d'histamine. La nature histaminique de la substance hypotensive des extraits est confirmée par la suppression de la dépression tensionnelle par un antihistaminique de synthèse (Phénergan: 5 mg/kg).

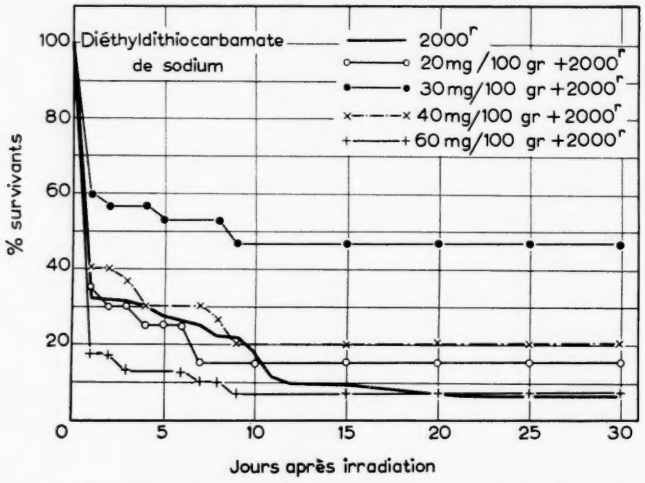

Fig. 3. Action du diéthyldithiocarbamate de sodium injecté chez le poussin irradié avant une dose de 2000 r. Effet variable suivant la quantité administrée.

Nous appliquons la loi de Bernoulli pour apprécier les différences entre les teneurs moyennes en histamine endogène des tissus prélevés chez des poussins normaux, irradiés ou traités par des substances histamino-libératrices:

$$\theta = M_t - M/\sqrt{(\sigma_{1t}^2 + \sigma_1^2)}$$

où M_t représente la moyenne arithmétique obtenue chez les témoins et σ_{1_t}, le σ_1 correspondant $\sigma_1 = \sigma/\sqrt{n}$. M et σ_1 représentent les valeurs correspondantes obtenues après traitements. Toute valeur de θ supérieure à 1,7 (probabilité d'arrivée supérieure à 0,9837) est statistiquement significative.

VOL 4 1958/

Ainsi qu'on peut le constater dans le Tableau 3, les rayons-X provoquent une déplétion des tissus en leur histamine constitutive. Celle-ci, faible au niveau de la peau, est nettement significative au niveau des poumons et très importante au niveau de l'intestin grêle.

2. Action des libérateurs de l'histamine tissulaire

(a) *Peptone* (*U.S.P. Lewis*). La peptone en solution à 20 pour cent dans du NaCl à 0,45 pour cent est administrée biquotidiennement durant 4 jours à raison de 1 ml à chaque injection; la dernière a lieu 12 heures avant l'irradiation. La même quantité est aussi injectée à d'autres poussins 5 min avant ou 5 min après celle-ci.

Les poussins traités par peptone présentent de la prostration durant quelques heures; elle s'intensifie au fur et à mesure que les injections se répètent. La libération d'histamine n'est importante qu'au niveau de l'intestin (Tableau 4).

Les poussins injectés de peptone sont en apparence normaux lorsqu'ils sont irradiés. Le Tableau 5 montre que seuls les effets précoces des rayons-X sont diminués après injection répétées de peptone. Une injection unique, immédiatement avant ou après l'irradiation, accroît l'intensité des manifestations pathologiques et 90 pour cent des poussins meurent au cours des 12 premières heures.

(b) *48/80* (*Wellcome*). L'injection de 1 mg de 48/80 dans 1 ml de NaCl 0,9% entraîne, 10 minutes plus tard, de la prostration et de la dyspnée, habituellement sans gravité. L'intestin est le seul organe dont la teneur en histamine est diminuée (Tableau 4).

Si cette injection précède de 12 heures l'irradiation, on n'observe qu'une réduction de la mortalité précoce (Tableau 5).

3. Action des antihistaminiques de synthèse

Les antihistaminiques de synthèse, Néoantergan (Mépyramine Spécia), Phénergan (Prométazine Spécia), Théphorine (Roche), dilués dans du NaCl 0,9%, déterminent des

TABLEAU 3. Teneur en histamine* (calculée en μg de bichlorhydrate par gramme de tissu frais) chez des poussins morts 1 à 5 heures après une irradiation avec 2000 r de R.X. (200 kV, 100 r/min)

Organes	Témoins			Après irradiation			θ de la différence
	Nombre	Moyenne	σ	Nombre	Moyenne	σ	
Peau	21	8,19	2,1	17	6,4	1,73	1,51
Poumon	21	22,33	5,65	17	11,24	2,73	7,46
Intestin	21	117,08	23,3	17	54,07	6,87	13,03

* Pour obtenir les teneurs en histamine-base, il suffit de multiplier les chiffres par le facteur 0,606 $= \frac{\text{Hist.-Base}}{\text{Hist.(2 HCl)}}$

TABLEAU 4. Teneur en histamine (calculée en μg de bichlorhydrate par gramme de tissu frais) de certains organes chez des poussins traités par des libérateurs d'histamine

Organes	Témoins			Peptone			θ de la différence	48/80			θ de la différence
	Nombre	Moyenne	σ	Nombre	Moyenne	σ		Nombre	Moyenne	σ	
Peau	21	8,19	2,1	18	8,5	2,87	0,21	10	10,53	3,73	1,18
Poumon	21	22,33	5,65	18	18,34	6,29	1,49	10	25,70	2,91	1,74
Intestin	21	117,08	23,3	9	63,33*	10,02	8,06	10	84,45*	3,19	3,98

* Ces valeurs sont seules statistiquement significatives.

TABLEAU 5. Action de substances histamino-libératrices et d'antihistaminiques de synthèse administrés chez le poussin avant ou après irradiation avec 2000 r de R.X. (200 kV, 100 r/min)

Lots et traitements	Nombre de poussins irradiés	Effet létal précoce		Effet létal tardif	
		Nombre de décès	P	Nombre de décès	P
Témoins non injectés	136	93		34	
Peptone: 200 (*mg*)					
inj. répétées avant R.X.	24	9	$P < 0{,}01$* dim.	9	$0{,}1 < P < 0{,}2$ dim.
inj. 5 min avant R.X.	20	18	$0{,}02 < P < 0{,}05$* augm.	2	$0{,}3 < P < 0{,}5$ augm.
inj. 5 min après R.X.	20	18	$0{,}02 < P < 0{,}05$* augm.	2	$0{,}3 < P < 0{,}5$ augm.
48/80: 1 (mg)					
inj. 12 h avant R.X.	25	11	$0{,}01 < P < 0{,}02$* dim.	13	$0{,}3 < P < 0{,}5$ augm.
Néoantergan: 2,5 (*mg*/100 *g*)					
inj. 5 min avant R.X.	49	25	$0{,}02 < P < 0{,}05$* dim.	13	$0{,}02 < P < 0{,}05$* dim.
inj. 30 min après R.X.	20	16	$0{,}2 < P < 0{,}3$ augm.	4	$0{,}2 < P < 0{,}3$ augm.
Théphorine: 2,5 (*mg*/100 *g*)					
inj. 5 min avant R.X.	30	24	$0{,}2 < P < 0{,}3$ augm.	3	$0{,}1 < P < 0{,}2$ dim.
Phénergan: 2,5 (*mg*/100 *g*)					
inj. 5 min avant R.X.	20	15	$0{,}5 < P < 0{,}7$ augm.	4	$0{,}95 < P < 0{,}98$ augm.

* Ces valeurs sont statistiquement significatives.

symptômes d'excitation légère s'ils sont injectés à la dose de 2,5 mg/100 g. Seul, le Phénergan à la dose de 5 mg/100 g est bien toléré.

Administrés immédiatement avant l'irradiation, à la dose de 2,5 mg, le Phénergan et la Théphorine n'exercent aucune action protectrice. Le Néoantergan réduit faiblement, mais de façon statistiquement significative, le nombre des décès survenant au cours des deux phases de létalité (Tableau 5). Injecté à la même dose 1/2 heure après l'irradiation, le Néoantergan devient inefficace.

En général, les antihistaminiques de synthèse raccourcissent la phase d'adynamie profonde qui précède le décès de l'animal irradié; les lésions cutanées, hémorragiques et oedémateuses, sont moins importantes au lendemain de l'irradiation. Cependant, l'examen anatomo-pathologique des poussins morts pendant les premières heures révèle des lésions viscérales identiques à celles des poussins non traités.

4. Action de l'histamine (bichlorhydrate Hoffman–La Roche)

L'injection de 1 mg/100 g d'histamine dans du NaCl 0,9% est peu toxique chez le poussin normal. Administrée 1 à 5 minutes avant l'irradiation, elle ajoute son action dépressive à celle des rayons-X, sans modifier toutefois l'importance de la mortalité.

Par contre, si l'injection est faite 5 à 10 minutes après l'irradiation, les décès sont plus précoces et plus nombreux (80 pour cent au cours des trois premières heures).

D. Rôle d'une éventuelle Hyperkaliémie chez le Poussin irradié

La mort précoce du poussin irradié avec un débit élevé présente de nettes analogies

avec celle du mammifère irradié avec des doses de rayons-X de l'ordre de 10.000 à 25.000 r. Le mammifère meurt alors en hyperkaliémie.[1]

Certains coqs adultes, irradiés dans des conditions expérimentales identiques (2000 r, débit: 100 r/min), montrent un accroissement du potassium plasmatique (de 137 mg/l à 280 mg/l) contemporain de l'apparition de l'hypotension et de l'hémoconcentration; la concentration du sodium plasmatique (3,76 g/l) et celle du calcium sérique (110 mg/l) étant par ailleurs inchangées.

Nous rechercherons:

(1) Si l'injection d'une quantité de KCl, calculée de façon à augmenter théoriquement de 8 à 10 fois environ la teneur en ions K^+ du plasma sanguin du poussin[29] (en supposant totale la résorption du K^+ injecté et l'excrétion rénale négligeable), accroît la mortalité précoce du poussin irradié;

(2) Si le glucono-galacto-gluconate de Ca et le NaCl corrigent les troubles dus à l'irradiation.

Les injections de quantités équimolé culaires de KCl (21 mg), de NaCl (16,5 mg) et de glucono-galacto-gluconate de Ca (167 mg) ne sont pas toxiques pour le poussin normal.

Pratiquée 5 minutes après l'irradiation, l'injection entraîne des effets variables suivant la substance utilisée. Le KCl est sans action, le NaCl et le glucono-galacto-gluconate de Ca aggravent les manifestations pathologiques et accroissent le nombre de décès.

E. Influence de l'ACTH et de certaines Hormones Cortico-surrénaliennes sur la Résistance à l'Irradiation

Les radiations ionisantes sont, chez le mammifère, des agents de stress. Elles augmentent la teneur de l'hypophyse en hormone corticotrope,[1] celle du sang en 17-hydroxystéroïdes,[12,30] tandis que le cortex surrénalien s'appauvrit en acide ascorbique et en cholestérol,[1] que le nombre des granulocytes éosinophiles diminue dans le sang circulant[3] et que l'excrétion urinaire des corticoïdes s'accroît.[1]

Chez l'oiseau, les réactions métaboliques qui accompagnent le stress n'ont pas encore fait l'objet d'une étude systématique. La plupart des critères de stimulation cortico-surrénalienne, applicables au mammifère, ne sont pas valables chez le poulet dont, en outre, les réactions à la surrénalectomie ne sont pas strictement comparables à celles du mammifère.[29]

Pour expliquer la pathogénie de la mort précoce du poussin irradié, STEARNER et ses collaborateurs[7,23] envisagent la possibilité d'un déficit des fonctions hypophyso-surrénaliennes. L'agression intense et brutale que constitue l'irradiation, la libération accrue de métabolites cellulaires peuvent être autant de facteurs de stimulation, puis d'épuisement du système neuro-endocrinien. De plus, l'hypothèse d'une déficience surrénalienne aiguë expliquerait les manifestations pathologiques observées lors du décès (adynamie, convulsions, dyspnée, uricémie élevée,[23] hyperkaliémie du coq adulte). Nous avons soumis cette hypothèse à certains contrôles expérimentaux: stimulation du cortex surrénalien par l'ACTH préalablement à l'irradiation, et traitements hormonaux substitutifs.[1]

L'évolution pondérale des poussins n'est pas modifiée par l'injection d'hormone corticotrope hypophysaire (ACTH Organon), pratiquée à raison de deux injections intrapéritonéales quotidiennes soit de 0,2 unité pendant les 15 jours, soit de 2 unités pendant les 7 jours qui précèdent l'irradiation.

Les animaux ainsi traités ne présentent, après exposition aux rayons-X, aucune modification de leur mortalité (précoce ou tardive). Une seule injection de 2 unités d'ACTH, 2 ou 12 heures avant l'irradiation, reste, elle aussi, sans effet sur la létalité.

Les thérapeutiques substitutives par désoxycorticostérone (DOCA sous forme de Percortène Ciba en suspension microcristalline), seule ou en association avec la cortisone (Ciba, en suspension microcristalline), ont été mises en train 3 à 4 heures avant l'irradiation. Les hormones, injectées de 12 en 12 heures dans les muscles pectoraux à raison de 2 × 500 mg de DOCA ou 2 × (250 mg de DOCA + 250 mg de Cortisone) le jour de l'irradiation, sont sans action sur la

VOL. 4 58/59

mortalité précoce. La poursuite du traitement à doses décroissantes durant 7 jours

1er jour: 2 × 500 mg de DOCA ou 2 × (250 mg de DOCA + 250 mg de Cortisone);

2me jour: 2 × 250 mg de DOCA ou 2 × (125 mg de DOCA + 125 mg de Cortisone);

3me jour: 2 × 100 mg de DOCA ou 2 × (50 mg de DOCA + 50 mg de Cortisone);

4me jour: 2 × 50 mg de DOCA ou 2 × (25 mg de DOCA + 25 mg de Cortisone);

5me, 6me et 7me jours: 50 mg de DOCA ou 25 mg de DOCA + 25 mg de Cortisone

ne réduit pas la proportion des décès qui caractérise la phase secondaire.

bactériens endo- et exogènes.[1] A ces lésions s'ajoutent, chez l'oiseau, les conséquences autotoxiques dues au passage à la chronicité de la néphrite aiguë installée au cours des premières heures qui suivent l'exposition aux rayons-X.

Les antibiotiques ont donné chez les mammifères irradiés des résultats variables avec l'antibiotique utilisé et l'animal traité.[1,20]

Nous avons traité le poussin à l'aide de la pénicilline, du chloramphénicol et de la streptomycine, celle-ci à petites doses en raison de sa néphrotoxicité. Les traitements débutent 12 heures après l'irradiation. Ils ont été administrés chez des poussins irradiés, traités au préalable par diéthyldithiocarbamate de sodium ou peptone. Les posologies sont indiquées dans le Tableau 6. Alors que la pénicilline (Pénaqua UCB) et

TABLEAU 6. Inefficacité et toxicité de certains antibiotiques administrés au cours de la phase de létalité tardive qui suit une irradiation avec 2000 r de R.X. (200 kV, 100 r/min)

Lots et traitements	Nombre d'animaux avant antibiotique	Létalité tardive	
		Nombre de décès au cours du traitement	*P*
Peptone + 2000 r			
Témoins	15	9	
20,000 U. Pénicilline	15	8	$0{,}7 < P < 0{,}8$
Diéthyldithiocarbamate de Na + 2000 r			
Témoins	17	4	
20,000 U. Pénicilline + 2 mg Streptomycine	11	9	$P < 0{,}01$*
Chloramphénicol (2 mg) + sol. à 0,2‰ *ad libitum per os*	13	3	$0{,}95 < P < 0{,}98$

* Valeur statistiquement significative.

F. Action de certains Antibiotiques sur la Létalité Tardive

Les causes de la mort du poussin irradié au cours de la phase de létalité *tardive* sont probablement identiques à celles que l'on décrit chez les mammifères: même syndrome intestinal, lésions hématopoïétiques identiques, sensibilité analogue aux agents

la streptomycine (Squibb) sont injectées biquotidiennement durant 15 jours dans les muscles pectoraux, le chloramphénicol (Erba) est administré *per os* en deux prises quotidiennes. L'eau de boisson* contient du chloramphénicol et un complexe vitaminique B; ce traitement est poursuivi durant 30 jours.

* *Composition de l'eau de boisson:* Chloramphénicol: 200 mg; Aneurine: 25 mg; Lactoflavine: 10 mg; Nicotinamide: 100 mg; Adermine: 10 mg; Pantothénate de Ca: 25 mg; Eau bidistillée: p.f. 1000 ml. Chaque poussin reçoit de cette manière environ 8 à 10 mg de chloramphénicol par 24 heures.

VOL 4 1958/

Les traitements par pénicilline et chloramphénicol sont dépourvus d'action sur le syndrome tardif post-irradiation. L'association streptomycine–pénicilline entraîne un nombre important de décès au cours d'une phase de convulsions toniques et cloniques qui suit de quelques minutes la fin de l'injection.

DISCUSSION

(1) Deux phases caractérisent la mortalité des poussins Rhode Island irradiés sous une intensité élevée (50 à 100 r/min) et recevant des doses de rayons-X comprises entre 1000 et 2000 r; l'une est *précoce* et caractérisée par la défaillance circulatoire et des lésions rénales, l'autre phase est *tardive*. Durant celle-ci, le comportement des poussins irradiés est analogue à celui des mammifères soumis aux mêmes agents physiques.

La mesure de la radiosensibilité du poussin de race Rhode Island nous permet d'établir:

(a) que la dose 100 pour cent létale en 30 jours est approximativement de 2000 r, pour un débit soit de 50 r, soit de 100 r/min;

(b) que le débit utilisé lors de l'irradiation de l'oiseau possède une importance capitale.

Chez le poussin Rhode Island, la D.L.100 est double de celle qu'utilisent les expérimentateurs américains pour tuer 100 pour cent des poussins de race Leghorn blanche, âgés de 2 semaines.[21] De telles variations de sensibilité selon la race existent aussi chez la souris.[1]

Dans nos expériences, l'intensité du rayonnement conditionne étroitement le décours de la mortalité et l'intensité des lésions purpuriques cutanées. Si le débit est de 100 r/min, la létalité précoce s'accroît lorsque la durée de l'irradiation augmente; s'il est de 50 r/min, la mortalité tardive varie de la même manière, tandis que la mortalité précoce reste constante dans tous les groupes.

Nous sommes la première à signaler l'existence de lésions hémorragiques précoces, localisées aux pattes et à l'extrémité céphalique. Ces hémorragies sont en effet fort discrètes après une irradiation débitée à 50 r/min, selon la technique utilisée par les auteurs américains.[14,21]

(2) Nous avons démontré que la plupart des substances radioprotectrices, chez la souris et le rat, sont dépourvues d'efficacité chez le poussin irradié sous une *intensité élevée*.

La toxicité, parfois importante, de ces substances, la potentiation de cet effet toxique par l'irradiation, et surtout les réactions très particulières de l'oiseau aux radiations ionisantes, pourraient sans doute expliquer nos échecs. Oftedal[19] a aussi démontré que la cystamine et les autres protecteurs à fonction soufrée sont dépourvus d'action protectrice chez l'embryon de poulet irradié *in toto*. Par contre, Wolff et Kirrmann[31] ont observé que la cystéamine atténue considérablement les effets tératogènes (cyclopie, anophtalmie) qui résultent, chez l'embryon de poulet, d'une irradiation localisée à certains segments céphaliques. L'âge de nos animaux d'expérience n'explique pas l'absence de radioprotection, puisque nous avons constaté que la cystamine, particulièrement toxique chez le poussin irradié, protège des ratons de 21 jours contre les effets létaux des rayons-X.

Seuls parmi les substances étudiées, la tryptamine et le diéthyldithiocarbamate de sodium sont protecteurs chez le poussin, mais cette protection est faible comparativement à celle que l'on observe chez la souris. Il est peu vraisemblable que l'hypoxie que ces corps semblent déterminer puisse expliquer leur pouvoir protecteur. En effet, la cystamine,[2] la cystéine[1] et le cyanure, tous trois agents d'hypoxie, sont dépourvus de propriété protectrice.

L'action radioprotectrice de la cystéamine, du cyanure et des autres protecteurs habituels, jusqu'à présent considérée comme généralé[1] est ici mise en défaut. Rappelons que Benson *et al.*[6] ont montré que le dérivé isothiouronium de l'éthylamine utilisé par Hollaender[13] pour protéger efficacement la souris, est totalement dépourvu d'action chez le chien exposé aux rayons-X.

(3) Les histamino-libérateurs, incapables de réduire la létalité du rat irradié,[4] préservent un certain nombre de poussins

contre la mort précoce sans modifier les effets tardifs des rayons-X.

La déplétion de certains organes, notamment l'intestin et les poumons, en leur histamine constitutive est très importante chez le poussin irradié. L'injection d'histamine après l'irradiation aggrave les manifestations pathologiques précoces. Il semble donc que la libération de l'histamine tissulaire qu'entraînent les rayons-X, puisse jouer un rôle dans la mort précoce du poussin, soit en induisant, soit en aggravant l'état de collapsus circulatoire observé dans les heures qui suivent l'irradiation.

Cependant, les antihistaminiques de synthèse, le Néoantergan excepté, sont incapables de réduire la mortalité du poussin irradié. De plus, ce dernier perd son action protectrice lorsqu'il est injecté à titre curatif.

Il faut donc admettre que d'autres substances libérées en même temps que l'histamine manifestent aussi leurs effets toxiques chez le poussin irradié, témoin l'hyperkaliémie qui apparaît chez le coq exposé aux rayons-X. Le pouvoir protecteur faible du Néoantergan, lorsqu'il est injecté avant l'irradiation, pourrait s'expliquer par son action sensibilisante à l'adrénaline[17,25] vraisemblablement libérée au cours du collapsus circulatoire qui suit l'irradiation.

(4) Nous n'avons pu confirmer le rôle éventuel de l'insuffisance cortico-surrénalienne aiguë dans la pathogénie du collapsus post-irradiation. Les injections répétées d'ACTH, avant l'exposition aux rayons-X, ne réduisent pas la mortalité des poussins irradiés. De plus, toutes les thérapeutiques substitutives par DOCA, seule ou en association avec de la cortisone, ont été vaines. D'ailleurs, selon Bloom,[8] Jacquez *et al.*[14] les surrénales de poussin ne subissent que peu de modifications histologiques lors de l'irradiation.

(5) Les antibiotiques ne modifient pas le nombre des décès qui surviennent tardivement. L'état cachectique des poussins survivant 48 heures après une forte irradiation ne semble pas dépendre de processus toxi-infectieux surajoutés.

Acknowledgements—Nous remercions vivement le Prof. Bacq et le Dr. Lecomte qui nous ont guidée dans ce travail, ainsi que les Prof. Liegeois, Granville et le Dr. Bienfait de l'Ecole de Médecine Vétérinaire de Cureghem.

Le Prof. Fredericq nous a accordé une généreuse hospitalité dans ses laboratoires.

Nous remercions le Dr. Herve qui, dans la laboratoire de Radiothérapie du Prof. Desaive, a procédé aux irradiations.

BIBLIOGRAPHIE

1. Bacq Z. M. et Alexander P., *Principes de Radiobiologie, Sciences et Lettres, Liège;* Masson, Paris (1955).
2. Bacq Z. M., Cuypers Y., Evrard E. et Soetens R., *Méd. Aéro.* **11,** 87 (1956).
3. Beaumariage M. L., *Arch. Int. Physiol. Biochem.* **63,** 132 (1955).
4. Beaumariage M. L. et Lecomte J., *C. R. Soc. Biol.* Paris, **150,** 1802 (1956).
5. Beaumariage M. L. et Lecomte J., *Rev. Belg. Pathol.* Bruxelles, **26,** 123 (1957).
6. Benson R. E., Michaelson S. et Howland J. W., *UR,* 452. Univ. Rochester, Atom. Energy Project (1956).
7. Bernstein E. K., Stearner S. P. et Brues A. M., *Amer. J. Physiol.* **186,** 543 (1956).
8. Bloom W. M. P., *Histopathology of Irradiation from External and Internal Sources* p. 736. McGraw-Hill Book Company, New York (1948).
9. Bryant T. H. E., Eisen V. D., Ellis R. E. et Wilson C. W. M., *J. Physiol.* **130,** 33 (1955).
10. Douglas W. W., Feldberg W., Paton W. D. M. et Schachter M., *J. Physiol.* **115,** 163 (1951).
11. Fisher R. A., *Statistical Methods for Research Workers* pp. 86–113. Oliver and Boyd, Edinburgh (1948).
12. French A. B., Migeon C. J., Samuels L. T. et Browers J. Z., *Amer. J. Physiol.* **182,** 469 (1955).
13. Hollaender A., *Science* **121,** 624 (1955).
14. Jacquez J. A. et Karnofsky D. A., *Amer. J. Roentgenol.* **64,** 289 (1950).
15. Koslowski L., Poppe H. et Walther E., *Strahlentherapie* **97,** 266 (1955).
16. Lea D. E., *Amer. J. Roentgenol.* **45,** 605 (1941).
17. Lecomte J. et Fischer P., *Arch. Int. Pharmacodyn.* **91,** 79 (1952).
18. Leitch J. L., Debley V. G. et Haley T. J., *Amer. J. Physiol.* **187,** 307 (1956).

VOL.
4
1958/5

19. Oftedal P., *First Report from Norsk Hydro's Institute for Cancer Research* p. 17 (1954–1956).
20. Smith W. W., Marston R. Q., Gonshery L., Aderman I. M. et Ruth H. J., *Amer. J. Physiol.* **183,** 98 (1955).
21. Stearner S. P., *Amer. J. Roentgenol.* **65,** 265 (1951).
22. Stearner S. P. et Christian E. J., *Amer. J. Roentgenol.* **65,** 272 (1951).
23. Stearner S. P., Christian E. J. et Brues A. M., *Proc. Soc. Exp. Biol. Med.* **78,** 676 (1951).
24. Stearner S. P., Christian E. J. et Brues A. M., *Rad. Res.* **1,** 270 (1954).
25. Stearner S. P., Christian E. J. et Brues A. M., *Amer. J. Physiol.* **176,** 455 (1954).
26. Stearner S. P. et Christian E. J., *Argonne National Laboratory Report,* ANL–5518, part II, p. 171 (1956).
27. Stearner S. P., Brues A. M., Sanderson M. et Christian E. J., *Amer. J. Physiol.* **182,** 407 (1955).
28. Stearner S. P., Sanderson M., Christian E. J. et Brues A. M., *Amer. J. Physiol.* **184,** 134 (1956).
29. Sturkie P. D., *Avian Physiology* pp. 25, 57, 308, 400. Comstock Publishing Associates, Ithaca, New York (1954).
30. Van Cauwenberge H., Fischer P., Vliers M. et Bacq Z. M., *Arch. Int. Physiol. Biochim* **65,** 143 (1957).
31. Wolff E. et Kirrmann J. M., *C. R. Soc. Biol.* Paris **148,** 1629 (1954).

OL.
4
8/59

International Journal of Applied Radiation and Isotopes, 1958, Vol. 4, pp. 84–88. Pergamon Press Ltd., London

Effect of Additives on the Radiation Induced Polymerization of *Iso*butene

R. WORRALL* and A. CHARLESBY†

(*Received* 20 *March* 1958)

The polymerization of certain monomers under the influence of high energy radiation is believed to proceed by an ionic mechanism. The yield is found to be greatly increased in the presence of fine powders of some metallic oxides, such as zinc oxide and silica. It is reduced by the presence of polyethylene powder, in which radicals are produced by radiation. Data on the effect of zinc oxide concentration, dose and radiation intensity are given. The increased yield is due to an increased initiation rate.

EFFET DES MATÉRIAUX ADDITIFS SUR LA RADIATION—LA POLYMÉRIZATION INDUITE DE L'ISOBUTÈNE

On croit que la polymérisation de certains monomères sous l'influence de la radiation à haute énergie a lieu par un mécanisme ionique. Le rendement se trouve fortement augmenté en la présence de certains oxydes métalliques, tels que l'oxyde de zinc et la silice, en forme de poudre fine. Il est diminué par le poly-éthylène en poudre, dans lequel des radicaux se produisent par la radiation. On présente des données sur l'effet de la concentration de l'oxyde de zinc, de la dose et de l'intensité de la radiation. L'augmentation du rendement vient d'une augementation du taux d'initiation de la réaction.

ДЕЙСТВИЕ ДОБАВОК НА РАДИАЦИОННО-ХИМИЧЕСКУЮ ПОЛИМЕРИЗАЦИЮ ИЗОБУТИЛЕНА

Считается, что полимеризация некоторых мономеров под действием излучения высокой энергии протекает по ионному механизму. Найдено, что в присутствии тонкоразмельченных порошков некоторых окислов металлов, например, окиси цинка или кремния, выход полимера значительно повышается. Понижение выхода наблюдается в присутствии полиэтиленового порошка, в котором под действием облучения образуются радикалы. Приводятся данные по влиянию концентрации окиси цинка, дозы и интенсивности облучения. Повышенный выход обуславливается увеличением скорости инициирования.

WIRKUNG VON BEIMENGUNGEN AUF DIE STRAHLUNGSINDUZIERTE POLYMERISATION VON ISOBUTAN.

Man nimmt an, dass die Polymerisation von bestimmten Monomeren unter dem Einfluss von hochenergetischer Strahlung über einen Ionenmechanismus vor sich geht. Es wurde gefunden, dass die Ausbeute bei Anwesenheit von feinem Pulver einiger Metalloxyde, wie z.B. Zinkoxyd oder Siliciumoxyd stark gesteigert wird. Die Ausbeute wird geringer bei Anwesenheit von Polyethlenpulver, in welchem durch Strahlung Radikale erzeugt werden. Zhalen für die Wirkung der Zinkoxydkonzentration, Dosis und Strahlungsintensität werden gegeben. Die gesteigerte Ausbeute hängt von einer vergrösserten Anfangsrate ab.

*Tube Investments Research Laboratories, Hinxton
†Royal Military College of Science, Shrivenham, Berkshire

VOL.
4
1958/5

INTRODUCTION

ALTHOUGH the primary effect of high energy radiation on organic systems is to produce ionization and excitation, published work on radiation-induced polymerization has shown that such reactions occur by a radical mechanism and are basically similar to reactions initiated by photochemical means. However, recent work in these laboratories has demonstrated that at low temperatures, radiation can also initiate polymerization reactions which are typical of an ionic mechanism. The polymerization of *iso*-butene[1] has been found to proceed rapidly at low temperatures with a high yield which increases as the temperature is lowered. Furthermore, the rate of reaction per unit radiation dose is substantially independent of dose-rate over a range of at least 5 decades from 10^3 to 10^8 rad/min showing that chain termination does not occur by bimolecular reaction.

Further work has shown that this polymerization reaction can show heterogeneous characteristics and that the rate of reaction can be considerably increased by the addition of many inorganic solids in the form of fine powders. This effect has also been observed with other monomers, but only the case of *iso*butene is reported here.

EXPERIMENTAL

Known weights of additives were introduced into glass tubes which were then sealed on to a high vacuum line. The additives were thoroughly de-gassed and pure de-gassed *iso*butene was distilled on to them. The tubes were sealed off under high vacuum.

Irradiations were carried out at −78·5°C (solid carbon dioxide–acetone) with Co^{60} γ-rays at a dose-rate of 930 rad/min or with pulses of 2 MeV electrons from a van de Graaff accelerator at an instantaneous dose-rate of ca. 10^8 rad/min. For the γ-ray work, dosimetry was based on the oxidation of ferrous sulphate, taking a G value of 15·5. For the electron irradiations, the doses were calculated from the output of the machine, allowing for back scatter and for absorption in the glass container. The effective beam penetration of 7 mm in material of unit density exceeded the wall thickness of the container and the depth of monomer irradiated.

After irradiation, the tubes were weighed and opened whilst frozen by liquid nitrogen. The unchanged *iso*butene was allowed to evaporate at room temperature and the contents of the tubes were dried to constant weight. From the weight of the empty tube, the weights of initial monomer and dry polymer were obtained.

Molecular weights were determined by viscometry in carbon tetrachloride solution, using a suspended level dilution viscometer at 30°C. Viscosity molecular weights (M_v) were calculated from the intrinsic viscosity ($[\eta]$) using the equation

$$[\eta] = kM_v^{\alpha}$$

where k and α have the values $2{\cdot}9 \times 10^{-4}$ and 0·68 respectively.[2]

RESULTS

The yield of polymer for a dose of 1 Mrad is shown in Tables 1 and 2, for both γ- (low intensity) and electron (high intensity) radiation, and for various concentrations of additive. The yield is expressed as a percentage of the *iso*butene, present in the mixture, which is converted to polymer. If the additive has no effect on the reaction, this figure should remain constant, while if all the energy absorbed by the mixture is transferred to the monomer which is then induced to polymerize, an increased yield should be observed, depending on the amount of additive present. The observed yields are however considerably greater than can be explained by this means; for example the addition of 25 per cent (by weight) of zinc oxide increases the yield by a factor of

TABLE 1. γ-irradiation of *iso*butene in the presence of solid additives
Radiation intensity 930 rad/min
Dose 1 Mrad
Temperature −78·5°C

Additive (% weight fraction)		Percent of *iso*butene converted	$M_v \times 10^{-3}$	*G* value (overall) for conversion (a)†	(b)‡	*G* value for initiation (maximum) (a)†	(b)‡
Nil	0	5·3	513	928	928	0·19	0·19
Calcium oxide	61·8	72·7	303	4750	12400	1·6	4·2
Magnesium oxide	47·9	40·1	469	3570	6850	0·8	1·5
Aerosil	1·9	12·9	607	2160	2200	0·32	0·33
	5·7	21·1	923	4290	4540	0·48	0·51
Sodium bicarbonate	57·3	21·6	662	1560	3650	0·24	0·56
Carbon black	32·4	4·8	456	551	815	0·13	0·19
Polyethylene powder	30·8	0·7	small	85	123	—	—
Zinc oxide*							

* See Table 2.
† (a) based on total energy absorbed in mixture.
‡ (b) based on energy absorbed directly in *iso*butene.

TABLE 2. Effect of additive concentration on polymerization of *iso*butene
Additive ZnO
Dose 1 Mrad
Temperature −78·5°C
2 MeV pulsed electron radiation; maximum intensity about 10^8 rad/min at 400 pulses/sec
1·3 MeV γ-radiation; uniform at 930 rad/min

Additive (% weight fraction)	Radiation	Percent of *iso*butene converted	$M_v \times 10^{-3}$	*G* value (overall) for conversion (a)*	(b)†	*G* value for initiation (maximum) (a)*	(b)†
0	Electron	4·9	541	830	830	0·16	0·16
14·4	Electron	20·6	538	3010	3510	0·56	0·65
23·1	Electron	43·2	402	5680	7400	1·5	1·9
28·1	Electron	45·9	399	5640	7830	1·5	2·1
36·2	Electron	53·8	342	5860	9170	1·8	2·8
45·7	Electron	59·9	342	5670	10,400	1·7	3·1
0	γ	5·3	513	928	928	0·19	0·19
13·5	γ	28·9	297	4270	4940	1·5	1·7
24·8	γ	55·4	404	7120	9460	1·8	2·4
41·0	γ	95·9	388	9600	16,300	2·6	4·4
53·0	γ	97·9	297	7930	16,900	2·8	6·0

* (a) based on total energy absorbed in mixture.
† (b) based on energy absorbed directly in *iso*butene.

VOL 4 1958/

ten. The G value for conversion represents the number of *iso*butene molecules polymerised, per 100 eV absorbed by the mixture, and equals the G value for initiation of the reaction, multiplied by the number average degree of polymerization u_1.

Measurements of the corresponding (viscosity) average molecular weights M_v are shown in the tables. Assuming that the molecular weight distribution is random, these values can be converted to number average degree of polymerization u_1.[3]

$$M_v = 1{\cdot}85\, M_n = 1{\cdot}85 \times 56{\cdot}1\, u_1$$
$$= 103{\cdot}5\, u_1$$

where 56·1 is the mol. wt. of the *iso*butene monomer. Then dividing the overall G value for the reaction by u_1, the G value for initiation based on the total energy absorbed has been derived.

This procedure is open to two serious objections. It assumes a random mol. wt. distribution, but it is known that the yield falls off with increase in dose, so that molecules formed later in the reaction will, on the average, be smaller, and the distribution will therefore be skew. Moreover radiation is known to result in main chain fracture (degradation).[3] A dose of 1 Mrad at −78·5°C degrades an infinite mol. wt. polymer to one whose M_v is about 550×10^3. In the polymer considered, the effective dose for degradation will vary from one molecule to another, depending on whether it was formed early on, or late in the reaction. As a result, the values of M_v quoted in Tables 1 and 2 are smaller than the viscosity average mol. wt. on formation: it is hoped to deduce the initial value in subsequent work. The G values for initiation quoted here are therefore maximum values.

Effect of additive concentration

The effect of the weight fraction of zinc oxide on the G value for overall conversion is shown in Fig. 1. Although the overall yield is increased, the differences in mol. wt. are small, and probably not significant. At zinc oxide weight fractions of up to 41 per cent, the initial mixture consists of a suspension of the additive, and a supernatant layer of *iso*butene, and the total yield may be expected to be the sum of reactions in the two phases. At 41 per cent the mixture forms a paste, and the maximum rate of reaction is observed. Beyond this concentration much of the energy absorbed in the oxide ceases to be effective, but this may be due to the almost complete polymerization of the *iso*butene when mixed with zinc oxide.

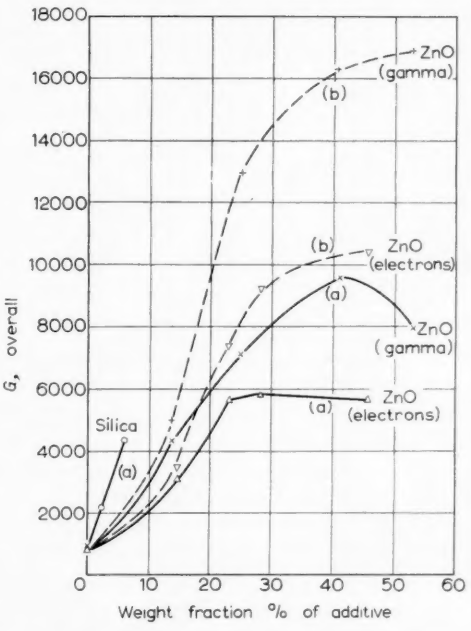

FIG. 1. Increase in polymerization rate of *iso*butene at −78·5°C due to presence of additives (a) G value based on energy absorbed in mixture (b) G value based on energy absorbed directly in monomer.

Powdered silica (Aerosil) and *iso*butene form a viscous system, even at low concentrations of silica (up to 6 per cent) and it is a much more efficient catalyst for the reaction than zinc oxide. Carbon black, which greatly increases the effect of radiation on rubber for example, has no effect. The reaction is virtually suppressed by polyethylene powder.

Effect of dose

The effect of radiation dose on a standard mixture containing 41 per cent of zinc oxide is shown in Table 3. The overall G values

TABLE 3. Effect of dose on polymerization in presence of zinc oxide (41%)
γ-radiation at 930 rad/min
Temperature −78·5°C

Dose (Mrad)	Percent of *iso*butene converted	*G* value (overall) for conversion	$M_v \times 10^{-3}$	*G* value for initation (maximum)
0·1	12·7	12,700	541	2·4
0·37	34·6	9430	390	2·5
0·54	59·2	11,100	404	2·9
0·80	86·6	10,800	407	2·8
1·00	95·9	9600	388	2·6

for the reaction are approximately independent of dose up to about one Mrad, although they do decrease at higher doses. This indicates that at the lower doses, the reaction is not seriously restricted by an inhibitor formed by radiation. Furthermore the values of M_v do not decrease rapidly with increasing dose in the same range, showing that radiation-induced degradation is not the major factor limiting the molecular dimensions, as it is at higher doses. The values given in Table 3 may therefore be taken as indicative of the polymerization reaction alone.

DISCUSSION

The experimental evidence summarized here shows that in the presence of an additive, the rate of polymerization per unit radiation dose of *iso*butene at −78·5°C can be increased tenfold or more. (Furthermore it is independent of radiation intensity over a very wide range.) The reaction is not due to an increase in radical formation, since polyethylene powder, which would be expected to provide such radicals, and form a graft polymer,[4] depresses the rate of the reaction.

The reaction is not due to a primary charge built up in the additive, since it occurs as readily with γ- as with electron radiation. It may however be due to static charges built up within the particles, or on their surface, following ionization.

An increased yield can be accounted for by an increased initiation, an increased propagation, or a reduced termination rate. The experiments at low doses (when radiation induced degradation is negligible) show that the average mol. wt. is not greatly affected by the presence of additive, so that the main effect is one of increased initiation. This conclusion may have to be modified if chain transfer is an important step in the reaction.

A number of suggested mechanisms for the effect of additives on yield may be advanced, including the trapping of the electrons emitted during ionization, the emission of electrons from the irradiated additive, or a surface polymerization. These will be discussed in a subsequent paper.

Acknowledgements—The authors of this communication wish to thank Mr. W. H. T. DAVISON and Dr. S. H. PINNER for stimulating and helpful discussions; they also thank the Chairman of Tube Investments Ltd. for permission to publish.

REFERENCES

1. DAVISON W. H. T., PINNER S. H. and WORRALL R., *Chem. & Ind. (Res.)* 1274 (1957).
2. FOX M. and FLORY P. J., *J. Phys. Chem.* **53,** 197 (1949).
3. ALEXANDER P., BLACK R. M. and CHARLESBY A., *Proc. Roy. Soc.* A**232,** 31 (1955).
4. CHARLESBY A. and PINNER S. H., *Industr. Plast. Mod.* (Dec. 1957).

VOL
4
1958/

International Journal of Applied Radiation and Isotopes, 1958, Vol. 4, pp. 89–95. Pergamon Press Ltd., London

A Survey of Chemical Dosimetric Systems*

JEROME WEISS
Health Physics Division, Brookhaven National Laboratory,
Upton, New York

(*Received* 17 *October* 1957)

This survey covers the literature published on chemical dosimetry for electrons, γ- and X-rays, during the past ten years. A brief discussion of ionization chamber measurements is given as well as the most recent values of W for various gases. The dosimeters listed include liquid, solid and gaseous systems with brief comments concerning each.

UNE ÉTUDE DES SYSTÈMES DE DOSIMÉTRIE CHIMIQUE

Ce résumé traite de la littérature sur la dosimétrie chimique pour les électrons, pour les rayons γ et X, qui a été publiée dans la dernière dizaine d'années. Y est donnée une brève discution des mesures à chambre d'ionisation, ainsi que les valeurs les plus récentes de W pour une variété de gaz. Les dosimètres nommés comprennent des systèmes liquides, solides et gazeux, chacun avec un bref commentaire.

ОБЗОР СИСТЕМ ХИМИЧЕСКОЙ ДОЗИМЕТРИИ

Данный обзор охватывает литературу по химической дозиметрии электронов, гамма и рентгеновских лучей, опубликованную за последние десять лет. Дается краткое описание измерений, проводимых в ионизационной камере, а также приводятся самые последние из полученных недавно значений W для различных газов. [Рассматриваются дозиметры для жидких, твердых и газовых систем, с краткими характеристиками каждой из них.

EIN UEBERBLICK ÜBER CHEMISCHE DOSIMETERMETHODEN

Die vorliegende zusammenfassende Arbeit bringt einen Ueberblick über die Veröffentlichungen der letzten 10 Jahre auf dem Gebiet der chemischen Dosimetrie für Elektronen, γ- und Röntgen-Strahlen. Sie enthält eine kurze Diskussion der Messungen mit Ionisationskammern, sowie die neuesten W-Werte für verschiedene Gase. Die Aufstellung enthält flussige, feste und gasförmige Dosimetersysteme mit kurzen Kommentaren zu der jeweiligen Methode.

VOL.
4
8/59

The study of radiation effects has now progressed to the point where scientists are becoming more and more concerned with quantitative measurements. As a consequence, the accurate measurement of radiation dose has become an important part of all radiation research. The measurement of dose has been a problem for many years, but many advances have been made in the field recently. New dosimetric systems have been devised and older systems have been re-investigated and modified to increase their accuracy.

There has been a general feeling among those concerned with radiation applications, and particularly among those wishing to enter the field, that a review covering the advances in chemical dosimetry during the past few years would be of great value. Since radiation dosimetry has grown so rapidly in the last ten years, it would be impossible to cover the entire subject or to describe the various methods in very great detail. This review is primarily intended to be a starting point for those interested in the problems of dosimetry, and will deal only

* Work performed under the auspices of the U.S. Atomic Energy Commission.

with electron, γ- and X-radiation. There are several excellent reviews of the field of dosimetry, which go into greater detail concerning particular aspects of dosimetric problems. The two most recent reviews are that edited by HINE and BROWNELL[1] and an article by MILLER.[2]

In dosimetric measurements, one is concerned with the amount of energy absorbed by the material being investigated rather than with the quantity of radiation impinging on the material. This review will therefore deal only with the measurement of energy absorption. While the major part of the paper will be taken up with discussion of chemical systems which can be used for measuring dose, a brief review of the principle and use of ionization chambers is also included since, in recent years, a great deal of work has been done on the measurement of W, the energy required to produce an ion pair.

IONIZATION MEASUREMENTS

In 1912, BRAGG[3] related the ionization produced in an ionization chamber to the electron-stopping power of the wall material. Later, GRAY[4] showed that the introduction of a small cavity at a point in a solid medium would not disturb the angular or energy distribution of secondary electrons at the point, providing the following conditions were fulfilled. There should be a negligible γ- or X-ray interaction with the gas, and the cavity should be small enough so that only a negligible fraction of the electrons, which are produced in the wall, are stopped in the gas.

If one wishes to apply the Bragg–Gray principle to a cavity or extrapolation chamber in order to obtain an absolute measure of absorbed dose, there are additional requirements which must be fulfilled. Except in the special case where the filling gas is of the same composition as the wall material, the thickness of the wall must be greater than the range of the most energetic secondary electrons. The γ- or X-ray absorption in the wall must be negligible, and the geometrical conditions of the irradiation must be such that the entire assembly is immersed in as uniform a beam as possible.

The result of the work of BRAGG and GRAY was to obtain a relation between the ionization current produced in the gas to the energy absorbed per unit volume per sec by the wall of an ionization chamber, when irradiated with γ- or X-rays. The relationship may be expressed as follows:

$$E_w = JW \,.\, S_{\text{wall}}/S_{\text{gas}} \qquad (1)$$

where E_w = energy absorbed per unit volume of wall material per sec, J = number of ion pairs per unit volume of the cavity per second, W = energy required to produce one ion pair in the gas, and S = stopping power for electrons of the wall or gas.

A more sophisticated study of cavity ion chamber theory[5,6] has shown that S, the stopping power, is a complex quantity, involving the cavity size and shape as well as many other factors. For the purpose of calculation, the stopping power can be approximated by using the relativistic equation derived by BETHE.[7] This equation is valid for electron energies greater than the binding energies of the electrons in the wall or gas, and below 1 MeV, where no polarization corrections are required. It may be written

$$S = -\frac{dE}{dx} = \frac{2\pi e^4 (NZ)}{m^2}\left\{\ln\frac{mv^2E}{2I^2(1-\beta^2)} - [2(1-\beta^2)^{\frac{1}{2}} - 1 + \beta^2]\ln 2 + 1 - \beta^2 + \tfrac{1}{8}[1-(1-\beta^2)^{\frac{1}{2}}]^2\right\} \qquad (2)$$

where m = rest mass of the electron, v = velocity of the electron, E = total energy minus rest energy of the electron, $\beta = v/c$, and I = average ionization potential of the absorbing material.

The values of I have been empirically determined for many elements from range–energy data for protons and α particles. Values of I for compounds can be computed using the Bragg rule, which states that the average ionization potential of a compound is the geometric mean of the average

ionization potentials of the constituent atoms; small corrections are necessary because of chemical binding. Since the stopping power is calculated per electron, when one combines the I values for different elements to calculate the I value for a compound, each element must be weighted by the number of electrons it contributes. For example, $I_{H_2O} = (I_H^2 I_O^8)^{1/10}$. Table 1 lists values of I for various materials. One of the main difficulties in using ionization chambers for the absolute measurement of γ- or X-radiation is that the S of equation (1) is strictly a somewhat more sophisticated function than the stopping power referred to in equation (2). However, it is quite possible to measure dose-rates to within a few per cent with ionization chambers, if they are properly designed and operated.

TABLE 1. The average ionization potentials of various substances

Substance	I (volts)
Air	83·2
N_2	80·5
O_2	92·0
CO_2	87·4
A	195·0
CH_4	40·5
C_2H_4	51·4
He	35·0
Ne	115·0
Kr	317·0
Xe	486·0
Polystyrene	61·0
H_2	15·6
Al	150·0
C	76·7
Cu	279·0
U	853·0

Recently a great deal of work has been done on the determination of W for air as well as for many other gases. In the past the W value used for air-filled chambers has been 32·5 eV. More recent work[8] has shown that this value is low and that the true value is nearer to 34·0 eV. At the last meeting of the International Commission on Radiological Units and Measurements, it was suggested that in all future work W for air be taken as 34·0 eV. Table 2 lists the more recent values W for air as well as W values for other gases.

In the construction of an ionization chamber the choice of wall material is dependent on whether the radiation is to be measured in terms of roentgens or rads. For a determination in roentgens the wall material must be "air equivalent"; i.e., it must have an effective atomic number close to that of air. If one wishes to measure an absorbed dose, however, both the wall and gas should be matched to the medium absorbing the energy. The thickness of the wall is also of great importance, as mentioned earlier, and should be capable of stopping the most energetic secondary particles.

TABLE 2. W values for various gases for electrons

Gas	W(eV)[32]
He	42·3
Ne	36·6
A	26·4
Kr	24·1
Xe	22·0
H_2	36·3
N_2	34·7
O_2	30·9
CO_2	33·0
C_2H_4	26·3
C_2H_6	24·8
CH_4	27·3
C_2H_2	26·1
Air	34·1[32]
Air	33·9[33]
Air	34·0[34]
Air	33·7[35]
Air	33·5[36]
Air	33·7[37]
Air	33·6[38]

CHEMICAL SYSTEMS

During the past decade much work has been done in the field of radiation chemistry. Chemists have been studying the initiation of chemical reactions, polymerization reactions, and oxidation–reduction reactions, using β-, γ- and X-radiation. In the course of these studies several chemical systems were found which could be used to measure

dose, and some of these systems have been developed into useful dosimeters. In addition to the usual requirements for a good dosimeter, a chemical dosimeter should have the following characteristics:

(1) It should be simple and convenient to use.

(2) The extent of reaction due to irradiation should be easily and accurately measurable.

(3) It should be reproducible and easily made from shelf reagents (insensitive to impurities).

(4) The amount of reaction should not be dependent on the concentration of the reagents.

(5) The amount of reaction should be proportional to dose.

Listed below is a group of dosimetric systems which meet some or all of these requirements. Certain systems are more fully described than others because in surveying the literature one finds that certain systems have been more completely investigated than have others, and consequently more information is available. Since each experimenter has his own opinion as to which system gives the best results, all systems used in the past decade are included in the listing.

1. *Fricke dosimeter* (*ferrous sulfate*).[9,10] This dosimeter system is probably the most widely used, and is generally considered the most reliable of all dosimetric systems. The dosimeter solution is prepared by dissolving 2 g of $FeSO_4$, 0·3 g of NaCl, and 110 ml of conc. H_2SO_4 in sufficient distilled water to make 5 l. of solution. The system is independent of concentration from 10^{-4} M to 5×10^{-2} M $FeSO_4$, and independent of sulfuric acid concentration above 0·1 N.[11] The useful range is from 4 to 40 krad (but it can be extended to 200 krad by saturating the solution with oxygen and increasing the ferrous sulfate concentration). The ferrous sulfate system is also independent of dose-rate from 6 to 10^8 rad/min. The yield of oxidation is 16·0 μM ferric iron formed per 1000 rad, and is independent of wavelength for γ-ray application.

The Fricke dosimeter can be modified for use at low doses (0–100 rad) by the addition of Fe^{59} to the solution as a tracer.[12] After irradiation, the ferric ions formed are separated from the ferrous ions by extraction of ferric thiocyanate with *iso*amyl alcohol and the activity of the two phases determined. As long as the concentration of the tracer is low enough so as not to increase the dose appreciably, the measurements can be carried out with an accuracy of better than 2 per cent.

For high total doses, the Fricke dosimeter can be modified to extend its upper limit. HART and WALSH[13] have developed a dosimetric system made up of 1 mM ferrous ions, 10 mM cupric sulfate and 0·01 N sulfuric acid. In this system the ferrous ion is oxidized without the consumption of oxygen and therefore the upper limit is extended to a total dose of at least 10^6 rad.

2. *Ceric sulfate.*[14,15] The production of cerous ions is a linear function of dose up to 100 per cent reduction of the ceric ion present in the initial solution. The dosimetric system is made by dissolving the desired amount of analytical grade ceric sulfate in 0·8 N H_2SO_4. Since this system is extremely sensitive to impurities, special care must be taken to ensure that all vessels are absolutely clean. A standard practice is to allow all glassware to be used to stand with dilute ceric sulfate solution when not in use. The system is independent of concentration from 3×10^{-2} to 10^{-5} M cerium, energy independent from 100 keV to 23 MeV, and independent of dose-rate from 0·5 rad/sec to 500 rad/sec. The yield of the radiation is 2·5 ions of cerium reduced per 100 eV absorbed, but if one adds thallous ion,[16] the yield is increased to 8·05 ions reduced per 100 eV absorbed.

3. *Sodium benzoate or benzene.*[17,18] The dosimeter solution is made either by dissolving sodium benzoate in distilled water to make a 0·5% solution, or by using distilled water saturated with benzene. Analysis is made by mixing 0·5 ml of irradiated solution with 0·5 ml of Folins reagent, and 1·5 ml of 18% Na_2CO_3 solution in sufficient

VOL.
4
1958/5

water to fill a 1 cm absorption cell. This system is useful from 10^4 to $7{\cdot}2 \times 10^4$ rad and the yield (one rad produces approximately 6×10^{-10} g/ml of salicylic acid) is not critically dependent on pH, concentration, or temperature. In the presence of air, the yield is directly proportional to dose up to about 60,000 rad; at higher doses the reaction proceeds at a slower rate. The sodium benzoate system is not being used at the present time since the ferrous sulfate system covers the same range of dose and is both more reliable and more convenient to use.

4. *Halogenated hydrocarbon–dye.*[19,20] This dosimeter solution consists of triply distilled water saturated with a reagent grade halogenated hydrocarbon such as chloroform, carbon tetrachloride or tetrachloroethylene. A reagent grade, water-soluble acidimetric dye is then added and the solution is standardized to a given pH and color. Acid production in this system is linear with dose up to 250,000 rad and is energy independent from 50 keV to 1·2 MeV. The system is also independent of dose-rate from 10 to 4250 rad per min. There is, however, a slight temperature effect and the acid production varies approximately 5 per cent between 5 and 50°C. The results of dose measurements with this system are reproducible to ± 2 per cent. The fast neutron response of this dosimeter is approximately 0·5 times the γ-response, although if one uses tetrachloroethylene the system is neutron insensitive.

In the chloroform–water solutions the production of acid can be followed by measuring the change in electrical conductivity of the solution,[21] using a Q-meter type of instrument, and reading the dose directly. The solution used in this case is three parts chloroform, from which the preservative alcohol has been removed, and one part doubly distilled water to which 0·15 per cent of alcohol has been added. The added alcohol improves the temperature stability of the solution. The system is useful from 50 to 1000 rad; above 600 rad the system loses some accuracy.

5. *Polyvinyl chloride film*[22] *with methyl violet.* Methyl violet is dissolved in chlorobenzene and a 4% solution of Geon-101 resin is made up using the chlorobenzene–methyl violet solution. The solution is then poured on to a mirror or other surface and the film formed. This system shows an energy dependence below 600 kV and its useful range is between 2×10^8 and 110×10^8 rad. This dosimeter has been replaced by a cellophane–dye system[23] due to the difficulty in preparing uniform polyvinyl chloride films. The cellophane system is a similar system and has been shown to be linear with dose up to 3×10^6 rad, with a probable error of 60 per cent in the 2×10^5 rad region and a probable error of 7 per cent at 3×10^6 rad.

Gel and solid dosimeters

6. *Resazurin in agar.*[24] This system is one of two which will be mentioned which are useful for depth dose measurements. The solution is made by mixing 8 ml of a 100 mg % solution of resazurin in 1500 ml of agar. Methylene blue has also been used instead of resazurin. The system has been investigated for electron energies between 300 and 3000 kV.

7. *Chloral hydrate–agar gel.*[25] This system has replaced the preceding dosimetric system in recent years. Radiation causes the formation of HCl and thus changes the pH and electrical conductivity of the gel. An acid–base indicator could be added and the system analyzed spectrophotometrically, or the system may be analyzed either by use of a pH electrode or a conductivity electrode pair. A minimum dose of 2000 rad is required for reasonable accuracy.

The gel is made by dissolving the agar in hot distilled water and adding the chloral hydrate when the gel has cooled to about 50°C. When the gel is prepared as described, it has a density of 1·04 g/cm^3. Since there is some diffusion effect, analysis of the gel must be carried out soon after irradiation. The reaction has a temperature dependence of about 2 per cent/° between 18°C and 24°.

The next two systems are not normally classified as chemical dosimeters, but it is

considered appropriate to include them in this review.

8. *Silver-activated phosphate glass.*[26,27] The glass used in this dosimeter is now commercially available, ready for use. The dosimeter is independent of dose-rate up to at least 170 rad/min, and energy independent from 200 keV to Co^{60} energies. Below 200 keV the sensitivity increases and at 65 keV is 18 times that for Co^{60}. The dose received can be determined in two ways: for doses between 10 and 600 rad, the reading is taken in a fluorimeter, while for high doses up to 2×10^6 rad, one uses a spectrophotometer and determines the change in optical density. At high doses the system has an accuracy of ± 5 per cent.

9. *Cadmium sulfide crystal detectors.* Several papers have appeared in the literature recently concerning the use of CdS crystals as radiation detectors.[28,29] A conventional photo-cell circuit will record the change in conductivity of the crystal with dose-rate. This type of dosimetric system is excellent for mapping radiation fields in a very short time. The detector does show an energy dependence below 200 keV, but this dependence can be substantially reduced by the use of a perforated lead filter. One criticism of this dosimeter has been its tendency to drift and to show a noticeable hysteresis effect. Some unpublished work by Weiss and Handloser shows that if the crystals are irradiated in a high radiation field prior to use as a dosimeter, the drift characteristics are greatly improved, and subsequent exposures are very reproducible with no detectable drift or hysteresis. The useful range of this system appears to have a lower limit of the order of 4000 rad/hr, but an upper limit has not as yet been determined.

Gas phase dosimeters

10. *Nitrous oxide.*[30] This is one of the two systems herein mentioned which have been used by workers studying chemical reactions in the vapor phase. Under irradiation nitrous oxide is decomposed and the products are measured by conventional vacuum techniques. In addition to decomposition products, nitrogen dioxide is formed and can be measured colorimetrically. The system has been used at very high doses (3×10^7 to 3×10^9 rad), and at doses as low as 10^6 rad may be measured colorimetrically by increasing the length of the light path from 2 to 50 in.

11. *Condensation of acetylene.*[31] This system appears to be preferred by workers in the vapor phase. The yield of benzene has been stated to be 5·1 molecules formed per 100 eV absorbed, and is independent of the initial acetylene pressure and radiation intensity.

Although all of the systems mentioned above have been in use during the past ten years, the following are the dosimeters most commonly used today. For the irradiation of solutions, the Fricke dosimeter is considered to be the most reliable. For high total doses (above 50,000 rad) either the ferrous–cupric system or the ceric sulfate system is recommended. The system most generally used for depth dose measurements is chloral hydrate–agar gel. As stated above, the condensation of acetylene is preferred by workers in the vapor phase. Silver-activated phosphate glass appears to be the only solid phase dosimeter in use at the present time and is quite reliable. For rapid mapping of radiation fields the simplest system to use is the cadmium sulfide dosimeter. It is felt that as more work is carried out on this system it may possibly replace some of the others, since it is the only direct reading dosimeter in use.

VOL
4
1958/

REFERENCES

1. Hine and Brownell (Editors), *Radiation Dosimetry* Academic Press, New York (1956).
2. Miller N. *Actions Chemiques et Biologique des Radiations 2me series.* p. 161, Mason, Paris (1956).
3. Bragg W. H. *Studies in Radioactivity* Macmillan, New York (1912).
4. Gray L. Y. *Proc. Roy. Soc.* A**156,** 578 (1936); *Brit. J. Radiol.* **10,** 600, 721 (1937).
5. Burch P. R. J. *Rad. Res.* **3,** 361 (1955).
6. Spencer L. V. and Attix F. H. *Rad. Res.* **3.** 239 (1955).

7. Segre E. (Editor) *Experimental Nuclear Physics* p. 257 John Wiley, New York (1953).
8. Weiss J. and Bernstein W. *Rad. Res.* **6,** 603 (1957).
9. Fricke H. and Morse S. *Phil. Mag.* **7,** 129 (1929).
10. Weiss J., Allen A. O. and Schwarz H. A. *Peaceful Uses of Atomic Energy*, United Nations, New York, Vol. **14,** p. 179 (1956).
11. Allen A. O. and Rothschild W. G. *Rad. Res.* **7,** 591 (1957).
12. Rudstam G. and Swedberg T. *Nature* **171,** 648 (1953).
13. Hart E. J. and Walsh P. D. *Rad. Res.* **1,** 342 (1954).
14. Hardwick T. J. *Canad. Chem. J.* **30,** 23 (1952).
15. Hummel R. W. *et al. Canad. Chem. J.* **31,** 1203 (1953).
16. Sworski T. J. *Rad. Res.* **4,** 483 (1956).
17. Day M. J. and Stein G. *Nucleonics* **8,** (2), 34 (1951).
18. Day M. J. and Stein G. *Nature* **164,** 671 (1949).
19. Sigoloff S. C. AEC Document AF-SAM-56-15.
20. Taplin G. *et al.* AEC Document UCLA2 97.
21. Kanwisher J. W. *Nucleonics* **10,** (5), 62 (1952).
22. Henley E. J. and Miller A. *Nucleonics* **9,** (6), 62 (1951).
23. Henley E. J. *Nucleonics* **12,** (9), 62 (1954).
24. Proctor B. E. and Goldblith S. A. *Nucleonics* **7,** (2) 83 (1950).
25. Andrews H. L. *et al. Rev. Sci. Instrum.* **28,** 329 (1957).
26. Schulman J. H. *et al. Nucleonics* **11,** (10), 52 (1953).
27. Schulman J. H. *et al. Nucleonics* **13,** (2), 30 (1955).
28. Mauldon G. F. *et al. Brit. J. Radiol.* **29,** 427 (1956).
29. Hollander L. E. Jr. *Research and Development of Photoconductive Dose-Rate Indicators*, Victoreen Inst. Co., Cleveland, O. (1956).
30. Dondes S. *Peaceful Uses of Atomic Energy*, Vol. **17,** p. 176 United Nations, New York 1956.
31. Dorfman L. M. and Shipko F. J. *J. Amer. Chem Soc.* **77,** 4723 (1955).
32. Jesse W. P. and Sadauskis J. *Phys. Rev.* **97,** 1668 (1955).
33. Weiss J. and Bernstein W. *Phys. Rev.* **98,** 1828 (1955); *Phys. Rev.* **103,** 1253 (1956).
34. Bernier J. P. *et al. Rad. Res.* **5,** 613 (1956).
35. Bay, Mann, Seliger and Wyckoff *Rad. Res.* **5,** 469 (1956); *Rad. Res.* **7,** 558 (1957).
36. Emery E. W. *Brit. J. Radiol.* **29,** 370 (1956).
37. Seliger H. H. *Int. J. Appl. Rad. Isotopes*, **1,** 215 (1955).
38. Gross, Wingate and Failla *Radiology* **66,** 101 (1956); *Rad. Res.* **7,** 570 (1957).

OL.
4
8/59

International Journal of Applied Radiation and Isotopes, 1958, Vol. 4, pp. 96–107. Pergamon Press Ltd., London

Contribution à l'Etude de Préparation des Sources de Coesium^{137}

J. TROCKER,* C. FISHER et A. RAGGENBASS
Commissariat à l'Energie Atomique, France

(*Received* 15 *December* 1957)

La fabrication de fortes sources de Cs^{137} est une réalisation qui pose de nombreux problèmes parmi lesquels figurent:

(1) Le choix du sel en fonction de sa bonne activité spécifique.

(2) Le choix de la méthode de "mise en forme" de ce sel qui peut être effectuée soit par fusion, soit par pastillage.

Le but de la présente étude a été de répondre à ces questions.

Nous avons étudié l'importance de la volatilisation lorsqu'on utilise la fusion pour la mise en forme des deux sels les plus intéressants: chlorure et sulfate de coesium, et trouvé que la volatilisation du sulfate de coesium est plus forte que celle du chlorure. En vue d'éliminer les inconvénients liés à la volatilisation et d'obtenir une densité, et donc une activité spécifique plus grande, on discute les avantages de la compression comme méthode d'encapsulage du sel de Cs^{137}.

La confection de fortes sources pose aussi le problème de l'auto-absorption du rayonnement-γ à l'intérieur de la source. Nous avons déterminé cette donnée dans le cas de sources réalisées à l'aide de chlorure et de sulfate de coesium.

On trouve que l'auto-absorption dans le chlorure de coesium est plus petite que dans le sulfate. La différence entre les activités mesurées d'une source de chlorure et d'une source de sulfate de coesium de mêmes dimensions, dûe à l'auto-absorption, varie avec la densité superficielle de la source: par exemple, pour une variation de 2 à 20 g/cm^2, elle est de 1 à 6 pour cent en faveur du chlorure. Considérant aussi l'activité spécifique plus grande du chlorure, cette différence s'élève à 8–13 pour cent.

CONTRIBUTION TO THE STUDY OF THE PREPARATION OF CAESIUM SOURCES

The manufacture of strong Cs^{137} sources is an operation which poses many problems; these include:

(a) The choice of salt with regard to its good specific activity and its stability under radiation.

(b) The preparation of this salt in suitable form, either by fusion or by pelleting.

The present study sets out to solve two of these problems.

We have investigated the importance of volatilisation when fusion is used as a means of preparing sources of the two most interesting salts: caesium chloride and caesium sulphate. Caesium sulphate has been found to be more volatile than the chloride. Nevertheless, taking into consideration the volatilisation of the two salts and the possibility of obtaining a higher density and thus specific activity by compression of the salts, the advantage of choosing compression as a method of encapsulation of the Cs^{137} salt is discussed.

The manufacture of strong sources also raises the problem of self-absorption in the source. This factor has been determined in the case of sources made up with caesium chloride and sulphate.

* Adresse actuelle: Commissariat à l'Energie Atomique, Israel.

VOL
4
1958/

Self-absorption has been found to be less in caesium chloride than in the sulphate. The difference between activities measured in a caesium chloride source and a caesium sulphate source of the same dimensions, due to self-absorption, varies with the superficial density of the source: for example for a variation of 2–20 g/cm^2 it amounts to 1–6 per cent in favour of the chloride. Considering also the higher specific activity of the chloride, this difference goes up to 8–13 per cent.

МАТЕРИАЛЫ К ИЗЧЕНИЮ ИЗГОТОВЛЕНИЯ ИСТОЧНИКОВ ЦЕЗНЯ

При производстве мощных источников Cs^{137} возникают многочисленные проблемы, среди которых, например:

(1) выбор соли цезия в зависимости от величины удельной радиоактивности ее и устойчивости при облучении,

(2) формовка этой соли либо плавлением, либо прессованием в таблетки. Целью настоящей работы является ответ на эти два вопроса.

Изучалось влияние испарения при применении плавки для формовки двух наиболее интересных солей: хлорида и сульфата цезия. Было найдено, что испарние сульфата цезия более значительно, чем хлорида. Принимая во внимание испаряемость обоих солей и возможность получения большей плотности, а следовательно и большей удельной радиоактивности, при прессовании, обсуждается преимущество выбора прессования, как метода для изготовления капсулей из солей Cs^{137}.

Производство высокоактивных источников ставит также проблему самопоглощения излучения внутри самого источника. Были проверены данные, относящиеся к случаю источников, изготовленных из хлорида и сульфата цезия.

Было найдено, что самополглощение в хлориде меньше, чем в сульфато. Разность радионктивностей хлоридного и сульфатного источников, измеренная для источников одинаковых размеров, одинакова и, вызываема ясамопоглощением, зависит от поверхностной плотности: так, например, при изменении плотности с 2 до 20 гр/см^2 она равнялась от I до 6% в пользу хлорида. Принимая во внимание большую радоактивность хлорида, общая разность доходила до 8-13%.

UEBER DIE HERSTELLUNG STARKER Cs^{137}-QUELLEN

Die Erzeugung starker Cs^{137}–Quellen stellt zahlreiche Fragen, u.a.:

(1) Die Wahl des Salzes in Abhängigkeit seiner guten spezifischen Aktivität und seiner Stabilität während der Bestrahlung.

(2) Die Gestaltgebung dieses Salzes, entweder durch Schmelzen oder durch Pastillenbildung.

Diese Untersuchung setzt sich als Ziel zwei von diesen Fragen zu beantworten. Wir haben die Bedeutung der Verfluchtigung bei Anwendung des Schmelzverfahrens bei der Formgebung für zwei der interessantesten Salzen untersucht: Caesiumchlorid und Caesiumsulfat.

Es wurde festgestellt dass die Verfluchtigung des Caesiumsulfates sträker ist als diejenige des Chlorids. Abei in Betrachtung des Verflüchtigung beider Salzen, sowie der Möglichkeit ein höheres spezifisches Gewicht, also eine höhere spezifische Aktivität durch Zusammenpressung der Salze zu erreichen, wird dieses Verfahren für das Einkapseln des Caesium^{137} Salzes untersucht.

Die Erzeugung starker Quellen stellt also die Frage der Selbstabsorption der Strahlung im inneren der Quelle. Wir haben diese Angabe, im Falle von Quellen welche mit Hilfe von Caesiumchlorid und Caesiumsulfat verwircklicht wurden, bestimmt.

Man fand dass die Selbstabsorption in Caesiumchlorid kleiner ist als im Sulfat. Der Unterschied zwischen den gemessenen Aktivitäten einer Caesiumchlorid- und einer Caesiumsulfatquelle derselben Abmessungen, welche der Selbstabsorption zuzuschreiben ist, ist mit dem oberflächlichem spezifischen Gewicht der Quelle veränderlich: zum Beispiel, für eine Veränderung von 2 bis 20 g/cm^2 ist sie dem Chlorid von 1 bis 6 Prozent gut zuschreiben. Ferner, in Betrachtung der höheren Aktivität des Chlorids steigt dieser Unterschied also auf 8–13 Prozent.

VOL. 4 58/59

INTRODUCTION

Dans la fabrication des sources intenses de Cs^{137}, le choix du sel avec lequel est confectionnée la source est conditionné par des facteurs qui dépendent, d'une part de la méthode de séparation chimique,[1] et d'autre part des propriétés de ce sel qui interviennent pour conférer à la source les qualités requises.[2,3] Parmi ces derniers on peut citer notamment:

(1) Une haute activité spécifique.
(2) Une faible volatilisation à une haute température.
(3) La stabilité chimique et resistance aux rayonnements.
(4) La facilité d'encapsulage.
(5) Une faible auto-absorption du rayonnement dans la source.

L'examen de ces différents facteurs, indique que les sels de coesium qui paraîssent convenir le mieux sont le chlorure et le sulfate. En effet, ces deux sels sont utilisés actuellement pour la préparation de sources de haute activité de Cs^{137}: le chlorure est la forme choisie à Oak Ridge,[4,5] tandis que le sulfate est choisi à Windscale.[6,7] Néanmoins, aucune étude expérimentale détaillée sur les avantages d'utilisation d'un de ces deux sels n'est pas apparue jusqu'à présent.

Nous avons entrepris de comparer ces sels en examinant deux des facteurs mentionnés ci-dessus, à savoir:

(a) La volatilisation des sels.
(b) L'auto-absorption du rayonnement.

VOLATILISATION DU CHLORURE ET DU SULFATE DE COESIUM

Afin de créer une couche dense et adhérente du sel de coesium au métal du récipient de la source, on peut envisager deux méthodes: la compression et la fusion. Il était donc intéressant d'étudier la volatilisation du chlorure et du sulfate de coesium à différentes températures, afin d'établir si la fusion comme méthode d'encapsulage ne conduirait pas à une perte d'activité et une contamination de l'atmosphère trop grandes. On voulait aussi établir lequel de ces deux sels est le moins volatile à la température de fusion et au-délà de cette température.

1. *Partie experimentale*

La volatilisation des sels de coesium a été étudiée par différentes méthodes:

(1) La thermobalance.
(2) La pesée des échantillons avant et après chauffage.
(3) L'analyse chimique du coesium dans les échantillons avant et après chauffage. Les matériaux utilisés dans nos essais étaient:
ClCs et SO_4Cs_2 purs ("Prolabo").
ClCs et SO_4Cs_2 préparés dans le laboratoire à partir de CO_3Cs_2 anhydre spectr. pur ("Johnson, Matthey & Co.") en utilisant le bleu de bromophenol comme indicateur.

Acide phospho-tungstique R.P. ("Prolabo") de formule

$$P_2O_5 \cdot 20WO_3 \cdot 27H_2O$$

Tous les sels ont été séchés à 110° avant les essais.

Volatilisation en thermobalance. La thermobalance utilisée a été de type Chevenard avec enregistrement graphique (No. 164) ou photographique (No. 16). Le cycle de chauffage a varié selon les différents paliers de température choisis pour étudier la volatilisation des sels à température constante. La température a été mesurée avec une précision de $\pm 5°$. Dans certains essais, l'échantillon a été introduit dans le four chauffé à une température plus élevée que la température ambiante. Le poids des échantillons a varié entre 150–400 mg sel.

Détermination de perte de poids par pesée. Comme la température maximum du four de la thermobalance a été de 1030°, et comme on a intérêt à étudier la volatilisation des sels à quelques dizaines de degrés au-dessus de la température de fusion (645° pour le chlorure et 1010° pour le sulfate), on a fait quelques essais dans un four électrique type "moufle", montant jusqu'à 1300°. On a chauffé durant différents temps, des échantillons de chlorure et sulfate de coesium

à des températures variées (précision de mesure $\pm 5°$) et on a déterminé la perte de poids par pesée, avant et après le chauffage. Le poids des échantillons a varié entre 0,4–2,0 g sel.

Détermination de perte de coesium par analyse chimique. Dans quelques autres essais, on a vérifié par analyse chimique du coesium résiduel et volatilisé si le produit volatilisé est le sel de coesium seulement. Dans ce but, on s'est servi d'un appareil en silice (Fig. 1) dans lequel on a introduit l'échantillon (0,2–0,3 g sel).

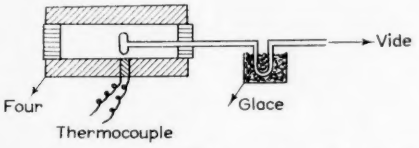

FIG. 1. Appareillage utilisé pour la condensation du coesium volatilisé.

L'appareil a été chauffé dans un four électrique type "moufle" à différentes températures et pendant des temps variés. En faisant le vide dans l'appareil et en refroidissant une partie de l'appareil extérieure au four, on a piégé par condensation les produits volatilisés pendant le chauffage. Après le chauffage, on coupe le tuyau de la capsule, on lave séparément résidu et produit volatilisé et on dose le coesium par précipitation avec l'acide phospho-tungstique, méthode utilisée pour la séparation du coesium des produits de fission.[1,2]

Dosage du coesium. On a étudié les conditions pour un rendement de précipitation optimum de petites quantités de coesium allant jusqu'à 0,2 mg Cs en solutions contenant 20–100 mg Cs/l. solution. Le coesium utilisé comme étalon a été sous forme de CO_3Cs_2 spectr. pur anhydre.

On a étudié:

(1) La quantité d'acide phospho-tungstique nécessaire pour la précipitation complète.
(2) La normalité de la solution.
(3) La nécessité de lavage du précipité.

Les quantités d'acide phospho-tungstique ajoutées sous forme de solution 0,01 M à la solution de Cs ont varié entre la quantité théorique et un excès de 230 pour cent.

La formule du précipité de phospho-tungstate de coesium, comme des autres métaux alcalins, étant[8]

$$3CsOH{\cdot}20WO_3{\cdot}P_2O_5{\cdot}2{,}5H_2O$$

on a établi le rapport:

$$\frac{3CsOH{\cdot}20WO_3{\cdot}P_2O_5{\cdot}2{,}5H_2O}{Cs} = 13{,}19$$

La normalité de la solution a été obtenue en ajoutant à la solution une quantité calculée d'acidenitri que; elle a varié jusqu' à 6N. La méthode d'analyse consistait à ajouter à la solution de Cs (10 ml) contenue dans un tube de centrifugeuse préalablement pesé, une quantité d'acide nitrique calculée, et une quantité calculée d'acide phospho-tungstique 0,01 M. On laisse le précipité se déposer pendant la nuit, on centrifuge pendant 15 min et on sépare le précipité par décantation. Les essais de dosage ont été faits en double, un des précipités étant lavé par une solution (10 ml) d'acide nitrique N, centrifugé et décanté de nouveau. Après la décantation, les précipités ont été séchés à 110° jusqu'au poids constant et le poids du Cs a été déduit.

Les courbes de rendement de précipitation en fonction de la normalité de la solution et de la quantité d'acide phospho-tungstique ajoutée (Fig. 2) ont été déterminées en utilisant une solution de 100 mg Cs/l. (1 mg Cs dans l'échantillon dosé).

On voit que les conditions de précipitation optimum sont:

(1) Solution 2N–3N d'acide nitrique.
(2) Excès d'acide phospho-tungstique d'environ 200 pour cent.
(3) Lavage du précipité après la décantation.

On a vérifié les conditions optimum de precipitation pour des solutions contenant des quantités plus petites de coesium et on a trouvé les résultats donnés dans le Tableau 1.

2. *Résultats*

Les résultats des essais avec la thermobalance pour le chlorure et le sulfate de coesium ("Prolabo" ou préparés au laboratoire), sont donnés dans la Fig. 3.

Les courbes construites avec ces données,

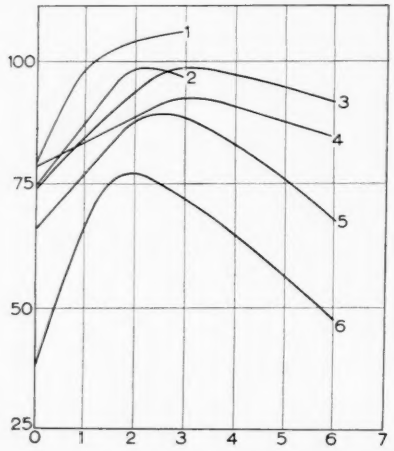

FIG. 2. Dosage du coesium par précipitation avec acide phospho-tungstique. Rendement de précipitation en fonction de la normalité de la solution et de la quantité d'acide phospho-tungstique ajoutée.
Abscisse: normalité de la solution
Ordonnées: rendement de précipitation (%)
Courbe 1. 230% excès d'acide phospho-tungstique (précipité non lavé)
Courbe 2. 230% excès d'acide phospho-tungstique (precipité lavé)
Courbe 3. 100% excès d'acide phospho-tungstique (précipité non lavé)
Courbe 4. 100% excès d'acide phospho-tungstique (précipité lavé)
Courbe 5. quantité théorique d'acide phospho-tungstique (précipité non lavé)
Courbe 6. quantité théorique d'acide phospho-tungstique (précipité lavé)

TABLEAU 1. Rendement de précipitation de Cs avec l'acide phospho-tungstique.
10 ml solution 2,5N, excès d'acide phospho-tungstique de 230%. Précipité lavé après la décantation

Concentration du Cs dans la solution (mg/l.)	Rendement de précipitation (%)
66	100,5
44	97,0
33	98,7
22	93,5

dans la Fig. 4, représentent les valeurs moyennes de volatilisation de ces deux sels à la température de fusion $\pm 10°$, en fonction du temps de chauffage. On voit que la

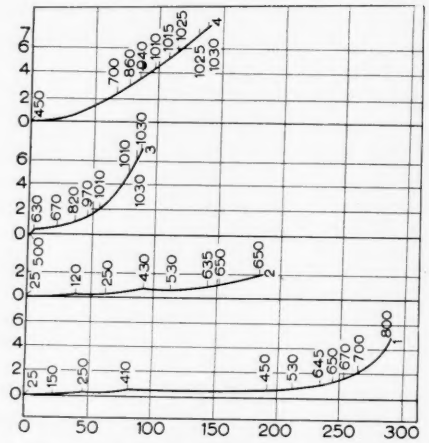

FIG. 3. Volatilisation du chlorure et sulfate de coesium en fonction de la température et du temps de chauffage (essais en thermobalance).
Abscisse: temps (min)
Ordonnées: perte en poids (%)
Les numéros sur les courbes indiquent la température correspondante.
Courbe 1. ClCs ("Prolabo")
Courbe 2. ClCs (préparation laboratoire)
Courbe 3. SO_4Cs_2 ("Prolabo")
Courbe 4. SO_4Cs_2 (préparation laboratoire)

volatilisation du SO_4Cs_2 atteint généralement le double de celle du chlorure: à la température de fusion, la volatilisation en 5 min est de 0,4 pour cent pour le chlorure et 0,8 pour cent pour le sulfate, tandis qu'en 30 min elle est de 1,0 pour cent pour le chlorure et 2,4 pour cent pour le sulfate.

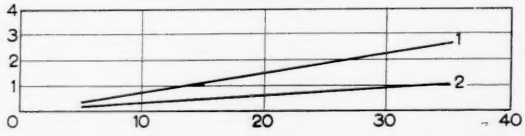

FIG. 4. Volatilisation du chlorure et sulfate de coesium. Valeurs moyennes de plusieurs essais de thermobalance à la température de fusion ($\pm 10°$) en fonction du temps de chauffage.
Abscisse: temps de chauffage (min)
Ordonnée: perte en poids (%)
Courbe 1. SO_4Cs_2 ($1010 \pm 10°$)
Courbe 2. ClCs ($645 \pm 10°$)

Des résultats semblables ont été trouvés après chauffage dans un four électrique des échantillons des sels préparés au laboratoire et détermination de la perte de poids par pesée (Fig. 5).

Les courbes de perte de poids de la Fig. 5 ont été tracées en fonction de la température de chauffage (10 min) allant jusqu'à environ 150° au-dessus de la température de fusion. Dans ces essais aussi, la volatilisation du sulfate de coesium a été le double de celle du chlorure: à 150° au-dessus de la température de fusion la volatilisation du chlorure est de 2,5 pour cent, tandis que celle du sulfate est de 5 pour cent.

La méthode de détermination de perte de coesium par analyse chimique a été utilisable seulement dans le cas du chlorure de coesium, car dans les essais faits avec le sulfate à des températures supérieures à 990°, l'appareil de silice a été attaqué par le sulfate de coesium.

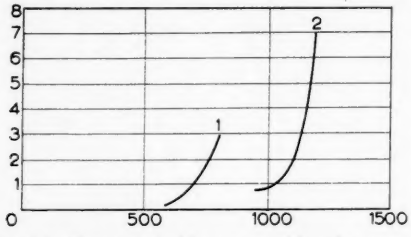

FIG. 5. Volatilisation du chlorure et sulfate de coesium en fonction de la température. (Détermination par pesée).
Temps de chauffage: 10 minutes
Abscisse: température (°C)
Ordonnée: perte en poids (%)
Courbe 1. ClCs (préparation laboratoire)
Courbe 2. SO_4Cs_2 (préparation laboratoire)

Dans le Tableau 2 sont donnés les résultats de dosage du coesium volatilisé et condensé après chauffage du chlorure de coesium à 645° pendant 15 et 60 min. Le total du coesium dosé dans le sel condensé et le sel résiduel a été de 98–99 pour cent.

La concordance des résultats trouvés dans ces essais, avec ceux trouvés dans les essais précédents, prouve que la perte de poids qu'on obtient par chauffage des sels de coesium, provient de la volatilisation de ces sels seulement.

3. *Discussion*

Dans les essais décrits plus haut, on a trouvé que si on envisage la fusion comme méthode d'encapsulage du sel de Cs^{137}, le chlorure est préférable au sulfate, car il se volatilise moins. Néanmoins, même les petites quantités de coesium volatilisées pendant la fusion du chlorure risquent de devenir gênantes quand il s'agira de la préparation de sources très actives, d'autant plus que pour faciliter la manipulation des sels de coesium fondus, il est nécessaire de les chauffer à une température d'environ 200° audessus de leur température de fusion.[7] Un dispositif de condensation des produits de coesium volatilisés diminuerait l'avantage de la simplicité et de la facilité de la technique de la fusion sur celle de la compression.

Pour comparer les avantages de la volatilisation et de la compression comme méthode d'encapsulage, nous avons mesuré aussi les densités des pastilles de chlorure et sulfate de coesium obtenus par les deux méthodes. La densité des pastilles de chlorure et de sulfate de coesium fondus a été pour les deux sels égale à 3,3 g/cm³, tandis que la densité des pastilles de ces sels obtenus par compression à 1500 kg/cm² a été de 3,6 g/cm³. Il est donc évident que, du point de vue de l'activité spécifique aussi, la compression est préférable comme méthode d'encapsulation.

TABLEAU 2. Volatilisation du chlorure de coesium par chauffage à 645°, déterminée par dosage chimique

Temps de chauffage (min)	Coesium volatilisé (% du poids initial)
15	0,52
60	2,10

AUTO-ABSORPTION DU RAYONNEMENT GAMMA DANS LE CHLORURE ET LE SULFATE DE COESIUM

Bien que l'auto-absorption du rayonnement-γ est plus faible que celle du rayonnement-β, elle peut atteindre des pourcentages élevés de l'activité réelle d'une source d'énergie de rayonnement moyenne surtout dans le cas des fortes sources dont la densité superficielle est grande.

Plusieurs auteurs, parmi lesquels

HUSHLEY,[9] PERRY,[10] DIXON,[11] WEISS,[12] et BRUCER[13] ont étudié l'atténuation du rayonnement-γ par l'auto-absorption et ont déterminé les coefficients d'absorption des divers matériaux pour des rayonnements d'énergie variée.

Dans l'étude des paramètres qui peuvent influencer le choix du sel de Cs^{137}, il était intéressant d'étudier aussi l'effet de l'auto-absorption du rayonnement-γ dans les sels de coesium. Cette étude a été effectuée sur le chlorure et le sulfate de coesium.

Le rayonnement-γ du Cs^{137} étant de 0,66 MeV, le coefficient d'absorption du chlorure et sulfate de Cs^{137} sera déterminé par l'effet photoélectrique et surtout par l'effet Compton. Il sera obtenu par la somme des coefficients d'absorption massique photoélectrique et Compton de chaque élément du composé, multiplié par la fraction en poids de l'élément correspondant.[14] Les valeurs théoriques approximatives des coefficients d'absorption massique peuvent être calculées en utilisant les formules données[15] pour les coefficients d'absorption photoélectrique et Compton des éléments:

$$\frac{\tau}{\rho} = \left(\frac{\tau}{\rho}\right)_{Pb} \cdot \frac{207{,}2}{A} \cdot \left(\frac{Z}{82}\right)^4$$

$$\frac{\sigma}{\rho} = \left(\frac{\sigma}{\rho}\right)_{Pb} \cdot \frac{207{,}2}{A} \cdot \frac{Z}{82}$$

où:

τ/ρ = le coefficient d'absorption photoélectrique (cm^2/g),

σ/ρ = le coefficient d'absorption massique Compton (cm^2/g).

Z = le numéro atomique de l'élément.

A = la masse atomique de l'élément.

Pour l'énergie de rayonnement-γ du Cs^{137}, on trouve[16] que les coefficients d'absorption photoélectrique et Compton du Pb ont les valeurs 0,045 et 0,062 cm^2/g respectivement. On calcule ainsi la valeur de 0,076 cm^2/g pour le coefficient d'absorption massique du chlorure de coesium et 0,077 cm^2/g pour celui du sulfate.

Considérant les sources de coesium de l'ordre de 1000 c et l'activité spécifique du Cs^{137} d'environ 22 c/g[7] on trouve que la nsi té superficielle du sel de coesium sera élevée et à cause du coefficient d'absorption important, l'auto-absorption sera aussi grande. Pour un diamètre déterminé de source, l'augmentation de poids du matériaux n'entraîne pas une augmentation proportionnelle de l'activité émise et au-délà d'une certaine densité superficielle, l'augmentation de poids n'augmente presque plus l'activité. La diminution de l'auto-absorption par l'augmentation du diamètre de la source n'étant pas toujours possible à cause des conditions imposées par les utilisateurs de la source, le seul moyen de la diminuer est le choix du sel de moindre coefficient d'absorption et d'activité spécifique la plus grande.

Dans nos essais, nous avons déterminé les coefficients d'absorption du sulfate et chlorure de Cs^{137} ($\beta = 0{,}51$ MeV, $\gamma = 0{,}66$ MeV) et du Cs^{134} dont le rayonnement est voisin ($\beta = 0{,}66$ MeV, $\gamma = 0{,}80$ MeV.).

1. *Partie experimentale*

Le chlorure et sulfate de Cs^{137} ont été préparés à partir d'une solution de Cs^{137} OH (30 μc/g Cs). Pour les essais avec les sels de Cs^{134}, on a irradié dans la pile une solution de CO_3Cs_2 spectr. pur ("Johnson Matthey & Co.") et à partir de cette solution (40 μc/g Cs) de $CO_3Cs_2{}^{134}$ on a préparé le chlorure et sulfate de coesium. Après la neutralisation, les sels ont été séchés, broyés en une poudre fine et séchés de nouveau jusqu'au poids constant.

La mesure de l'atténuation de l'activité par l'auto-absorption a été faite en mesurant l'activité des quantités croissants de sels de coesium (exprimées pour la comparaison en g Cs/cm^2) et en extrapolant la courbe d'activité spécifique à la densité superficielle zéro. Ainsi, on a obtenu une courbe d'activité réelle qui comparée avec la courbe d'activité mesurée a permis le calcul de l'atténuation dûe à l'auto-absorption.

Pour ces mesures, on a utilisé l'appareillage suivant (Fig. 6).

(1) Une porte source cylindrique en Plexiglas, de 60 mm de diamètre et de 50 mm de hauteur avec une cavité centrale de 7 mm de diamètre, la paroi inférieure de cette cavité étant de 1 mm.

VOL.
4
1958/5

(2) Un compteur à scintillation contenant un crystal de INa "Harshaw" de 38 mm de diamètre et 25,4 mm de hauteur, un phototube EMI 6260 et préamplificateur Gabon Aff 9050 en montage DCS–1 No 014, associé à une échelle de 1000.

Comme le montre la Fig. 6, le compteur a été placé à une distance de 60 cm du porte

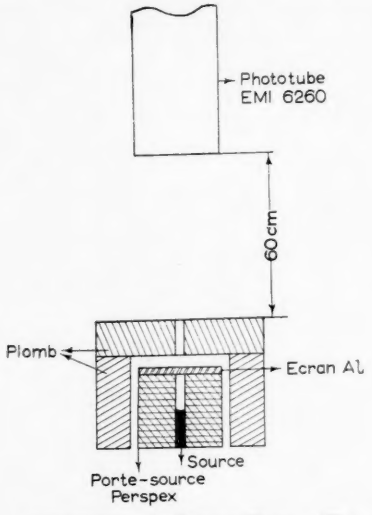

FIG. 6. Arrangement de l'appareillage utilisé pour les mesures d'activité.

source afin que le changement de géométrie par l'augmentation de poids de sel et, par conséquent, de la hauteur de la source n'influence pas les mesures. Le porte-source a été couvert d'un écran d'aluminium (1400 mg/cm²) pour absorber les $-\beta$ du Cs. Ainsi, on s'est assuré que l'atténuation de l'activité trouvée est dûe à l'absorption du rayonnement-γ seulement. On a aussi entouré le porte-source de briques de plomb de 50 mm d'épaisseur, la brique supérieure ayant un trou cylindrique de 7 mm de diamètre, concentrique avec la cavité du porte-source, pour faire sortir de la source un faisceau collimaté de rayons-γ dans lequel la probabilité que les rayons diffusés arrivent au compteur est très petite.

Les mesures d'activité de chaque échantillon ont été faites pendant 5 min. Les activités ont été corrigées pour le mouvement propre. On n'a pas tenu compte de la correction dûe au temps mort de l'appareillage qui vérifié par la méthode des deux sources[17] a été inférieure à 0,1 pour cent. Les mesures d'activité du chlorure et sulfate de coesium ont été faites en utilisant le même porte-source et en gardant rigoureusement la même géométrie. Le poids des échantillons des sels a été déterminé avec une précision de 0,1 mg.

2. *Résultats et discussions*

Les Figs. 7 et 8 donnent les résultats des activités mesurées du Cs^{137} et Cs^{134} sous forme de chlorure et sulfate, les activités réelles correspondants et l'atténuation dûe a l'auto-absorption. La densité superficielle étant exprimée en g Cs/cm², on peut comparer l'activité correspondante du Cs actif sous forme de sulfate ou de chlorure.

On constate que l'activité d'une quantité donnée de coesium actif sous forme de chlorure est plus grande que celle du sulfate, celà à cause de l'auto-absorption qui, comme on le voit dans les courbes d'absorption, est plus grande dans le sulfate que dans le chlorure.

Le coefficient d'absorption massique (cm²/g) résultant de nos mesures a été déterminé à l'aide de la formule donnée par DIXON[11] pour l'auto-absorption des $-\gamma$ dans le cas des sources linéaires:*

$$\frac{I}{I_0} = \frac{1}{\mu x} \cdot (1 - e^{-\mu x}) \qquad (1)$$

où:

I = l'activité mesurée
I_0 = l'activité réelle
μ = coefficient d'absorption massique (cm²/g)
x = densité superficielle (g/cm²)

Pour les petites valeurs de μx, le coefficient d'absorption peut être calculé avec une assez bonne précision selon une formule modifiée:

$$\frac{I}{I_0} = e^{-\mu x/2} \qquad (2)$$

Les valeurs des coefficients d'absorption

* Une source ayant l'axe placé sur la ligne qui joigne la source et le détecteur.

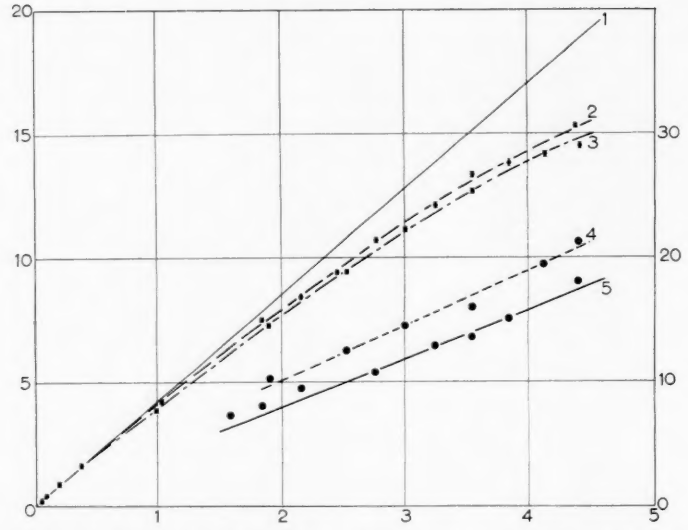

FIG. 7. Activités de chlorure et sulfate de coesium^{137} en fonction de la densité superficielle du coesium.
Abscisse: densité superficielle du Cs (g/cm^2)
Ordonnée gauche: activité (c/min $\times$ 10^3)
Ordonnée droite: absorption (%)

Courbe 1. Activité réelle du ClCs et du SO_4Cs_2
Courbe 2. Activité mesurée du ClCs
Courbe 3. Activité mesurée du SO_4Cs_2
Courbe 4. Absorption dans le SO_4Cs_2
Courbe 5. Absorption dans le ClCs

VOL
4
1958/

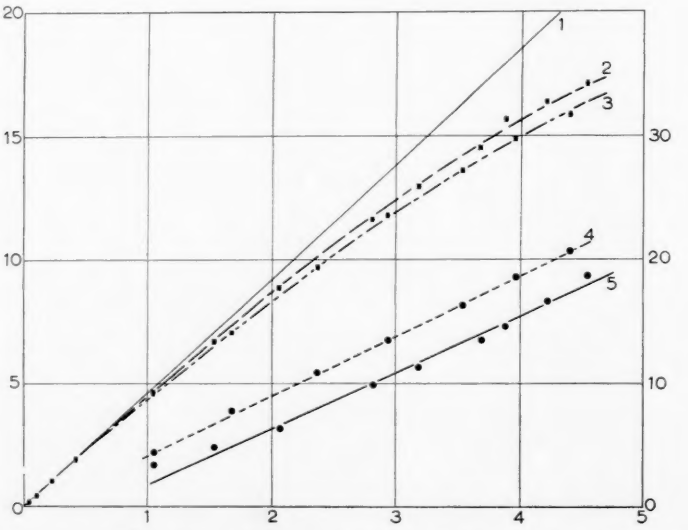

FIG. 8. Activités de chlorure et sulfate de coesium^{134} en fonction de la densité superficielle du coesium.
Abscisse: densité superficielle du Cs (g/cm^2)
Ordonnée gauche: activité (c/min $\times$ 10^3)
Ordonnée droite: absorption (%)

Courbe 1. Activité réelle du ClCs et du SO_4Cs_2
Courbe 2. Activité mésurée du ClCs
Courbe 3. Activité mésurée du SO_4Cs_2
Courbe 4. Absorption dans le SO_4Cs_2
Courbe 5. Absorption dans le ClCs

massique obtenus dans nos mesures et leur valeur approximative théorique sont données dans le Tableau 3.

TABLEAU 3. Valeurs du coefficient d'absorption massique du chlorure et sulfate de coesium

Sel	μ mesuré (cm²/g)	μ théorique (cm²/g)
$ClCs^{137}$	0,071 ± 0,005	0,076
$SO_4Cs_2{}^{137}$	0,078 ± 0,006	0,077
$ClCs^{134}$	0,063 ± 0,005	0,067
$SO_4Cs_2{}^{134}$	0,070 ± 0,005	0,068

On voit que les valeurs mesurées des coefficients d'absorption sont en assez bon accord avec les valeurs théoriques approximatives et que la petite déviation pour les différentes densités superficielles utilisées dans nos mesures vérifie la validité de la loi exponentielle formulée par DIXON.[9] En utilisant cette formule et les valeurs des coefficients d'absorption mesurés, on peut calculer les épaisseurs moitié d'auto-absorption du chlorure et sulfate de coesium pour le rayonnement-γ du Cs^{137}. Elles sont d'environ 20,5 g/cm² pour le sulfate et 22,5 g/cm² pour le chlorure de coesium. La comparaison de ces valeurs avec les épaisseurs moitié des mêmes matériaux utilisés comme écrans extérieurs à la source (8,9 g/cm² pour le sulfate et 9,75 g/cm² pour le chlorure), montre que l'épaisseur moitié d'auto-absorption est plus grande que celle d'absorption extérieure du rayonnement d'un facteur d'environ 2,3.

En utilisant l'activité spécifique du coesium^{137}, 22 c/g[7] et les valeurs des coefficients d'absorption trouvés pour le chlorure de coesium^{137} (0,071 cm²/g) et sulfate de coesium^{137} (0,078 cm²/g) on a construit (Fig. 9) des courbes d'activité que l'on peut obtenir pour des sources cylindriques de différentes dimensions et on a comparé ces activités avec les activités réelles que l'on obtient sans tenir compte de l'auto-absorption. Le groupe des courbes 1 représente les activités des sources de l'ordre de 1000 c, en supposant un diamètre de source de 2,76 cm (S = 6 cm²) et le groupe 2, les activités des sources de l'ordre de quelques centaines de curies, en supposant un diamètre de source de 1,6 cm (S = 2 cm²). Nous avons considéré la densité du chlorure et sulfate de coesium, obtenus par compression, égale, pour les deux sels, à 3,6 g/cm³. La densité superficielle correspondante à 1 cm de hauteur est donc de 3,6 g/cm².

Considérant l'utilisation des sources linéaires, on s'aperçoit qu'à cause de l'auto-absorption une augmentation de poids de source au-delà d'une hauteur d'environ 5 cm (densité superficielle de 18 g/cm²) augmente très peu l'activité obtenue de la source. C'est pourquoi le choix du sel de moindre coefficient d'absorption et d'activité spécifique plus grande, devient important. On voit aussi des courbes de la Fig. 9 que, tandis

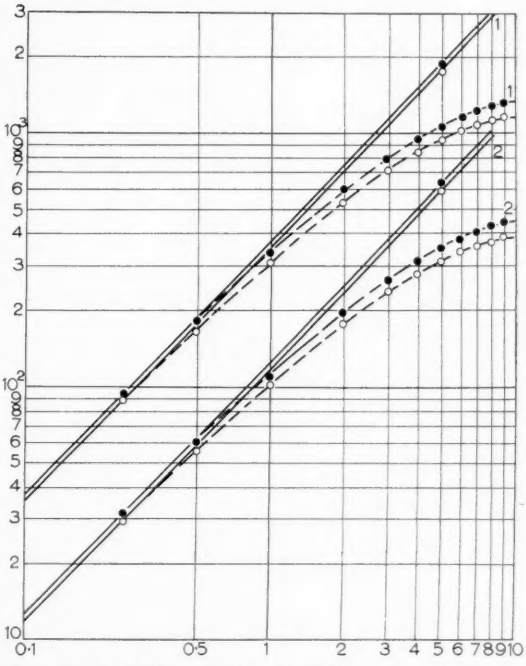

FIG. 9. Activités calculées de chlorure et sulfate de coesium^{137} en fonction de la hauteur de la source.
Abscisse: hauteur de la source (cm)
Ordonnée: activité (curies)
. : chlorure
o : sulfate
Ligne continue: activité non corrigée pour l'auto-absorption.
Ligne discontinue: activité corrigée pour l'auto-absorption.
Courbe 1. Diamètre de la source: 2,76 cm (S = 6 cm²)
Courbe 2. Diamètre de la source: 1,6 cm (S = 2 cm²)

que les différences entre les activités d'une source de même dimension de chlorure ou sulfate de coesium, à cause de l'activité spécifique, est de 7,5 pour cent en faveur du chlorure, cette différence augmente avec la croîssance de la densité superficielle des sels à cause de leur auto-absorption différente.

Tableau 4. Différence d'activité (%) obtenue avec des sources de mêmes dimensions en chlorure et sulfate de coesium. Densité des sels = 3,6 g/cm³

Hauteur de la source (cm)	Densité superficielle du sel (g/cm²)	Auto-absorption dans le chlorure (%)	Auto-absorption dans le sulfate (%)	Activité sulfate* / Activité chlorure (%)
1	3,6	12,2	12,8	91,3
2	7,2	21,7	23,4	90,0
3	10,8	30,2	32,3	89,0
4	14,4	37,3	39,8	88,2
5	18,0	43,5	46,2	87,3
6	21,6	48,8	51,5	86,7
7	25,2	53,5	56,2	85,9
8	28,8	57,4	60,1	85,3
9	32,4	60,8	63,5	84,8
10	36,0	63,9	66,6	84,2

* Compte tenu de la différence des activités spécifiques (7,5%) en faveur du chlorure.

Dans le Tableau 4 sont données quelques valeurs des différences d'activités obtenues des sources de mêmes dimensions, de chlorure et sulfate de Cs^{137}, en fonction de la densité superficielle du sel.

Dans ce tableau on trouve aussi les valeurs de l'auto-absorption dans le chlorure et le sulfate de coesium correspondants à une hauteur de source variant de 1 à 10 cm.

Considérant que par les avantages qu'il présente du point de vue de l'activité spécifique et de l'auto-absorption, le chlorure de coesium sera utilisé dans la préparation des sources, on a construit pour le chlorure de Cs^{137} un nomographe des activités corrigées et non corrigées pour l'auto-absorption correspondantes à différents diamètres et hauteurs de source (Fig. 10).

Le nomographe des activités non corrigées a été construit en utilisant la formule:

$$A_0 = \frac{\pi d_0^2 \, h_0 \times \rho \times A_S}{4} = 49{,}2 \, d_0^2 \qquad (3)$$

où:

A_0 = activité (curies) non corrigée pour l'auto-absorption
d_0 = diamètre de la source (cm)
h_0 = hauteur de la source (cm)
ρ = densité du ClCs = 3,6 g/cm³
A_S = activité spécifique du ClCs = 17,5 c/g.

Le nomographe des activités corrigées pour l'auto-absorption a été construit en utilisant la formule:

$$A_1 = \frac{\pi d_1^2 \times h_1 \times \rho \times A_S \times (1 - e^{-\mu \rho h_1})}{4 \times \mu \rho h_1} = 193{,}5 \, d^2 \, (1 - e^{-0{,}256 h_1}) \qquad (4)$$

où:

d_1, h_1, ρ, A_S ont respectivement la signification de d_0, h_0, ρ, A_S dans la formule (3) et

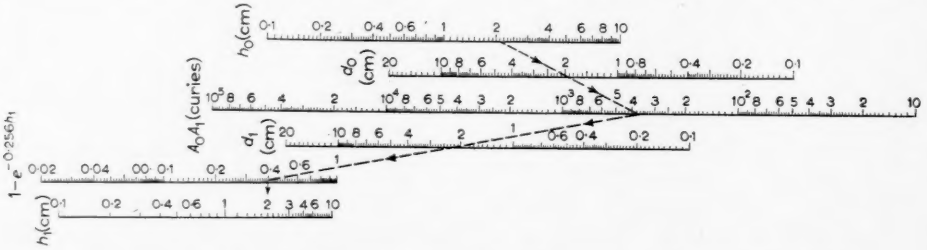

Fig. 10. Nomographe des diamètres et hauteurs des sources de $ClCs^{137}$ correspondants à différentes activités.

A_1 = activité (curies) corrigés pour l'auto-absorption
μ = coefficient d'absorption massique = 0,071 cm²/g

L'échelle $(1 - e^{-0{,}256 h_1})$ est une échelle intermédiaire a partir de laquelle, en traçant

une perpendiculaire, on trouve la hauteur correspondante sur l'échelle h_1.

On voit que pour choisir les dimensions d'une source d'activité désirée, compte tenu de l'auto-absorption, on a, selon les points que l'on joint sur l'échelle A_0, A_1, d_1, $(1 - e^{-0,256h_1})$, différents choix de diamètre et hauteur de source. Ainsi, par exemple, pour une source d'environ 340 c, on trouve comme posibilité (ligne pointillée avec flèche) de choisir une source de 2 cm de diamètre et 2 cm de hauteur. En joignant les valeurs de hauteur et de diamètre trouvés auparavant sur les échelles h_0, d_0, on trouve sur l'échelle A_0, A_1 l'activité que aurait la même source en absence d'auto-absorption.

3. *Conclusions*

L'auto-absorption dans les sels de Cs^{137} joue un rôle important dans le choix de sources de coesium. Autant que possible on choisira une densité superficielle faible afin de diminuer cet effet.

Dans ce même but, on a aussi intérêt à choisir comme matériau le chlorure de coesium, étant donné sa plus grande activité spécifique et son moindre coefficient d'absorption.

BIBLIOGRAPHIE

1. Fisher C. et Raggenbass A., *Int. Conf. on Radioisotopes in Scientific Research, Paris*, 1957. UNESCO/NS/RIC/13.
2. Eastwood W. S. AERE C/R 1231, p. 137.
3. Carter P. E. et Myerscough L. C. *Peaceful Uses of Atomic Energy* **14,** 96 (1955).
4. Sunderman D. N. AECU 3159.
5. Rupp A. F., *Int. Conf. on Peaceful Uses of Atomic Energy, Geneva*, 1955. A/CONF 8/P/315.
6. Warner G. F., The manufacture of kilocurie Cs^{137} from fission product wastes. *Congrès de Chimie Industrielle, Paris*, 1956.
7. Saddington K., *Int. Conf. on Radioisotopes in Scientific Research, Paris*, 1957. UNESCO/NS/RIC/16.
8. Kirk R. E. et Othmer D. F. *Encyclopedia of Chemical Technology* **14,** 369 (1955).
9. Hushley W. J. et Dixon W. R. *Canad. J. Res.* A 25, 210 (1947).
10. Perry W. E. *Proc. Phys. Soc.* **57,** 178 (1945).
11. Dixon W. R. *Nucleonics* **8,** 68 (1951).
12. Weiss H. F. et Weiss C. *Phys. Z.* **36,** 486 (1935).
13. Brucer M., TID 5086.
14. Fano U. *Nucleonics* **11,** No. 8, 8 (1953).
15. Goodman C. *et al. Science and Engineering of Nuclear Power* p. 38. Addison Wesley (1947).
16. Evans R. D. *The Atomic Nucleus* p. 716. McGraw-Hill, New York (1955).
17. Beers Y. *Rev. Sci. Instrum.* **13,** 72 (1942).

OL.
4
8/59

technical notes

Use of RIHSA in Differentiating Ascites due to Nephritis and Cirrhosis

(*Received* 17 *February* 1958;
in revised form 5 *March* 1958)

THE author during the determination of human blood volume using radio-iodinated human serum albumin also plotted the plasma clearance curves of several patients. After an intravenous injection of RIHSA diluted in isotonic saline, the isotope level in plasma may be said to remain more or less constant for about 30 min; then it is cleared out, first rather

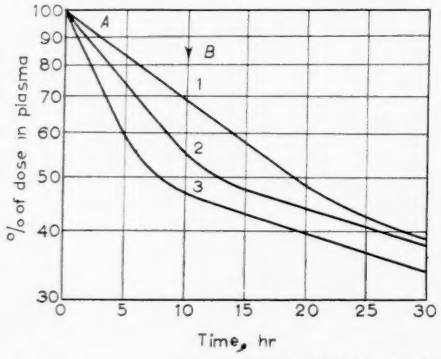

FIG. 1. Mean plasma clearance of RIHSA; (1) cirrhosis, (2) normal, (3) nephritis.

rapidly, then slowly. A semi-logarithmic plot of the distribution of the concentration of the isotope with time for 3 days shows a superposition of two exponential curves; the bending occurs within 24 hr.

A closer study, collecting blood samples at intervals of 3–4 hr for 30 hr, shows a definite bending of the curve at about 12th hr for the normal subjects, and this time factor is different for patients suffering from nephritis and cirrhosis. The initial slope is also different for normal, nephritis and cirrhosis cases, and the statistical variation in any group does not interfere with other groups. Fig. 1 shows the mean curves for a number of normal subjects and patients suffering from nephritis and cirrhosis. This suggests the possibility of differentiating the cases and the condition of the cases. Initial rapid disappearance of albumin is due to the diffusion into the lymphatic system before it comes into equilibrium with the vascular and extra-vascular albumin.

The method can further be simplified by choosing two fixed points like A and B at intervals of 10 min and 10 hr. The point A corresponds to the stage of mixing of the isotope with blood and the point B gives a convenient resolution of blood isotope level for different cases. Now, the deviation of the ratio of A to B from the normal value gives the condition of kidney and liver if either of the two is damaged, the mean normal value being $1{\cdot}8 \pm 0{\cdot}2$. The values of the ratio of A to B for 12 normal subjects range from 1·62 to 1·94 and those for 6 nephritis cases lie between 2·10–2·18 and 8 cirrhosis cases from 1·24 to 1·42. So, this method may be applicable to some extent in kidney and liver functional tests.

The present observation is mainly confined to healthy normal subjects and clinically established subacute nephritis and Laennec's cirrhosis cases. This work has been done both using conventional tracer doses of 10–20 μc of I^{131} tagged human serum albumin and low doses between 1–2 μc. For conventional doses a thin-walled endwindow β-counter and for lower doses a gas flow geiger counter in anticoincidence[1] have been used. A counting time of 15–30 min has been found suitable to keep the statistical error less than 3 per cent. Samples same in quantity are counted under similar geometrical conditions and corrected for any radioactive decay from the time of collection of the blood to the time of radioactive measurement of the plasma. This is essential for obtaining correct values of the ratio.

Acknowledgements—I wish to thank Prof. B. D. NAG CHAUDHURI for his continued interest and advice and the Department of Atomic Energy, Government of India for awarding a research fellowship.

FAZLE HOSAIN

Institute of Nuclear Physics,
Calcutta 9 *(India)*

Reference

1. HOSAIN F. *Naturwissenschaften* **45,** 107 (1958).

VOL.
4
1958/5

On the Spatial Distribution of the Gamma-ray Dose from a Plane Source*

(*Received* 26 *October* 1956)

Much thought has been given in recent years to the problems of employing powerful sources of artificially radioactive isotopes in γ-irradiation installations. The applications of this branch of technology include research into the interaction of radiation with living matter, the cold sterilization of foodstuffs and medical supplies, and the speeding-up of polymerization and

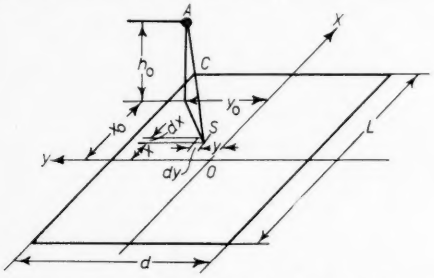

Fig. 1. A coordinate system for calculating the dose rate above a plane rectangular source.

halogenation processes.[1,2,3] A point source of radiation is normally unsuitable for irradiating bulk matter, owing to the inverse square dependence of the dose rate on distance; a more uniform exposure is obtained with a source in the form of a plane. Calculations and measurements for such a plane source are described below.

Calculation of the dose from a plane source

Consider the rectangular plane source of Fig. 1, which we suppose to be of negligible thickness so that self-absorption may be ignored. If the specific (per unit area) activity be q, the accumulated dose D_A at the point $A(x_0,y_0,h_0)$ after a time t will be given by

$$D_A = kqt\int_{-L/2}^{+L/2} \frac{1}{\sqrt{(x-x_0)^2+h_0^2}} \times \left(\tan^{-1}\frac{y_0 - d/2}{\sqrt{(x-x_0)^2+h_0^2}} + \tan^{-1}\frac{y_0 + d/2}{\sqrt{(x-x_0)^2+h_0^2}}\right) dx. \quad (1)$$

As shown in Fig. 1, L and d are the length and breadth of the rectangle; k is the ionisation constant of the source.

If $d/L \doteq 1$, the dose at a point directly over the centre of the rectangle can alternatively be calculated by an approximate procedure. The dose from any one of the isosceles triangles into which the rectangle is divided by its diagonals is roughly equal to the mean of the two doses which would be calculated for the

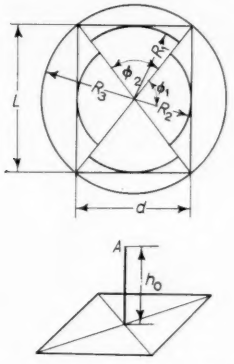

Fig. 2. Illustrating an approximate method of calculating the dose above the centre of the rectangle.

inscribed and circumscribed circular sectors. Using the magnitudes defined in Fig. 2, the dose rate at $A(h_0)$ from one sector is

$$P_{AR_i} = kq\int_0^{\varphi_0}\int_0^R \frac{r\,d\varphi\,dr}{r^2+h_0^2} = \tfrac{1}{2}kq\varphi_0 \ln\left(1+\frac{R^2}{h_0^2}\right), \quad (2)$$

and from the whole source

$$P_A = 2\left(\frac{P_{AR_3}+P_{AR_1}}{2}\right)_{\varphi_2} + 2\left(\frac{P_{AR_3}+P_{AR_2}}{2}\right)_{\varphi_1}$$
$$= \frac{1}{2}\frac{kQ}{Ld}\left[(\varphi_2+\varphi_1)\ln\left(1+\frac{R_3^2}{h_0^2}\right) + \varphi_2\ln\left(1+\frac{R_1^2}{h_0^2}\right) + \varphi_1\ln\left(1+\frac{R_2^2}{h_0^2}\right)\right] \text{r.hr}^{-1}. \quad (3)$$

Q here is the total activity in mg equiv. of radium. If $1 > d/L > 0{\cdot}6$, this formula gives a figure within 10 per cent of equation 1.

The dose at a point a distance h_0 above the centre of a source of strength $Q = 1000$ mg equiv. of radium and having $L = 100$ cm has been calculated as a function of d by numerical integration of equation 1, with the result shown in Fig. 3.

Measurements

Sources simulating the rectangular plane of the preceding section were constructed from 1 metre rods of Co^{60}, 6 mm in diameter and sheathed in 0·5 mm aluminium. The total activity of such a source was

* Translated by R. D. Lowde from *Atomnaya Energiya* **3**, 338 (1957).

675 mg equiv. of radium (418 mc). Measurements were made by the ILK luminescence method, using activated phosphor dosimeters which were simultaneously exposed for 5 min. Since the accuracy of a single observation by this method is only 10–15 per cent, each measurement was made three to five times with different indicators. Figures 4, 5 and 6 show surveys of the distribution of dose rate D in air between two similar parallel rectangular sources having $L = 100$ cm and $d = 60$ cm, separated by a distance H cm. The dose rate is expressed as the fraction of the value D_0 found at the geometrical centre of the system.

From these and other measurements, isodose curves have been constructed for the dose distributions between sources of $L = 100$ cm, $d = 20$, 40 and 60 cm and $H = 10$ and 15 cm. One family of curves is reproduced in Fig. 7. They are of interest particularly from the point of view of deciding the maximum size of object which can be given an irradiation of prescribed uniformity. It was found that the variation of dose with h is very similar to that which is observed along the diameter of a hollow cylindrical source of the same length L. The region in which the dose is constant within 10 per cent extends longitudinally over 0·7 L in both cases; in the transverse direction it is 0·5 H with the parallel plates and 0·5 δ for a cylinder of diameter δ. Along the y-axis, the parallel

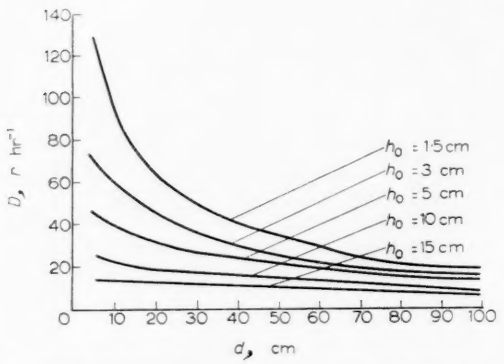

FIG. 3. Computed dose rates at a point a distance h_0 above the centre of a plane rectangular source of total activity 1 g equiv. of radium and $L = 100$ cm, as a function of d.

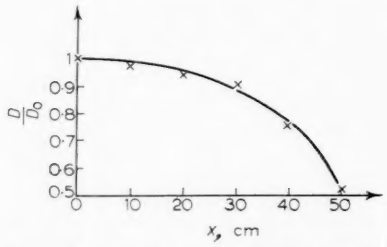

FIG. 4. The observed dose rate distribution along the (lengthwise) x axis centrally between two parallel rectangular sources separated by $H = 20$ cm.

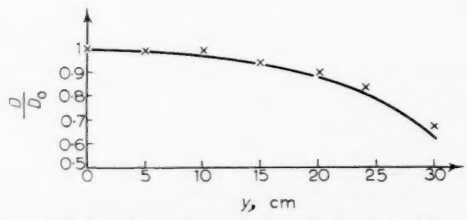

FIG. 5. The observed dose rate distribution along the (transverse) y axis centrally between two parallel rectangular sources separated by $H = 20$ cm.

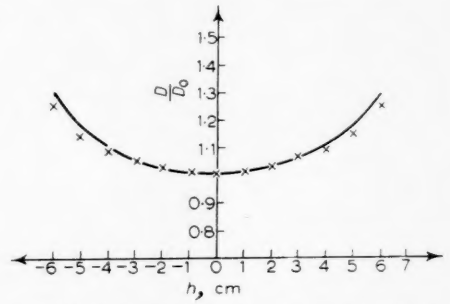

FIG. 6. The observed dose rate distribution along the h axis between two parallel rectangular sources separated by $H = 15$ cm.

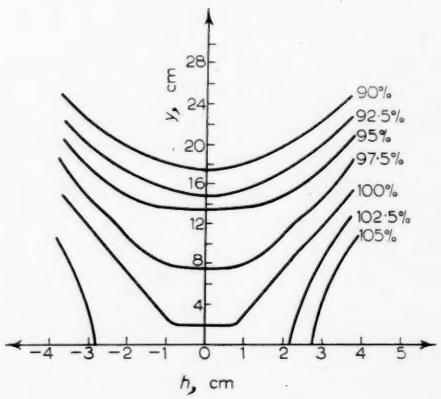

FIG. 7. Isodose curves for the region between two parallel rectangular sources of $L = 100$ cm and $d = 60$ cm separated by $H = 10$ cm.

VOL. 4 1958/5

plates give a distinct advantage, uniformity of dose rate being found within 10 per cent over $0{\cdot}7\ d$; this is again to be compared with $0{\cdot}5\ \delta$ in the case of the corresponding cylinder.

A comparison of the irradiation facilities offered by two parallel rectangular plates and by a hollow cylinder

The uniformity of the dose distribution within an irradiation enclosure is one of its most important characteristics; the greater the volume of uniform exposure, the greater the productivity of the unit. For special purposes such as the irradiation of rabbits and dogs, whose bodies are roughly cylindrical in shape, the cylindrical enclosure finds a natural application. However, for flat objects the arrangement with two parallel rectangles is preferable on account of its greater capacity in the y direction. This may be illustrated by comparing the outputs of the two alternative installations in a case where it is desired to irradiate, uniformly within 10 per cent, an object having the shape of a right rectangular parallelepiped. Suppose the enclosure is 1 metre long and the time taken to pass through is one minute. We consider a cylinder of diameter $\delta = 25{\cdot}44$ cm; the allowed transverse dimension is then $0{\cdot}5\ \delta$, i.e. 12·72 cm. Putting the density $\rho = 1$ for simplicity, the capacity is

$$P = 0{\cdot}5\delta \times 0{\cdot}5\delta \times L\rho = 12{\cdot}72 \times 12{\cdot}72 \times 100 \times 1 = 16{\cdot}18 \text{ kg}$$

If the total activity of the cylinder is $Q = 1000$ mg equiv. of radium, the dose rate at the centre will be 0·291 r min^{-1}. The corresponding rectangular array is of spacing $H = 25{\cdot}44$ cm and has the same surface area as the cylinder; the plates are therefore of width $d = \frac{1}{2}\pi\delta = 40$ cm. The required uniformity of dose can be obtained over a cross-section of $0{\cdot}5H \times 0{\cdot}7d$; the capacity is accordingly

$$P = 0{\cdot}5H \times 0{\cdot}7d \times L\rho = 35{\cdot}616 \text{ kg}$$

with a dose rate at the centre of 0·21 r min^{-1}. The productivity of the rectangular array is seen to be 1·6 times that of the equivalent hollow cylinder.

U. Ia. Margulis
A. V. Khrustalev

References

1. *Industrial Uses of Radioactive Fission Products.* USAEC (1951).
2. Duffey D. *Nucleonics* **11,** 10, 8 (1954).
3. Lewis G. J. *et al. Nucleonics* **12,** 1, 40 (1954).

All-glass Apparatus for Micro-synthesis of Radioactive Solids

(*Received* 6 *January* 1958)

The preparation of milligram amounts of radioactive organic compounds frequently calls for elaborate apparatus and shielding devices which are not always readily available in small laboratories. Syntheses resulting in 15–30 mg of radioactive solids of high specific activity, using relatively short lived radioisotopes, and involving reaction with continuous stirring, precipitation, washing and drying of the resultant compound in a short period of time, usually involve several pieces of apparatus, several manipulations, or a reaction train. We have recently developed an inexpensive all-glass apparatus to handle such preparations. The preparation of radioiodinated 2-amino-3,4-di-iodobenzoic acid (specific activity 400 μc per mg) is described as an example of the use of this apparatus.

Materials and methods

Construction of apparatus

Fig. 1 is an exploded view of the apparatus. The reaction chamber consists of a filter stick (Corning No. 39570–10F) cut down to $2\frac{1}{2}$ in. length and having a capacity of about 5 ml. It is sealed below the sintered glass disc to a 14/20 male standard taper joint, which fits into a 14/20 female joint at the bottom of a small glass cup. The latter has a male 24/40 joint at its lower extremity, and serves as a receptacle for circulating hot or cold water, or for crushed ice. The entire assembly fits into the neck (24/40) of a 50 ml filtration flask. The assembled apparatus is $6\frac{1}{2}$ in. high, which allows efficient shielding with a minimum number of lead bricks.

The sintered glass plate in the reaction chamber serves as a floor for reacting solutions. This plate will not allow the passage of liquids by gravity over a period 2–3 hr. Continuous stirring is performed by slight positive pressure (air or inert gas) through the side of the filtration flask; slight positive pressure is necessary to eliminate passage of liquids through the filter plate over periods longer than 3 hr. Waste liquors or reaction products in solution are drawn off into the flask by suction via the same route. Washing and drying of precipitates is readily performed by the same means. Glass hooks on the apparatus allow the use of spring clips between components, to permit the use of positive pressure.

Use of apparatus in the preparation of radio-iodinated 2-amino-3,4-di-iodobenzoic acid

In a separate container, 130 mc of NaI^{131} (carrier free) was evaporated to about 0·2 ml at 110°C; a

gentle flow of nitrogen was allowed to impinge on the liquid surface, to eliminate boiling. When cool, 0·45 ml of a solution of iodine monochloride in glacial acetic acid (0·04 ml ICl in 0·75 ml acetic acid) was introduced and mixed; $I^{131}Cl$ was rapidly formed by exchange. 0·25 ml of a solution of anthranilic acid in glacial acetic acid (30 mg anthranilic acid in 0·25 ml acetic acid) was placed in the reaction chamber, and stirred with a gentle air current. 0·45 ml $I^{131}Cl$ in glacial acetic acid was added dropwise, (using a distance pipette) over a 5 min period, after which the $I^{131}Cl$ container was washed out twice with 0·5 ml volumes of glacial acetic acid, these washes being combined in the reaction chamber. After 20 min of continuous stirring, 3 ml water were added, mixed thoroughly, air stirring stopped, and negative pressure applied to draw the precipitate down on the filter disc. The sides of the reaction vessel were washed down with a thin stream of water, and the washed precipitate allowed to dry over a 20 min period, by suction. The crude radioactive 2-amino-3,5-di-iodobenzoic acid can be purified by solution in ammonium hydroxide and reprecipitation with hydrochloric acid, the process being repeated as often as necessary. The method used is a modification of the original method of WHEELER and JOHNS[1].

Results

By the method described, 20 to 25 mg of radioactive 2-amino-3,5-di-iodobenzoic acid can be prepared and purified in a total time of a little over an hour, in a single reaction vessel. The specific activity of the compound was 400 μc/mg.

Discussion

The preparation described above is an example of a multistage microsynthesis which can be performed rapidly and with a minimum of manipulation in the apparatus described.

The flexibility of the apparatus is considerable. The material prepared can be subjected to several further reactions yielding a solid product, or a liquid form or solution of a further reaction product, in the same reaction vessel, the product in the latter instance being collected merely by substituting a clean 50 ml flask. For example, the substituted benzoic acid could be diazotized after drying and coupled with proteins for immunological studies. Replicate units can easily be set up simultaneously, or reaction vessels can be interchanged indefinitely by substituting fresh reaction chambers. Conversion for use with volatile solvents, involving positive pressure, is accomplished by modification of the top of the reaction vessel to accommodate a female 19/38 socket, engaging with a lead-in line ending in a male 19/38 plug (not shown in the illustration).

P. C. RAJAM
MARGARET E. WIRGAU

Department of Bacteriology
University of Michigan Medical School
Ann Arbor, Michigan

Pediatrics Laboratory U. M. TSAO
University Hospital
University of Michigan
Ann Arbor, Michigan

Reference

1. WHEELER H. L. and JOHNS C. O. *J. Amer. Chem. Soc.* **43,** 398 (1910).

Micro Counter Tubes for Beta-gamma Measurements

(*Received* 30 *December* 1957)

BETA–GAMMA sensitive micro counter tubes of the Maze type have been developed for radioisotope tracer work. The tubes can be sterilized and used in humans for medical diagnosis by radioisotope uptake and for biological research. Flexible lead wires are hermetically sealed to the metal-encased glass tubes. Volumes range from 2 mm^3 to 850 mm^3, and wall thicknesses range from 0.4 MeV to 0.2 MeV. Thinner windows have been made in some types. Life is $>10^7$ counts, with helium filling. Practical beta detection sensitivity is 0.001 to 0.01 μc at 1.0 cm distance in air. Similar tubes 1.0 mm o.d., 6 mm to 30 mm long have been made for interchangeable use in needle-type probes. Techniques of construction and typical β response characteristics to Sr–Y^{90}, Co^{60}, Y^{90}, and Ra γ-rays are given.

1. Introduction

An obvious requirement for the measurement of the weakest radioactivity is that the sensing element respond to individual particles or quanta. Some form of counter that gives digital indication is accordingly required, rather than a macroscopic device such as an ionization chamber or semiconductor. Detectors for internal use in medical diagnosis by radioisotope uptake in humans, or for biological experiments in animals, must be as small and mechanically flexible as possible. Scintillation detectors have limitations due to the size of the multiplier tube and the necessity for use of a rigid probe; otherwise they would be ideal for this work.

VOL
4
1958/5

VOL.
4
8/59

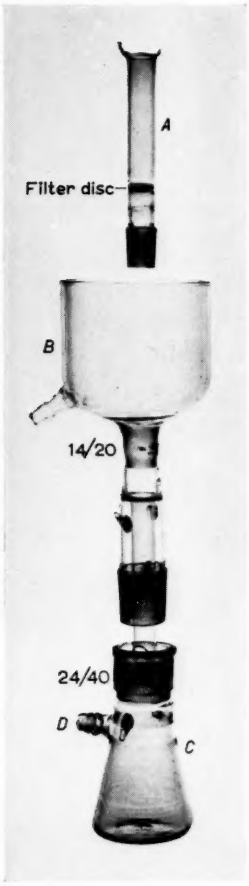

FIG. 1. Exploded view of apparatus
A. Reaction chamber with 14/20 standard taper joint.
B. Bath with 14/20 joint and 24/40 joint.
C. 50 ml Erlenmeyer filtration flask with 24/40 joint.
D. Side arm for application of positive or negative pressure.

VOL
4
1958/

Geiger–Mueller counters hitherto described have usually incorporated a gas reservoir external to the counting volume, to minimize the rate of deterioration of characteristics resulting from discharges of the tube or from chemical reaction of the quenching agent with the electrodes.

NAKAYAMA[1] has reported use of Geiger–Mueller tubes, without gas reservoirs, for studies of P^{32} uptake in cases of gastric cancer. Tubes 5 mm in diameter by 20 mm long, and smaller tubes, were successfully used on flexible leads to show preferential uptake of the radioisotope by certain cancerous tissues.

This paper describes sub-miniature counter tubes developed for measurements of local concentrations of beta or gamma emitters in humans, or for other applications requiring maximum flexibility of the detector. The tubes are beta–gamma sensitive, and the gas is wholly contained in the sensitive volume. Two flexible leads, hermetically sealed to the tube, serve as electrical leads and as a mechanical means of inserting the tube in a surgical manipulator, or directing it to the point of application through plastic or metal tubing. The counter tube walls are gold-plated nickel sheaths electroformed over very thin glass tubing, and can be sterilized for use in direct contact with tissue. Life in excess of 10 million counts, without significant deterioration of tube characteristics has been obtained, even for tubes whose volume is less than 3 mm^3. Work reported here is based on production of 135 successful tubes by techniques considered satisfactory. Production techniques have been adopted as satisfactory when the rejection rate due to all causes fell to less than 20 per cent of tubes assembled. About 600 experimental tubes were consumed in all phases of this work, principally for studies of variations of characteristics with gas content, with especial reference to tube life. For this purpose it was necessary to seal tubes off the pump system and to run life tests with a digital scaler, with intermittent evaluation of performance.

VOL. 4 58/59

2. Structure

Diameters of tubes range from 1 to 6 mm. Lengths range from 5 mm to 30 mm. It is evident that construction of a 1 mm diameter beta counter tube of conventional Geiger-Mueller form would be very difficult, although it is not impossible. Consequently the method of MAZE[2,3] has been adopted. Electrical characteristics of Maze tubes are especially good when the envelopes are of very thin glass. Elimination of an internal metallic cathode is also advantageous from the standpoint of maintaining gas cleanliness.

A polished chromium–iron–nickel alloy wire 0.127 mm in diameter, thermally compatible with the glass, is used for the anode. This wire is tipped with a glass bead 0.5 mm in diameter and beaded for sealing in the envelope. Due to the thinness of the glass, a micro-flame about 1 mm in diameter is used for assembly of the tube. The flame does not touch the glass, but melts it by convection and radiation. All glassblowing is done under magnification.

Tubing for the envelopes is hand-drawn, except for those of 6 mm diameter. Suitable tubing is selected by visual inspection of wall thickness and uniformity and annealed in a furnace. The glass walls range from 0.035 to 0.064 mm thick. When a metal sheath is electroformed over this, the total beta absorption is of the order of 0.20 to 0.25 MeV for small tubes. For tubes 6 mm diameter, the total absorption is approximately 0.38–0.40 MeV, with the standard wall. Concave bubble windows have been made in a few 6 mm o.d. tubes, to pass betas of still lower energies.

Since the functional cathode of a Maze tube is believed to be an ionic layer on the internal surface of the glass, formed and maintained by electrolysis through the wall, selection of suitable glass is important. Of many types tested, Kimble flint glass gave the best performance and was used for production. After sealing the anode wire, a cathode layer of graphite from a colloidal dispersion in alcohol is applied, and the tube is sealed in a larger manifold-connecting tube with thermosetting resin or hard wax. No constriction is used for seal-off purposes, due to the thinness of the glass wall. Outgassing is done on the vacuum system with radiant heat and repeated gas flushing with hydrogen, followed by helium.

The most satisfactory gas filling tested was tank helium at 36 cm of Hg pressure, 25°C. Condensable vapors and gases are removed or reduced in pressure by a cold trap refrigerated with liquid nitrogen. The pressure is not very critical, but fillings under 10 cm of Hg led to shorter tube life and to occasional discharges of the entire gas content of the tube, instead of the limited conical-volume discharge of a normal counter. The same filling is used in all tubes of this type, through an electrode radius ratio of about 6.

After filling, the tubes are sealed off the vacuum manifold with a micro-flame, stored under heat as an accelerated test for microscopic leakage, and tested for performance. The principal production loss is at seal-off, where atmospheric pressure and surface tension of the softened glass combine to shrink cavities in the ends of the tubes. Irregularity of the tip is later smoothed by adding thermosetting resin.

A cathode connection is formed by attaching a stainless steel wire of 0.127 mm diameter along the entire length of the tube wall. This is fixed at each end with an epoxy resin and provides an electrical

ground connection to the cathode and a firm mechanical grip on both ends of the tube. The wire is later incorporated in an electroformed metal sheath and serves to hold all parts of the tube together, in case of accidental breakage in use.

An external cathode is formed by coating the wall and tip of the tube with a baked graphite film 0.007–0.01 mm thick. A total thickness of not more than 0.025 mm of metal is next electroformed over the tube. Successive layers are: graphite, metallic silver paint, nickel, and pure gold. The gold is applied to protect the nickel sheath from chemical attack. Plating current densities are kept below the point of gas evolution at the cathode, and baths of good throwing-power are used, with rapid agitation of the work. Electroformed deposits cannot safely be polished, due to the delicacy of the glass. In earlier tubes, rhodium plating was used instead of gold. But rhodium sometimes tended to peel at the edge or to crack, whereas gold retains good ductility.

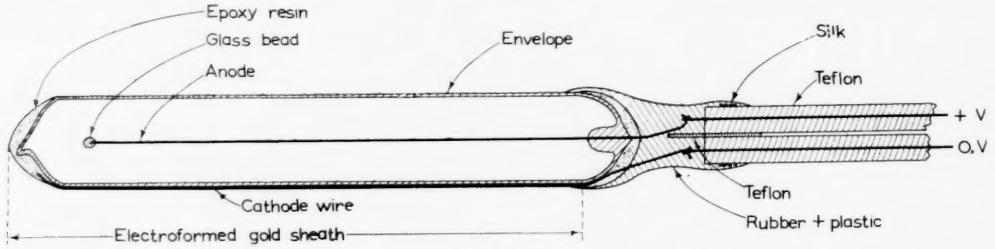

FIG. 1

3. Attachment of leads

The lead wires are stranded silver-plated copper with teflon* insulation, 1.0 mm o.d. This insulation has excellent chemical inertness, electrical resistivity, heat resistance, and tensile strength. Insulation of the soldered junctions between the tube wires and the leads presents problems almost as difficult as production of the tubes themselves. Clearance between the wires is usually only 0.3–1.0 mm, the field strength in this region is 3000 to 10,000 V/cm, and the wires must be allowed to flex while immersed in conducting fluids. Since the counter tube is usually used with an amplifier whose sensitivity is in the low millivolt range, it is necessary to maintain insulation resistance of many thousands of megohms. Leakage currents observed under such conditions are often sporadic, leading to spurious counting not arising in the tube itself. Insulating materials were accordingly adopted only after they are studied for leakage while immersed in conducting fluid for 6 hr. The water absorption properties of thermosetting resins, for example, may be affected by the amount of catalyst used, and by the completeness of curing. Diffusion of water through solid insulators is slow, and the moisture can gradually be expelled by heating in a stream of air above 120°C for 5–10 hr.

Composite insulation has been found most successful for covering the soldered joints. A separator of teflon sheet, 0.15 mm thick, is used between the soldered joints to prevent short-circuiting, and the wires are firmly tied together with silk thread, about 5 mm from the joints. A rubber–plastic insulating compound is applied over the connections and cured for 6 hr in an air stream at 130°C. Complete drying is essential, since solvents often show electrolytic conductivity. For larger tubes, stiffness may be added at desired places by applying epoxy resin and curing, followed by additional rubber–plastic insulation. Resistance measurement is the best indicator of the condition of the seal: resistances of 10^{11} to $5 \times 10^{12}\ \Omega$ are regularly obtained in finished tubes. The rubber–plastic compound is soluble in chloroform, butyl acetate, and ketones, but insoluble in water, alcohols, xylene, benzene, or petroleum hydrocarbons. Penetration of solvents is important in connection with wet sterilization of the tube, since autoclaving would probably damage the insulating compound. Sterilizing agents such as tincture of benzalkonium chloride do not attack the insulation.

Fig. 1 shows the structure of the micro-tube. Fig. 2 shows a collection of tubes ranging from 6.0 mm o.d. × 25 mm long to 1.0 mm o.d. × 5 mm long. The wires of one tube are encased in polyethylene surgical tubing 2.37 mm o.d. × 1.65 mm i.d. The internal volume of the smallest tube shown is approximately 2·0 mm^3.

Fig. 3 shows a hypodermic needle type probe and a collection of 1 mm o.d. tubes for use in the needle. These tubes range from 6 mm to 30 mm active length. The probe may have either a sharp or rounded point. In either case, the closure is a short length of Pt–Ir wire silver-soldered in the end of the stainless steel tube. Only one wire is attached to the counter tube, since the gold-tipped cathode is held in contact with the end of the grounded needle. Tubes

* Tensolite 30221A1. Polytetrafluoroethylene insulation.

VOL 4 1958/5

VOL.
4
8/59

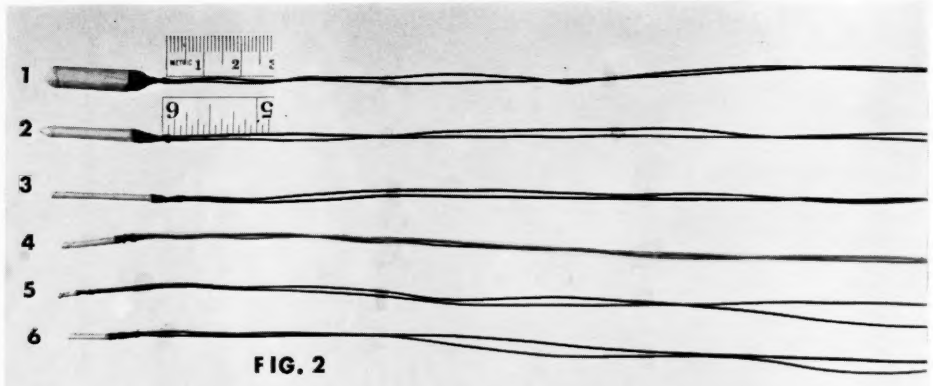

FIG. 2

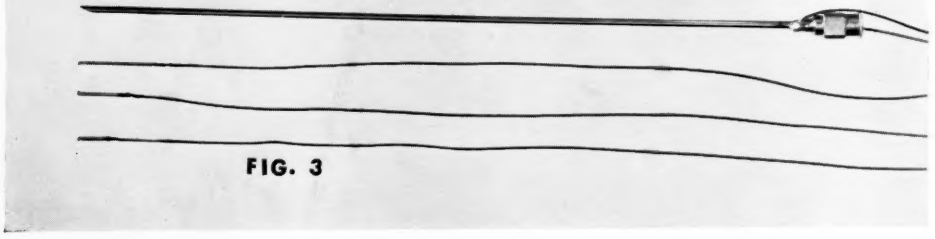

FIG. 3

VOL.
4
1958/5

of various lengths can be interchanged in this probe in a few seconds, to vary the volume being explored for radioactivity, with minimum loss of time.

4. Electrical characteristics

Operating voltages are of the order of 325–400 V, with a practical plateau lengths of 50–75 V. Variations in optimum operating voltage are observed, due to variable cave-in when the tubes are sealed off and gas evolution during subsequent baking. Since the background rates of the small tubes are under 1 count/min, threshold and plateau tests must be made in the presence of a beta or gamma source.

In addition to reduction of field strength in the insulating compound over the soldered joints, use of low voltage reduces rate of damage to the gas in normal use. The latter can be further reduced by insertion of a series resistor of 20 to 100 MΩ in the positive high-voltage supply line to the tube anode. Loss of pulse-height at high counting speeds, resulting from use of the resistor is easily offset by slight increase of gain of the pulse amplifier. At low rates, the resistor has no effect on pulse-height.

Decline of pulse-height with increasing counting rate is characteristic of Maze tubes. It is therefore desirable to use a pre-amplifier of sufficient gain ahead of the multivibrator stage of the indicating instrument. In practice, the writer has mainly used an amplifier with 12 mV sensitivity, with filaments operated on d.c. to eliminate hum. A coaxial input cable 200 cm long, with polyethylene insulation and capacity of 150 $\mu\mu$f is used to separate the electronic equipment from the area of use of the tube. For low counting rates, an amplifier sensitivity of 0.25 to 0.5 V suffices.

The output meter may be either a digital scaler or rate-meter. If a rate-meter is used, it should have adequately low minimum ranges and a choice of time constants. A loud speaker is often a convenient indicator when rapid exploration is necessary, but it should not be relied upon to make fine intensity discriminations at low rates, because of illusory effects arising from randomness of time-distribution of counts.

Other electrical characteristics resemble those of Maze tubes, in general. On the basis of several thousands of Maze tubes of forty to fifty structural forms, the writer finds that:

(1) Maximum counting rate in the presence of a strong source increases with amplifier gain.

(2) Maze tubes can be used from 0°C to 120°C; the plateau shortens with rising temperature.

TABLE 1. Response of tubes to β- and γ-radiation

(A) *Dimensions.* Tube numbers same as in Fig. 2

Tube No.	Diameter (mm)	Active length (mm)	Total length (mm)
1	6.0	25.0	30.0
2	3.0	25.0	30.0
3	1.8	27.0	32.0
4	1.5	14.0	27.0
5	1.0	3.5	6.0

(B) *β and γ Response.* β sources at 1·0 cm distance

Tube No.	Sr–Y^{90}* (counts/min per μc)	Co^{60}* (counts/min per μc)	Y^{90}† (counts/min per μc)	Ra γ‡ (counts/min per mr per hr)
1	5.5×10^4	3.0×10^3	1.4×10^5	141.2
2	2.0×10^4	1.2×10^4	2.7×10^4	41.5
3	1.1×10^4	5.1×10^3	1.7×10^4	28.7
4	4.8×10^3	1.3×10^3	6.5×10^3	7.4
5	8.0×10^2	4.9×10^2	7.9×10^2	0.42

* Source diameter 1·0 cm. Covering <2 mg/cm^2. Strength 0·0045/μc.
† Source diameter 2·5 cm. Sr^{90} β's removed by filtration. Strength 0·012 μc.
‡ Filtered through 0·5 mm Pt–Ir needle wall.

(3) Light should be excluded by black lacquer or other opaque coating. Photosensitivity may develop with use, especially with H_2 fillings. This is attributed to free sodium or other low work-function cathode layer generated by electrolysis.

(4) Rigidity and centering of the anodes are less important than in conventional G–M tubes.

(5) Many variant forms can be made. For example a tube formed like a Dewar flask can be operated without internal electrodes; a Maze tube can be made by painting conducting rings around a gas-filled glass tube.

(6) Action of quenching agents and position of the Geiger threshold are approximately identical with those of analogous G–M tubes.

5. Radiation response

Table 1 shows response of typical tubes to three types of beta source distributed over circular areas at a minimum distance of 1.0 cm in air.

Due to increase of projected wall thickness arising from curvature of the glass envelope, the effective window area is obviously smaller than the nominal area, for low-energy betas. This is shown by comparing Co^{60} and Y^{90} counting rates. Any of the tubes is capable of detecting 0.001 to 0.01 μc of beta emitter at 1.0 cm distance if the beta energy exceeds the tube window thickness, on arrival at the window.

Acknowledgements—The writer wishes to acknowledge the skilled assistance of E. Fountain, who did much of the delicate glass work.

G. L. Locher

Western Radiation Laboratory,
1107 W. 24th Street Los Angeles,
California, U.S.A.

References

1. Nakayama K. *Surgery* **39,** 736 (1956).
2. Maze R. *J. Phys. Radium* **7,** 164 (1946).
3. Curran S. C. and Craggs J. D. *Counting Tubes,* Academic Press, New York; Butterworths, London (1949).

Absolute Counting of β-Particles by Means of a Plastic Scintillator

(*Received* 18 *December* 1957; *in revised form* 12 *February* 1958)

4π geometry is obtained by the use of a split plastic scintillator. The absolute counting rate is determined by extrapolating to zero voltage the bias curves measured with three different values of the high voltage on the photomultiplier tube.

The method to be discussed in the following was developed at Kjeller in the years 1952 and 1953. It is fully described in a *Jener* Publication,[1] but otherwise no description exists. Since the method is a rather simple one, it might perhaps be of some interest for other people working in this field and a short description will be given here.

Description and procedure

The first experiments were carried out with small crystals of NaI(Tl) which were irradiated with neutrons. It was found that the activities induced in sodium and iodine could be measured absolutely by extrapolation of the discriminator bias curves to zero bias.[1,2] Thus neutron densities may be measured in an easy and fairly accurate way by means of small crystals of sodium iodide, but the crystals cannot be used for β-counting in general, since only the activities induced in the crystals themselves can be measured.

However, experiments have shown that the extrapolation method may be applied to a number of active materials other than iodine and sodium when a split plastic scintillator is used instead of sodium iodide crystals. The plastic scintillator used in the present experiments was a French product.[3] Two pieces were used, shaped like half cylinders or rectangular prisms. The active material in the form of a foil or a powder was placed between the two pieces which were pressed together and put on the photocathode of a photomultiplier tube. The plane between the two plastic pieces was standing normal to the photocathode and thus 4π geometry was obtained. The weight of the material was determined directly in the case of foils. When a powder was used it was placed on one of the plastic pieces and its weight determined as the difference between the weight of the plastic piece with and without the powder. Small amounts of active material were used, varying from 3 to 13 mg. It is estimated that the thickness did not exceed 10 mg/cm^2.

To determine the absolute counting rate a discriminator was used which passed only pulses higher than a certain fixed voltage or bias. The counting rate was measured as a function of discriminator bias for three different settings of the high voltage on the photomultiplier tube. If the activity decreased significantly during the measurements, all measured values of the counting rate were referred back to the end of the irradiation in order to obtain the correct functions. Then the functions were drawn as curves (called bias curves). An example of such a set of curves obtained from a measurement on sodium carbonate is shown in Fig. 1. The bias curves are drawn so as to cut the ordinate axis at the same point. Therefore each single curve is

VOL.
4
1958/5

not necessarily the best fit to the set of experimental points obtained for a specific value of the high voltage. If the bias curves gave a true picture of the β-spectrum they should not be straight lines since the integrated β-spectrum is not a linear function. Actually, a

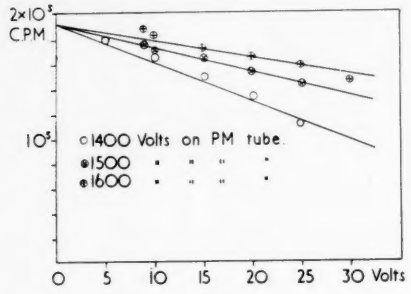

FIG. 1.

number of cases have been observed when the bias curves were not straight lines, but in most cases they had the form shown in Fig. 1. The extrapolation to zero bias could be carried out easily also in the case of non-linear bias curves.

Results

Now let N be the counting rate at the end of the irradiation corresponding to zero bias. This quantity, of course, is not measured directly, but determined from the measured curves. The mass m of the sample is known, and thus the number N/m can be calculated. It is clear that if N is equal to the absolute counting rate, then N/m must be a constant for samples which have been simultaneously irradiated. On the other hand, if N is less than the absolute counting rate because of losses of soft β-particles, one would expect N/m to decrease somewhat with increasing mass, since the loss of β-particles would probably be greater with a greater mass of the sample. The experiments indicate definitely that N/m is a constant for samples simultaneously irradiated. In twenty-six cases two such samples were examined and in 21 of them the difference in N/m was less than 5 per cent. In one case five aluminium foils were simultaneously irradiated and the standard deviation obtained was 7·5 per cent. In another case nine aluminium foils gave a standard deviation of 3·6 per cent, whereas nine samples of phosphorus in the form of red powder gave a standard deviation of 4·0 per cent. A number of other cases with three or four samples simultaneously irradiated gave similar results. For sample weights between 3 and 13 mg no correlation was observed between N/m and m. If now, S is the true specific activity one may put $N/m = fS$, and it is clear that for the cases mentioned above f is a constant which does not depend upon the sample weight. It is difficult to see how this could be the case unless f is equal to or at least very nearly equal to one. It is concluded, therefore, that N/m is the true specific activity of the sample within an error of 5 per cent, and from this follows that N is the absolute counting rate given with the same accuracy. In fact it has been verified also by comparison with other measurements that N is the absolute counting rate.

Discussion

The results referred to above were all obtained from measurements of samples emitting β-particles with maximum energies of 0·96 MeV or more. Some experiments were made with iron samples emitting two groups of β-particles, one with a maximum energy of 0·46 MeV and another one with a maximum energy of 0·257 MeV. The accuracy was poor in this case, probably not better than 30 per cent. There are two main reasons for this. First of all, the self-absorption will be quite substantial with such soft β-particles and secondly it is necessary to work with a high amplification, with a resulting increase in the background. This background is due mainly to some sort of phosphorescence induced in the scintillator when it is exposed to light. There seem to be two components of this phosphorescence, one which decays with a half-life of about 1·5 min and one which decays with a half-life of about 150 min. It might be possible to reduce the effect of the phosphorescence if the scintillator were exposed to red light only. This, however, would require a special room for the countings and the weight determinations, and would thus reduce the simplicity of the method. Since the phosphorescence is not constant it is difficult to make the proper corrections for it. Therefore, the absolute activity of the sample should not be smaller than 10000 disintegrations/min, otherwise the accuracy will become poorer. Even then one will often observe irregularities at the end of the bias curves, corresponding to low discriminator voltage, especially for the highest values of the high voltage. This is seen in Fig. 1.

Normally about 45 min are required to make a complete measurement of a powder sample. First the scintillator is washed with alcohol to remove any active powder from the previous measurement. Paraffin oil, which is used to secure good optical contact between the scintillator and the photocathode, is also removed by the washing. Then the weight of the new sample is determined and the scintillator is placed on the photocathode. It is left there a few minutes before the countings are started so that the short lived component of the phosphorescence will go down to a reasonable level.

The photo tube used during the present investigations was of the type EMI 5311. This tube is no longer in production, but certainly any photomultiplier tube with a flat cathode could be used for this sort of measurements.

It should be emphasized that other methods exist for absolute counting of β-particles by means of scintillation counters, which are more accurate than the one discussed in this paper. However, these methods are certainly not so simple as the present one. One of them requires that the correct β-spectrum be measured[4,5] and this is not such an easy task as the simple determination of the bias curves referred to above. Another method requires the use of two multiplier tubes.[6] Both tubes face the scintillator and any light pulse there gives electron pulses in the two photo tubes. These are coupled in coincidence and thus any light pulse in the scintillator gives an output pulse, whereas noise pulses due to dark current will give no output pulses unless they appear in coincidence in the two tubes. In order to obtain the lowest possible background due to dark current, the whole set-up is placed inside a deep freezer. Thus the apparatus used by this method is rather complicated and a deep freezer is certainly not available at all laboratories.

The apparatus required for the extrapolation method discussed above is the simplest possible one to be used in connection with scintillation counters, and the measurements are easily made. Hence the method might be useful in cases where high accuracy is not needed.

B. GRIMELAND

Joint Establishment for Nuclear Energy Research, Kjeller per Lillestrøm, Norway

References

1. GRIMELAND B. *Jener Publication* No. 12 (1956).
2. GRIMELAND B. *Phys. Rev.* **86,** 937 (1952).
3. PICHAT L. and KOECHLIN Y. *J. Chim. Phys.* **48,** 225 (1951).
4. KETELLE B. H. *Phys. Rev.* **80,** 758 (1950).
5. GOOD M. I. *Phys. Rev.* **83,** 1054 (1951).
6. KOFOED-HANSEN O. *E.A.E.S. Symposium* VIII–57, Zurich (17/18 October, 1957).

An Automatic Sample Changer for Well-type Scintillation Counters

(*Received* 26 *December* 1957; *in revised form* 21 *March* 1958)

A simple and reliable automatic sample changer for use with well-type scintillation counters has been constructed. A maximum of 25 samples may be assayed at one time by placing them in special carrier assemblies which are then inserted in a turntable mounted above the counter. A moving platform engages each carrier assembly in turn and positions it in the well. Although designed to operate directly with, and without modification of, specific commercially-available equipment, its principle of operation permits it to be readily modified for use with other counters, scalers or ratemeters.

Résumé

Il s'agit d'un simple changeur d'essais automatique et éprouvé à l'usage des compteurs de scintillation du type réservoir. Un maximum de 25 essais peuvent être mis à l'épreuve simultanément en les mettant dans des montures porteuses lesquelles sont ensuite introduites dans une plaque tournante, fixée au-dessus du compteur. Une base mouvante embraie chaque monture porteuse successivement er l'assigne son endroit dans le réservoir. Bien que le changeur soit construit pour fonctionner directement, sans modification, avec des appareils spécifiques qui peuvent être achetés, néanmoins son mode d'opération comporte sa prompte modification à l'usage d'autres compteurs, échelles graduées et instruments de mesure.

Zusammenfassung

Es handelt sich hier um einen neuen, ganz einfachen und zuverlässigen selbsttätigen Probenwechsler zum Gebrauch mit behälterähnlichen Szintillationszählern. Ein Höchstbetrag von 25 Proben kann gleichzeitig geprüft werden, indem man sie in besondere Traggestelle einsetzt, die dann ihrerseits in eine über dem Zähler angebrachte Drehscheibe eingefügt werden. Ein sich bewegender Untersatz nimmt der Reihe nach jedes Traggestell auf und weist ihm seinen Platz im Behälter an. Obgleich der Probenwechsler so hergestellt ist, dass man ihn unmittelbar mit besonderen, käuflichen Einrichtungen oder Apparaten ohne irgendwelche Abänderung verwenden kann, lässt es seine Arbeitsweise doch zu, dass er ganz leicht mit anderen Zählern, Anzeigern und Messgeräten benutzt werden kann.

КРАТКИЙ ОБЗОР

Речь идет о простом и надежном автоматическом приборе для смены образцов, применяющемся с сцинтилляционными счетчиками колодцеобразного типа. При помощи этого прибора можно подвергнуть испытанию до двадцати пяти образцов одновременно путем помещения их в специальные агрегатные носители, которые после этого вставляются в вращающийся стол, установленным над

VOL 4 1958/

VOL.
4
58/59

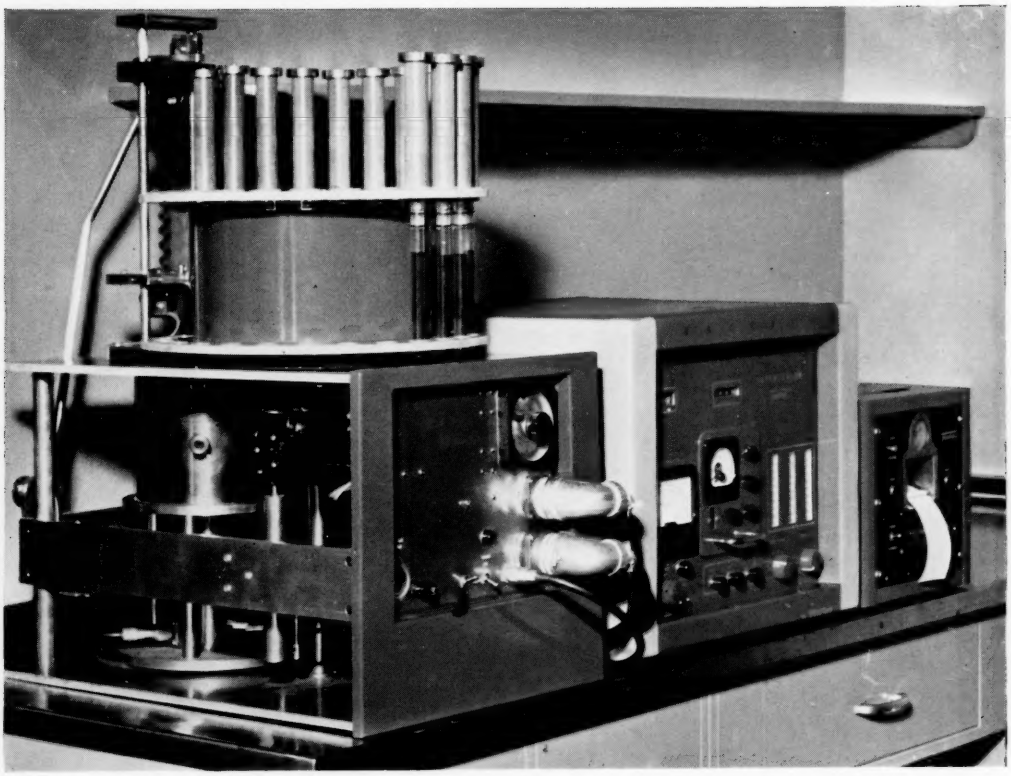

FIG. 1. Automatic sample changer and associated equipment. The well-type counter and shield are in place within the framework of the changer.

VOL
4
1958/

счетчиком. Движущаяся платформа включает каждый агрегатный носитель по очереди и помещает его в колодец. Хотя прибор предназначен для непосредственного действия оборудованием имеющемся в продаже, который не нуждается в модификации, принцип, на котором построено его действие, дает возможность его приспособления для употребления с другими счетчиками, пересчетными приборами и измерителями скорости счета.

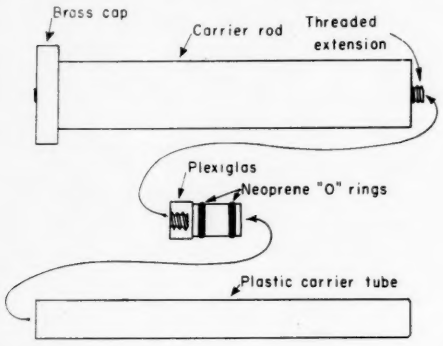

The widespread use of well-type scintillation counters has emphasized the need for an automatic sample changer for use with this type of detector. Demorest and Erickson[1] described an ingenious machine to perform this function which employed electromagnets to position and transfer samples. The present paper describes a sample changer of simple design, modest cost and reliable performance which employs mechanical rather than magnetic positioning. It incorporates readily available commercial components, consisting of a well-type scintillation counter and shield* scaler† and printer-timer‡ (Fig. 1).

A maximum of 25 samples at a time may be assayed by placing them in special carrier assemblies, the loaded carriers being inserted in a turntable which rotates above the well-type counter. A lifting platform engages each carrier assembly in turn and positions it in the well.

* Nancy Wood model SC2L
† Tracerlab model SC-18
‡ Tracerlab model SC-5C

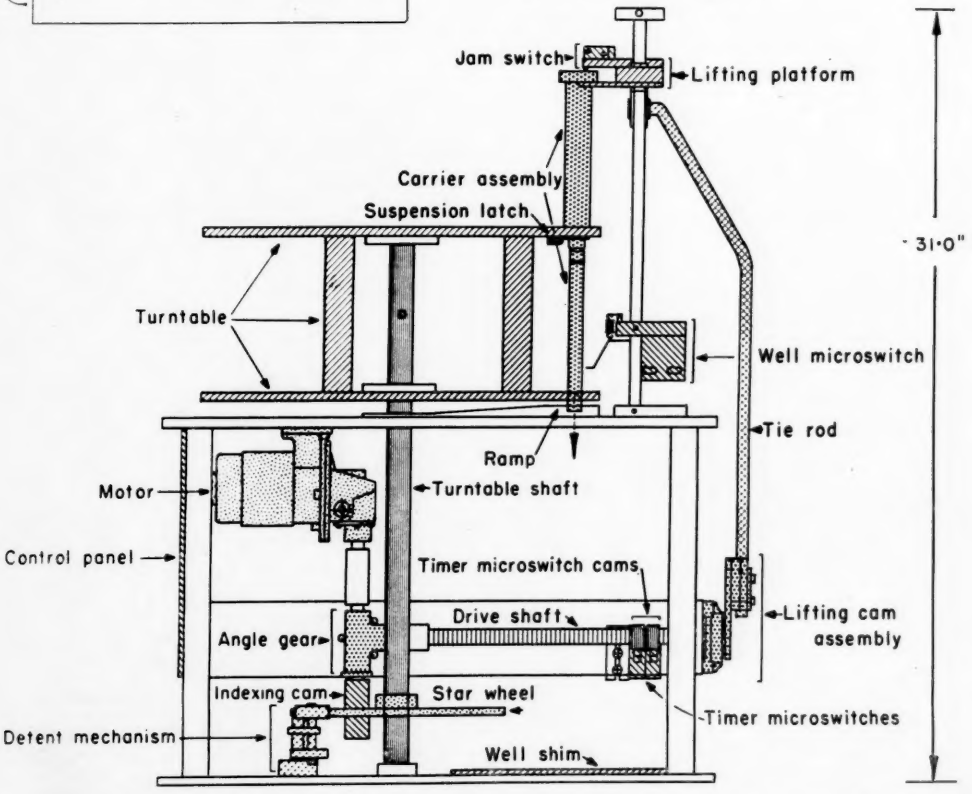

Fig. 2. Automatic sample changer showing principal items in its construction. Insert shows carrier assembly showing the individual units disassembled.

Construction

The major items in the construction are shown in Fig. 2. Each of the 25 carrier assemblies consists of a plastic tube,* a threaded Plexiglas tube cap with two concentric neoprene "O"-rings and a formica carrier rod with an oversize brass cap on top and a short threaded extension below. These units can be seen inset in Fig. 2.

A turntable with 25 holes lined with polyethylene is supported above an aluminum framework by a brass shaft. Twenty-five suspension latches are mounted beneath the top disc of the turntable, one at the periphery of each hole. These support the carrier assemblies and prevent the sample tubes from riding on the framework. A single aperture in the framework located at the counting position permits the sample tube to pass through to the counter well which is mounted between the frame-work on a spacing shim.

A 3.6 rev/min 1/70 h.p. capacitor motor performs all power functions. It is coupled to the input of a 1 : 1 ratio right angle gear drive which has two outputs. The horizontal output is coupled to a drive shaft which rotates a lifting cam. The vertical output rotates a cam which indexes a 25-position star wheel fastened to the turntable shaft; hence the turntable moves one position for each rotation of the motor.

*Celluplastic Corporation, 50 Avenue L., Newark, New Jersey.

A spring-loaded detent mechanism locks the star wheel at each position. Coupled to the lifting cam by a tie rod is a lifting platform consisting of a ledge and an overhanging pushing bar. The ledge accommodates the carrier assembly in counting position as well as the carriers on either side; the pushing bar, however, covers the central carrier assembly only. Mounted on the framework directly beneath the turntable is a positively inclined (in the direction of turntable rotation) formica ramp. In horizontal distance it covers an arc corresponding to 6 positions of the turntable. The ramp is placed so that its highest elevation is one position from the aperture in the framework.

The electronic assembly (Fig. 3) is confined primarily to a control panel mounted on one end of the framework. It contains the necessary circuitry including relays, switches and cable connectors. Two microswitches feeding voltage to the printer–timer are mounted beside the drive shaft and are activated by cams on the drive shaft. Mounted above the aperture in the framework is a spring-loaded lever attached to a microswitch. In the pushing bar of the lifting platform is an "anti-jam" safety-switch.

Sequence of operation

Starting approximately 4 positions before the counting position, the bottom of the plastic tube of the carrier assembly contacts the inclined ramp. With each index of the turntable the carrier assembly is

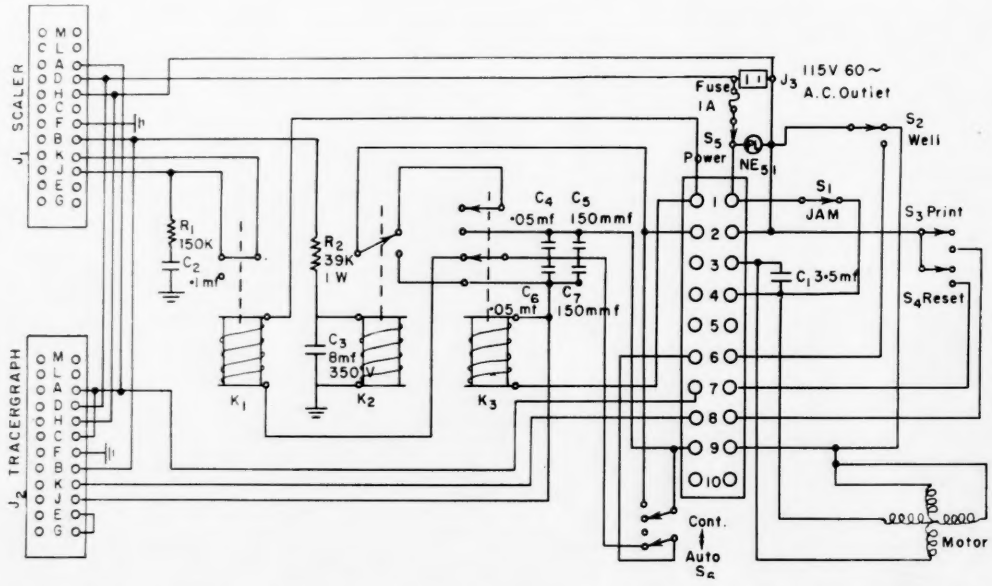

FIG. 3. Schematic diagram of electronic circuit. The cables from the printer–timer and scaler are connected directly to the individual jacks to complete the electronic assembly.

raised a few millimeters so that at one position before counting position the carrier is resting on the highest elevation on the ramp and the guide rod cap is above lifting platform ledge.

When the turntable indexes, the carrier assembly drops off the ramp and the guide rod cap slides along the lifting platform ledge and comes to rest beneath the pushing bar. The lifting platform then begins to descend and at half distance the printer–timer prints zero. When the tube is resting on the bottom of the well, the well microswitch is activated. This de-energizes the motor and simultaneously initiates the electronic sequence which starts the scaler and timer. At a predetermined number of counts scaling ceases, the timer prints and the motor is re-energized so that the sample is lifted out of the well. During the lifting operation the register of the printer–timer is reset, which completes one cycle of operation.

Normal cycling of the changer is interrupted only when the well microswitch, S2, is depressed. Hence, empty positions on the turntable are bypassed. In order to move the turntable rapidly through positions which do contain carrier assemblies a "continuous-automatic" switch is included. In the "continuous" position, the action of the well microswitch is negated.

As a safety precaution the jam-switch S1 was introduced. At any time during the lowering cycle should pressure on the pushing bar become excessive, S1 is activated and current to the motor is interrupted.

Although the sample changer was designed for the associated equipment mentioned above, relatively minor changes in dimensions need be made for other well-type counters. For example, with taller counters the height of the framework could be increased. Alternatively, a section of the lower plate of the framework could be removed to permit the counter to protrude from beneath the changer. The circuitry could also be adapted to permit operation with other scalers and timers. Thus, the automatic sample changer has been used successfully with a rate-meter and a strip chart recorder. In this operation an interval timer* (seen on the control panel in Fig. 1) is incorporated in a simpler circuit to provide a fixed delay following activation of the well microswitch. The delay is adjusted to be of sufficient length to permit the counting rate for each sample to reach an equilibrium reading on the rate-meter. A continuous tracing of the rate-meter deflection on the strip chart then gives the activity for each sample.

The geometric arrangement of the carriers in the turntable together with the shielding of the counter adequately prevent the contribution of significant radioactivity to the well by samples not in counting position. In practice it was found that the background was raised by an amount equivalent to only 0.01 per cent of the counting rate of samples immediately adjacent to the counting position.

In several months of continuous use, the sample changer has performed in a reliable fashion requiring, in the main, only periodic lubrication.

Radioisotope Service,
Veterans Administration Hospital,
Kansas City, Missouri, U.S.A.
DAVID V. COHN
WILLIAM E. CARTER
RICHARD ANDERSON
and
Department of Biochemistry,
University of Kansas Medical School,
Lawrence, Kansas, U.S.A.

* Eagle model HP25A6—Eagle Signal Corporation, Moline, Illinois.

Reference

1. DEMOREST H. L. and ERICKSON J. H., *Nucleonics* **12,** 68 (1954).

A Remotely Operating Flowmeter*

RADIOACTIVE isotopes find applications in the design of several types of measuring instruments.[1–3] We have used radioactive cobalt for making a remote-reading flowmeter for small liquid and gas flows, based on the usual rotameter.[4]

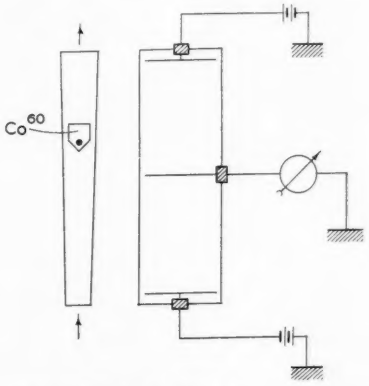

FIG. 1. The principle of the radioactive flowmeter.

Remote reading has until now been achieved by making use of changes in inductance, but experience shows that such flowmeters can not be used for small rates in the range 0·2–2 l/hr. Their sensitivity is small and can only be increased by introducing complex, stabilized electronic equipment. The necessity of making the rotameter tube of non-magnetic material can also be an inconvenience.

* Translated from *Atomnaya Energiya*.

These shortcomings can be overcome in a radioactive remote-reading flowmeter.

The apparatus is shown schematically in Fig. 1. The γ-source is contained in the float, the position of which is determined from the difference current in a compensated ionization chamber, e.g. of type filled with air at atmospheric pressure. Cylinder 1 is the collector electrode and 2 is the high voltage electrode. Cylinder 2 is cut in half and each half is fed with 200 V of opposite sign through the leads 3. Cylinders 4 and 5 are the chamber walls. The rotameter tube is inside the inner cylinder and is

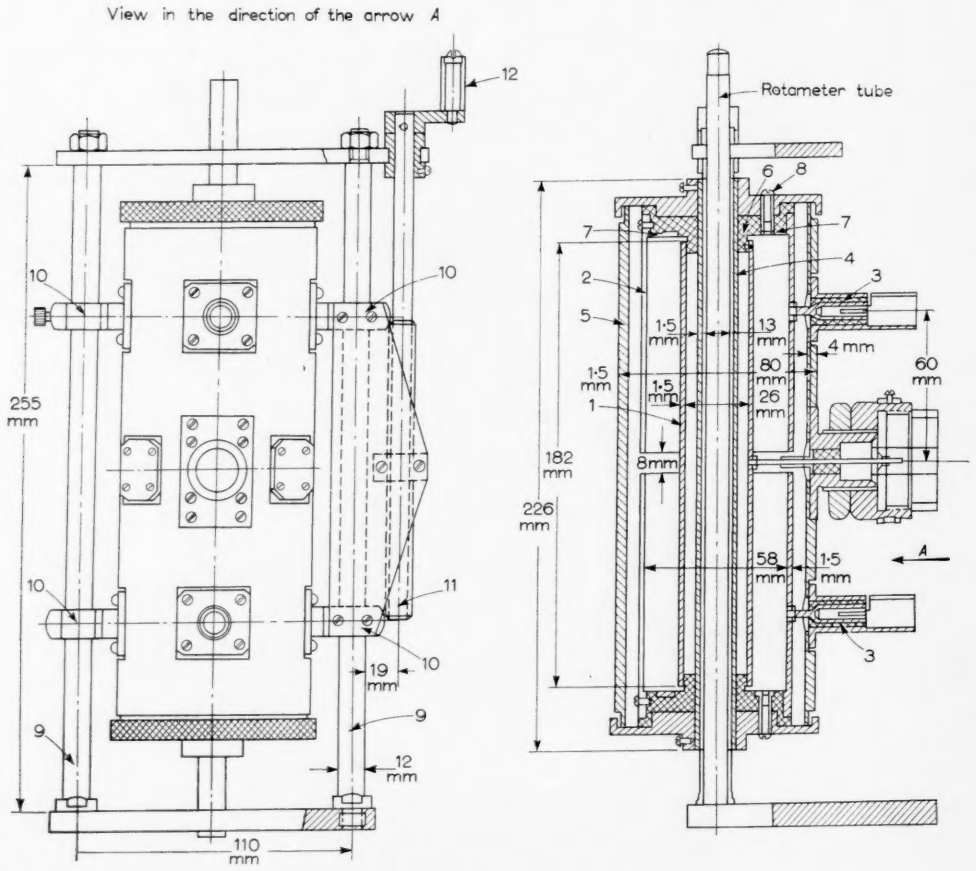

FIG. 2. The construction of the ionization chambers. 1, 2—electrodes, 3—leads, 4, 5—cylinders, 6—insulator, 7—ring, 8—screw, 9—supports, 10—nuts, 11—lifting screw, 12—handle.

SP. The amplifier scale is graduated in flow units and, if required, the signal can be fed to a recorder or to some regulator from a d.c. amplifier. Co^{60} is used as the γ-source in the form of a metal wire of 0·7–0·8 mm diameter; the strength is 2–5 mc. A piece is housed in the teflon float and the rotameter tube can be made of any material which suits the technological requirements.

The construction of the ionization chamber is shown in Fig. 2. It consists of four coaxial cylinders, sealed with rubber gaskets. The collector and high voltage electrodes are fixed to the Plexiglas insulators, 6, through which all leads from the electrodes pass. A guard ring 7, is fixed to insulator 6 and is connected to the case by a screw 8. The case of the chamber is fixed on two supports, 9, by the nuts, 10, and the chamber can be moved vertically by the screw and handle, 11 and 12, to alter the range of the flowmeter.

The dependence of the difference current on the

position of the float is given by the following expression:

$$\Delta I = 2\pi K\left\{R\left(\tan^{-1}\frac{H-Z}{R} + 2\tan^{-1}\frac{Z}{R} - \tan^{-1}\frac{H+Z}{R}\right) - r\left(\tan^{-1}\frac{H-Z}{r} + 2\tan^{-1}\frac{Z}{r} - \tan^{-1}\frac{H+Z}{r}\right) - \frac{1}{2}\left[(H-Z)\ln\frac{(H-Z)^2}{(H-Z)^2+R^2} + 2Z\ln\frac{Z^2+r^2}{Z^2+R^2} - (H+Z)\ln\frac{(H+Z)^2+r^2}{(H+Z)^2+R^2}\right]\right\}$$

where K is the constant of proportionality. The other terms are explained in Fig. 3 and the analysis shows that for $Z = 0$, $\Delta I = 0$, i.e. there is no current when the float is in the centre of the chamber. The function $f(Z)$ is odd, i.e. $f(-Z) = -f(Z)$ so that the current is symmetrical about the origin. Fig. 4 shows the curves $\Delta I = f(Z)$; curve 2 is calculated from the formula, while 1 is obtained experimentally. Over some ranges the function is

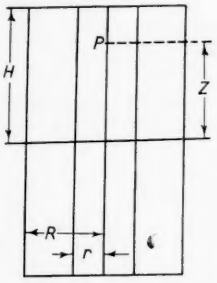

Fig. 3. Explanation of symbols used in the formula.

almost linear, with a corresponding linear scale for the flowmeter. The high sensitivity of the compensated chamber enables the position of the float to be fixed to within 0·5 mm or less.

Two types of flowmeter were made with this construction, one with 100 mm movement (RDR–1–100) and the other 50 mm (RDR–2–50). The flow range is determined by the rotameter tube and the float parameters. Under laboratory conditions experiments showed that the errors in determining flows were not greater than ±2·5 per cent for a range of 0·015–0·06 l/hr of carbon tetrachloride and of 0·2–2 l/hr of water.

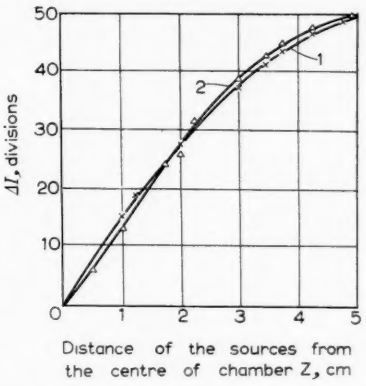

Fig. 4. Calibration curve for the flowmeter.

Similar instruments were tried under semi-industrial conditions 20 m from the control panel. The apparatus worked perfectly, with errors of not more than 2·5 per cent.

A model for automatic control of small liquid flows (0·5–3 l/hr) was based on the radioactive float principle and the small scale instruments were developed at IAT. The time required to determine a given flow rate is 50–60 sec.

N. S. Korshunov
M. V. Khatskevich

References

1. Shteibok, N. I. *Uspekhi Fizicheskikh Nauk* **4**, 231 (1954).
2. Jordan, G. G. *Priborostroeniye* **1**, 4 (1956).
3. Neiman M. B. *Izmeritel'naia Tekhnika* **1**, 10 (1955).
4. Korshunov N. S. *Avtorskoe Udostovereniye* No. 01971.

book reviews

Ionising Radiations and Cell Metabolism. A Ciba Foundation Symposium. Edited by G. E. W. Wolstenholme and Cecilia M. O'Connor, J. and A. Churchill, London, 1956. 318 pp. 45s.

One of the basic questions in radiobiology is whether radiation damage to the cell is primarily of structure or of process. In either case, metabolic disturbances must ensue. This volume surveys recent work in this field, often in a most pertinent manner. It records the proceedings of a small symposium held in March 1956 and of the high standard now expected of the Ciba Foundation. When a biochemist refers to 8000 r as a comparatively small dose of radiation (p. 60), the biologist is apt to smile, but recent findings have suggested that only a few tens of roentgens are needed to produce detectible changes in DNA. The biological relevance of this must still be in doubt, because nuclear control of metabolic processes seems normally to be at one or two removes (Brachet). Correlation of *in vitro* and *in vivo* effects depends on a knowledge of submicroscopic cellular organization (Dale), which emphasizes how ambitious it is to attempt to explain radiation damage in biochemical terms.

It is clearly much more widely appreciated than it used to be, that biochemical changes cannot be interpreted without parallel microscopic observations. There is no confirmed example of a change in enzymatic activity preceding visible cellular change (Pirie). Surveys included such generally important fields as protein synthesis, DNA synthesis, biochemical reactions during cell division, pacemakers of metabolic processes. It seems to the reviewer, however, that the effects of ionizing radiation on cellular metabolism are not likely to be based on processes common to all living matter. The amounts of radiation required to damage different kinds of cells, even in the same organism, may differ by several orders of magnitude: the biochemical lesion should therefore be closely linked to the metabolic differences between different types of cell rather than to what they have in common.

R. H. Mole

William H. Beierwaltes, Philip C. Johnson, and Arthur J. Solari: **Clinical Use of Radioisotopes,** W. B. Saunders Company, Philadelphia, 1957. 457 pp. 80s. 6d.

This well-organized and clearly written volume is designed to serve the needs of both the medical student and the clinician who is concerned with the practical clinical application of various radioisotopes. Following a complete reproduction of the regulations and requirements which must be met in the establishment of an isotope laboratory and the application of radioisotopes to human use in the U.S.A., there is a section devoted to the essential physical quantities involved and the way in which nuclear radiations may be detected and measured.

Four chapters are devoted to the use of iodine-131 in the study of thyroid function and in the diagnosis and treatment of thyroid disease. As a preliminary to the more technical applications, an entire chapter is devoted to thyroid physiology, the relation of the thyroid hormone to the endocrine system generally, and the effects of specific drugs on thyroid action. On this basis the subsequent discussions of tests of thyroid function and the other uses of radio-iodine in thyroid disease are presented in much more precise perspective than is usually the case.

A separate chapter is devoted to the various clinical uses of iodine-131 other than those concerned with the thyroid gland and its functions. Here the applications are largely those dealing with the use of a tag for protein which may be followed functionally in various regions of the body.

Radioactive phosphorus is given a separate chapter, as is also the case with radioactive gold. These isotopes, which have had extensive use in clinical medicine, have been very useful in a limited number of situations. The limitations of the uses are explicitly stated and the rationale of the applications in particular diseases has been generally clearly developed.

The remaining isotopes are covered in two chapters, chromium, cobalt, and iron in the radioactive forms being described in applications in hematology. These are tools of remarkable precision in the functional measurements upon which modern concepts of blood dyscrasias depend. Again, not only the techniques but the phyisological bases for the procedures have been stated.

The fact that all of the remaining isotopes are considered in a single chapter of incidental notes is probably an indication of the comparatively undeveloped state of our knowledge in this field. As an example, approximately one page of text is devoted to tritium, the radioactive isotope of hydrogen, and this concerns the measurement of body water, an important application. However, it is probably true that, along with carbon-14, tritium will become one of the most valuable of isotopes for the tagging of complex compounds for diagnostic purposes. It is a fair prediction that one of the measures

VOL 4 1958/

of the progress of knowledge in the next decade will be the degree to which the material of this one chapter will grow in volume as new and important applications not at present established become realized.

The volume concludes with a brief review of the fundamental aspects of radiobiology which form the basis for the procedures in health physics and general principles of radiation safety. Practical information on establishing and managing a clinical radioisotope unit should be of substantial assistance to those confronted with the problem of actually putting radioisotopes where they may be most effectively employed in medicine.

J. C. BUGHER

Basic Foundations of Isotope Technique for Technicians. Edited by W. C. SMULLEN. Blackwell Scientific Publishers, Oxford, and Charles C. Thomas, Illinois, 1956. 163 pp. 36s.

VOL. 4 58/59

THIS book is based on a series of lectures given by the various contributors at a training course for medical laboratory technicians at Decatur, Illinois. As AEBERSOLD points out in the first chapter, the increasingly wide spread use of radioisotope techniques in hospitals and clinics other than those associated with large Universities and Medical Schools has resulted in an increasing requirement for technical personnel who are familiar with these procedures. It is a comparatively simple matter to teach an untrained individual to carry out a given test as a drill by numbers, but it is important in clinical work that the data obtained should be reliable. This implies that the work should be done conscientiously, and the best guarantee of this is that the individual concerned should know not only how to carry out the necessary procedures but also why he is carrying them out.

The expressed purpose of the present volume is "to tempt the beginner into exploration of the various facets of isotope knowledge, rather than to overwhelm him with tedious technical ramifications." Consequently, it is rather unfortunate that a claim is made on the dust cover that it is a practical manual, because this is not the case. It can be assumed that the main emphasis of the course was on practical work and that the lectures were supplementary; this probably accounts for a certain lack of balance between the various subjects covered and for a number of important omissions. For example, it is difficult to see how various measurement techniques can be discussed intelligently without bringing in the question of statistical fluctuations and the effect of the background on experimental accuracy. As it is, the reader is likely to interpret a statement on p. 30 as implying that a scaler is more accurate than a ratemeter because it is not necessary to read a fluctuating needle. He might also accept without question the necessity for giving the decay correction of Au^{198} to six significant figures on p. 102 when the half life is quoted as $2{\cdot}697 \pm 0{\cdot}003$ days and the dose to be dispensed is in any case "decided clinically".

On the whole, the best chapters are those written by clinicians dealing with their individual subjects, and in this connexion LITTLE's chapter on the use of iodine in the diagnosis of thyroid disease is outstandingly well done. Not only is the rationale of the various possible tests discussed, but attention is given to some of the possible sources of error. G. W. MORGAN's discussion on the elements of radiation protection is also a particularly clear presentation of a difficult subject.

Some of the other chapters raise doubts about the desirability of choosing contributors who are identified with individual commercial firms for a volume of this nature.

In Great Britain the term "medical technician" is used in a rather more restricted sense than appears to be the case in the U.S.A. Most of the chapters in this volume would provide useful background reading for radiographers. The technician in the pathology department who is the person most likely to be carrying out low level tracer tests is not so well served. To such a person even the section on radiation protection is largely of academic interest, since the first new thing he must learn in practice is that the level of contamination which can make a laboratory impossible to work in, is considerably lower than the level which may constitute a health hazard.

The book is extremely well produced, and profusely illustrated, though the few drawings are far more informative than the many photographs. The present writer has submitted the book to a group of interested technicians who expressed the opinion that it was interesting to look through in the library, but they, as individuals, would not buy it. Thus the authors' main objective appears to have been achieved, and the acquisition of this book by hospital libraries might be recommended.

N. VEALL

Radioéléments artificiels. (Commissariat à l'Energie Atomique, Gif-sur-Yvette, 1957;) Imprimerie Hemmerlé, Petit & Cie, Paris, 1957. 137 pp.

THIS interesting catalogue is very similar in form to the Harwell catalogue (shortly to be reviewed in this journal). The chief difference is that in the main body of its catalogue the Commissariat a l'Énergie Atomique

unfortunately gives no reference to the sources of the data quoted. Thus under cobalt-60 a reference for the gamma ray energies of 1·1715 and 1·3316 MeV wou'd have been interesting; the National Research Council's *Nuclear Level Schemes* (1955) gives only three values, with references, for each, namely 1·1728, 1·1726 and 1·1724 MeV for the one and 1·3325, 1·3329 and 1·3309 MeV for the other. The catalogue is, however, somewhat more conservative in giving the half-life of this nuclide as 5·3 years (5·25 years and 5·27 years in the Harwell and Oak Ridge catalogues respectively).

In addition to its list of artificially radioactive nuclides available, there is catalogued a considerable number of different chemicals that can be obtained with hydrogen-3, carbon-14, nitrogen-15, sulphur-35, cobalt-60 and iodine-131 as tracers. The section dealing with health hazards and the precautions that can be taken in the use of radioactive materials is somewhat less comprehensively treated than in the Harwell catalogue but is adequate to draw the attention of new users both to the need for care and also to some of the less recent of the U.S. National Committee on Radiation Protection and Measurements Handbooks which are pertinent to the subject. Handbooks 54, 56 and 59 might perhaps also have been included. However, in spite of its recent date of publication the section on tolerance dose neglects to mention the most recent recommendations of the International Commission on Radiological Protection and dose is still referred to in terms of external radiation field in roentgens rather than the more recently accepted unit of RBE dose, the rem. The accumulated dose for radiation workers and the average dose for the population might also perhaps have been referred to. It appears, in fact, that the five sections in the chapter on "Precautions" have been taken from the March 1955 edition of the catalogue without any revision!

The Commissariat à l'Énergie Atomique is, however, to be congratulated on the standard that it has set in the production of this catalogue, and also on its convenient and useful form.

W. B. MANN

Radiation Biology. Edited by ALEXANDER HOLLAENDER. Vol. 1: **High Energy Radiations** 1265 + ix pp. 131s. 6d. 1954; Vol. II: **Ultraviolet and Related Radiations** 593 + x pp.; 60s. 1955; Vol. III: **Visible and Near-visible Light** 765 + viii pp. McGraw-Hill, New York, Toronto, London. 75s. 1956.

It has been suggested that the interest and fascination of radiobiology lies in the way in which it draws together scientists of differing disciplines and outlook. No better demonstration of this breadth of interest could be found than these 3 volumes under review. The authors range from agriculturists to zoologists (even including a psychologist) and their subjects from physics to sunburn. The books are prepared under the auspices of the National Research Council and Dr. Hollaender has been assisted in the editing by a number of distinguished helpers. Each of the 58 contributors to the 3 volumes is well known in his field. Most of them are from the United States but representatives from Great Britain, New Zealand, the Netherlands, Israel and Sweden are included.

The first volume is devoted to the effects of high energy radiation. The principles of radiological physics are dealt with in the opening chapter and this is followed by considerations of the relevant aspects of radiation chemistry and linear energy transfer. A detailed account is given of the effects of ionizing irradiation on cells both from the morphological and the genetic aspects. The results of irradiating the intact animal are well described in a series of chapters on embryology, physiology, and haematology and histology. The volume ends with a valuable summary of the facts which have accumulated on the cancer producing effects of ionizing radiation.

Vol. II is concerned primarily with ultra-violet light but many of the chapters contain material on high energy irradiation. The chapters on bacteria, viruses, fungi and protozoa cover both types of irradiation and as the principal editor points out, in this respect Vol. I and II should be regarded as a single unit. Ultra-violet light itself is considered in its physical aspects and is action on genes and chromosomes. Its effect on the skin, in the way of sunburn, and its cancer producing qualities also receive full attention. Chapters on photochemistry, photoreactivation and cytochemical methods are also included.

The third volume concerns visible and near-visible light and may not therefore be of such immediate interest to readers of this journal. The physical and chemical aspects are again fully dealt with including a consideration of the biologically important polyenes and porphyrins. Plant physiology naturally takes up a good deal of the volume with such subjects as photosynthesis in its various aspects, seed germination, and phototropism, photoperiodism, nitrate reduction and the various structural changes produced in protoplasm by visible light. Animal effects are covered by chapters on vision and the volume ends with a section on photodynamic action.

The appearance of these volumes and their imposing list of contents encourage one to expect an authoritative text but the chapters are more in the nature of a series of reviews. Only rarely is a chapter suitable to recommend to someone just entering the

VOL
4
1958/

field it covers and the majority of the sections will be found more useful to the experienced worker in search of references. The literature reviewed is very extensive but although the volumes were published from 1954 to 1956 few of the chapters were written after 1952. The lag in publication is unfortunate but no doubt unavoidable. In spite of this these volumes will be a valuable work of reference for radiobiologists, and others interested in the subjects they cover, for many years to come. Few of the chapters can be praised for their interesting style or attractive presentation but perhaps the reader should not expect such refinements in what are virtually review articles.

The twelve hundred or so pages of Vol. I would have made a very weighty book and the publishers have been wise in binding it in two parts. Their decision to do so however appears to have been made too late during production to provide any indication in the contents and index of whereabouts the division occurs and, what is more important, only one index and one list of contents is provided. Consequently this volume is not as convenient to use for reference purposes as it might otherwise be. In other ways the book production is very satisfactory, the printing is clear and the binding is well suited to the hard usage which these volumes will undoubtedly have to withstand.

E. V. HULSE

K. W. STENSTROM: **Manual of Radiation Therapy.** C. C. Thomas, Springfield, U.S.A., 1957 94 pp. 34s.

THIS little book is a working manual of basic radiotherapy techniques in use at the University of Minnesota, compiled as a guide for graduate students in radiology. A few of the more common medical uses of radioactive isotopes are mentioned but are not described in any detail.

The methods of radiation treatment outlined cover all the common conditions seen in a radiotherapy department. The dosage levels and fields prescribed are sound and conservative guides for a junior radiotherapist, especially when read in conjunction with Dr. OHLFELT's preface: "Actually, one of Dr. STENSTROM's most definite principles . . . is to treat each patient individually, varying the treatment as the patient and the disease respond." There is the usual difference from British practice in prescribing skin doses as roentgens measured in air, which we think may be misleading. There are only a few treatment policies advocated that might cause disagreement. For example, some therapists would not agree that surgery offers the best chance of cure of carcinoma of the tongue, and would use interstitial implants of radium, cobalt-60 or tantalum-182 in this and other sites more often than suggested by Dr. STENSTROM. A few selected references are included which are meant for American readers (the American publishers of Sir STANFORD CADE's book are quoted, and an American paper from Professor MCWHIRTER) and are not always the most accessible references for European radiologists.

There is a very good concise introduction to the *Basic Elements of Radiation Therapy* which would be even better with a selected bibliography, similar to that in the main body of the book. It might be extremely annoying to read, for instance, on page xiii about L. H. GRAY's views on radiochemistry without being given the reference to the paper being quoted. This is perhaps the fault of the publishers rather than the author. The reviewer has found only one minor printing error—on page 74 sub-heading "3. Malignant Melanoma" seems to be incorrectly positioned under "(2) Leukaemic infiltration" rather than under "2. Secondary skin cancer."

In general therefore this book is a good summary of the radiotherapy techniques in use at one centre in the United States, with emphasis on well tried methods of X-ray, radium and telecobalt treatment.

K. E. HALNAN

WILLIAM H. SULLIVAN: **Trilinear Chart of Nuclides.** U.S. Government Printing Office, Washington 25, D.C., 1957, 4 pp. + chart $2.00.

THE second edition of the *Trilinear Chart* needs no introduction, for its predecessor, the first edition of 1949, is already well-known. In this new edition the most important changes are to be found in a slight increase in size of the hexagonal plaques for each nuclide and the discarding of color in favor of black and white presentation. These changes have been accompanied by a very pleasing and quite definite transition above the threshold of legibility.

The mechanics of the new chart are similar to the old and it can, with a lot of fun with scalpel and gum, be assembled into a continuous concertina-like structure for very easy reference. It would however have been easier to hold if the mass numbers had been somewhat less ambitiously terminated, as might seem safe for the next decade at least, at 269 instead of 270! For those who have an uninterrupted study wall it will make an admirable $17\frac{1}{2}$ ft frieze!

From the technical point of view the chart contains a wealth of information and it is doubtful whether even Dr. SULLIVAN could squeeze anything more into

the space available. As a ready means of obtaining information quickly about any nuclide in the context of its neighbours and for rapid orientation the chart is ideal, especially after it has been removed from its cover and assembled by cutting and gumming. It contains far more information than the conventional wall charts and it is carefully assessed information by an outstanding authority in the field of nuclear data. If one desires detailed published data on a particular nuclide one would turn to the cards published by the National Research Council's Nuclear Data Group in which the reporting is objective and comprehensive. But for a great many purposes it is extremely useful to have most probable values and although there may be some who might hesitate to delegate their assessment of the most probable to anyone, there are many occasions where one is only too pleased to relax in the assurance of Dr. SULLIVAN's wide and encyclopedic knowledge.

It is planned to keep the new edition up-to-date by a periodic distribution of gummed hexagonal labels. This should be a most useful service to owners of the chart provided that no attempt is made to correct quite trivial mistakes by too frequent distributions of these labels.

This new edition of the *Trilinear Chart* will be a great asset to all those who wish to have readily accessible and up-to-date nuclear data.

W. B. MANN

Fortschritte der angewandten Radioisotopie und Grenzgebiete Band II. Edited by Dr. ALFRED HUTTIG, Verlag Heidelberg 1957. Preis: DM 32.00.

WIE im ersten Band sind die einzelnen Aufsätze zusammenfassende Berichte über allgemein interessierende Themen wie auch Berichte über die experimentelle Behandlung spezieller Probleme. Dass dabei Gebiete der Medizin und Biologie zunächst im Vordergrund stehen, ist verständlich.

In der Aufsätzen "*Isotope in der Technik*" von MONTENS und über Bau und Einrichtung von Radioisotopenabteilungen "von GRAUL und DREIHELLER" werden dem Interessenten, der sich in das Gebiet einarbeiten will sicher zahlreiche wertvolle Anregungen geboten. Es wäre aber zu erwägen, ob bei einer Neuauflage nicht ein Hinweis darauf erfolgen sollte, dass bei der Verwendung von langlebigen Isotopen in der Technik gelegentlich beträchtliche Störungen in messtechnischer Hinsicht auftreten können. Die Verwendung langlebiger Strahler (einige Hunderttausend Impulse pro Minute!!) zur Vermeidung elektrostatischer Aufladung bei guten analytischen Waagen, macht diese Instrumente für den Gebrauch in der Praxis völlig ungeeignet und da sie bisher nicht gekennzeichnet waren, sogar gefährlich. Co^{60} im Stahl oder Sr^{90} in Glasschmelzen sind weitere Beispiele für ernsthafte Störungsmöglichkeiten. Was den Bau von Isotopenlaboratorien betrifft, so könnte bei einer Neuauflage meines Erachtens ein Hinweis nicht schaden, dass man zwar mit einer Gruppe von ausgezeichnet geschulten und disziplinierten Mitarbeitern ohne Schaden anzurichten die meisten radioaktiven Arbeiten auch in einem normal eingerichteten Laboratorium ausführen kann, während auch das grösste Mass an Hilfsmitteln und Vorsichtsmassnahmen keinen ausreichenden Schutz gegen unsachgemässes Verhalten der Mitarbeiter bietet.

Für die speziellen Fragen, die in den Aufsätzen von H. BILLION über den "*Radiotest der Schilddrüsenfunktion*", E. H. GRAUL über "*Inkorporierung und Dekorporierung radioaktiver Spaltprodukte*", und W. KOCH über "*Die spezifische Strahlenreaktion des Knochens*" behandelt werden liegt der besondere Wert in der ausgezeichneten Literaturzusammenstellung und ihrer kritischen Auswertung. Da immer wieder festgestellt werden kann, wie stark die Reproduzierbarkeit experimenteller Daten schon von der jeweiligen Beschaffenheit der Versuchstiere abhängt, muss die Beschaffung eines möglichst reichhaltigen Zahlenmaterials ja dringend erwünscht sein. Einige Schönheitsfehler könnten vermieden werden. Auf Seite 33 soll es wohl heissen 0,1 g NaJ statt 1,0 cm^2 NaJ. Die Beschreibung auch "gebräuchlicher" Verfahren sollte bis in Einzelheiten gehen im Interesse einer Reproduzierbarkeit der Ergebnisse und ihrer Beurteilungsmöglichkeit durch Interessenten.

Folgerungen wie sie auf Seite 104 gezogen werden, dass z.B. die Halbwertszeit von $1{,}5 \cdot 10^9$ a beim Thorium es unwahrscheinlich macht, dass es innerhalb von 8 Tagen nach einer Thoriuminjektion zu einer genügenden ThX Ablagerung im Knochengewebe kommen kann, verraten, wenn sie ernst gemeint sind, einen bedenklichen Mangel an Überblick über Zerfall und Nachbildung radioaktiver Elemente. Es trifft diese Bemerkung nur für Radiothoriumfreie Thorium-Präparate zu, von denen vermutlich höchstens noch 1 auf der Erde existiert. Im übrigen ist bei genügend langlebiger Muttersubstanz die Geschwindigkeit der Nachbildung der Tochtersubstanz ausschliesslich von deren Halbwertszeit abhängig. In den meisten Fällen darf man also selbst bei frischen Thorium-Präparaten nach 8 Tagen mit einem erheblichen Prozentsatz ThX rechnen, der bei sehr alten Präparaten nach 8 Tagen auf 75% steigen kann.

F. STRASSMANN

VOL.
4
1958/

International Journal of Applied Radiation and Isotopes, 1959, Vol. 4, pp. 129–143. Pergamon Press Ltd. Printed in Northern Ireland

Rates of Transfer of Rb^{86}, K^{42}, K^{39}, Cl^{36}, Cl^{35}, Na^{22}, and Na^{23} across a Blister Surface on the Forearm of Normal Man and Patients with Chronic Congestive Heart Failure*

C. T. RAY and G. E. BURCH

Department of Medicine, Tulane University School of Medicine and the Charity Hospital of Louisiana at New Orleans

(*Received* 25 *March* 1958)

VOL. 4 8/59

The base of a cantharides blister on the forearm of man was utilized as a living membrane for the study of kinetics of electrolyte transfer. This preparation provided a readily reproducible and reliable model for such studies. Studies were made of transfer of Na^{23}, Na^{22}, Cl^{35}, Cl^{36}, K^{39}, K^{42} and Rb^{86} both into and out of the experimental extracorporeal compartment. Since the electrolytes and radioisotopes entered and left the extracorporeal compartment by way of capillaries, this model provided an approach to the study of transfer across capillary walls without the limitations of circulation and mixing which interfere with such studies from within the vascular tree. Transcapillary transfer of electrolytes was found to be very rapid. Estimation of the amount of electrolytes crossing the capillaries of man per day revealed enormous amounts: sodium chloride 60,000 lb and potassium 1900 lb at normal seral concentrations.

TAUX DE TRANSMISSION DU Rb^{86}, K^{42}, K^{39}, Cl^{36}, Cl^{35}, Na^{22} ET Na^{23} À TRAVERS LA SURFACE D'UNE AMPOULE SUR L'AVANT-BRAS DE L'HOMME NORMAL ET DE MALADES SOUFFRANT DE LA DÉFAILLANCE CARDIAQUE CHROMIQUE CONGESTIVE

Le fond d'une ampoule à cantharide sur l'avant-bras de l'homme fut employé comme membrane vivante pour l'étude de la kinétique du transfert électrolytique. Cette préparation donna un modèle facilement reproductible et sûr pour de telles études. On examina le transfert du Na^{23}, Na^{22}, Cl^{35}, Cl^{36}, K^{39}, K^{42} et Rb^{86} entrant dans et sortant de ce compartiment extra-corporel expérimental. Vu que les électrolytes et les radioisotopes entraient dans le compartiment extra-corporel, et le quittaient, par les capillaires, ce modèle donnait un rapprochement à l'étude du transfert à travers les parois capillaires sans les limitations de circulation et de mélangement qui gênent les études semblables faites dans l'arbre vasculaire. Il parut que le transfert des électrolytes à travers les parois capillaires était très rapide. L'estimation de la quantité par jour des électrolytes traversant les capillaires de l'homme décela des quantités énormes: 27.000 kg de chlorure de sodium et 860 kg de potassium aux concentrations normales dans le sérum.

* Aided by grants from the Public Health Service (H143), the Upjohn Co., and the Thibodeaux Research Foundation.

СКОРОСТИ ПЕРЕНОСА Rb^{86}, K^{42}, K^{39}, Cl^{36}, Cl^{35}, Na^{22} И Na^{23}, ЧЕРЕЗ ПОВЕРХНОСТЬ ПУЗЫРЯ НА ПРЕДПЛЕЧЬЕ ЗДОРОВОГО ЧЕЛОВЕКА И У ЛИЦ С ХРОНИЧЕСКОЙ КОРОНАРНОЙ НЕДОСТАТОЧНОСТЬЮ

Основание пузыря, образованного на предплечье человека под действием порошка из шпанских мушек, использовалось в качестве живой мембраны для изучения кинетики переноса электролитов. Этот метод дает легко воспроизводимую и надежную модель для изучения проницаемости. Исследовали проникновение Na^{23}, Na^{22}, Cl^{35}, Cl^{36}, K^{39}, K^{42} и Rb^{86} как внутрь, так и из области экспериментального пузыря. Так как электролиты и радиоизотопы проникают в содержимое пузыря и выходят из него через капилляры, эта модель позволяет исследовать явление проницаемости капилляров в чистом виде, неосложненное зависимостью от скорости кровообращения и перемешивания веществ в крови, в то время как при исследовании выхода веществ из кровеносных сосудов последние два фактора влияют на полученные результаты.

Обнаружен очень быстрый переход электролитов сквозь капиллярную стенку. При оценке общего количества каждого электролита, проникающего сквозь капиллярные стенки всей капиллярной сети человека за сутки, получились огромные цифры: для хлористого натрия—60,000 фунтов и для калия 1900 фунтов при нормальных их концентрациях в плазме крови.

TRANSPORT VON Rb^{86}, K^{42}, K^{39}, Cl^{36}, Cl^{35}, Na^{22} UND Na^{23} DURCH DIE OBERFLÄCHE EINER BLASE AUF DER HAUT DES UNTERARMES BEI NORMALEN VERSUCHSPERSONEN UND BEI PATIENTEN MIT CHRONISCHEN HERZERKRANKUNGEN

Die Basis einer Cantharides Blase am menschlichen Unterarm wurde als lebende Membran beim Studium der Kinetik des Transportes von Elktrolyten verwendet. Diese Methode liefert ein leicht reproduzierbares und verlässliches Modell für solche Untersuchungen. Der Transport von Na^{23}, Na^{22}, Cl^{35}, Cl^{36}, K^{39}, K^{42} und Rb^{86} aus dem extrakorporalen Versuchsraum in den Körper hinein, wie auch in umgekehrter Richtung war Gegenstand der Untersuchungen. Da Eindringen bzw. Austreten der Elektrolyte und Radioisotopen beim extrakorporalen Versuchsraum auf kapillarem Wege erfolgt, liefert dieses Modell annähernd die für Transportstudien durch kapillare Wände erforderlichen Versuchsbedingungen ohne die Einschränkung von Zirkulation und Vermischung, welche sich bei Untersuchungen, die von Inneren der Gefässe aus durchgeführt werden, störend auswirkt.

Es zeigt sich, dass der transkapillare Transport äusserst rasch vor sich geht. Abschätzungen der Elektrolytmengen, welche pro Tag die menschlichen Kapillaren durchsetzen, ergaben folgende enorme Werte: bei normalen Serumkonzentrationen 60.000 Pfund für NaCl und 1900 Pfund für Kalium.

VOL. 4 1958/5

The mechanisms which control the kinetics of exchange of electrolytes across surfaces composed of living cells are little understood and need investigation. Unfortunately, living surfaces of greatest interest are not readily accessible in intact man. Because it was readily accessible the base of a blister[1,2] of the skin of the forearm was employed even though it is not a normal cellular surface. Nevertheless, it can serve a useful purpose in an approach to an understanding of the kinetics of exchange of electrolytes across living membranes. The cantharides blister surface is relatively uniform and reproducible, and lends itself to the study of aspects of the influence of solvents, solutes, drugs and disease states such as congestive heart failure upon transfer of electrolytes and water across "membranes" as shown previously in this laboratory.[3,4,5] With these points and obvious limitations in mind an investigation of aspects of rubidiokinetic, kaliokinetic, chlorokinetic and natriokinetic phenomena were undertaken.

METHODS

1. *Preparation of the blister membrane*

Cantharides create (0·5–0·6 g) was spread evenly on circular filter paper discs (Whatman No. 2), 33 mm in diameter and was applied to the skin of the volar surface of the forearm at the junction of the middle and upper thirds. It was held in place for 10–12 hr by adhesive tape, then the top of

the vesicle was removed by cutting as close to its edge as possible. The exposed blister surface was irrigated with isotonic NaCl and a circular lucite cup, 38 mm in diameter, was sealed over the blister with an inert cement.* The test solutions were introduced into the cup through a hole stoppered at all times except for sampling of test fluid.

The application of the cantharides disc to the forearm resulted in a blister of rather uniform depth.[1] The size of the blister was intentionally varied (2·6–10·2 cm^2) to test the effect of the area of the blister surface on the rates of exchange of the isotopes.

2. *Tracer material*

Rb^{86}, Na^{22}, Cl^{36} and K^{42} were the tracers employed. Aliquots of test fluid, usually 0·5 ml, were removed at 30 min intervals for assay as previously described.[6] At the end of the observation all remaining test fluid (except for 0·1–0·2 ml which could not be removed) was aspirated and the volume noted. In experiments in which two isotopes were studied simultaneously, the tracers were separated either by suitable aluminum filters or by allowing sufficient time for physical decay of the tracer with the shorter physical half-life. The amount of each isotope added to the test fluid in each lucite extracorporeal chamber varied from 0·1 to 0·25 μc.

3. *Subjects*

The subjects were from the wards of the Charity Hospital. Control subjects consisted of patients who had convalesced from infections, peptic ulcers and other diseases without cardiovascular or renal disturbances, whereas patients were selected with varying degrees of edema, heart failure and venous hypertension for representative disease states.

The subjects rested supine in a comfortable room in a hospital type bed with the blister surface at about heart level. Occasionally gentle passive movement of the forearm maintained mixing of the test fluid.

In most experiments both forearms were studied so that one served as a control. The initial volume of the test fluid was 10 ml except when varied to study the effects of volume. The subject's serum, 5% glucose in water, and distilled water with added tracers and electrolytes served as test fluids. The experiments lasted 210 min initially but later the time was reduced to 120 min.

The content of chloride in the test fluid and blood serum was determined by the method of Schales and Schales[7] and sodium and potassium by flame photometry.

4. *Analysis of data*

For convenience, the blister membrane was considered a functionally single membrane. The extracorporeal compartment, the plastic cup, was considered to be a single compartment on the external surface of the membrane and the remainder of the body a single large compartment on the other side. The mathematical methods of analysis employed in these experiments are now well known.[8,9,10,11]

RESULTS

For convenience of presentation, these studies are divided into five sections. All rates of transfer are expressed in terms of 10 cm^2 of blister surface unless otherwise stated.

Group I *experiments*

In these experiments the test fluid consisted of 10 ml of the patient's serum containing approximately 50,000 counts/min of Rb^{86}. Half ml samples of test fluid were removed simultaneously from both extracorporeal compartments at 15 and 30 min intervals over a period of 120–210 min. The samples were analyzed for Rb^{86}, K^{39}, Cl^{35} and Na^{23}. The concentration of the stable elements was measured in a sample of blood (serum) collected at the beginning of each experiment. The subjects consisted of 12 controls and 6 with chronic congestive heart failure.

Results. The mean rate of disappearance of Rb^{86} from the extracorporeal compartment

* Miracle, Brite Magic, Miracle Adhesive Co., New York.

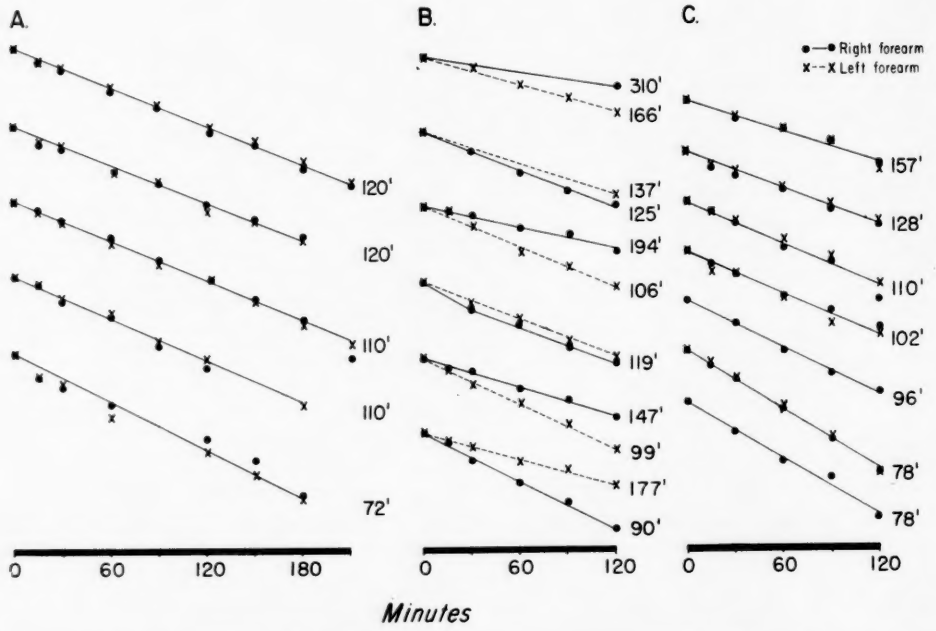

FIG. 1. Concentration–time course of Rb^{86} in the extracorporeal compartment containing serum with the $T_{1/2}$ value for concentration in minutes shown at the end of each curve. There was no change in rate of disappearance during 6 observations lasting 120–210 min (Group A). In the 6 observations shown in Group B, the slower rates of change in concentration in four subjects were associated with the smaller surface area but all were equal when reduced to unit area and equal volume. In two subjects in this group such corrections are shown, 137′ and 125′ $T_{1/2}$ and 119′ $T_{1/2}$. The similarity of right and left sides is apparent when the blister membranes were equal in size (Group A and C). In all illustrations of this type, ordinate values are not shown because of variations in amount of tracer material employed. Because the curves are exponential and the $T_{1/2}$ values for concentration are shown to the right of each curve, absolute ordinate values are unnecessary.

expressed as $T_{1/2}$ (time required to reach half the initial concentration) was $91{\cdot}3 \pm 21{\cdot}7$ min/10 cm² of blister surface ($0{\cdot}71 \pm 0{\cdot}12$ per cent of Rb^{86} in the test fluid transferred/min) for all forearms of all subjects (Fig. 1), a mean rate of 88·8 min (0·73 per cent of Rb^{86} in the test fluid/min) for the 6 subjects with congestive heart failure and 94·6 min (0·70 per cent of Rb^{86} in the test fluid/min) for the control subjects. The mean values were not significantly different for both groups. The mean rates of disappearance were $91{\cdot}4 \pm 24{\cdot}5$ min ($0{\cdot}69 \pm 0{\cdot}12$ per cent of Rb^{86} in the test fluid/min) for the left forearm and $91{\cdot}3 \pm 16{\cdot}6$ min for the right ($0{\cdot}72 \pm 0{\cdot}13$ per cent of Rb^{86} in the test fluid/min).

Except for sampling, there were not significant net gains or losses of water, Na^{23}, K^{39} or Cl^{35} in the extracorporeal compartment during the course of these experiments. The rates of disappearance were not altered by reducing the initial volume of the test fluid to 5 ml. Likewise variations in size of the blister surface from 2·6 to 10·2 cm² did not alter the rates of disappearance per unit area. The duration of the experiments (120–210 min) did not influence the rates (Fig. 1).

The rate of disappearance of Rb^{86} was not measurably related to variations in the seral concentration of sodium (127–149 meq/l.), potassium (3·1–4·6 meq/l.) or chloride (100–114 meq/l.).

Comment. The substances studied traversed a membrane composed of several layers of cells and intercellular substances.[1] Monitoring of the forearm near the blister area, as well as along the main lymphatic trunks draining the forearm, failed to reveal

accumulations of Rb^{86}. It would appear, therefore, that the Rb^{86} was removed mainly by the blood.

The studies of other investigators as well as other experiments from this laboratory[12–23] showed Rb^{86} to trace K^{39} in man sufficiently well to justify calculation of certain kaliokinetic phenomena from these data on Rb^{86}. Employing rough estimations of total capillary surface area based on KROGH's studies[24] it was possible to estimate the quantity of potassium which exchanges across the capillaries of an average-size man per day. For example, it was found in these studies that the average unidirectional transfer of K^{39} was 0·00031 meq/10 cm^2 blister base/min. When it is estimated that each cm^2 of blister base was in functional contact with 0·1 cm^2 of capillary and venular surface area,[25] the mean rate of transfer of K^{39} was 0·00031 meq/cm^2 capillary/min. Therefore, if all the capillaries and venules of the body were exchanging at a rate observed for the blister base then approximately 1880 lb (about 1 ton) of potassium would transfer back and forth across the walls of these vessels per day. The quantity which would cross back and forth through the vessels of the skin per day was found to be about 0·13 lb.

With healing of the blister surface the rate of exchange might be expected to decline, but during the course of these studies there were no indications that healing influenced the rate of exchange of Rb^{86}.

These experiments showed the preparations on the right and left arms to serve as reproducibly reliable controls for each other, a fact utilized in subsequent experiments. In addition, the rate of disappearance of Rb^{86} from the extracorporeal compartment (test fluid) for any forearm was uniformly constant throughout an entire experiment. Therefore, changes in the time course of the rate of disappearance were used to study the effect of various factors upon the exchange phenomena with each forearm of the same subject serving as its own control.

Group II *experiments*

(a) Blister surfaces were prepared on both forearms of 11 subjects and a test fluid of 5% glucose in distilled water with Rb^{86} was added to the left extracorporeal compartment and 5% glucose and Rb^{86} with varying amounts of potassium chloride (4 to 50 meq of K^{39}/l.) was added to the right. The net rates of entry of Na^{23} and Cl^{35} into both extracorporeal compartments were determined simultaneously with the rates of loss of Rb^{86}. The net rates of loss of K^{39} from the right cup were also measured.

(b) In 5 other subjects 5% glucose in distilled water with Rb^{86} was placed in both extracorporeal compartments and histamine (0·2 ml of 1 : 1000 dilution) was added to the right side at the beginning of the observation. Two additional unpaired observations were conducted in the same manner with added histamine. The extra corporeal compartments were studied as noted in (a) above.

Results. The mean rate of disappearance of Rb^{86} from the extracorporeal compartment, expressed as $T_{1/2}$, was 106·5 $\pm$ 22·1 min (a percentile decline of 0·60 $\pm$ 0·10 per cent/10 cm^2 blister base/min) for all 32 forearms (Figs. 2 and 3). The addition of potassium to the test fluid had no detectable influence on the rate of disappearance of Rb^{86}. In these experiments with added potassium, the rate of disappearance of Rb^{86} from the right side was 103·6 $\pm$ 24·1 min, from the left 104·9 $\pm$ 22·7 min and 104·9 $\pm$ 22·9 min for both (Fig. 2). The addition of histamine to the test solution resulted in a more rapid rate of disappearance of Rb^{86} for the first 30 min in four of seven experiments, however, following this interval the rates tended to be slower than for the control side (Fig. 3).

Sufficient potassium was added to the extracorporeal compartment on the right side of 10 preparations to allow its rate of disappearance to be measured as rate of change in the difference between the concentration of K^{39} in the extracorporeal compartment (K_e^{39}) and K^{39} in the serum (K_s^{39}),

$$\Delta K^{39} = K_e^{39} - K_s^{39}.$$

The time required for the ΔK^{39} value at

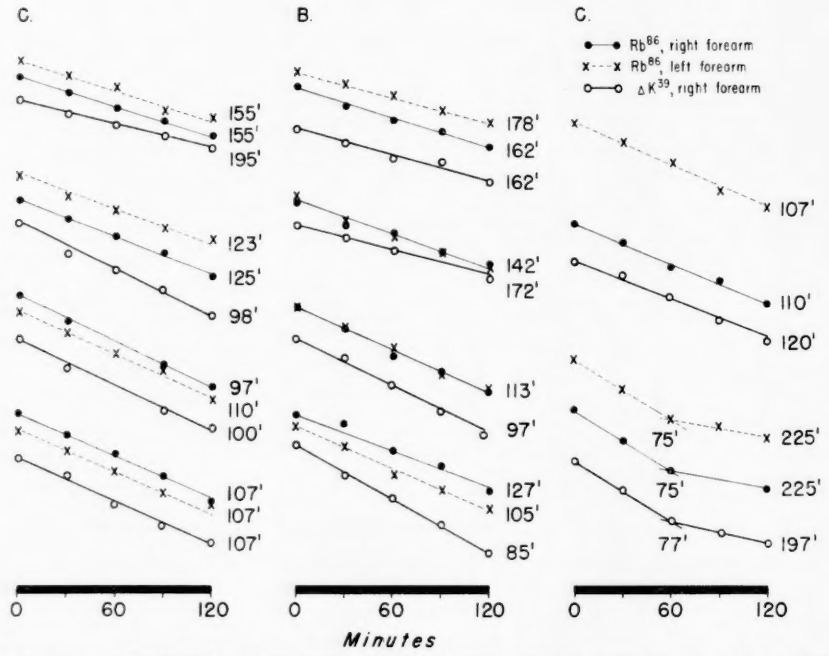

FIG. 2. The simultaneous concentration–time course of Rb^{86} in extracorporeal compartment for both forearms. The left compartment contained 5% glucose in distilled water as the test fluid and the right contained 5% glucose in distilled water with KCl (4–50 meq/l. added). The time course of ΔK^{39} represents the change with time in the difference between the concentration in extracorporeal compartment and that in the serum. $T_{1/2}$ values for concentration in minutes are shown to the right of each curve.

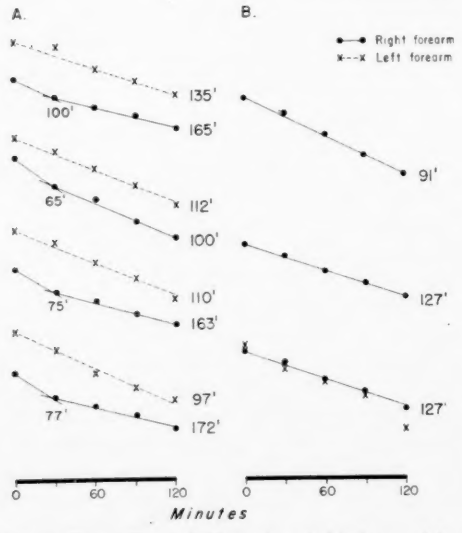

FIG. 3. The effect of histamine (added to right side) on the rate of disappearance of Rb^{86} in 5% glucose from the extracorporeal compartment in 7 subjects.

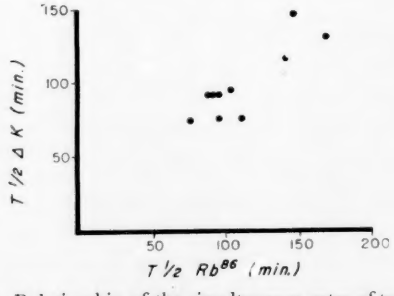

FIG. 4. Relationship of the simultaneous rates of transfer of K^{39} to that of Rb^{86} from the same extracorporeal compartment expressed as $T_{1/2}$ values. The high correlation further supports the adequacy with which Rb^{86} traces K^{39}.

VOL 4 1958/

t_0 to be reduced to one-half was the $T_{1/2}$ of ΔK^{39}. The $T_{1/2}$ value, 106·0 ± 32·6 min, was not significantly different from the $T_{1/2}$ value of Rb^{86}, 103·6 ± 24·1 min, measured simultaneously for the same extracorporeal compartments (Figs. 2 and 4). Thus the mean rate of transfer of K^{39} was 0·0027 ± 0·0009 meq K^{39}/10 cm² blister/min for the initial 30 min, and 0·0016 ± 0·0007 meq K^{39}/10 cm² blister/min for the entire 120 min of study. The $T_{1/2}$ values for ΔK^{39} and Rb^{86} were not influenced by the initial concentration of potassium in the extracorporeal compartment except that the mass of K^{39} which transferred was increased by adding potassium.

Since the test fluid was sodium-free initially, it was also possible to determine the rate of entry of sodium into the extracorporeal compartment. The mean rate was 0·0052 ± 0·0007 meq/10 cm² blister/min for all blisters. In paired experiments, the addition of potassium to the right side did not change the rate of sodium transfer, the mean rate for all forearms being 0·0052 ± 0·0006 meq Na/10 cm² blister/min with 0·0051 ± 0·0008 for the right and 0·0053 ± 0·0006 for the left side without added potassium.

Since this method of analysis ignored the transfer of sodium from the extracorporeal compartment back into the body, a second method of analysis was utilized, i.e. the time course of the difference (ΔNa^{23}) between the concentration of sodium in the serum (Na_s^{23}) and that in the extracorporeal compartment (Na_e^{23}) expressed as

$$\Delta Na^{23} = Na_s^{23} - Na_e^{23}$$

was employed to determine the rate of exchange of Na^{23}. This was expressed as $T_{1/2}$ or time in minutes required to reach one-half the concentration in the serum. The addition of potassium or histamine to one side (right) did not influence this rate (Fig. 5). The mean $T_{1/2}$ values were: 120·0 ± 25·1 min/10 cm² blister base (0·0078 ± 0·0018 meq Na/10 cm²/min) for all observation, the right and left sides having values of 121·3 ± 28·1 min (0·0077 ± 0·0019 meq/10 cm²/min) and 123·2 ± 24·7 min (0·0076 ± 0·0017 meq/10 cm²/min) respectively in the paired observations. The rates remained constant throughout the experimental period (Fig. 5).

Since there was no chloride in the extracorporeal compartment in 20 blister preparations, the rate of entry of chloride into the extracorporeal compartment was also determined. In these experiments, chloride was measured in the extracorporeal compartment only at the beginning and end of each experiment. The methods of analysis were the same as those utilized for Na^{23}.

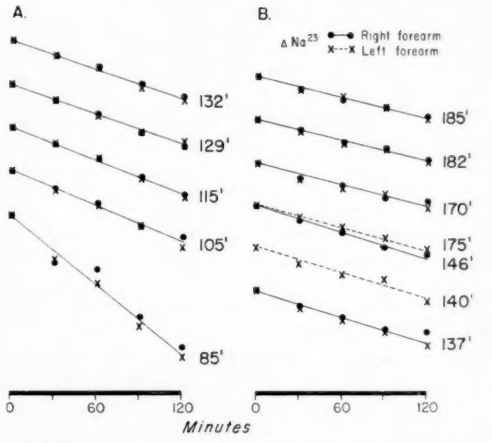

FIG. 5. Time course of the change in the difference between concentration of Na^{23} in the serum and in the blister compartment containing 5% glucose in distilled water (ΔNa^{23}). This is an expression of the rate of transfer of Na^{23} into the extracorporeal compartment. The $T_{1/2}$ values in minutes are shown to the right of each curve.

The mean rate of net transfer of chloride was 0·0046 ± 0·0006 meq Cl/10 cm²/min. The mean $T_{1/2}$ value for ΔCl^{35} was 97·6 ± 17·6 min, a rate of entry of chloride into the extracorporeal compartment of 0·0075 ± 0·0014 meq Cl/10 cm² blister base/min.

Comment. The two forearms served as good controls for each other. The rate of disappearance of Rb^{86} from the extracorporeal compartment with 5% glucose in distilled water as test fluid ($T_{1/2}$ 106·5 ± 22·1 min) was about the same as that found with serum as the test fluid ($T_{1/2}$ 91·3 ± 21·7 min). Potassium was added to the test fluid in concentrations varying from 4 to 50 meq/l.

in an attempt to overload existing transport mechanisms for K^{39}, Rb^{86}, Cl^{35} and Na^{23}. There was no evidence of overloading at any of the concentrations employed and there was no evidence of selective competition between the potassium and Rb^{86}. In these

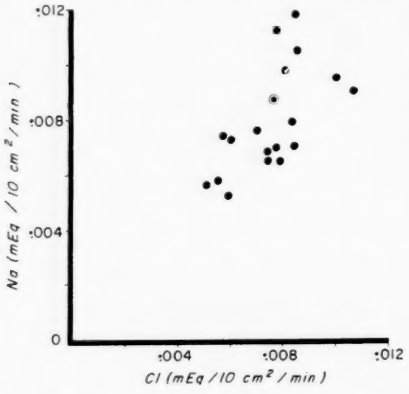

FIG. 6. Illustration showing the high degree of relationship of the rate of transfer of Na^{23} and Cl^{35} into extracorporeal compartment containing 5% glucose in distilled water as the test fluid. The circled point is a double point.

preparations the greater the concentration gradient across the membrane, the greater was the mass of electrolyte transferred. Therefore the rate of disappearance of Rb^{86} from the side with added potassium was not expected to differ from the side without added potassium since overloading of the exchange mechanisms was not obtained. The rates of entry of sodium and of chloride into the test solution varied directly with each other (Fig. 6), the mean rate of transfer of sodium and chloride (one direction) for all observations being $0{\cdot}0079 \pm 0{\cdot}0018$ meq/10 cm^2 blister base/min for each.

With certain rough estimations, it was possible to calculate the masses of the various electrolytes that were transferred across the capillary surfaces of the body of man. For example, if the area of capillaries and venules in the blister base is considered to be one-tenth of the area of the blister base[25] and the total area of capillaries in the body is considered to be 5000 m^2[24] and functionally similar to the capillaries of the blister base, there is a transfer across the capillaries of the body of 60,000 to 70,000 lb of sodium chloride daily at normal seral concentrations. At the high concentrations employed in the test solution, the transfer for potassium was 16,400 lb or 31,207 lb of potassium chloride. In addition to these electrolytes, the total mass of substances transferred back and forth across the capillary walls includes such substances as H_2O, Mg, Ca, glucose, as well as others.

Group III *experiments*

Blister surfaces were prepared on both forearms of 6 subjects. The test solution contained K^{42}, Rb^{86} and K^{39} (35·5 meq/l.) and Cl^{35} (41·0 meq/l.) in distilled water. Separation of K^{42} and Rb^{86} was accomplished by allowing K^{42} to decay and recounting the samples. The rates of disappearance of K^{42}, Rb^{86} and K^{39} were measured along with the rates of entry of sodium and chloride into the extracorporeal compartment.

Results. The concentration–time course curves of K^{42}, K^{39} and Rb^{86} for all 6 subjects are shown in Fig. 7. The parallelism of all curves for each subject is apparent. The curves indicate an increasing rate of disappearance of K^{42}, K^{39} and Rb^{86} with time in all experiments, a phenomenon observed only in this group of experiments in which the initial test fluid was hypotonic to serum. The loss of a constant amount of the Rb^{86}, K^{39} and K^{42}, rather than a constant percentage of that remaining in the extracorporeal compartment, could result in this type of concentration–time course curve. A theoretic (calculated) concentration–time course curve was obtained based upon the rate of loss of Rb^{86} during the first 30 min interval and measured decrements in volume of the test fluid during the entire experiment. The calculated and observed curves were strikingly similar (Fig. 7). For the 6 subjects, the average mass of Rb^{86} leaving per minute throughout the experiment was $0{\cdot}037 \pm 0{\cdot}011$ per cent of that present at the beginning of the experiment. Since the curves for Rb^{86}, K^{39} and K^{42} for each subject were essentially parallel, it was not necessary to make such calculations for K^{39} and K^{42}. Analysis of the data for the average net loss of Rb^{86}, K^{42}

VOL 4 1958/

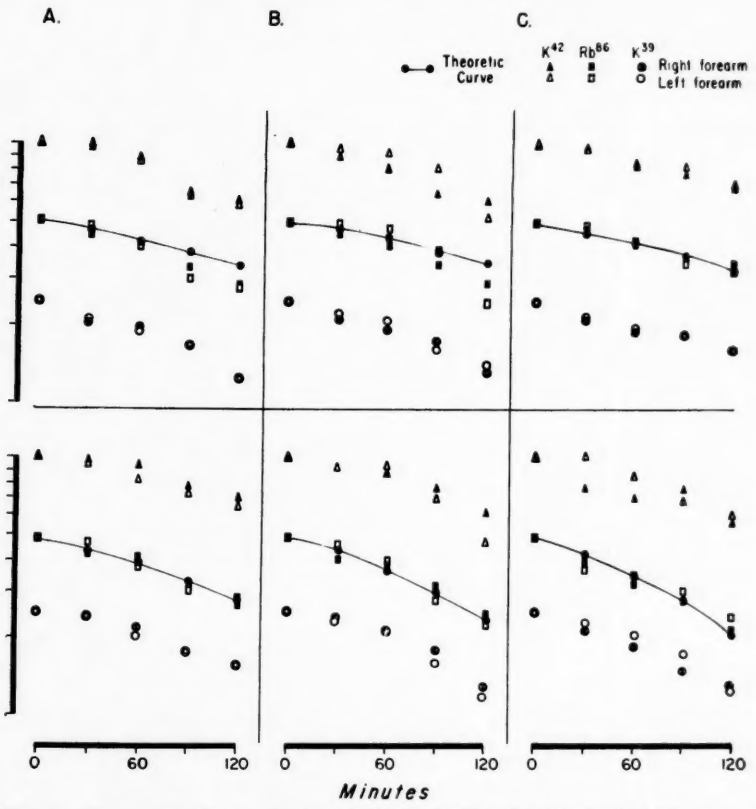

FIG. 7. The simultaneous time course of concentration of Rb^{86} and K^{42} and of K^{39} in the blister compartment of both forearms. Both right and left compartments contained Rb^{86} and K^{42} in distilled water with 50 meq/l. of KCl. K^{39} represents the difference between concentration of K^{39} in the blister compartment and that in the serum. See text for derivation of theoretic curve. All points are observed values.

and K^{39} per minute expressed as a percentage of that present at the beginning of each 30 min period revealed a mean net loss for the 6 subjects of: Rb^{86}, $0{\cdot}52 \pm 0{\cdot}12$ per cent/10 cm² blister/min; K^{42}, $0{\cdot}46 \pm 0{\cdot}14$ per cent; and K^{39}, $0{\cdot}46 \pm 0{\cdot}10$ per cent; thus 0·0016 meq of potassium transferred per 10 cm² of blister per minute.

Fig. 8 shows that Rb^{86} traced K^{39} about as well as K^{42}. Therefore, if it is assumed that Rb^{86} traced K^{39} in these observations, there was an average of $0{\cdot}0013 \pm 0{\cdot}0004$ meq K^{39} that left the extracorporeal compartment/10 cm² blister/min.

The time course of the rates of change in concentration of sodium, Na^{23}, and of chloride, Cl^{35}, in the blister compartment were determined and found to be constant and the same as those observed when the extracorporeal compartment contained isotonic solutions of glucose (Fig. 5). The mean rate of entry of Na^{23} was $0{\cdot}0074 \pm 0{\cdot}0014$ meq Na/10 cm² blister/min and for chloride the mean rate of entry was $0{\cdot}0070 \pm 0{\cdot}0014$ meq Cl/10 cm² blister/min.

Comment. The rates of disappearance of Rb^{86}, K^{42} and K^{39} from the extracorporeal compartment in a hypotonic solution with a high concentration of potassium differed from those in isotonic solutions with similar concentrations of potassium. The type of concentration–time course curves observed in this group of experiments could be due to a fixed quantity of transfer of Rb^{86}, K^{42} and K^{39}. Although the amount of potassium transferred per minute in this group of

experiments was less than that transferred from isotonic glucose solutions, chemical transport mechanisms could exist and function at a fixed rate. It is likely that

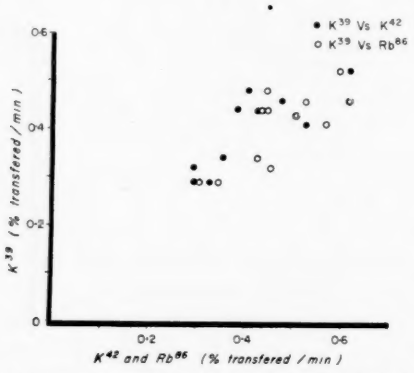

FIG. 8. Illustration showing the high degree of relationship of the rates of transfer of K^{39} to K^{42} and to Rb^{86} from the extracorporeal compartment containing hypotonic solution of KCl.

several factors were operative. In hypotonic test fluids, the slower rate of decline in concentration initially could have been due, in part, to loss of electrolyte-free water from the blister compartment. Physiologically it would be expected that electrolyte-free water would more likely be lost from the hypotonic solution during the early part of the observation before sodium, chloride and other substances entered the blister compartment. As the osmolality of the test solution rose in consequence of transfer of sodium and chloride into the compartment, the physiologic need for removal of electrolyte-free water would diminish. Although the loss of water from the test compartment may have contributed to this type of disappearance curve, the measured loss of water was not sufficient to explain these findings. The injurious effects of hypotonicity and high concentrations of potassium were doubtless important. The state of the barrier of cells and intercellular substances interposed between the test fluid and the capillary lumen must have influenced the loss of tracers and electrolytes.

The rate of entry of sodium and chloride into the hypotonic test solution was the same as that observed for isotonic test solutions, being 0·0074 meq/10 cm^2 blister/min for the hypotonic solutions and 0·0078 meq/10 cm^2/min for the isotonic solution. The rate of change in concentration of sodium in the two types of test solutions remained constant in each experiment. The factors influencing the rate of transfer of Rb^{86} K^{42} and K^{39} from the hypotonic test solution had no detectable influence either on rate or quantity of sodium and chloride entering the blister compartment.

Group IV *experiments*

These experiments were designed to compare the amount of Rb^{86}, and therefore potassium, which entered the extracorporeal compartment (A) of one forearm with that which left a similar compartment (B) of the opposite forearm in 4 subjects. The test solution in A was the subject's serum and that in B was serum with 10,000 counts/min/ml of Rb^{86}. A relatively constant arterial concentration of Rb^{86} was maintained by a rate of infusion of the isotope as previously described.[26] The test solutions from both extracorporeal compartments were sampled simultaneously at 6, 10, 14, 18, 22, 26, 30 and 34 min after onset of the infusion of Rb^{86}.

Another study of the same general design was made utilizing a single intravenous injection of Rb^{86} administered relatively slowly (approximately 2 min injection time) so that the concentration of Rb^{86} in arterial blood declined fairly rapidly with time.

Results. The concentration–time course of Rb^{86} in arterial blood following a single intravenous injection of the tracer was defined by the general equation:[26]

$$C_t = C_{o1}e^{-b_1 t} + C_{o2}e^{-b_2 t} + C_{o3}e^{-b_3 t} \text{ (Fig. 9).}$$

From the concentration–time course curves of Rb^{86} in the arterial blood and in the test fluid it was possible to calculate a fractional rate of exchange of Rb^{86} in the extracorporeal compartment. This was defined by the following equation:

$$S = \frac{KC_{o1}}{K - b_1}(e^{-b_1 t} - e^{-Kt}) + \frac{KC_{o2}}{K - b_2} \times (e^{-b_2 t} - e^{-Kt}) + \frac{KC_{o3}}{K - b_3}(e^{-b_3 t} - e^{-Kt})$$

where K represents the fraction of the tracer in the compartment under observation which either entered or left per minute, and S represents the specific activity in that compartment.[26] A fractional rate of exchange of 0·0086 parts of that in the

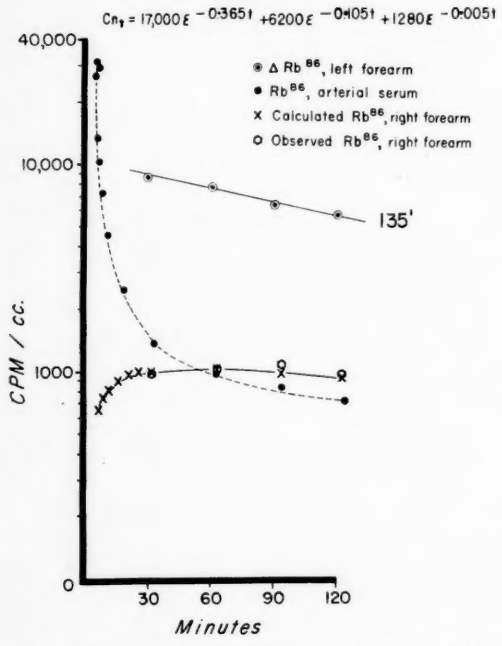

FIG. 9. Simultaneous concentration–time course of Rb^{86} in serum and in extracorporeal compartments following single intravenous injection of the tracer.

extracorporeal compartment per minute resulted in the calculated curve shown in Fig. 9. Assuming Rb^{86} traced K^{39} then 0·00039 meq K/10 cm²/min transferred unidirectionally into the extracorporeal compartment A. The rate of loss of potassium simultaneously from extracorporeal compartment B was 0·00028 meq K/10 cm²/min.

The time course of concentration and rate of change in concentration of Rb^{86} in the extracorporeal compartment in experiments in which the arterial concentration of Rb^{86} was constant are shown in a typical subject in Fig. 10. The amounts of potassium entering compartment A and simultaneously leaving compartment B respectively were 0·00054 and 0·00038, 0·00046 and 0·00045, 0·00044 and 0·00044 meq/10 cm²/min for 3 subjects. In the fourth subject only compartment A was studied, showing the rate of entry of potassium to be 0·00093 meq/10 cm²/min. These rates of transfer were essentially of the same magnitude as observed

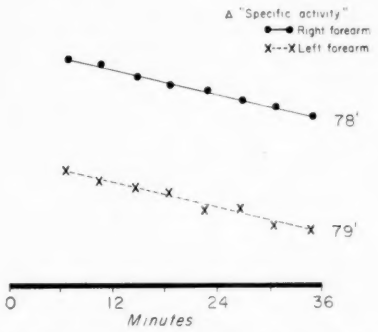

FIG. 10. Simultaneous time course of the Δ "specific activity" (Rb^{86}/K^{39}) in extracorporeal compartment of right and left forearm of a representative subject in whom the "specific activity" in serum was maintained essentially constant by appropriate continuous intravenous infusion of the tracer.

in the Group I experiments in which serum was the test fluid in the extracorporeal compartment.

Comment. This group of observations show conclusively that Rb^{86} entered the extracorporeal compartment across the vascular walls as rapidly as it traversed them on leaving the compartment. The exchange with the test fluid must be almost entirely across the walls of capillaries. Therefore, if Rb^{86} can traverse the capillary, interstitial spaces and/or cells including other intervening structures and substances, to enter the compartment from the blood stream there is no reason to believe that it could not move in the opposite direction with equal facility, especially since the two rates noted above were remarkably similar. Thus, there is little need to expect any significant role of the lymphatics in removal of such tracers and electrolytes from the extracorporeal compartment. Undoubtedly, some of the loss of tracers and electrolytes from the test fluid was through lymphatics. From a consideration of the expected rate and volume of dermal lymph flow, one

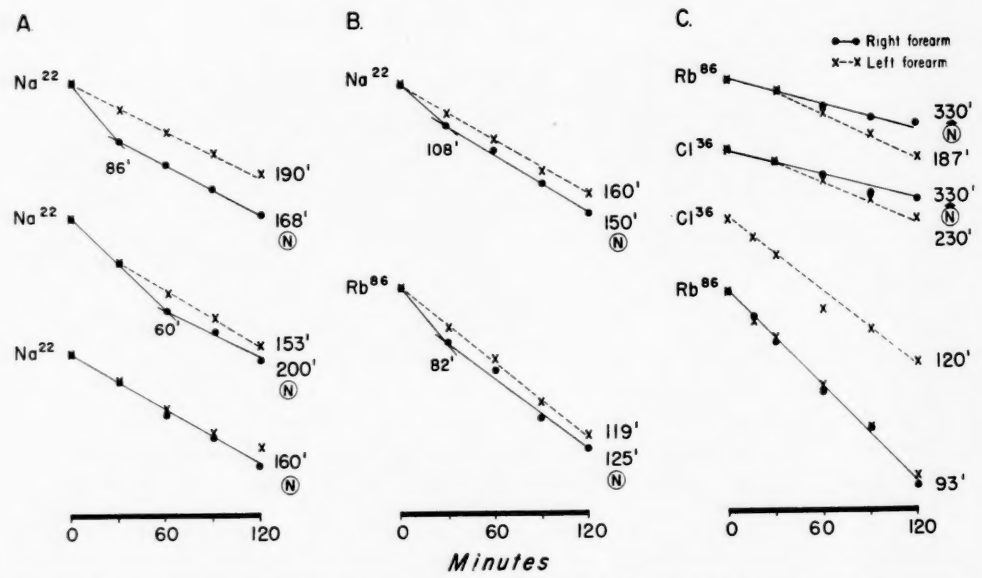

FIG. 11. The effect of norepinephrine on the rates of transfer of Na^{22}, Cl^{36} and Rb^{86} from the extracorporeal compartment containing serum. The norepinephrine (N) was added to the right side in each instance. See text for details.

would not expect these vessels to remove a significant amount of tracer in the time periods involved. Furthermore, monitoring over the major lymphatic vessels and lymph nodes draining the blister area failed to reveal any accumulation of isotope in the lymphatic system. Therefore, these experiments show that the Rb^{86} and K^{39} of the test fluid of the extracorporeal compartment exchange directly with that in the plasma of the capillaries.

Group V *experiments*

In this series of experiments, the blister membranes were prepared as before and the subject's serum was used as the test fluid. Na^{22} alone was used in three experiments, Na^{22} combined with Rb^{86} in one and Cl^{36} combined with Rb^{86} in two. Norepinephrine (1·6 to 3·2 γ) was added to one side in five experiments. Where isotopes were combined, their separation was achieved by allowing time for physical decay of Rb^{86} and recounting.

Results and comments. This series of experiments was designed to investigate

(1) the rates of transfer of sodium across the blister surface as measured by Na^{22} (Fig. 11A),

(2) the rates of transfer of chloride as measured by Cl^{36} (Fig. 11C),

(3) the simultaneous rates of loss of Rb^{86} with Na^{22} (Fig. 11B) and of Rb^{86} with Cl^{36} (Fig. 11C) and

(4) the effect of norepinephrine on the rates of transfer of these isotopes (Fig. 11). The results of experiments utilizing Na^{22} and Rb^{86} are shown in Fig. 11A and B. The average unidirectional rate of transfer of sodium determined from the measurements of Na^{22} was 0·0079 meq/10 cm^2 blister/min, which was exactly the same as the average rate of Na^{23} entering the compartment containing 5% glucose determined previously (Fig. 5). In the two experiments with Cl^{36} (Fig. 11C), the rate of loss of chloride as determined by the tracer method was also of the same general magnitude as determined previously by measuring the changes in concentration of Cl^{35} in the extracorporeal compartment. These observations on Na^{22} and Cl^{36} support the reliability of determining the rate of transfer of Na^{23} and Cl^{35} by means of concentration changes in the

extracorporeal compartments containing 5% glucose.

The effects of norepinephrine on the transfer of these tracers was variable (Fig. 11). This series was small but the most consistent effect of norepinephrine was to increase the rate of transfer of Na^{22} and Rb^{86} from the compartment during the first part of the experiment. There was no evident blanching of the blister base in response to norepinephrine. The transient increased rate of transfer of Na^{22} and Rb^{86} in response to norepinephrine may have resulted, in part, from an influence of this agent on a chemical ion transport mechanism. In the one experiment with Na^{22} and Rb^{86} in both test compartments, there were distinct differences in rates of loss of these two isotopes (Fig. 11B). Also in one of the two experiments combining Cl^{36} and Rb^{86} there were significant differences in simultaneously observed rates of transfer of the two isotopes (Fig. 11C). Although the number of subjects studied was small, each individual served as his own control.

These experiments show the membrane, in spite of its complexity, to be a convenient preparation for investigating aspects of transfer of electrolytes and water. Furthermore, it is a living membrane in man which is available for the study of various normal and disease states.

GENERAL DISCUSSION

The membrane studied is complex. Although the lymphatics probably participated in the removal of electrolytes and water from the blister base, these studies showed that, in the time intervals involved, their role was negligible. To gain access to the capillary lumen, the electrolytes must have traversed cells and/or intercellular substances. The effect of the vasodilatation of inflammation on the rates of transfer of electrolytes and water in these observations is not known. Healing of the blister base had no detectable effect on these rates during the relatively short duration of these experiments. In spite of the complexity of this membrane, this simple preparation is a useful experimental model for the study of transfer phenomena in intact man. Furthermore, hypotonic test solutions of these same electrolytes resulted in concentration–time course curves of similar configurations and rates for these blister preparations as for the normal pericardial sac of dogs.

These studies lend further evidence to the usefulness of Rb^{86} as a tracer of K^{39} since no differences were detected between Rb^{86} and K^{42} studied simultaneously. Therefore, studies of "specific activity" calculated with Rb^{86} and K^{39} reflected accurately the kinetics of K^{39}. Since transcapillary exchange of K^{39} in this blister model was accurately traced by Rb^{86}, transcapillary exchange of K^{39} elsewhere in the body can be observed satisfactorily utilizing Rb^{86}. In fact, it is possible that the blister membrane reflects adequately the role of the capillaries of the entire body in kaliokinetic, natriokinetic, chlorokinetic and hydrokinetic phenomena. The rate of blood flow could have been one of the main factors limiting the rate of removal of water and electrolytes. The capillaries of the blister membranes were all fully dilated whereas in normal resting tissues of the body, such a state of dilatation would not be expected. However, electrolytes and water must pass through the wall of the capillaries even though they are closed. Whether or not electrolytes are removed from the area by the circulating blood as rapidly as they enter the lumen of the capillaries depends upon the rate of blood flow. Therefore, the enormous magnitudes of exchange of electrolytes and water across the capillary walls estimated for normal man are valid within the limits of the assumptions necessary for the calculations. It would appear that large quantities of electrolytes and water traverse the capillary walls per unit of time, but the net quantities retained in the various compartments at steady state are determined by Donan equilibrium and many other poorly understood factors such as types of and quantities of proteins, membrane potentials and many physicochemical phenomena which are highly integrated and regulated to ensure a

healthy environment for the living cells. Extremely small and immeasurable percentile changes in the rates of exchange of these substances could quickly result in abnormal distribution in the quantities of water and electrolytes located in any compartment.

Because of these magnitudes of rates of exchange, it would be anticipated that no differences in transfer rates could be found between the control subjects and those with chronic congestive heart failure. That net quantities of transfer into the interstitial compartments were different was evident by the edema of the patients with heart failure. It is for such reasons that a study of the size, composition and regulating mechanisms of the respective compartments rather than the rates of exchange continue to provide the tangible data related to differences between patients with congestive heart failure and control subjects.

SUMMARY AND CONCLUSIONS

(1) Although complex, the blister membrane has been shown to provide a reproducible and reliable model for the study of exchange phenomena for electrolytes and water across a living membrane in intact man.

(2) Rb^{86} has been shown to trace K^{39} across the capillary wall of man with high degree of reliability.

(3) The rate of disappearance, expressed as a $T_{1/2}$ value of Rb^{86} from the extracorporeal compartment across the blister membrane with the subject's own serum as a test fluid was $91{\cdot}3 \pm 21{\cdot}7$ min. The percentile rate of disappearance was $0{\cdot}71 \pm 0{\cdot}12$ per cent per 10 cm^2 of blister base per minute. The right and left forearms were identical. The controls and the subjects with congestive heart failure had the same rates.

(4) When glucose was used as the test fluid, the findings were essentially the same, the $T_{1/2}$ value was $106{\cdot}5 \pm 22{\cdot}1$ min. The percentile rate of loss was $0{\cdot}60 \pm 0{\cdot}10$ per cent per 10 cm^2 of blister surface per minute.

(5) K^{39} concentrations up to 50 meq/l. in the test fluid did not alter these rates of exchange.

(6) The mean rate of transfer ($T_{1/2}$) of Na^{23} into the extracorporeal compartment containing 5% glucose was $120{\cdot}0 \pm 25{\cdot}1$ min. This was 0·58 per cent of that present at equilibrium in the compartment for 10 cm^2 of blister surface per minute. When the subject's plasma was used as test fluid, the amount of Na leaving was essentially the same.

(7) The mean rate of entry ($T_{1/2}$) of Cl^{35} into the extracorporeal compartment was $97{\cdot}6 \pm 17{\cdot}6$ min. This represented 0·61 per cent of the Cl^{35} present in the compartment at equilibrium per 10 cm^2 of blister surface per minute.

(8) The effects of histamine and noradrenaline were described.

(9) If the state of electrolyte transfer across the blister surface existed for the capillary surface of the entire body then roughly 1900 lb of K^{39} and 60,000 to 70,000 lb of NaCl traverse the capillary walls of an average size normal person per day. Such magnitudes of exchange make it impossible to measure with present day methods minute alterations in rates of exchange which would be sufficient to result in abnormal accumulations in the extracellular and intercellular compartments in disease states.

REFERENCES

1. Benedek T. *J. Trop. Med.* **42,** 81 (1939).
2. Petersen W. F. *A.M.A. Arch. Internal Med.* **39,** 19 (1927).
3. Winsor T. and Burch G. E. *A.M.A. Arch. Internal Med.* **74,** 428 (1944).
4. Burch G. E. and Winsor T. *Amer. J. Med. Sci.* **209,** 226 (1945).
5. Kelly F. J., Svedberg A. H. and Harp V. C., Jr. *J. Clin. Invest.* **29,** 988 (1950).
6. Burch G. E., Reaser P. B., Ray C. T. and Threefoot S. A. *J. Lab. Clin. Med.* **35,** 626 (1950).
7. Schales O. and Schales S. S. *J. Biol. Chem.* **140,** 879 (1941).

VOL
4
1958/

8. Burch G. E., Threefoot S. A. and Cronvich J. A. *J. Lab. Clin. Med.* **34,** 14 (1949).
9. Burch G. E., Ray C. T. and Threefoot S. A. *J. Lab. Clin. Med.* **42,** 34 (1953).
10. Sheppard C. W. and Householder A. S. *J. Appl. Phys.* **22,** 510 (1951).
11. Solomon A. K. *J. Gen. Physiol.* **36,** 57 (1952).
12. Love W. D. and Burch G. E. *J. Lab. Clin. Med.* **41,** 351 (1953).
13. Wilbrandt W. *J. Gen. Physiol.* **20,** 519 (1937).
14. Mann P. J. G., Tennenbaum M. and Quastel J. H. *Biochem. J.* **33,** 822 (1939).
15. Mitchell P. H., Wilson J. W. and Stanton R. E. *J. Gen. Physiol.* **4,** 141 (1921).
16. Follis R. H. *Amer. J. Physiol.* **138,** 246 (1943).
17. Roberts R. B., Roberts I. Z. and Cowie D. B. *J. Cellular Comp. Physiol.* **34,** 259 (1949).
18. Lorente de No Rafael A study of nerve physiology, studies from the Rockefeller Institute for Medical Research, **131,** 31 (1947).
19. Burch G. E., Threefoot S. A. and Ray C. T. *J. Lab. Clin. Med.* **45,** 371 (1955).
20. Threefoot S. A., Ray C. T. and Burch G. E. *J. Lab. Clin. Med.* **45,** 395 (1955).
21. Ray C. T., Threefoot S. A. and Burch G. E. *J. Lab. Clin. Med.* **45,** 408 (1955).
22. Love W. D., Cronvich J. A. and Burch G. E. *J. Clin. Invest.* **34,** 61 (1955).
23. Love W. D., Romney R. B. and Burch G. E. *Circulation Research* **2,** 112 (1954).
24. Krogh A. *The Anatomy and Physiology of Capillaries* Yale University Press, New Haven (1922).
25. Wetzel N. C. and Zotterman Y. *Heart* **13,** 357 (1926).
26. Love W. D. and Burch G. E. *J. Clin. Invest.* **36,** 468 (1957).

VOL.
4
58/59

International Journal of Applied Radiation and Isotopes, 1959, Vol. 4, pp. 144–153. Pergamon Press Ltd. Printed in Northern Ireland

Comparative Metabolism of Strontium and Calcium in Man*†

ARTHUR R. SCHULERT and EDWIN A. PEETS
Lamont Geological Observatory of Columbia University, Palisades, New York
and
DANIEL LASZLO,‡ HERTA SPENCER, MARTIN CHARLES, and JOSEPH SAMACHSON
Division of Neoplastic Diseases, Montefiore Hospital, Bronx, New York

(*Received* 11 *May* 1958)

The metabolic fate of intravenously administered Sr^{85} and Ca^{45} was studied in man. It was found that the isotopes were somewhat equally divided between bone and soft tissue shortly after administration, but that after four months, more than 99 per cent of the fraction of each isotope remaining in the body resided in bone. The initial specific activity (isotope concentration per gramme calcium) was far greater in soft tissue than bone with the values approaching uniformity in about four months. The retention among the bones in the interval studied was greatest in vertebrae and least in long bone shaft and skull. The bone exhibits no marked preference in the uptake of the isotopes initially. However, as Sr^{85} is preferentially excreted by the kidneys, the relative ratio of Ca^{45} to Sr^{85} remaining in bone gradually increases. The net retention of Ca^{45} is about 60 per cent whereas that for Sr^{85} is about 25 per cent.

VOL
4
1958/

LE MÉTABOLISME COMPARATIF ENTRE LE STRONTIUM ET CALCIUM DANS L'HOMME

Le résultat métabolique de Sr^{85} et Ca^{45} administré intraveineusement fut étudié dans l'homme. Il fut découvert que les isotopes étaient divisés prèsque également entre l'os et le tissulaire peu après l'administration, mais après quatre mois, plus de 99 pour cent de la fraction de chaque isotope restant dans le corps se trouvait dans l'os. Au dèbut, la radioactivité spécifique (la concentration d'isotope par gramme de calcium) était plus grande dans le tissulaire que dans l'os, les valeurs approchant de l'uniformité apres environ quatre mois. La retention entre les os dans l'interval étudié, était la plus grande dans les vertèbres et était la moindre dans les longs os et le crâne. L'os ne montre aucune préférence initialement entre les isotopes. Néanmoins comme le strontium est excreté par les reins de préférence, le rapport rélatif entre le Ca^{45} et le Sr^{85} restant dans l'os augmente graduellement. La retention nette du Ca^{45} est près de 60 pour cent et près de 25 pour cent pour le strontium.

СРАВНИТЕЛЬНЫЙ ОБМЕН СТРОНЦИЯ И КАЛЬЦИЯ В ЧЕЛОВЕКЕ

Изучалась судьба введенных человеку внутривенно стронция-85 и кальция-45. Показано, что вскоре после введения оба изотопа распределяются более или менее равномерно между костями и мягкими тканями. Однако, через 4 месяца после введения

* A report of the early phases of this work was presented before the 3rd annual meeting of the Society of Nuclear Medicine at Salt Lake City in June 1956.

† This work was conducted under U.S. Atomic Energy Commission contract number AT (30–1) 1656 with Columbia University (Lamont contribution No. 312) and contract number AT (30–1) 1763 with Montefiore Hospital.

‡ Deceased 7 June, 1958.

в костях обнаруживается более 99% от общего количества изотопа, содержащегося во всем теле. Начальная удельная активность (концентрация изотопа на грамм кальция) в мягких тканях значительно выше, чем в костях, однако по истечении 4-х месяцев удельные активности практически выравниваются. При сравнении содержания изотопа в различных костях отмечено самое высокое поглощение в позвоночнике и самое низкое—в длинных трубчатых костях и в черепе. В начальный период для костей не наблюдается заметной избирательности поглощения вводимых изотопов; однако, с течением времени отношение содержания в костях кальция-45 к стронцию-85 постепенно увеличивается, так как через почки преимущественно выделяется стронций-85. При этом поглощение в костях кальция-45 достигает приблизительно 60% и стронция-85—около 25%.

METABOLISCHER VERGLEICH VON STRONTIUM UND CALCIUM IM MENSCHLICHEN KÖRPER

Der metabolische Ablauf von intravenös verabreichten Sr^{85} und Ca^{45} wurde erprobt im menschlichen Körper.

Es wurde festgestellt, dass die Isotopen kurz nach Verabreichung gleichmässig verteilt waren zwischen Knochen uns Geweben, jedoch nach vier Monaten, mehr als 99 prozent jedes einzelnen Isotopen die im Körper verblieben, waren in den Knochen enthalten. Die ursprüngliche Tätigkeit (Isotopen Konzentration per Gramm Calcium) war bedeutend grösser in weichen Geweben als in den Knochen; nach vier Monaten waren die Auswertungen beinahe einheitlich. Die Behaftung zwischen den Knochen während der Versuchszeit war am grössten in der Wirbelsäule und am geringsten in Röhren- und Schädelknochen. Ursprünglich zeigt der Knochen keine lange markante Bevorzugung in der Aufnahme von Isotopen. Jedoch, da Sr^{85} durch die Nieren bevorzugt ausgeschieden wird, vergrössert sich das relative Verhältnis von Ca^{45} zu Sr^{85} allmählich. Der Netto-Rückstand von Ca^{45} ist etwa 60 prozent wogegen der des Sr^{85} etwa 25 prozent beträgt.

INTRODUCTION

STRONTIUM represents a trace element in the human body, having an average concentration of 4·5 parts per 10,000 parts of calcium in bone.[1]

Widespread interest in strontium today is due to the presence of the long-lived radioisotope Sr^{90} among the products of nuclear fission.[2] Strontium-90 is generally regarded as the principal health hazard among the fission products since it is selectively taken up by the human skeleton where it remains deposited for many years.[3] In order to be able to evaluate the radiotoxicity of Sr^{90} in man, the knowledge of the metabolism of the element in humans is of paramount importance. Extensive work has been done to determine the absorption and excretion of administered strontium and calcium isotopes.[4] The present study was designed to show the relative retention of strontium compared to calcium in man and to determine the distribution of administered isotopes within the body including both bone and soft tissue.

EXPERIMENTAL PROCEDURES

1. *Clinical design and sampling*

Tracer quantities of Sr^{85} [$T\frac{1}{2}$ 65 days] and Ca^{45} [$T\frac{1}{2}$ 163 days] in chloride form were administered in a single dose simultaneously to ten terminal cancer patients by the intravenous route [Table 1]. The average dose was 1·5 μc/kg for Sr^{85} and 0·4 μc/kg for Ca^{45}. The intravenous route of administration was selected since it excludes the parameter of gastro-intestinal absorption. Since autopsy analyses were employed, the patients were, of necessity, of limited life expectancy with cancer involvement, and cannot be considered as normal healthy adults. Survival times of patients studied varied from 3 hr to 124

TABLE 1. List of patients studied

Patient	Age	Sex	Wt. (kg)	Time interval isotope admin.–death (days)	Clinical diagnosis	Skeletal involvement
H. H.	62	F	45	1/8	Carcinoma of pancreas	None
S. K.	50	M	54	2	Hodgkins disease	All vertebrae
S. J.	60	F	54	3	Carcinoma of colon	Moderate
C. C.	59	F	73	3	Carcinoma of breast	Diffuse
J. Z.	72	M	73	6	Carcinoma of lung	Diffuse
G. B.	70	F	54	18	Carcinoma of breast	None
S. G.	49	M	50	30	Multiple myeloma	Moderate
T. M.	70	M	43	39	Carcinoma of lung	Single area of skull
A. W.	63	M	61	65	Carcinoma of kidney	Thoracic vertebrae
M. S.	70	F	56	124	Carcinoma of lung	None
J. T.	67	M	76	251	Multiple myeloma	Moderate
I. J.	55	F	53	960	Multiple myeloma	Diffuse

days. In addition, samples were obtained from one patient who received Sr^{85} only, 251 days prior to death and from one patient who received Ca^{45} only, 960 days before death. At autopsy, samples of many soft tissues and of bone were taken for analysis. As many as twenty-five soft tissue samples were obtained in the early studies while later sampling and analysis of soft tissues were restricted to four major organs, namely, muscle, liver, kidney, and lung. Except for muscle, these organs were obtained *in toto* and only small sections were removed for histologic analysis. In regard to bone, samples of vertebrae and ribs were obtained from all patients and in seven of the ten cases either femur shaft, iliac crest, and skull were obtained. Particular attention was given to the variation among bones of the skeleton as well as the distribution within single bones.

2. *Radiochemical assay*

Strontium-85 is readily assayed, since it emits a γ-ray of moderate energy. The sample is merely dried, ashed, and counted in a well-crystal γ-ray spectrometer. The isotope counted with an efficiency of approximately 10 per cent with an associated background of about 10 counts per min. (Slight variations in both of these values were constantly checked by appropriate blanks and standards.)

Two chemical procedures were used in the Ca^{45} assay, one adapted to bone and the other for soft tissue.

Ashed bone is dissolved in HCl after which the pH is adjusted to 3·0–3·5 with ammonium hydroxide. A mixture of oxalic acid and ammonium oxalate is then added to precipitate the calcium oxalate. (Care is taken to avoid a pH higher than 3·5 since this precipitates some calcium as the phosphate.) The calcium oxalate is filtered and converted to the oxide by heating in a muffle furnace. The calcium oxide is weighed, dissolved in HCl, and diluted to 100 ml in a volumetric flask. A convenient aliquot is taken, the pH adjusted, and the calcium again precipitated as the oxalate. After digestion the precipitate is filtered on 29 mm diameter No. 42 Whatman filter paper which is then placed on a brass planchet, covered with a thin piece of pliofilm and placed in a low-level end window β-counter.

For the determination of Ca^{45} in soft tissue, the sample is ashed in platinum and then fused with sodium carbonate at 1200°C. The fusion mixture is leached with water, filtered to remove sodium phosphate and soluble carbonates, and the residue dissolved in hot HCl. After cooling, ammonium hydroxide is added to pH 7, precipitating ferric hydroxide which also occludes remaining phosphate ion. The precipitate

VOL.
4
1958/5

is filtered with the calcium remaining in the filtrate. To remove traces of calcium which may have been carried with the ferric hydroxide, the precipitate is redissolved in HCl and again precipitated, the filtrate being combined with the previous one. Excess ammonia is expelled by boiling. Oxalic acid and ammonium hydroxide are added to precipitate the calcium oxalate. After digestion and cooling, the oxalate is filtered and counted in the same manner as the bone samples.

The β-counter in which the Ca^{45} samples are counted is equipped with an anti-coincidence ring so that background is about 2 counts per min. The counting efficiency for Ca^{45} varies with particular counters from 8 to 12 per cent so that 10^{-6} μc can be adequately detected in a sample. The Sr^{85} which follows the calcium through the chemistry, registers on the β-counter with an efficiency of only 0·3 per cent. As the Sr^{85} concentration is known from the γ-assay, this small correction for the Sr^{85} is made in the β-count.

PRECISION ANALYSIS AND TREATMENT OF DATA

In order to properly evaluate the experimental findings, it is necessary to know the relative precision of each particular result. The problem may be considered in three categories:

(1) the precision of the radiochemical determinations,

(2) the biological precision of different portions of the same tissue, and

(3) the precision between the tissues of two individuals treated in an identical manner.

There is also the matter of statistical error of counting but the counting time was almost always sufficient to reduce this to below 1 per cent, making it negligible compared to the other variations.

The chemical precision is of concern primarily in the Ca^{45} determination, since essentially no chemistry is involved in the Sr^{85} assay. Duplicate and in some cases triplicate samples were analysed. The average of the mean deviations for the Ca^{45} determinations in these small groups is 4·8 per cent and 7·5 per cent in bone and soft tissue respectively.

In comparing the biological variation in two or more parts of the same tissue, an effort was made to obtain representative samples, e.g. a cross section of bone or the half of a kidney cut along its major axis. (In subsequent discussion, systematic variations within bone are noted.) The average of the mean deviations for the Ca^{45} determinations in these groups is 22·0 per cent for soft tissue and 16·4 per cent for bone.

The corresponding values for Sr^{85} are 14·5 per cent for soft tissue and 17·1 per cent for bone.

There is insufficient direct information to assess the biological variation from one individual to another. However, the relative distribution of isotopes in the skeletons of different individuals gives some indication. Thus the standard deviation in the vertebra/rib concentration ratio for Sr^{85} is 30 per cent showing, as expected, that variation among individuals is somewhat greater than variation in representative samples in a single tissue. The concentration ratio of one bone to another is changing in time, as subsequently discussed, but the change is slight over a four month interval.

These facts account for a large amount of the "scatter" in the data and underline the need for caution in its interpretation. Nevertheless, certain generalizations and a number of significant facts can be drawn from the experimental results.

In order to give a gross overall picture of the behavior of the isotopes in the human body in time, the total body load is calculated for each patient. A standard procedure, which admittedly involves considerable approximation, is employed as follows:

Soft tissues

(1) The weights of lung, liver, and kidney were obtained at autopsy. Muscle weight is estimated from the total body weight using the body composition data of MITCHELL *et al.*[5]

(2) The total content of each tissue is then calculated by multiplying the estimated tissue weight by the tissue concentration.

(3) Accordingly, these four tissues constitute 40·3 per cent of the total body weight, whereas the total soft tissue comprises 85·2 per cent. On the assumption that the tissues analysed are representative of all the soft tissue, the total isotopic content of these 4 tissues is multiplied by 85·2/40·3 to give the total estimated isotopic content for soft tissue.

Bones

The bones are divided into three groups, which according to the data of TROTTER,[6] comprise the following percentages of the total skeleton:

I	"Long" bone: limb, hip, skull (and mandible)	70·6%
II	Rib	5·7%
III	Vertebra and sternum	8·9%
	Total	85·2%

(1) The weight of each bone analysed is estimated from the body weight and the data of TROTTER[6] together with the data of MITCHELL *et al.*[5] for the percentage of total skeletal mass.

(2) Bones within a group which are not represented are assumed to have the same value as the average of the others in order to estimate the total isotopic content for each group.

(3) When an entire group is not represented, its value is estimated by using the femur/rib ratio (for "long" bone) and the vertebra/rib ratio (for the vertebra/sternum group) as obtained from the average on all patients.

(4) The total estimated isotopic content of the three groups is multiplied by 100/85·2 to get the estimated total skeletal content.

RESULTS AND DISCUSSION

The distribution of Sr^{85} and Ca^{45} in the body, the percentage of the isotopes accounted for, and the ratios of each isotope contained in bone and soft tissues are listed in Table 2. Also shown are the ratios of Ca^{45}/Sr^{85} in bone and soft tissues. In spite of the problems of representative sampling the approximations entering in the calculations, and the fact that the extent and degree of the cancer involvement varied markedly, a fairly consistent pattern is obtained. The limitations of this analysis are demonstrated most sharply by the calculated Ca^{45} retention in patient C. C. at three days (127 per cent). There is a partial explanation for this since the patient (a female weighing 72·6 kg) had a higher percentage of adipose tissue than normal. Thus the standard assumption that the skeleton represents 14·8 per cent of the body undoubtedly gives an estimated bone weight in this case which is in excess of the true value. Since the concentration of the isotopes per gramme of bone is much greater than of soft tissue, the standard procedure results in a high value for total body retention. It is noted that both isotopes are somewhat equally divided between bone and soft tissue shortly after their administration and that the proportion gradually shifts so that less than one-half per cent of the body load of each isotope is retained in the soft tissues by 124 days. This is primarily due to the more rapid removal of the isotopes from the soft tissues. The data also suggest some translocation from soft tissue to bone, particularly of Ca^{45} as previously noted by others in animals over short intervals.[7] This translocation is shown graphically in Fig. 1. Whereas the skeletal Sr^{85} retention begins to decline within the first few days and

TABLE 2. Distribution of Sr^{85} and Ca^{45} in soft tissues and bone; tissue concentrations expressed in per cent of administered dose

	Patient days*	H. H. 1/8	S. K. 2	S. J. 3	C. C. 3	J. Z. 6	G. B. 18	S. G. 30	T. M. 39	A. W. 65	M. S. 124
Sr^{85}	Soft tissue	55	31	44	35	26	22	1·2	1·4	1·5	0·15
	Bone	33	47	36	45	42	41	20	26	30	26
	Total	88	78	80	80	68	63	21	27	32	26
	Sr^{85} ratio bone/soft tissue	0·60	1·5	0·82	1·3	1·6	1·8	17	19	20	173
Ca^{45}	Soft tissue	33	28	28	53	32	14	3·0	5·5	1·9	0·27
	Bone	30	42	55	74	59	36	35	71	79	60
	Total	33	70	83	127	91	50	38	76	81	60
	Ca^{45} ratio bone/soft tissue	0·91	1·5	2·0	1·4	1·8	2·6	12	14	42	222
Ca^{45}/Sr^{85}	Soft tissue	0·60	0·90	0·64	1·5	1·2	0·64	2·5	3·9	1·3	1·8
	Bone	0·91	0·89	1·5	1·6	1·4	0·88	1·8	2·7	2·6	2·3

* Days elapsed between the injection of the isotopes and *exitus* of patients.

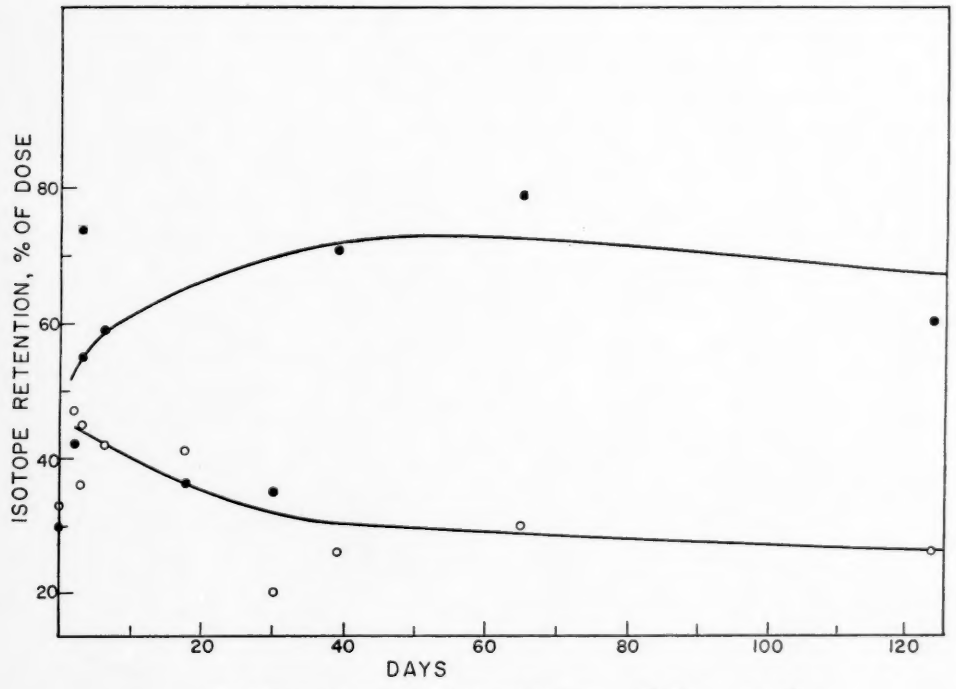

FIG. 1. Isotopic content of the total skeleton. ● Ca^{45} ○ Sr^{85}

approaches a plateau at about 25 per cent, the Ca^{45} appears to rise for the first month and levels off at about 65 per cent. Three experimental points are badly off the Ca^{45} curve, but these are the three least valid values of the ten: the high 3 day point [C. C.] is subject to question as previously mentioned, and the low points at 18 and 30 days represent the only skeletons for which just two bones were obtained for analysis. The retention values for the two isotopes are consistent with those obtained in balance studies over shorter intervals by other investigators.[4, 8, 9, 10]

The ratios of Ca^{45}/Sr^{85} of the individual tissues are listed in Table 3. Although these ratios are somewhat more variable for soft tissues than for bone, both show an increase with time; the values for bone being generally 2 or above after 30 days. This is a reflection of the fact that Sr^{85} is preferentially eliminated from the body and thus has a shorter average biological residence time than calcium.

The enrichment in favor of calcium is not apparent in the bones until several days after the administration of the isotopes. Thus the bone tissue as a whole shows no preference in accepting both isotopes immediately after administration in agreement with the conclusion of BAUER *et al.*[11] and COMAR *et al.*[12] The subsequent increase in the Ca^{45}/Sr^{85} ratio in time reflects the preferential excretion of strontium by the kidneys. It has been stated that the overall calcium enrichment from diet to bone is governed primarily by the calcium/strontium discrimination factor across the intestine and by that of urinary excretion.[13, 14] In the course of time, the renal discrimination factor is reflected by the retention of the isotopes in the body, i.e. primarily in the skeleton. Whereas the intestinal discrimination is essentially a one step process (disregarding the endogenous fecal strontium) in that the isotopes which reach the intestinal tract are either taken across the intestinal wall or eliminated from the body, the kidney discrimination is a cyclic process in which ions that have been retained in the body during one circulatory cycle and via the renal tubules are presented to the kidney again during the next circulatory cycle. This repetitive renal process leads to continued preferential excretion of radio-strontium and therefore to increased relative retention of radio-calcium. The factor of net effective enrichment from blood to bone for Ca^{45} in the two to four month interval is approximately 2–3. An appreciable increase in the enrichment over longer periods of time is not expected since the *loci* of isotope deposition become more and more inaccessible with time due to the fact that:

(1) The isotope is cleared early from the more accessible sites and

(2) Some accessible sites will be made

TABLE 3. Ca^{45}/Sr^{85} ratios in bone and soft tissues as a function of time

Soft tissue	Days									
	1/8	2	3	3	6	18	30	39	65	124
Kidney	0·46	0·86	0·81	0·74	0·91	1·2	1·3	1·5	0·58	0·87
Liver	0·34	0·84	0·63	1·3	1·6	1·7		1·9	1·2	3·0
Lung	0·28	0·68	0·67	0·74	1·4	0·50	4·6	1·2	1·1	0·44
Muscle	0·72		0·88		1·7	0·70	0·28	8·0	1·4	1·7
Bone										
Femur		0·81		1·9				1·8	2·1	
Iliac crest	0·86	1·0								2·7
Skull				1·7	1·5					2·3
Sternum	0·94	0·90	1·1	1·4		1·0	2·4	2·2	3·5	2·0
Rib	0·74	0·82	0·76	1·4	1·3	1·3	1·0	3·6	2·2	
Vertebra	0·86	0·94	2·1	1·5	1·3	0·94		2·7	3·8	1·9

unavailable by the continued deposition of new bone mineral.

Although extensive data on the excretion of Sr^{85} and Ca^{45} in man have been obtained,[4, 15] these excretions have not been followed for prolonged periods of time. One would expect the elimination of administered Sr^{85} and Ca^{45} to follow a power function as in the case of radium.[16] While the present data on bone retention of the isotopes are inconclusive, they suggest that only slight changes are occurring after the second month, compatible with such an elimination pattern.

Since the Ca^{45}/Sr^{85} retention ratio reaches two in two months, and since these isotopes present in bone remain there for years, it is concluded that this enrichment will also occur under continuous intake of Sr^{90} due to fallout. A comparison of average Sr^{90} content of diet and human bone in northeastern United States by ECKELMANN *et al.*[17] indicates that the overall calcium/strontium discrimination from diet to bone is four. Since the discrimination against strontium across the intestinal barrier has been reported to be two[4] and the discrimination from blood to bone is also two, the present data are in general agreement with those reported in the literature.

The specific activity of Sr^{85} (concentration of Sr^{85} per gramme stable calcium) of bones and of the major soft tissues are listed in Table 4. The average specific activity of vertebrae and rib are respectively 5·4 and 2·3 times that of femur. This distribution must clearly change in time as evidenced by the fact that common strontium is uniformly distributed throughout the skeleton.[1] However, this approach to uniformity proceeds very slowly since Sr^{90}, which has been in our environment for several years, is reported to be more greatly concentrated in vertebrae and rib than in long-bone shaft by factors of about four and two respectively.[17] It is apparent that while the isotopes are largely concentrated in the skeletal tissue, the specific activity of the soft tissue greatly exceeds that of bone throughout the initial two month period following injection. It is noted in the 124 day and 251 day samples, however, that the specific activities are of the same order of magnitude. This indicates that about four months are required for the soft tissue to be cleared of the strontium initially deposited therein. Subsequently the isotopic content of the soft tissue probably reflects that which is resorbed from the bone into the blood stream, (the blood probably being in near equilibrium with the soft tissue). Further evidence that this must be the case comes from the data from one patient who was given Ca^{45} alone, 960 days before death. Samples of the four major soft tissues were obtained and showed an average specific activity of one-twentieth that shown by the 124 day

TABLE 4. Specific activity of Sr^{85} in bone and soft tissue (% administered dose/g Ca)

	Days										
	1/8	2	3	3	6	18	30	39	65	124	251
Kidney	21	8·1	8·8	7·6	0·29	2·3	0·69	0·47	0·57	0·17	0·092
Liver	8·0	12	7·4	1·7	5·8			0·54	0·25	0·070	0·043
Lung	8·0	9·5	1·8	5·1	4·8	3·2	1·6	1·4	0·36	0·32	0·019
Muscle	11	3·3	12	4·0	2·9	4·1	0·24	0·25	0·42	0·053	0·056
Femur		0·036						0·024	0·016		
Iliac crest	0·048	0·070								0·11	0·073
Skull		0·031		0·017	0·012					0·027	
Sternum	0·18	0·067	0·21	0·10		0·25		0·067	0·062	0·099	0·14
Rib	0·071	0·035	0·077	0·035	0·052		0·052	0·078	0·056		0·044
Vertebra	0·17	0·095	0·16	0·13	0·16	0·14	0·070	0·16	0·116	0·14	0·11

case. Therefore it may be concluded that at intervals greater than four months, urinary excretion reflects bone resorption. The excretion may also give an index of the isotopic bone concentration, although the relationship is complex. For example, animal experiments have shown that the specific activity of soft tissue may ultimately become much less than that of bone.[18, 19] Thus the relation is largely an empirical one.

It is evident that in the practical experimental evaluation of agents for their effect on removing strontium from the skeleton, the most meaningful results would be obtained at long periods after strontium administration when the specific activity of the soft tissue approximates that of bone, or at least does not greatly exceed it. The induced enhancement of urinary radio-strontium excretion achieved in the early phase[20] will largely represent clearing of soft tissues, whereas a sustained effect produced at later periods will represent removal of the isotope from bone. Studies carried out in our laboratories on the relationship of urinary radio-strontium excretion and bone concentration determined at time intervals of varying length following the administration of the tracer are in progress at the present.

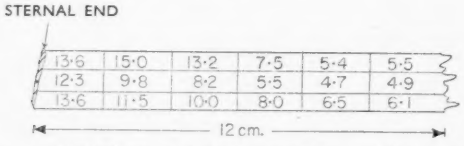

FIG. 2. Variations of Sr^{85} concentration within a rib section.

Fig. 2 shows that the isotope concentration varies greatly within a single bone. For example, Sr^{85} concentration decreases by a factor of greater than two in a section of rib as one proceeds from the sternal end for 12 cm toward the axillary portion of the rib. This finding indicates the biological variation one may expect to encounter in rib samples taken at random.

Table 5 lists the data of radio-strontium concentration in successive one mm layers of the femur which were taken from the external surface and were followed towards the marrow cavity. It is noted that the samples taken after three hours and two days show high activity in the outermost layer followed by a marked decline in the second and third mm. The value then gradually rises with the layer adjacent to the marrow having the highest concentration of all. However, the samples obtained 65 days after the administration of the isotopes show a progressive unidirectional decrease of activity from the outermost layer which has the highest concentration to the inner layer which has the lowest. This may suggest a greater resorption of the isotope through the marrow cavity than from the outer surface of the bone.

TABLE 5. Sr^{85} concentration in various layers of the femur

Time	Depth of bone mm	Concentration in % of dose/kg bone
3 hr	1	4·11
	2	1·64
	3	1·72
	4	1·84
	5	2·25
	Marrow	11·16
2 days	1	6·00
	2	3·96
	3	3·95
	4	4·48
	5	4·57
	Marrow	7·41
65 days	1	2·91
	2	2·01
	3	1·57
	4	1·35
	5	1·21

SUMMARY AND CONCLUSIONS

(1) Tracer quantities of Sr^{85} and Ca^{45} were administered simultaneously to ten cancer patients by the intravenous route and samples of bone and four major soft tissue organs were obtained at autopsy for radio-assay.

(2) The isotopes are approximately equally distributed between bone and soft

tissue for the first few days after administration; after four months about 99·5 per cent of the isotopes which are retained in the body are found in bone.

(3) The net retention of the isotopes appears to level off at about 60 per cent for Ca^{45}, and 25 per cent for Sr^{85}.

(4) There is a gradual increase in the Ca^{45}/Sr^{85} ratio in bone, which reaches a value of two or more in the two to four month interval.

(5) The specific activity of the isotopes is much greater in soft tissue than in bone throughout the first two months after administration, but the values approach the same order of magnitude at four months.

Acknowledgements—The authors gratefully acknowledge the role of J. Laurence Kulp, who along with Daniel Laszlo, initiated this cooperative effort and gave valuable counsel throughout the investigation. Walter Eckelmann was integrally associated with the early phases of the work. Important assistance in the radiochemical analysis was provided by Marian Wampler and Dorothy Walton.

REFERENCES

1. Thurber D. L., Kulp J. L., Hodges E., Gast P. W. and Wampler J. M. *Science* **28,** 256 (1958).
2. *Hearings before the Special Subcommittee on Radiation of the Joint Committee on Atomic Energy*, The nature of radioactive fallout and its effects on man, May 27–29–June 3–7, (1957), U.S. Government Printing Office, Washington, D.C. (1957).
3. Hamilton J. G. *Rev. Mod. Phys.* **20,** 718 (1948).
4. Spencer H., Laszlo D., and Brothers M. *J. Clin. Invest.* **36,** 680 (1957).
5. Mitchell H. H., Hamilton T. S., Steggerda F. R. and Bean H. W. *J. Biol. Chem.* **158,** 625 (1945).
6. Trotter M. Personal communication.
7. Norris W. P. and Kisieleski W. *Cold Spr. Harb. Symp. Quant. Biol.* **13,** 164 (1948).
8. Bellin J. and Laszlo D. *Science* **117,** 331 (1953).
9. Bronner F., Harris R. S., Maletskos C. J. and Benda C. E. *J. Clin. Invest.* **35,** 78 (1956).
10. Harrison G. E., Raymond W. H. A. and Tretheway H. C. *Clin. Sci.* **14,** 681 (1955).
11. Bauer G. C. H., Carlsson A. and Lindquist B. *Acta Physiol. Scand.* **35,** 56 (1955).
12. Comar C. L., Whitney I. B. and Lengemann F. W. *Proc. Soc. Expl. Biol. Med.* **88,** 232 (1955).
13. Commar C. L., Russel R. S. and Wasserman R. H. *Science* **126,** 485(1957).
14. *Deposition and retention of ingested strontium-90 in the skeleton.* Committee Report Washington, D.C., April 23, (1957). Official use only.
15. Spencer H., Samachson J. and Laszlo D. *Fed. Proc.* **17,** 154 (1958).
16. Norris W. P., Speckman T. W. and Gustafson P. W. *Amer. J. Roentgenol.* **73,** 661 (1955).
17. Eckelmann W. R., Kulp J. L. and Schulert A. R. *Science* **127,** 266 (1958).
18. Neuman W. F. and Neuman M. W. *The Chemical Dynamics of Bone Minerals*, U. of Chicago Press (1958).
19. Comar C. L. *Radioisotopes in Biology and Agriculture*, McGraw-Hill (1955).
20. Spencer H., Samachson J., Kabakow B. and Laszlo D. *Clin. Sci.* **17,** 291 (1958).

VOL. 4 58/59

International Journal of Applied Radiation and Isotopes, 1959, Vol. 4, pp. 154–161. Pergamon Press Ltd. Printed in Northern Ireland

A Versatile, High-Contrast Photoscanner for the Localization of Human Tumors with Radioisotopes

MERRILL A. BENDER and MONTE BLAU
Department of Radioisotope Research, Roswell Park Memorial Institute, Buffalo, New York

(*Received* 18 *April* 1958)

Isotope scanning permits the non-traumatic localization of several types of human tumors. To obtain satisfactory visualization, a scanner must be capable of resolving small differences in isotope content between target and non-target tissues and presenting this data in a readily interpretable form. In addition, it must have sufficient flexibility to be adaptable to the variety of activity levels and target : non-target ratios encountered clinically. Since for the most part isotope scanning is a diagnostic screening procedure, the overall counting efficiency must be high so that the administered radioactivity can be kept as low as possible.

A scanner meeting these needs has been constructed. The data presentation system, based upon the marked voltage dependence of the light output of a tungsten filament provides the high contrast necessary for visualizing small changes in count rate. It is possible to adjust the contrast and gain of the recording system to match the clinical requirements. A focusing collimator and large NaI crystal provide high efficiency, good resolution, and adequate depth response.

This instrument has been successfully used for the localization of human tumors of the brain, liver, and thyroid.

VOL
4
1958/

UN PHOTO-EXPLORATEUR À CONTRASTE ÉLEVÉ, DE CAPABILITÉ ÉTENDUE, POUR LA LOCALISATION DES TUMEURS HUMAINES AU MOYEN DES RADIO-ISOTOPES

L'exploration isotopique permet la localisation non-traumatique de plusieurs formes de tumeurs humaines. Pour donner une bonne visualisation, un explorateur doit pouvoir résoudre de petites différences de contenu isotopique entre les tissus targes et les tissus non-targes, et présenter ces données en une forme facile à interpréter. De plus, il doit pouvoir s'adapter à la variété de niveaux d'activité et de proportions targe : non-targe qui se trouve dans la clinique. Puisque pour la plupart l'exploration isotopique est une méthode de séparation diagnostique, l'efficacité générale du compteur doit être élevée afin que la radioactivité administrée puisse être aussi peu que possible.

Un explorateur a été construit de telle façon. Le système de présenter les données, qui dépend de la dépendance marquée sur la tension de l'émission lumineuse d'une lampe à tungstène, donne le grand contraste nécessaire pour observer de petites variations du taux de compte. Il est possible d'ajuster le contraste et l'amplification du système enregistreur selon les besoins cliniques. Un collimateur ajustable et un grand cristal de NaI donnent une forte efficacité, une bonne résolution et une réponse en profondeur suffisante.

Cet instrument a servi avec succès à la localisation des tumeurs humaines du cerveau, du foie et de la thyroïde.

МНОГОСТОРОННЕЕ ФОТОСКАНИРУЮЩЕЕ УСТРОЙСТВО ВЫСОКОЙ КОНТРАСТНОСТИ ДЛЯ ВЫЯВЛЕНИЯ ЛОКАЛИЗАЦИИ ЧЕЛОВЕЧЕСКИХ ОПУХЛЕЙ

Для определения местоположения опухоли в теле человека требуется сканирующее устройство, обладающее следующими свойствами: высокая контрастность (с возможностью ее регулировки), хорошая разрешающая способность и возможность обнаружения изотопа глубоко под поверхностью тела.

Отвечающее этим требованиям устройство недавно создано. Контрастирующая система основана на изменении напряжения, подаваемого на вольфрамовую нить лампы накаливания, что обеспечивает высокую контрастность световой регистрации, необходимую для выявления даже незначительных изменений скорости счета. Конрастность и чувствительность регистрирующей системы можно регулировать в соответствии с клиническими требованиями. Фокусирующий коллиматор и большой кристалл NaI обеспечивают высокую эффективность, хорошую разрешающую способность и адекватную глубинную реакцию.

Установка была с успехом применена для выявления локализации опухолей мозга, печени и щитовидной железы человека. Приведены типовые примеры.

EIN VIELSEITIGER, KONTRASTREICHER PHOTOSCANNER ZUR LOKALISIERUNG VON MENSCHLICHEN TUMOREN MIT HILFE VON RADIOISOTOPEN

Isotopen-Scanning erlaubt eine untraumatische Lokalisierung verschiedener Arten von menschlichen Tumoren. Für ein zufriedenstellendes Sichtbarmachen muss ein Scanner imstande sein, geringe Unterschiede der Isotopen-Konzentration zwischen Tumor und umgebenden Gewebe anzuzeigen und die erhaltenen Werte in einer leicht interpretierbaren Form liefern. Darüber hinaus muss es möglich sein, ihn für einen weiten Bereich von Aktivitätsstärken und auch für sehr unterschiedliche Aktivitätsdifferenzen zwischen Tumor und umgebenden Gewebe, welche klinisch auftreten können, zu verwenden. Da Isotopen-Scanning meist zur diagnostischen Überprüfung des gesamten Körpers verwendet wird, muss die Zählausbeute des Scanners sehr gross sein, damit die verwendeten Aktivitäten so niedrig wie möglich gehalten werden können.

Ein Scanner, welcher allen diesen Erfordernissen entspricht, wurde entwickelt. Das System der Messwertanzeige, welches auf der Voltabhängigkeit der Lichtemission eines Wolframdrahtes beruht, liefert den nötigen Kontrast beim Sichtbarmachen kleiner Anderungen der Zählrate. Es ist möglich Kontrast und Verstärkung des Anzeigesystems den jeweiligen klinischen Erfordernissen anzupassen. Ein fokusierender Kollimator und ein grosser NaJ-Kristall liefern grosse Empfindlichkeit, gutes Auflösungsvermögen und eine adäquate Tiefenanzeige.

Dieses Instrument wurde mit Erfolg zur Lokalisierung von Gehirn-, Leber- und Schilddrüsentumoren verwendet.

INTRODUCTION

The selective deposition of radioisotopes in specific anatomical sites can provide a convenient and non-traumatic method for the localization of normal and abnormal tissues. Scanning devices furnish a graphic representation of the *in vivo* distribution of γ-emitting isotopes. Cassen *et al.*[1] described an instrument with a scanning scintillation probe and a coupled mechanical stylus that printed at a rate proportional to the detected γ-ray intensity. Anger[2] and Horwitz and Lofstrom[3] replaced the mechanical stylus with a flashing light, thereby permitting data presentation on a photographic emulsion. Kuhl *et al.*[4] developed a high contrast, pulsed light, photographic recording system and reported its use for the visualization of I^{131} in the thyroid and the distribution of therapeutic amounts of I^{131} and Au^{198} used in the treatment of metastatic disease. Bender[5] published a preliminary report on a photoscanning system which was based on a continuously energized tungsten filament. This instrument permitted the visualization of brain tumors and normal and malignant thyroid tissues with minimal dosages. The present report discusses the principles of operation and presents a detailed description of this instrument.

RATIONALE

Satisfactory external localization is primarily dependent upon the relative levels of detected activity between the area of interest and the surrounding tissues. Many factors contribute to this target: non-target ratio including:

(1) the specificity of deposition of the tracer agent,

(2) the size and anatomical location of the lesion,
(3) the contribution of cosmic ray and body background to the total count-rate.

The metabolic specificity of the thyroid gland for iodide ion and its favorable anatomical location combine to permit scanning of this organ with relatively unrefined apparatus. On the other hand, brain tumor localization is extremely difficult. Several tracer agents, di-iodo fluoroscein, iodinated human serum albumin and various inorganic ions[6,7,8,9] show some degree of specificity for these lesions. Unfortunately, none of these approaches the specificity of iodide ion for the thyroid. The localization of brain tumors is further complicated by their relative inaccessibility within the cranial vault and high background resulting from the non-localized total body distribution of the tracer agent. Experience with fixed counter techniques has indicated that under these circumstances the count-rate over a tumor area is usually elevated only 10 to 25 per cent above the count-rate from the adjacent normal tissue.[10] To be useful under these conditions, a scanning device must be capable of resolving these small differences and presenting the data in a readily interpretable form.

High contrast

In our system, the contrast necessary to visualize small changes in count-rate is obtained by utilizing the marked dependence of the light output of a tungsten filament on small changes in applied voltage. The pulses from a scanning scintillation probe are integrated by a count-rate meter and the output of this instrument controls the voltage applied to a light bulb. The response of the light bulb is such that a 30 per cent increase in count-rate is translated into a ten-fold increase in photographic film density. There is no darkening of the film until 70 per cent of a preselected count-rate has been reached. The full dynamic range of the film is used for the presentation of the data from 70 per cent to 100 per cent of this count-rate. This gives a markedly non-linear (high contrast) response over this limited but crucial range. Background erase circuits[11] also reject data below a given level but if this level is exceeded the total count-rate is recorded without contrast amplification. The differences between these two systems of data recording can best be understood by considering the visualization of a tumor that elevates the detected count-rate 10 per cent above the adjacent normal tissue. With background erase circuits, the tumor will be detected only when the rejection level is set above the count-rate of normal tissue and below the count-rate of the tumor. If the reject level is set too low, the full count-rate over both normal tissue and tumor is recorded, and it is impossible to visually resolve 10 per cent differences with linear data presentation. If the reject level is set above the count-rate over the tumor, no data is recorded. With our high contrast photoscanning system, gain settings are also critical, but diagnostic scans can be attained over a much wider range. Because of the high contrast, the tumor is visualized with any setting which permits the film to record differences of a few per cent. The extremes of the range of usable settings for visualization of the above tumor are with minimal film density set to correspond to count-rates between 70–110 per cent of the count-rate over the normal brain tissue. While in practice, the extremes of this range are not usable, settings within the 75–105 per cent limits provide easily interpretable scans. In the clinical situation where the normal tissue count-rate is not a fixed value, but changes from point to point because of anatomic variations, a data presentation range of 10 per cent is totally inadequate.

Variable gain

With high contrast recording, a 30 per cent change in count-rate covers the full dynamic range of the film; from white to black. If the film is to record the desired data, the light output must be adjusted to give minimal film darkening when the probe is over normal brain tissue. Small increases in count-rate over tumor areas will then

VOL
4
1958/

produce marked darkening of the film. Since the absolute count-rate varies from patient to patient, it must be possible to adjust the instrument to obtain minimal film darkening with any count-rate. This is achieved by a variable gain control in the integrated output of the count-rate meter. This adjustment is not possible with other high contrast photoscanning systems based upon non-integrated pulsed light sources.[4]

Variable contrast

In addition to the detection of brain tumors, the photoscanner has been used for the localization of liver metastases with I^{131}-labeled Rose Bengal, and for the visualization of functioning thyroid tissue with NaI^{131}. The specificity of these tracers results in relatively high target: non-target ratios of detected activity, eliminating the need for extreme contrast amplification. In fact, limiting the range of data presentation to 30 per cent variations in count-rate may result in the loss of significant information. To adapt to these counting situations, provision has been made for lowering the contrast. An almost linear response is used for thyroid scans and an intermediate contrast for liver metastases localizations.

Counting geometry

For the detection of small tumors, it is necessary to use a probe capable of good resolution with high counting efficiency. In addition, the response pattern must be such that deep-seated lesions can be detected with the same efficiency as superficial ones. Previously, these criteria have been approached only by coincidence counting of positron-emitting isotopes.[9] The expense and complexity of coincidence counting equipment and limited availability of positron-emitting isotopes restrict the applicability of this technique. Utilizing recent advances in collimator design and pulse-height analysis, it is possible to achieve comparable results with γ-emitting isotopes.

INSTRUMENTATION

Fig. 1 illustrates the basic operational principles of the Roswell Park photoscanner. Pulses from the scanning scintillation probe are fed through the pulse-height analyzer

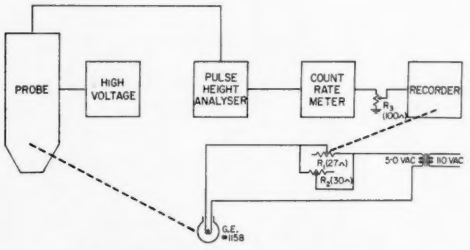

FIG. 1. Block diagram and schematic.

into the count-rate meter. A fraction of the integrated output drives the recorder which in turn lowers the resistance (R_1) in series with the light bulb increasing the light output when the count-rate increases. This bulb is mechanically coupled to the probe and exposes film to provide a photographic image of the distribution of the tracer.

Detector

Fig. 2 is a cross-sectional diagram of the scintillation probe. The focusing collimator is based upon the principle advanced by NEWELL *et al.*[12] and is similar to that constructed by FRANCIS *et al.*[13] This collimator has sixty-one tapered, hexagonal channels and a focal point 3 in. beyond the face. The 3 in. diameter, 2 in. thick NaI(Tl) crytsal is optically coupled with silicone oil to a Dumont No. 6363 3 in. photomultiplier tube. The crystal is shielded with a minimum of 1 in. of lead which extends the full length of the photomultiplier tube. The collimator differs from the original Oak Ridge design in that there is additional lateral shielding to reduce the contribution from the total body distribution of the tracer. A small light (Welch-Allen No. 9) in the central channel of the collimator makes it possible to index the probe properly. High voltage for the photomultiplier tube is supplied by a Technical Measurement Corp. Model HV-4A voltage supply. The

large crystal and multiple channel collimator assure high efficiency. Fig. 3, a photoscan of 6 glass tubes having an internal diameter of 4 mm and filled with a solution of I^{131}, demonstrates the high resolution possible with this collimator.

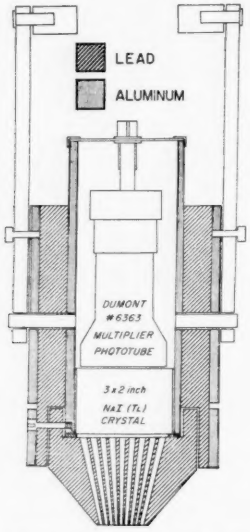

FIG. 2. Cross-section of scintillation probe.

In addition to high resolution and efficiency, the ideal collimator for brain tumor localization should provide uniform sensitivity for any tumor location, i.e. the count-rate from a given tumor should remain the same whether the tumor is at the surface or deep within the skull. With this in mind, the response patterns of three collimators were investigated. These included a long, narrow cylindrical aperture; a nineteen channel, 2 in. focusing collimator, and the sixty-one channel 3 in. focusing collimator. To simulate clinical conditions, isocount lines were measured using a plastic "tumor" 2 cm in diameter containing I^{131} in a skull filled with water. The data are presented in Fig. 4. None of these collimators has the ideal characteristic of uniform response from the surface to a depth equal to the maximum diameter of the skull. However, the 90 per cent response line of the 3 in. focusing collimator extends almost to the mid-line, providing essentially uniform response over one hemisphere. By scanning bilaterally, the entire brain volume can be uniformly covered.

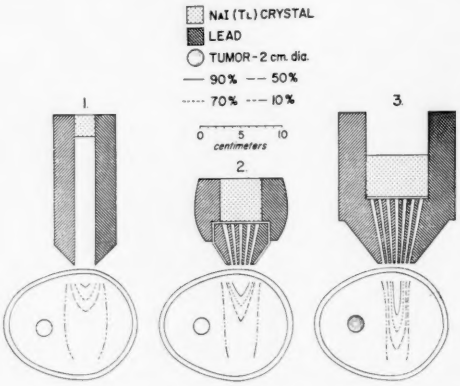

FIG. 4. Comparison of collimator depth response and resolution under simulated clinical conditions.
1. Single cylindrical hole, $\frac{3}{8}$ in. diameter, 6 in. long.
2. Two-inch focusing collimator, 19 channel.
3. Three-inch focusing collimator, 61 channel.

Pulse-height analyzer

Pulses from the photomultiplier tube are fed directly into the amplifier section of a Radiation Instrument Development Laboratory Model 115 amplifier–pulse-height analyzer. Pulses are selected for counting through a nine-volt window centered on the 0·36 MeV photo-peak of I^{131}. The full spectrum of this isotope covers a seventy-volt range. γ-rays outside the field of collimation reach the crystal only after losing energy through scattering processes. By counting only the primary radiation, the contribution from these scattered photons is minimized. Pulse-height analysis also reduces the background due to cosmic rays and local γ-sources. With the crystal and shield used in these studies, this background is reduced to 50–75 counts per min. With a simple discriminator set to count all pulses above 0·36 MeV the background is approximately 500 counts per min. This background reduction coupled with the high efficiency of the large crystal and focusing collimator permits scanning with minimal dosages.

OL.
4
8/59

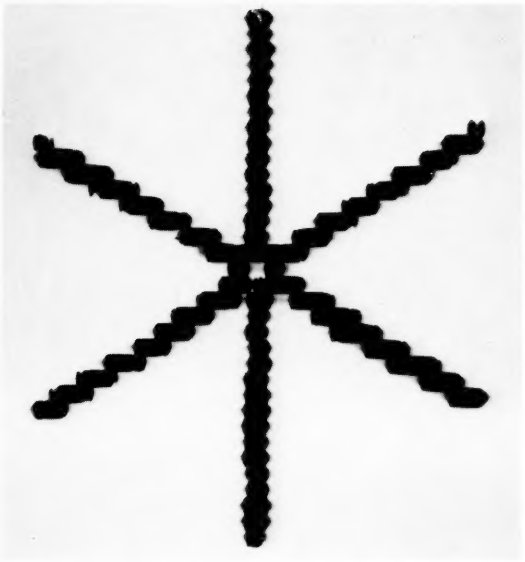

FIG. 3. Photoscan of six glass tubes filled with I^{131} solution. Inner diam. = 4 mm; Length = 10 cm.

VOL
4
1958/

Rate-meter and recorder

A model RB-1A Technical Measurement Corporation count-rate meter integrates the pulses that pass the pulse-height analyzer. The resistance-capacitance time constant for the 1000 count per min scale has been changed to 2 sec. The dosages used are such that almost all scanning can be done on this single scale. The output circuit of the count-rate-meter was changed to provide an output of 0–100 mV rather than the standard 0–10 mV. This was accomplished, as noted in Fig. 1, by replacing the 10 Ω output resistor by 100 Ω, ten-turn helipot (R_3). The potential developed across the resistor drives a Minneapolis Honeywell 10 mV Brown recorder with a 1 sec response time. By varying the output potentiometer of the rate-meter, full-scale deflection of the recorder can be obtained with any count-rate above 10 per cent of full scale.

Light circuit

A 70 Ω three-turn helipot (R_1) is mechanically coupled through a universal joint to the shaft of the pen drive wheel of the recorder. This potentiometer is in series with the fine filament of the scanning light bulb (GE No. 1158, a standard automobile tail-light bulb). The filament is energized by a 5 V a.c. transformer capable of delivering 5 A. When the recorder reading is 0, the portion of the potentiometer in series with the filament has a resistance of 27 Ω. When the recorder is driven to full-scale deflection, this resistance is decreased to 0 Ω. A multiple turn helipot was necessary because the pen drive shaft of the recorder revolves $1\frac{1}{8}$ turns for full-scale deflection.

The scanning light is mounted on the scanner in place of the printing stylus. The light exposes Kodak Blue Brand X-ray film (screen type) held in an X-ray cassette. The opaque bakelite face of the cassette is replaced with $\frac{1}{8}$ in. thick ruby, transparent Plexiglas covered by a sheet of window glass for mechanical protection. By using the ruby Plexiglas cassette, it is possible to scan in a room with subdued light without any fogging of the film. This avoids the complications associated with the use of a light-tight box. The coarse filament of the scanning bulb is used to mark the film for anatomical orientation. The light box and cassette are shown in Fig. 5.

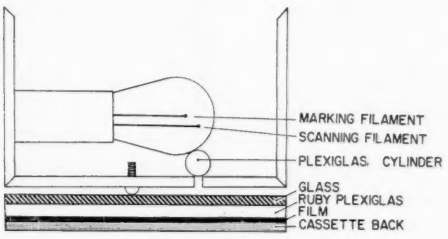

FIG. 5. Cross-section of light-box and cassette.

The voltage on the light bulb varies with the count-rate, and light output of the tungsten filament is sharply dependent on the applied voltage. As the light exposes the film, some of the high contrast achieved

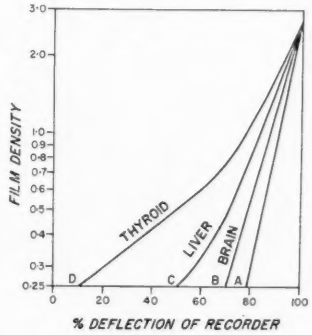

FIG. 6. Contrast curves.

by the use of the tungsten filament is lost due to the exponential response of the film to the light source. However, as shown by curve A in Fig. 6, the end result is high contrast and the full dynamic range of the film is used exclusively for presenting 20 per cent of the count-rate between 80–100 per cent of maximum.

To provide for clinical situations where the significant count-rate varies through a wider range than 20 per cent, a 30 Ω variable resistor (R_2) was placed in parallel with R_1 (Fig. 1.) Curves B, C, and D in Fig. 6 show film response data for various settings of the "contrast" control R_2. Based on

clinical experience, curve B was found to be optimal for the localization of brain tumors with I^{131} human serum albumin. Curve C is used for the localization of liver tumors with I^{131}-Rose Bengal and curve D for the visualization of thyroid tissue with I^{131}.

Scanning mechanism

The scintillation probe and the light box are mounted on a Nuclear Chicago Model No. 1700 isotope scanner. To achieve reasonable statistical accuracy with low doses, it is necessary to scan at a speed of 10–12 cm/min or less. Despite this relatively low scanning speed, the photographic image is displaced in the direction of the scan due to the necessarily slow response of the count-rate meter. If the data is recorded with the probe moving in alternating directions this results in a stepped effect with each line off-set in opposite directions. To prevent this, data is recorded only when scanning from left to right. A relay is activated when the probe reaches the right margin, simultaneously turning off the scanning light and switching to maximum scanning speed for fast return. Efforts to compensate for this "stepped effect" by means of two scanning bulbs appropriately off-set or an alternating shift in the position of the cassette were unsatisfactory because the degree of off-set is a function of count-rate and target: non-target ratio and these factors could not be predicted with sufficient accuracy to permit suitable adjustment.

CLINICAL APPLICATIONS

To date, three routine clinical procedures have been evolved using this apparatus. All of these procedures utilize I^{131} as the radioactive tracer:

(1) brain tumor localization with iodinated human serum albumin,
(2) liver tumor localization with Rose Bengal, and
(3) thyroid studies with sodium iodide.

The present report will only describe the techniques and a detailed evaluation of the clinical result will be published elsewhere.

Brain tumor localization

The uptake of radio-iodine by the patient's thyroid is blocked by the oral administration of 7 drops of Lugol's solution twice daily for three days, beginning the day before the administration of the tagged albumin. A dose of 5 μc per kg of body weight of I^{131}-labeled human serum albumin (RISA–Abbott Laboratories) is administered intravenously 16–48 hr before scanning. The patient lies on the scanning bed with his head fixed in a true lateral position. The head is immobilized with a dilatancy bag (Flexicast–Picker X-ray Corp.). The adjustment of the variable gain control (R_3, Fig. 1) to obtain proper film density is accomplished as follows: As the probe passes over Reid's baseline, the gain control is adjusted so that the recorder is just driven to full scale deflection along this entire line. A second trial pass is then made over the center of the cerebral region and if the first adjustment was correct, the recorder will read 70–80 per cent of full scale deflection except when the probe is over a region of abnormal deposition. The adjustment for the anterior and posterior views is made in the same manner. In the anterior view, the supra-orbital ridge serves as the baseline, and in the posterior view the initial pass is made at the level of the nuchal prominence. The contrast control is set to provide the response shown in Fig. 6, curve B. The exact location of a lesion is established by correlating abnormal densities on the lateral and anterior or posterior views.

Approximately 150 unselected patients suspected of having intracranial pathology have been examined. Preliminary evaluation indicates an accuracy of diagnosis and localization of 80–90 per cent. The scans were interpreted without access to clinical data or the results of other diagnostic procedures. Representative scans are shown in Fig. 7.

VOL
4
1958/

TOL. 4 8/59

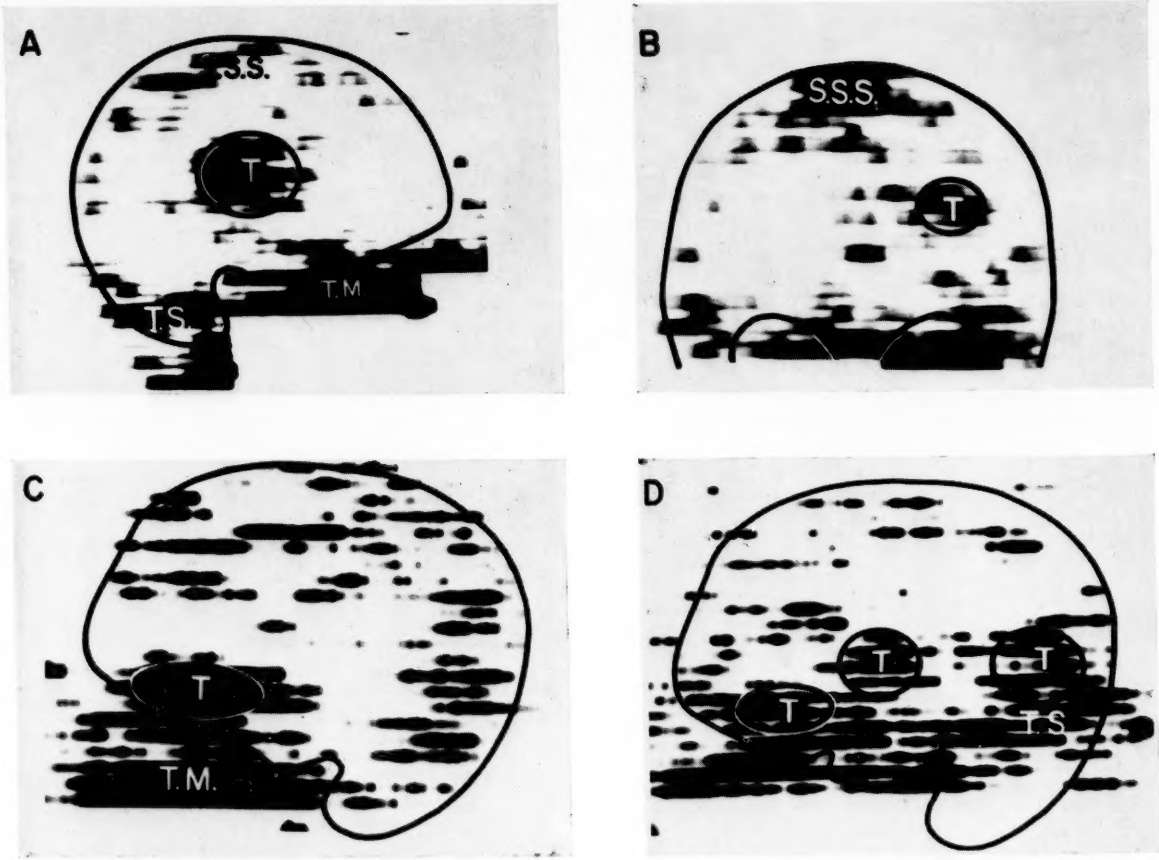

FIG. 7. Brain tumor localization studies, 24 hr after the intravenous administration of 5 μc/kg of I^{131} labeled human serum albumin, showing deposition in normal and tumor tissue.

T = tumor; T.M. = temporal musculature; T.S. = transverse sinus; S.S.S. = superior sagittal sinus.

A. Right lateral scan showing single 2 cm diameter metastasis from a carcinoma of the bronchus. B. Anterior scan of the same patient. C. Left lateral scan showing a 3 cm diameter astrocytoma at the mid-line in the anterior fossa. D. Left lateral scan showing multiple metastases from a malignant melanoma.

FIG. 8. Liver tumor localization studies following the intravenous administration of 50 μc of I^{131} labeled Rose Bengal.
T = tumor.

A. Normal liver.
B. Single metastasis from a carcinoma of the stomach.
C. Multiple metastases from a carcinoma of the colon.
D. Diffuse metastatic involvement with lymphosarcoma.

VOL.
4
1958/5

OL.
4
8/59

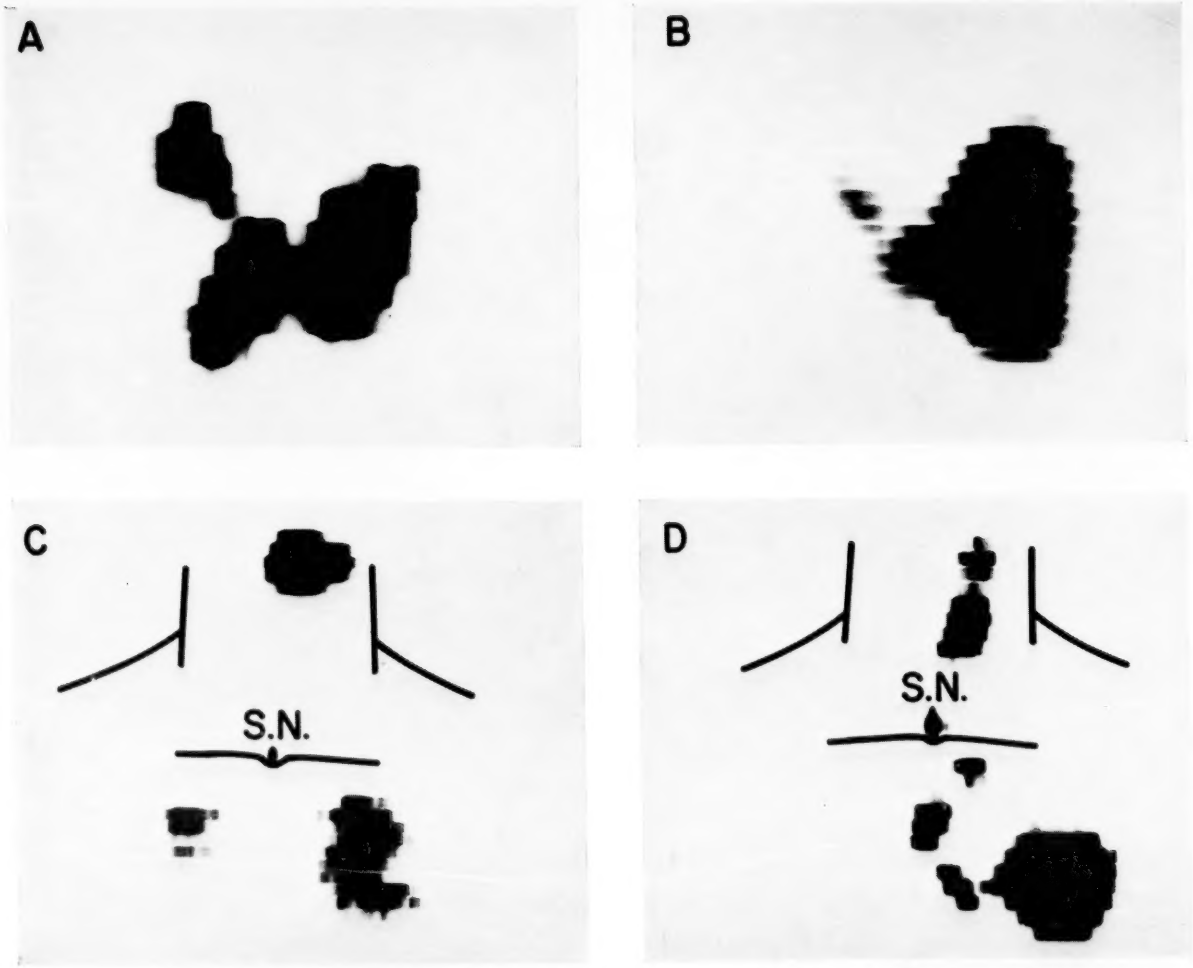

FIG. 9. Thyroid tumor localization studies 24 hr following the oral administration of 7–10 μc of NaI^{131}.
S.N. =sternal notch.

A. Single non-functioning adenoma of the right lobe.
B. Hemithyroidectomy.
C. Carcinoma of the thyroid metastatic to the lungs.
D. Carcinoma of the thyroid metastatic to mediastinal lymph nodes.

VOL
4
1958/5

Liver tumor localization

Rose Bengal[14] is removed from the blood by normally functioning liver parenchyma. Areas of non-functioning tissue within the liver are visualized on the scans as zones of radioisotope deficit. To prevent the rapid clearance of radioactive Rose Bengal through the liver, a blocking dose of 100 mg of non-radioactive Rose Bengal is injected intravenously. Ten minutes later, 50 μc of I^{131}-labeled Rose Bengal (Abbott Laboratories) are administered. Scanning is started 20 min after the injection of the radioisotope. For liver scans, the gain control is set to provide full-scale deflection of the recorder (maximum film density) over the majority of the liver. The contrast control is set to give the response shown in Fig. 6, curve C.

Sixty-five patients suspected of having metastatic liver disease, have been examined. Thirty-two of these cases have been evaluated at the time of surgery or autopsy. The scan findings were confirmed in 29 of the 32 cases. Fig. 8 shows several typical liver scans.

Thyroid tumor localization

The overall efficiency of this system is such that routine thyroid scanning can be accomplished with administered doses of 7–10 μc of I^{131}. Satisfactory scans have been obtained with as little as 0·5 to 1·0 μc localized in the gland. Metastatic sites giving count rates 10–20 per cent above background are readily visualized. For thyroid scans the gain control is adjusted to give maximum film density over the majority of the thyroid gland. The contrast control is set to provide the response shown in Fig. 6, curve D. Fig. 9 shows typical thyroid scans.

REFERENCES

1. Cassen B., Curtis L., Reed C. and Libby R. *Nucleonics* **9,** 46 (1951).
2. Anger H. O. *Amer. J. Roentgenol.* **70,** 605 (1953).
3. Horwitz N. H. and Lofstrom J. E. *Nucleonics* **13,** No. 7, 56 (1955).
4. Kuhl D. E., Chamberlain R. H., Hale J. and Gorson R. O., *Radiology* **66,** 730 (1956).
5. Bender M. A. *Science* **125,** 443 (1957).
6. Moore G. E. *Science* **107,** 569 (1948).
7. Chou S. N., Aust J. B., Moore G. E. and Peyton W. T. *Proc. Soc. Exp. Biol.* **77,** 193 (1951).
8. Selverstone B., Solomon A. K. and Sweet W. H. *J. Amer. Med. Ass.* **140,** 277 (1949).
9. Brownell G. L. and Sweet W. H. *Nucleonics* **11,** 40 (1953).
10. Planiol T. *Thérapie* **12,** 747 (1957).
11. Friedell H. L., MacIntyre W. J. and Rejali, A. M. *Amer. J. Roentgenol.* **77,** 455 (1957).
12. Newell R. R., Saunders W. and Miller E. *Nucleonics* **10,** 36 (1952).
13. Francis J. E., Bell P. R. and Harris C. C. Personal communication.
14. Taplin G. V., Meredith O. M., Jr. and Kade H. J. *J. Lab. Clin. Med.* **45,** 665 (1955).

International Journal of Applied Radiation and Isotopes, 1959, Vol. 4, pp. 162–168. Pergamon Press Ltd. Printed in Northern Ireland

Le Rôle de la Phagocytose Reticuloendotheliale dans L'Organisme Multicellulaire Irradié—I

L'Etude de l'Action à Distance des Radiotoxines au Moyen de Techniques de Parabiose

FREDERIC LUDWIG*

Service de Biologie du Commissariat à l'Energie Atomique, Saclay, France

(*Received* 23 *June* 1958)

Après une irradiation unique, l'activité des radiotoxines, telle que l'on peut la suivre au moyen d'une tumeur d'ascite, est progressivement réduite. L'injection intraveineuse d'une suspension aqueuse de particules de carbone permet de prolonger et d'accentuer l'activité des radiotoxines. De même, l'introduction des particules de carbone dans le courant sanguin de deux rats en parabiose permet, après l'irradiation de l'un des deux animaux, la réalisation d'un effet à distance au niveau d'une tumeur d'ascite inoculée à l'animal non irradié. De telles injections de systèmes granulaires chimiquement inertes réduisent temporairement la granulopexie du système reticuloendothélial et aggravent les états pathologiques faisant appel au pouvoir phagocytaire de celui-ci. Nous en concluons que des fractions appréciables des radiotoxines sont neutralisées par le système reticuloendothélial.

VOL.
4
1958/5

THE ROLE OF THE RETICULOENDOTHELIAL PHAGOCYTOSE IN THE IRRADIATED MULTICELLULAR ORGANISM—I. EXAMINATION OF THE REMOTE ACTION OF RADIOTOXINS BY MEANS OF PARABIOSE TECHNIQUES

After one single irradiation the activity of the radiotoxins, as followed by an abscopal effect produced in an ascites tumor, is progressively reduced. Furthermore, by introduction of carbon particles in the bloodstream of parabiotically united rats, it is possible to achieve an abscopal effect in an ascites tumor of the non-irradiated partner, after previous irradiation of the other animal. Such injections of chemically inert granular systems in the blood stream of experimental animals reduce temporarily the granulopectic activity of the reticuloendothelial system and aggravate pathological conditions involving phagocytosis. We therefore conclude that appreciable fractions of the radiotoxins are neutralized by the reticuloendothelial system.

РОЛЬ РЕТИКУЛОЭНДОТЕЛИАЛЬНОГО ФАГОЦИТОЗА В ОБЛУЧЕННОМ МНОГОКЛЕТОЧНОМ ОРГАНИЗМЕ—I. ИССЛЕДОВАНИЕ ДЕЙСТВИЯ НА РАССТОЯНИИ РАДИОАКТИВНЫХ ТОКСИЧЕСКИХ ВЕЩЕСТВ ПРИ ЭКСПЕРИМЕНТАЛЬНОМ ИАРАБИОЗЕ

Радиоактивность токсических веществ, приводящая к абскопальному эффекту, наблюдающемуся в опухоли брюшной полости, прогрессивно уменьшается после одного облучения. Далее, путем введения частиц угля в кровоток крыс, соединенных между собой парабиотически, можно вызвать абскопальный эффект в опухоли брюшной полости необлученного партнера, после предварительного облучения другого животного. Введение таких химически инертных гранулированных веществ в кровоток подопытных животных временно снижает гранулопектическую активность ретикулоэндотелиальной ситемы и способствует ухудшению паталогического состояния, вызываемого фагоитозом. Отсюда выводится эаключение, что эаметные количества радиоактивных токсических веществ нейтрализуются ретикулоэндотелиальной системой партнера.

* Chargé de recherches à l'Institut National d'Hygiène. *Present address:* Radiological Laboratory, University of California Medical Center, San Francisco 22, California U.S.A.

DIE ROLLE DER RETICULOENDOTHELIALEN PHAGOZYTOSE IM BESTRAHLTEN, VIELZELLIGEN ORGANISMUS—I. UNTERSUCHUNG DER INDIREKTEN WIRKUNG VON RADIOTOXINEN MITTELS DER PARABIOSE-METHODE

Fortlaufende Messungen an Aszitestumoren deuten darauf hin, dass die Aktivität der im Gefolge einer einzeitigen Bestrahlung auftretenden Radiotoxine stetig abfällt. Durch intravenöse Zufuhr einer wässrigen Suspension von Kohlepartikeln wird der Abbau der Radiotoxine verlangsamt. Intravenöse Zufuhr von Kohlesuspension in den Blutestrom parabiotisch vereinigter Ratten ermöglicht es ausserdem, nach Bestrahlung eines der beiden Tiere einen Distanzeffekt im Aszitestumor des unbestrahlten Tieres herbeizuführen. Durch die Einführung chemisch inerter Partikelsysteme in den Blutstrom von Versuchstieren wird deren retikuloendotheliale Phagocytose temporär herabgesetzt und alle solchen Zustände aggraviert, bei denen es zu parenteralem Abbau krankhaften Materials kommt. Wir schliessen daraus, dass das retikuloendotheliale System nennenswerte Fraktionen der Radiotoxine neutralisiert.

Des expériences précédentes nous avaient montré que l'irradiation à la lumière visible, après photosensibilitation de l'organisme considéré, peut provoquer un effet à distance appréciable au niveau d'une tumeur d'ascite inoculée dans cet organisme.[1] L'évolution d'un tel effet à distance peut être suivie par des mesures successives du taux des cellules nécrobiotiques de cette tumeur, vérifié au moyen de l'effet Strugger.[2,3] On peut admettre que ce phénomène est du à l'action de produits d'histolyse toxiques apparaissant au niveau du tissu ayant absorbé l'énergie radiante, emportés par le courant sanguin et agissant sur des structures spécialement réceptives.[4,5,6] Nous appelons "radiotoxines" l'ensemble de ces substances capablés de produire des effets biologiques ailleurs qu'à l'endroit de leur formation. Dans la présente étude, comme dans celles entreprises précédement, nous renonçons à l'analyse chimique des radio-toxines pour appliquer des méthodes permettant une appréciation quantitative de leur action globale.

Aprés un choc photodynamique provoqué chez la souris ou le rat porteur d'une tumeur d'ascite, le pourcentage de la tumeur en cellules nécrobiotiques ("Strugger-positives") augmente brusquement et redescend aux valeurs de contrôle en une semaine environ. La teneur en cellules nécrobiotiques de la tumeur inoculée est plus basse quand cette tumeur a été transplantée après l'irradiation. Plus le décalage entre irradiation et transplantation augmente, plus le pourcentage initial en cellules nécrobiotiques baisse (Fig. 1). Dans les tumeurs inoculées 9 jours après l'irradiation, aucun effet à distance n'est décelable.[7] On peut en déduire que, après une irradiation unique, l'activité des radiotoxines est progressivement réduite;[8] autrement dit, l'organisme multicellullaire semble disposer d'un mécanisme d'épuration des radio-toxines. Les expériences suivantes ont pour but de déterminer la nature de ce mécanisme.

L'injection intraveineuse d'une suspension aqueuse de particules de carbone accentue et prolonge l'effet à distance vérifié au niveau d'une tumeur d'ascite.[9] Des systèmes granulaires chimiquement inertes, introduits dans le courant sanguin, réduisent temporairement la granulopexie du système réticuloendothélial[10] et accentuent les états pathologiques faisant appel au pouvoir phagocytaire de celui-ci.[11]

On pourrait en déduire que des fractions appréciables des radio-toxines sont neutralisées par le système réticuloendothélial. Cette conclusion nécessite, il est vrai, une confirmation. Nous savons que le carbone introduit dans le courant sanguin produit un blocage temporaire de la phagocytose réticuloendothéliale. Mais ce blocage, si bien établi soit-il, n'est peut être pas le seul effet provoqué par le carbone; il est concevable que celui-ci provoque des altérations métaboliques inconnues, qui compliquent le syndrôme d'irradiation autrement que par une intensification de l'activité des radiotoxines. Il est connu que le stress non spécifique et la fatigue musculaire accentuent la radiosensibilité des animaux d'expérience.

Pour obtenir des renseignements plus

précis sur le mécanisme neutralisateur des radiotoxines, nous avons eu recours à des techniques de parabiose. On sait déjà depuis quelques temps que les effets à distance instantanés sont irréalisables chez le partenaire non irradié d'un couple de rats en parabiose.[15] Ceci a été attribué à l'intervention d'un mécanisme d'épuration qui s'opèrerait évidemment plus vite que le passage des radiotoxines d'un animal dans l'autre.[16] Si l'on admet que l'épuration qui prévient l'apparition des effets à distance dans l'animal parabiotique non irradié est identique à celle qui assure la réduction progressive de l'action des radiotoxines dans l'animal irradié indépendant, des techniques de parabiose peuvent être un moyen élégant pour mettre en relief la nature de cette clearance: pour provoquer l'action des radiotoxines chez le partenaire parabiotique non irradié, il faudrait donc, en dehors d'une irradiation efficace de l'autre partenaire, inhiber la phagocytose réticuloendothéliale des deux animaux.

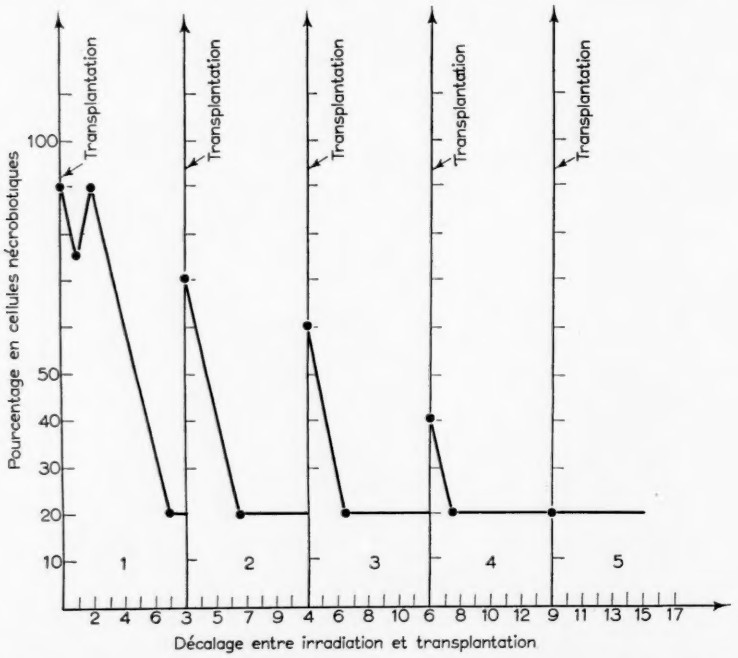

FIG. 1. Evolution du nombre des cellules Strugger-positives (nécrobiotiques) dans les tumeurs d'ascite inoculées à des animaux préalablement irradiés. Chaque courbe représente la moyenne obtenue à partir de 8–10 souris blanches inoculées par voie intrapéritonéale avec 0,25 ml d'ascite tumorale (Ehrlich). 12 hr après la transplantation, on détermine par 10 numérations successives le pourcentage des cellules Strugger-positives, chaque numération individuelle représentant la moyenne de 10 numérations du meme prélèvement. On effectue une numération journalière jusqu'à la mort de la souris, causée par la cachexie tumorale. Dans la première courbe, on a suivi l'évolution du pourcentage des cellules necrobiotiques dans une tumeur inoculée 5 hr après la réalisation du choc photodynamique (0,25 ml d'une solution aqueuse d'éosine rendue isotonique par le NaCl, irradiation, pendant 2 hr par une lampe Philips HP 125, (120 W), distance 90 cm, filtre verre ordinaire 15 mm). Les courbes représentent l'évolution du pourcentage en cellules nécrobiotiques de la tumeur telle qu'elle apparait dans des tumeurs inoculées 3, 4, 6 . . . jours après le choc photodynamique. Le deuxième maximum que l'on constate dans la première courbe ne se produit pas chez les souris surrénalectomisées.[1] Elle reflète l'intervention de la corticosurrénale dans le mécanisme de cet effet à distance. Nous avons constaté que 16 mg/C/100 g animal sous forme de 0,5 ml de suspension aqueuse n'augmentent pas le pourcentage en cellules Strugger-positives de la tumeur d'ascite, sauf si la suspension injectée contient du shellac. Puisque celui-ci accentue et prolonge le blocage du système réticuloendothélial, le blocage obtenu dans nos expériences ne dure guère plus de 3 jours (comp. 10). La suspension de carbone utilisée par nous est préparée à partir du produit 77/702 de la maison Günther Wagner. Cette solution a été stabilisée par 2 pour cent de gelatine blanche, la suspension pure provoquant des embolies chez les animaux injectés.

VOL
4
1958/

Nos expériences portent sur 51 couples de rats en parabiose. L'opération a été réalisée suivant la technique classique[17] améliorée par la suture des omoplates préconisée par SAUERBRUCH et son école.[18] La technique habituellement employée par les endocrinologistes prévoit la création d'une fenêtre péritonéale[19,20] permettant le contact direct des surfaces viscérales des séreuses. Pour nous, la réalisation d'une telle fenêtre est impossible en raison de la présence de la tumeur d'ascite. Celle-ci doit évidemment rester limitée à l'animal auquel elle a été inoculée sans se mélanger avec celle inoculée dans la cavité péritonéale de l'autre. C'est pourquoi nous avons suturé l'incision péritonéale de telle manière que les cavités respectives se referment (Fig. 2). Nos animaux ont été opérés à l'age de trois semaines quand ils pèsent 60 g. Ils ont été anesthésiés par injection intrapéritonale de 0,6 ml d'une solution saturée de α-chloralose. Avant et après l'opération, chaque rat reçut 40.000 U.I. de pénicilline. C'est surtout le traitement aux antibiotiques *avant* l'opération qui nous permit de réduire la mortalité à 20 pour cent.

Pour assurer un nombre suffisant d'expériences de contrôle, ces 51 couples de rats en parabiose ont été répartis de la façon suivante:

(1) 5 couples . . . vérification du pourcentage des cellules nécrobiotiques d'une tumeur A–A[21] inoculée à un rat en parabiose.

(2) 5 couples . . . vérification du pourcentage des cellules necrobiotiques de la tumeur A–A, inoculée à un rat en parabiose, après blocage du système réticuloendothélial des deux animaux par 16 mg C/100 g rat,

(3) 5 couples . . . vérification du pourcentage des cellules nécrobiotiques de la tumeur A–A du rat en parabiose dont le partenaire a subi un choc photodynamique, (Fig. 3. courbe A).

(4) 5 couples . . . vérification du pourcentage des cellules nécrobiotiques de la tumeu A–A du rat en parabiose dont le partenaire a subi une irradiation par 600 r de rayons-X (100 kV 12 mA, 50 r/min.) (Fig. 3, courbe B)

(5) 12 couples . . . vérification du pourcentage des cellules necrobiotiques de la tumeur A–A du rat en parabiose dont le partenaire a subi un choc photodynamique après blocage du système réticuloendothélial, (Fig. 3. courbe C)

(6) 12 couples . . . vérification du pourcentage des cellules necrobiotiques de la tumeur A–A du rat en parabiose dont le partenaire a subi une irradiation aux rayons-X (600 r, 100 kV, 12 mA, 50 r/min), après blocage du système réticuloendothélial. (Fig. 3, courbe D)

(7) 7 couples . . . vérification de l'épilation d'un rat en parabiose dont le partenaire a subi une irradiation par 600 r de rayons-X (100 kV, 12mA, 50 r/min).

Chez le rat en parabiose, il semble que le taux des cellules necrobiotiques de la tumeur A–A non traitée, qui est de l'ordre de 20 pour cent chez l'animal indépendant, est seulement de l'ordre de 15 pour cent. Cependant, le nombre restreint des animaux disponibles pour les expériences de contrôle, ne nous a pas permis d'affirmer qu'il s'agit là d'un effet protecteur de la part de l'animal associé par la parabiose, tel qu'il a été constaté par un certain nombre d'auteurs.[22]

Comme nous l'avons vu chez l'animal indépendant, l'injection intraveineuse de 16 mg C/100 g rat dans 0,5 ml de suspension aqueuse stabilisée par 0,01 g de gélatine blanche, ne modifie pas le taux des cellules nécrobiotiques de la tumeur A–A.

L'irradiation exclusive d'un seul des deux rats en parabiose pose le problème de la protection de l'animal chez lequel on se propose d'observer des effets à distance.

Dans ce but, nous utilisons une chambre à deux compartiments, dont les dimensions correspondent à celles des rats adultes et qui est construite de la façon suivante: la base et les deux faces antérieure et postérieure sont en Plexiglas. La face antérieure présente deux évidements sur lesquels reposent les museaux des rats. La séparation entre les deux compartiments est assurée par une paroi de laiton de 12 mm d'épaisseur qui présente une fente rectangulaire destinée au passage du pont tissulaire entre les deux rats en parabiose. L'un des deux compartiments est recouvert sur toute sa longueur d'un couvercle de laiton de 12 mm d'épaisseur,

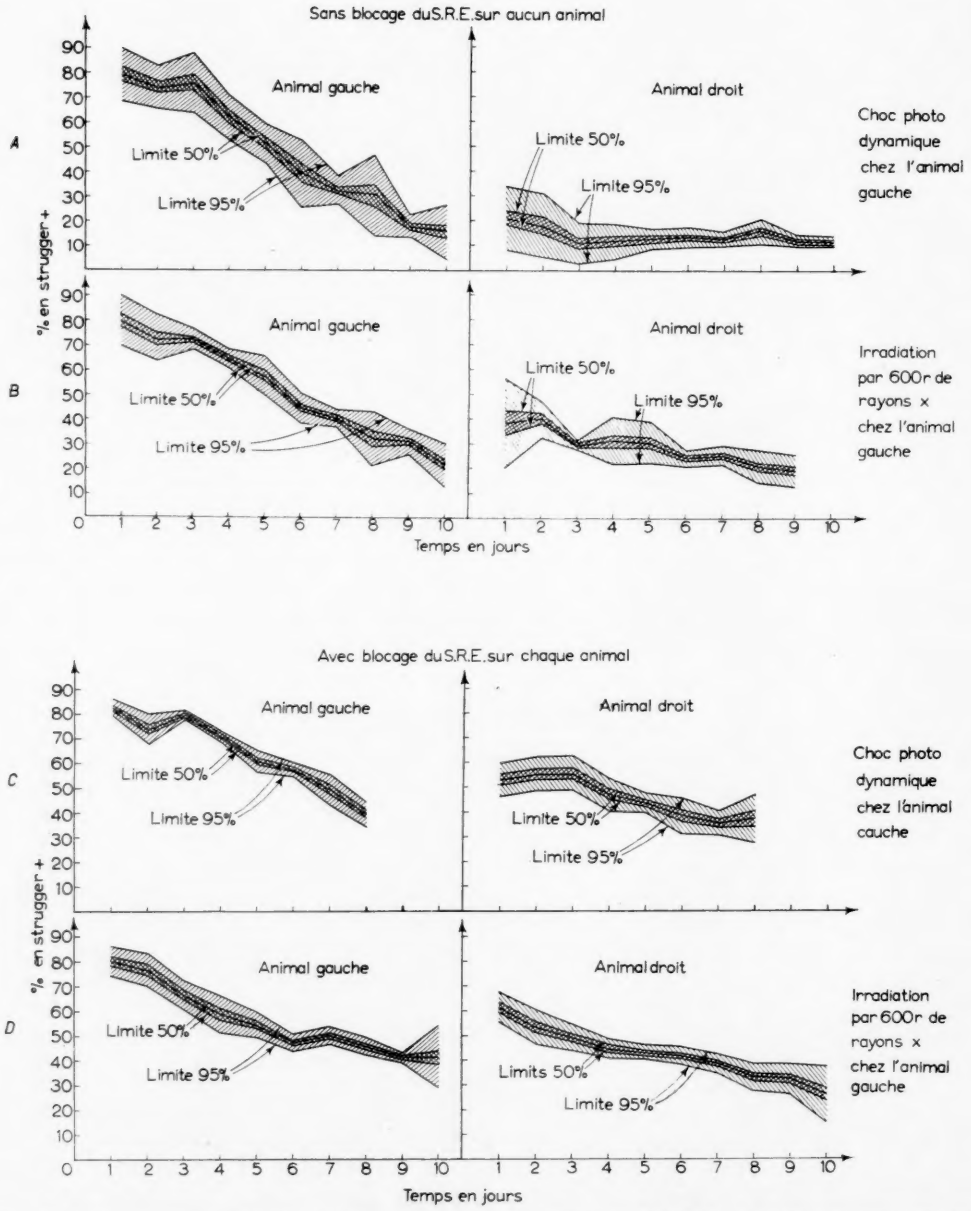

FIG. 3. Les rapports entre l'activité phagocytaire du système réticuloendothélial, l'inhibition de cette activité par les particules de carbone injectées par voie intraveineuse et le passage des radiotoxines d'un animal en parabiose irradié dans l'animal non irradié. Animal gauche: irradié, animal droit: effet à distance en fonction du blocage du système réticuloendothélial.

perpendiculaire au rayonnement incident.

L'introduction de cet appareil dans un chateau de plomb permet, lors de l'utilisation des rayons-X, d'éviter toute pénétration d'un rayonnement diffusé dans le compartiment de l'animal protégé, à l'exception de celui qui prend naissance au niveau de l'animal irradié et qui passe par la fente destinée au passage du pont tissulaire.

Pour évaluer l'importance relative de ce rayonnement diffusé, nous avons, à l'intérieur du compartiment destiné à l'animal protégé, installé trois sacs de cellophane mince, remplis de sulfate ferreux (concentration: 10^{-3} mol.) après avoir enfermé dans le compartiment d'irradiation un rat. L'un de ces sacs s'appuyait contre la fente de telle sorte que celle-ci était obstruée, le deuxiéme se trouvait dans le coin entre la face postérieure et celle présentant la fente, le troisième s'appuyait contre la paroi en face de cette fente.

L'application de 6000 r de rayons-X (100 kV, 12 mA 50 r/min) au rat enfermé dans le compartiment d'irradiation, produisait, au niveau du sac obstruant la fente, un rayonnement de l'ordre de 750 r. Toutefois, étant donné la différence considérable entre l'énergie du rayonnement incident et celle du rayonnement diffusé, une telle évaluation est sujette à caution. Le contenu des deux autres sacs ne présentait aucune oxydation radiochimique mesurable. La dose prévue pour l'irradiation du rat en parabiose étant de 600 r (100 kV, 12 mA, 50 r/min) et compte tenu de la limite de sensibilité de la dosimétrie à base de sulfate ferreux, nous admettons que le rayonnement diffusé au niveau de la fente ne peut pas dépasser 75 r. De plus, ce rayonnement diffusé, bien qu'il attaigne le pont tissulaire entre les parabionts, semble trop mou pour pouvoir atteindre l'intérieur du compartiment protégé.

La Fig. 3 montre que le choc photodynamique, appliqué à l'un des deux rats en parabiose, ne provoque aucun effet à distance chez l'animal non irradié (courbe A), alors que l'irradiation aux rayons-X entraine une augmentation significative du taux des cellules necrobiotiques de la tumeur d'ascite de l'animal protégé (courbe B). C'est cette différence qui est difficile à interpréter. Faut-il admettre que l'action des rayons-X, contrairement à celle des rayons lumineux agissant sur un tissu photosensibilisé, engendre la formation de substances capables de franchir la "barrière parabiotique" ou s'agit-il d'une radiolésion locale provoquée par le rayonnement diffusé, dont l'action, compte tenu de nos études dosimétriques, n'est peut-être pas négligeable? Pour l'instant, cette question reste sans réponse.

La courbe C par contre, représentant l'effet du blocage du système réticuloendothélial sur les phénomènes consécutifs au choc photodynamique, montre un effet à distance marqué au niveau de la tumeur de l'animal en parabiose non irradié. C'est l'injection de la suspension de carbone qui permet le passage des radiotoxines d'un animal à l'autre, ce qui indique que la présence du carbone dans le mesenchyme actif compromet un mécanisme de neutralisation. On peut correctement attribuer ce mécanisme de neutralisation aux structures qui captent les systèmes granulaires injectés et dont les propriétés phagocytaires sont solidement établies, c'est à dire au système réticuloendothélial. Pour ce qui est des rayons-X, le blocage du système réticuloendothélial accentue sensiblement l'effet au niveau de la tumeur de l'animal enfermé dans le compartiment protégé (Fig. 3, courbe D). On peut en déduire, compte tenu de ce que nous avons dit au sujet de la courbe B, Fig. 3, que, chez l'animal protégé, un effet à distance s'ajoute à un effet dont l'explication reste incertaine.

La chute du poil du rat en parabiose dont le partenaire a été irradié aux rayons-X, signalée par VAN DYKE et HUFF en 1949[23] a été vérifiée par nous sur 7 couples de rats en parabiose. L'épilation du rat protégé survient après 15 jours, peut durer une ou deux semaines et coïncide avec celle constatée chez l'animal irradié. VAN DYKE et HUFF signalent que la chute du poil du rat protégé se produit un peu avant celle du rat irradié et que sa durée est moins longue. Nous n'avons pas pu constater cette différence.

Etant donné l'intervalle considérable entre l'irradiation et la chute du poil, la longue

durée de cette dernière et la brève inhibition de la phagocytose réticuloendothéliale, nous n'avons pas essayé d'influencer ce phénomène par l'injection d'une suspension de carbone.

VAN DYKE et HUFF, eux aussi, ont fait des mésures dans le compartiment protégé du dispositif qu'ils ont employé et signalent une dose de 27 r, sans préciser la qualité de ce rayonnement. Une dose aussi faible, il est vrai, ne produit pas d'épilation, mais les expériences personnelles que nous venons d'exposer nous incitent à être prudent quant à l'explication définitive de l'épilation à distance. Peut-être des irradiations partielles au moyen d'un rayonnement non pénétrant ionisant permettront un jour des expériences plus concluantes.

BIBLIOGRAPHIE

1. LUDWIG F. *Int. J. Appl. Rad. Isotopes* **2,** 44 (1957).
2. LUDWIG F. *C. R. Acad. Sci., Paris* **239,** 957 (1954).
3. LUDWIG F. *C. R. Acad Sci., Paris* **239,** 453 (1954).
4. JOLLES G. *Nature* **164,** 63 (1949).
5. HEVESY G. V. *Rev. Mod. Phys.* **17,** 102 (1945).
6. RAPER J. R., ZIRKLE, R. E., and BARNES, K. K. *Comparative lethal effects of external β-irradiation. Effects of external β-irradiation* (Edited by ZIRKLE R. E.) McGraw Hill, New York (1951).
7. LUDWIG F. Regression de tumeurs d'ascite inoculées à des animaux préalablement irradiés. *C. R. Soc. Biol., Paris* (22me Juin, 1957).
8. LUDWIG F. La nature et la signification biologique des effets à distance dans les organismes multicellulaires irradiés. Conf. Soc. d'Anatomie, Section d'Anatomie Pathologique, Paris 1957.
9. LUDWIG, F. *C. R. Soc. Biol., Paris* **152,** 467 (1958)
10. HALPERN B. N., BENACERRAF B., BIOZZI G. et STIFFEL C. *Rev. Hémat.* **9,** 621 (1954).
11. BIOZZI G., BENACERRAE B. and HALPERN B. N. *Brit. J. Exp. Path.* **36,** 226 (1955).
12. HORNYKIEWITSCH TH., SOHRE W. und STENDRE H. ST. *Strahlentherapie.* **95,** 527 (1954).
13. STAPLETON G. E. and CURTIS H. J. Atomic Energy Comm. Techn. Inform. Dir. Abstr. of Clas. Doc. MDC-696 (Nov. 10, 1947).
14. QUASTLER H. *Mort consécutive à une irradiation brève. L'utilisation de l'énergie atomique à des fins pacifiques.* Actes de la Conference Internationale de Genève Vol. XI, p. 137 août 1955, Nations Unis, Genève (1946).
15. EDWARDS J. L. and SOMMERS S. G. *J. Lab. Clin. Med.* **40,** 342 (1952).
16. JONES J. B. Some physiological factors related to the effect of radiation in mammal. *Symposium on Radiobiology. The basic aspects of radiation effects in living systems.* (Edited by NICKSON J. J.) John Wiley, Chapman & Hall, New York–London (1952).
17. MILNE-EDWARDS M., FLOURENS C., COSTE F., BRONGIART J. et. BERNARD C. L. (rapporteur). *C. R. Acad Sci., Paris* **62,** 515 (1866).
18. SAUERBRUCH F. und HEYDE M. *Münch. Med. Wschr.* **55,** 153 (1908).
19. FINERTY J. C. *Physiol. Rev.* **32,** 277 (1952).
20. ZIZINE L. *Ann. Endroc.* **16,** 708 (1955).
21. APTEKMAN, P. M. and BOGDEN, A. E. *Cancer Res.* **15,** 89 (1955).
22. BINHAMMER R. T., METZ G., SCHNEIDER M. and FINERTY J. C. *Arch. Path (Lab. Med.)* **59,** 594 (1955).
23. VAN DYKE, G. and HUFF R. L. *Proc. Soc. Exper. Biol.* **72,** 266 (1959).

VOL.
4
1958/5

VOL.
4
8/59

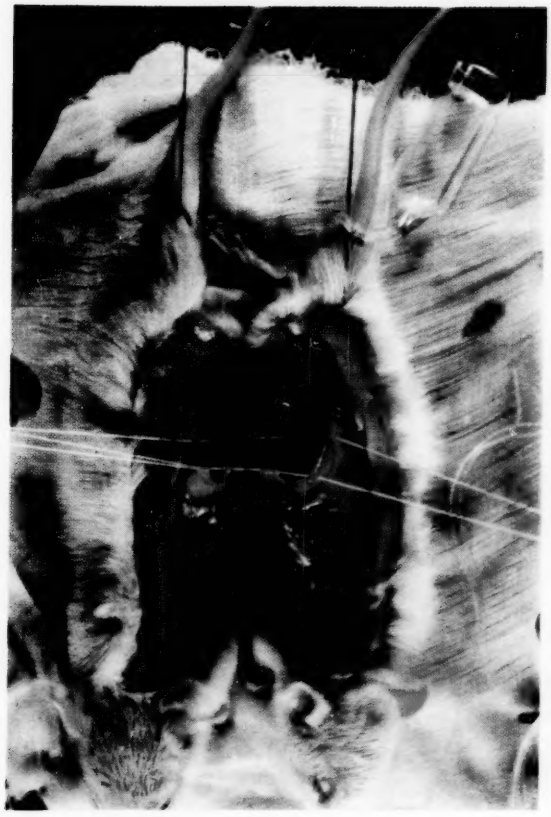

FIG. 2. Opération de parabiose. Les incisions péritonéales sont suturées de telle manière que les cavités péritonéales, au lieu de communiquer, se referment.

VOL.
4
1958/5

International Journal of Applied Radiation and Isotopes, 1959, Vol. 4, pp. 169–172. Pergamon Press Ltd. Printed in Northern Ireland

A Method for the Determination of Water Intake of Grazing Sheep*

J. R. LUICK, D. T. TORELL and W. SIRI
Department of Animal Husbandry and the Donner Laboratory, University of California, Davis and Berkeley, California

(*Received* 5 *May* 1958)

A method is described by which the moisture content of grazed pastures may be calculated. Sheep, fitted earlier with esophageal fistulas, were dosed with tritiated water, and the saliva water, which had been added to the egesta, was calculated by the isotope dilution technique. Forage water was then calculated as the difference between total water in the egesta and the saliva water. The validity of this method was verified by feeding ewes a ration of known water content. The results obtained by the isotope dilution technique and by dehydration were in close agreement. This method may be especially useful on ranges where it is impossible to obtain representative samples of the grazed forage.

OL.
4
8/59

UNE MÉTHODE DE MESURER L'ABSORPTION D'EAU DANS LES MOUTONS PAISSANTS

On décrit une méthode pour calculer le contenu d'humidité des prairies pâturées. Des moutons munis au préalable de fistules ésophagéales furent dosés d'eau tritiée, et l'eau salivaire, déjà ajoutée à l'égesta, se calcula par la technique de la dilution isotopique. L'eau de fourrage fut alors calculée comme la différence entre le total d'eau dans l'égesta et l'eau salivaire. La validité de cette méthode fut vérifiée en donnant à des brebis une ration de contenu aqueux connu. Les résultats donnés par la technique de dilution isotopique et par la déhydratation étaient très rapprochés. Cette méthode pourra servir particulièrement sur des prairies telles qu'il est impossible d'obtenir des échantillons représentants du fourrage pâturé.

МЕТОД ДЛЯ ОПРЕДЕЛЕНИЯ ДОЗЫ ВОДЫ ПОГЛОЩАЕМОЙ ОВЦАМИ НА ПАСТБИЩЕ

Описан метод определения влаги на пастбище. Овцам с фистулой пищевода вводили определенную дозу тритиевой воды. Затем методом изотопного разведения определяли количество воды в слюне, применявшейся к проглоченной пище. Далее содержание воды в корме определяли как разность между количеством воды в проглоченной пище и в смочившей ее слюне. Надежность метода была проверена путем кормления овец кормом с заранее известным содержанием воды. Результаты, полученные методом изотопного разбавления и методом обезвоживания хорошо согласуются между собой. Этот метод может быть особенно полезен в тех случаях, когда нет возможности взять на анализ пробы подножных кормов.

EINE METHODE ZUR BESTIMMUNG DER WASSERAUFNAHME WEIDENDER SCHAFE

Es wird eine Methode beschrieben, mit deren Hilfe Kalkulationen über den Feuchtigkeitsgehalt des abgeweideten Grasfutters angestellt werden können. Schafe, denen schon vorher Ösophagus-Fisteln angebracht worden waren, wurde Tritium-hältiges Wasser eingeflösst und das Speichelwasser, welches der Egesta beigefügt worden war, wurde durch die

* This investigation was supported by the U.S. Atomic Energy Commission.

Isotopenverdünnungsmethode berechnet. Das Futterwasser wurde dann als die Differenz zwischen dem Gesamtwasser der Egesta und dem Speichelwasser berechnet. Die Gültigkeit dieser Methode wurde durch Verfütterung einer Protion bekannten Wassergehaltes an Mutterschafe verifiziert. Die Ergebnisse, die man durch die Isotopenverdünnungsmethode und durch Dehydrierung erzielt wurden, stimmten gut überein. Diese Methode ist besonders für solche Gebiete geeignet, in denen es unmöglich ist, charakteristische Proben des abgegrasten Futters zu erhalten.

INTRODUCTION

THE moisture content of the forage which a sheep eats while grazing is in general not well known. The most widely used method to date for making this determination has been the analysis of forage specimens which have been clipped by hand. This procedure is both tedious and time consuming. Furthermore, it is quite unlikely that one would obtain by clipping, a sample which would represent exactly the food which a sheep eats. A sheep may be highly selective, not only in the species of grasses or legumes eaten on mixed pastures, but also on the parts (leaves, stems, blossoms, etc.) of the selected plant.

Recently, TORELL[1] described an esophageal fistula technique by means of which one may obtain a sample of forage that a sheep actually eats. It appeared to us that we could use this technique to determine the moisture content of pasture, provided we could separate egesta water into food water and saliva water. We have shown that such a separation can be made by the use of tritium-labeled salivary water [HTO].

VOL 4 1958/

METHODS AND PROCEDURES

Two mature white-faced ewes of approximately 55 kg body weight were fitted with esophageal fistulas as described earlier.[1] A metal cannula was inserted through the esophageal fistula and into the rumen 12 hr before the first collection period. Fifty ml of tritiated water containing approximately 5 mc of H^3 were injected into the rumen through a plastic tube which had been previously threaded through the metal cannula. Collections were taken at 0·5 and 4·5 days after injection.

Prior to each collection, a 5 ml saliva sample was obtained by removing the esophageal fistula plug and placing a 20 dram shell vial against the inner wall of the esophagus. After the saliva sampling, the sheep were fitted with an egesta collection bag and allowed to graze lawn clippings for 20 min. The saliva and egesta samples were stored in the frozen state for subsequent radiochemical analysis.

Later the egesta samples were weighed, thawed, and thoroughly kneaded while inside the plastic collecting bag to ensure thorough mixing. These samples were then rolled to form a tube of approximately 4 cm diameter and refrozen. They were sawed into 2 cm thick rings, and alternate rings were taken for isotope analysis and for dry matter determination. The entire saliva sample was lyophilized while frozen. Dry matter content of the egesta, forage, and lawn clippings was determined by drying at 105°C for 48 hr.

Preparation of water samples for radiochemical analysis

Water was removed from the frozen egesta rings and was trapped quantitatively in the cold finger* of a lyophilizing apparatus. This apparatus is shown in Fig. 1. The sample was placed in a 2 l. reaction flask† which was fitted with a manometer, and was lyophilized for at least 12 hr. An infra-red heat lamp was used during the last 2 hr of lyophilization to complete the drying process. The shell vials containing the

* Vacuum trap No. 7525, Ace Glass Inc., Vineland, New Jersey.
† Reaction flask No. 6486, Ace Glass Inc., Vineland, New Jersey.

VOL.
4
58/59

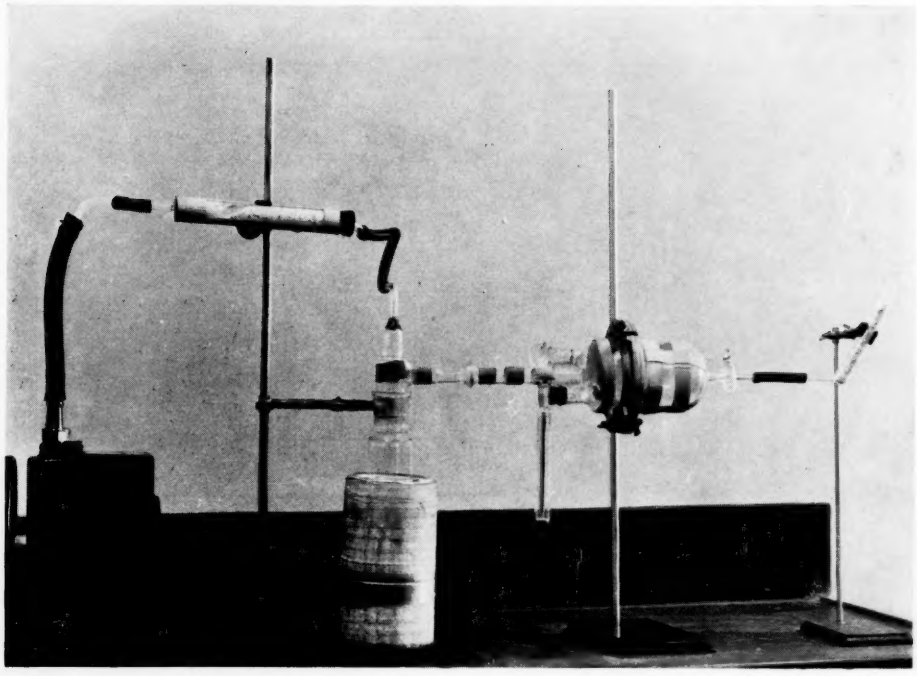

FIG. 1. Apparatus used for the low-temperature recovery of water from large egesta samples.

VOL
4
1958/

frozen saliva were attached directly to the apparatus in place of the reaction flask. The tritium concentration in the water samples was determined by means of a vibrating-reed electrometer.

RESULTS AND DISCUSSION

The calculation of the water intake of grazing sheep is based on the principle of isotope dilution. Thus, after ingestion, tritiated water is rapidly absorbed from the digestive tract, and is distributed throughout the total body water.[2] A portion of the labeled water is trapped by the salivary glands and is secreted as saliva. The food which is eaten by the sheep travels only a few cm down the esophagus before it falls through the esophageal fistula into the collection bag. We assume that the tritium which is found in the egesta must come from the saliva since the foodstuff does not contain tritium.

If σ is the specific activity of the saliva, expressed as μc of tritium per ml water, and S the amount of salivary water (ml) which is added to the egesta, then σS indicates the amount of tritium (in μc) which is secreted as saliva water into the egesta. This amount of tritium may also be expressed as εE where ε is the specific activity of the egesta and E is the total egesta water.

Thus

$$\sigma S = \varepsilon E$$

and the amount of added salivary water may be calculated as:

$$S = \frac{\varepsilon}{\sigma} E$$

If food water is expressed as W, and the dry matter intake as D,* then

$$W = E - S = E - \frac{\varepsilon}{\sigma} E = E\left(1 - \frac{\varepsilon}{\sigma}\right)$$

and the per cent water content of the food is equal to:

$$\left(\frac{W}{W + D}\right) 100.$$

This method of calculating the per cent moisture in a food stuff was tested by feeding lawn clippings to two ewes. Collections were made at 0·5 and 4·5 days after ingesting 5 mc of tritiated water into the rumen of each ewe. A saliva sample was taken immediately

TABLE 1. A comparison of the direct and indirect methods of determining % moisture in the feed of sheep

Category of interest	Collection 1		Collection 2	
	Sheep no. 4777	Sheep no. 4387	Sheep no. 4777	Sheep no. 4387
Collection time from injection (days)	0·5	0·5	4·5	4·5
Egesta water, E, (g)	314	157	483	385
Food water, W, (g)	174	52·5	237	175
Saliva water, S, (g)	140	104	246	210
Dry matter in egesta, D, (g)	41·7	14·5	63·5	35·5
Specific activity of saliva, σ (μc H^3/ml H_2O)	0·0734	0·0733	0·0305	0·0305
Specific activity of egesta, ε (μc H^3/ml H_2O)	0·0327	0·0487	0·0156	0·0166
% Moisture in feed				
isotope analysis	80·05	79·0	79·0	82·8
direct measurement	80·2	80·2	78·5	78·5

* In this formulation, D is measured as the dry matter content of the egesta. We assume that the contribution of dry matter from the saliva is negligible since saliva is reported to contain more than 99 per cent water.[3]

before the collection of the egesta and a dry matter determination of the lawn clippings was made to compare with the results obtained by isotope analysis. These results are shown in Table 1.

During the first collection period the lawn clippings were found to have a moisture content of 80·2 per cent by desiccation as compared with 80·5 per cent and 79·0 per cent by isotope analysis. Similarly, in period 2, we found a moisture content of 78·5 per cent (desiccation) as compared with 79·0 per cent and 82·8 per cent (isotope analysis).

The close agreement between the two methods justifies the use of this technique for the determination of the moisture content of pasture grasses where it is impossible to obtain representative samples of the forage.

REFERENCES

1. Torell D. T. *J. Anim. Sci.* **13,** 878 (1954).
2. Thompson R. C. *Nucleonics* **12,** 31 (1954).
3. Dukes H. H. *The Physiology of Domestic Animals* (6th Ed.) p. 270. Comstock, New York (1947).

VOL
4
1958/

International Journal of Applied Radiation and Isotopes, 1959, Vol. 4, pp. 173–178. Pergamon Press Ltd. Printed in Northern Ireland

Ermittlung von Spurenverunreinigungen im Reinstphosphor durch Aktivierungsanalyse

W. GEBAUHR und J. MARTIN
Forschungslaboratorium der Siemens–Schuckertwerke AG, Erlangen, Germany

(*Received* 13 *January* 1958; in revised form 28 *April* 1958)

Es sollte versucht werden, den Verunreinigungsgrad des für Halbleiterzwecke benötigten Reinstphosphors zu ermitteln. Hierzu diente die Aktivierungsanalyse als Übersichtsanalyse, deren Fehlerbreite $2^{\pm 1}$ betragen konnte.* Aus dem 42 Tage lang bestrahlten Phosphor wurden verschiedene Nuklide auf chemischem Wege abgetrennt und die Absolutaktivität der radiochemisch reinen Präparate aus den Daten einer allgemein üblichen Messanordnung rechnerisch ermittelt. Zur Identifizierung der erhaltenen Aktivitäten dienten neben ihrem chemischen Verhalten auch die physikalischen Eigenschaften. Zur Ermittlung von E_{max} bei β-Strahlern musste wegen der geringen Aktivitätsraten die Halbwertsdicke herangezogen werden, die sich auch hier gut bewährte.

ESTIMATION OF TRACE IMPURITIES IN HIGH-PURITY PHOSPHORUS BY ACTIVATION ANALYSIS

An attempt was made to estimate the degree of impurity of high-purity phosphorus, needed for semi-conductor work. Activation analysis was used as a general method, thus the deviations could be $2^{\pm 1}$ of the true values. After pile irradiation for 42 days the radionuclides produced in the phosphorus were separated chemically. The true activities of the radiochemically pure samples, were determined by a mathematical method, from measurements with a conventional counting assembly. The radionuclides were identified by their chemical and physical properties. In view of the low counting rates, E_{max} of the β-emitters was estimated by means of half-thickness, a method which was found to be excellent in this case.

RECHERCHE DES TRACES D'IMPURETÉS DANS LE PHOSPHORE LE PLUS PUR PAR ANALYSE PAR ACTIVATION

Le problème consistait à rechercher le pourcentage d'impuretés contenues dans le phosphore le plus pur nécessaire pour les semi-conducteurs. La méthode employée a été l'analyse par activation servant dans le cas présent d'analyse synoptique, dont la marge d'erreurs peut être de $2^{\pm 1}$. Différents nuclides ont été isolés par voie chimique du phosphore irradié pendant 42 jours, et l'activité absolue des préparations radiochimiquement pures a été recherchée à l'aide d'un procédé de calcul, en partant des données d'un montage usuel de mesure. L'identification des activités a été faite en se basant sur leur comportement chimique et sur leurs propriétés physiques. Pour la recherche de E_{max} sous les rayons-β il a fallu employer, à cause de la petitesse des activités, la méthode de l'absorption de moitié qui a donné dans ce cas de bons résultats.

ОПРЕДЕЛЕНИЕ ЗАГРЯЗНЕНИЙ В ХИМИЧЕСКИ ЧИСТОМ ФОСФОРЕ ПРИ ПОМОЩИ АКТИВАЦИОННОГО АНАЛИЗА

Требовалось определить загрязнения в химически чистом фосфоре, применявшемся для полупроводников. Для этого был выбран активационный анализ, погрешность которого находится в пределах $2^{\pm 1}$. Из фосфора, подвергнутого 42-дневному облучению, были выделены химическим путем различные изотопы и абсолютная активность радиохимически чистых препаратов вычислялась из данных обычных измерений. Идентифицирование полученных активных веществ производилось как по их химическому поведению, так и по физическим свойствам. Вследствие малых значений активности β-излучателей, определение E_{max} для этих веществ пришлось производить по половинной толщине слоя, что в данном случае вполне оправдало себя.

* Dies bedeutet, dass der wahre Wert die Hälfte oder das Doppelte der gegebenen Zahl betragen kann.

REINSTER Phosphor wird für die Halbleiter-Verbindungen vom Typ A(III)–B(V), z.B. InP, benötigt, da nur reinste Substanzen die gewünschten physikalischen Effekte zeigen. Diese hängen im einzelnen von der Natur der Verunreinigungen ab, so dass eine Aufklärung über deren Art und Konzentration erwünscht ist. Eine solche Spurenanalyse ist nicht nur für die physikalische Seite, sondern auch für die Weiterentwicklung der chemischen Präparation von Bedeutung.

Bei dem in unseren Laboratorien hergestellten, hochreinen elementaren Phosphor konnte als sicher angenommen werden, dass der Gehalt der meisten Verunreinigungen weniger als 10^{-4} Prozent betragen würde. Hierüber mit den üblichen Analysenverfahren genauere Aussagen zu erhalten, erschien, zumal in dieser Grundsubstanz, nur in einzelnen Fällen nach langwieriger Entwicklungsarbeit erfolgversprechend. Mehr Aussichten bot dagegen die Methode der Aktivierungsanalyse, welche die gerade bei der Ermittlung geringer Konzentrationen so hinderliche Empfindlichkeitsbegrenzung durch den Blindwert aufhebt. Sie ermöglicht fernerhin nach Zugabe von inaktiven Isotopen eine Vereinfachung der Arbeitstechnik, so dass das betreffende Element auf Grund der resultierenden Mengen eine geringe Selbstabsorption in den Endpräparaten mit sich bringt.

Im allgemeinen lässt man mit der zu analysierenden Probe einen Standard mitbestrahlen, der aus der gleichen Grundsubstanz, jedoch mit definiertem Gehalt an dem zu bestimmenden Element besteht. Mitunter werden auch die zu bestimmenden Elemente in geeigneter Form, von der Probe getrennt, doch in der gleichen Bestrahlungseinheit mitgegeben. Die gezielte Dotierung stösst bei elementarem Phosphor auf erhebliche Schwierigkeiten, so dass allenfalls die zweite Möglichkeit für uns in Frage gekommen wäre. Aber wir besassen keinerlei Anhaltspunkte für die Art und Menge der Verunreinigungen. Sowohl den physikalischen als auch den chemischen Belangen genügte zunächst eine Übersichtsanalyse mit einer Genauigkeit von $2^{\pm 1}$. Dieser Forderung musste auch ohne die Beigabe von Standards nachzukommen sein, so dass wir auf eine solche verzichteten und den radiochemisch reizvolleren Weg einschlugen, mit Hilfe anderer Methoden die wahre spezifische Aktivität der abgetrennten Elemente und damit ihren Gehalt zu ermitteln.

Es erschien nach überschlägiger Rechnung möglich, von einer Reihe von Elementen noch Konzentrationen von 10^{-7} Prozent bei einer Einwaage von 1–2 g Phosphor zu erfassen, sofern eine siebenwöchige Bestrahlung bei einer thermischen Neutronenflussdichte von mindestens $1 \cdot 10^{12}$ Neutronen/cm^2/sec erfolgte. Unter diesen Bedingungen erreicht der Phosphor eine spezifische Aktivität von ca. 85 mc/g. Die Handhabung solch relativ stark aktiver Substanzmengen erfordert zwar besondere Schutzmassnahmen, wird jedoch durch den Umstand erleichtert, dass es sich um einen reinen β-Strahler von 1,7 MeV handelt. Da ein besonders eingerichtetes radiochemisches Laboratorium mit mehreren Arbeitsräumen zur Verfügung stand, ergaben sich von dieser Seite keine Schwierigkeiten. Die zu erwartenden geringen Mengen an Verunreinigungen machten die Zugabe von inaktiven Trägern notwendig, um Adsorptionsverluste, Mitreisseffekte u.ä. bei den chemischen Trennungen auszuschliessen. Zu diesem Zweck setzten wir der eingewogenen Phosphor-Probe vor dem Lösen eine Reihe verschiedener Kationen zu, die zum Teil als Träger, zum Teil auch als Rückhalte-Träger fungieren sollten.

Eine Reihe von Elementen, die als Verunreinigungen u.U. enthalten sein konnten, besitzen relativ kurzlebige Isotope. Die Erfassung derselben konnte nicht in allen Fällen mehr erfolgen, da der Transport vom Reaktor* auch per Flugzeug einen Tag in Anspruch nahm. Nach kritischer Durchsicht der in Frage kommenden Elemente erschien es möglich, die eventuell noch messbaren Radionuklide des As, Cu und Na in einem sogenannten Schnellgang vor den übrigen, längerlebigen Radionukliden

* Die Bestrahlung erfolgte im Reaktor "BEPO" in Harwell, England.

VOL. 4 1958/5

zu erfassen. Dabei war die wahrscheinlich noch merkliche Aktivität des Si^{31} ($t_{1/2}$ = 2,5 hr) zu berücksichtigen, die auch beim Fehlen einer Silicium-Verunreinigung infolge der (n,p)-Reaktion des P^{31} auftreten musste.

Für alle analytischen Operationen wurden solche Reaktionen gewählt, die einfach durchzuführen sind, daneben aber genügende Spezifität und hohe Ausbeute sichern. Letzteres erschien im Hinblick auf die zu erwartenden geringen Impulsraten notwendig. Die Forderung nach radiochemischer Reinheit bedingte die Wahl umfällbarer Niederschläge. Zur Verringerung des Arbeitsaufwandes strebten wir Gruppenumfällungen an. Im Hinblick auf die Hauptaktivität P^{32} war es zweckmässig, Niederschläge zu wählen, die in sauren Lösungen umgefällt werden können, wobei selbstverständlich inaktives Phosphat zuzugeben war.

Der Schnellgang begann 34 hr nach Entnahme aus dem Reaktor und sei hier wegen des vom üblichen abweichenden chemischen Verfahrens kurz erläutert: 2,6 g roter Phosphor wurden mit einer Lösung versetzt, die die Ionen folgender Elemente in definierten Mengen von je 2–3 mg enthielt: Si, As, Sb, Sn, Te, Se, Cd, Cu, Fe, Cr, Ni, Co, Zn, Ca, Na. Nun erst erfolgte durch Zugabe von 20 ml konz. HNO_3 und—tropfenweise—0,5 ml Br_2 das Lösen des Phosphors und seine quantitative Überführung zum Phosphat. Die Kieselsäure wurde in üblicher Weise unter mehrmaligem Abrauchen unlöslich gemacht. Im eingeengten Filtrat erfolgte die H_2S-Fällung bei steigendem pH Wert bis pH 3. Aus dem erhaltenen Niederschlag wurden die Sulfosäuren mittels 5% iger Na_2S-Lösung in Lösung gebracht. Nach Oxydation des Sulfidschwefels zum Sulfat und Zugabe von konz. H_2SO_4, etwas NaN_2PO_4 sowie Hydrazinsulfat und Borax wurde Arsen quantitativ abdestilliert. Aus der ursprünglich natron-alkalischen Vorlage erfolgte nach Oxydation mit H_2O_2 und Ansäuern schliesslich in 6 N HCl die Fällung des As_2S_5.

Zur quantitativen Entfernung des Phosphors war bei den Sulfobasen eine nochmalige Umfällung notwendig. Das Kupfer wurde schliesslich vom mitgegebenen Cadmium durch Fällung aus essigsaurer Lösung als Cu-Oxinat getrennt und zur Messung, gebracht. Für die Anreicherung des Natriums im Filtrat der H_2S-Gruppe wählten wir das Ausfällen des NaCl durch Einleiten von HCl-Gas in die gekühlte Lösung. Nach zweimaliger Umfällung unter Phosphatzusatz erwies sich auch dieses Präparat als radiochemisch rein.*

Die übrigen Prüfungen wurden 8 Tage nach Entnahme durchgeführt. Die Endmessungen erfolgten am zehnten Tage, so dass die kurzlebigen Aktivitäten nicht weiter berücksichtigt zu werden brauchten.

Für die möglichst quantitative Abtrennung aller Kationen von der Hauptmenge des Phosphats in einer Operation fiel die Wahl auf ein Ionenaustauschverfahren. Aus Vorarbeiten ergab sich, dass die gewählten Ionen von dem Kationenaustauscher Amberlite IR–120 (H-Form) aus einer Lösung von pH 4 quantitativ zurückgehalten werden. Das dabei schon weitgehend hydrolysierte Sb verbleibt gleichfalls quantitativ auf der Säule. Durch Nachwaschen mit inaktiver Phosphatlösung vom pH 5 bei sehr geringer Durchflussgeschwindigkeit gelingt es, ohne Verluste an Kationen die Phosphatkonzentration im salzsauren Eluat noch weiter herabzusetzen.

Für die Trennung der Vielzahl von Elementen legten wir das Arbeitsschema des qualitativen Trennungsganges, wie es z.B. von BÖTTGER[1] angegeben wird, zu Grunde und führten dieses wegen der anzustrebenden hohen Ausbeute sehr sorgfältig durch. Die hierbei erhaltenen Niederschläge mussten selbstverständlich entsprechend dem hohen Anfangsgehalt an radioaktivem Phosphor noch etwas P^{32}-Aktivität besitzen. Die notwendigen Reinigungsoperationen wurden in der üblichen radiochemischen Arbeitsweise unter Zusatz entsprechender "Rückhalter" so lange durchgeführt, bis die Impulsraten konstant

* Nach Abklingen der Na-Aktivität konnte keine längerlebige Strahlung gemessen werden, was zunächst überraschte, da mit der Möglichkeit des Mitreissens von Fe, Co oder Ca zumindest in geringem Masse zu rechnen war.

blieben. Beim Eisen ergab sich die Notwendigkeit, eine Ätherextraktion einzuschieben, welche die letzten Phosphatspuren wirksam entfernte. Der Impulsmessung, wurde, soweit möglich, eine Mengenbestimmung angeschlossen, um ein Mass für die chemische Ausbeute zu erhalten.

Die Einwaage von 2,6 g wurde in gleicher Weise wie beim Schnellgang gelöst; die vorher zugegebene Kationenlösung enthielt, ausgenommen die Elemente mit kurzlebigen Isotopen, die gleichen Komponenten. An das Verkochen des überschüssigen Broms schloss sich die Einstellung auf pH 4 mit NaOH an. Die Durchflussgeschwindigkeit bei dem folgenden Ionenaustausch-Prozess betrug 30 Tropfen/min (Säule: 400 mm, 20 mm Durchmesser). Das noch zurückgebliebene Phosphat konnte mit 50 ml 1% iger NaH_2PO_4-Lösung und weiteren 300 ml H_2O weitgehend ausgewaschen werden. Zum Eluieren dienten 250 ml 6 N HCl.

Die so erhaltene Lösung der Kationen wurde eingeengt, ihre Acidität auf 2N eingestellt und die H_2S-Fällung, Abtrennung der Sulfosäuren sowie die Isolierung der einzelnen Elemente mit den üblichen chemischen Verfahren durchgeführt. Se und Te wurden gemeinsam mit SO_2 gefällt und wegen der für eindeutige Identifizierungen zu geringen Gesamtaktivität nicht weiter getrennt.

Die in der Ammoniakgruppe ausgefallenen Hydroxyde des Fe und Cr wiesen eine Gesamtaktivität von ca. 2500 cpm auf. Die Reinigung des mittels $NaOH + H_2O_2$ abgetrennten $Fe(OH)_3$ durch Umfällen konnte hier keinen Erfolg bringen. Am wirksamsten erschien die Äther-Extraktion; der nach Rückschütteln in wässriger Lösung erhaltene Niederschlag zeigte eine Aktivität von 221 ± 5 cpm. Bei Wiederholung der Operation wurden 215 ± 5 cpm gemessen. Das Chrom konnte nach mehrfachem Umfällen aus essigsaurer Lösung als $BaCrO_4$ schliesslich auch rein erhalten werden.

Aus dem Sulfidniederschlag der $(NH_4)_2$ S-Gruppe wurde ZnS mit 2 N HCl herausgelöst. Nach gemeinsamer radiochemischer Reinigung der verbliebenen Sulfide des Ni und Co wurden diese als Dimethylglyoxim-bzw. als α-nitroso-β-naphtholverbindung isoliert. Die nahezu gleiche Aktivitätsrate des letzten Sulfidniederschlags und des Co-Niederschlags bestätigt die nur mit Hilfe eines fensterlosen Zählrohres wahrnehmbare geringe Nickel-Aktivität.

Die Aktivitätsmessungen wurden somit in folgenden Präparaten vorgenommen: CdS, Sb_2S_3, SnS_2, Se + Te, $Fe(OH)_3$, $BaCrO_4$, ZnS, $CaC_2O_4 \cdot 2H_2O$, $NiC_8H_{14}N_4O_4$, $Co(C_{10}H_6ONO)_3 \cdot 2H_2O$. Wenn auch diese Substanzen in Bezug auf die radioaktive Messung nicht immer die geeignetsten sind, so ergaben sie sich jedoch aus dem chemischen Gang und den in erster Linie zu berücksichtigenden Forderungen nach Spezifität bzw. radiochemischer Reinheit.

Die Messung der β-Strahlung wurde mit einem Endfensterzählrohr in üblicher Anordnung durchgeführt. Um von den so erhaltenen Ergebnissen zu den benötigten Absolutaktivitäten zu kommen, folgten wir dem von BURTT[2] vorgeschlagenen Weg. In der von ihm gegebenen Beziehung zwischen gemessener Aktivität und absoluter Zerfallsrate können einige Korrekturglieder vernachlässigt werden,* so dass schliesslich nur Zählausbeute, Rückstreuung und Gesamtabsorption zu berücksichtigen sind. Eine kurze Überprüfung ergab, dass dieses auch für unsere Messanordnung zulässig ist. Damit war für alle β-strahlenden Präparate die Bestimmung der Absolutaktivitäten mit ausreichender Genauigkeit gegeben.

Die Absolutaktivität der reinen γ-Strahler Cr^{51} und Sn^{113} wurde in einem Bohrloch-Scintillationszähler ermittelt, dessen Zählausbeute vorher bestimmt worden war.

Die exakte Durchführung der chemischen Trennungen und Reinigungen machte es unwahrscheinlich, in den auszumessenden Niederschlägen merkliche Mengen an Fremdaktivitäten zu finden. Diese Annahme bestätigten die durchgeführten Untersuchungen der Strahlung in den einzelnen

* Siehe hierzu auch die Überprüfung der Formel von ZUMWALT[8] durch GLEASON *et al.*[7]

VOL. 4 1958/5

Präparaten. Wegen der zum Teil sehr niedrigen Impulsraten wurde die Ermittlung von E_{max} mit Hilfe der Halbwertsdicke vorgenommen. Dieses verschiedentlich vorgeschlagene Verfahren[3–7] erwies sich auch hier bis herunter zu 0,5 cps als ausserordentlich genau.* Bei einigen γ-Strahlern war das zugehörige Spektrum auch bei Impulsraten von weniger als 200 cpm noch gut mit den Spektren entsprechender Eichpräparate vergleichbar. Schliesslich wurden auch, soweit möglich, die Halbwertszeiten zur Identifizierung herangezogen, die gut mit den in der Literatur zu findenden Werten übereinstimmten.

Erfreulicherweise war in allen Präparaten keine Fremdaktivität, insbesonders keine P^{32}-Aktivität festzustellen, so dass die Berechnung der Mengen bzw. Konzentrationen direkt mittels der bekannten Aktivierungsformel vorgenommen werden konnte. Es ist hier ohl überflüssig, näher darauf einzugehen.

Nach der geschilderten Methode wurden die folgenden Elemente mit den nachstehend aufgeführten Konzentrationen in einer Reinstphosphorprobe gefunden:

Tabelle 1. Spurenvereinigungen in Reinstphosphor

Elemente	%
Eisen	$8 \cdot 10^{-5}$
Calzium	$3 \cdot 10^{-5}$
Zink	$2 \cdot 10^{-5}$
Natrium	$1 \cdot 10^{-5}$
Zinn	$3 \cdot 10^{-6}$
Antimon	$1 \cdot 10^{-6}$
Kupfer	$8 \cdot 10^{-7}$
Kadmium	$5 \cdot 10^{-7}$
Chrom	$3 \cdot 10^{-7}$
Arsen	$3 \cdot 10^{-7}$
Kobalt	$1 \cdot 10^{-7}$
Nickel	$<10^{-6}$
Tellur	$<10^{-6}$
Selen	$<10^{-8}$

Die Angabe von Höchstgehalten bei Ni, Se und Te geht darauf zurück, dass die Aktivitätsraten der entsprechenden Präparate zu gering waren, um eine nähere Identifizierung der Strahlung vornehmen zu können.† Auf Grund des chemischen Trennungsganges dürfte jedoch die gemessene Aktivität mit ziemlicher Sicherheit dem betreffenden Element zuzuordnen sein.

Der Fehler dieser Werte liegt im Mittel bei ± 50 Prozent; im ungünstigsten Fall, d.h. bei Summierung aller Fehler im Sinne gleichen Vorzeichens kann er $2^{\pm 1}$ nicht überschreiten. Das geht aus folgendem hervor:

Die erprobten Operationen des chemischen Ganges wurden so sorgfältig durchgeführt, dass die erzielten Ausbeuten mehr als 90 Prozent betrugen. Desgeleichen ist die radiochemische Reinheit als gewährleistet anzusehen. Die radiochemische Fehlerquelle der Möglichkeit von Kernreaktionen im Reaktor, die die hier zur Messung herangezogenen Nuklide aus einem anderen Element zu bilden vermögen, kann nach Durchsicht der bisher aufgefundenen Reaktionen und zugehörigen Wirkungsquerschnitte und im Hinblick auf die niedrigen Konzentrationen ausgeschlossen werden. Die Messungen wurden so durchgeführt, dass der durch die Statistik begründete wahrscheinliche Fehler nicht mehr als ± 5 Prozent beträgt.

Gewisse Unsicherheiten bringt die Berechnung der spezifischen Aktivität mit sich. Wir haben die nach dem Vorschlag von Burtt angewandte Extrapolation auf die Absolutaktivität überprüft, indem radioaktive Schwefel- und Phosphor-Präparate einmal in einem 4π-Zähler, das andere Mal in unserer normalen Zählanordnung ausgemessen wurden. Dabei ergab sich eine Übereinstimmung der beiden Absolutwerte innerhalb ± 10 Prozent.

Des weiteren sind die zur Berechnung der spezifischen Aktivität notwendigen Grössen der Neutronenflussdichte und des Wirkungsquerschnittes nicht genau bekannt. Die erste wird im allgemeinen von Reaktorseite mit ± 20 Prozent angegeben. Der von uns benutzte Wert stammt aus der gemessenen Absolutaktivität der

* Eine mit einer Reihe bekannter β-Strahler aufgenommene Kurve ergab mit unserer Messanordnung die Beziehung $d_{1/2} = 44{,}5 \cdot E_{max.}^{1506}$

† Die Aktivität des Ni-Präparates konnte nur im Durchfluss-Zähler beobachtet werden.

Phosphor-Grundsubstanz und lag unter Berücksichtigung der nur geringen Selbstabschirmung der Probe 15 Prozent niedriger als der von Harwell angegebene Wert. Für die Wirkungsquerschnitte wurden die im neuesten Katalog der Isotope Division, Harwell, angegebenen Grössen eingesetzt, deren Schwankungsbreite auch in ungüstigen Fällen 25 Prozent nicht überschreiten dürfte.

Wir haben darauf verzichtet, einen mittleren Fehler o.ä. an Hand einer Fehlervergleichsrechnung anzugeben, da es fraglich bleibt, ob alle Fehlerquellen gleiches Gewicht haben. Aus vorstehendem kann aber mit Recht abgeleitet werden, dass die oben erwähnte Fehlerbreite von $2^{\pm 1}$ auch in ungünstigen Fällen nicht überschritten wird. Da eine solche bei diesen niedrigen Konzentrationen für viel Zwecke, wie z.B. die eingangs erwähnten, ausreicht, stellt die Aktivierungsanalyse auch als Übersichtsanalyse ein wertvolles Hilfsmittel zum Erkennen von Spurenverunreinigungen dar, die nun mit der gleichen Methode unter Zuhilfenahme von Standards mit weitaus grösserer Genauigkeit ermittelt werden können.

LITERATUR

1. Böttger W. *Qualitative Analyse* (1925).
2. Burtt B. P. *Nucleonics* **5,** (2), 28 (1949).
3. Pery M. *J. Phys. Rad.* **1,** 28 (1945).
4. Huber O., Lienhard O., Scherrer P. und Wäffler H. *Helv. Phys. Acta* **18,** 221 (1945).
5. Libby W. F. *Analyt. Chem.* **19,** 2 (1947); **27,** 921 (1955).
6. Libby W. F. *Phys. Rev.* **103,** 1900 (1956).
7. Gleason G. J., Taylor J. D. und Tabern D. L. *Nucleonics* **8,** (5), 12 (1951).
8. Zumwalt L. R. AECU-567.

VOL
4
1958/

International Journal of Applied Radiation and Isotopes, 1959, Vol. 4, pp. 179–188. Pergamon Press Ltd. Printed in Northern Ireland

Use of Radioactive Isotopes in Studying the Spatial Distribution of Elements in Direct Current Arc Plasma During Spectrochemical Determination of Impurities in Uranium

E. E. VAINSTEIN and YU. I. BELYAEV
V. I. Vernadsky Institute of Geochemistry and Analytical Chemistry, Academy of Sciences, Moscow

VOL.
4
58/59

(*Received* 11 *May* 1958)

Radioactive tracers were first used for experimental investigation of the longitudinal distribution of elements in the plasma of a d.c. arc. Active isotope distribution in the plasma was recorded in γ-rays by means of a pin-hole camera.

The spatial distribution of atoms of various elements in the plasma of a d.c. arc was proved to be different and to depend essentially on their volatility at the temperature of the source which has set in during the experiment.

The causes of the effect of the carrier on the sensitivity of spectrochemical determination of impurities in uranium have been ascertained. A symmetrical dome-like distribution of the atoms in the arc space with a sharp maximum in the centre is characteristic of the carrier, irrespective of the method of its introduction into the analytical gap of the arc. Its presence in the sample does not result in any change in the velocity of feeding impurities into the arc plasma. The carrier affects only the distribution of the elements in the analytical gap of the source and brings about forced concentration of impurities in the central region of the plasma in accordance with carrier distribution. This accounts for a reduced removal of the impurity atoms from the discharge zone. The effect of the carrier in determining impurities in uranium is not of a selective nature. It may be considerably reduced through the presence of large amounts of elements in the sample with a spatial atom distribution differing from that of the carrier.

L'EMPLOI DES ISOTOPES RADIOACTIFS DANS L'ÉTUDE DE LA DISTRIBUTION EN ESPACE DES ÉLÉMENTS DANS LE PLASMA D'UN ARC À COURANT DIRECTE PENDANT LE DOSAGE SPECTROCHIMIQUE DES IMPURETÉS DANS L'URANIUM

L'emploi des indicateurs radioactifs servit d'abord pour l'examen expérimental de la distribution longitudinale des éléments dans le plasma d'un arc à courant directe. La distribution isotopique active dans le plasma fut enregistrée en rayons γ au moyen d'une chambre noire à ouverture minuscule.

On démontra que la distribution en espace des atomes des différents éléments dans le plasma d'un tel arc différait selon les éléments, dépendant au fond de leur volatilité à la température de la source qui s'est établie pendant l'expérience.

On a reconnu les causes de l'effet du porteur sur la sensibilité du dosage spectrochimique des impuretés dans l'uranium. Une distribution symmétrique en forme de coupole dans l'espace de l'arc, ayant un maximum net au milieu, est typique du porteur, quelle que soit

la méthode de son introduction dans l'espace analytique de l'arc. Son existence dans l'échantillon ne donne aucun changement dans la vitesse d'alimentation des impuretés dans le plasma de l'arc. Le porteur n'influence rien que la distribution des éléments dans l'espace analytique de la source et produit une concentration artificielle d'impuretés dans la région centrale du plasma selon la distribution du porteur. Ceci explique une diminution de la vitesse d'enlèvement des atomes d'impuretés hors de la zone de décharge. L'effet du porteur dans le dosage des impuretés dans l'uranium n'a aucun caractère sélectif. Il peut se diminuer de beaucoup par la présence de grandes quantités d'éléments dans l'échantillon ayant une distribution atomique en espace différente à celle du porteur.

ПРИМЕНЕНИЕ РАДИОАКТИВНЫХ ИЗОТОПОВ ДЛЯ ИССЛЕДОВАНИЯ ПРОСТРАНСТВЕННОГО РАСПРЕДЕЛЕНИЯ ЭЛЕМЕНТОВ В ПЛАЗМЕ ДУГИ ПОСТОЯННОГО ТОКА ПРИ СПЕКТРАЛЬНОМ ОПРЕДЕЛЕНИИ ПРИМЕСЕЙ В УРАНЕ

С помощью радиоактивных индикаторов впервые проведено экспериментальное исследование распределения элементов в плазме дуги постоянного тока. Распределение активного изотопа в плазме фотографировалось с помощью камеры-обскуры.

Показано, что пространственное распределение атомов различных элементов в плазме дуги постоянного тока не одинаково и зависит в первую очередь от их летучести при той температуре, которая устанавливается в источнике в условиях проведения анализа.

Выяснены причины влияния «носителя» на чувствительность спектрального определения примесей в уране. Независимо от способа введения в междуэлектродный промежуток «Носитель» характеризуется симметричным куполообразным распределением атомов в пространстве дуги с резким максимумом в центре. Его присутствие в пробе не приводит к изменению скорости поступления примесей в плазму. «Носитель» влияет лишь на распределение элементов в межэлектродном промежутке источника и приводит к их принудительной концентрации в центральной области плазмы в соответствии со своим распределением. Благодаря этому происходит уменьшение степени выноса атомов примесей из зоны разряда. Действие «носителя» при определении примесей в уране не имеет селективного характера. Оно может быть значительно уменьшено присутствием в пробе больших количеств элементов с иным, чем у «носителя», пространственным распределением атомов.

DIE VERWENDUNG VON RADIO-ISOTOPEN ZUR UNTERSUCHUNG DER RÄUMLICHEN VERTEILUNG VON ELEMENTEN IM PLASMA DES GLEICHSTROMBOGENS WÄHREND DER SPEKTROCHEMISCHEN UNTERSUCHUNG DER VERUNREINIGUNG DES URANS

Radioaktive Indikatoren wurden erstmalig für die Untersuchung der Longitudinalverteilung von Elementen im Plasma des Gleichstrombogens verwendet. Die Verteilung der aktiven Isotopen wurde mit Hilfe ihrer γ-Strahlung und mittels Lochcamera festgestellt. Es wurde gezeigt, dass die räumliche Verteilung im Plasma des Gleichstrombogens für verschiedene Elemente verschieden ist und wesentlich von deren Flüchtigkeit bei der während des Versuches herrschenden Temperatur abhängt. Die Ursachen für den Einfluss des Trägers auf die Empfindlichkeit der spektrochemischen Bestimmung der Verunreinigung des Urans wurde festgestellt. Für den Träger charakteristisch ist eine symmetrische, kuppelförmige Verteilung der Atome im Gebiet des Lichtbogens mit einem scharfen Maximum in der Mitte, unabhängig von der Methode nach welcher der Träger in die analytische Lücke in den Bogen eingebracht wurde. Seine Gegenwart in der Probe verursacht keineswegs eine Veränderung der Geschwindigkeit mit welcher die Verunreinigungen in das Plasma des Bogens transportiert werden. Der Träger beeinflusst lediglich die Verteilung der Elemente im analytischen Spalt der Quelle und verursacht eine starke Konzentrierung der Verunreinigungen im mittleren Teil des Plasma in Übereinstimmung mit der Trägerverteilung. Dies ist die Ursache für einen langsamen Abtransport der Fremdatome aus der Entladungszone. Der Einfluss des Trägers auf die Bestimmung der Verunreinigungen im Uran ist nicht selektiv und kann bedeutend herabgesetzt werden, wenn in der Probe Elemente vorhanden sind, deren räumliche Verteilung von der des Trägers stark verschieden ist.

VOL. 4 1958/5

SOME of the ways of using radioactive isotopes in studying the processes of evaporation and excitation of elements in various sources used in spectrochemical analysis were dealt with in a previous communication.[1] Attention was notably drawn to the possible use of traced atoms in studying the spatial distribution of elements in the d.c. arc plasma. First results of these investigations are given in this paper. New evidence obtained permits judgment of the part played by the carrier, which is often used to raise the sensitivity of spectrochemical analysis of many materials, as has been proposed by SCRIBNER and MULLIN.[2]

The nature of distribution of various elements in the d.c. arc space was studied by photographing the analytical gap of the source in γ-rays of radioactive isotopes of the elements to be determined. The isotopes were introduced into uranium dioxide–oxide as oxide powders or nitric acid solutions with subsequent calcination and grinding of the uranium base in a mortar. After evaporation into the analytical gap of the arc the isotopes distributed together with the atoms of corresponding impurities in accordance with some law. The longitudinal distribution of the elements in the d.c. arc plasma was recorded on a photographic film in the γ-rays of a radioactive isotope by means of a pin-hole camera. To study the arc space distribution of the excited atoms of the same elements, the analytical gap was simultaneously photographed through an interference filter. Comparison of the arc photographs obtained simultaneously in γ- and monochromatic rays emitted by atoms or ions of the element, leads to some deductions on the course of changes in the intensity of their luminescence in various regions of the arc plasma and on the law of temperature distribution. In making the photographs through a light filter, the optical system was so diaphragmed that the exposure required to obtain satisfactory photographs of the arc in the rays of excited elements and in γ-rays was the same.

All chemical operations connected with the preparation of the standards and samples, as well as packing of the electrodes, were carried out in a protective lead chamber with the aid of manipulators. The arc with the radioactive isotopes (activity = 400–600 mc and more) was placed in a lead pin-hole camera made as a box and furnished with protectors and manipulators providing for safe remote displacement of the electrodes and operation of the arc electrode-holder by the experimenter. The operation was observed by means of a periscope system. A container with electrodes prepared for the experiments was placed into the camera prior to operation. To prevent the laboratory ventilation system from being polluted with radioactive dust from the substance evaporating in the arc, the air was sucked out from the camera through a protective absorbing filter. A general view of the experimental set is shown diagramatically in Fig. 1. The carton adapter with the photographic film recording the arc image in γ-rays was placed in a box beyond the pin-hole camera and was irradiated only by γ-rays coming from the hole of the camera. Optimum dimensions of the camera hole and the distance between the latter and the film were selected experimentally and were as follows: hole diameter—1 mm, distance—100 mm, analytical gap—4 mm. Under such conditions and using samples of the above activity it was possible to obtain sufficiently contrasted and distinct images of the arc at irradiation of the film for 18–20 min. The time that the element spends in the arc plasma depends on its volatility. Hence in the case of highly volatile elements being present in the arc space only for a short time, it was necessary to photograph successively several samples on one and the same spot of the film, to obtain sufficiently contrasted arc images at the available specific activity. To prevent the real picture of longitudinal distribuuion of the elements in the arc plasma (analytical gap) from being distorted, the distance between electrodes in successive experiments had to be maintained constant by means of special precautionary measures. Thus the photographs obtained of distribution of various

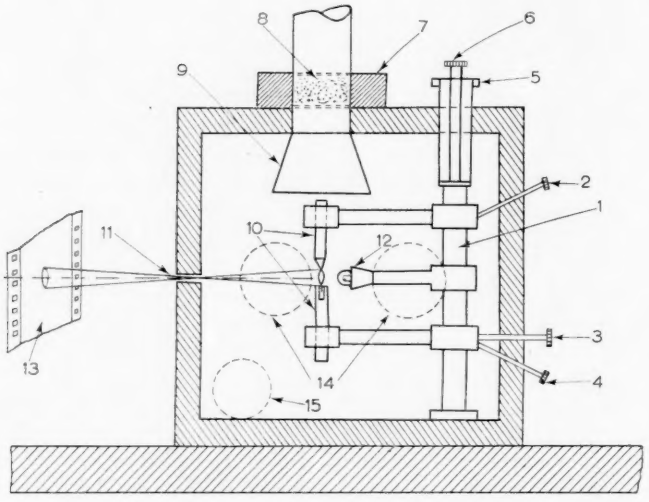

FIG. 1. Schematic diagram of experimental set. 1—electrode-holder; 2, 3, 4—holder remote control knobs for horizontal shifting of the upper and lower electrodes; 5, 6—control knobs for separate vertical shifting of electrodes; 7—protective lead ring of the filter; 8—protective filter in ventilation system; 9—ventilation funnel; 10—arc electrodes; 11—pin-hole of the camera; 12—lamp for accurate setting of electrodes on optical axis by shade projection; 13—film (adapter not shown); 14—openings for manipulators to change the electrodes; 15—opening to charge the camera with containers with electrodes.

elements in the plasma of the arc source (Fig. 2) give an idea only of the average element distribution during the exposure. Some changes in the experimental technique and in particular the use of more active samples are envisaged with a view to study the changes in spatial element distribution with time and the effect of various factors. Sensitometric curves of the used photographic emulsion for γ-rays were obtained for quantitative photometry of the photographs and for plotting the curves for spatial distribution of the elements in the d.c. arc plasma. The photometric marks were recorded on every film from a point source of γ-rays by exposing various sections of the film at different distances (r) from the radiation source. The sensitometric curves (Fig. 3) were plotted in co-ordinates S, lg r.

Curves were obtained for spatial distribution in the plasma of a large number of elements. Fig. 4 for example gives the most typical of them, representing elements of different volatility (Sb, Ga and Ta) and having different values of the ionization potential. Thus it can be seen that the volatility of the element at a temperature existing in the d.c. arc plasma under analytical conditions exerts a decisive influence on the shape of the distribution curves. The curve for sodium spatial distribution (Fig. 4d) distinctly shows the effect of cathode layer enrichment of its ions in the d.c. arc, which is naturally not obtained in experiments with an a.c. arc (Fig. 10b). The shape of distribution curves for given elements and the position of their points are well reproduced from experiment to experiment and do not depend (Fig. 5) on the content of the element in the sample to be analysed, for concentrations more than 0·05 per cent.

VOL. 4 1958/5

OL.
4
8/59

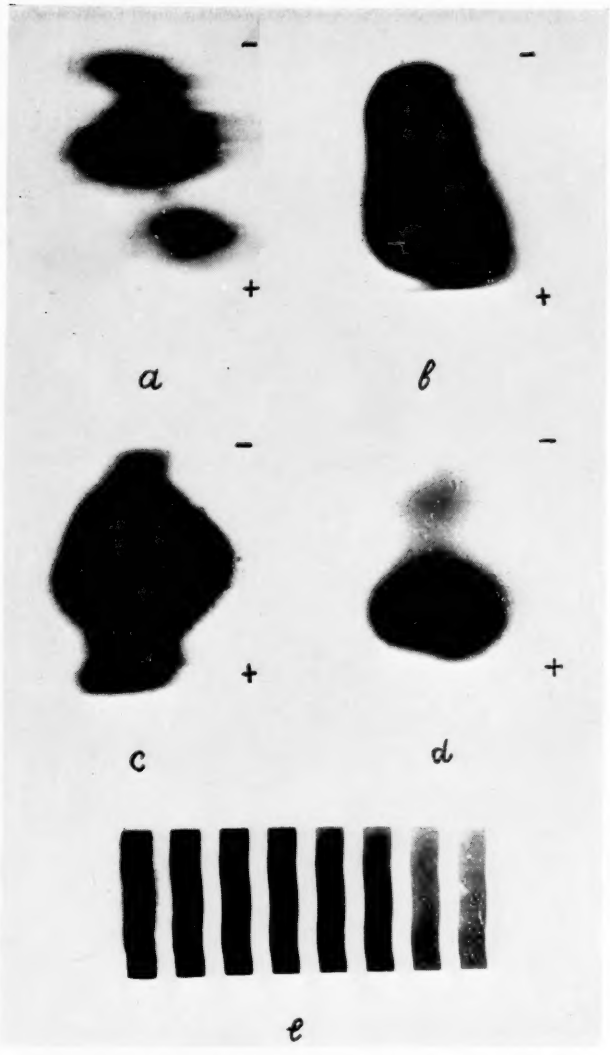

FIG. 2. Photograph of radioactive isotopes Zn^{65}, Na^{24}, Ga^{72} and Co^{60} in γ-rays, defining the longitudinal distribution of the elements in the d.c. arc plasma during their evaporation from uranium dioxide–oxide. Amperage—8 A.
(a) for sodium; (b) for cobalt; (c) for gallium; (d) for zinc; (e) photometric marks.

VOL
4
1958/

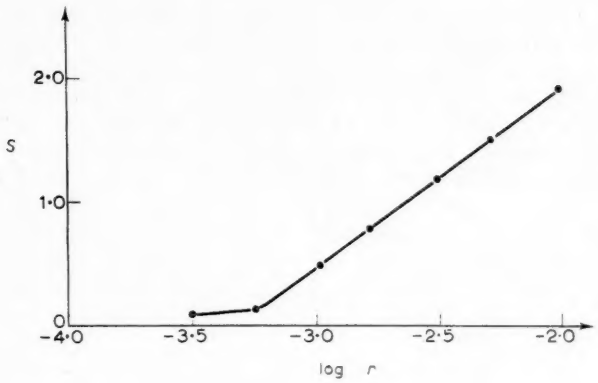

FIG. 3. Characteristic curve of film emulsion for γ-rays.

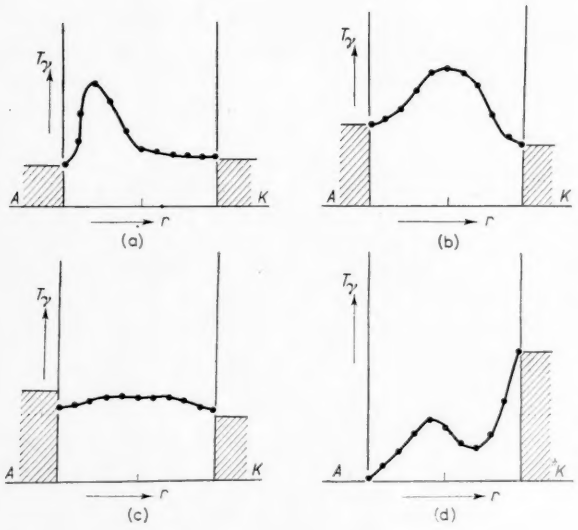

FIG. 4. Typical curves of spatial distribution of various elements in the analytical gap of the d.c. arc during evaporation of impurities from uranium dioxide–oxide: (a) for antimony; (b) for gallium; (c) for tantalum; (d) for sodium; A—anode, K—cathode.

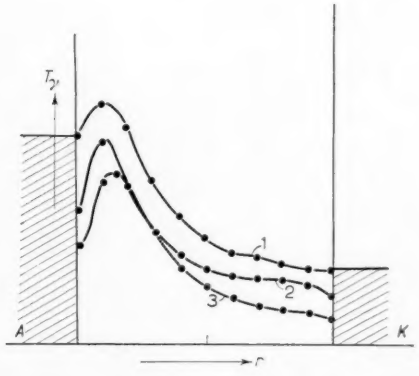

FIG. 5. Curves of spatial distribution of antimony with its varying content in uranium dioxide–oxide: 1–10%; 2–2% and 3–0·1%. A—anode, K—cathode.

Of considerable interest was the study of the effect of the carrier on the shape of impurity atoms distribution during their evaporation from the uranium dioxide–oxide. As is well known, the mechanism accounting for higher sensitivity of spectrochemical determination of impurities in the presence

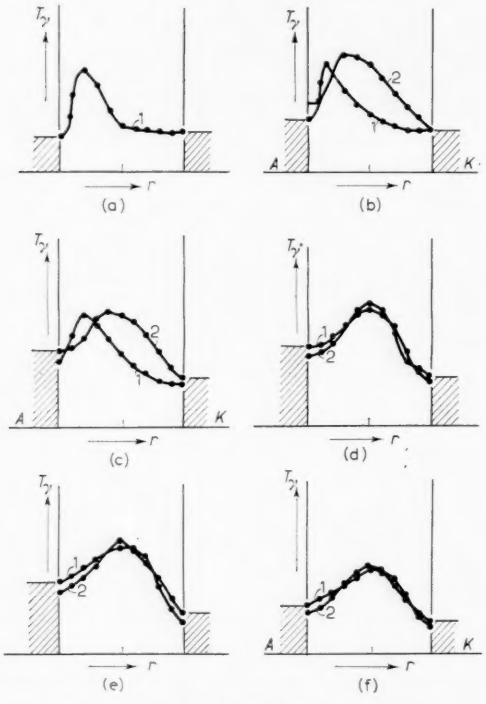

FIG. 6. Curves of spatial distribution of antimony (1) and gallium (2) in samples with different content of carrier (gallium oxide): (a) in the absence of the carrier in the sample, (b) Ga_2O_3—0·1%, (c) Ga_2O_3—0·5%, (d) Ga_2O_3—1%, (e) Ga_2O_3—2%, (f) Ga_2O_3—3%. A—anode, K—cathode.

of the carrier (for instance Ga_2O_3 or AgCl) has not yet been established, and the hypothesis suggested by the authors of the carrier method[2] for an explanation of its effect does not appear to be confirmed experimentally.[3] Contradictory evidence obtained by various researchers in studying the degree of effectiveness of the carrier method in raising the sensitivity of spectrochemical analysis of various materials under different conditions should also be noted. The curves shown in Fig. 6 illustrate the effect of introducing various amounts of the carrier (Ga_2O_3) into the analysed sample of uranium dioxide–oxide on the distribution of an impurity, namely antimony ($\approx$ 0·15 per cent) in the analytical gap of the d.c. arc source. The curves of antimony distribution in the arc plasma at a relatively low content of the carrier in the sample, greatly differing from those for gallium, when gallium oxide content exceeds 1 per cent, can be seen to reproduce fully the curve for spatial distribution of the latter element in the arc plasma. Due to the dome-like curve of spatial distribution of atoms with a sharp maximum in the centre of the analytical gap, typical of the carrier, the presence of carrier atoms in the plasma of the arc consequently results in a forced concentration of impurity atoms in the central region of the plasma, in accordance with the carrier distribution. This accounts for the reduced degree of scattering of the atoms of impurity elements and of their removal from the discharge zone, and consequently for the higher intensity of their spectral lines. The authors have shown by direct experiment that the shape of longitudinal distribution of carrier atoms in the arc space and the distribution connected with various impurity atoms in the plasma do not depend on the method of introducing of the carrier into the analytical gap. Neither is the joint presence of the impurity atoms and the carrier in the sample required for such a forced distribution in the arc space under the influence of the carrier. The evaporation of impurities and the carrier (taken in a corresponding proportion to the impurity) into the plasma may be done separately as well, with the same effect.

Analysis of the data represented in Fig. 7 leads to the assumption that the above mechanism of the effect of gallium oxide on the shape of distribution of impurity atoms in the plasma and on the intensity of the lines of these elements in the spectrum will also be responsible, fully or at least partly, for the effect of other carriers used in spectral analysis, including such as AgCl. The same data indicate that the

curves for distribution of silver atoms in the analytical gap of the d.c. arc source and the possible manifestation of the carrier effect, other things being equal, depend on the kind of the compound and the form of the given

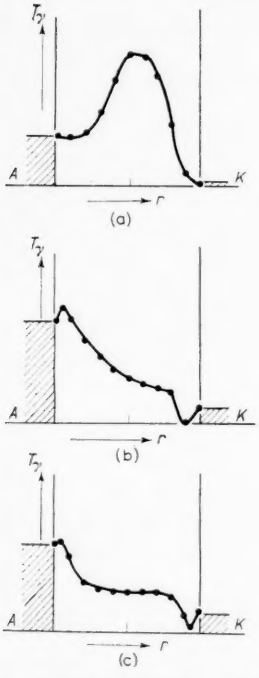

FIG. 7. Curves of spatial distribution of silver during its evaporation from uranium dioxide–oxide as AgCl (a), Ag_2O (c) and metal (b). A—anode, K—cathode.

element in the sample to be analysed. It may be assumed that the condition in which the silver atoms are to be found in the arc plasma during their evaporation from the uranium dioxide–oxide, in which they are as chlorides, and in the two other cases considered (metal and oxide) is not equivalent. This problem is now being studied by the authors in greater detail. It should only be noted that the shape of the curves for decrease of activity of the base containing radioactive AgCl with traced Ag^{110} or Cl^{36}, depending on the time of the arc burning,* was shown to be quite identical.

Interesting results were obtained in investigating the spatial distribution of impurities during their evaporation from the uranium dioxide–oxide containing, together with the carrier, large amounts of other elements, such as calcium and copper, whose atoms are distributed in the arc space in

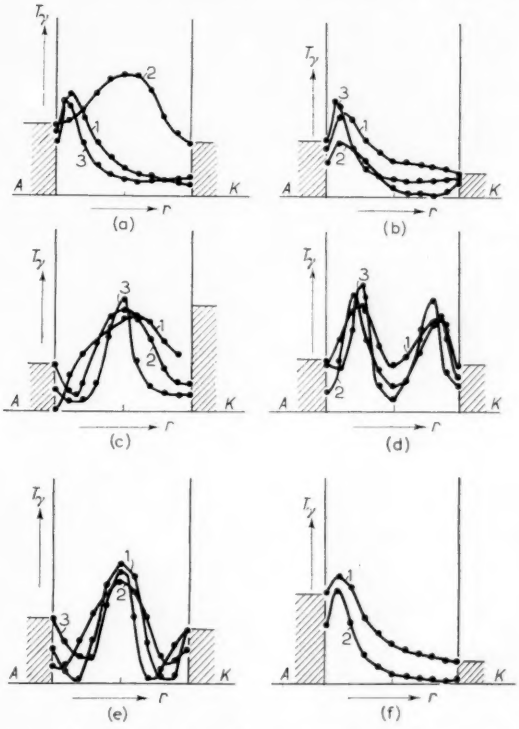

FIG. 8. Spatial distribution of antimony (1), gallium (2) and copper (3) during their joint presence in uranium dioxide–oxide in various ratios: (a) curves for antimony, gallium and copper during their separate evaporation:
(b) Sb_2O_3—0·1%, CuO—1%, Ga_2O_3—0·1%;
(c) Sb_2O_3—0·1%, CuO—1%, Ga_2O_3—2%;
(d) Sb_2O_3—0·1%, Ga_2O_3—2%, CuO—2%;
(e) Sb_2O_3—0·1%, Ga_2O_3—30%, CuO—10%;
(f) Sb_2O_3—10%, Ga_2O_3—2%.
A—anode, K—cathode.

accordance with a substantially different law than that for gallium atoms. The results seem to be important for understanding the part played by the carrier and also some other phenomena observed in spectrochemical analysis. Some experimental data are plotted in Figs. 8–11. They illustrate with evidence the arbitrariness of the term "carrier"

* For the method of obtaining such curves, see Ref. 1, 4.

VOL. 4 58/59

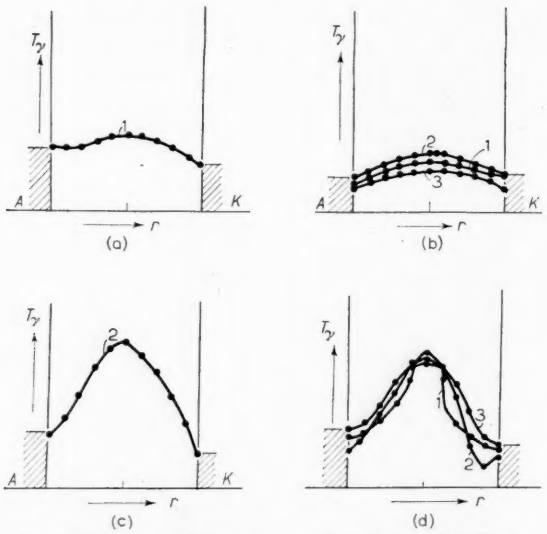

FIG. 9. Influence of the presence of calcium and gallium on the curves of longitudinal distribution of sodium in the d.c. arc plasma. Curves (a) and (c) for calcium and gallium themselves. Curves 1, 2 and 3 of Figs. (b) and (d) refer to calcium, gallium and sodium respectively. A—anode, K—cathode.

and the strong dependence of the results of its effect on the spatial distribution of impurity atoms in the d.c. arc plasma upon the presence and relative content of other elements in the sample. In the presence of two macrocomponents with a different arc space atom distribution, the distribution of impurities follows that of the atoms of the macrocomponent present in the sample in prevailing amounts. The curves related to sodium (Fig. 10a,c,d) give a particularly vivid example of the effect of macrocomponents on the shape of distribution of impurities and elements contained in the sample in subordinate amounts. Comparison of the gallium distribution curves given in Fig. 11 permits observation of a peculiarity common to all curves, namely the dependence of the width of the element concentration region in the d.c. arc plasma on the relative content of elements in the sample.*

In summing up the following basic conclusions may be drawn:

(1) Spatial distribution of the atoms of various elements in d.c. arc plasma (and apparently also in other sources) is different. The distribution shape depends essentially on the volatility of the element (or of its compound) at the temperature which occurs in the source under analysis conditions. In the case of elements with low ionization potentials and under favourable conditions in the d.c. arc there occurs a concentration of ions of the elements near the cathode. The shape of the curve for spatial element distribution does not in practice depend on its content in the sample to be analysed.

(2) In case of a low volatile base containing, together with the impurity to be analysed, larger amounts of another element (denoted as a macrocomponent), whose atoms are distributed in the analytical gap by a law different from that for the impurity atoms, the macrocomponent predetermines a law of distribution, obligatory for the atoms of all other elements, beginning at a certain content. In the presence of two

* It should be noted that all described processes proceed before the uranium vapour feeds into the plasma. Therefore uranium distribution does not affect the distribution of other elements under consideration.

VOL 4 1958/

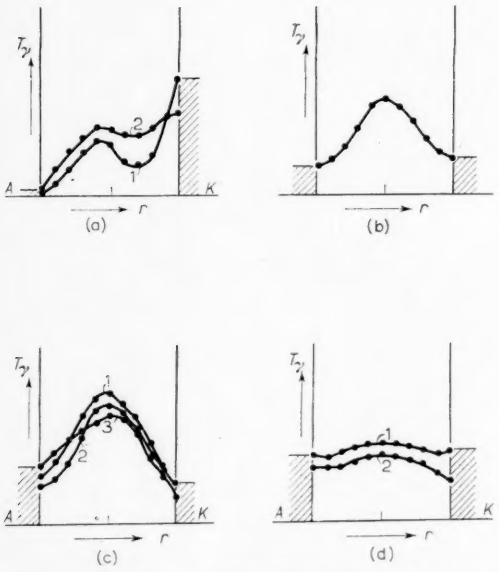

FIG. 10. Spatial distribution of sodium, calcium and gallium during their evaporation from uranium dioxide–oxide with a varying content of the elements:

(a) for sodium (1) by γ-rays in the absence of the two other impurities and during analysis in a d.c. arc; curve (2) by the line 5688 Å. (b) for sodium by γ-rays in an a.c. arc; (c) for gallium (1) and sodium (2) with their content in the sample amounting to 2% and 0·01% respectively. Curve (3) for sodium by the line 5688 Å; (d) for calcium and sodium with their content in the sample amounting to 10% and 0·01% respectively. A—anode, K—cathode.

macrocomponents with a different arc space atom distribution, the impurity elements (irrespective of the law of spatial distribution of atoms in the source, peculiar to them) follow the distribution of the atoms of the macrocomponent prevailing in the sample to be analysed. When relative contents of macrocomponents in the sample are approximately equal, the impurities are captured by each of them to an approximately equal degree.

(3) The elements representing compounds, which are generally used in spectrochemical analysis as carriers and participate in raising its sensitivity, are characterized by a symmetrical dome-like law of the arc space atom distribution, with a maximum in the centre. In this case the shape of distribution of the carrier atoms in the arc space does not depend on the method of feeding into the analytical gap. The higher intensity of the impurity element lines, observed under favourable conditions, is by no means related to a change in the velocity of evaporation of the elements to the plasma. As has been proven by direct experiments conducted by the authors and by existing evidence[3] the velocity remains invariable. The carrier affects only the distribution of the impurity elements in the analytical gap of the source and brings about their forced concentration in the central region of the plasma, in accordance with the carrier distribution. This results in a reduced degree of scattering and in removal of the impurity elements from the discharge zone. It is the reason why the effect of the carrier on the intensity of spectral lines is not a selective one. In some cases, for instance in the presence in the sample of large amounts of elements with more asymmetric atom distribution than that of the carrier, the effect of the latter may be considerably weakened or altogether eliminated.

(4) The differences in spatial distribution of the elements in the analytical gap of the source, and the effect of composition of the substances to be analysed on this distribution, are likely to be important factors

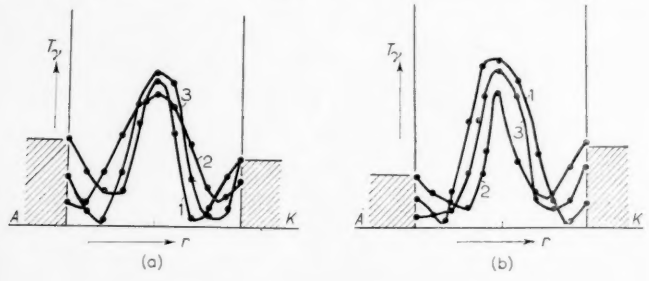

FIG. 11. Spatial distribution of antimony (3), gallium (2) and copper (1) in the d.c. arc plasma during their evaporation from uranium dioxide–oxide samples with 0·1% of antimony and a varying content of the two other components: (a) Ga_2O_3—30%, CuO—10%, (b) Ga_2O_3—50%, CuO—10%. A—anode, K—cathode.

accounting for the dependence of spectrochemical analysis results on the composition of the samples and the presence of the so-called "third components" in them.

However this effect has not yet been sufficiently taken into account and deserves further special systematic investigation.

REFERENCES

1. Vainstein E. E., Pavlenko L. I. and Belyaev Yu. I. The use of radioactive isotopes in spectral analysis. *Proceedings of the International Conference on Radioisotopes in Scientific Research.* Paris (1957). In English.
2. Scribner B. F. and Mullin H. R. *J. Res. Nat. Bur. Standards* **37,** 379 (1946).
3. Zaidel A. N., Kaliteyevsky N. I., Kundt G. G. and Fratkin Z. T. *Optica i Spectroscopiya* **2,** 28 (1957) In Russian.
4. Vainstein E. E. and Pavlenko L. I. *Zh. Anal. Khim.* **11,** 410 (1956). In Russian.

VOL
4
1958/

International Journal of Applied Radiation and Isotopes, 1959, Vol. 4, pp. 189–195. Pergamon Press Ltd. Printed in Northern Ireland

The Influence of Chain Length on the Luminescent Output of Plastic Scintillators

B. LIONEL FUNT and ARLENE HETHERINGTON
Chemistry Department, University of Manitoba

(*Received* 21 *April* 1958)

The influence of chain length on the luminescent efficiency of plastic scintillators was studied over a wide range of molecular weights.

By varying the temperature of polymerization and by employing chain transfer agents, samples with molecular weights ranging from 10^3 to 10^6, determined by intrinsic viscosity measurements, were obtained.

The results indicate that the chain length has negligible influence on the luminescent efficiency for molecular weights in excess of 100,000. For lower molecular weights a sharp dependence of light output on chain length is found. The use of polymerization initiators does not lower the molecular weight to the region of critical dependence and it is concluded that the quenching effects of such substances are not due to the lower molecular weights that are concomitant with their use. The influence of various solutes on the molecular weight of resultant polymers was investigated. No evidence of chemical interaction could be found from molecular weight determination or from absorption spectra of the purified polymers. These results weighed against the acceptance of copolymerization or chain transfer as a significant factor in the polymerization process.

L'INFLUENCE DE LA LONGUEUR DE CHAÎNE SUR LE RENDEMENT LUMINEUX DES SCINTILLATEURS PLASTIQUES

L'influence de la longueur de chaîne sur le rendement lumineux des scintillateurs plastiques fut étudiée par une grande rangée de poids moléculaires.

En variant la température de polymérisation et en employant des agents de transfert de chaîne, on a obtenu des échantillons ayant des poids moléculaires dans la rangée 10^3–10^6, déterminés par des mesures de la viscosité intrinsèque.

Les résultats indiquent que la longueur de chaîne a une portée négligeable sur l'efficacité lumineuse pour les poids moléculaires au delà de 100.000. Pour les poids inférieures, il se trouve une dépendance définie de l'émission de lumière sur la longueur de chaîne. L'emploi des amorceurs de la polymérisation ne réduit pas le poids moléculaire à la région de dépendance critique et on déduit que les effets éteignants de tels corps ne suivent pas des poids moléculaires inférieurs que comporte leur emploi. On rechercha l'influence des différents solutés sur le poids moléculaires des polymères qui en résulte. Aucune indication d'interréaction chimique se montra, soit de la caractérisation du poids moléculaire soit des spectres d'absorption des polymères purifiées. Ces résultats disputent l'acception de la copolymérisation ou du transfert de chaîne comme facteur signifiant dans le procédé de la polymérisation.

ВЛИЯНИЕ ДЛИНЫ ЦЕПИ НА ИНТЕНСИВНОСТЬ ЛЮМИНИСЦЕНЦИИ ПЛАСТМАССОВЫХ СЦИНТИЛЛЯТОРОВ

Было исследовано влияние длины молекулярной цепи на интенсивность люминисценции пластмассовых сцинтилляторов в широких пределах молекулярных весов.

Путем изменения температуры полимеризации и применения переносчиков цепи были получены образцы с молекулярным весом в пределах от 10^3 до 10^6, определяемым по измерению вязкости.

Результаты показывают, что для молекулярных весов выше 100,000 влияние длины

цепи на интенсивность люминисценции ничтожно. Для низких молекулярных весов была обнаружена резкая зависимость выхода света от длины цепи. Применение инициаторов полимеризации не снижает молекулярный вес до тех значений, когда наблюдается критическая зависимость; поэтому делается заключение, что тормозной эффект таких веществ не связан с уменьшением молекулярного веса. Исследовано влияние различных растворителей на молекулярный вес образующихся полимеров. Ни определение молекулярного веса, ни рассмотрение спектра поглощения очищенного полимера не свидетельствуют о наличии химического взаимодействия. Эти результаты говорят против признания сополимеризации или переноса цепи как существенных факторов в процессе полимеризации.

DER EINFLUSS DER MOLEKÜLKETTENLÄNGE AUF DIE LUMINESZENZAUSBEUTE VON PLASTIKSZINTILLATOREN

Der Einfluss der Molekülkettenlänge auf die Lumineszenzausbeute von Plastikszintillatoren wurde über eine weite Reihe von Molekulargewichten untersucht. Durch Veränderung der Polymerisationstemperatur und Verwendung von Kettenumlagerungsmitteln wurden Proben mit Molekulargewichten von 10^3 bis 10^6, bestimmt durch innere Viskositätsmessungen, erhalten.

Die Ergenisse zeigen, dass die Kettenlänge bei Molekulargewichten über 100.000 einen vernachlässigbaren Einfluss auf die Lumineszenzausbeute hatten. Für niedrigere Molekulargewichte wurde eine starke Abhängigkeit der Lichtausbeute von der von der Kettenlänge gefunden. Der Gebrauch von Polymerisation auslösenden Katalysatoren senkt das Molekulargewicht solcher Stoffe nicht in den Bereich der kritischen Abhängigkeit und es wird daraus geschlossen, dass der Löscheffekt solcher Stoffe nicht vom niedrigeren Molekulargewicht, das eine Begleiterscheinung der Anwendung dieser Auslöser ist, veruracht wird. Der Einfluss verschiedener Szintillatorsubstanzen in der Lösung auf das Molekulargewicht der resultierenden Polymere wurde untersucht. Weder bei der Molekulargewichtsbestimmung, noch aus den Absorptionsspektren der gereinigten Polymere konnte ein Beweis für chemische Wechselwirkung gefunden werden. Diese Ergebnisse sprechen gegen die Copolymerisation und Kettenumlagerung als charakteristische Faktoren im Polymersiationsprozess.

VOL. 4 1958/5

PREVIOUS studies of plastic scintillators have been largely devoted to the development of superior activator systems which would provide enhanced light output. It has generally been assumed that the activator system was dispersed as a solid solution in the polystyrene or polyvinyltoluene plastic base. The mechanism of light emission was thus believed to be similar to that postulated for liquid scintillator compositions or gels, which often employed the same types of scintillating solutes, but usually at much lower concentrations.[1,2,3,4]

It is a noteworthy fact, however, that monomeric styrene and vinyl toluene containing dissolved scintillating chemicals are extremely poor scintillators with negligible light emission, whereas the polymerized product has a relatively high luminescent efficiency.

Published descriptions of the formation of plastic scintillators have included conditions which would be expected to result in products of widely differing molecular weight. In some instances polymerization was completely effected at reflux or higher temperatures, which for styrene and vinyl toluene represent temperatures in excess of 140°C and 175°C respectively.[5] This should produce relatively low molecular weight material, incidentally, with poor mechanical and machining properties. The use of initiators such as benzoyl peroxide has been reported to produce products of both superior[6] and inferior[7,8,9] performance. Such initiators will produce a decrease in the molecular weight of the polymer formed at any given temperature. Furthermore, one can infer that with certain scintillating solutes some interference with the polymerization process can take place since the solutes are chemically changed during the reaction.[10,11] Chain transfer has been suggested by KOSKI[12] in his studies of the styrene–anthracene system, whereas copolymerization can be inferred from the data reported for some solutes containing ethylenic bonds. BASILE[13] has reported both an increase and

a decrease in luminescent efficiency on increasing the polymerization temperature. This work was devoted to the study of the range of molecular weights at which the transition from poor to good scintillation efficiency is obtained. In view of the discrepancies and uncertainties noted above, a separate study of the relationships of molecular weight to light output efficiency in plastic scintillators appeared well warranted.

EXPERIMENTAL

Vinyl toluene, obtained from the Dow Chemical Co., was purified by fractional distillation under reduced pressure. A scintillating solute composition was chosen which did not contain *p*-terphenyl, since the latter material crystallized out of solution at temperatures under 80°C preventing low temperature–high molecular weight studies.

The molecular weights of plastic scintillators were varied by changing the temperature of the polymerization reaction and by the use of chain transfer agents. For the latter the usual halogen derivatives were avoided and α-methyl styrene dimer* was employed.

Twenty ml samples of plastic scintillators of various molecular weights were prepared in 25 × 200 mm test-tubes sealed under vacuum. The samples were degassed by repeated freezing and thawing cycles before being sealed. The samples were polymerized a minimum of 7 days at 125°C and periods of up to 3 weeks were employed for samples prepared at lower temperatures to ensure complete polymerization.

Molecular weights were determined by dissolving part of the sample in methyl ethyl ketone to form a 1% solution, and precipitating the polymer by dropping the solution into methanol. The polymeric powder was dried and weighed, and a 1% solution in methyl ethyl ketone was prepared. Intrinsic viscosities of the samples were measured using an Ubbelohde suspended level viscometer which permitted the addition of increments of solvent *in situ*. The molecular weights were determined from the intrinsic viscosities by the application of the Staudinger equation.[14]

$$(*n)_{c\to 0} = KM^{\alpha}$$

where n = intrinsic viscosity $= \left(\frac{n_{sp} - 0}{c}\right)_{c\to 0}$

where n_{sp} is the ratio of flow time of solute to solvent.

Values of $K = 3{\cdot}9 \times 10^{-4}$, $\alpha = 0{\cdot}58$[15] were employed from the data for styrene.

The light output of the samples were measured relative to a plastic scintillator standard using a Cs^{137} source. A conventional scintillation counter assembly, consisting of a Dumont 6292 photomultiplier, cathode follower, linear amplifier, differential discriminator and scaler was used.

Most samples were machined to a standard length of 15 in. and were mounted with powdered MgO reflector for the light output measurements. Very low molecular weight samples could not be machined and were measured in flat bottomed glass vials.

RESULTS

The results are shown in Fig. 1 and Table 1. In the general range of molecular weights from 100,000 to 1,000,000 the light output appears independent of the chain length. Plastic scintillators prepared at temperatures between 80°C and 150°C fall within this range of molecular weights. Increase of temperatures over 175°C brings the molecular weights to the knee of the molecular weight curve and a reduction of light output is observed. Typical data obtained with 2,2-azo-bis*iso*butyronitrile are shown in Table 2. For the molecular weights found, reduction in light output must be attributed to quenching effects rather than the shortening of the polymer chain.

* Furnished through the courtesy of Dr. R. Forbes of Polymer Corporation, Sarnia, Ontario.

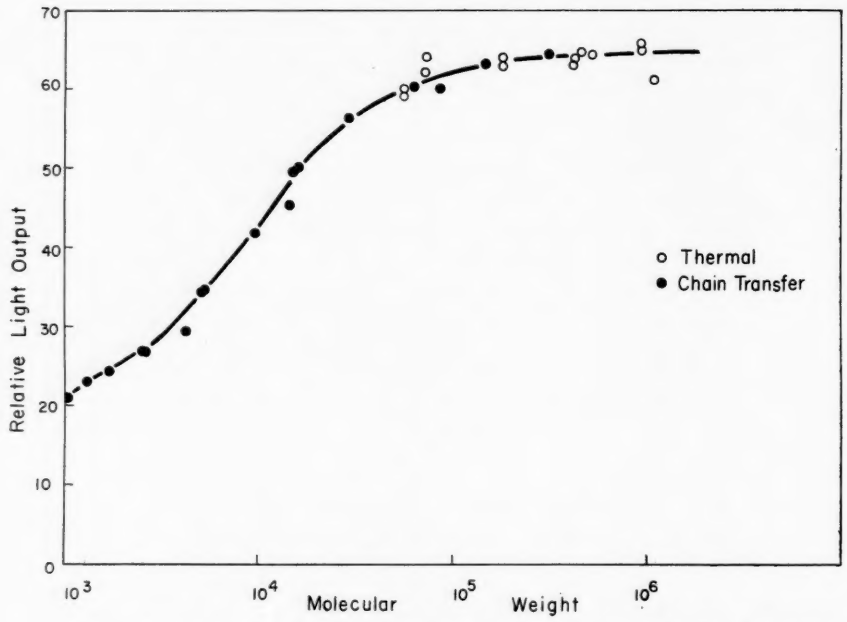

FIG. 1. Effect of molecular weight on the relative light output of plastic scintillators.

When chain transfer agents were incorporated much lower molecular weights could be produced. A sharp dependence of light output on molecular weight is observed for the region below a molecular weight of 50,000. The results may be influenced by slight quenching action due to the α-methyl styrene dimer. Attempts to compression mold samples of low molecular weight material with added scintillation solutes yielded irreproducible results and were eventually abandoned. However, a Stern–Volmer plot[16,17] of the light output vs. the concentration of dimer does not give a straight line and it is evident that quenching, although a possible complicating factor, cannot account for the reductions in light output observed. Furthermore, reasonable agreement was obtained in the molecular weight region where samples prepared by chain transfer and by high temperature polymerization overlapped.

The data indicate that initiators such as 2,2-azo-bis*iso*butyronitrile or benzoyl peroxide reduce the light output as a result of quenching action and not from the lowering of molecular weight. On the other hand, samples prepared at reflux temperatures of polyvinyl toluene gave reduced light output and molecular weights below 100,000. This indicates that procedures recently suggested for production of large scintillators[5] would result in products with an inferior light output efficiency. The mechanical properties of such plastics were also poor, as was evidenced by the brittleness of these materials during machining operations. It is likely that in the preparation of large units by these procedures, the heat evolved during polymerization could further increase the temperatures in the central portion of the samples to above 200°C.

A study was made of several solutes and their influence on the molecular weight of the resulting polymer. The data are summarized in Table 3. It can be seen that the molecular weight is unchanged in systems containing *p*-terphenyl, 2,5-diphenyloxazole [PPO] and 1,4-di-[2-(5-phenyloxazolyl)]-benzene [POPOP] when compared to pure polymer prepared under the same conditions. These results weigh heavily against the

VOL.
4
1958/5

TABLE 1. Relative light output of plastic scintillators arranged in order of decreasing molecular weight

Sample	% Chain transfer agent (α-Me styrene dimer)	Polymerization temperature (°C)	Relative light output (arbitrary units)	Molecular weight
VT-62	—	80	61·2	1,080,000
VT-64	—	100	66·1	933,000
VT-65	—	100	65·4	933,000
CL-141	—	125	64·6	515,000
CL-197	—	125	65·0	454,000
VT-66	—	125	63·3	417,000
VT-67	—	125	64·1	417,000
CL-198	0·1	125	64·8	311,000
VT-68	—	150	63·6	179,000
VT-69	—	150	64·0	179,000
CL-199	0·5	125	63·4	147,000
CL-200	1·0	125	60·1	86,000
VT-71	—	175	64·3	71,000
VT-72	—	175	62·3	71,000
CL-142	1·0	125	60·3	61,700
VT-75	—	200	60·3	56,000
VT-76	—	200	59·5	56,000
CL-201	3·0	125	56·7	28,600
CL-143	5·0	125	50·0	15,600
CL-202	5·0	125	49·9	15,000
CL-144	10·0	125	45·4	14,400
CL-203	10·0	125	42·2	9,600
CL-145	20·0	125	34·9	5,200
CL-204	20·0	125	34·6	5,100
CL-146	30·0	125	29·4	4,100
CL-147	40·0	125	27·0	2,500
CL-148	50·0	125	24·6	1,700
CL-149	60·0	125	23·2	1,300
CL-150	70·0	125	21·3	1,050

TABLE 2. Molecular weights of plastic scintillators containing 10·0 g/l. PPO and 0·1 g/l. POPOP prepared with and without 2,2′-azo-bis*iso*butyronitrile as initiator

Sample	Initiator concentration (%)	Polymerization temperature (°C)	Molecular weight
VT-17	0·1	60	889,000
VT-18	—	60	1,824,000
VT-29	0·1	80	470,000
VT-23	—	80	958,000
VT-30	0·1	100	426,000
VT-26	—	100	809,000

TABLE 3. Comparison of molecular weights with scintillating solute concentration and atmosphere used during polymerization reaction

Sample	Concentration of scintillating solute (g/l.)	Atmosphere	Molecular weight
VT-1	no solutes	nitrogen	411,000
P-1	no solutes	vacuum	480,000
P-3	*p*-terphenyl (20·0)	vacuum	501,000
P-5	*p*-terphenyl (20·0) POPOP (0·1)	vacuum	426,000
P-7	*p*-terphenyl (20·0) POPOP (0·5)	vacuum	547,000
P-9	*p*-terphenyl (20·0) POPOP (1·0)	vacuum	574,000
CL-141	PPO (10·0) POPOP (0·1)	nitrogen	426,000
CL-197	PPO (10·0) PPOPOP (0·1)	nitrogen	515,000
CL-140	PPO (10·0) POPOP (0·1)	nitrogen	454,000
VT-27	PO (10·0) POPOP (0·1)	vacuum	468,000
VT-67	PPO (10·0) POPOP (0·1)	vacuum	417,000
VT-66	PPO (10·0) POPOP (0·1)	vacuum	417,000

acceptance of chain transfer or copolymerization as a necessary condition in the formation of efficient plastic scintillators, although it is probable that such interaction can take place in certain systems.

An investigation was also performed to determine whether 1,1,4,4-tetraphenyl-1,3-butadiene [TPB], a commonly employed solute, could be detected in the purified and precipitated polymer by absorption spectrophotometry. From its structure this solute might be expected to enter into copolymerization reaction with the growing polymer radicals. To check this possibility absorption spectra were taken of solutions of vinyl toluene polymer in chloroform in the ultra-violet region. A polyvinyl toluene sample containing 2 per cent TPB was dissolved in methyl ethyl ketone and precipitated three times in methanol. A 5% solution of dried polymer was prepared in chloroform and absorption spectra were determined on a DK recording spectrophotometer in the ultra-violet region. The same procedure was employed for pure polyvinyl toluene and for polyvinyl toluene with 2 per cent TPB added during the precipitation procedure. Although a slight absorption was found corresponding to the presence of TPB this proved to represent a very small portion of the original material. Due to an overlap of absorption bonds a Beer's Law plot could not be obtained. However, the preparation of samples of known amounts of TPB permitted an empirical determination of the concentration remaining in the polymer. This was found to be less than 10^{-4} per cent TPB for a sample which originally contained 2 per cent of this solute. Recent work by PANI, *et al.*[18] indicates a similar result. Although they did not form a quantitative estimate of the TPB remaining in the polymer, their conclusion that no appreciable amount of copolymerization can take place with this diene solute is in agreement with our observations. It was concluded that the main bulk of the TPB was not incorporated in the polymer chain. Similar measurements with samples containing *p*-terphenyl–POPOP showed no absorption peaks in the polymer solution corresponding to the solutes employed, thus

indicating that these solutes were not present in the polymer chain.

Molecular weights of samples prepared *in vacuo* were compared against those polymerized under pure nitrogen. No difference in molecular weight was found, as shown by the data in Table 3.

CONCLUSIONS

This work indicates that, in general, the solutes are not chemically bonded to the chain, and that chemical interaction between the growing polymer radical and scintillating solute is not essential for the production of an efficient scintillating system. The optimum region of chain length has been determined and it is concluded that the molecular weight region over 100,000 is satisfactory. The reason for decrease in light output at low molecular weights has not been established in this work but may be attributed to greater ease of solute diffusion and self quenching which could be expected to accompany the lower viscosity concomitant with shorter polymer chains.

Acknowledgements—We are indebted to the National Research Council of Canada for a grant-in-aid in support of this work.

REFERENCES

1. Swank R. K. and Buck W. L., *Phys. Rev.* **91,** 927 (1953).
2. Swank R. K., *Nucleonics* **12,** No. 3, 14 (1954).
3. Brooks F. D., *Progr. Nucl. Phys.* **5,** (1956).
4. Funt B. L., *Nucleonics* **14,** No. 8, 83 (1956).
5. Clark G. W., Scherb F. and Smith W. B., *Rev. Sci. Instrum.* **28,** 433 (1957).
6. Schorr M. G. and Torney F. L., *Phys. Rev.* **80,** 474 (1950).
7. Eichholz G. G. and Horwood J. L., *Rev. Sci. Instrum.* **23,** 305 (1952).
8. Swank R. K. and Buck W. L., *Nucleonics* **11,** No. 11, 48 (1953).
9. Koton M. M., *Zh. Tekh. Fiz.* **26,** 1741 (1956).
10. Carlson T. and Koski W. S., *Phys. Rev.* **85,** 697 (1952).
11. Prins W., de Waard H. and Prins A., *Appl. Sci. Res., Hague* **B3,** 372 (1953).
12. Koski W. S., *Phys. Rev.* **82,** 230 (1951).
13. Basile J., *J. Chem. Phys.* **27,** 801 (1957).
14. Kraemer E. O. and Lansing W. D., *J. Phys. Chem.* **39,** 156 (1935).
15. Outer P., Carr C. I. and Zimm B., *J. Chem. Phys.* **18,** 830 (1950).
16. Stern O. and Volmer M., *Phys. Z.* **20,** 183 (1919).
17. Funt B. L. and Neparko E., *J. Chem. Phys.* **60,** 267 (1956).
18. Pani I. E., Baroni E. E. and Shoniya V. M., *Zh. Fiz. Khim.* **31,** No. 3, 732 (1957).

International Journal of Applied Radiation and Isotopes, 1959, Vol. 4, pp. 196–200. Pergamon Press Ltd. Printed in Northern Ireland

Metal Loaded Scintillator Solutions*

A. R. RONZIO†

Los Alamos Scientific Laboratory, University of California, Los Alamos, New Mexico

(*Received* 5 *May* 1958)

The scintillation efficiency of various scintillating solutions containing hydrocarbon soluble salts of cadmium, lead, bismuth, uranium, and iron was compared. The directions for the preparation of the salts are given. The pulses obtained from cesium-137 were compared by means of a pulse height analyser.

SOLUTIONS SCINTILLANTES CHARGÉES DE MÉTAL

L'efficacité de scintillation de différentes solutions scintillantes contenant des sels de cadmium, de plomb, de bismuth, d'uranium et de fer, solubles en hydrocarbure, fut mis en comparison. On donne les avis nécessaires à la préparation des sels. La comparaison des pulsations du Césium 137 se fit au moyen d'un analysateur de force de pulsations.

ЗАГРУЖЕННЫЕ МЕТАЛЛОМ СЦИНТИЛЛИРУЮЩИЕ РАСТВОРЫ

Сравнивалась эффективность различных сцинтиллирующих растворов, содержащих соли кадмия, свинца, висмута, урана и железа, растворимые в углеводороде. Даны способы приготовления солей. Импульсы, получаемые от цезия-137 сравнивались при помощи амплитудного анализатора импульсов.

VOL.
4
1958/5

INTRODUCTION

The use of large liquid scintillation detectors for free neutrino studies[1] has focussed attention on the incorporation of metals into hydrocarbon scintillator solutions as a means of adjusting the sensitivity of liquid scintillation detectors for other applications such as neutron detection and increased γ-ray absorption. A large number of experiments were conducted in the study of types of metal derivatives soluble in aromatic hydrocarbons and the effect upon pulse height obtained from the loaded scintillating solutions. The efficiency of scintillation was studied by comparing the pulse height of the solution being investigated with the pulse height obtained from a solution of purest toluene containing terphyenyl and POPOP as a band shifter. Cesium-137 was used as a standard source of radiation. The solutions under test were contained in a quartz thimble with a capacity of one milliliter which was placed at the center of the photocathode of a 2 in. end window photomultiplier tube. The Cs^{137} was placed at the apex of a silvered glass hemisphere, the diameter of which was equal to that of the

* Work performed under the auspices of the U.S. Atomic Energy Commission.

† Now with the Radiological Research Institute, Inc., Denver, Colorado.

cathode surface of the photomultiplier tube. The entire assembly was enclosed in a light-proof soft iron chamber one-fourth inch in thickness to shield the photomultiplier against the action of external magnetic fields. The photomultiplier signals were fed through a preamplifier and amplifier to a single channel pulse-height analyzer.

1. NAPHTHENATES

Naphthenic acids are a class of acidic organic compounds isolated from the base soluble fraction of petroleum in which they occur to the extent of 0·1–3·0 per cent. The acids do not show any appreciable unsaturation and have been classified as *cyclo*-paraffin carboxylic acids.

The heavy metal salts of the naphthenic acids are insoluble in water but are soluble in hydrocarbons.

The lowest boiling members of the acid mixture containing 8–10 carbon atoms, have the type formula $C_nH_{2n-2}O_2$ and are *cyclo*-hexane derivatives in which the cyclic group is attached to either a carboxyl group or to an α-carbon of a fatty acid.

The crude naphthenic acid mixture when extracted from petroleum is a dark colored liquid with a characteristic and unpleasant odor. Several vacuum distillations will yield a clear product with a trace of yellow color. Attempts to remove the last traces of color by repeated vacuum distillations were without success.

It was observed that 80% sulfuric acid solution would extract color from a solution of naphthenic acid when dissolved in petroleum ether.

A solution of 100 ml of naphthenic acid in 300 ml of petroleum ether was extracted 3 times with 50 ml of 80% sulfuric acid. The petroleum ether raffinate was then washed twice with 100 ml of water and once with 50 ml of 5% sodium acetate solution.

Removal of the petroleum ether by distillation followed by a distillation under the vacuum from a mechanical pump gave an almost water-white product which remained unchanged upon standing three months in the laboratory in an open container.

Lead naphthenate

Fifty grammes of purified naphthenic acid in a separatory funnel were treated with 100 ml of clear 25% sodium hydroxide solution. This concentration of base is sufficient to form sodium naphthenate and also serves to salt out the sodium salt. The two layers were separated and the naphthenate was washed in succession with sodium chloride solution, petroleum ether, and with hexane.

The sodium naphthenate was poured into a vigorously stirred solution of lead acetate (to which had been added sufficient glacial acetic acid to keep the solution clear). The precipitate of lead naphthenate in the form of a thick oil was washed with water, placed in a Petri dish and dried. The yield of lead naphthenate was 45·5 g.

Cadmium naphthenate may be prepared in a similar manner with comparable yields.

The scintillation efficiency of lead naphthenate was 28 per cent of that of the standard toluene solution while cadmium naphthenate was below 20 per cent as efficient, both at 5% concentrations calculated as the salt.

The metal naphthenates prepared in the manner described always contained an appreciable amount of brown color. Since a water-white solution was desired, other salts were tested.

2. OCTOATES

An acid used for the same purpose as naphthenic acid in the paint industry is octoic acid, or more correctly, 2-tehyl-hexanoic acid. The acid is colorless and easily forms metal salts which are soluble in hydrocarbons and are stable upon standing.

Cadmium octoate (*cadmium 2-ethyl-hexanoate*)

This compound was particularly useful in the neutrino studies and has also been used

in neutron detectors. Sodium octoate was prepared by adding the calculated amount of iron-free and carbonate-free sodium hydroxide to the weighed amount of octoic acid suspended in water. The octoic acid dissolved completely upon stirring the mixture. The sodium octoate solution was then

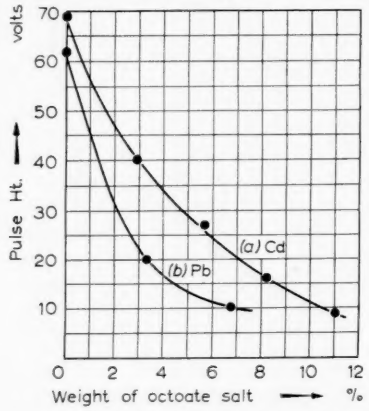

FIG. 1. All solutions contained 4 g/l. of terphenyl in pure toluene. Curve (a) shows the pulse height in volts as a function of percentage by weight of Cd as an octoate salt. Curve (b) shows the pulse height in volts as a function of percentage by weight of Pb as an octoate salt.

added to a well stirred solution containing the calculated amount of cadmium acetate. A thick oily layer of cadmium octoate separated and settled to the bottom of the container. The compound prepared in this manner is in the form of a hydrate and is insoluble in hydrocarbons. A sample of the salt will crystallize in the course of several months.

The aqueous layer was removed by decantation. The octoate was suspended in toluene and the water was removed by distilling off the water-toluene azeotrope. An anhydrous solution of cadmium octoate remained in the distilling flask.

Cadmium octoate and toluene are miscible in all proportions at room temperature. At concentrations greater than 10% cadmium octoate, the solutions become viscous, and are very difficult to pour at concentrations greater than 20%.

The scintillation efficiency of cadmium octoate solutions in toluene is shown in Fig. 1(a).

The effect upon scintillation caused by using other salts of cadmium than the acetate for the preparation of the octoate was also studied. Cadmium octoate was prepared from the nitrate and the sulfate. The scintillation properties were compared with the cadmium octoate prepared from the acetate. No difference was observed between salts prepared from the acetate and nitrate. An appreciable lowering in pulse height was obtained in the salt prepared from the sulfate. No cadmium octoate was prepared from cadmium chloride because of the well known quenching effect of chlorides upon scintillation.

It was observed for an ambient temperature of 25°C that terphenyl begins to crystallize out of cadmium octoate solutions in toluene when the concentration of cadmium approaches 10 per cent.

The method described above for the preparation of heavy metal salts of octoic acid may conceivably lead to solutions containing small amounts of free octoic acid.

The effect upon scintillation efficiency of both the standard toluene solution and a solution of cadmium octoate in toluene caused by adding 20 ml of free octoic acid per liter of solution was determined. The change observed was within experimental error. A difference of only one volt between the pulse heights from the two solutions was observed.

Lead octoate was prepared from lead acetate by the method described. The salt separates without hydration but is distilled with toluene to remove small amounts of occluded water. The scintillation efficiency of various concentrations of lead octoate in toluene solutions is shown in Fig. 1(b).

Solutions of bismuth octoates and uranium octoates were prepared. The scintillation efficiency was not studied sufficiently to be reported.

Solutions of the metal octoates in carefully purified tri-ethyl-benzene can be made which exceed the scintillation efficiency attainable with toluene solutions. The presence of iron should be rigorously excluded from all scintillating solutions prepared from octoate salts, since this element leads to

VOL. 4 1958/5

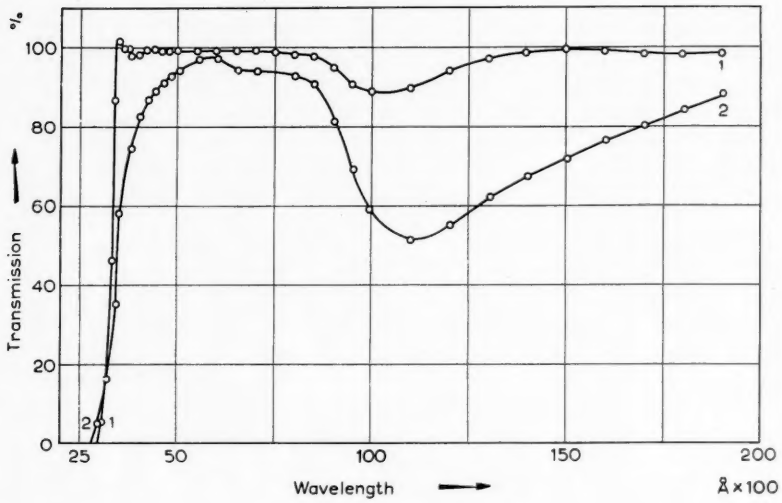

FIG. 2. Absorption spectra

Curve 1. 2-ethyl-hexanoic acid (octoic acid), anhydrous, in pure toluene, 5 g/l. Compared with pure toluene in reference cell. 10 cm cell.

Curve 2. Cadmium 2-ethyl-hexanoate (octoate) anhydrous in pure toluene, 5 g/l. Compared with pure toluene in reference cell.

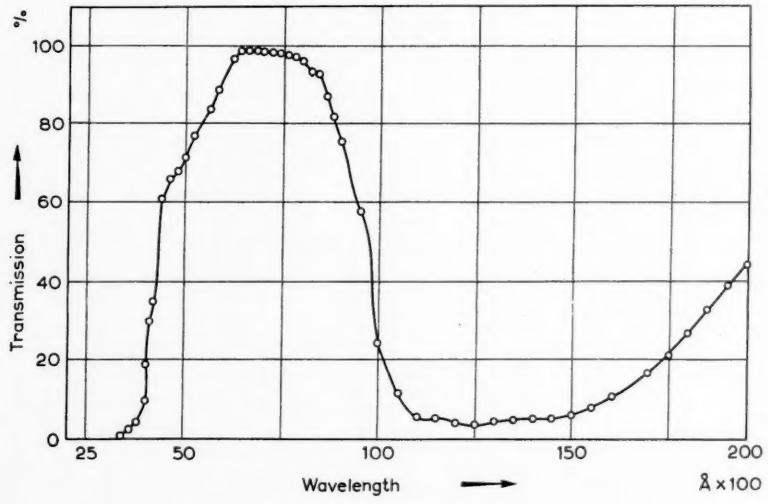

FIG. 3. Absorption Spectra

Ferric 2-ethyl-hexonate in pure toluene. $8{\cdot}03 \times 10^{-7}$ g/ml 10 cm cell.

colored solutions of iron octoate which absorbs light strongly in the region of greatest sensitivity of photomultiplier tubes.

The transmission curves shown in Figs. 2 and 3 for solutions of octoic acid, iron octoate, and cadmium octoate in toluene solutions were obtained by A. D. McGuire using a Beckman Model DU spectrophotometer.

All analyses for percentage metal of the heavy metal octoate solutions were performed by oxidizing weighed quantities of the solutions with sulfuric acid followed by gentle ignition. The residues were weighed as the sulfates.

CONCLUSION

Heavy metals have been incorporated into liquid scintillators such as toluene and triethyl-benzene in quantities sufficient to be useful for neutron detection, but thus far the quantities are too small to enhance γ-ray absorption greatly.

Acknowledgements—The author wishes to thank C. L. Cowan, Jr., F. B. Harrison, A. D. McGuire, and F. Reines for their help with various parts of the work, but especially for indicating the uses for scintillators with heavy metal loading.

REFERENCE

1. Ronzio A. R., Cowan C. L. Jr. and Reines F. *Rev. Sci. Instrum.* **29,** 146 (1958).

VOL.
4
1958/5

International Journal of Applied Radiation and Isotopes, 1959, Vol. 4, pp. 201–209. Pergamon Press Ltd. Printed in Northern Ireland

Stability of the Cation Exchange Resins

V. A. NIKASHINA, A. Kh. BREGER, M. M. SENYAVIN and A. V. GORDIEVSKY
Institute of Physics, Academy of Sciences of the USSR, Moscow

(*Received* 26 *August* 1958)

OL.
4
8/59

The chemical stability to X-, β-, and γ-radiation of air-dry cation exchange resins in the H form has been studied in connexion with the use of ion-exchange resins for absorption and separation of radioactive substance mixtures. Variations in the exchange capacity, degree of swelling and chemical stability of the resins have been investigated experimentally.

The nature of these variations in properties of the cation-exchange resins investigated has been shown to be similar on exposure both to X- and γ-rays and to fast electrons. Decrease in exchange capacity and chemical stability and variations in swelling are observed after exposure. Most affected by irradiation are ion-exchange resins of aliphatic structure. A higher degree of degradation is observed on irradiation of cation-exchange resins in the presence of air.

LA STABILITÉ CONTRE LA RADIATION DES RÉSINES À ÉCHANGE DE CATIONS

On a étudié la stabilité contre la radiation X, β et γ des résines à échange de cations dans la forme H, séchées à l'air, portant sur l'emploi des résines à échange d'ions pour l'absorption et la séparation des mélanges de matières radioactives. On a fait un examen des variations dans la capacité d'échange, dans le degré de gonflement et dans la stabilité contre la radiation des résines.

La nature de ces variations de propriétés des résines à échange de cations ainsi examinées se montre pareille lors de leur exposition également aux rayons X et γ et aux électrons rapides. Il se montre une diminution de la capacité d'echange et de la stabilité contre la radiation et des variations de gonflement suivant exposition. Les plus affectées par l'irradiation sont les résines à échange d'ions de structure aliphatique. La dégradation se fait voir à un niveau plus élevé lorsque les résines à échange de cations sont irradiées en présence de l'air.

РАДИАЦИОННО-ХИМИЧЕСКАЯ УСТОЙЧИВОСТЬ КАТИОНИТОВ

В связи с применениями ионообменных смол для поглощения и разделения смесей радиоактивных веществ изучена радиационно-химическая устойчивость отечественных воздушно-сухих катионитов в Н-форме к дейтвию ренгеновского (КУ-1, КУ-2, КБ-4), а также β- и γ-излучений (КУ-1, КУ-2, КБ-4, РФ, СБС). Экспериментально определялись изменения в результате облучения обменной емкости, набухаемости и химической устойчивости катионитов.

Показано, что характер изменения свойств изученных катионитов в результате действия рентгеновских лучей, γ-лучей и быстрых электронов одинаков. Под действием облучения падает обменная емкость, уменьшается химическая стойкость и изменяется набухаемость. Особенно сильные изменения претерпевают ионообменные смолы алифатического строения. Более глубоко деструкция протекает при облучении катионитов на воздухе.

THE problem of chemical stability of the cation and anion exchange resins becomes important in connection with the variety of ion-exchange resin applications, in particular to the absorption and separation of radioactive substances.

Published evidence on such investigations is very scarce. Studying the effect of γ- and β-radiation on Dowex-1, Dowex-30 and Dowex-50, Cathers[1] had found that after exposure at a dose of approximately 4×10^8 rep the loss in capacity of Dowex-1 and Dowex-50 was 40 and 15–35 per cent respectively, while for Dowex-30 it amounted only to 1 per cent.

This work is a continuation of previous investigations on the chemical stability of cation exchange resins of Russian trade marks KU-2, KU-1, SBS, RF, KB-4 to X-ray irradiation.[2] Air-dry cation exchange resins in the H form were investigated.

Exchange capacity, the degree of swelling and chemical stability were determined before and after irradiation by means of conventional techniques described later.

VOL. 4 1958/5

EXPERIMENTAL

Determination of the exchange capacity (EC) was carried out as follows. Titrated alkali solution was poured over a resin sample (about 0·2 gr) dried to a constant weight at 93–95°, and left to stand for 40 hours in a tightly closed conic vessel. An aliquot part of the solution (10 ml) was taken and its excess of alkali was titrated with a hydrochloric acid solution of a definite composition. Phenol phtalein was used as indicator. EC was expressed in mg. eq./gr. resin.

In order to determine the degree of relative swelling the dried resin was placed into a graduated flask, centrifuged, covered by distilled water and left to stand for 24 hours. Then it was again recycled and the relative swelling in the course of the process was computed by formula $100(V_k/V_H - 1)$, where V_k is the volume of swollen resin in ml, and V_H of the dry resin.

On determining the chemical stability by the degree of filtrate oxidation, 15 ml of H_2SO_4 (1 : 4) and a fixed volume of the $KMnO_4$ solution (0·01 N) were added to the remaining part of the filtrate (5 ml) which was transferred into a conic vessel. The mixture was boiled for 5 minutes, 5 ml of an oxalate acid solution (0·01 N) were added to the hot solution and its excess was removed by titration with the same $KMnO_4$ solution until the appearance of a rosy coloration. The degree of filtrate oxidation was expressed in mg of oxygen, in accordance with formula $X = 0{\cdot}64(V_1 - V_2)$, where V_1 is the total amount of the potassium permanganate solution used, in ml, and V_2 is the amount of the oxalate acid solution in ml.

In order to determine the exchange capacity by means of the potentiometric method, a number of resin samples of 0·1 gr each were placed in separate conic vessels and a NaCl solution with an NaOH content increasing from vessel to vessel was poured over them. The resin containing vessels were allowed to stand for 40 hours and their pH was then measured by means of a lamp potentiometer.

X-ray radiation was obtained in a laboratory of the Institute of Physical Chemistry of the USSR Academy of Sciences from high power X-ray tubes with a cylindric anode of the Russian mark TRZ-3A, at a voltage of 80 kV and a loading of 200 μA. The resins

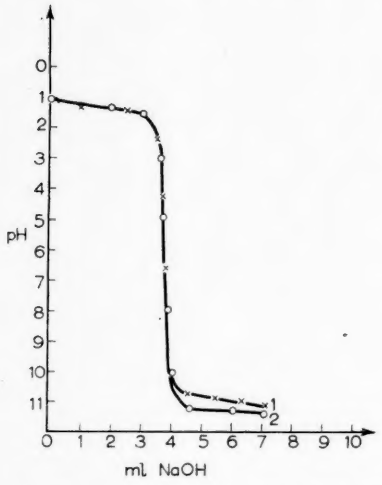

FIG. 1. Curves for potentiometric titration of the KU-2 cation exchange resin: 1—before irradiation, 2—after X-irradiation.

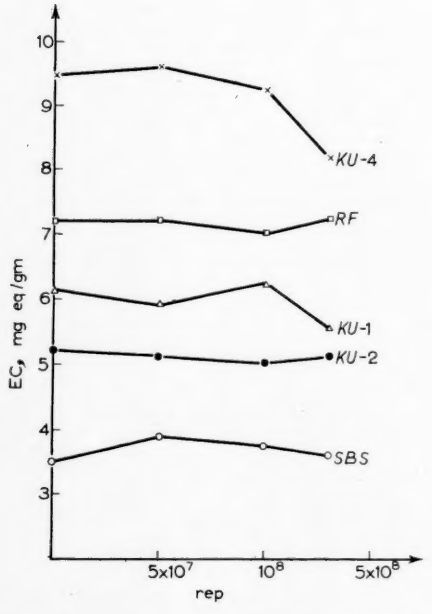

FIG. 2. Dependence of the exchange capacity of the cation exchange resins on the integral γ-radiation dose.

were then placed into cells of a 30 mm diameter, 7 mm high; the lateral walls of the cells were made from polyethylene, the wall joints were stuck up by polystyrene. The amount of energy absorbed in samples was determined by means of a thermistor calorimeter, designed at the Institute of Physical Chemistry by V. I. Petrovsky.

Chemical oxidizability of cation exchange resins resulting from X-ray exposure was not determined.

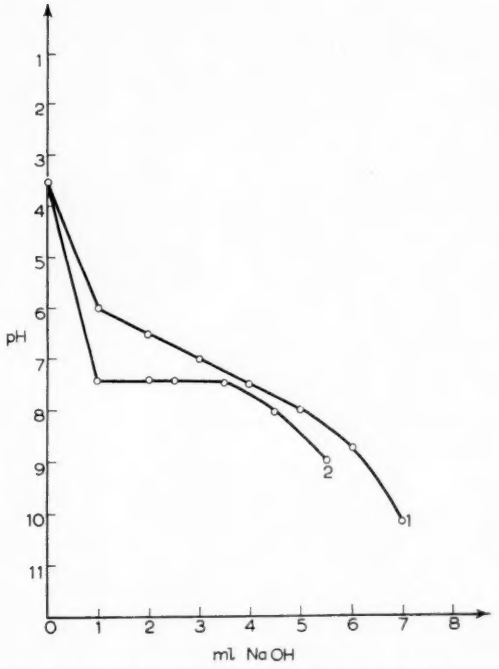

FIG. 3. Curves for potentiometric titration of the KB-4 cation exchange resin: 1—before irradiation, 2—after γ-irradiation.

The data obtained are given in Table 1 and Fig. 1.

Study of the X-ray damage to cation exchange resins was of a preliminary nature. More detailed evidence was obtained on the stability of cation exchange resins to γ- and β-radiation.

A K-20,000 apparatus designed by the Karpov Physico-Chemical Institute was used for irradiation of the resins. A Co^{60} source with an activity of 21000 gr. eq. radium

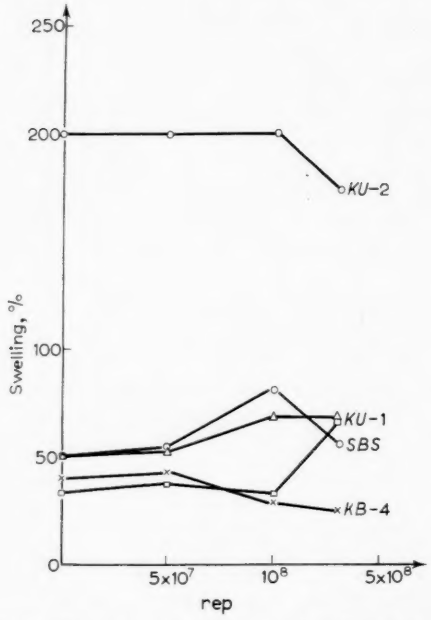

FIG. 4. Dependence of the degree of swelling of the cation exchange resins on the integral γ-radiation dose.

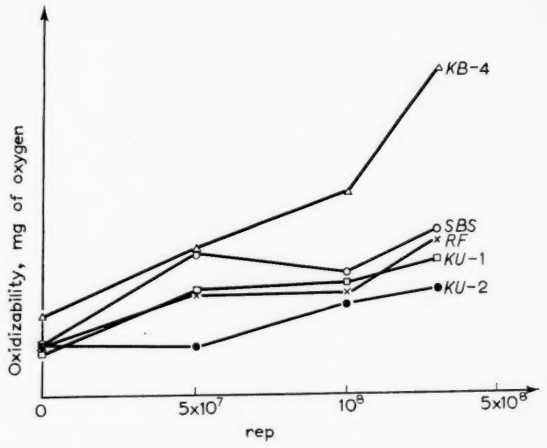

FIG. 5. Dependence of the filtrate oxidizability on the integral γ-radiation dose.

permitted to carry out investigations at high doses up to 1000 r/sec. Thus considerable integral doses could be obtained over reasonably short periods of time. The radiation dose was about 400 r/sec. The integral doses were varied from 5×10^7 to 3×10^8 rep. The dose was determined by means of the conventional dosimetry oxidation reaction of a Mohr salt solution (0·01 M) in 0·8 N HCl, yielding 15·6 mole/100 eV. Water was used to prevent heating of the samples irradiated.

Some results of these investigations are given in Table 2 and Figs. 2, 3, 4, 5.

As can be seen from Table 2 and Fig. 2 the loss in capacity of the resins investigated varies in a more or less considerable degree, being insignificant in the case of KU-2, KU-1 and RF (from 3 to 9 per cent).

At a dose of 5×10^7 rep the SBS capacity is increased by 11 per cent, but with larger doses it decreases again. Yet even at a dose of 3×10^8 rep it exceeds that of an unexposed resin. The lowest chemical stability to γ-radiation was observed for a carboxyl resin of an aliphatic structure (KB-4). At a dose of 3×10^8 rep it loses 17 per cent of its capacity. Different rates of capacity loss in carboxyl resins on the one hand, and in sulfo- and phosphoric acid resins on the other, are

TABLE 1

Type of the cation exchange resin	Properties to be determined	Integral dose, rep		
		0	$\sim 2{\cdot}5 \times 10^8$	10^9
KU-1	EC in mg. eq./gr	6·80	6·01	—
	degree of swelling, %	72	53	—
KU-2	EC in mg. eq./gr	4·08	4·16	5·38
	degree of swelling, %	215	167	162
KB-4	EC in mg. eq./gr	9·10	8·20	—
	degree of swelling, %	53	32	—

Table 2

Type of the cation exchange resin	Properties to be determined	Integral dose, rep			
		0	5×10^7	10^8	3×10^8
KU-1	EC, mg. eq./gr	6·15	5·94	6·25	5·59
	Degree of swelling, %	50	53	70	67
	Oxidizability, mg of oxygen	14·3	33·3	35·8	43·52
KU-2	EC, mg. eq./gr	5·20	5·12	5·00	5·10
	Degree of swelling, %	200	200	210	175
	Oxidizability, mg of oxygen	16·3	16·3	29·6	33·7
SBS	EC, mg. eq. /gr	3·51	3·90	3·76 (3·74)	3·60
	Degree of swelling, %	50	55	82	52
	Oxidizability mg of oxygen	16·3	45·6	39·2	53·0
RF	EC, mg. eq./gr	7·20	7·20	7·00 (6·90)	7·20
	Degree of swelling, %	33	38	33	66
	Oxidizability, mg of oxygen	16·3	32·6	32·6	48·9
KB-4	EC, mg. eq./gr	9·45	9·51	9·20 (8·45)	8·14 (7·87)
	Degree of swelling, %	40	43	29	26
	Oxidizability, mg of oxygen	25·2	46·9	65·3 (29·2)	104·0 (72·8)

apparently accounted for by different chemical stability of the COOH—, SO_3H— and H_2PO_3 groups. Elimination of CO_2 as a result of exposure could conceivably take place.

Variation of swelling is apparently due to degradation (increase in swelling) or to cross-linking (decrease in swelling) of the cation exchange resins. The swelling variations are especially pronounced at doses above 10^8 rep (Fig. 4, Table 2). The swelling of the phenol-formaldehyde cation exchange resins (RF, KU-1) raises with larger doses, i.e. degradation of these resins takes place. The swelling of the SBS cation exchange resin (a sulfo-resin with a butadiene cross-linking agent) increases over the dose range of 5×10^7–10^8 rep, whilst that of KU-2 (a sulfopolystyrene resin with divinil benzene as a cross-linking agent) remains constant at the same doses. A sharp decrease in swelling of SBS and KU-2 is observed at doses above 10^8 rep. The difference in chemical stability of the aromatic and aliphatic cross-linking agents can be seen from comparison of the SBS and KU-2 degree of swelling.

The degree of degradation can also be established by the filtrate oxidation (Fig. 5, Table 2). As had to be expected, the maximum value of the filtrate oxidation was observed for the aliphatic resin KB-4. At a dose of 3×10^8 rep the degree of oxidation is raised 4-fold, and that of SBS 3·5-fold. This can also be considered as a proof of the low chemical stability of the aliphatic components. Maximum stability was observed for KU-2. Thus the results obtained are in full agreement with the evidence available on chemical stability of high polymers.[3]

Further investigations were concerned with the effect of fast electrons* on air-dry samples of KU-1, KU-2, SBS, RF and

* The effect of β-emitting radioactive isotopes is in principal similar to that of fast electrons.

TABLE 3

Type of the cation exchange resin	Properties to be determined	Integral dose, rep			
		0	5×10^7	$3{\cdot}4 \times 10^8$	$1{\cdot}2 \times 10^9$
KU-1	EC, mg. eq./gr	6·15	6·10	6·07	6·00 (5·95)
	Degree of swelling, %	50	63	35	42
	Oxidizability, mg of oxygen	14·3	33·3	28·8	33·3
KU-2	EC, mg. eq./gr	5·20	—	5·12	4·92
	Degree of swelling, %	200	—	124	72
	Oxidizability, mg of oxygen	16·3	—	19·2	23·7
SBS	EC, mg. eq./gr	3·51	3·39	3·36	3·30 (3·16)
	Degree of swelling, %	50	55	50	42
	Oxidizability, mg of oxygen	16·3	28·2	35·8	46·1 (32·6)
RF	EC, mg. eq./gr	7·20	7·20	7·20 (6·75)	7·65 (6·3)
	Degree of swelling, %	33	26	33	32
	Oxidizability, mg of oxygen	16·3	41·6	44·2 (33·9)	55·1 (35·8)
KB-4	EC, mg. eq./gr	9·45	9·32	7·72 (7·50)	5·20 (2·10)
	Degree of swelling, %	40	41	12	0
	Oxidizability, mg of oxygen	25·2	70·4	97·3 (63·4)	112·6 (28·8)

KB-4. The samples were irradiated in an electron accelerator of the Karpov Physico-Chemical Institute at a current of 20 μA and a voltage of 200 kV. Integral radiation doses were varied from 5×10^7 to $1{\cdot}2 \times 10^9$ rep depending upon time. The results obtained are given in Table 3.

As can be seen from Table 3 and Figs. 6 and 7 a loss in capacity with larger doses was observed for all cation exchange resins investigated. Increase of the RF capacity (at an integral dose of about 10^9 rep) was only apparent; washed resin taken from the same sample displayed a fairly considerable loss in capacity (about 12 per cent), as compared to that of an unexposed sample. The smallest loss (about 2·5 per cent) was observed for the KU-1 sulfo-cation exchange resin (of the phenolformaldehyde type), the greatest (about 45 per cent) for the KB-4 resin (of aliphatic structure).

At a dose of 5×10^7 rep the swelling of KU-1, SBS and KB-4 is slightly more pronounced (showing the predominance of the degradation process). On further increase of the dose the cross-linking apparently becomes stronger than degradation and the swelling decreases. In the case of RF the processes are inverse (up to 5×10^7 rep the swelling diminishes, above this value it begins to raise.) The KU-2 swelling decreases with increase of the dose. Apparently cross-linking is in this case predominant over the whole dose range from 5×10^7 to $1{\cdot}2 \times 10^9$ rep (Fig. 8).

The evidence on chemical stability of the resins is in good agreement with the results obtained for swelling. Considerably

VOL. 4 1958/5

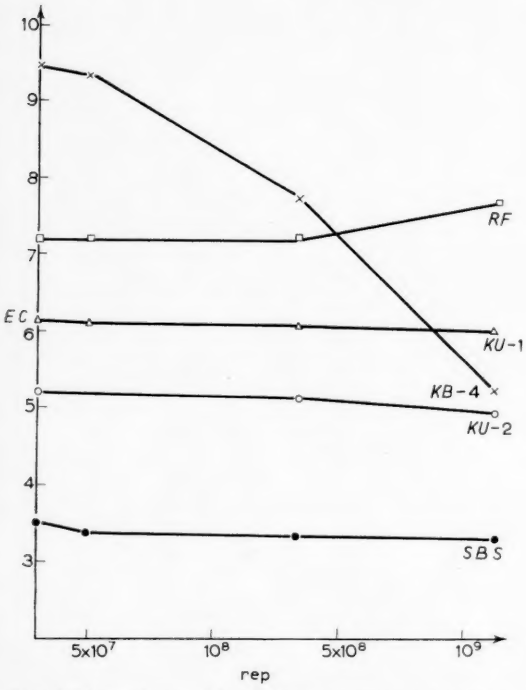

FIG. 6. Dependence of the exchange capacity of the cation exchange resins on the integral fast electron radiation dose.

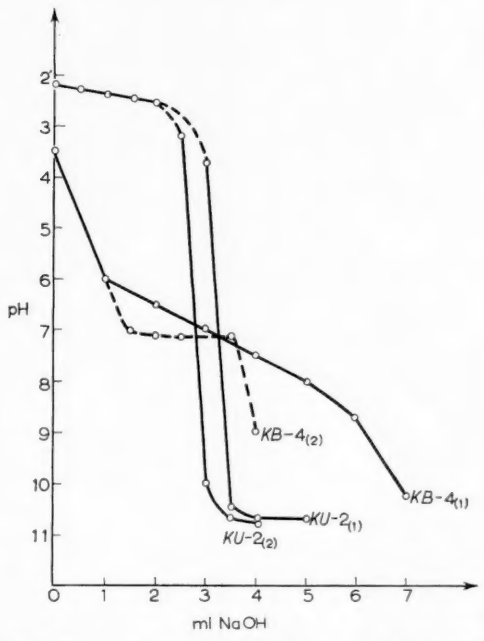

FIG. 7. Curves for potentiometric titration of the KB-4 and KU-2 cation exchange resins: 1—before irradiation 2—after irradiation with fast electrons (the integral dose for KB-4 being 3×10^8 rep, for KU-2 $\sim 10^9$ rep).

greater oxidizability of KU-1, SBS, and KB-4 filtrates can be considered as a proof of the degradation of these resins at a given dose.

The cross-linking of KU-1 over the dose range from 5×10^7 to 3×10^8 was confirmed by corresponding oxidation decrease. Maximum chemical stability was observed for KU-2 (Fig. 9).

As can be seen from evidence obtained for exposure of cation exchange resins both to fast electrons and to γ-rays, deeper degradation takes place in the latter case (at equal integral doses).

Loss in the exchange capacity of cation exchange resins exposed to fast electrons indicated on a lesser number of functional groups and on their qualitative chemical stability. The casually observed increase in the exchange capacity can be accounted for by the formation of soluble oxidation products and may therefore be considered as only apparent.

CONCLUSIONS

1. A loss in capacity, especially of the KB-4 resin, decrease in chemical stability, and variation of the swelling degree (decreasing for KU-2 and KB-4 and increasing for KU-1 and RF) are observed as a result of γ-exposure.

2. Variation of chemical stability and of the degree of swelling can be considered as a proof of competing degradation and cross-linking processes.

3. The functional groups of cation exchange resins investigated are qualitatively stable, though their quantity is somewhat decreased with increase of the dose.

4. Aromatic structure resins are more chemically stable than aliphatic ones.

5. Variation of EC, of the degree of swelling and of the chemical stability of the cation exchange resins investigated appears to be of the same nature both on

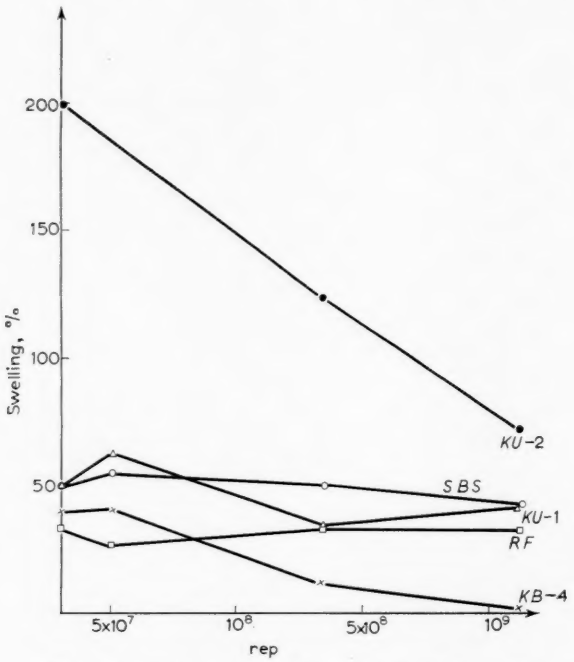

FIG. 8. Dependence of the degree of swelling of the cation exchange resins on the integral fast electron radiation dose.

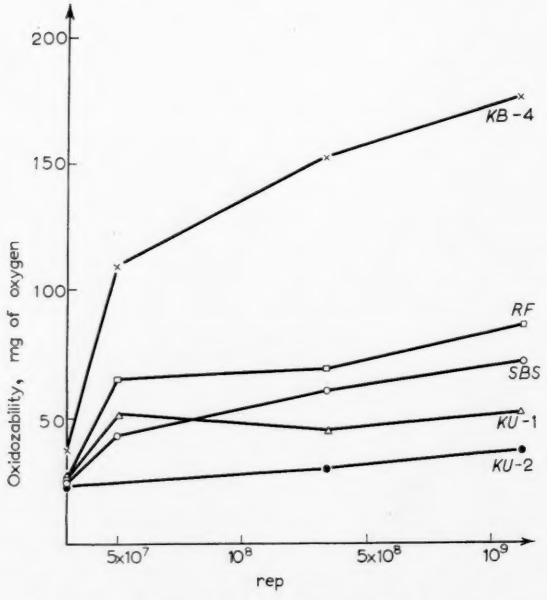

FIG. 9. Dependence of the filtrate oxidizability on the integral fast electron radiation dose.

VOL. 4 1958/5

exposure to fast electrons and to γ-rays.

6. On γ-exposure in the presence of air the degradation is deeper.

7. A study of the gas-phase and of the filtrate composition, as well as structural analysis of the resins would be necessary for establishing the mechanisms of radiation induced processes in resins.

Acknowledgements—The authors are indebted to E. B. TROSTYANSKAYA and A. S. TEVLINA for the resin samples they gave and also for the valuable information on their composition and structure; to V. L. KARPOV for his helpful advices in discussing the results obtained, and to V. B. OSIPOV and L. A. VASSILIEV, who have irradiated the preparations by means of a K-20,000 device.

REFERENCES

1. CATHERS G. I. *International Conference on the Peaceful Uses of Atomic Energy*, **7,** 1956.
2. SENYAVIN M. M., KOLOSOVA G. M. and NIKASHINA V. A. *Zh. Neorgani Khim.* **3,** 1 (1958).
3. KUZMINSKY A. S. *Uspekhi Khim.* **24,** 863 (1955).

OL.
4
8/59

International Journal of Applied Radiation and Isotopes, 1959, Vol. 4, pp. 210–213. Pergamon Press Ltd. Printed in Northern Ireland

Preparation of Carrier Free Radiofluoride with a New Estimate of the Half-life of F^{18}*

C. H. CARLSON†, L. SINGER, D. H. SERVICE and W. D. ARMSTRONG
Department of Physiological Chemistry and Department of Physics of the University of Minnesota

(*Received* 12 *May* 1958)

A method for producing carrier free radiofluoride in aqueous solution using proton bombardment of O^{18} enriched water is described together with a new estimate of 109·7 minutes for the half-life of F^{18}.

LA PRÉPARATION DE RADIOFLUORURE SANS PORTEUR AVEC UNE NOUVELLE ESTIMATION DE LA PÉRIODE DE DEMI-VALEUR DE F^{18}

On décrit une méthode pour la production de radiofluorure sans porteur en solution aqueuse au moyen du bombardement à protons de l'eau enrichie en O^{18}, ainsi qu'une nouvelle estimation de 109,7 minutes pour la période de demi-valeur de F^{18}.

ПОЛУЧЕНИЕ РАДИОАКТИВНОГО ФТОРА БЕЗ НОСИТЕЛЯ И НОВЫЙ РАСЧЕТ ПОЛУПЕРИОДА ЖИЗНИ F^{18}

Описывается метод получения радтоактивного фтора без носителя из водного раствора посредством протоннрй бомбардировки воды, обогащенной O^{18}, а также приводится новое значение полупериода жизни F^{18}, равное 109,7 мин.

HERSTELLUNG VON TRÄGERFREIEN RADIOFLUORID UND NEUE BESTIMMUNG DER HALBWERTSZEIT VON F^{18}

Im Vorliegenden wird beschrieben wie tragerfreies Radiofluorid in wässriger Lösung durch Protonenbestrahlung von O^{18} angereichertem Wasser hergestellt werden kann. Ausserdem wurde eine neue Bestimmung der Halbwertszeit von F^{18} durchgeführt. Es ergab sich ein Wert von 109,7 Minuten.

INVESTIGATIONS of the kinetics of tissue distribution and excretion of fluoride are best carried out with a radioisotope of fluorine. For these purposes the only radionuclide of useful properties is F^{18}. Even in this case the short half-life of F^{18} limits its use to relatively short-term experiments conducted near its site of production. The usefulness of F^{18} as a tracer can be enhanced through improved methods of preparation of the radioisotope and through a better delineation of its properties. This paper describes techniques for the convenient preparation of high yields of carrier-free F^{18} in small volumes of aqueous solution and presents the results of a new estimate of the half-life of F^{18}.

At least ten nuclear reactions, exclusive of spallation reactions, have yielded F^{18}[1]. The availability of 10 MeV protons through the use of the University of Minnesota Linear Accelerator determined our use of the O^{18} (p, n) F^{18} reaction. This reaction was first described in 1938[2] and has been previously used[3] to give useful quantities of F^{18}.

* Supported by U.S. Public Health Service Grant A-592 (Physiological Chemistry) and U.S. Atomic Energy Commission Contract AT (11-1)-50 (Physics-Linear Accelerator).

† U.S. Public Health Service Post-Doctoral Fellow.

VOL. 4 1958/5

METHODS

The radioactivity measurements were made with 2 ml aqueous samples counted in a well-type crystal scintillation counter except in one case, as indicated below, when a flow type Geiger counter was used.

Water enriched to 3% O^{18} abundance* was routinely used as the target material. The bombardments were carried out with the water enclosed in polyethylene cells, improvised for each run, as illustrated in Fig. 1,A. A circular section 3–4 mm high was cut from polyethylene tubing of 32–35 mm outside diameter and 29–32 mm internal diameter. The ends of the cylinder were closed by sealing around the entire circumference of each end of the cylinder a piece of polyethylene film 5×10^{-3} cm thick. The seals were made by applying heat from a small soldering iron to soft aluminum foil pressed into firm contact with the film and cylinder. The latter was deformed, before attaching the film, to the approximate dimensions shown in Fig. 1,A to permit better accommodation of the water and gas volumes. An 18-gauge syringe needle, positioned as shown, was used to introduce 1·8–2·0 ml of water leaving about 0·5 ml of air volume in the cell. The needle, with its tip located in the air space, was left in place during the bombardment to permit the escape of gases.

The excess of film shown in Fig. 1,A was used to attach the cell with adhesive tape to the aluminum plate of the beam current integrator. The cell was positioned 4–8 mm from the linear accelerator port which had an aluminum window 0·1 mm thick. The cell was cooled by an air stream during the bombardment which was normally continued until a charge collection of 120 microcoulombs had been registered. This charge, representing the accumulated proton bombardment of the target, was selected because it could be delivered in a time (20–60 min) relatively short to that of the half-life of F^{18}.

The other illustrations in Fig. 1 indicate the method used to remove the contents of the cell. B and C were cut from separate 2 oz polyethylene bottles in the proportions shown. In use a 20 ml beaker was placed

* Water of this and higher O^{18} concentration has been obtained from the Weizmann Institute of Science, Rehovoth, Israel.

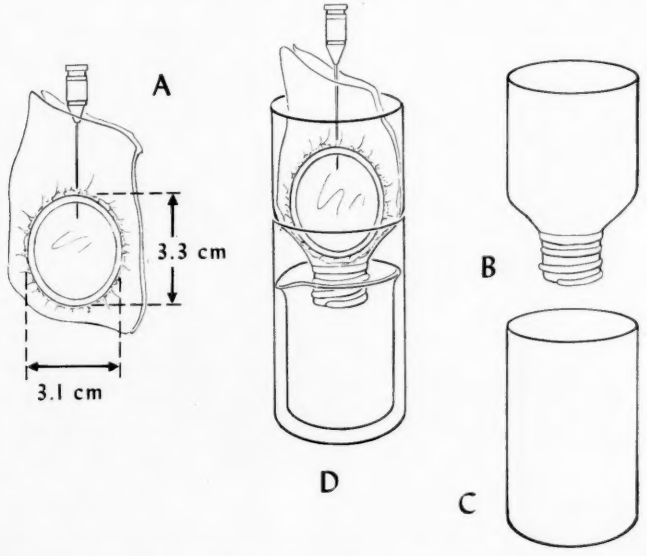

FIG. 1. Equipment for bombarding O^{18} enriched water with protons. A, Polyethylene cell with needle vent. B and C, Polyethylene components of D. D, Assembly prepared for centrifugation to remove water from cell.

in C, B was inserted into C and the cell with its contents was placed into the assembly as shown in D. The polyethylene faces of the cell were punctured and the whole assembly was centrifuged at 800 rev/min. The liquid contents of the cell were thereby thrown into the beaker and were diluted to the desired volume.

Total activities of 6 to 9 $\times$ 10^7 counts/min as of the end of the bombardment period were usually obtained. Based upon the lower yields obtained when ordinary water (0·2% O^{18}) was used it appears that the use of water with an O^{18} abundance greater than 3 per cent would yield proportionally higher quantities of F^{18}. Higher proton intensities will also increase the yield if these are delivered without unduly prolonging the bombardment time.

Counts of dilutions of new prepared target solutions showed the presence of a radioactive species which decayed with a half-life of about 10 minutes and is therefore assumed to be N^{13}. The N^{13} is believed to be formed by the reaction $C^{12}(p, \gamma)N^{13}$ since bombardment of empty polyethylene cells with protons produced what was apparently the same radioactive isotope in the polyethylene and its washings. The radioactive contaminant causes no interference since it effectively decays before (2–3 hr) the assays for F^{18} concentration are made. It can also be removed, as indicated below, by distillation from perchloric acid or by precipitation of fluoride as lead chlorofluoride.

The half-life of F^{18} is commonly accepted to be 112 min[5] but estimates have varied from 107 min[2] to 115 min.[4] Table 1 gives a summary of our estimates of half-life of this radioisotope. All counts were made for 2-minute periods and all were in excess of 10,000 counts/min. Corrections for resolving time losses were made when applicable. All points fell in a straight line when plotted on large scale semi-log paper. Equations were derived to fit each set of observations by a

VOL 4 1958/

TABLE 1. Estimates of half-life of radiofluoride—F^{18}

Sample preparation	Period observed (min)	Number of points	Half-life (min)
a Aged 12 hours before counts started	273	26	109·6
	353	39	109.3
b Distilled from $HClO_4$; Carrier fluoride added	373	27	110.0
	383	27	109·2
	597	39	109·1
	599	41	109·5
c Distilled from $HClO_4$; Precipitated as PbFCl; Carrier fluoride added	476	45	110·8
	614	50	110·4
d Aged 5 hours before counts started*	375	19	109·6
		Mean	109.7 ±0·54 (S.D.)

* Geiger-Mueller (particle) counts; all other crystal scintillation (gamma ray) counts.

method of least squares. The slope of this equation (log c/m *vs* time) gave the decay constant from which was calculated the separate values of half-life given in the table. The possible effect of the presence of a gamma ray emitting radioisotope of shorter half-life than that of F^{18} on the results had to be considered. The results in section "a" were obtained with samples which had been aged for a time which would have allowed N^{13} to have decayed through approximately 70 half-lives. Those in section "b" were obtained with material which had been purified by distillation of fluoride from perchloric acid as in the procedure commonly employed for separation of fluoride from interfering elements in the chemical determination of fluoride.

The results in section "c" were obtained with material which had, after distillation, been further purified by precipitation of the fluoride as lead chlorofluoride.[6] In order to eliminate the effect of an unrecognized bias consequent to the radiometric measurement of the annihilation gamma rays with crystal scintillation counters in sections a, b and c, the data summarized in section d were obtained. A sample with carrier fluoride was neutralized, evaporated on a metal planchet and counted in a flow type Geiger counter. It is assumed that the counts thus obtained were mainly due to positrons. At any rate a system markedly different from crystal scintillation counters was used.

We find that results calculated to zero time through the use of the decay constant related to a half-life of F^{18} of 109·7 min are more consistent than when a half-life of 112 min is employed and give time–zero values which are more closely and randomly distributed about the mean.

VOL. 4 58/59

REFERENCES

1. Bernstein R. B. and Katz J. J. *Nucleonics* **11** (10) 46 (1953).
2. Dubridge L. A., Barnes S. W., Buck J. H. and Strain C. V. *Phys. Rev.* **53,** 447 (1938).
3. Volker J. F., Sognnaes R. F. and Bibby B. G. *Amer. J. Physiol.* **132,** 707 (1941).
4. Huber O., Lienhard O., Scherrer P. and Wäffler H. *Helv. Phys. Acta* **16,** 33 (1943).
5. Hollander I. M., Perlman I. and Seaborg G. T. *Rev. Mod. Phys.* **25,** 469 (1953).
6. Stark B. *Z. Anorg. Chem.* **51,** 173 (1911).

International Journal of Applied Radiation and Isotopes, 1959, Vol. 4, pp. 214–220. Pergamon Press Ltd. Printed in Northern Ireland

The Determination of Copper and Zinc in Biological Material by Activation Analysis

H. J. M. BOWEN
Technological Irradiation Group, Isotope Division,
Wantage Radiation Laboratory, Grove, Berkshire

(*Received* 2 *July* 1958; *in revised form* 14 *August* 1958)

A method is described for the determination of copper and zinc in biological material using the technique of activation analysis. The limit of detection of the method is 4×10^{-10} g for copper, and 5×10^{-8} for zinc. The method has been used to determine copper and zinc in single seeds and in human blood. The seeds of tomato plants grown under controlled conditions contained about 8 p.p.m. of copper and 150 p.p.m. of zinc. The mean copper in the blood of 16 subjects was found to be 75·5 μg/100 ml, and the mean zinc 0·77 mg/100 ml.

LE DOSAGE DU CUIVRE ET DU ZINC DANS LES MATIÈRES BIOLOGIQUES PAR L'ANALYSE À ACTIVATION

On décrit une méthode pour le dosage du cuivre et du zinc dans les matières biologiques en employant la technique de l'analyse à activation. La limite d'observation de la méthode est 4×10^{-10} g. pour le cuivre, et 5×10^{-8} g. pour le zinc. La méthode a servi au dosage du cuivre et du zinc dans des graines uniques et dans le sang humain. Les graines de plantes de tomate, cultivées sous des conditions contrôlées, continrent environ 8 p.p.m. de cuivre et 150 p.p.m. de zinc. La moyenne pour le cuivre dans le sang de 16 sujets se trouva à 75,5 μg/100 ml., et la moyenne pour le zinc 0,77 mg/100 ml.

ОПРЕДЕЛЕНИЕ МЕДИ И ЦИНКА В БИОЛОГИЧЕСКИХ МАТЕРИАЛАХ ПРИ ПОМОЩИ АКТИВАЦИОННОГО АНАЛИЗА

Описывается метод определения меди и цинка в биологических материалах, с использованием методики активационного анализа. Пределом метода является 4×10^{-10} г для меди и 5×10^{-8} г для цинка. Метод был применен для определения меди и цинка в отдельных семенах и в крови человека. В заданных условиях семена томатов содержали около 8 частей на миллион меди и 150 частей на миллион цинка. Среднее содержание меди в крови 16 объектов было 75,7 μг/100, а цинка 0,77 мг/100 мл.

DIE BESTIMMUNG VON KUPFER UND ZINK IN BIOLOGISCHEM MATERIAL MITTELS AKTIVIERUNGSANALYSE

Eine Methode zur Bestimmung von Cu und Zn in biologischem Material mit Hilfe der Aktivierungsanalyse wird beschrieben. Die untere Grenze, der nach dieser Methode auffindbaren Mengen sind 4.10^{-18} g Cu und 5.10^{-8} g Zn. Die Methode wurde verwendet, um Cu und Zn in einzelnen Samen und im menschlichen Blut zu bestimmen. Samen von Tomatenpflanzen, welche unter kontrollierten Bedingungen gezogen wurden, enthielten ungefähr 8 p.p.m. Cu und 150 p.p.m. Zn. Als mittlerer Kupfergehalt des Blutes von 16 Personen wurden 75,5 μg/100 ml aufgefunden, als mittlerer Zinkgehalt 0,77 mg/100 ml.

INTRODUCTION

COPPER is an essential element in both animals and plants but occurs there only in minute quantities. It is a constituent of numerous enzymes (e.g. polyphenol oxidase, laccase and ascorbic acid oxidase) and is an essential catalyst in the biosynthesis of both haemoglobin and chlorophyll. There are a number of established methods which can be used to determine microgram quantities of the metal but these are liable to error owing to losses

and contamination which may be introduced during the analysis. The dry-ashing of organic matter may lead to irreproducible results, perhaps on account of volatilisation or absorption of copper on the crucible (COMRIE;[1] BAILEY *et al.*;[2] MALTBY.[3]) BORCHARDT *et al.*[4] suggest that wet-ashing with a mixture of nitric and perchloric acids is more reliable, but the reagents must be carefully purified to avoid contamination, as strong acids can leach traces of copper from glass containers. CRAWLEY[5] and RUSSELL *et al.*[6] consider that some wet-ashing reagents interfere with the polarographic determination of traces of copper. Neutron activation analysis is not subject to these errors since the sample can be activated before it is ashed and the only contamination hazard occurs before the activation process.

Zinc is also an essential element in both animals and plants where it forms the prosthetic group of carbonic anhydrase, dehydropeptidase, glycyl glycine dipeptidase and probably other enzymes. It is not an easy metal to determine by conventional methods since it forms few coloured complexes, has only one valency state and does not give a strong arc or flame spectrum. Although zinc is not activated so strongly as copper by thermal neutrons, very small quantities can be determined by activation analysis.

Natural copper consists of two isotopes, Cu^{63} and Cu^{65}, which on activation by thermal neutrons are converted to Cu^{64} and Cu^{66} respectively. Cu^{66} has a half-life of only 5·1 min and one hour after activation the only countable activity from the pure element comes from the Cu^{64}, which decays with a half-life of 12·8 hr.

The cross-section of copper for neutrons is relatively high and SMALES *et al.*[7] suggest that 10^{-10} g amounts should be detectable after activation.

Natural zinc consists of five isotopes, which on activation by thermal neutrons give rise to five radioisotopes. Some characteristics of these isotopes are shown in Table 1.

TABLE 1. Zinc radioisotopes produced by neutron activation
(Activated for 12 hr in a flux of $1{\cdot}5 \times 10^{12}$ n/cm²/sec)

Isotope	Half-life	mc/g produced	mc/g after 10 hr decay	Emission
Zn^{65}	245 day	0·13	0·13	$\beta\gamma$
Zn^{69}	14 hr	3·0	1·82	γ
Zn^{69b}	52 min	67·0	0·02	β
Zn^{71}	3 hr	0·19	0·02	$\beta\gamma$
Zn^{71b}	2 min	0·19	0·00	$\beta\gamma$

It will be seen that by activating for 12 hr and then allowing 10 hr for decay 90 per cent of the activity left is caused by the isotope Zn^{69}. It proved possible to detect as little as 5×10^{-8} g of the element by counting this isotope after activation.

The present work was initiated because it was required to determine the copper and zinc content of certain seeds. Since each seed contained about 4×10^{-8} g of copper and 5×10^{-7} g of zinc, it was obvious that no existing method was sufficiently sensitive for the purpose. The method was then tested on blood, which can be collected under cleaner conditions than most biological samples, with the results described below.

EXPERIMENTAL

The ideal method of analysing seeds would be to activate a whole pod and dissect out the seeds after activation. In the present instance this method was not used. Tomato fruits were cut transversely with a quartz knife and the seeds and pulp squeezed into clean polystyrene tubes. The mass was allowed to ferment at 25°C for five days, after which the mucus adhering to the seeds could be washed away through clean terylene netting. The seeds were air dried before storing at constant humidity. They were transferred to clean polythene packets with perspex forceps and then sealed prior to activation.

Blood samples were obtained as described in a previous publication[8] and sealed in clean polythene tubes.

Samples were packed, together with standards of about 0·1 μg spectrographically pure copper and 20 μg spectrographically pure zinc in solution, in a polythene bag inside an aluminium can. The can was then irradiated for 12 hr in the Harwell pile B.E.P.O. in a flux of about 10^{12} thermal neutrons/cm^2/sec. After irradiation, the tube or packets were cut open and the contents dissolved in hot fuming nitric acid. The seeds were washed twice in dilute hydrochloric acid containing a detergent to dissolve any metals adhering to the seed coat before the wet-ashing process.

Chemical separation of copper

10 mg of copper carrier was added to each sample and the standard and a chemical procedure was carried through to isolate the Cu^{64} free from all radioactive impurities. Sodium, calcium, strontium, chlorine, bromine, potassium, chromium, manganese, cobalt, yttrium and phosphorus carriers were added and the copper reduced to the colourless cuprous state with sodium sulphite in normal nitric acid. It was precipitated in boiling solution with potassium thiocyanate and the precipitate spun off in a centrifuge and washed twice with the diluted reagents. The precipitate was dissolved in hot nitric acid, carrier iron, manganese and phosphorus were added and the whole was made strongly alkaline with ammonia. The ferric hydroxide was spun off, dissolved in nitric acid and reprecipitated with ammonia. The two deep blue supernatants were united and acidified until 1 N in nitric acid and cuprous thiocyanate was precipitated as before. The thiocyanate was destroyed by boiling with nitric acid and the solution brought to pH 5 with ammonia and acetic acid. Alcoholic salicylaldoxime was added and the solution boiled till the precipitate coagulated. It was thoroughly washed with water and acetone, and finally slurried onto an aluminium counting tray, dried, weighed and counted with an end window counter. Chemical yields were generally about 70 per cent or higher and blanks were small for the blood and quite negligible for the seeds.

The whole procedure took about 2 hr for eight samples. Losses of copper were tested using dummy runs, and the purity of the separated copper by plotting a decay curve. Counting rates were of the order of 2000 counts/min.

Table 2 shows the losses in the chemical steps in a dummy run replicated four times, together with losses in other steps which were initially considered for purification.

TABLE 2. Losses in the chemical steps

Chemical step	Purpose	% Cu lost
CuSCN precipitation	Removal of all metals but Pb	6·7
$Fe(OH)_3$ scavenge	Removal of traces of Mn, P and La	0·8
CuSCN precipitation	Removal of final traces of metals	6·7
Cu salicyl aldoxime precipitation	Obtaining Cu in weighable form	4·0
TOTAL for separation procedure		18·2
Cu thionalide precipitation		11·3
Cu dithio-oxamide precipitation		4·2
Cu precipitation with Fe dust		3·7

These losses were largely mechanical, as organic precipitates generally give rise to a scum which cannot be centrifuged off. They did not affect the accuracy of the method because the chemical yield was measured in every case.

There are a number of sources of error in the activation procedure, but fortunately none of them is particularly serious for the analyses reported here. The neutron flux used was homogeneous to ± 2 per cent, and the statistical counting errors were of the same order. A small self-absorption correction was found to be necessary in counting the Cu^{64}, but no correction was necessary for long-lived impurities since these were present in completely negligible amounts. Cu^{64} is produced by other nuclear reactions than the Cu^{63} $(n\gamma)$ reaction, for example the Zn^{64} (n,p) reaction, but the cross-section for the latter is probably exceedingly small compared with

the former. The method might give spurious results if very large amounts of zinc were present in the sample.

Chemical separation of zinc

20 mg of zinc was added to each sample and also carrier copper and manganese. The following chemical procedure was used to isolate the activated zinc from other radioactive material. Sodium sulphite was added, and cuprous thiocyanate was twice precipitated and spun off to ensure complete removal of radio-copper.

The zinc was then precipitated from the supernatant by adding 5 ml of potassium mercury thiocyanate and a little nitric acid and oxalic acid, and standing in ice for 15 min. The precipitate was dissolved in strong nitric acid and reprecipitated by diluting to 1 N and adding more of the potassium mercury thiocyanate reagent. It was washed and dissolved up in strong nitric acid. Cobalt, manganese and phosphorus carriers were added and cobalt hydroxide was precipitated by boiling with excess potassium hydroxide containing a little hydrogen peroxide. The supernatant was brought to pH 5 with glacial acetic acid and boiled with 2% sodium quinaldate till the precipitate coagulated. Zinc quinaldate was spun off, dissolved in hot nitric acid and reprecipitated as before, and then thoroughly washed with water and acetone. It was slurried onto a counting tray with acetone, dried, weighed and counted with an end window counter. Chemical yields were generally in the region of 70 per cent, and blanks did not exceed 10^{-7} g: for the seeds the blanks were negligible. Counting rates varied from 100 to 1000 counts/min and would have been higher if a scintillation counter had been employed.

The whole procedure took about 2·5 hr for eight samples. Losses of zinc were tested using dummy runs, and the purity of the separated zinc by plotting a decay curve. Occasionally samples were contaminated with long-lived impurity which was shown to have a fourteen day half-life and was almost certainly phosphorus-32.

Table 3 shows the losses in the chemical steps in a dummy run replicated four times.

TABLE 3. Losses in the chemical steps

Chemical step	Purpose	% Zn lost
2 × CuSCN precipitations	Removal of Cu	2·0
2 × Zn HgSCN precipitations	Removal of Na, Fe, Ni, Cr and La	0·6
$Co(OH)_3$ scrub	Removal of Co, Mn, P and La	1·6
2 × Zn quinaldate precipitations	Removal of traces of Co, Mn and La: gives Zn in weighable form	0·6
		—
TOTAL for separation procedure		4·8

These losses did not affect the accuracy of the method because the chemical yield was measured in every case. The neutron flux used was homogeneous to ± 2 per cent and statistical counting errors were kept below 5 per cent. No self-absorption correction was found to be necessary in counting the zinc-69. This isotope is produced by other reactions than the Zn^{63} (n, γ) reaction, for example the Ga^{69} (n, p) reaction and the Ge^{72} (n, α) reaction. However, the cross-sections for these side reactions are very small and the concentrations of gallium and germanium in biological material are so small that their effects are probably negligible.

RESULTS

Copper and zinc were determined in the seeds of tomato (*Lycopersicon esculentum*) and in human blood. The tomato seeds were obtained from plants of the variety "Moneymaker", grown in sand culture using the complete culture solution recommended by HEWITT[9] and collected truss by truss. Copper was also determined in seeds of red campion (*Silene dioica*) which were obtained from a variety of sources via the Director of the Chelsea Physic Garden. The results are shown in Tables 4–7. Replicate determinations did not vary by more than 20%, and generally agreed within 10 per cent.

TABLE 4. Copper content of tomato seeds
(Data are means of 5 replicates)

Truss	Wt. of 2 seeds (g)	Cu content (μg)	Cu content (μg/g)
1	0·00901	0·0778	8·64
2	0·00815	0·0730	8·95
3	0·00776	0·0647	8·34
4	0·00724	0·0621	8·58
5	0·00723	0·0632	8·74
6	0·00666	0·0581	8·73
7	0·00687	0·0576	8·38

TABLE 5. Zinc content of tomato seeds
(Data are means of 2 replicates)

Truss	Mean weight of 10 seeds (g)	Zinc content (μg)	Zinc content (μg/g)
1	0·0387	5·06	131
2	0·0331	6·01	182
3	0·0431	5·48	127
4	0·0343	5·39	157
5	0·0289	5·92	205
6	0·0330	5·12	155
7	0·0283	4·30	164

TABLE 6. Copper content of *Silene dioica* seeds
(Data are means of 2 replicates)

Origin	Mean weight of 20 seeds (g)	Copper content (μg)	Copper content (μg/g)
Cologne	0·01045	0·070	6·70
Budapest	0·0162	0·135	8·39
St. Andrews	0·01615	0·178	11·02
Lugduno	0·0186	0·074	3·98

TABLE 7. Copper and zinc content of human blood
(Data are means of 2 replicates)

Sex	Blood used (g)	Cu content (μg)	Cu content (μg/g)	Zn content (μg)	Zn content (μg/g)
M	0·1063	0·1002	0·943	0·902	8·49
M	0·0346	0·0330	0·955	0·226	6·52
M	0·0412	0·0259	0·628	0·316	7·67
M	0·1415	0·0975	0·689	1·08	7·62
M	0·0598	0·0374	0·626	0·391	6·54
M	0·0356	0·0286	0·802	0·239	6·71
M	0·0461	0·0387	0·840	0·409	8·88
M	0·0198	0·0185	0·935	0·176	8·88
M	0·0596	0·0497	0·834	0·415	6·96
M	0·0367	0·0221	0·601	0·223	6·08
M	0·0588	0·0403	0·685	0·604	10·27
M	0·0317	0·0273	0·860	0·293	9·25
F	0·0248	0·0198	0·797	0·249	10·06
F	0·0235	0·0196	0·832	0·241	10·26
F	0·0501	0·0442	0·883	0·421	8·40
F	0·1159	0·1063	0·917	0·816	7·04
Mean (M)			0·781 ± 0·232		7·82 ± 1·63
Mean (F)			0·846 ± 0·091		9·06 ± 1·50
Overall Mean			0·797 ± 0·116 (75·5 μg/100 ml)		8·13 ± 1·38 (0·77 mg/100 ml)

VOL.
4
1958/5

DISCUSSION

A number of workers have used activation analysis to determine traces of copper and zinc in pure metals and samples of geochemical interest, and reference to these may be obtained in a recent excellent bibliography.[10] TOBIAS *et al.*[11] have discussed methods employed for copper and zinc in mouse tissue, and TIPTON *et al.*[12] briefly mention the use of the method to determine copper in human hearts. HALL[13] and HELWIG *et al.*[14] have determined zinc in biological material by activation. Chemical separation procedures are summarised by MEINKE.[15]

For blood, the *Handbook of Biological Data*[16] quotes 98 μg Cu and 0·88 mg Zn per 100 ml whole blood: our figures are slightly lower but fall well within the rather wide range of variation already known. The relatively high zinc content of the blood of female subjects measured here is probably not significant. There is no correlation between the amounts of the two metals present in blood.

The copper and zinc contents of seeds found by this method agree in order of magnitude with earlier values. The *Handbook of Biological Data*[16] gives a copper content of about 10 p.p.m. and a zinc content ranging from 13 to 360 p.p.m. for a number of plant seeds. The analyses from which these figures were obtained used 1–10 g samples of tissue where the present method requires 10–100 mg only. STOUT *et al.*[17] fed tomato plants with Zn^{65} of known specific activity and estimated that each seed contained 0·03 μg of zinc from their radioactivity. This is much less zinc than we have found here.

The tomato seeds all contained about the same amount of zinc although the mean weight of seeds from different trusses varied considerably. In contrast, the copper content of the tomato seeds was markedly dependent on seed weight. Although the absolute amount of copper per seed falls off in the higher trusses where the seeds are smaller and lighter, the content in μg/g remains remarkably constant. The Campion seeds show an unexplained variation in both dry weight and copper content, but do not contain unusual amounts of the element, despite the fact that *Silene dioica* is a copper indicator plant,[18] at least in the northern part of its range.

A cursory survey of the literature indicates that the activation method compares favourably with conventional methods of analysis in sensitivity. Recent colorimetric methods are not applicable for less than microgram amounts of copper[4,6,19] or zinc[20] and polarographic methods[6,21,22] have about the same limit of applicability. STITCH[23] considers that the arc spectrograph cannot detect less than 10^{-7} g copper in tissue, and the microbiological assay of NICHOLAS *et al.*[24] cannot be used to determine less than this.

The present method could be applied to the majority of biological materials with very little modification. It was estimated that 4×10^{-10} g of activated copper, or 5×10^{-8} g of activated zinc, would double the background of an end window counter, so these are the smallest amount of the elements that could reasonably be detected. In order to detect or determine still smaller amounts one would have to use higher neutron fluxes for activation, or lower the counter background by some method.

Acknowledgements—I should like to thank DR. D. GIBBONS, DR. G. E. HARRISON and DR. D. MAPPER for much helpful discussion.

REFERENCES

1. COMRIE A. A. D. *Analyst* **60,** 532 (1935).
2. BAILEY L. F. and MCHARGUE J. S. *Plant Physiol.* **20,** 79 (1945).
3. MALTBY J. G. *Nature* **160,** 468 (1947).
4. BORCHARDT L. G. and BUTLER J. P. *Analyt. Chem.* **29,** 414 (1957).
5. CRAWLEY R. H. A. *Analyt. Chim. Acta.* **13,** 373 (1955).
6. RUSSELL G. and HART P. J. *Analyst.* **83,** 203 (1958).
7. SMALES A. A., MAPPER D. and WOOD A. J. *Analyst* **82,** 75 (1957).

8. Bowen H. J. M. *J. Nuclear Energy* **3,** 18 (1956).
9. Hewitt E. J. Sand and water culture methods used in the study of plant nutrition. C.A.B. (1952).
10. Gibbons D., Loveridge B. A. and Millett R. J. A.E.R.E. I/R 2208 (1957).
11. Tobias C. A., Wolfe R., Dunn R. and Rosenfeld I. *Acta Unio Intern. Contra Cancrum* **7,** 874 (1952).
12. Tipton I. H., Foland W. D., Bobb F. C. and McCorkle W. C. CF53-8-4 (1954).
13. Hall T. A. *Nucleonics* **12,** No. 3, 34 (1954).
14. Helwig H. L., Ashikawa J. K. and Smith E. R. UCRL 2655 (1954).
15. Meinke W. W. AECD 2738 (1949).
16. Spector W. S. *Handbook of Biological Data* (1956).
17. Stout P. R., Overstreet R., Jacobson L. and Ulrich A. *Proc. Soil Sci. Soc. Amer.* **12,** 91 (1947).
18. Rune O. *Acta Phytogeogr. Suec.* **31,** 1 (1953).
19. Stark G. R. and Dawson C. R. *Analyt. Chem.* **30,** 191 (1958).
20. Jackson R. K. and Brown J. F. *Proc. Amer. Soc. Hort. Sci.* **68,** 1 (1956).
21. Hinsvark O. N., Houff W. H., Wittwer S. H. and Sell H. M. *Analyt. Chem.* **26,** 1202 (1954).
22. Verdier E. T., Steyn W. J. A. and Eve D. J. *Agric. Food. Chem.* **5,** 354 (1957).
23. Stitch S. R. *Biochem. J.* **67,** 97 (1957).
24. Nicholas D. J. D. and Fielding A. H. *J. Hort. Sci.* **26,** 125 (1951).

VOL
4
1958/

International Journal of Applied Radiation and Isotopes, 1959, Vol. 4, pp. 221–226. Pergamon Press Ltd. Printed in Northern Ireland

Micro-Determination of Zinc in Blood and Other Tissues by Neutron Activation Analysis

T. E. BANKS, R. TUPPER, E. M. A. WHITE and A. WORMALL
Departments of Biochemistry and Physics, The Medical College of St. Bartholomew's Hospital, London

(*Received* 17 *July* 1958; *in revised form* 7 *August* 1958)

A method is described for the determination, by radioactivation analysis, of zinc in small amounts of blood and tissues (e.g. 50–100 mg of blood containing 0·3–0·8 μg of zinc). The method gives results in good agreement with those determined by a standard chemical technique. Excellent recoveries of zinc added to blood samples were obtained.

MICRO-DÉTERMINATION DU ZINC DANS LE SANG ET LES AUTRES TISSUS PAR L'ANALYSE NEUTRONACTIVATION

On a décrit une méthode pour la détermination, par l'analyse radioactivation, du zinc dans les quantités petites du sang ou des tissus (par exemple 50–100 mg du sang contenissant 0·3–0·8 μg du zinc). Lá méthode donne les résultats en bon accord avec ceux là déterminé par une classique technique chimique.

Recouvrements excellents étaient obteni du zinc ajouté à echantillons du sang.

МИКРО-ОПРЕДЕЛЕНИЕ ЦИНКА В КРОВИ И РАЗЛИЧНЫХ ТКАНЯХ ПРИ ПОМОЩИ НЕЙТРОННОГО АКТИВАЦИОННОГО АНАЛИЗА

Описывается метод определения цинка в небольших количествах крови и тканей (а именно 50–100 мг крови, содержащей 0,3–0,8 г цинка) при помощи радиоактивационного анализа. Метод дает результаты, находящиеся в хорошем согласии с результатами, полученными при обычном химическом анализе. Количественное определение вводимого в кровь цинка также оказалось весьма удовлетворительным.

MIKROBESTIMMUNG VON ZINK IM BLUT UND ANDEREN GEWEBEN MIT HILFE DER NEUTRONENAKTIVIERUNGSANALYSE

Eine Methode für die Messung von Zink in kleinen Blut-oder Gewebequantitäten (z.B. 50–100 mg Blut mit 0·3–0·8 μg Zink) mittels Radioaktivationsanalyse wird beschrieben. Die Resultate dieser Methode sind in Ubereinstimmung mit denen der üblichen chemischen Technik. Vorzügliche Zurückgewinnung von Blutproben zugefügtem Zink wurde erreicht.

INTRODUCTION

The presence of zinc in living tissues and the essential nature of this element as a nutrient for plants and animals have been recognized for many decades, but the precise role of zinc compounds in metabolism has not been fully elucidated.

It has been established that zinc is a structural component of certain enzymes, for example, carbonic anhydrase,[1] pancreatic carboxypeptidase,[2] alcohol dehydrogenase[3] and a few other dehydrogenases, and it has also been shown that zinc ions can

markedly stimulate some enzymic reactions.

There appears to be no doubt that this element has important biochemical functions, and further information about the nature of the zinc compounds present in living tissues might help to explain these functions. Apart from the zinc in the above mentioned enzymes, there is not much precise information about the nature of the zinc compounds in the tissues of the animal body, though it has been shown by VALLEE *et al.* that the individual leucocytes of human blood contain about twenty-five times as much zinc as do the individual red cells, and about 4/5 of this leucocytic zinc is in the form of a hitherto undescribed zinc protein.[4] Other studies by VALLEE *et al.*[5] have shown that leucocytes from leukaemic subjects contain much less zinc than do normal leucocytes, with a return to a more normal value following successful therapy.

For an investigation of the metabolic role of zinc and the possible significance of deficiencies in zinc compounds, it is essential that methods should be available for the micro-determination of zinc in small amounts of blood, blood fractions and other animal tissues.

Several methods have been described for the measurement of zinc in blood, but most of these methods are not sufficiently sensitive for reliable determinations to be made on very small samples. One chemical method of this type is the dithizone method, involving the formation and separation of a zinc–dithizone complex and this technique has been modified in such a way that reliable results can be obtained with samples containing only a few μg of zinc;[6] usually it is advisable, however, to make determinations on 2 or 3 ml of blood, or a corresponding amount of other tissue, and it is necessary to take special precautions to reduce the "blank" values by using reagents and glassware from which all dissociable zinc has been removed;[7] it is also essential that there should be no contamination from laboratory dust or from contact of the reagents with rubber tubing or with filter paper. The microdetermination of zinc or any other "trace element" thus presents many problems which do not normally arise in biochemical analysis.

The technique of activation analysis is being applied in many biochemical investigations and is proving of great value for the measurement of submicrogram amounts of elements which, when exposed to a neutron flux, are converted into radioactive isotopes which can be separated from, or otherwise measured in the presence of, other radioactive material in the irradiated sample.

For many of our investigations we require to estimate the amount of zinc in very small samples (e.g. 0·10 ml) of blood or leucocyte suspensions, and we therefore decided to examine the possibility of using radioactivation analysis for this purpose. The method described in this paper is based in principle on that described by BOWEN[8] for the determination of manganese in biological material by activation analysis. An excellent bibliography on radioactivation analysis is given by GIBBONS *et al.*[12]

EXPERIMENTAL DETAILS

Materials

(1) *Zinc-free reagents and glassware.* Reagents and glassware were freed from zinc if intended for use in the chemical determination of the metal or in the stages of the radioactivation analysis prior to irradiation of the sample in the pile.

Zinc-free water was prepared by passage through a mixed ion exchange column.

Hydrochloric acid (conc.) and ammonia (S.G. 0·880) were re-distilled in all-Pyrex glass stills. A special sodium acetate buffer pH 5·5 (GETTLER *et al.*[9]) and sodium potassium tartrate solution (20% w/v) were freed from zinc by extraction with a solution of dithizone in carbon tetrachloride.

Glassware and silica crucibles were soaked in 2 N HCl for at least 24 hr. The apparatus was then thoroughly washed with zinc-free water and dried.

Polythene pill packs and sleeves were soaked for 24 hr in conc. HNO_3, thoroughly

washed with zinc-free water and finally dried in a vacuum desiccator.

(2) *Standard zinc solution.* This was prepared by dissolving a weighed amount of "Analar" zinc foil in hydrochloric acid and diluting with water to yield a final solution containing 20 μg Zn/ml.

METHODS

(1) *Chemical determination of zinc.*

The method used for the chemical determination of zinc in blood and tissue samples was a slight modification of that described by VALLEE *et al.*[6] Silica instead of platinum crucibles were used and were found to give satisfactory results. The ashing temperature for samples was reduced from 600°C to 450°C in order to reduce the risk of loss by volatilization of zinc salts.

Determinations were made on samples of blood or tissue weighing about 3 g and usually containing 12–30 μg of zinc, and the results recorded in this paper are the mean values for triplicate determinations. The "blank" values were about 1 μg of zinc.

(2) *Determination of zinc by radioactivation analysis*

Principle. The weighed blood or other tissue samples (e.g. about 0·10 g) are inserted in polythene pill packs and these packs, together with others containing known amounts of zinc of the same order as that present in the biological samples, are dried and exposed to neutron irradiation in an atomic pile. The irradiated pill packs are dissolved in H_2SO_4 and a relatively large amount of carrier zinc is added to the solution, which is then buffered at pH 5·5. At this pH and in the presence of cyanide and thiosulphate, the only metals extracted by dithizone are tin and zinc.[7] The zinc, including the ^{69m}Zn produced during the irradiation of the sample, is quantitatively extracted by dithizone solution and freed from radioactive contaminants. The amount of ^{69m}Zn is then determined by a scintillation counter.

The preparation of samples and standards. BOWEN[8] has described the use of polythene pill packs as containers for samples to be irradiated in the nuclear pile. The pill packs used in our experiments were 18 mm high with an i.d. of 6 mm. The packs were numbered by writing on them with a red-hot needle. The packs were enclosed in polythene envelopes or sleeves made from thin polythene sheeting, to protect them from contamination. After the pill packs had been acid-washed as described above, they were only handled with stainless steel forceps. The pill packs in their sleeves were mounted in holes drilled in wooden blocks, each block holding six packs.

Samples of blood or liver brei were carefully pipetted into weighed pill packs, which were then reweighed. Great care was taken to avoid bubble formation which can cause frothing during the drying stage.

Pill packs containing known amounts (2 or 4 μg) of zinc to act as standards were prepared by pipetting in with a micro-pipette 0·1 or 0·2 ml of the standard zinc solution. Zinc sulphate (20–30 mg) was weighed into an additional pack to serve as a very high standard for calibration of the pulse-height analyser.

Pill packs and contents were dried over conc. sulphuric acid in a vacuum desiccator. The vacuum was increased in stages to avoid frothing in the samples. The packs when dry were closed with small polythene stoppers.

Irradiation. It was found possible to place twelve pill packs in the standard 30 ml irradiation can, the composition of the twelve being as follows: six packs containing dried blood or other tissue, two with 2 μg Zn, one with 4 μg Zn, two empty to act as "blanks" and one containing the large zinc sulphate standard.

The can and contents were irradiated with neutrons for 28 hr in BEPO at the maximum pile factor obtainable, and the can was normally received by us about 6 hr after its removal from the pile.

Separation of zinc from irradiated samples. Owing to the fact that the sodium, potassium and chlorine in the blood samples had become highly radioactive, it was necessary to carry out these separation procedures behind lead screening.

The polythene envelopes were stripped from the pill packs and discarded. The stopper of the pill pack was removed and the pack was dropped into a 100 ml Kjeldahl flask containing conc. sulphuric acid (10 ml) to which had been added about 50 μg of Zn as $ZnCl_2$ to act as "carrier". The top of the stopper was sliced off with a scalpel and the remainder of the stopper was added to the contents of the flask. In this way any material which may have become attached to the inside of the stopper was not lost, but the top, which might have become contaminated, was discarded.

The contents of the pill pack containing the large zinc sulphate standard were washed directly with water into a volumetric flask and the resulting solution made up to a total volume of 50 ml.

The Kjeldahl flasks and contents were heated on an electric rack until the pill packs had dissolved. Nitric acid (conc.) was then added at intervals (0·5–1 ml at a time) until digestion was complete. At this stage the contents of the flasks were straw coloured. The solutions were allowed to cool, a few ml of water were cautiously added to each and the flasks were re-heated to drive off oxides of nitrogen. The flasks were removed from the rack when fumes of sulphur trioxide appeared.

Methyl red solution (1 or 2 drops of a 1% solution in alcohol) was added to the cooled contents of each flask and ammonia (S.G. 0·880) was added cautiously drop by drop until the indicator just turned yellow. The contents of each flask were then transferred to a 150 ml separating funnel containing a mixture of the special acetate buffer pH 5·5 (20 ml), 2% sodium potassium tartrate solution (2 ml) and a solution containing 1% NaCl and 1% KCl (10 ml). (The NaCl and KCl were added as carriers for the radioactive sodium, potassium and chlorine present in the irradiated samples). Although we reported in our earlier investigations,[10] that the extraction of zinc with dithizone from an acid-digested tissue was most satisfactory at pH 8·5–9, we have used in our present investigations extraction at pH 5·5 in the presence of the special acetate buffer advocated by GETTLER *et al*;[9] we have found that under these conditions complete extraction of zinc from the acid-digested blood samples plus pill packs is obtained).

A solution of dithizone (diphenylthiocarbazone) in carbon tetrachloride (100 mg/l.; 4 ml) was added to the separating funnel (A) and compressed air was blown in through a fine jet to agitate the contents. When the dithizone solution had turned red, the agitation was stopped, and the dithizone extract was run into another separating funnel (B) mounted directly below the first funnel (A). This extraction with dithizone solution was repeated until a dithizone layer remained green. The aqueous phase in funnel (A) was then washed with carbon tetrachloride (10 ml) to remove the last traces of dithizone and the washings were added to the pooled dithizone extracts in funnel (B). The aqueous phase in funnel (A) was discarded.

The contents of funnel (B) were washed three times with water (20 ml each time) in in order to remove traces of radioactive elements other than zinc. The aqueous washings were discarded. Hydrochloric acid (2 ml; 2 N) was added to the funnel which was then vigorously shaken for 2 min. The lower (dithizone–CCl_4) layer was run off and the acid extract pipetted into a 5 ml volumetric flask. This extraction of the dithizone solution was repeated with a further 2 ml of HCl. At this stage, the dithizone solution was green, indicating complete transfer of the zinc to the HCl phase. The extracted dithizone solution was discarded and the funnel washed with 2 N HCl (1 ml). This acid washing was added to the pooled acid extracts in the volumetric flask and the solution made up to 5 ml with water. This solution was then ready for measurement of ^{69m}Zn activity. The contents of the flask were transferred to a 10 ml glass dish, the flask was washed with water (1 ml) and the

VOL. 4 1958/59

washings added to the contents of the dish.

Measurement of the ^{69m}Zn. Neutron activation of zinc produces several radioactive isotopes of this element but most of these are short lived and the only one which will contribute a significant amount to the radioactivity of the sample, 10–12 hr after the irradiation, is ^{69m}Zn, an isotope which emits 94 per cent of its radiation as γ-rays with an energy of 0·44 MeV. Measurements of activity were made with the scintillation counter described by BANKS *et al.*[11] In order to avoid counting errors which might be introduced by traces of radioactive isotopes other than ^{69m}Zn, a single channel pulse-height analyser (Type 672, Isotope Developments Ltd.) was included in the circuit.

The optimum bias voltage on the analyser for counting the ^{69m}Zn was determined using as source a solution prepared from the irradiated zinc sulphate sample. Oscillator type power packs were found to be insufficiently stable for use in conjunction with the pulse-height analyser, and a pentode stabilized pack (Panax Ltd. Type P 3000 C) was used.

Since ^{69m}Zn has a short half-life, it was found necessary to limit the period of "counting" the samples and as a general rule the radioactivity of each sample was measured for two periods, with a total count of about 1000 each time. A standard was counted at frequent intervals and a decay curve was constructed to facilitate correction of the counts of the samples. The half-life determined from these curves was invariably in agreement with that recorded for ^{69m}Zn, i.e. 14 hr.

RESULTS AND DISCUSSION

TABLE 1. Micro-determination of zinc in blood

Sample	Zinc content (μg/g blood)	
	Radioactivation analysis	Chemical determination
Rabbit blood	3·15	3·65
	3·35	3·65
	4·2	4·3
	4·25	4·0
Rabbit blood (with added zinc)	13·1	13·0
Human blood	4·7	4·8
	4·2	4·7
	4·6	4·8
	4·7	5·0

The results recorded above are the mean values for duplicate and in some cases triplicate determinations. The blood samples used for the radioactivation analysis weighed 87–313 mg.

The radioactivation method described here has been repeatedly tested on samples of human and rabbit blood, and for comparison the zinc contents of these bloods were also measured by chemical determination; triplicate determinations by the chemical method required about 9 ml of blood, whereas three determinations by radioactivation analysis could be made with as little as 0·25 ml. A representative set of results by the two methods is given in Table 1. In all our experiments radioactivation analysis has given results which are in complete agreement with the values obtained by chemical analysis. Furthermore, small amounts of zinc (0·8–2·0 μg) added as zinc chloride to blood samples (0·15–0·28 g of rabbit blood containing 0·5–1·0 μg of zinc) were estimated with satisfactory results (see Table 2). The mean percentage recovery of this added zinc was $102 \pm 1{\cdot}8$.

This method for the determination of zinc

TABLE 2. Recovery, by radioactivation analysis, of zinc added to blood

Blood sample (mg)	Additional zinc (μg)	
	Added	Found
281	0·78	0·80
148	1·00	1·11
218	1·00	1·02
243	1·50	1·50
207	1·50	1·43
135	2·00	1·95
156	2·00	2·01

in blood and other tissues is sensitive to about 0·04 μg of zinc and a reliable determination can be carried out on 0·10 ml of blood, an amount containing 0·3–0·8 μg of zinc. The amount of zinc in the pill packs used was very small and the "blank" determinations gave values of slightly less than 0·1 μg of zinc.

The method is applicable to other animal tissues. Determinations were made on samples of a brei prepared from the pooled livers of six normal mice, and a mean value of 27·0 $\pm$ 0·6 μg of Zn per gramme of wet tissue was obtained in five determinations by radioactivation analysis (with samples of 50–70 mg); measurements made with much larger samples, and using the chemical method, gave a mean value of 28·4 μg of zinc per gramme of wet tissue.

Acknowledgements—The authors are indebted to Dr. H. J. M. Bowen for much helpful information about polythene pill packs suitable for radioactivation analysis and details about neutron activation. Part of the expenses of this work has been covered by grants from the British Empire Cancer Campaign.

REFERENCES

1. Keilin D. and Mann T. *Biochem. J.* **34,** 1163 (1940).
2. Vallee B. L. and Neurath H. *J. Amer. Chem. Soc.* **76,** 5006 (1954).
3. Vallee B. L. and Hoch F. L. *J. Amer. Chem. Soc.* **77,** 821 (1955).
4. Hoch F. L. and Vallee B. L. *J. Biol. Chem.* **195,** 531 (1952).
5. Vallee B. L. *J. Amer. Med. Ass.* **162,** 1053 (1956).
6. Vallee B. L. and Gibson J. G. *J. Biol. Chem.* **176,** 435 (1948).
7. Malmstrom Bo G. *Methods Biochem. Analysis* **3,** 327 (1956).
8. Bowen H. J. M. *J. Nuclear Energy,* **3,** 18 (1956).
9. Gettler A. O. and Bastian R. *Amer. J. Clin. Path.* **17,** 244 (1947).
10. Banks T. E., Tupper R. L. F., and Wormall A. *Biochem. J.*, **47,** 466 (1950).
11. Banks T. E., Tupper R., Watts R. W. E. and Wormall A. *Biochem. J.* **59,** 149 (1955).
12. Gibbons D., Loveridge B. A. and Millett R. J. A.E.R.E, I/R 2208 (1957).

VOL. 4 1958/5

International Journal of Applied Radiation and Isotopes, 1959, Vol. 4, pp. 227–231. Pergamon Press Ltd. Printed in Northern Ireland

Radio-iodine Counting in Unanesthetized Mice

DAVID L. JOFTES
Cancer Research Institute, New England Deaconess Hospital, Boston, Massachusetts

(*Received* 21 *July* 1958; *in revised form* 15 *August* 1958)

Unanesthetized mice have been immobilized in special holding devices so that direct counting of I^{131} taken up by the thyroid could be accomplished by means of a well collimated scintillation counter. The method was tested by recounting the radiation from the thyroids which were surgically removed *en bloc* with trachea immediately following the counting of the I^{131}-containing thyroids in the intact animals. Extirpated thyroid recounts were begun within 5 min of the end of the *in vivo* counts in every case. The 6 mm collimation aperture excluded nearly all counts originating in the salivary glands or other non-thyroidal tissue. Seventy-three Swiss albino (Rockland All Purpose) male mice were used. Counts were performed within 2–7 hr after injection of 2 μc of I^{131}. The per cent uptakes were calculated against counts from standards prepared from aliquots of the injected I^{131} solution. The mean of the uptakes in the intact mice was 11 per cent $\pm$ 3·7 and the corresponding mean of the extirpated thyroids was 12 per cent $\pm$ 4·6. The difference is statistically insignificant, and therefore the method appears to be very accurate. This high accuracy is attributed to the close correspondence in area between the frontal projection of the thyroid and the cross-section of the collimator aperture when the animal is placed very close to the collimator.

COMPTER LE RADIO-IODE DANS LES SOURIS NON-ANESTHÉSIÉES

Des souris non-anesthésiées ont été immobilisées dans des appareils spéciaux de sorte qu'on a pu compter directement l'I^{131} recueilli par la thyroïde, au moyen d'un compteur à scintillation bien collimé. On a fait épreuve de la méthode en comptant de nouveau la radiation des thyroïdes retirées chirurgiquement en bloc avec trachéa directement après le comptage des thyroïdes contenant I^{131} dans les animaux intacts. Le recomptage des thyroïdes extirpées commençait dans les 5 minutes suivant la fin du comptage *in vivo* en chaque cas. L'ouverture de 6 mm. du collimateur excluait presque toutes les pulsations venant des glandes salivaires et d'autre tissu non-thyroïdien. On employa soixante treize souris mâles, albinos suisses (Lockland All Purpose). On acheva les comptes dans les 2 à 7 heures après l'injection de 2 μc d'I^{131}. Le pour-cent d'absorption fut calculé vis-à-vis les comptes d'étalons préparés d'aliquotes de la solution d'I^{131} injectée. La moyenne d'absorption dans les souris intactes fut 11 pour-cent $\pm$ 3,7 et la moyenne correspondante pour les thyroïdes extirpées fut 12 pour-cent $\pm$ 4,6. La différence est insignifiante statistiquement, donc la méthode parait très précise. Cette précision élevée est attribuée à la correspondance rapprochée en aire entre la projection frontale de la thyroïde et la section transversale de l'ouverture du collimateur lorsque l'animal est situé très près du collimateur.

ОПРЕДЕЛЕНИЕ ВКЛЮЧЕНИЯ РАДИОАКТИВНОГО ИОДА У НЕАНЕСТЕЗИРОВАННЫХ МЫШЕЙ

Для непосредственного определения при помощи счетчика с коллиматорной щелью включения I^{131} щитовидной железой неанестезированные мыши помещались в специальные держатели. Для проверки метода щитовидные железы удалялись одновременно с дыхательными путями и производилось повторное определение включения, непосредственно вслед за определением включения у интактных животных. В каждом случае повторные определения начинались не позже чем через пять минут после окончания счета *in vivo*. Ширина коллиматорной щели в 6 мм почти полностью исключала регистрацию счетчиком радиоактивности слюнных желез и других тканей, не относящихся к щитовидной железе. Для опытов были использованы 73 белых швейцарских мыши

(Роклэнд). Определение включения производилось по истечении от 2-х до 7-ми часов после введения 2 μc I^{131}. Процент включения определялся в зависимости от результатов определения включения эталонными образцами, изготовленными из аликвотных частей вводимого раствора I^{131}. Среднее включение у интактных мышей было 11 $\pm$ 3,7%, а соответствующее среднее включение в удаленных железах было 12 $\pm$ 4,6%. Статистически эта разница не имеет значения и метод можно счтать очень точным. Высокая точность объясняется близким совпадением размеров фронтальной выпуклости щитовидной железы и поперечного сечения коллиматорной щели при приближении счетчика вплотную к подопытному животному.

RADIOJOD-MESSUNG BEI UNANÄSTHESIERTEN MÄUSEN

Nicht anästhesierte Mäuse wurden in einer Spezialhalterung fixiert, sodass die Messung des durch die Schilddrüse aufgenommenen J^{131} mit Hilfe eines gut kollimierten Szintillationszählers auf direktem Wege vorgenommen werden konnte. Die Methode wurde überprüft durch Messung der Strahlung von Schilddrüssen, welche en bloc zusammen mit der Trachea, unmittelbar nach Messung des J^{131} am lebenden Tier, chirutgisch entfernt worden war. Die Wiederholung der Messung an der exstirpierten Schilddrüse wurden in allen Fällen 5 Minuten nach Beendigung der in vivo Messung durchgeführt. Die Apertur des Kollimators betrug 6 mm und verhinderte die Mitregistrierung von Strahlung aus den Speicheldrüsen und anderen Nicht-Schilddrüsen-gewebe fast vollständig. 73 schweizer Albino Männchen (Rockland All Purpose) wurden verwendet. Die Messungen wurden zwischen 2 bis 7 Stunden nach der Injektion von 2 μC J^{131} durch geführt. Die perzentuelle Aufnahme wurde berechnet aus den Messwerten von Standards, welche aus aliquoten Mengen der injizierten J^{131} Lösung hergestellt wurden. Die Aufnahme, gemessen an intakten Mäusen, betrug im Mittel 11 $\pm$ 3,7%, der entsprechende Mittelwert der exstirpierten Drüsen war 12 $\pm$ 4,6%. Der Unterschied liegt innerhalb des statistischen Fehlers, weshalb die Methode sehr genau erscheint. Diese Genauigkeit wird der guten flächenmässigen Übereinstimmung zwischen Frontalprojektion der Schilddrüse und dem Querschnitt der Kollimatorapertur zugeschrieben, die sich ergibt, wenn das Tier sehr nahe an den Kollimator herangebracht werden kann.

VOL.
4
1958/5

INTRODUCTION

Determination of radio-iodine uptake by the thyroid involves some method of accounting for, or eliminating the radiation which reaches the counter from the non-thyroidal radio-iodine. For humans the usual method is to subtract from the thyroid count a count obtained in the leg or thigh.[1] In small animals it is not possible to find an area comparable to the neck such as the leg or thigh, so that other expedients such as recounting after thyroidectomy or establishing the ratio of the counts from the thyroidectomized neck to some other structure[2,3] have been used. Other workers[4] have waited until the count of non-thyroidal radio-iodine has dropped to negligible levels. At best, all of these procedures add extra steps to the determination and at worst they are inaccurate.

In the mouse the problem is compounded by the very small (approximately 3 mg) thyroid and the proximity of iodide-concentrating salivary gland tissue.[5] The small size of the gland demands a much smaller tracer dose (lest undesirable radiation damage be done) which in turn requires a detector of great sensitivity. Separation of the counts originating in the salivary tissue from those in the thyroid demands careful collimation and positioning of the animal with respect to the counter.

The scintillation counter is sensitive enough to make possible the use of a very small aperture in the collimator and still obtain an accurate count in a practical counting time. Thus great sensitivity and the means of separating the thyroid iodine counts from non-thyroid iodine counts are available.

MATERIALS AND METHODS

A scintillation detector with a thallium activated NaI crystal 0·5 in. in diameter and 1 in. long was used. Since it was estimated that the longest diagonal of the frontal projection of the mouse thyroid was just under 6 mm, the collimator aperture was

made 6 mm in diameter. The collimator was made of lead 5 cm thick and the aperture was machined to be concentric with the sensitive crystal. Adding a 2·5 cm thick cylinder of lead extending from 2·5 cm in front of the crystal to 18 cm behind it reduced the background from a rated 120 counts/min to 35–45 counts/min. With this background, a statistical error of counting of less than 3 per cent was attained by counting 2048 counts.[6] The arrangement yielded approximately 1000 counts/min/1 μc of I^{131}.

The tracer dose selected was 2 μc which was taken as a compromise between a true tracer dose of perhaps 0·1–0·25 μc and the practical requirement of a dose large enough to be counted in a reasonable length of time. It is thought that the 2 μc dose did not cause any damage or detectable change during the 7 hr period of interest.

Identical doses of 2 μc of carrier-free I^{131} in 0·2 ml were administered intraperitoneally by means of a B–D Cornwall syringe and Metal Pipetting Holder. The same dose was delivered into a standard holder, which was made by drilling a 0·25 in. hole through 0·25 in. thick Plexiglas and cementing a 1/16 in. thick Plexiglas sheet on the bottom. Creation of a mouse thyroid phantom was not attempted since all that was required was a reproducible reference standard of an aliquot dose which would permit calculation of comparable per cent uptakes. It is possible that the uptake figures may contain an error, but the error is constant and therefore negligible, at least for this purpose.

Seventy-three male Rockland All Purpose albino mice were used. Before being injected the mice were kept 7–10 days on a diet supplying 3–9 μg of iodine per day. This intake is adequate but does not load the thyroid with iodine. The mice were 7–8 weeks old and weighed between 19 and 21 g when used.

In order to avoid the use of anesthetics[7] the mice were confined in Plexiglas chambers such as the one shown in Fig. 1. The bottom of the chamber is 1/16 in. thick, as is the bottom of the standard holder. The mouse was induced to enter the chamber A. The

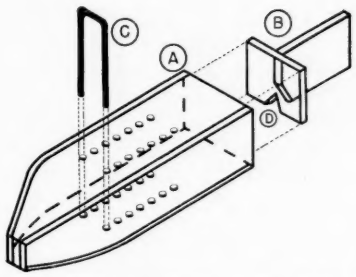

FIG. 1. Immobilization chamber. Description in text.

"plunger" B was used to press the mouse gently to the end of the chamber. The U-shaped bar C was then dropped through the holes of the chamber behind the front plate D to hold it in place. The notch at the bottom of the plate of the plunger accommodates the tail. Once the mouse is in position and the bar is dropped behind the plunger, the mouse is relatively immobile. It was found that the animals did not resent being compressed in these chambers as long as they were allowed enough space to breathe. The chambers are fairly comfortable, for in experiments during which mice were placed in these holders thirty times in thirty hours, most animals entered them voluntarily after the first few trials. Several sizes of chambers were used to accomodate mice of different sizes.

When the animal had been confined in the chamber, he was positioned so that his thyroid was over the aperture in the collimator (Fig. 2) and the chamber was shifted about until the maximum counting rate was observed. The animal was separated from the top of the collimator only by two layers of Plexiglas totaling 1/8 in. in thickness. Two counts were taken in every case. In order to check the accuracy of the *in vivo* count, the animals were immediately sacrificed and the thyroids extirpated *en bloc* with a section of trachea and placed upon a slip of Plexiglas of the same thickness as the bottom of the mouse holder. The extirpated thyroids were also counted twice, always within 5 min of the time the counts of the intact animal were taken. The intact mice were counted at intervals varying from 2 to 7 hr after injection of the radio-iodine. Uptakes were calculated

as the percentage of the standard for both the intact and extirpated thyroid of each animal. No correction for extrathyroidal radio-iodine was made in the counts of the intact animals.

It was observed that the intact mice held their heads above the bottom of the holders, so that the thyroid rested at approximately 56–57 mm above the sensitive crystal, whereas the extirpated thyroids rested at 54 mm above it. The influence of this positional difference was investigated by placing a standard at each of these positions and obtaining the counts.

RESULTS

Fig. 3 shows the frequency distributions of the per cent uptakes of both the intact and the extirpated thyroids. The mean uptake calculated for the intact thyroids was 11 per cent $\pm$ 3·7 (standard deviation) and the mean uptake of the extirpated thyroids was 12 per cent $\pm$ 4·6. The extirpated thyroid mean is one percentage point but relatively 9 per cent (1/11) higher than the mean of the intact mice.

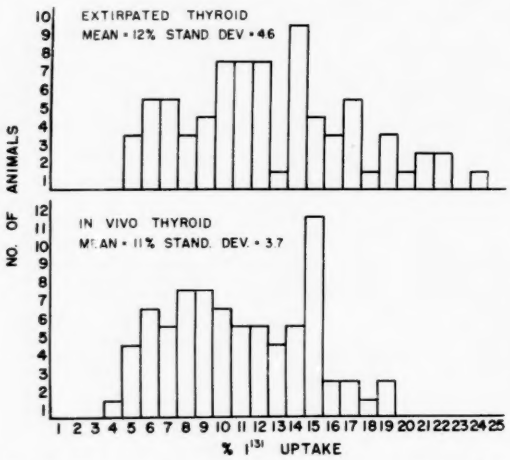

FIG. 3. Frequency distribution curves of per cent uptakes of I^{131} by intact and extirpated thyroids.

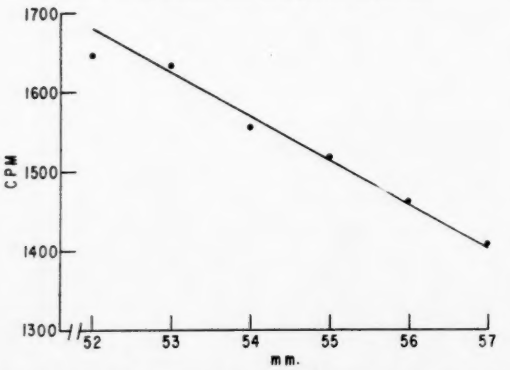

FIG. 4. Effect of increasing distance between thyroid and scintillation crystal. Each point represents the mean of thirty determinations.

Fig. 4 shows the effect of increasing the distance between the radioactive source and the crystal. Each point represents the mean of thirty determinations with the same standard. The count at 54 mm was used as the base, and the percentages of the difference between it and the counts at 56 and 57 mm were found to be 6 per cent and 9 per cent respectively. Thus it can be seen that the 9 per cent relative difference in the counts was due to the positional difference.

Discussion and conclusions

The data show that the apparent difference between the intact and extirpated thyroid uptakes was actually due to the slight difference in geometry which occurred in the two parts of the experiment. Furthermore the observed difference was found to be statistically insignificant when tested by the formula for the significance of differences of means. The accuracy of the method is attributed to the close correspondence in area between the frontal projection of the thyroid and the cross-section of the collimator aperture, which results in the exclusion of most counts originating in extrathyroidal tissue when the animal is placed close to the end of the collimator.

Whether this method would work as well in a larger animal is open to question. Presumably a larger thyroid would require a larger aperture, which would survey a larger volume of extrathyroidal tissue with a consequent increase in the number of extrathyroidal counts picked up. Some extrathyroidal radio-iodine counts were no doubt picked up with the mice, too, but apparently

VOL.
4
58/59

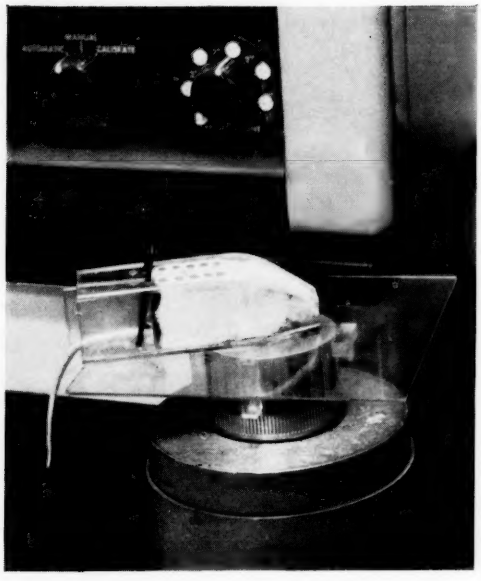

FIG. 2. Mouse immobilized in chamber and positioned over collimator on scintillation probe. Chamber rests on Plexiglas table which provides stability and prevents contamination of probe by excreta.

VOL.
4
1958/5

not enough to influence the determination of the uptake. For practical purposes then, this method permits determination of thyroid I^{131} uptakes in mice to an accuracy limited almost exclusively by the statistical error of counting.

Summary

Unanesthetized mice have been immobilized in special holding devices so that direct counting of I^{131} taken up by the thyroid could be accomplished by means of a well collimated scintillation counter. The method was tested by recounting the thyroids which were surgically removed *en bloc* with trachea immediately following the counting of the thyroid in the intact animal. No significant statistical difference was found between the means of the intact animal and extirpated thyroid counts, which were 11 per cent and 12 per cent respectively. The accuracy of the method is attributed to the close correspondence in area between the frontal projection of the thyroid and the cross-section of the collimator aperture.

Acknowledgements—The author gratefully acknowledges the technical assistance of LAURA MERRILL DONNENWIRTH.

This investigation was supported by the United States Atomic Energy Commission contract No. AT(30–1)–901 with the New England Deaconess Hospital.

REFERENCES

1. BURNS F. J., FISH W. A., HACKETT J. W. and HICKEY F. C. *J. Appl. Physiol.* **4,** 15 (1951).
2. STEVENS C. E. and D'ANGELO S. A. *Proc. Soc. Exp. Biol.* **85,** 633 (1954).
3. FREDRICKSON D. S., GANONG W. F. and HUME D. M. *Proc. Soc. Exp. Biol.* **89,** 416 (1955).
4. NYGAARD O. and ELDJARN L. *Arch. Int. Physiol.* **62,** 528 (1954).
5. LOGOTHETOPOULOS J. H. and MYANT N. B. *J. Physiol.* **134,** 189 (1956).
6. LOEVINGER R. and BERMAN M. *Nucleonics* **9,** 26 (1951).
7. WASE A. W., REPPLINGER E. and FOSTER W. C. *Endocrinology* **53,** 630 (1953).

International Journal of Applied Radiation and Isotopes, 1959, Vol. 4, pp. 232–248. Pergamon Press Ltd. Printed in Northern Ireland

The Standardization of Radioisotopes by the Beta–Gamma Coincidence Method Using High Efficiency Detectors

P. J. CAMPION
Nuclear Physics Branch Atomic Energy of Canada, Limited

(*Received* 3 *March* 1958; *in revised form* 18 *June* 1958)

VOL.
4
1958/5

In Part I of this paper the corrections pertaining to absolute disintegration rate determinations by the $4\pi\beta$–γ coincidence method are discussed. It is demonstrated that because of the high efficiency of the 4π detector most corrections are small. In general, the largest corrections, apart from background, are those due to the accidental coincidence rate and dead time losses, expressions for which are derived. In Part II a $4\pi\beta$–γ coincidence apparatus which was developed in this laboratory is described. An account of the performance of this instrument is given, together with the experimental verification of the accidental coincidence rate and dead time corrections discussed in Part I. The performance suggests that accuracies of the order 0·1 per cent are now feasible.

СТАНДАРТИЗАЦИЯ РАДИОИЗОТОПОВ МЕТОДОМ БЕТА-ГАММА СОВПАДЕНИЯ, ДЕТЕКТОРАМИ ВЫСОКОЙ ЧУВСТВИТЕЛЬНОСТИ

В первой части этой статьи обсуждаются поправки, относящиеся к определению абсолютных скоростей распада методом совпадений $4\pi\beta$–γ. Показано, что благодаря высокой эффективности детектора 4π поправки большей частью малы. Вообще говоря, наибольшие поправки, не считая фона, обусловлены скоростью случайных совпадений и потерями на мертвое время. Выведены уравнения для таких поправок. Во второй части рассматривается счетчик совпадений $4\pi\beta$–γ, разработанный в данной лаборатории. Даны описание работы этого счетчика и экспериментальная проверка поправок на скорость случайных столкновений и мертвое время, которые рассматривались в части I. Работа счетчика свидетельствует о возможности достижения точности до 0,1%.

INTRODUCTION

The technique of β–γ coincidence counting as an absolute method of standardization is well known and has been reviewed by several authors.[2,5,17] The characteristic advantage of the coincidence method lies in the fact that the result is, in principle, independent of the efficiency of either detector. Thus the fundamental problem of $4\pi\beta$ counting, namely the self absorption correction, is avoided. However, this merit is often outweighed by the uncertainties in several corrections which must be applied before

the true disintegration rate can be determined. The purpose here is to point out the advantages to be gained by the use of the coincidence method when the β-detector has 4π geometry. It will be shown (Part I) that under these conditions most corrections are small and hence the error introduced by these corrections must also be very small. The use of the coincidence method using 4π geometry is illustrated in Part II by reference to a $4\pi\beta$–γ coincidence unit which was developed in this laboratory. This unit is described and details of its performance are given.

In this paper the following general notation will be adopted: N_0 is the absolute disintegration rate of the source under study, while N_β, N_γ, and N_c are the observed counting rates less background and accidental coincidences in the β-, γ- and coincidence channels respectively. The overall efficiencies of the β- and γ-detectors are ε_β and ε_γ; these efficiencies include all factors leading to an observed counting rate less than N_0 except those due to dead time losses and due to an emission probability different from one per disintegration, unless otherwise stated.

PART I

In this part the various corrections which may apply to $4\pi\beta$–γ coincidence counting will be considered. Since decay schemes differ so widely no attempt is made here to derive a universal set of "coincidence equations" which can be applied to any isotope. Instead the form of the correction is indicated and it is left to the reader to set up the equations with the appropriate corrections for any particular isotope.

Finite source size

In discussing the applicability of the coincidence method for the measurement of extended sources PUTMAN[16] has shown that the method is valid provided that either the β-detector or the γ-detector is equally sensitive to all parts of the source. The absolute disintegration rate is given by PUTMAN as

$$N_0 = \frac{N_\beta N_\gamma}{N_c}\left[\frac{\overline{\varepsilon_\beta \varepsilon_\gamma}}{\bar{\varepsilon}_\beta \bar{\varepsilon}_\gamma}\right]$$

where $\overline{\varepsilon_\beta \varepsilon_\gamma}$ is the mean of the product of the β- and γ-detector efficiencies integrated over the extension of the source while $\bar{\varepsilon}_\beta$, $\bar{\varepsilon}_\gamma$ are the means of the individual efficiencies. The last two quantities are identically equal to ε_β, ε_γ respectively, as defined above. If either of the detectors is equally sensitive to all parts of the source the ratio in the square brackets reduces to unity. Clearly this is the case when the β-detector is 100 per cent efficient. The possibility remains, however, that the ratio may differ appreciably from unity for β-detector efficiencies of less than 100 per cent.

A simple order of magnitude estimate of this correction may be made as follows: The source is assumed to be a disc deposit of radius R and to possess radial symmetry. The activity per unit area, ρ, of any point on the source is assumed to be a function of the radius r such that

$$\rho = ar^n$$

where a and n are constants. Such a variation of activity is extreme but is not completely unreasonable since the usual technique for source preparation by the evaporation of an aliquot of active solution tends to produce a "ring" source unless a spreading agent is added to make the deposit more even. A more realistic distribution may be of the form $\rho = ar^n + \text{constant}$, but since the β-efficiency is determined primarily by self absorption such a distribution would tend to make this efficiency more uniform across the source and hence reduce the correction. The variation of the efficiency of a $4\pi\beta$ detector with respect to the position of a point source has been shown to be small[6,12] (see also Part II). Let the β-efficiency with respect to any point on an

extended source be e_β and suppose for sake of argument that it may be written*

$$e_\beta = e_{\beta 0}(1 - br^m)$$

where b and m are constants and $e_{\beta 0} = 1{\cdot}0$, since $\rho = 0$ at $r = 0$ for the distribution assumed. The average β-efficiency integrated over the area of the source is therefore

$$\epsilon_\beta = e_{\beta 0}\left[1 - \frac{R^m b(n+2)}{m+n+2}\right]$$

For spectra whose maximum β-ray energy is below about 0·3 MeV self absorption effects become appreciable and losses up to 10 or even 15 per cent may occur.[10,18] Hence, in extreme cases we have

$$R^m b\left(\frac{n+2}{m+n+2}\right) = 0{\cdot}15$$

Similarly, let the γ-efficiency with respect to any point on the source be e_γ, such that

$$e_\gamma = e_{\gamma 0}(1 - cr^p)$$

where c, p, and $e_{\gamma 0}$ are further constants. In contrast to the previous case this efficiency is determined primarily by the geometry since the self absorption of the source for γ-rays is negligible. The variation of this efficiency for a particular instrument is shown in Part II to be about 0·5 per cent. Let us assume that at the worst $cR^p = 0{\cdot}01$.

Using these premises:

$$\frac{\overline{e_\beta e_\gamma}}{\bar{e}_\beta \bar{e}_\gamma} \simeq 1 + \frac{bcR^{m+p}}{A} \times \left\{\frac{n+2}{m+n+p+2} - \frac{(n+2)^2}{(m+n+2)(p+n+2)}\right\} \quad (1)$$

where

$$A = \left\{1 - \frac{b(n+2)}{(m+n+2)} R^m - \frac{c(n+2)}{(p+n+2)} R^p\right\}$$

and if we assume linear variations, i.e. $n = m = p = 1$, the correction amounts to 9×10^{-3} per cent for the extreme case cited. Further, any other reasonable choice for n, m, and p alters this by less than an order of magnitude. It is concluded, therefore, that one is justified in neglecting this correction at least for instruments similar to that described in Part II.

The stability of counting systems

The coincidence method can also be shown to be valid for fluctuating detector efficiencies if one or other detector is stable over the period of measurement. The proof of this is analogous to that used by Putman[16] except that the variable parameter, distance, is replaced by that of time.

It has been demonstrated that a correctly operated gas-flow proportional counter is a very stable device[6,11,12] and hence the coincidence method is valid without correction for instruments which employ at least one of these detectors irrespective as to whether the efficiency of the other detector is constant or not. The gain of a scintillation detector is more susceptible to change, and hence, for those coincidence arrangements which rely on these detectors entirely, such fluctuations may be important. However, simple considerations show that quite large fluctuations can be tolerated.

Beta–gamma angular correlation

For β-detector efficiencies of 100 per cent there is obviously no correction required for any angular correlation between the β-particle and γ-ray. For those cases in which the β-detector efficiency is less than 100 per cent two cases obtain. It has been already noted that evaporated sources generally consist of local aggregates.[14] If these approximate to spheres and are well separated from

* The evaporation of an aliquot yields deposits of local aggregates[14] the average size of which is roughly constant over the source but the number per unit area increases towards the circumference. If the specific activity is such that these aggregates are well separated the variation of β-efficiency with radius is questionable. If on the other hand the aggregates overlap appreciably then some variation of efficiency with radius might be expected.

VOL. 4 1958/5

each other one can assume that any self absorption will be isotropic and hence no correction is required even for efficiencies of less than 100 per cent. For aggregates which have considerable extension in one direction it is possible that a correction may be necessary. Since source deposits vary so greatly it is not very meaningful to attempt to evaluate such a correction. However, it should be noted that an angular correlation can be expected only for first and higher order forbidden β-transitions and that its magnitude is dependent on the actual energy of the β-particle, the asymmetry being weaker for lower energies. Since the correction to the coincidence method due to this phenomenon arises from the absorption of the lower energy β-particles the pertinent angular correlation will be small.

Internal conversion of the gamma-ray

If the internal conversion process follows the β-decay in a time short compared with the dead time of the β-channel the conversion electrons add nothing to the counting rate unless the β-detector efficiency is less than 100 per cent. In this case a correction must be applied to take into account those conversion electrons which produce a signal in the β-detector when the associated β-ray was not observed. Omitting dead time corrections, which are discussed later, we have

$$N_\beta = N_0\left[\varepsilon_\beta + \frac{\alpha(1-\varepsilon_\beta)}{1+\alpha}\,\varepsilon_{ce}\right]$$

and hence

$$\frac{N_\beta N_\gamma}{N_c} = N_0\left[1 + \frac{\alpha(1-\varepsilon_\beta)\varepsilon_{ce}}{\varepsilon_\beta(1+\alpha)}\right] \qquad (2)$$

where α is the total internal conversion coefficient and ε_{ce} is the probability for detecting the conversion electron in the β-counter. Since these electrons are monoenergetic ε_{ce} is generally indistinguishable from unity. However, the usually small value of α together with the $(1-\varepsilon_\beta)$ term reduce the correction to a very small value.

Gamma-sensitivity of the beta-detector and gamma–gamma coincidences

For those isotopes which have a single γ-ray transition following β-decay the correction has the simple form

$$\frac{N_\beta N_\gamma}{N_c} = N_0\left[1 + \frac{(1-\varepsilon_\beta)}{\varepsilon_\beta}\,(\varepsilon_\beta)_\gamma\right] \qquad (3)$$

where $(\varepsilon_\beta)_\gamma$ is the sensitivity of the β-detector for counting the γ-ray of the isotope under study and provided that the process giving rise to a signal in the β-detector cannot produce a coincidence signal. If, on the other hand, such coincidences can occur, or if a second γ-ray is present in the spectrum, the equation becomes

$$\frac{N_\beta N_\gamma}{N_c} \simeq N_0\left[1 + \left(\frac{1-\varepsilon_\beta}{\varepsilon_\beta}\right)\{(\varepsilon_\beta)_\gamma - \varepsilon_e/\varepsilon_\gamma\}\right], \qquad (4)$$

where ε_e is the probability that a coincidence will be observed when the β-particle is undetected. The γ-efficiency in this case may include contributions from the two (or more) γ-rays in cascade. The quantities $(\varepsilon_\beta)_\gamma$ and ε_e are dependent on the experimental conditions and should, in principle, be determined for each nuclide if the correction is to be made. In Part II some values for $(\varepsilon_\beta)_\gamma$ and ε_e are given for a particular $4\pi\beta$–γ instrument and they serve to show that in most practical cases the correction can be neglected.

The beta-sensitivity of the gamma-detector and bremsstrahlung effects

The wall of the $4\pi\beta$-detector and that of the γ-detector are in general sufficiently thick to prevent β-particles entering the latter. It is however possible that the lower bias of the pulse-height analyser is set at a sufficiently small value to allow the detection of bremsstrahlung quanta in the γ-counter. Let N be the emission rate of β-particles having energy E, and e_β the β-detector efficiency for these particles. The counting

rates in the three channels are thus:

$$N_\beta = \int_0^{E_{\max}} N e_\beta dE$$

$$N_\gamma = \varepsilon_\gamma \int_0^{E_{\max}} N\,dE + (1 - \varepsilon_\gamma) \int_0^{E_{\max}} N e_\gamma' dE$$

$$N_c = \varepsilon_\gamma \int_0^{E_{\max}} N e_\beta\,dE + (1 - \varepsilon_\gamma) \times \int_0^{E_{\max}} N e_\beta e_\gamma' dE$$

where for simplicity e_γ' is the probability that a particle of energy E will emit a quantum which is subsequently detected. Since the bremsstrahlung effect is small, we find

$$\frac{N_\beta N_\gamma}{N_c} \simeq N_0 \left[1 - \frac{(1 - \varepsilon_\gamma)}{\varepsilon_\gamma} \times \left\{ \left(\int_0^{E_{\max}} N e_\beta \varepsilon_\gamma' dE \right) \Big/ \left(\int_0^{E_{\max}} N e_\beta\,dE \right) - \left(\int_0^{E_{\max}} N e_\gamma' dE \right) \Big/ \left(\int_0^{E_{\max}} N\,dE \right) \right\} \right] \quad (5)$$

Let the lower energy limit for detection in the γ-channel be E_1. Since the bremsstrahlung intensity decreases rapidly with increasing energy the position of any upper limit is unimportant unless a narrow energy range is used. Equation (5) can thus be rewritten with the integrals in the numerators evaluated between energies E_1 and $E_{\max}$. If now E_1 is such that all β-particles of this energy and greater (which are the only ones contributing to the bremsstrahlung counting rate in the γ-detector) are detected with 100 per cent efficiency then equation (5) reduces to

$$\frac{N_\beta N_\gamma}{N_c} = N_0 \left[1 - \frac{(1 - \varepsilon_\gamma) N_{\gamma B}}{\varepsilon_\gamma N_\beta N_0} \times \left\{ \int_0^{E_1} N\,dE - \int_0^{E_1} N e_\beta\,dE \right\} \right]$$

$$= N_0 \left[1 - \frac{(1 - \varepsilon_\gamma)(1 - \varepsilon_\beta) N_{\gamma B}}{\varepsilon_\gamma \varepsilon_\beta N_0} \right] \quad (6)$$

where $N_{\gamma B}$ is the bremsstrahlung counting rate in the γ-channel. The quantity $N_{\gamma B}/N_0$ may be calculated from external bremsstrahlung theory and the response probability of the γ-detector, or found experimentally using pure β-emitters. As an example the value of $N_{\gamma B}/N_0$ for bremsstrahlung quanta from a P^{32} source was found to be 2×10^{-3} above 100 keV and 6×10^{-5} above 500 keV for the apparatus described later. However, for the large maximum β-transition energy of P^{32}, ε_β is expected to be close to unity, while for lower transition energies the value of $N_{\gamma B}/N_0$, for the same energy ranges in the γ-channel, is greatly reduced, and hence the correction may be neglected in most cases.

Complex decay schemes

PUTMAN[15] has shown that the coincidence method is valid for isotopes having several β-branches if the efficiency of either the β- or γ-detector is the same for all branches. The use of 4π geometry is the obvious approach to this condition and the magnitude of the correction involved may be found by considering the following hypothetical case. Suppose an isotope decays by two β-branches of fractional intensity a and b, such that $a + b = 1$. Let the efficiency of the β-detector for each branch be $\varepsilon_{\beta a}$ and $\varepsilon_{\beta b}$ respectively, and similarly the efficiency of the γ-detector be $\varepsilon_{\gamma a}$ and $\varepsilon_{\gamma b}$. These γ-efficiencies may include the contributions from several γ-rays in each branch. The expression is thus:

$$\frac{N_\beta N_\gamma}{N_c} = N_0 \left\{ 1 - \frac{ab(\varepsilon_{\beta a} - \varepsilon_{\beta b})(\varepsilon_{\gamma a} - \varepsilon_{\gamma b})}{a\varepsilon_{\beta a}\varepsilon_{\gamma a} + b\varepsilon_{\beta b}\varepsilon_{\gamma b}} \right\} \quad (7)$$

The correction is zero[15] if $\varepsilon_{\beta a} = \varepsilon_{\beta b}$ or $\varepsilon_{\gamma a} = \varepsilon_{\gamma b}$. If any of the γ-rays are internally converted the correction is zero for the first condition only. The efficiency of the β-detector is mainly determined by absorption in the source and mount, that in the mount being small if thin films are used. A most unfavourable case may involve losses of 10–15 per cent in one branch only.

In view of the small variation[22] in the efficiencies of NaI crystals over the range of

VOL. 4 1958/5

γ-ray energies usually involved, ε_γ may lie between 10 and 20 per cent for the instrument described in Part II. Finally the maximum value of ab is 0·25 for $a = b = 0{\cdot}5$. Using these extreme values the correction is about 2·7 per cent. In practical examples it is usually less than one-tenth of this and can be ignored. The most pessimistic values for the corresponding efficiencies in the case of Au^{198} lead to a correction of 0·01 per cent. Thus, the serious restriction of the beta–gamma coincidence method to simple decay schemes is largely removed by the use of 4π geometry in the β-detector. With the present apparatus sources of such complexity as U^{237}, Rh^{106} and I^{131} have been standardized.

The accidental coincidence rate

Owing to the finite resolving time of the mixer it is always possible to obtain a coincidence pulse from two unrelated events unless both detectors are 100 per cent efficient. An expression for this accidental rate may be derived as follows: It is assumed that the background rates are negligible, which is well justified for those instances in which the accidental rate is important. Let the probabilities of detection due to dead time losses be p_β and p_γ for the two channels respectively. The probability for the β-counter to detect a disintegration when the associated γ-ray is not recorded in the γ-detector is $p_\beta\varepsilon_\gamma \times (1 - p_\gamma\varepsilon_\gamma)$. The probability that a second disintegration will occur and be recorded in the γ-detector (the β-channel being dead due to the previous disintegration) within τ_R, the resolving time of the mixer unit, is $N_0\tau_R p_\gamma\varepsilon_\gamma$. Hence, the accidental rate due to this type of event is

$$\tau_R N_0^2 p_\beta p_\gamma \varepsilon_\beta \varepsilon_\gamma (1 - p_\gamma\varepsilon_\gamma)$$

A similar expression obtains for the type of accidental coincidence in which the first disintegration is recorded in the γ-detector and the second in the β-detector. Thus the total random rate N_{Acc} is given by the sum of these two rates.

$$\begin{aligned} N_{\text{Acc}} &= \tau_R N_0^2 p_\beta p_\gamma \varepsilon_\beta \varepsilon_\gamma (2 - p_\beta\varepsilon_\beta - p_\gamma\varepsilon_\gamma) \\ &\simeq \tau_R N_0^2 \varepsilon_\beta \varepsilon_\gamma (2 - \varepsilon_\beta - \varepsilon_\gamma) \end{aligned} \qquad (8)$$

if dead time corrections can be neglected. Equation (8) can be readily transformed into an expression involving observed quantities only, giving for the true coincidence counting rate*

$$N_c = \frac{N_c' - 2\tau_R N_\beta N_\gamma}{1 - \tau_R(N_\beta + N_\gamma)} \qquad (9)$$

where N_c' is the observed coincidence counting rate including accidentals.

Although expression (9) is obtained from equation (8) in the derivation of which the background rates were assumed to be negligible it can be shown that equation (9) is quite general, as follows: Consider a decay scheme of any degree of complexity. Let the observed counting rates, including backgrounds, be N_β', N_γ', and N_c'. The counting rate in, say, the β-channel of those pulses for which no true coincident pulse was recorded in the γ-channel is just $(N_\beta' - N_c)$. Thus the accidental rate due to this type of event is $(N_\beta' - N_c)N_\gamma'\tau_R$. A similar expression obtains for the type of event in which the roles of the two channels are reversed. Hence the total accidental coincidence rate is

$$\begin{aligned} N_{\text{Acc}} = N_c' - N_c = \tau_R N_\gamma'(N_\beta' - N_c) \\ + \tau_R N_\beta' (N_\gamma' - N_c) \end{aligned}$$

whence

$$N_c = \frac{N_c' - 2\tau_R N_\beta' N_\gamma'}{1 - \tau_R(N_\beta' + N_\gamma')}$$

which is the form of equation (9). This is seen to be independent of the complexity of the decay scheme or the magnitude of the background rates. It should be noted that this expression takes no account of a genuine but unwanted background rate in the coincidence channel which must be subtracted in the usual manner.

These expressions for the accidental coincidence rate corrections, although derived from a rather different approach, are essentially the same as that given by WESTCOTT *et al.*[21]

The efficiency ε_β for the instrument described below normally lies between 90–100 per cent depending upon the isotope and its specific activity while ε_γ is about 10 per cent and depends upon the isotope and the

* The author is grateful to MR. J. G. V. TAYLOR for first pointing out this form of the correction.

energy response of the γ-channel. Hence, for a disintegration rate of 10^4 disintegrations/sec and a resolving time $\tau_R = 7 \times 10^{-7}$ sec, the accidental coincidence rate is less than 0·7 per cent of the true coincidences.

The dead time and background corrections

We shall assume that the dead times of both channels are the same, non-extendable, and equal to τ and that there is no dead time associated with the coincidence channel greater than τ. Further, the source strength is assumed to be such that the probability of two disintegrations occurring within a time τ can be neglected compared with the probability of occurrence of one disintegration, i.e. $(N_0\tau)^2$ is very much less than $N_0\tau$.

The probability of no disintegration occurring in an interval τ is thus $(1 - N_0\tau)$. The detection efficiency in the β-channel, for example, is therefore:

$$\varepsilon_\beta[(1 - N_0\tau) + N_0\tau(1 - \varepsilon_\beta)]$$

where the first term in the square brackets expresses the chance that there was no disintegration in the preceding interval τ while the second term is the chance that there was a disintegration in this interval but that it was undetected owing to the inefficiency of the β-counter. After simplification the observed counting rate becomes:

$$N_\beta = N_0\varepsilon_\beta(1 - N_0\varepsilon_\beta\tau) \qquad (10)$$

Within the limits of the initial assumption this correction is the same as that generally adopted (see for example PUTMAN[17]).

The argument may be extended to the coincidence channel. If a distintegration, occurring within a time τ prior to one which would normally result in a coincidence count, is registered in either detector the coincidence channel will be blocked for the second disintegration. Hence we find for the detection efficiency

$$\varepsilon_\beta\varepsilon_\gamma[(1 - N_0\tau) + N_0\tau(1 - \varepsilon_\beta)(1 - \varepsilon_\gamma)] \quad (11)$$

The second term in square brackets is the chance that a disintegration did occur in the interval τ before a further disintegration but was not registered by either detector.

Adopting an equation similar to (10) for the γ-channel and rewriting expression (11) we have the following equations:

$$\begin{aligned} N_\beta &= N_0\varepsilon_\beta(1 - N_0\varepsilon_\beta\tau) \\ N_\gamma &= N_0\varepsilon_\gamma(1 - N_0\varepsilon_\gamma\tau) \\ N_c &= \\ &\quad N_0\varepsilon_\beta\varepsilon_\gamma[1 - \{1 - (1 - \varepsilon_\beta)(1 - \varepsilon_\gamma)\}N_0\tau] \end{aligned} \qquad (12)$$

and therefore

$$\frac{N_\beta N_\gamma}{N_c} = N_0\left[1 - \frac{N_0\tau\varepsilon_\beta\varepsilon_\gamma(1 - N_0\tau)}{1 - N_0\tau(\varepsilon_\beta + \varepsilon_\gamma - \varepsilon_\beta\varepsilon_\gamma)}\right]$$

which, since $N_0\tau \ll 1$, reduces to

$$\frac{N_\beta N_\gamma}{N_c} = N_0[1 - N_0\tau\varepsilon_\beta\varepsilon_\gamma] \qquad (13)$$

A simple extension of the above derivation can be carried out for the case of unequal dead times. If the β- and γ-channel dead times are designated τ_β and τ_γ it can be readily shown that for $\tau_\beta > \tau_\gamma$

$$\frac{N_\beta N_\gamma}{N_c} = N_0\left[1 - N_0\varepsilon_\beta\varepsilon_\gamma\tau_\gamma \times \left\{\frac{1 - N_0\tau_\beta}{1 - N_0(\tau_\gamma\varepsilon_\gamma + \tau_\beta\varepsilon_\beta - \varepsilon_\beta\varepsilon_\gamma\tau_\gamma)}\right\}\right]$$

For the $4\pi\beta$–γ coincidence method ε_β tends to unity and the above expression immediately reduces to equation (13) with the τ replaced by τ_γ. The case $\tau_\gamma > \tau_\beta$ leads to a similar expression with the β- and γ-subscripts interchanged, but in this case the term in the curly brackets does not reduce to unity as $\varepsilon_\beta \to 1$. If however quadratic terms can be neglected equation (13) is again obtained with τ replaced by τ_β. No attempt has been made to increase the range of validity of these formulae since in practice it is difficult to impose a dead time which is truly "non-extending".

WESTCOTT *et al.*[21] have derived an empirical expression for the dead time correction to the coincidence channel in terms of the true coincidence rate and the side channel counting rates of pulses which are not components of a coincident pair. It is difficult to compare their equation with the appropriate formula above, except for the

VOL. 4 1958/5

simplifying case of 100 per cent efficiency in one channel, for which the two expressions give essentially the same result.

Let us now return to equations (12) and (13) and suppose that the efficiency of the β-detector is 100 per cent. The dead time correction for the coincidence channel is then just that for the β-channel while the correction appearing in equation (13) is that for the γ-channel. Further, no appreciable error is introduced if the more usual expression for the dead time correction, $(1 - N_\gamma\tau)$, is used. In order to obtain a quantitative estimate of the error thus introduced the ratio

$$R = \frac{1 - N_0\tau\varepsilon_\beta\varepsilon_\gamma}{1 - N_\gamma\tau}$$

has been calculated for a range of values of $N_0\tau$, ε_γ and ε_β. The results are shown in Table 1 from which it is seen that, for the range of parameters chosen, the value of R differs from unity by less than 0·1 per cent for the most unfavourable case, viz. $\varepsilon_\beta = 0{\cdot}9$ and $\varepsilon_\gamma = 0{\cdot}2$. Clearly the more exact expression (13) need only be considered when much higher efficiencies are attained in the γ-detector than are available at present. We may write therefore:

$$N_0 = \frac{N_\beta N_\gamma}{N_c(1 - N_\gamma\tau)} \qquad (14)$$

and to the same approximation

$$\varepsilon_\beta = \frac{N_c(1 - N_\gamma\tau)}{N_\gamma(1 - N_\beta\tau)}, \qquad \varepsilon_\gamma = \frac{N_c}{N_\beta} \qquad (15)$$

Besides the one dead time factor, equation (14) contains only observed counting rates corrected for background and, in the case of the coincidence channel, for the accidental coincidence rate. It is convenient therefore to apply the two individual channel dead time corrections to the background rates measured when no source is present and to subtract these corrected backgrounds from the observed rates. The coincidence channel background rate in any well-shielded system is extremely small and may be subtracted directly. The accidental coincidence rate is taken into account by the use of either equation (8) or (9).

Comparison of the $4\pi\beta$–γ-coincidence and $4\pi\beta$ counting methods

The relative merit of the $4\pi\beta$–γ coincidence method can be compared with that of straight $4\pi\beta$ counting on the basis of the corrections involved. Considering first the counting rate-dependent corrections, both methods are limited at the upper end of the useful counting rate range by the inapplicability of simple dead time theory. In the $4\pi\beta$ method the correction in this region of the range is simply that due to the dead time losses. In the $4\pi\beta$–γ coincidence method there are two corrections, viz. that due to dead time losses, and that due to the accidental coincidence rate. The ratio of the (fractional) corrections in the two methods may be written, for this purpose, as

$$\frac{4\pi\beta\text{–}\gamma \text{ correction}}{4\pi\beta \text{ correction}} \simeq \frac{\tau_R N_0(2 - \varepsilon_\beta - \varepsilon_\gamma) + \tau_D N_0\varepsilon_\gamma}{\tau_D N_0\varepsilon_\beta}$$

$$= \frac{\tau_R}{\tau_D}(1 - \varepsilon_\gamma) + \varepsilon_\gamma \qquad \text{for } \varepsilon_\beta = 1{\cdot}0$$

TABLE 1. Values of the ratio R for various values of $N_0\tau$, ε_β, and ε_γ

$N_0\tau$	$\varepsilon_\beta = 1{\cdot}0$ $\varepsilon_\gamma = 0{\cdot}10$	$\varepsilon_\beta = 0{\cdot}95$ $\varepsilon_\gamma = 0{\cdot}10$	$\varepsilon_\beta = 0{\cdot}90$ $\varepsilon_\gamma = 0{\cdot}10$	$\varepsilon_\beta = 1{\cdot}0$ $\varepsilon_\gamma = 0{\cdot}20$	$\varepsilon_\beta = 0{\cdot}95$ $\varepsilon_\gamma = 0{\cdot}20$	$\varepsilon_\beta = 0{\cdot}90$ $\varepsilon_\gamma = 0{\cdot}20$
0·03	1·0001	1·0002	1·0003	1·0000	1·0003	1·0006
0·02	1·0000	1·0001	1·0002	1·0000	1·0002	1·0004
0·01	1·0000	1·0001	1·0001	1·0000	1·0001	1·0002
0·005	1·0000	1·0000	1·0001	1·0000	1·0001	1·0001

where τ_R and τ_D are the resolving time of the mixer circuit and the dead time of the system (assumed to be the same in both methods), respectively. Since the coincidence resolving time can generally be made somewhat smaller than the dead time the corrections are of comparable magnitude, with the coincidence method slightly more favoured.

The lower limit of the counting rate range is set by the background rates, and for the $4\pi\beta$–γ coincidence method the controlling rate is that in the γ-detector. Hence any arbitrary signal to background limit is reached first in the coincidence method. Thus the $4\pi\beta$ method can accommodate a greater range of activities and is therefore particularly useful for determining half lives.

In the $4\pi\beta$–γ coincidence method it has been shown that the remaining corrections are usually very small (a few tenths of one per cent for reasonable efficiencies in the β-detector) and can be readily calculated to a fair degree of accuracy. On the other hand, in the $4\pi\beta$ method there are corrections due to film and self absorptions. The former correction has been treated by SMITH,[20] HAWKINGS *et al.*,[6] MANN and SELIGER,[9] and more recently by PATE and YAFFE.[13] The self absorption however still remains in general an unknown quantity unless determined experimentally.

PART II

The apparatus

Fig. 1 shows a general view of the $4\pi\beta$–γ coincidence unit and shielding which is in current use in this laboratory. A more detailed drawing of the counters is shown in Fig. 2(a). The β-detector consists of a $4\pi\beta$ proportional counter sandwiched between two 3 in. by 3 in. NaI crystals coupled to Dumont 6363 photomultiplier tubes. The shielding consists of 4–6 in. of lead and part of the shielding may be rolled back along the supporting table to allow easy access to the $4\pi\beta$ counter. This counter, which is a flow type using methane gas, is shown in an exploded view in Fig. 2(b). Each half consists of an aluminium pill box counter, 3 in. i.d. and 1 in. deep. In order to avoid regions of reduced electrical field strength which might well exist in such a geometry, two shaped lucite pieces, whose surfaces are rendered conducting, are inserted to form a cathode as shown in Fig. 2(b). A 0·0005 in. stainless steel wire forms the anode. The two halves of the counter are separated by a thin Dural turntable on which sources may be placed and rotated into the apparatus, a gas-tight seal being effected by two "0" rings mounted in the top and bottom pill boxes. The turntable avoids the necessity to open the counter directly to the atmosphere when inserting a source and thereby greatly reduces the flushing time required before a measurement can be taken.

The source mount is formed from a thin ring of copper, 1·5 in. o.d., 1·0 in. i.d., and 0·022 in. thick. Following the technique of PATE and YAFFE,[12] a thin plastic film (VYNS, about 5 μg/cm^2 thick) is stretched across this ring and subsequently rendered conducting by the vacuum distillation of gold on to both surfaces. It has been found necessary to put down a total of at least 30 μg/cm^2 of gold in order to obtain consistent plateaux in the β-channel.

The β-detector is operated in the proportional region in order to avoid the long dead times inherent in Geiger Müller counters, and is used in conjunction with a non-overloading amplifier. A well stabilized power supply employing a standard cell for a reference voltage is used for the photomultiplier tubes and this also forms a convenient supply for the β-detector.

A block diagram of the electronic circuitry is shown in Fig. 3. The outputs of the crystal detector units are fed each to an amplifier and single channel pulse-height analyser. The signals from these are normally added before entering the coincidence mixer. Although any variation in the efficiency of the γ-channel also affects the coincidence channel in the same ratio it is nevertheless desirable to avoid counting rate-dependent gain shifts. The γ-ray background spectrum exhibits a decrease in intensity with energy and a large gain change may result in an

VOL.
4
1958/5

OL.
4
8/59

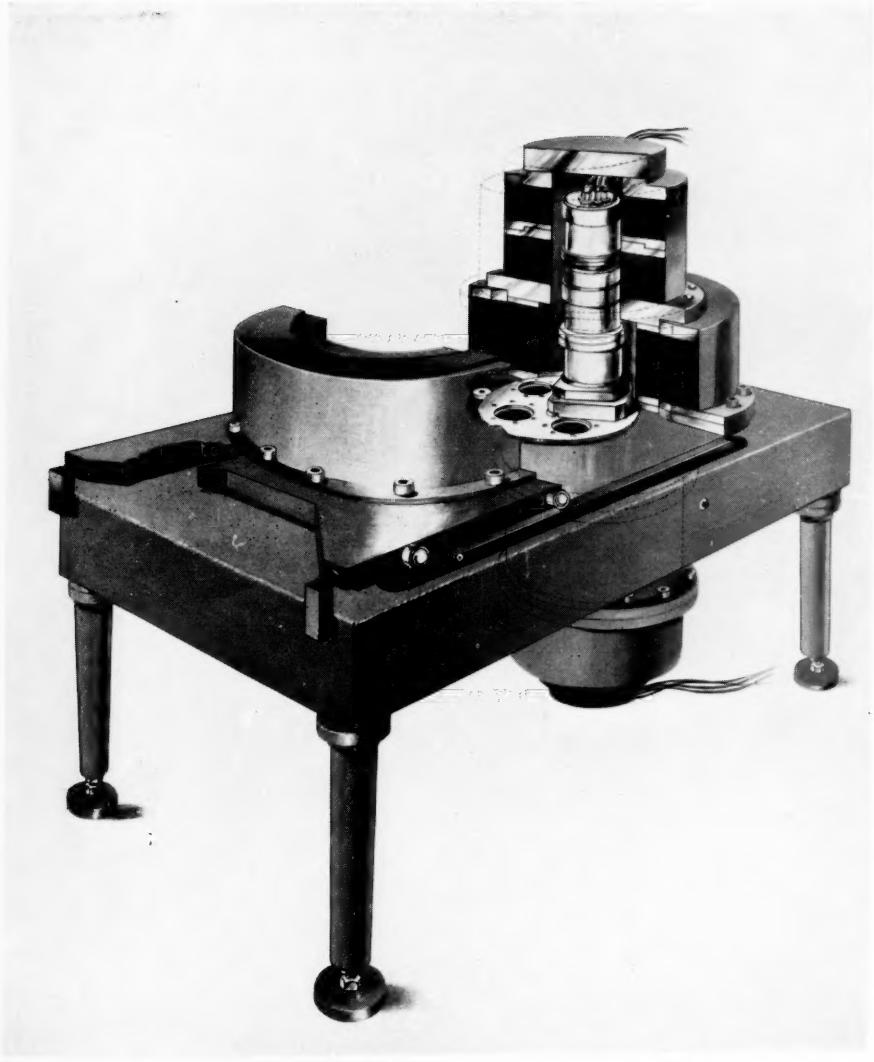

FIG. 1. Sketch of the $4\pi\beta$–γ coincidence instrument and shielding.

VOL.
4
1958/5

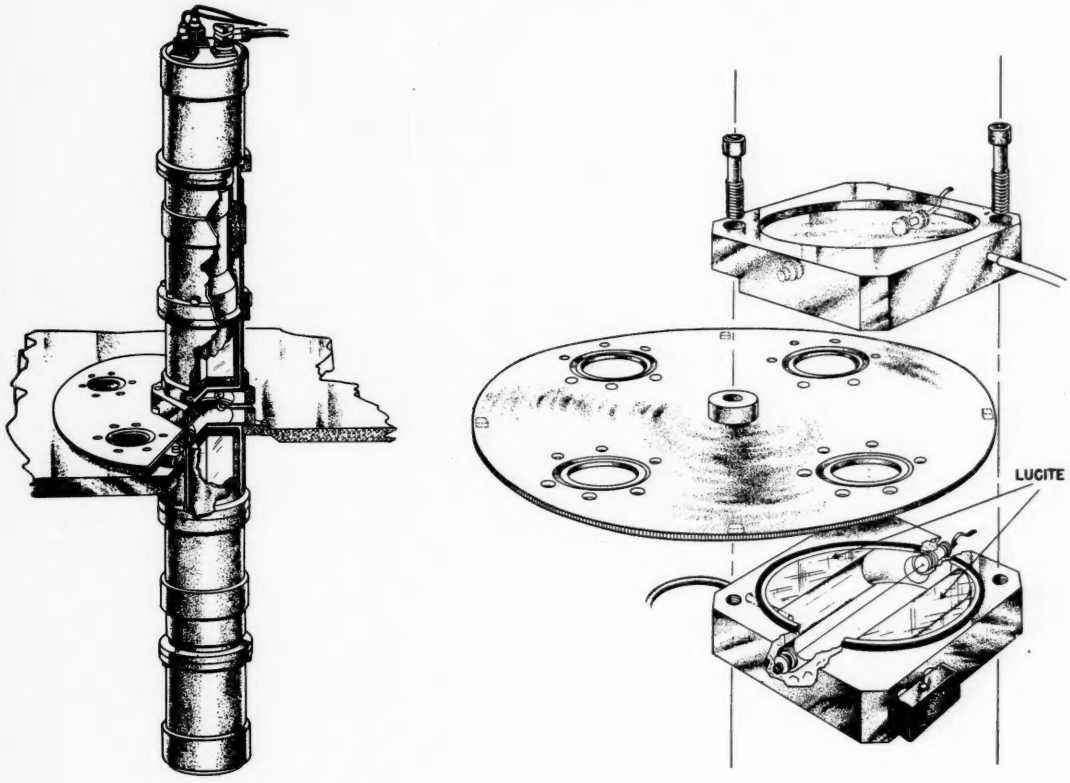

FIG. 2. (a) Sketch of the detectors and turntable. (b) Exploded view of the $4\pi\beta$ detector.

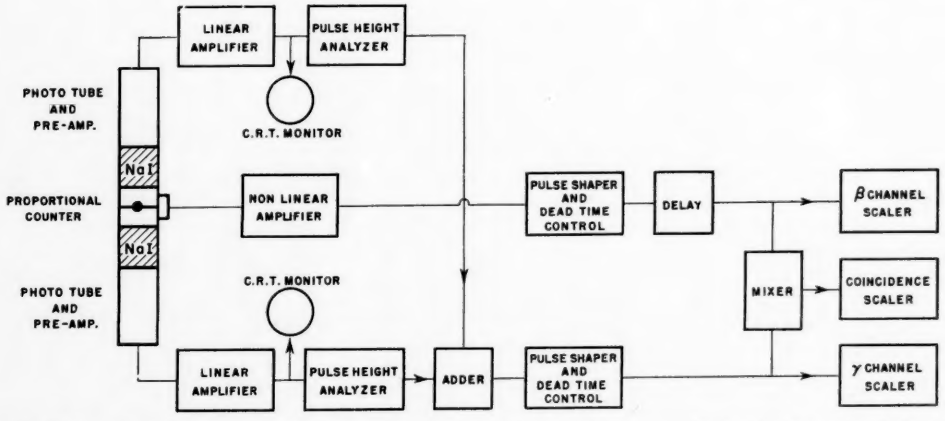

FIG. 3. Block diagram of the electronic circuitry. For triple coincidences a third pulse-shaper and dead time control unit is available.

incorrect background subtraction. The photomultipliers are therefore run at a low h.t. voltage (~800 V) with a suitable increase in the gain of the amplifier to compensate for the loss in pulse-height. For similar reasons the equipment is installed in a temperature-controlled laboratory in order to reduce the fluctuations of the γ-efficiency resulting from the temperature dependent diodes in the pulse-height analysers. Further the electronics should be such that no long positive overshoot appears after a signal. Although such overshoots may not by themselves be sufficient to be recorded, small background pulses superimposed on them may be, thus giving a higher background rate than measured in a direct background run. The counting rate due to electronic noise in the 110 VAC line is made negligible by the provision of filter circuits to all units dealing with low level signals.

Since there is an inherent delay of 0·25 μsec in each pulse-height analyser the β-pulse must be delayed before entering the mixer. The value of this delay is determined experimentally in order to eliminate any further relative delays between the channels. The mixer may be operated as either a double or triple coincidence unit, and when used in the latter role the signal from each analyser is fed to a separate pulse-shaper and input channel. The pulse-shapers have a continuously variable dead time control and are usually operated with equal dead times of 2·0 μsec. This value is sufficiently large to be the determining dead time in both channels, and is measured by the use of a double pulse-generator and calibrated oscilloscope, or by the paired source technique. The resolving time of the mixer is determined by shorted delay cables and can be measured by introducing a variable delay in each channel and observing the coincidence counting rate as a function of the relative delay. It is essential that no coincidences are lost due to the use of too short a resolving time. Accordingly, a family of such resolving time curves was plotted for different lengths of shorted cables. The curves showed flat plateaux, the counting rates of which were practically independent of the resolving time down to 0·3 μsec. Below this value the curves ceased to show a plateau. This is the expected limit that can be obtained with the present arrangement, since the rise time of pulses from sodium iodide crystal detectors is 0·25 μsec and these signals are in coincidence with the output of a saturated amplifier. The resolving time currently used is 0·7 μsec and has been measured more exactly by the use of a S^{35} source to produce random pulses in the β-detector and a Nb^{95} source placed outside the $4\pi\beta$ counter but close to the sodium iodide crystals to produce random pulses in the γ-channel. The windows of the pulse-height analysers accepted only the photopeak of the 760 keV radiation from Nb^{95}. This reduced the number of true coincidences due to scattered γ-rays and entirely prevented those due to bremsstrahlung quanta from the S^{35} source. Subsidiary experiments were performed with each source removed in turn in order to determine the true coincidence rate. This amounted to less than one per cent of the random rate. The measured resolving time, 0·70 μsec ($\pm$3 per cent), agreed well with that found by inserting variable delays.

Performance details

The background counting rate in the β-detector is about one count per sec while the corresponding rate in the coincidence channel is less than one-tenth of this. The combined background rate of the two NaI crystals above 60 keV is 16 counts/sec. In a determination of absolute activity a window is set to bracket part of the γ-ray spectrum of the isotope to be measured and hence the actual background rate in this detector is much less than 16 counts/sec. This is however the greatest background correction, and in order that the error in this correction should be negligible the background to signal ratio in the γ-channel is always kept to less than one per cent and usually less than 0·3 per cent.* In general there is no particular

* *Note added in proof*—Recently copper and brass have been substituted for aluminium in the construction of the 4π counter, turntable and crystal housings. This has resulted in a decrease, by a factor of 2, in the background counting rate in the γ-channel.

VOL.
4
1958/5

virtue in setting a narrow window across a photopeak unless a very weak activity is to be measured or an exceptional decay scheme demands it. On the other hand, the use of a wide window results in an increased γ-efficiency, particularly if several γ-rays are present in the spectrum, and hence enables a given statistical accuracy to be reached in a shorter time.

To determine the efficiency of the 4π counter for detecting γ-radiation, $(\varepsilon_\beta)_\gamma$, sources of Ce^{141}, Hg^{203}, Nb^{95}, and Co^{60}, each of known activity, were sandwiched between polythene sheets sufficiently thick to absorb the β-rays emitted by the respective isotopes. The outer surfaces of the sandwiches were coated with gold in a similar way to normal source mounts. The response of the β-detector to each of these sources was then observed but before calculating $(\varepsilon_\beta)_\gamma$ it was necessary to examine two possible effects, namely the response of the β-detector to the interaction of the γ-radiation with the polythene absorber and to bremsstrahlung. The former was measured, for those isotopes whose γ-ray energy greatly exceeded their maximum β-particle energy, by doubling the thickness of the absorber and was found to be negligible. For Ce^{141} and Hg^{203} it was assumed to be negligible. For the bremsstrahlung effect it was assumed that Nb^{95} and S^{35} have the same maximum β-particle energies and similarly Co^{60} and Pm^{147}. Sources of S^{35} and P^{147} were therefore sandwiched between polythene absorbers of the same thickness as used for the Nb^{95} and Co^{60} sources respectively, and the response of the β-detector observed. The correction amounted to only 0·3 per cent of $(\varepsilon_\beta)_\gamma$ in these cases. A similar experiment was carried out using a standardized Mn^{54} source* sandwiched between two thin foils of titanium to absorb the X-rays. The result is in very good agreement with the interpolation of the data obtained from β-active sources. The efficiency $(\varepsilon_\beta)_\gamma$ per γ-ray is shown in Fig. 4 as a function of the energy of the γ-radiation. The general features of this curve are in agreement with the results of other workers[3,5] using external sources.

Measurements of the probability of detecting a coincidence when the β-particle is undetected, ε_c, as a function of the setting of the pulse-height analyser windows, were made using the same techniques as described above. The results are shown in Fig. 5 where values of $\varepsilon_c/\varepsilon_\gamma$ are plotted against ε_γ for various γ-ray energies. From the results

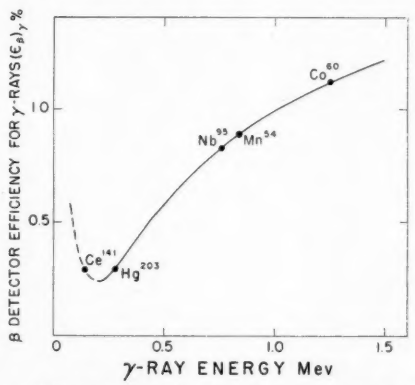

FIG. 4. The efficiency of the $4\pi\beta$ detector for γ-radiation as a function of energy.

of Figs. 4 and 5 it is seen that for high overall γ-efficiencies the term $(\varepsilon_\beta)_\gamma - \varepsilon_c/\varepsilon_\gamma$ appearing in equation (4) is small and thus the total correction is very small. It is emphasized that these results depend strongly on the

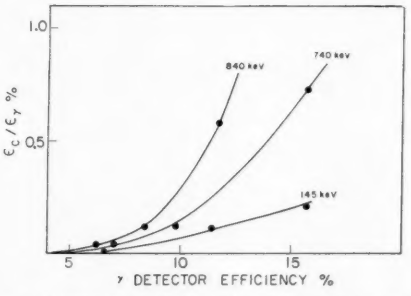

FIG. 5. Values of the ratio $\varepsilon_c/\varepsilon_\gamma$ as a function of the γ-detector efficiency ε_γ for various energies.

experimental conditions and are therefore only strictly applicable to the instrument described here. They illustrate however the small magnitude of these effects.

The variation of the γ-detector efficiency

* The author is indebted to MR. R. C. HAWKINGS for this standardization.

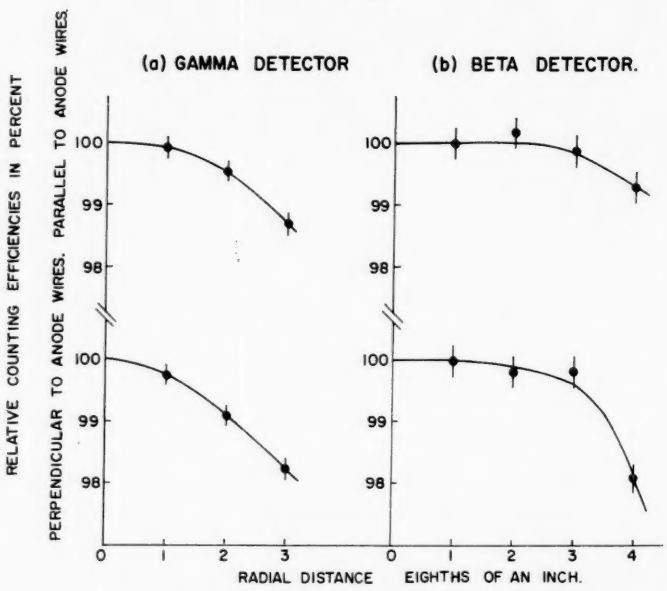

FIG. 6. The variation of (a) the γ-detector efficiency and (b) the β-detector efficiency with respect to a point radiator. The results for (a) are obtained with a Hg^{203} source, and for (b) with a Tl^{204} source. The radius of a source deposited in the normal way is about $\frac{1}{8}$ in.

as a function of the position of a point radiator was determined using both Hg^{203} and Co^{60} sources. Each isotope was deposited in a small depression in a slide which could be moved along a radial groove in a thin aluminium disc which was placed on the turntable. The γ-detector counting rate was observed as a function of the radial distance of the source from the centre of the disc.

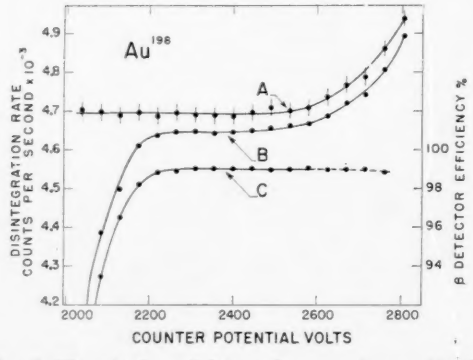

FIG. 7. The absolute disintegration rate (curve A), the β-detector counting rate (curve B) and the efficiency of the $4\pi\beta$ detector (curve C, right-hand ordinate) as a function of the potential applied to the $4\pi\beta$ detector, for a typical source of Au^{198}.

Measurements were made in directions parallel and perpendicular to the anode wires of the 4π counter. The results for Hg^{203} are shown in Fig. 6(a) where the relative counting rate is plotted as a function of radial distance. The results for Co^{60} are similar and will not be given here. Since a 100 μl aliquot yields a deposit some 0·25 in. diameter it is seen that the efficiency of the γ-detector varies by less than 0·5 per cent over the dimension of a source.

A similar experiment was performed using Tl^{204} to determine the response of the β-detector to the position of a point radiator. Fig. 6(b) summarizes the results.

The β-channel counting rates obtained with sources of Au^{198} and Na^{22} as a function of the voltage applied to the anode of the proportional counter are shown as curves B in Fig. 7 and 8 respectively. Both curves show an essentially flat portion and are typical of the plateaux obtained with this counter. The maximum slope allowed by the errors is less than 0·2 per cent per 100 V for the Au^{198} source and less than 0·07 per cent per 100 V for the Na^{22} source. The β-particle disintegration rates, calculated

according to equation (8) with corrections for the accidental coincidence rates, are shown as curves A in both Figs. while curves C represent the β-detector efficiencies.

In the case of the Au^{198} source the pulse-height analyser windows were set to accept pulses from the γ-detectors in the energy interval 200–450 keV. The average value of ε_β along the plateau was 99·1 per cent. In order to determine the contribution of the source mount to this departure from 100 per cent a similar film was laid on top of the source and the value of ε_β was then found to be reduced to 99·0 per cent. Attempts were made to increase the value of ε_β by the consideration of the following points:

(a) the field strength at the source was increased by using a 0·001 in. wire as the counter anode with a corresponding increase in the potential required to reach the plateau,
(b) the thickness of the source ring was reduced to 0·010 in. and the i.d. increased to 1·25 in., and
(c) a mixture of 90 per cent argon and 10 per cent methane was used as the counter gas.

Since all these attempts yielded the same value of ε_β as before, i.e. about 99 per cent, it is very probable that this departure from 100 per cent efficiency results from self absorption.

Because of the inability of the proportional counter to detect the electron capture transition in Na^{22}, it is found that in this isotope the coincidence equations take a relatively simple form provided that the pulse-height analyser windows are set to accept only sum events due to the simultaneous detection of a 1·28 MeV γ-ray and an annihilation quantum.* The equations then become, neglecting dead time and γ–γ coincidence corrections,

$$N_\beta = N_0 a \varepsilon_\beta$$

$$N_\gamma = N_0 a \varepsilon_{\gamma 1{\cdot}79}$$

$$N_c = N_0 a \varepsilon_\beta \varepsilon_{\gamma 1{\cdot}79}$$

whence $$\frac{N_\beta N_\gamma}{N_c} = a N_0$$

where a is the number of positrons emitted per disintegration, and $\varepsilon_{\gamma 1{\cdot}79}$ is the efficiency of the γ-detector for the sum peak at 1·79 MeV. The value for a has been measured experimentally[1,7,19] and found to agree with the theoretically predicted value[23] of 0·900 which was the quantity used here. The results shown in Fig. 8 were obtained with

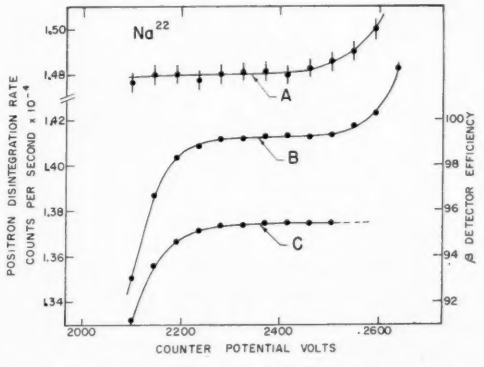

FIG. 8. The positron disintegration rate (curve A), the β-detector counting rate (curve B), and the efficiency of the $4\pi\beta$ detector (curve C, right-hand ordinate) as a function of the potential applied to the $4\pi\beta$ detector, for a Na^{22} source.

windows covering the energy interval 1·68–1·90 MeV. Using equation (9) the accidental coincidence rate correction was found to be 1·0 per cent in the positive direction, while that due to the dead time was in this case negligible. The background correction in the γ-detector amounted to 0·3 per cent in the negative direction. The internal conversion in this isotope is extremely small[8] and therefore the only other instrumental correction to be considered is the γ-sensitivity of the β-detector. Neglecting dead

* The absolute disintegration rate may also be determined by gating on the 1·28 MeV γ-ray. In this case account must be taken of a sum event correction which is difficult to evaluate unless rather complex subsidiary experiments are performed. In order to avoid the uncertainties in such a correction it is more convenient to use the method proposed above. For relatively low efficiency γ-detectors, in which the counting rate in the sum peak would be prohibitively low, the method of gating on the 1·28 MeV γ-ray must be used. However, in such cases the sum event correction and the associated uncertainty are correspondingly smaller.

time corrections the relevant equations are:

$$N_\beta = N_0[a\varepsilon_\beta + a(1 - \varepsilon_\beta)(\varepsilon_\beta)_{\text{tot}} + \\ + (1 - a)\,(\varepsilon_\beta)_{1\cdot28}]$$

$$N_\gamma = N_0 a\varepsilon_{\gamma 1\cdot79}$$

$$N_c = N_0[a\varepsilon_\beta + a(1 - \varepsilon_\beta)(\varepsilon_\beta)_{0\cdot511}]\varepsilon_{\gamma 1\cdot79}$$

where a is again the number of positrons emitted per disintegration. The subscripts "0·511," "1·28," and "tot" refer to the 0·511 MeV, 1·28 MeV γ-rays and the total electromagnetic radiation emitted by the source respectively. The efficiencies ε_β and ε_γ can be calculated from equation (15) after making the accidental rate correction. The value of $(\varepsilon_\beta)_{\text{tot}}$ was determined in a subsidiary experiment, similar to those already described in this Part, to be two per cent, while $(\varepsilon_\beta)_{0\cdot511}$ and $(\varepsilon_\beta)_{1\cdot28}$ were found from Fig. 4 to be 0·6 and 1·1 per cent respectively. The correction amounted to 0·2 per cent in the negative direction when the β-detector was operating on the plateau. Thus the total instrumental corrections, irrespective of sign, for Na^{22} at this counting rate amount to about 1·5 per cent. Finally the disintegration rates shown in Fig. 8 must be multiplied by a^{-1} in order to obtain the absolute disintegration rate of the source. The good agreement between the experimental and theoretical values suggests that this quantity is known to about 0·5 per cent.

The dead time and accidental coincidence rate corrections

A suitable check on the accuracy of those corrections which are a function of counting rate is the observation of a source, decaying with a known half life, over as great a range of activities as practicable. The most suitable isotope is perhaps Na^{24}, since its large maximum β-energy permits sources to be prepared whose efficiencies are close to 100 per cent, for which equation (14) is exact. It has a sufficiently short half life so that the observations may be completed within a reasonable period of time. Further, it may be readily purified by ion exchange techniques. However, the half life must be well known and although several measurements of this quantity appear in the literature it was felt that a more accurate measurement could be made. The details of this determination have been published elsewhere;[4] the result obtained was 14·959 $\pm$ 0·010 hr.

A source of about 2×10^4 disintegrations/sec of Na^{24}, which had been purified by passing it through an ion exchange column of Dowex 50, was mounted on a standard source mount. The absolute activity of this source, corrected to a zero reference time, was measured in the $4\pi\beta$–γ instrument as a function of elapsed time from zero. The results are shown in Fig. 9 in which curve (a) was obtained by using equation (14) with corrections for the accidental coincidence rate according to either equation (8) or (9). Curve (b) was obtained by including the accidental rate correction only. Curve (c) is the result obtained without any correction. The absolute activity is independent of the time of observation and hence the counting rate, provided that both the dead time and accidental rate corrections are included. It should be pointed out that the shape of these curves depends on the value adopted for the half life of the source. For example, a half life of 14·97 hr would move the curves downwards by about 0·2 per cent at 70 hr elapsed time while there would be no change at zero elapsed time. Since the source used for this experiment was prepared from one of the master solutions used in the half life determination it is felt that the adopted half life is not in error by more than the quoted value.

A further check on the validity of the dead time and accidental coincidence rate corrections was provided by the following experiment, which does not rely heavily on an accurate knowledge of a half life. The absolute activity of a Br^{82} source, free from any Br^{80} activity, was observed as a function of the efficiency of the γ-detector. This was achieved by varying the width of the pulse-height analyser windows and since there are several γ-rays emitted per disintegration, the γ-detector efficiency could be varied from 2 to 37 per cent. The results, corrected for the accidental coincidence rate, dead time and background, together with a small

VOL. 4 1958/9

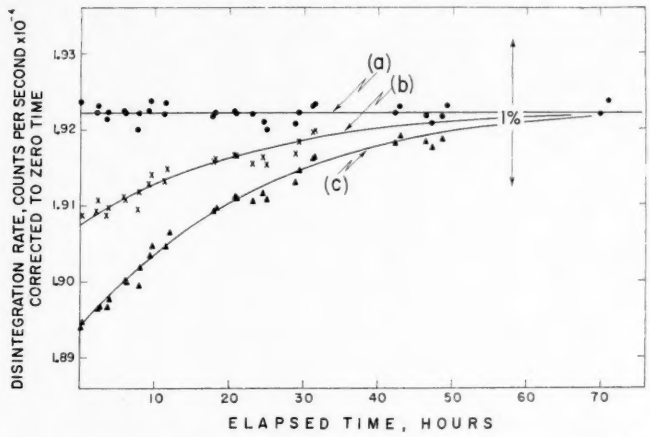

FIG. 9. The absolute disintegration rate, corrected to zero elapsed time, of a Na^{24} source as a function of elapsed time. See text.

correction for decay from a zero reference time, are shown by curve (a) in Fig. 10. Curve (b) shows the result obtained if the dead time correction is neglected. This is asymptotic to curve (a) at low values of the γ-detector efficiency but deviates by up to one per cent at large values, whereas curve (a) is independent of the γ-detector efficiency. Curve (c) was obtained by omitting the accidental coincidence rate correction from the calculation.

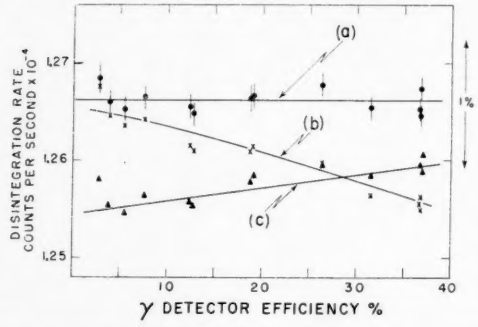

FIG. 10. The absolute disintegration rate of a Br^{82} source as a function of the γ-detector efficiency. See text.

These experiments show that the dead time and accidental coincidence rate corrections discussed in Part I are correct and should be included in the calculation of absolute activities by the $4\pi\beta$–γ coincidence method. The Na^{24} experiment also shows that an extensive range of activities can be accommodated in this instrument.

Acknowledgements—The author wishes to acknowledge the assistance of Mrs. J. S. MERRITT in the preparation and counting of the sources used in the experimental part of this report and of MR. R. L. BROWN for the construction and maintenance of some of the electronic equipment.

REFERENCES

1. ALLEN R. A., BURCHAM W. E., CHACKETT K. F., MUNDAY G. L. and REASBECK P. *Proc. Phys. Soc.* **68A,** 681 (1955).
2. BARNOTHY J. and FORRO M. *Rev. Sci. Instrum.* **22,** 415 (1951).
3. BRADT H., GUGELOT P. C., HUBER O., MEDICUS H., PREISWERK P. and SCHERRER, P. *Helv. Phys. Acta.* **19,** 77 (1946).
4. CAMPION P. J. and MERRITT J. S. *Canad. J. Phys.* **36,** 983 (1958).
5. DUNWORTH J. V. *Rev. Sci. Instrum.* **11,** 167 (1940).
6. HAWKINGS R. C., MERRITT W. F. and CRAVEN J. H. *Proceedings of Symposium: Maintenance of Standards, National Physical Laboratory.* H. M. Stationery Office, London (1952).
7. KREGER W. E. *Phys. Rev.* **96,** 1554 (1954).
8. LEAMER R. D. and HINMAN G. W. *Phys. Rev.* **96,** 1607 (1954).
9. MANN W. B. and SELIGER H. H. *J. Res. Nat. Bur. Stand.* **50,** 197 (1953).

10. Merritt J. S., Taylor J. G. V. and Campion P. J. Unpublished.
11. Merritt W. F., Campion P. J. and Hawkings R. C. *Canad. J. Phys.* **35,** 16 (1957).
12. Pate B. D. and Yaffe L. *Canad. J. Chem.* **33,** 610 (1955).
13. Pate B. D. and Yaffe L. *Canad. J. Chem.* **33,** 929 (1955).
14. Pate B. D. and Yaffe L. *Canad. J. Chem.* **34,** 256 (1956).
15. Putman J. L. A.E.R.E. Report N/R 318 (1949).
16. Putman J. L. A.E.R.E. Report I/M 26 (1953).
17. Putman J. L. Chapter 26: *Beta- and Gamma-Ray Spectroscopy*. Edited by K. Siegbahn. North-Holland Publishing Co. (1955).
18. Seliger H. H. and Schwebel A. *Nucleonics* **12,** 54 (1954).
19. Sherr R. and Miller R. H. *Phys. Rev.* **93,** 1076 (1954).
20. Smith D. B. A.E.R.E. Report I/R 1527.
21. Westcott C. H., Greenberg J. S. and Kirkaldy J. S. *Canad. J. Phys.* **31,** 859 (1953).
22. Wolicki E. A., Jastrow R. and Brooks F. N.R.L. Report 4833.
23. Zweifel P. F. *Phys. Rev.* **96,** 1572 (1954).

VOL.
4
1958/5

International Journal of Applied Radiation and Isotopes, 1959, Vol. 4, pp. 249–252 . Pergamon Press Ltd. Printed in Northern Ireland

Mesure Absolue des Emetteurs β de Faible Energie et de Faible Activité Spécifique

Y. LE GALLIC et M. THENARD
Service de Biologie du Commissariat à L'Energie Atomique, Saclay, France

(*Received* 25 *August* 1958)

Description d'une méthode de mesure particulièrement adaptée à la détermination de l'activité d'émetteurs β peu énergiques (S^{35}, C^{14}, Ca^{45} . . .) de faible activité spécifiqué.

La technique décrite utilise les solutions elles-mêmes sans qu'il soit nécessaire de préparer des sources solides. La solution est déposée dans une cuvette à mince paroi, placée ensuite entre deux compteurs à fenêtre ou dans une cuvette à fond plat épais lorsqu'on n'utilise qu'un seul compteur. Dans le premier cas, le seuil de détection correspond à $5 \cdot 10^{-4}$ $\mu c/cm^3$ et le seuil de mesure (plus faible activité mesurable) correspond à 10^{-3} $\mu c/cm^3$. La précision de la méthode varie de 4 à 6 pour cent pour des activités comprises entre 1 $\mu c/cm^3$ et $5 \cdot 10^{-3}$ $\mu c/cm^3$.

ABSOLUTE MEASUREMENT OF β-EMITTERS OF LOW ENERGY AND LOW SPECIFIC ACTIVITY

Description of a method of measurement particularly suited to determining the activity of low energy β-emitters (S^{35}, C^{14}, Ca^{45}. . . .) of low specific activity.

The technique described employs the solutions themselves without the need of preparing solid sources. The solution is placed in a thin-walled container between two window counters, or in a bowl with a thick flat bottom, in which case only one counter is used. In the former case, the threshold of detection corresponds to $5 \cdot 10^{-4}$ $\mu c/cm^3$ and the threshold of measurement (weakest measurable activity) corresponds to 10^{-3} $\mu c/cm^3$. The accuracy of the method varies from 4 to 6 per cent for activities between 1 $\mu c/cm^3$ and $5 \cdot 10^{-3}$ $\mu c/cm^3$.

АБСОЛЮТНЫЕ ИЗМЕРЕНИЯ β-ИЗЛУЧАТЕЛЕЙ С НИЗКОЙ ЭНЕРГИЕЙ И НИЗКОЙ УДЕЛЬНОЙ АКТИВНОСТЬЮ

Описан способ измерений особенно подходящий-для определения активности эмиттеров небольшой энергии (S^{35}, C^{14}, Ca^{45} . . .) со слабой удельной активностью.

Описанная технология позволяет употреблять сами растворы, без необходимости приготовления источиков в виде твердых тел. Раствор помещают в тонкостенный кювет, который устанавливается между двумя торцовыми счетчками, или в плоский сосуд с толстым дном если измерения производят только одним счётчиком. В первом случае порог чувствительности соответствует $5 \cdot 10^{-4}$ $\mu c/cm^3$ тогда как порог измерен ний (наименьшая активность которую можно измерить), соответствует 10^{-3} $\mu c/cm^3$. Точность метода состовляет 4–6% для активностей от 1 $\mu c/cm^3$ до $5 \cdot 10^{-3}$ $\mu c/cm^3$.

UNBEDINGTE MESSUNG DES β-STRAHLEN DER SCHWACHEN ENERGIE UND DER SCHWACHEN SPEZIFISCHEN AKTIVITÄT

Beschreibung eines zur Messung der Radioaktivität von schwachen β-Strahlern (S^{35}, C^{14}, Ca^{45} . . .) mit schwacher spezifischer Aktivität besonders geeigneten Messverfahrens.

Dieses Verfahren benützt die Lösungen selbst, man braucht also keine festen Lösungen herzustellen. Man schüttet die Lösung in ein dünnwandiges Gefäss, das man sodann zwischen zwei mit einem Fenster versehenen Zähler stellt oder, wenn man einen einzigen Zähler benützt, in einen Behälter mit dickem flachem Boden. Im ersten Falle ist die Detektionsschwelle gleich $5 \cdot 10^{-4}$ $\mu c/cm^3$ und die Messungsschwelle (das heisst die geringste messbare Radioaktivität) gleich 10^{-3} $\mu c/cm^3$ Die Empfindlichkeit des Verfahrens schwankt zwischen 4% und 6% für Radioaktivitäten zwischen 1 $\mu c/cm^3$ und $5 \cdot 10^{-3}$ $\mu c/cm^3$.

Parmi les nombreux radioisotopes utilisés tant en médecine et en biologie que dans l'industrie, le S^{35}, le C^{14} et le Ca^{45} occupent une place importante. Par suite, la mesure absolue de leur activité s'avère indispensable dans de nombreux cas.

Plusieurs méthodes conviennent à la mesure des solutions de faible activité specifique:

(1) Les compteurs à liquides

Mais ils ne conviennent pas à la mesure des émetteurs β de faible énergie, du fait de l'épaisseur de leur paroi de verre (25 mg/cm²).

(2) Les scintillations liquides

Méthode idéale en théorie mais présentant un certain nombre de difficultés pratiques. En effet, elles s'accommodent difficilement des solutions aqueuses et d'autre part l'importance des bruits de fond rend difficile la mesures des faibles activités.

(3) Le compteur 4π

Le compteur 4π enfin, qui est le meilleur appareil de mesure absolue β, présente quand même certains inconvénients. En effet, la mesure repose sur la préparation de sources sèches, ce qui rend difficile d'une part la mesure de radioisotopes en solutions organiques, d'autre part la mesure d'émetteurs β de faible énergie si les solutions contiennent une forte proportion d'entraineur, la correction d'autoabsorption devenant dans ce cas trop importante.

La méthode décrite plus loin utilise les solutions elles-mêmes sans qu'il soit nécessaire de passer par l'intermediaire de sources solides. Elle permet de mesurer rapidement, avec une précision satisfaisante les émetteurs β de faible énergie et de faible activité spécifique.

VOL. 4 1958/5

DISPOSITIF EXPERIMENTAL

Il est essentiellement constitué par un compteur à fenêtre mince (1 à 1,5 mg/cm²) et une cuve contenant la solution (Fig. 1).

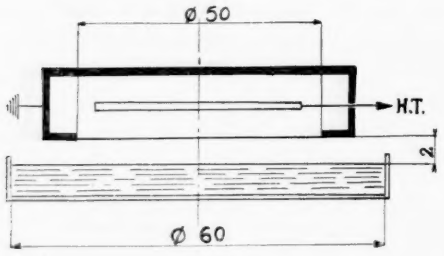

Fig. 1.

Choix du compteur

Quoique les compteurs français L.C.T. soient très satisfaisants nous avons préféré un compteur Anton type 1.017, compteur à fenêtre, plat, dont le diamètre plus grand (50 mm au lieu de 32 mm) permet un angle solide d'utilisation plus grand.

Caractéristiques du compteur utilisé

Palier: 200 volts
Pente: 0 pour cent.
Mouvement propre: 20 c/min
Tension de fonctionnement: 950 volts

Le dispositif électronique associé comprend une haute-tension pouvant débiter 3 à 4 mA et un préamplificateur à temps mort défini de $7 \cdot 10^{-4}$ sec.

Cuve

Céntrée sur l'axe du compteur et de diamètre nettement supérieur à celui du compteur. Ceci est nécessaire pour être assuré de travailler à angle solide constant.

Pour qu'une bonne reproductibilité soit atteinte, un certain nombre de conditions doit être respecté.

(1) La solution doit être en couche "épaisse". Pour des émetteurs tels que S^{35} et C^{14}, ceci correspond à une épaisseur d'eau de 0,5 mm; le volume correspondant, dans la cuve utilisée est de 0,8 cm³.

(2) La surface libre de la solution doit être parfaitement plane et parallèle à la fenêtre des compteurs. On évite la formation d'un ménisque en essuyant la cuve, avant remplissage, avec un coton imbibé d'un agent mouillant. Nous avons comparé les résultats obtenus avec les agents mouillants suivants: Insuline (Endopancrine 40 UI/cm³)—Tween

20 (Polyoxyéthylène sorbitan monooleate)—Cetavlon (Bromure de cetyltriméthylammonium + acétone + éthanol). De cette étude il ressort que les deux agents mouillants qui conviennent le mieux sont dans l'ordre le Tween 20 et le Cetavlon. Le tableau ci-après indique la reproductibilité des résultats, pour une prise de 2 cm³, après rinçage de la cuve avec les agents mouillants étudiés.

Si on ne prend pas la précaution d'essuyer la cuve avec un mouillant, la quantité de solution doit être telle qu'on soit en couche épaisse au centre de la cuve; ceci conduit à des quantités au moins égales à 3 cm³.

Prise No.	Insuline 40 UI/cm³ (c/min)	Tween 20 (c/min)	Cetavlon (c/min)
1	5.304	5.320	5.297
2	5.347	5.301	5.310
3	5.234	5.340	5.340
4	5.387	5.337	5.316
5	5.280	5.320	5.289
Valeur moyenne:	5.310	5.324	5.310
Ecart maximum:	77	23	30

ETALLONNAGE DU DISPOSITIF POUR LE S^{35}

Nous avons réalisé cet étalonnage avec deux solutions de S^{35} sans entraîneur (densitié = 1), dont l'activité a été déterminée avec précision au compteur 4π.

Solution 1

Activité mesurée au 4π: 0,874 μc/g ±3%
Activité moyenne abtenue avec le dispositif: 9.850 c/min.
Par suite, 1 μc/cm³ correspond à 11.180 c/min/2 cm³.

Solution 2

Activité mesurée au 4π: 0,175 μc/g ± 3%
Activité moyenne obtenue avec le dispositif: 1.960 c/min.
Par suite, 1 μC/cm³ correspond à 11.200 c/min/2 cm³.

Etalonnage

1 μc/cm³ correspond à 11.190 c/min/2 cm³.

Dans les mêmes conditions, mais avec un compteur L.C.T. de 1,4 mg/cm², 1 μc/cm³ donne 5.300 c/min. La sensibilité est donc environ deux fois plus faible, ainsi que nous l'avons vérifié pour des solutions de S^{35} dans le dioxane et l'alcool.

Cette technique est naturellement utilisable pour des solutions organiques, à condition seulement qu'elles ne soient pas trop volatiles. Elle est donc, pensons-nous, particulièrement appelée à rendre des services en recherche biologique où les composés organiques de S^{35} et C^{14} sont fréquement utilisés.

ETALLONNAGE POUR D'AUTRES RADIOISOTOPES

(1) Ca^{45}(*β de 0,25 MeV*)

1 μc/cm³ donne 94.000 c/min (volume de solution: 2 cm³)
Limite inférieure mesurable: $2 \cdot 10^{-4}$ μc/cm³.

(2) Co^{60}(*β de 0,3 MeV*)

1 μc/cm³ donne 159.000 c/min (volume de solution: 2 cm³)
Limite inférieure mesurable: 10^{-4} μc/cm³.

LIMITES DE LA METHODE

Les activités mesurables avec le dispositif étudié précédemment sont comprises entre $2 \cdot 10^{-3}$ et 1 μc/cm³.

La limite inférieure, $2 \cdot 10^{-3}$ μc/cm³, est encore relativement élevée, c'est pourquoi nous avons essayé d'abaisser ce seuil en modifiant légèrement notre dispositif.

(1) *Mesure avec deux compteurs* (*Fig. 2*)

Afin d'augmenter le rendement de notre

dispositif nous avons utilisé un deuxième compteur Anton que nous avons placé en regard du premier, la cuve étant interposée entre les deux.

Il est nécessaire dans ce dispositif d'utiliser une cuve à fond à la fois suffisamment mince pour laisser passer le plus possible de β et suffisamment résistant mécaniquement.

Nous avons utilisé le modèle de cuve représenté sur la Fig. 3 nous avons obtenu avec ce nouveau dispositif l'étalonnage suivant pour le S^{35}:

1 $\mu c/cm^3$ correspond à 17.670 c/min/2 cm^3 ce qui permet d'abaisser le seuil de mesure à 10^{-3} $\mu c/cm^3$ et le seuil de détection à $5 \cdot 10^4$ $\mu c/cm^3$.

Ces seuils peuvent encore être abaissés de moitié si l'on associe aux compteurs un dispositif à anticoincidences.

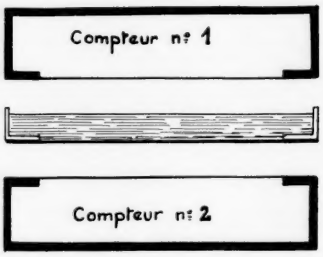

FIG. 2.

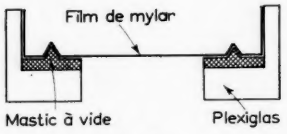

FIG. 3.

PRECISION DE LA METHODE

(1) *Erreur sur le volume*

La prise de 2 cm^3 est obtenue par pipettage; l'erreur maximum admissible est de 1/20 cm^3. En faisant varier le volume de 2 à 3 cm^3, on a constaté que pour Dv = 1/20 cm^3 la variation apparente d'activité est de 0,27 pour cent.

(2) *Pertes de comptage*

Le temps mort étant déterminé à 5 pour cent près les erreurs dues aux pertes de comptage seront de:

—0,7% pour des solutions de 1 $\mu c/cm^3$

—0,3% pour des solutions de 0,1 $\mu c/cm^3$

—moins de 0,1% pour des solutions de moins de 0,1 $\mu c/cm^3$.

(3) *Erreur statistique*

Négligeable pour les activités supérieures à 0,5 $\mu c/cm^3$; devient importante aux très faibles activités (0,7 pour cent 0,1 $\mu c/cm^3$, 2,5 pour cent pour 10^{-2} $\mu c/cm^3$).

CONCLUSION

Compte tenu de ce qui précède et de ce que la précision sur l'étalonnage des solutions de référence est de l'ordre de 3 pour cent pour S^{35} et C^{14}, de 2,5 pour cent pour Ca^{45} et Co^{60}, on peut admettre que la précision de la méthode—qui varie selon les activités—est comprise entre 4 et 6 pour cent lorsque celles-ci sont elles-mêmes comprises entre 1 $\mu c/cm^3$ et $5 \cdot 10^{-3}$ $\mu c/cm^3$.

Cette méthode qui a l'avantage d'être relativement rapide semble donc convenir particulièrement aux émetteurs β peu énergiques et de faible activité spécifique.

VOL
4
1958/

International Journal of Applied Radiation and Isotopes, 1959, Vol. 4, pp. 253–255. Pergamon Press Ltd. Printed in Northern Ireland

Porosity Detection in Magnesium Alloys Using Paraffin Containing Pd^{109}

S. M. MAKIN
Isotope Division, Atomic Energy Research Department, Harwell

(*Received* 3 *March* 1958; *in revised form* 16 *July* 1958)

VOL. 4 8/59

Surface porosity in magnesium alloys has been detected by autoradiography. Pores extending from a surface area of $1{\cdot}5 \times 10^{-5}$ cm² and within 0·4 mm of the surface can be detected on samples which have been soaked in hot oil containing Pd^{109}. A polished surface and a finish equivalent to 0000 grade emery gave satisfactory autoradiographs, but roughly turned samples were unsuitable.

ОПРЕДЕЛЕНИЕ ПОРИСТОСТИ МАГНЕЗИЕВЫХ СПЛАВОВ ПРИ ПОМОЩИ ПАРАФИНА, СОДЕРЖАЩЕГО Pd^{109}

С помощью радиоавтографии определялась пористость поверхности магнезиевых сплавов. Порын на поверхности размером $1{,}5 \times 10^{-5}$ см² и на глубину 0,4 могут быть определены на образцах, которые были погружены в горячий парафин, содержавший Pd^{109}. Удовлетворительные результаты были получены на полированных поверхностях, а также на поверхностях, подвергнутых финишной обработке, эквивалентной 0000; грубо обработанные поверхности были неприменимы.

AUFFINDUNG VON POREN IN MAGNESIUMLEGIERUNGEN MITTELS Pd^{109}—HÄLTIGEM PARAFFIN

Oberflächenporosität von Magnesiumlegierungen wurden autoradiographisch aufgefunden. Poren mit einer Oberflächenausdehnung von $1{,}5 \cdot 10^{-5}$ cm² und innerhalb von 0,4 mm der Oberfläche können an Proben nachgewiesen werden, welche einige Zeit hindurch in heisses, Pd^{109} enthaltendes Öl getaucht waren. Eine polierte Oberfläche und ein Finish entsprechend 0000 Schmiergel gaben zufriedenstellende Autoradiographien, während rauh geformte Proben sich als ungeeignet erwiesen.

INTRODUCTION

Magnesium alloy castings, especially of the magnesium–zinc alloy type, are prone to grain boundary microporosity. If the castings will be subject to severe bending moment, assessment of porosity near the surface in tension is important. The defect can be detected by X-ray or γ-radiography but more than one radiograph is required to locate them within the casting. Non-destructive microscopic examination cannot reveal directly how the pores extend below the surface. Fluorescent penetrants are found to be insufficiently sensitive and are not usually used. Ultrasonic testing does not give sufficiently detailed information on the distribution of porosity.[1]

METHOD

In the radioactive method the pores which lead to the surface of the sample are filled with radioactive oil and autoradiographs are taken of the surface of the sample. The density distribution on the photographic film shows the extent of the porosity in the surface layers of the sample to a depth depending upon the penetration of the radiation used.

Pd^{109} was chosen for these experiments because the 1·02 MeV β-radiation, which has a half-thickness of 0·02 cm in magnesium, gives a reasonable compromise between the soft radiation for good definition in autoradiography and the harder radiation required to penetrate the surface layers of the sample. Palladium was also chosen because it forms complexes soluble in paraffin, and in benzene and chloroform which were used as solvents.

The material tested was a magnesium alloy containing 3·5–5·5 per cent zinc, and 0·4–1·0 per cent zirconium to specification DTD 711A. A good polished surface was obtained by using an automatic polisher working with diamond dust in graded sizes down to 0–1 μ diameters on well lubricated pads revolving at slow speeds. The specimens were degreased and then put in a radioactive oil bath at 97°C for 1 hr. Three kinds of oil baths were tried; their compositions are listed in Table 1. On removing the sample from the bath the free oil was cleared from the surface with benzene on a soft camel hair brush. Autoradiographs were then taken using Industrial G X-ray film. Chemical interaction between the film and metal surface was prevented by covering the sample with formvar applied from a 2% solution in chloroform.

Table 1. Composition of tracer oils

Complexing agent for 0·5 g Pd	Volume of paraffin (ml)	Volume of solvent (ml)
1. 50 ml α-benzoin oxine	225	50 (benzene)
2. 50 ml sodium diethyldithiocarbonate	150	125 (benzene)
3. 50 ml salicylaldoxime	150	50 (chlorform)

RESULTS AND CONCLUSIONS

Autoradiographs taken on Industrial G X-ray film of the polished surface of a casting showed active regions that corresponded to the porosity seen in the micrograph (Fig. 1). Blackening on the autoradiograph corresponding to concentrations of activity in the sample is found to match all but the smallest regions of porosity visible on the micrograph. Pores spreading out from a surface area of $2{\cdot}5 \times 10^{-5}$ cm^2 are visible on this film. An enlargement of some of the pores beneath the surface would explain greater blackening produced by the crack beneath B, for example, compared with that produced by a crack of apparently similar width to the right of A.

Another autoradiograph was taken to test the possibility of detecting cracks with packed X-ray film. The envelope packing was retained between the sample and the lower part of the film. Blackening was produced on both parts of the film but the resolution was reduced in the lower half due to β-particle scattering and the geometrical effect of increasing the separation of the specimen and film by two layers of packing paper.

Autoradiography of the surface in a roughly turned condition was found to be very difficult to interpret. The activity clung to any surface imperfections and in particular to the turning marks. The occlusion of activity also prevented the use of counting techniques. Unfortunately a cleansing technique rigorous enough to free the rough surface of activity was likely to extract it from the pores also. It was impossible to make a direct comparison between the autoradiograph and a micrograph as the rough surface used in the autoradiograph was removed during polishing.

A casting was also polished, scribed with

VOL 4 1958/5

VOL.
4
58/59

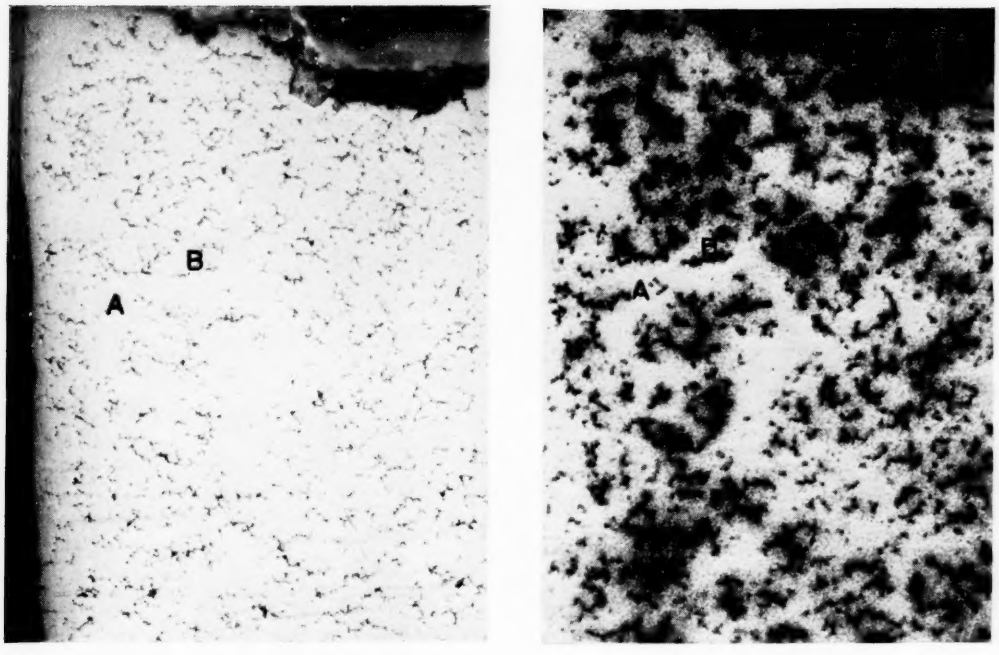

(a) (b)

FIG. 1. Porosity in magnesium alloy casting. ×6·6 (a) micrograph, (b) autoradiograph.

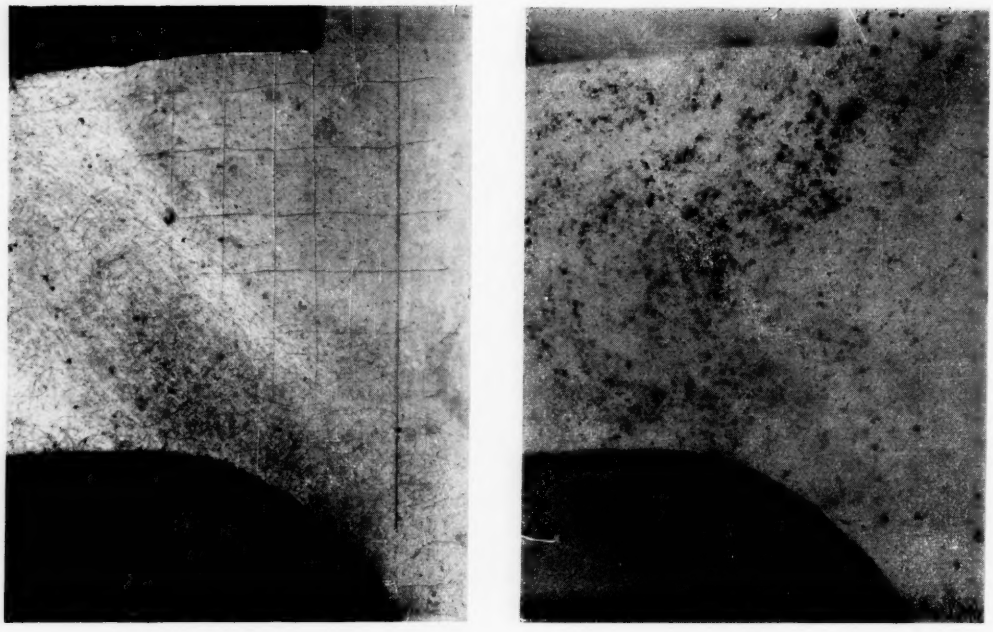

(a) (b)

FIG. 2. Porosity on a part polished, part emery finished surface. ×3·3 (a) micrograph, (b) autoradiograph.

VOL.
4
1958/5

reference marks and the part below the diagonal joining the top left and lower right corners of the sample finished with 0000 emery paper. Fig. 2 shows a micrograph of this surface and an autoradiograph taken on X-ray film which shows the active oil with equal clarity in the regions having a polished and 0000 emery finish.

An autoradiograph was also taken on Kodak AR50 stripping film. The grains in this film were visible at ×90 magnification and their number increased with activity until they coalesced to form generally darkened regions through which the microporosity was just visible. Porous regions spreading out from a surface area of $1{\cdot}5 \times 10^{-5}$ cm were just detectable on this film.

There was little to choose between the oil containing α-benzoin oxine used in Fig. 1 and that containing salicylaldoxime used in Fig. 2. Although the former precipitated a little it was easier to handle as it evaporated less readily than the latter. The oil containing sodium diethyldithiocarbonate corroded the specimens. The specific activity used was 4·8 μc/ml at the time of exposure and gave a photographic density of 0·9 from the activity in a porous region covering a surface area of 4×10^{-5} cm². Greater sensitivity, still within the limits of resolution of the film, could be attained with a higher specific activity.

Microporosity, in which individual pores cover a surface area of $1{\cdot}5 \times 10^{-5}$ cm² and spread out within 0·4 mm below the surface, has been detected in some magnesium castings by autoradiography using radioactive oil. Autoradiographs taken on surfaces which have been polished or finished on 0000 emery paper showed the porosity with equal clarity. Those taken on roughly machined surfaces were difficult to interpret owing to the activity which clung to the turning marks. Autoradiographs suitable for general overall inspection can be taken on samples prepared with 0000 emery paper using Industrial G X-ray film and if precise localization is not required wrapped film can be used.

Acknowledgements—I would like to express my gratitude for the co-operation of the Dunlop Rim and Wheel Co. Ltd., who suggested the work. This firm has also kindly supplied the alloys and financed the work. My thanks are due to Mr. B. R. Payne who supplied the paraffin complexes.

REFERENCE

1. Emley E. F. and Fisher P. A. *J. Inst. Metals* **85,** 236 (1957).

VOL. 4 8/59

International Journal of Applied Radiation and Isotopes, 1959, Vol. 4, pp. 256–260. Pergamon Press Ltd. Printed in Northern Ireland

Leak Detection in an Underground Gasification System

C. G. CLAYTON
Isotope Division, Atomic Energy Research Establishment, Harwell

(*Received* 5 *March* 1958; *in revised form* 23 *June* 1958)

Confirmation of a suspected leak in an underground gasification system operating under conditions which preclude the use of conventional leak detection methods has been established. The leak was between co-axial pipes at 130 ft depth. The velocities in all sections of the system were sufficiently large to ensure turbulent conditions.

The magnitude and position of a leak were determined by injecting 100 mc of krypton-85 in the form of a short pulse into the down-flowing air stream and observing the time interval and character of the pulse on its return to the surface.

Factors governing the interpretation of the results are discussed and it is suggested that the technique has general application in other fields of chemical and steam engineering.

VOL.
4
1958/5

LA DÉTERMINATION DES FUITES DANS UN SYSTÈME À GAZÉIFICATION SOUTERRAINE

On a pu vérifier une fuite soupçonnée dans un système à gazéification souterraine fonctionnant sous des conditions qui empêchent l'emploi des méthodes conventionnelles pour la détermination des fuites. La fuite se trouva entre des tuyaux co-axiaux à une profondeur de 130 pieds (40 mètres). Les vitesses étaient assez grandes dans toutes les parties du système pour assurer les conditions turbulentes.

La grandeur et la location de la fuite furent observées en injectant 100 mc de krypton-85 en forme d'une pulsation brève dans le courant d'air descendant et en observant l'espace de temps et le caractère de la pulsation lors de son retour à la surface.

On discute les facteurs réglant l'interprétation des résultats, et on propose que la technique trouverait une application générale dans des autres domaines du génie chimique et du génie de la vapeur.

ОПРЕДЕЛЕНИЕ ТЕЧИ В ПОДЗЕМНОЙ СИСТЕМЕ ГАЗИФИКАЦИИ

Приводится способ определения предполагаемой течи в подземной системе газификации, работающей в условиях, исключающих возможность применения обычных методов обнаружения течи. Утечка происходила на стыке двух коаксиальных труб на глубине 130 футов. Скорость прохождения газа во всех участках системы была достаточно велика для создания условий турбулентности.

Величина и местоположение утечки определялись путем впрыскивания коротким импульсом одной дозы криптона-85 активностью в 100 милликюри в направленный книзу поток воздуха и определения промежутка времени и характера импульса по возвращении его к поверхности.

Обсуждаются факторы, на которые опирается толкование полученных результатов, и высказывается мнение, что данная методика может найти применение и в других областях химической технологии и теплотехники.

INTRODUCTION

THE underground gasification[1] system consists of a network of pipes carrying air to a gasification reactor where coal is burnt in the seam, the hot gases from the reaction being fed back to the surface where they are available as a source of heat. To increase the combustion efficiency the temperature of the injected air arriving at the reactor is increased by arranging that the horizontal air inlet pipe to the reactor lies inside the exhaust pipe, so forming a simple heat exchanger (Fig. 1). However, fracture of the inlet air pipe may be caused by differential expansion between pipes, localized corrosion or roof fall and subsidence, and under such circumstances air is introduced directly into the exhaust stream, thus by-passing the reactor. Apart from the possibility of local combustion such an occurrence reduces the gas quality. A rapid and simple method of determining the magnitude and position of a suspected leak is thus required.

The method adopted enables the magnitude and position of a leak to be determined from a single observation and is applicable to systems where turbulent conditions prevail. It consists in introducing a short pulse of radioactive gas into the downflowing air stream and in determining the time interval and spread of the pulse on its return to the surface by measurement of the radioactivity and display on a timed chart as in Fig. 2. The time interval depends on flow velocity and length of pipe: the pulse spread is governed by dispersion in the pipe and the dynamic characteristics of the gasification reactor.

If the system is free from leak a single pulse will be observed and its transit time in the pipe alone can easily be determined by measuring the time taken from injection to the appearance of the leading edge of the pulse. It is also possible to estimate this time, or the time spent in any fraction of the system, by dividing the known length of pipe by the mean flow velocity, which can be determined by direct observation, using conventional flow meters.

If a fracture occurs in the air inlet pipe where it lies inside the return flow, some fraction of the injected pulse will leak directly into the return stream, preceding the main pulse on its arrival at the surface. If the transit time of such a leak pulse is compared with the calculated time in each section of the pipe network, the position of the leak can be readily established.

The magnitude of the leak is given by comparing the area under the curve in Fig. 2 corresponding to the leak pulse with that corresponding to the main pulse.

The radioactive gas most suitable for this purpose was considered to be krypton-85 which is available as a fission product with high specific activity. It emits 0·7 per cent of its energy as gamma rays and the beta spectrum has a maximum energy of 0·67 MeV. The half-life is 10·6 years, but, as it is an inert gas, there is no metabolism or specific absorption by the body. The maximum permitted concentration of krypton-85 in the atmosphere is thus relatively high, and approximately 5×10^{-6} μc per cm^3.[2]

TECHNIQUE

A simplified diagram of the system is shown in Fig. 1. It consists of a 12-inch diameter vertical air pipe leading to a gallery approximately 130 ft below ground level, air being injected at 23,200 ft^3 per hour. At the end of the gallery the vertical pipe is connected to a narrower, horizontal pipe, 180 ft long, leading into the coal seam. This latter pipe is constructed of heat resistant chrome-iron sections, each $2\frac{1}{2}$ ft in length and 3 in. in diameter, and lies inside a $10\frac{3}{4}$-inch diameter borehole which is the return gas line. The whole comprises an annular system which is open ended in the combustion chamber and terminated at the gallery. A separate 8-inch diameter pipe carries the gas to ground level.

100 mc of krypton-85 occupying a volume of 2·5 cm^3 at N.T.P. was injected into the input air stream at point *A*, Fig. 1, injection being accomplished by smashing a small glass ampoule containing the krypton with a heavy, knife-edged, plunger. The injection

system was designed so that the gas was released only into the air stream.

To detect the activity in the return gas stream an end-window, halogen-quenched, Geiger counter* having its window flush with the inside wall of the pipe was inserted at point *B*, Fig. 1. The temperature of the return gas was reduced below 75°C, which was the safe operating temperature of the counter, by water-cooling the counter and the previous 4 ft of pipe. The counter was operated in conjunction with a counting rate meter and pen recorder running at a speed of 12 inches per minute.

In order to confirm that the shape and duration of the injected pulse did not influence the result, a number of separate injections were made, and the shape of the pulse was determined at a point 20 ft downstream. The counter was mounted in a similar manner but the output in this case was displayed on a recorder operating at a speed of 70 in. per minute.

In all these experiments the return gases, including the radio-krypton, were discharged to the atmosphere from the top of a 20 ft high tower.

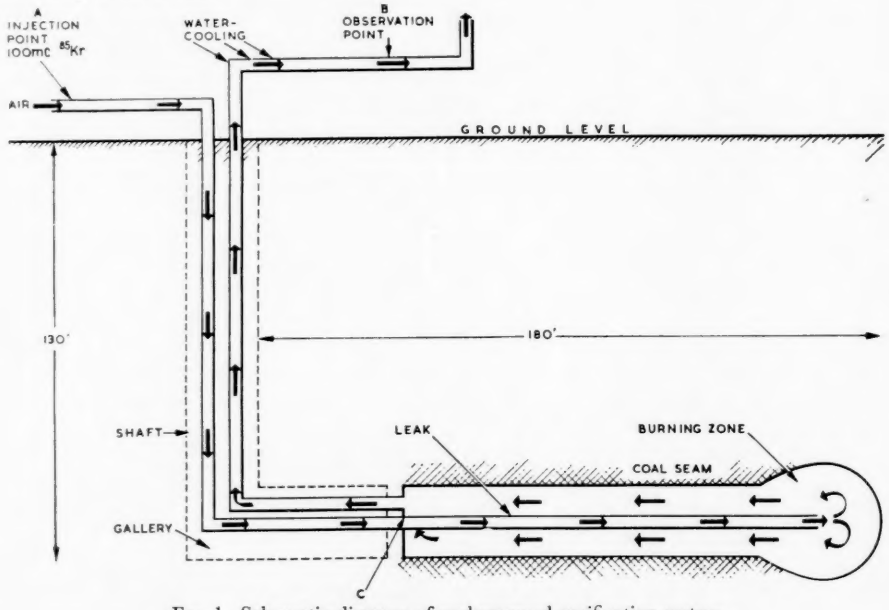

FIG. 1. Schematic diagram of underground gasification system.

RESULTS AND DISCUSSION

The waveform observed at point *B*, Fig. 1, is shown in Fig. 2 where it is seen that most of the radioactive gas returns within the first 3 minutes following injection. The very long duration of this pulse indicates dispersion of gas in the reactor.

The sharp pulse preceding the main pulse is associated with a fracture between input and output streams at some point in the system.

The position of the fracture was determined in the manner outlined, by subtracting the sum of the calculated values for the transit times in the forward and return sections up to the point *C*, Fig. 1, from the observed transit time of the leak pulse. The difference was the time spent in the section beyond *C*, and as the velocity of gas in this section was known, the position of the leak could then be established.

It was in fact found afterwards, by visual inspection, to be within 10 ft of that predicted.

* Mullard Ltd., Type MX. 123.

A small error is likely to be introduced in this type of measurement when relating the true mean flow to some parameter of the pulse shape. On experimental and theoretical grounds TAYLOR[3] has suggested that it should be the peak of the wave, whereas YOUNG and WILSON,[4] from a series of absolute determinations, have concluded that either the centroid or a point midway between points on the rise and decay of the pulse where the ordinates are half the maximum, give a more accurate result.

From the point of view of these experiments it was considered that TAYLOR's assumptions were more relevant and hence the mean velocity was based on a measurement to the peak of the pulse.

It was possible to measure the areas associated with the two pulses to within 4 per cent and this resulted in a value for the magnitude of the leak, determined from the ratio of the areas, of $4{\cdot}1 \pm 0{\cdot}16$ per cent.

From the width of the pulse it is clear that significant dispersion has taken place during transit, and it is necessary to confirm that this is simply due to turbulence in the pipeline. A series of fractures could, for instance, produce a similar result if a smaller degree of dispersion were coupled with a detecting apparatus of poor resolution. The possibility that the output pulse width might be influenced by the finite duration of the injected pulse can be ignored, as four observations made on the width of the injected pulse were found to lie between 75 and 85 msec.

To discriminate between the two most likely possibilities, the dispersion expected in the input pulse due to turbulent flow up to the estimated position of leak and back to the surface was calculated from the known constants of the pipe using the equation

$$C = At^{-\frac{1}{2}} \exp -\frac{(x - ut)^2}{4Dt}$$

where t = time between injection and observation of the pulse.
x = distance from point of injection to point of observation.
u = mean velocity of gas in the pipe.
C = concentration of gas at the observation point.
A = initial concentration of the gas.
D = diffusion coefficient.

The value of the diffusion coefficient was calculated in the manner described by TAYLOR.[3] The calculated value for dispersion of the leak pulse was 4·3 second which is in reasonable agreement with that observed, so that it seemed very likely that only a single fracture occurred.

(a) THE ENTIRE PULSE ILLUSTRATING AN INITIAL LEAK PULSE PRECEDING THE MAIN PULSE THE SLOW DECAY OF THE MAIN PULSE IS DUE TO THE DISPERSION CHARACTERISTICS OF THE GASIFICATION REACTOR

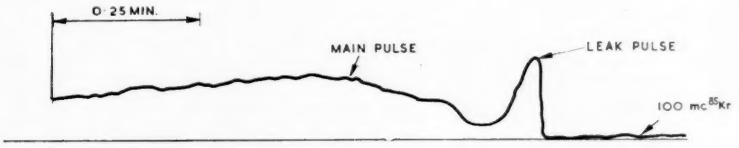

(b) THE INITIAL PART OF THE OBSERVED WAVEFORM, AS RECORDED

FIG. 2.

The method described is generally applicable to the detection of leaks in pipes where there is a common boundary between two fluids. The annular arrangement with the return pipe lying inside the delivery pipe is a particular example but the method is not restricted to a single ended system such as that described. More generally if the system is open ended and if the fluid velocity in each pipe is known, or can be measured, it is a simple matter to locate the position of the leak in the manner described, and provided that each end of the system is available for injection and observation, the remainder may be inaccessible. It is advisable to confirm by calculation that the pulse width observed is simply due to dispersion of the injected pulse. The low radiation hazard and inert nature of krypton-85 makes it particularly useful in this connexion.

Acknowledgements—These experiments were carried out at the Newman Spinney Site, Derbyshire, England, of Messrs. Humphreys and Glasgow Ltd., and the writer is greatly indebted to this firm for permission to use the information obtained. The valuable help and advice given by Messrs. J. Welsh, H. B. Hunter and G. C. Partridge of Messrs. Humphreys and Glasgow and by Dr. E. J. Wilson of A.E.R.E. is gratefully acknowledged. Thanks are also due to Messrs. Isotope Developments Ltd., for the loan of a high speed recorder.

REFERENCES

1. Masterman C. A. *J. Met. Min. Mech. Engrs.* In Press.
2. Recommendations of the International Commission on Radiological Protection. *Brit. J. Radiol.*, Supplement 6 (1955).
3. Taylor G. I., *Proc. Roy. Soc.* A **220,** 446 (1954).
4. Young L. and Wilson G., D.S.I.R. Mech. Eng. Res. Lab., Fluid Report No 60 (1957).

VOL
4
1958/

technical notes

Liquid Scintillators containing Metallic Ions*

(*Received* 13 *March* 1958)

A liquid scintillator that dissolves salts without being prohibitively quenched would make possible a simple internal sample (4π) counter for α- or β-particles. Although liquid scintillators respond to γ-rays chiefly through Compton interactions, a significant amount of high Z material in the liquid would raise the effective photoelectric effect cross-section whereby both the efficiency and energy discrimination for γ-rays would be improved. Moreover, liquid scintillators that contain neutron-absorbing or fissionable isotopes might make superior neutron counters of low γ-sensitivity.

We have been studying the properties of a series of liquid scintillators that contain tri-*n*-butyl phosphate (TBP). TBP is an organic extractant that dissolves a large number of the salts of the actinide and rare earth elements as well as many salts of the lighter elements. Although TBP, by itself, scintillates only weakly, it is a good energy transfer agent in liquid scintillation systems: a solution of 50 parts TBP, 50 parts toluene and 3·0 g/l. of 2,5-diphenyloxazole (DPO) gave rise to a pulse height from electrons that was over one half as high as the pulse height obtained from the toluene and DPO alone.

We have been able to introduce as much as 3·2 g/l. of uranium as the sulfate and 15 g/l. of thorium as the nitrate into a scintillator solution containing 15 parts toluene, 5 parts TBP, 4·5 g/l. *p*-terphenyl and 0·75 g/l. 2-(1-napthyl)-5-phenyloxazole (α-NPO) before reducing the pulse height from α-particles by more than 50 per cent of that of the solution without the salts.

After the data reported above were obtained, KALLMANN and BRUCKER published data on several liquid scintillators that consisted of TBP containing 200–300 g/l. of napthalene with small amounts of scintillator solutes such as DPO.[1] They did not report having dissolved any inorganic salts in their recipes. We have found that typical recipes given by KALLMANN and BRUCKER will dissolve 7·5 g/l. of bismuth as the nitrate or 5 g/l. of thorium as the nitrate before quenching reduces the original pulse height by more than 50 per cent. The solution containing 5 g/l. of thorium, however, gave a pulse height only about one half as big as that of our toluene recipe containing 15 g/l. of thorium.

R. C. AXTMANN
Savannah River Laboratory LECONTE CATHEY
E. I. du Pont de Nemours and Company
Aiken, South Carolina

* The information contained in this report was developed during the course of work under contract AT(07-2)-1 with the U.S. Atomic Energy Commission, whose permission to publish is gratefully acknowledged.

Reference

1. KALLMANN H. and BRUCKER G. J. *Phys. Rev.* **108,** 1122 (1957).

The Irradiation of Indigocarmine with α-Particles and X-rays

(*Received* 26 *February* 1958)

IN recent years the radiolysis of dyes has been studied by a number of investigators.[1–6] These studies have been mainly carried out with γ- and X-rays. In many of them the eventual practical application of the experimental results to the chemical dosimetry of the radiation has also been considered. Few such studies have been made with rays of higher specific ionization, such as α-particles.

The initial purpose of the present investigation was to compare the effects of the α-particle irradiation of aqueous solutions of indigocarmine with the γ-ray induced decomposition as observed by MONGINI and ZIMMER in 1953.[7]

Experimental procedure

1. *Materials.* The indigocarmine, the sulphuric acid, and the other reagents used in these experiments were Merck products of A. R. grade. No further purification was made.

All solutions were prepared from specially purified water. Laboratory distilled water was first

redistilled in a Pyrex apparatus from acid potassium permanganate and then from potassium bisulphate. The product was again distilled from baryta in a silica apparatus. The conductivity of the final water was of the order of 10^{-6}/ohm per cm at the temperature of 25°C.

The experiments were made in 0·8 N sulphuric acid under atmospheric pressure and at a room temperature of 19–21°C.

2. *Analytical methods.* The concentration of indigocarmine was determined spectrophotometrically on a Universal Coleman 14.

The absorption spectrum of indigocarmine in the range 350–800 mμ exhibits a maximum at 610 mμ (see Fig. 2) for which Beer's Law is obeyed; the molar extinction coefficient was found to be 12×10^3.

The spectrum of indigocarmine in the range 210–800 mμ was obtained on a Beckman DU spectrophotometer.

The hydrogen peroxide was measured by cerimetry using *o*-phenanthroline–ferrous salt as indicator. The ceric ion concentrations in 0·8 N sulphuric acid were also determined on a Beckman DU spectrophotometer (at 320 mμ).

The organic peroxides in the irradiated solutions were determined using the reduction of ceric salts at 0°C and at room temperature.[8] At room temperature ($\approx$20°C) both the hydrogen peroxide and some organic peroxides reduce rapidly the ceric ions, while at 0°C only the hydrogen peroxide reacts quickly with Ce^{IV}, the quantity reduced corresponding, thus, practically to the hydrogen peroxide.

3. *Irradiation with α-particles.* Polonium-210 was used for the α-particle irradiations. The sources were prepared from a solution of Ra-D by spontaneous deposition on silver, purified by anodic deposit on gold, and dissolved in the solutions to be irradiated following the techniques previously described.[9,10]

The dose measurements in the irradiated solutions were made by chemical dosimetry on an aliquot part of the Po^{210} solution, using ferrous sulphate in 0·8 N sulphuric acid as dosimeter, and the value of $G_{Fe^{III}} = 6{\cdot}0$.[11]

As a standard of purity of the polonium sources, use was made of the reduction yield of the ceric sulphate in 0·8 N H_2SO_4 solution, in an aliquot part of the utilised sources.[12] For this reduction G yields of 3·2 were obtained.

4. *Irradiation with X-rays.* A Philips Metalix X-ray tube with a tungsten anticathode was used for X-ray irradiation. The tube was run at 18 kV and at a current intensity of 30 mA, with no filtration, except the inherent filtration of the tube window.

The absorbed energy was measured by chemical actinometry using the ferrous sulphate in 0·8 N sulphuric acid as dosimeter.[13]

Results

1. *α-particles.* Fig. 1 shows the results obtained by irradiation of a solution of indigocarmine 10^{-4} mole/l.

It was observed that, under the action of α-particles, the indigocarmine becomes completely

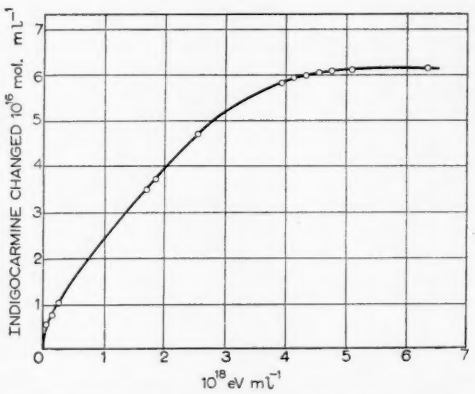

FIG. 1. Irradiation of indigocarmine solutions with polonium α-particles in 0·8 N sulphuric acid; dose-rate $1{\cdot}65 \times 10^{15}$ eV/ml per min; initial indigocarmine concentration 10^{-4} mole/l.

bleached for a sufficient dose. For a given dose-rate ($1{\cdot}65 \times 10^{15}$ eV/ml per min) the bleaching yield decreases as the dose absorbed by the solution increases. This yield, expressed as the number of molecules of the dye transformed by 100 eV of absorbed energy, is $G = 5{\cdot}2$ for the dose $1{\cdot}02 \times 10^{17}$ eV/ml, and $G = 1{\cdot}0$ for the dose $6{\cdot}35 \times 10^{18}$ eV/ml.

TABLE 1. Initial concentration of indigocarmine 10^{-4} mole/l; dose-rate $1{\cdot}65 \times 10^{15}$ eV/ml per min

Total dose eV/ml	Dose absorbed after solution completely bleached eV/ml	Ce^{IV} used $\times 10^{16}$ ions/ml	H_2O_2 $\times 10^{16}$ mol./ml
$13{\cdot}85 \times 10^{18}$	$7{\cdot}50 \times 10^{18}$	at 0°C 28·0	14
		at 20°C 31·2	
$30{\cdot}01 \times 10^{18}$	$23{\cdot}66 \times 10^{18}$	at 0°C 56·4	28·2
		at 20°C 56·8	
$38{\cdot}99 \times 10^{18}$	$32{\cdot}64 \times 10^{18}$	at 0°C 76·8	38·4
		at 20°C 77·6	

VOL. 4 1958/5

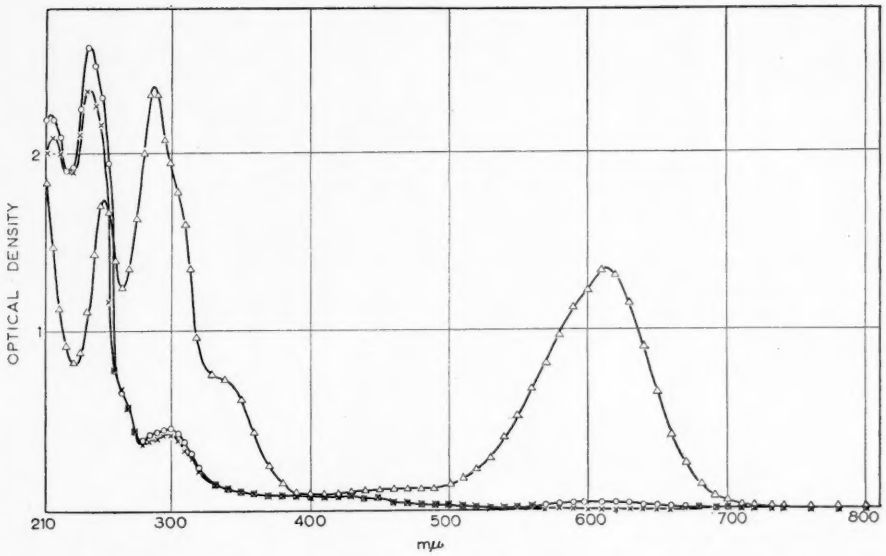

FIG. 2. Absorption spectra of indigocarmine and the products obtained by irradiating with α-particles indigocarmine in 0·8 N sulphuric acid; initial indigocarminecon centration 10^{-4} mole/l

—△—△— indigocarmine
—○—○— indigocarmine during irradiation
—×—×— after total bleaching during irradiation

For irradiation times longer than those corresponding to the total bleaching of indigocarmine, the hydrogen peroxide and the organic peroxides eventually formed in the solutions were determined. The results of these measurements are given in Table 1.

The rather high G values obtained for the hydrogen peroxide ($G \approx 1$) after total bleaching of indigocarmine — $G_{H_2O_2}$ in 0·8 N sulphuric acid being 1·15[9] — and a comparison of the absorption spectra of these solutions and of others containing the dye not yet completely transformed (see Fig. 2), suggest that there was also hydrogen peroxide in these latter solutions. This led us to consider the possibility of there being an after-effect in the radiochemical transformation of the solutions of indigocarmine.

This hypothesis could only be confirmed by submitting the solutions to external radiation. As we were lacking the necessary experimental conditions to undertake experiments with α-particles, studies were made with X-radiation.

2. *X-rays.* Fig. 3 shows two dotted curves each of them relating the quantity of indigocarmine bleached to the total dose absorbed. The yield of the chemical change observed immediately after irradiation decreases with an increase of the dose absorbed by the solution.

The effect of dosage rate is also shown in Fig. 3. The quantity decomposed decreases when the

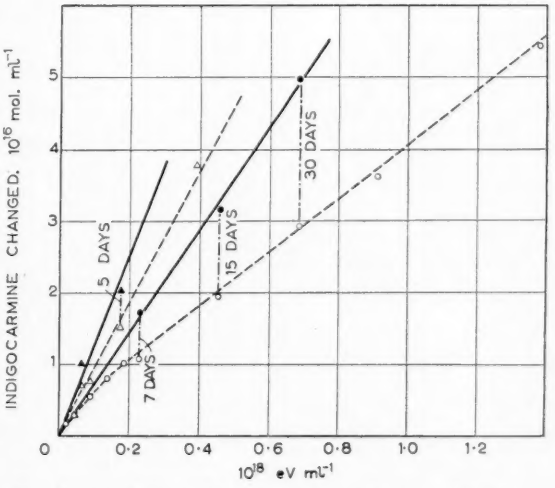

FIG. 3. Irradiation of indigocarmine solutions with X-rays in 0·8 N sulphuric acid; dose-rate 46 × 10^{15} eV/ml per min: ○ immediately after irradiation, ● with after-effect; dose-rate 1·47 × 10^{15} eV/ml per min: △ immediately after irradiation, ▲ with after-effect; initial indigocarmine concentration 10^{-4} mole/l.

dosage rate increases. Thus, for a total dose of $0{\cdot}4 \times 10^{18}$ eV the corresponding G values are: $G = 4{\cdot}5$ for a dose-rate of 46×10^{15} eV/ml per min and $G = 9{\cdot}0$ for a dose-rate of $1{\cdot}47 \times 10^{15}$ eV/ml per min.

The transformation of the dye continues after the irradiation is finished. The importance of this *after-effect* depends on the irradiation time, the effect being always very slow (several days) and it may correspond to about 60 per cent of the transformation observed immediately after the irradiation.

Taking account of this effect, the transformation is in each case represented by a straight line. The yields are independent of total dose and for the dose-rates used are respectively $G = 7{\cdot}4$ and $G = 13{\cdot}2$.

Conclusion

At this time any attempt at detailed interpretation of the results of these experiments would be premature. However, the data already obtained, in particular the influence of the dose-rate in the yield and the observation of an after-effect, led us to conclude that the particularities of the transformation of the indigocarmine by the ionizing radiations are much more complex than might have been inferred from previous experiments.

At a later time we shall refer to any further development of this work.

Summary

The study of the bleaching of indigocarmine in aqueous solutions by ionizing (α- and X-) radiations, leads us to the conclusion that the yield of the chemical change depends on the type of radiation and on the dose-rate. This transformation continues after the irradiation is finished, and the after-effect may be attributed, in part, to the hydrogen peroxide formed in the irradiated solutions.

Acknowledgements—We wish to thank Professor Herculano de Carvalho, President of C.E.E.N. for his support of this work, and Professors Pereira Forjaz and Torre de Assunção of the F.C.L., for all the experimental facilities granted.

M. C. Anta
M. L. Roda Santos

Instituto de Alta Cultura—C.E.E.N.,
Lisbon, Portugal

References

1. Collinson E. and Swallow A. J. *Chem. Rev.* **56,** 471 (1956).
2. Day M. and Stein G. *Nature* **166,** 146 (1950). *Nucleonics* **8,** 34 (1951). *Rad. Res.* **6,** 666 (1957).
3. Proctor B. and Goldblith S. *Nucleonics* **7,** 83 (1950).
4. Henley E. J. and Miller N. *Nucleonics* **9,** 62 (1951). Henley E. J. *Ibid.* **12,** 62 (1954).
5. Clark G. L. and Bierstedt P. E. *Rad. Res.* **2,** 199, 295 (1955).
6. Suttle J. F. *U.S. Atomic Energy Commission* Report no. LA-1615 (1953).
7. Mongini L. and Zimmer E. L. *J. Chim. Phys.* **50,** 491 (1953).
8. Greenspan F. P. and McKellar D. G. *Analyt. Chem.* **20,** 1061 (1948).
9. Anta M. C. and Lefort M. *J. Chim. Phys.* **51,** 29 (1954).
10. Anta M. C. Theses, Paris, 1955.
11. Haïssinsky M. and Anta M. C. *C.R.* **236,** 1161 (1953).
12. Anta M. C. and Haïssinsky M. *J. Chim. Phys.* **51,** 33 (1954).
13. Cottin M. and Lefort M. *J. Chim. Phys.* **53,** 267 (1956).

An Inexpensive Metabolism Apparatus for collecting CO_2, Excreta and Blood from Small Experimental Animals

(*Received* 24 *March* 1958)

Summary

A simple, inexpensive metabolism apparatus for the simultaneous and intermittent collection of CO_2, urine, feces and blood from small experimental animals is described.

During the course of experiments with C^{14} labelled compounds, it is frequently desirable to obtain samples of CO_2, urine and feces at intervals during the course of the experiment to follow the metabolism of the administered compound. Previous publications have presented such data from separate animals sacrificed at desired intervals. The metabolism apparatus described herein makes possible the simultaneous collection of samples from one animal. It permits:

(1) intermittent and quantitative collection of expired CO_2;
(2) withdrawal of blood samples at specific times during the course of the experiment; and
(3) intermittent collection of urine and feces.

The apparatus is inexpensive and has been used successfully with rats in experiments in which 10 or more samples were obtained during a 24 hr interval.

VOL. 4 1958/5

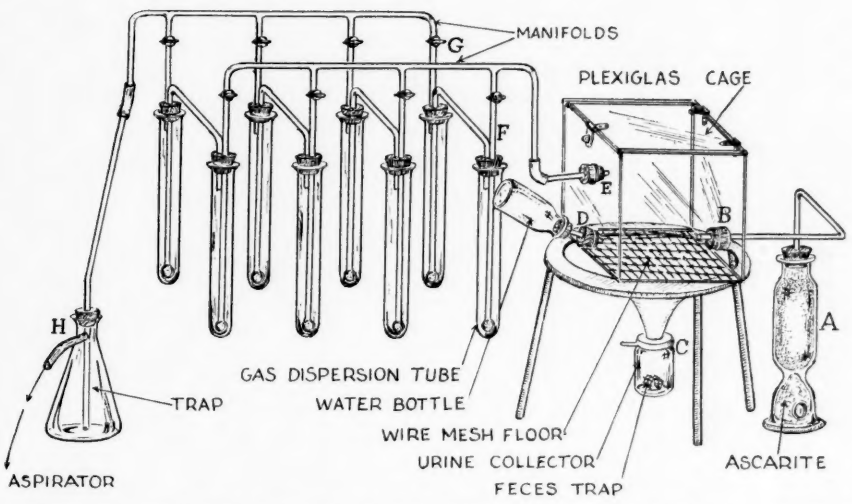

FIG. 1. Inexpensive metabolism apparatus for the intermittent collection of CO_2, excreta and blood.

A metabolism cage meeting some of these requirements has been described by ROTH.[1] However, the apparatus constructed by this worker is costly. Furthermore, the entire animal must be enclosed.

Experimental

The 8 × 8 × 8 in. cage shown in Fig. 1 was made of $\frac{1}{4}$ in. Plexiglas, a transparent plastic material which can be cut and drilled. The junctions are joined with cement (Plexiglas dissolved in chloroform) and reinforced with small steel corner braces which were bolted to the cage. The top of the cage is supplied with hinges and a latch to permit the animal to be placed in position in the cage on a $7\frac{1}{2} \times 7\frac{1}{2}$ in. 2 gauge wire platform.

The bottom of the cage was molded into the shape of a funnel, thus permitting the drainage of urine and feces from the apparatus. To construct the funnel an 8 × 8 in. piece of Plexiglas with a drilled center hole 1 in. in diameter was placed in a wooden frame press which covered one-half inch of the four edges. The press was made of eight 1 in. strips of masonite cut and bolted in such a manner to allow expansion of the Plexiglas. This device prevented the edges from warping and provided a flat ridge for attachment to the cage sides and a ledge for the wire gauze floor. The Plexiglas was then supported in an air oven at 270°F. A round bottom flask weighted with lead shot and placed in the center of the Plexiglas caused a funnel-shaped depression as the material softened. When the desired degree of softness was reached the sheet was removed and pressure applied to the center weight to produce a depression of the desired depth. After the sheet had cooled, a piece of Plexiglas tubing, 1 in. in diameter, was attached to the funnel with Plexiglas cement.

Baby-food jars were used to collect excreta. Into these were placed 4 gauge wire circles to catch feces. The wire was cut with 2 legs which were bent beneath the circle to suspend the feces trap above the urine. Less than 1 sec was required to change these containers. A circle of 1 in. diameter was cut from a plastic cover (sold in the local stores for strained baby-food jars) and inserted over the funnel end. This air-tight cap held the jar in place. After the collection of samples, solid plastic caps were placed on the jars to provide tight fitting covers during storage of the samples.

Water was supplied through a hole (D) into which a drinking bottle was suspended by means of a rubber stopper. Food can be supplied from a cup covered with a wire screen and connected to the wire cage bottom. However, in our experiments, the ration was fed by stomach tube prior to placing the rat in the cage. For the collection of blood the tail of the rat was inserted through a hole in the No. $6\frac{1}{2}$ rubber stopper which also held the air inlet. The hole was large enough to loosely retain the tail which was bound lightly with adhesive tape and secured to the outside of the tubing which served as the air inlet. The adhesive tape also served to seal the tail in the rubber stopper. The cage was placed on a tripod, approximately 10 in. above the floor of the fume hood. A 2 × 4 in. wood block, 11 in. high, provided a surface on which the tail of the rat rested during periods when blood samples were obtained.

Atmospheric CO_2 was removed by allowing the air to pass through the bottom of an Ascarite tower

(A) through a 10 mm glass tubing connection (B) into the bottom of the cage. The air left the cage through a 10 mm glass tubing connection contained in a rubber stopper in an opening near the top of the cage (E). The air then passed to a series of tubes for the collection of CO_2.

Pyrex test tubes, 300 × 35 mm, fitted with rubber stoppers into which were placed inlets and outlets from glass manifolds, were used for the collection of CO_2. The inlet tube (F) was provided with a stopcock above the rubber stopper. Below the stopper, it was connected with tygon tubing to a gas dispersion tube (medium porosity, 20 mm) which extended below the surface of 0·1 N sodium hydroxide. The dispersion disc was suspended in a vertical plane.

A second hole in the rubber stopper of the collection tube enclosed a Pyrex tubing arm which led to a second tube in the set, equipped in the same manner as the first. The outlet of the second tube (G), however, was connected by means of a stopcock to the second manifold. Each manifold contained connections to four such sets of tubes. This permitted collection of CO_2 in the two tubes of each set independently of the other tubes and made possible the intermittent collection of samples during any desired time interval without loss of CO_2. The second manifold was connected with tygon tubing to a trap (H) and thence to an aspirator to provide a source of suction.

In our work it was desirable to connect four sets of two tubes to the manifolds because of the short time intervals for the collection of CO_2 during the early part of the experiments. However, one set of two tubes will suffice in instances where one total collection is desired.

The cost of all materials used in the construction of the metabolism apparatus, using only one set of two CO_2 collection tubes, did not exceed $20, whereas commercially available metabolism cages of similar construction for rats cost approximately $300. The parts of the apparatus, with the exception of the Plexiglas, are normally found in chemistry laboratories.

The hole in the rubber stopper (B) containing the tail of the rat can be plugged when it is not necessary to collect blood samples. The apparatus can be checked for air-tightness prior to use by placing a small beaker containing a few ml of concentrated hydrochloric acid on the floor of the cage and passing a beaker of ammonium hydroxide over the junctions, as gentle suction is applied. If a cloud of ammonium chloride vapor forms at any Plexiglas junction, it can be resealed with the Plexiglas cement. The authors found the cage to be perfectly airtight when the lid was sealed with adhesive tape.

The rate of flow of air is regulated by the flow of water through the aspirator. The cage was operated in an air-conditioned room. Where this convenience is not available, a thermometer can be inserted through one of the rubber stoppers and the temperature controlled with fans and moist towels in difficult weather conditions. Additional holes can be drilled as desired for other purposes. The cage floor and all other components can be separated for easy cleaning.

This investigation was supported in part by a research grant from the National Institute of Arthritis and Metabolic Diseases, National Institutes of Health, Public Health Service. The animal experiments will be published at a later date.

GERALD A. EDWARDS
Department of Chemistry CECILE H. EDWARDS
Department of Home Economics EVELYN L. GADSDEN
The Agricultural and Technical College of North Carolina, Greensboro, North Carolina

Reference

1. ROTH L. J. *Nucleonics* **14,** 104 (1956).

VOL. 4 1958/5

An Apparatus for the Intracavity Administration of Radioactive Colloidal Gold

(*Received* 27 *March*, 1958; *in revised form* 1 *September*, 1958)

AN earlier paper[1] described equipment for the intracavity administration of radioactive colloidal gold. With this equipment it was possible to dilute a sterile preparation of gold aseptically to any volume and to run it into the patient by gravity feed, the whole operation being remotely controlled.

Experience with this equipment suggested certain improvements which might be made on grounds of radiation protection. These relate principally to the method of removing the gold from the ampoule in which it is delivered and to the taps used to control the flow of radioactive solution. These improvements, and other minor ones, have now been incorporated in the apparatus described here, the working of which may be understood by reference to Fig. 1.

The essential glass part is a reservoir,* of volume about 100 ml, with a ground-glass Luer nozzle and a side-arm. To the side-arm is attached a length of silicone-rubber tubing bearing a sphygmomanometer bulb with its air-intake port stopped. The lower outlet tube of the reservoir carries a T-piece, one

* Specially made by Messrs. Aimer Ltd.

arm of which leads to the patient, whilst saline can be introduced into the reservoir to any degree required by means of the other. The reservoir, with its attendant tubes and T-piece is sterilized as a unit together with a Luer serum needle of suitable dimensions *in situ* on the nozzle.

The two taps referred to in Fig. 1 as "quick-action" form one of the novel features of this apparatus. Their working may be understood by reference to Fig. 2. Each consists of a clamp *A* which can be opened or closed by action of a cam, (shaded) which is itself actuated by means of half a turn of the operating handle. The clamp may be held firmly in any position (fully open or shut, or at any point intermediate between the two) by means of the friction provided by a cork friction-plate *B* loaded against the inside face of the case by means of a spring *C*. A forked slide (not shown in diagrams) holds the rubber tube in the correct position under the clamp.

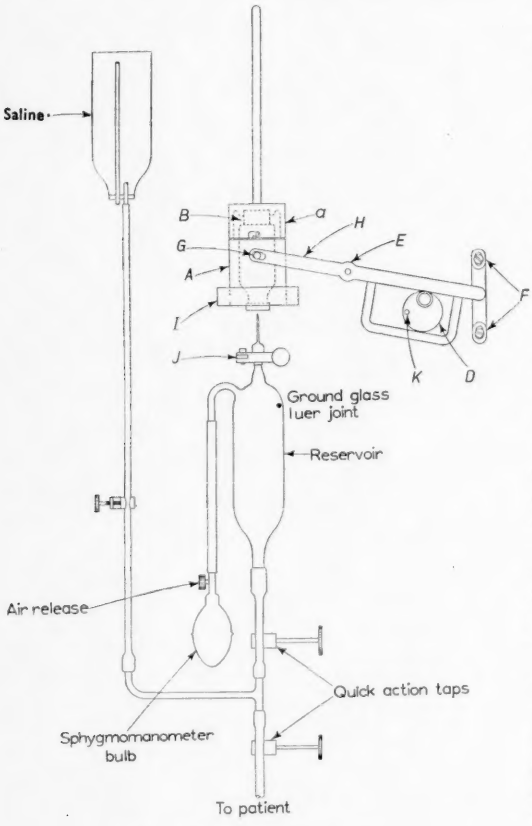

FIG. 1. General arrangement.

The second major improvement concerns the mechanism by which the gold solution is extracted from the sterile ampoule in which it is delivered. This may be understood by reference to Figure 1 and the accompanying photograph.

The ampoule is held upside-down in forceps and placed in the Perspex carrier *A* where it is firmly held by the bayonet cap *a*, which carries a sponge rubber pad *B* for the purpose. The carrier is brought down onto the needle point by half a turn of the operating handle (shown in the photograph); this is also sufficient to cause the needle to penetrate the rubber ampoule-cap. The movement is transmitted from the operating handle by means of the cam *D* moving in the rocker-arm about the pivot *E*; the degree of movement required can be adjusted by means of the movable stops *F*.

The Perspex carrier is pivoted at *G* in the yoke *H* and supported vertically in the bearing *I*. When the ampoule-carrier is at its highest point its movement is held by a spring-loaded ball *K* in a dimple on the operating cam.

This mechanism is very robustly built since the rubber caps supplied on U.K.A.E.A. ampoules are much harder to puncture than those on normal pharmaceutical ampoules, a fact which can be a source of hazard unless special precautions are taken. The needle itself is locked into a metal clamp *J*.

When the needle has punctured the rubber cap, the reservoir being empty, the sphygmomanometer bulb is compressed. Air is forced up the needle and into the ampoule; and on releasing the bulb some of the radioactive solution is sucked into the reservoir. Repetition of this operation 3 to 6 times transfers all the gold aseptically to the reservoir. The

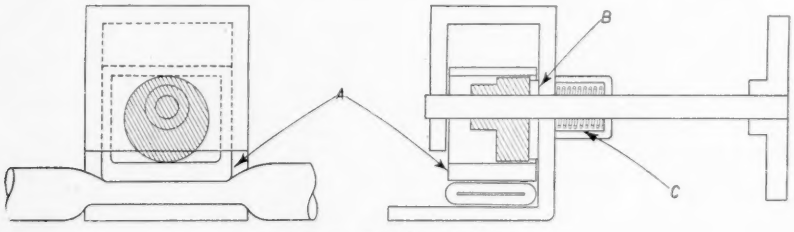

FIG. 2. Quick-action tap.

air-release valve on the sphygmomanometer bulb is then unscrewed to act as an airway, after which saline can be run in to dilute the colloidal gold to the extent required. It may be readily observed from the colour of the gold solution that mixing is instantaneous and complete.

The diluted gold solution is then run into the patient at whatever speed is required together with such further washings of saline as may be necessary.

The apparatus is mounted on a board the lower edge of which is at a height of approximately 5 ft, the saline bottle being at about 6 ft 6 in.; this gives sufficient head of pressure for efficient running of the preparation into the patient.

The equipment is fully shielded by lead when in operation, and observation and control of the process are maintained by indirect vision using a lamp-house and mirror.

It is claimed that incidental radiation hazard to the operator has been eliminated as fully as practicable in this equipment.

Reference

1. Arnott D. G. and Joy A. R. *Brit. J. Radiol.* **29,** 337 (1956).

The London Hospital D. G. Arnott
London E1 H. R. Knight

Effects of Ionizing Radiations on Tissue Mast Cells*

(*Received* 16 *May* 1958)

It is believed that the radiation sickness is due to liberation of histamine in the body.(1) Histamine liberation is thought to be one of the main functions of tissue mast cells. With this idea in view, an attempt was made to see the effects of different kinds of radiations both from external and internal sources on tissue mast cells. Results of this study form the subject matter of this communication.

Methods and materials

The mesenteric spread of 40 adult healthy albino rats weighing from 175 to 225 g were used in this study. The abdomen was opened after killing the animal with nembutal and a loop of jejunum and ileum was draped over a slide. Once the mesentery and its vessels had adhered to the glass the guts and the mesenteric attachments were cut away. All the slides were fixed in absolute alcohol for 6 hr and stained with 0·25% toluidin blue in 35% alcohol for 2–3 min. On each slide from each animal 20 fields, 4·4196 mm^2 each, were covered using a magnification factor of 150. The variation in the total mast cell count per unit area of mesenteric window along with the percentage of morphological variations were noted. Morphological characters were recorded with the *camera lucida* drawing and actual changes in the size were measured with a planimeter. Autoradiographic studies of the peritoneal spread were done. Doses of isotopes were injected intraperitoneally. X-rays were given from 10^6 V and 250 kV machines.

Results

Number. Table 1 shows that in the control group the average number of mast cells per 20 fields was 310·4. This number was increased in all the irradiated groups. Remarkable increase was seen after irradiation with 10^6 V X-rays and Fe^{59}, namely 528 and 413 respectively.

The average number after treatment with P^{32}, Au^{198}, and 250 kV X-rays did not show much difference, the numbers being 344·7, 387, and 378·5 respectively.

Size. The average area of cross section of the mast cells in control group was 423·8 μ^2. The remarkable change was seen again for Fe^{59} with or without X-ray. Here most of the cells were very small, the average area being 151·1 μ^2 for Fe^{59} and 140·3 μ^2 for Fe^{59} along with 250 kV X-ray. The average area for P^{32} was 212·9 μ^2, for Au^{198} 225·7 μ^2 and for both 250 kV and 10^6 V X-rays 161·1 μ^2.

Percentage of morphological variations. The various morphological characters observed were placed in 3 categories:

1. Normal—cells with uniform distribution of metachromatic granules with or without visible nucleus.

2. Small hyperchromatic—cells smaller than the average of the above described normal cells and stained so deeply that nuclei were not seen and the granules were found to be clumped together.

3. Others—those which show granular shifting, bipolar giving a dumb-bell shape, unipolar shifting of granules, small cells with nucleus filling almost the whole of the cells, cells with eccentric nucleus, cells with vacuolation and granular spilling, clumping of the granules in groups, cells having peculiar shapes and cells showing degranulation. It is

* This paper was presented at the 7th Annual Conference of the Indian Association of Pathologists held in November 1956 at Mysore (South India).

VOL. 4 1958/5

OL.
4
8/59

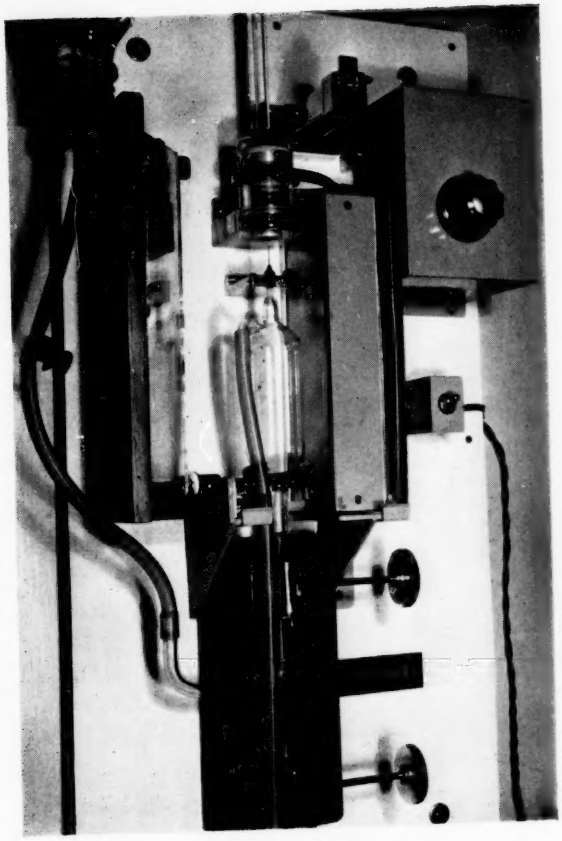

FIG. 3. General view of equipment.

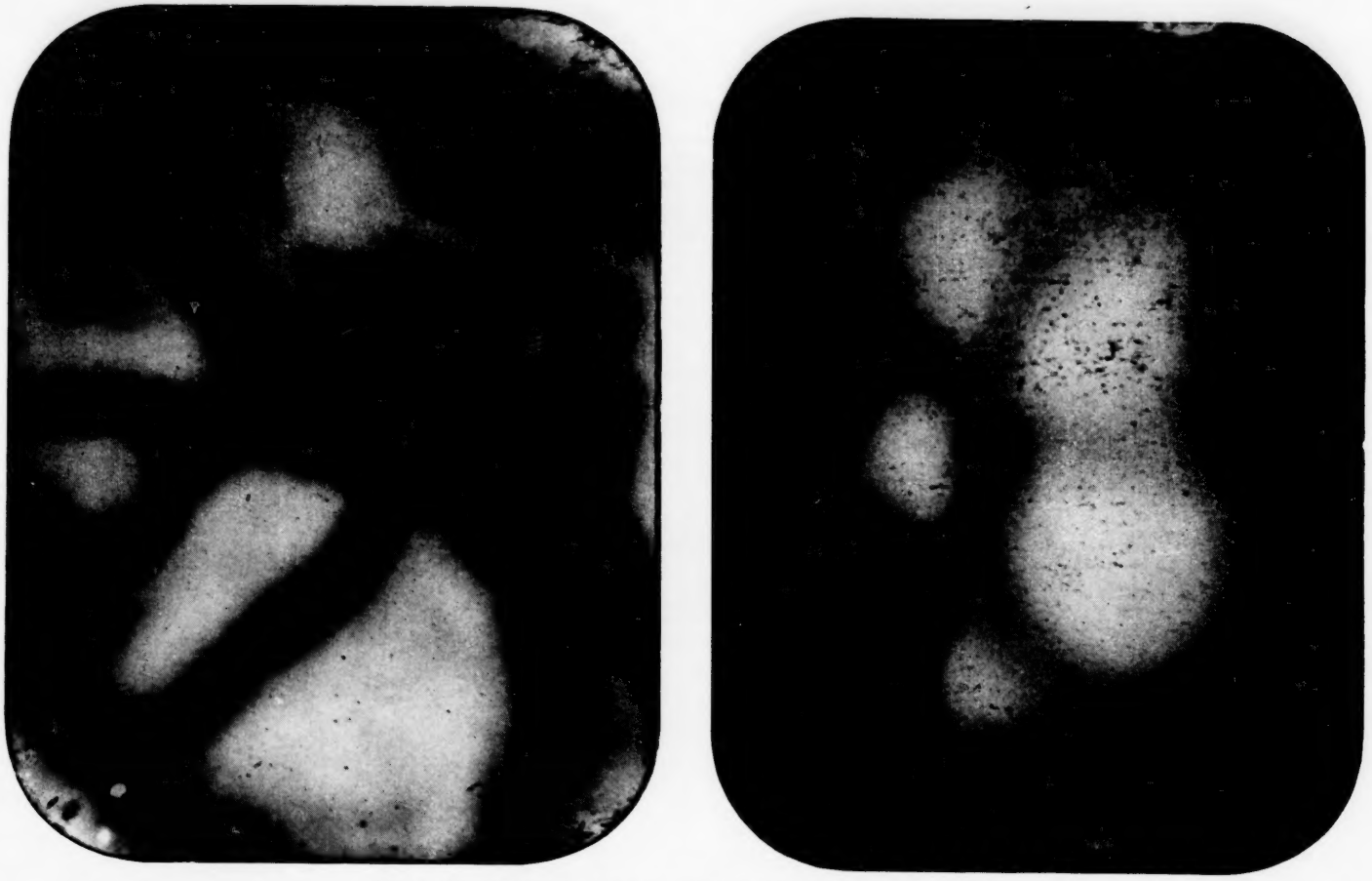

FIG. 2. Autoradiographs showing uptake of isotopes in P^{32} and Au^{198}.

VOL.
4
1958/5

TABLE 1. Showing the results of different types of ionizing radiations on tissue mast cells

No. of animals	Nature of radiation	Concentration of radioactive materials (μc/g body wt.)	Dose of radiation (rads)	Duration in days	No. of cells in 20 fields $\times$150	Cross-section in μ^2			Variation in %		
						biggest	smallest	average	normal	small hyperchromatic	others
11	None				310·4	666·6	222·2	423·8	72·4	7·6	19·9
4	Fe^{59}	0·0017	0·112	5	413·5	222·2	55·5	151·1	20·9	33·0	46·1
3	P^{32}	0·1	9·3	3	344·7	333·3	111·1	212·9	14·9	25·9	59·2
2	Au^{198}	2·0	117	8	387·0	333·3	55·5	225·7	10·8	16·2	73·0
2	X-ray 250 kV		332	5	378·5	222·2	55·5	761·1	22·5	14·2	63·3
2	X-ray MV		83	5	528·0	333·3	55·5	161·1	13·9	4·9	81·2
2	X-ray 250 kV + Fe^{59}	0·0017	332 (X-ray) + 0·112 (Fe^{59})	*10 + 3†	377·9	295·5	55·5	140·3	14·6	55·7	29·7
5	X-ray MV + Fe^{59}	0·0017	82 (X-ray) 0·112 (Fe^{59})	*10 + 3†	472·4	222·2	55·5	161·1	7·9	13·9	78·2
9	X-ray 250 kV + P^{32}	0·1	332 (X-ray) + 9·3 (P^{32})	*13 + 3†	332·0	444·4	55·5	396·8	16·2	12·2	76·6

* Days following X-irradiation after which radioactive material was administered.
† Days after administration of respective radioactive materials after which animal was sacrificed.

evident from histogram (Fig. 1) that there is a marked increase in the number of abnormal mast cells in all the irradiated groups. The abnormal cells described under the third category are less marked after exposure to Fe^{59} than to P^{32}, Au^{198} and X-rays. Fe^{59} also causes a remarkable increase in the number of small hyperchromatic cells. Variation in size and shape along with granular spilling are most marked after exposure to 10^6 V X-rays. In Au^{198} it was also observed that the granules of the majority

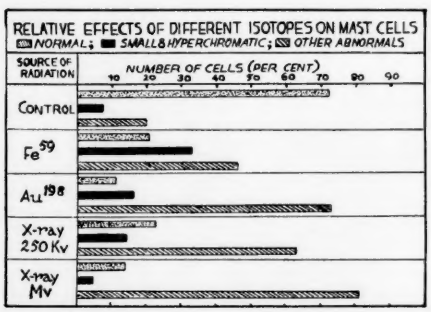
RELATIVE EFFECTS OF DIFFERENT ISOTOPES ON MAST CELLS
NORMAL; SMALL & HYPERCHROMATIC; OTHER ABNORMALS
SOURCE OF RADIATION
NUMBER OF CELLS (PER CENT)
10 20 30 40 50 60 70 80 90
CONTROL
Fe 59
Au 198
X-ray 250 Kv
X-ray Mv

FIG. 1. Histogram showing the relative incidence of different types of mast cells for various types of radiations.

of cells, instead of taking the usual characteristic stain with toluidin blue, looked black. The black granules were distinct, refractile and of bigger size. Autoradiographic study shows (Fig. 2) there was uptake of isotopes in the peritoneal windows of Au^{198} and P^{32} cases; but there was no uptake in Fe^{59} cases.

Discussion

It is evident from the above observations that though the numbers of cases in different groups are not sufficient to justify a detailed conclusion at this stage, the effect of ionizing radiation on tissue mast cells is certainly to increase their population along with a relative increase of abnormal types of cells.

Summary

Forty albino rats were treated with Fe^{59}, Au^{198}, X-ray (10^6 V and 250 kV) and their effects on the morphology of peritoneal mast cells were studied. It is observed that the effects of ionizing radiation on tissue mast cells is to increase their population along with relative increase of abnormal types of cells.

Acknowledgements—Our thanks are due to Dr. SUBODH MITRA, Director, Chittaranjan Cancer Hospital, Calcutta for his kind interest in this work and also to SRI ARABINDA BOSE, Physicist, for helping us to calculate the dose of radiation.

R. DUTTA-CHOUDHURI
H. ROY
Department of Pathology, Chiltaranjan Cancer Hospital and National Medical College, Calcutta, India

Reference

1. ELLINGER F. *Schweiz. Med. Wschr.* **81,** 55 (1951).

The Use of Radioactive Isotopes in the Study of the Kinetics of Scrap Melting and Slag Formation in a Scrap Ore Process*

A DESCRIPTION is given of the use of radioactive isotopes for a new method of studying the rate of melting and slag formation in a scrap ore process. The method allows the absolute weight of the slag to be determined while melting is in progress.

The kinetics of scrap melting

The melting rate of scrap in 130 ton and 350 ton open hearth furnaces was determined by measuring the specific activity of metal samples taken from test melts containing Co^{60}. Under the conditions of the experiment, Co^{60} does not oxidize or volatilize and does not enter the slag, and consequently, the number of atoms of Co^{60} in the metal remains constant. To ensure even distribution, Co^{60} preparation was poured into the ladle while it was being filled with iron from the mixer. An initial sample was taken from the Co^{60}-bearing iron in the ladle, and further samples were drawn from the furnace during smelting.

The values of the specific counting rate of all the samples were reduced to that of an ideal standard specimen of 400 g weight. Measurement of the activity of the metal samples was done with 12 gas-filled counters of type MS-4, assembled as described previously.[1]

The specific counting rate and weight of the iron sample in the ladle, and those of the samples extracted from the furnace during the melting, are related in the following manner,

$$A_t = A_0 i_0 / i_t, \tag{1}$$

where A_t is the weight of the liquid metal in the furnace at a time t, A_0 is the weight of liquid iron containing Co^{60} in the ladle, i_0 is the specific counting rate of the iron sample in imp/min g, and i_t is the specific counting rate of the metal samples withdrawn from the furnace at a time t, in imp/min g.

Taking into account the amount of oxidized impurities, the actual weight x, of the scrap which has been melted up to time t, will be

$$x = \frac{A_0 i_0}{i_t}\left(1 - \frac{\Sigma C_t}{100}\right) - A_0\left(1 - \frac{\Sigma C_0}{100}\right) \tag{2}$$

where ΣC_t is the total percentage content of impurities in the metal at time t, and C_0 is the total percentage content of impurities in the iron when it is poured into the furnace.

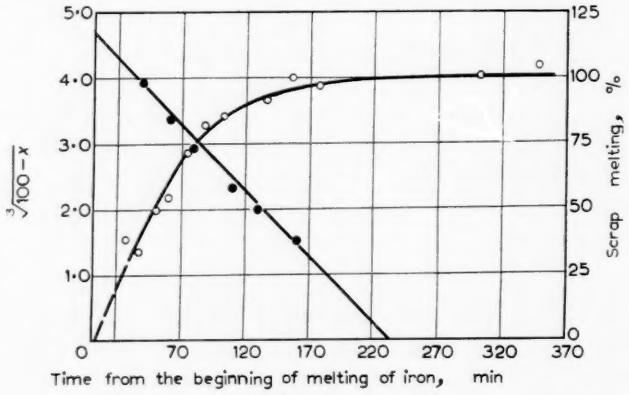

FIG. 1. Dependence of the amount of scrap melted on time.
○—percentage of overall weight.

Calculations of x, from measurements of the activity of the metal samples and from chemical analyses, thus allows the kinetics of the melting to be determined. The relationship of the amount of scrap melted, as a percentage of the overall weight, to the time, forms a regular fusion curve such as that shown in Fig. 1. The flattening of the curve indicates the completion of melting and the flat portion can be used to determine the total weight of the metal. Similar results have been obtained for 20 experimental melts.

In the present paper the authors have confined themselves to finding a kinetic equation that describes the melting of the scrap in a scrap-ore process. If it is supposed that the rate of melting (dG/dt), where G

* *Translated by* Mrs J. AGRELL from *Atomnaya Energiya* **3**, No. 10, 352 (1957).

VOL. 4 1958/5

is the weight of the melted scrap, is taken as proportional to the surface area G of the scrap, then

$$(dG/dt) = KS, \tag{3}$$

where K is the coefficient of proportionality. For a solid, the relationship between its weight and surface can be written,

$$S = \alpha G^{2/3} \tag{4}$$

where α is a coefficient whose value depends on the shape. Since scrap consists of pieces of various shapes, α is some average value. Therefore

$$(dG/dt) = K\alpha G^{2/3} \tag{5}$$

The rate at which the scrap melts can be expressed as a function of the weight of melted scrap. Obviously the percentage weight of scrap that remains solid at time t is $(100 - x)$. Therefore, the rate of melting is, in accordance with the surface relationship,

$$(dx/dt) = K_M(100 - x)^{2/3} \tag{6}$$

where $K_M = K\alpha$.

Integration of equation (6) gives

$$3(100 - x)^{1/3} = K_M t + C, \tag{7}$$

where C is the integration constant. It follows from equation (7) that the quantity $(100 - x)^{1/3}$ is a linear function of the time. Fig. 1 shows that values of $(100 - x)^{1/3}$ derived from the smoothed kinetic curve fit very satisfactorily on a straight line.

The introduction of the rate constant K_M allows the intensity of the smelting process to be estimated for each melt and allows conditions of melting in different furnaces to be compared. Furthermore, if K_M is known for a given melt, the amount of scrap which has been melted at a given moment is easily calculated, and from it the actual rate of oxidation of impurities during the melting can be estimated.

The kinetics of slag formation

The method of isotope dilution has also been used to study the formation of liquid slag during melting. CaO, containing Ca^{45}, was used because, in the smelting conditions of the open-hearth process, CaO is not reduced, does not dissolve in the metal and is found only in the slag.

Before the smelting began, the calcium oxide preparation was placed in a closed metal tube and put into the furnace as the iron began to melt. A sample was taken 30 to 35 minutes after the isotope had been placed in the furnace, a period long enough for it to be distributed uniformly throughout the entire volume of the slag.

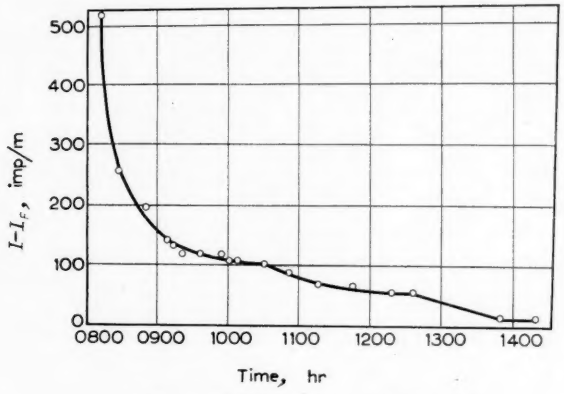

FIG. 2. Solubility curve of Ca^{45} in slag.

The quantity of slag in the furnace was determined from the formula:

$$G_i = \frac{I_0 Q_i G_0}{I_i Q_0} \tag{8}$$

where G_i is the amount of liquid slag in the furnace at a given time, I_0 is the activity of a "standard" slag in imp/min, Q_1 is the activity of the Ca^{45} in the slag of the test melt in μc, G_0 is the weight of a standard slag, I_i is the counting rate of a slag sample from the test melt at a given time, and Q_0 is the activity of the Ca^{45} in the "standard" slag in μc. If a known amount of slag is taken out of the furnace and gives an average counting rate I_{sl}^{av}, then formula (8) becomes

$$G_i = \frac{I_0 Q_i G_0}{I_i Q_0} - \frac{G_{sl} I_{sl}^{av}}{I_i} \tag{9}$$

where G_{sl} is the weight of slag withdrawn. The dilution curve of Ca^{45}, for one of the test melts, is shown in Fig. 2.

As a first assumption it can be taken that, after the oxidation of the silicon and manganese in the iron

and the melting of the ores, the further development of slag formation is determined by the rate of solution of the lumps of limestone in melt in the system FeO–Fe_2O_3–SiO_2–MnO.

Solution goes on for rather a long time and may therefore be the factor limiting the slag formation.

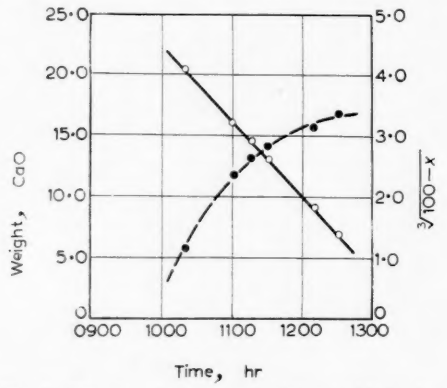

FIG. 3. Kinetics of solution of calcium oxide in slag.
● —weight of CaO.

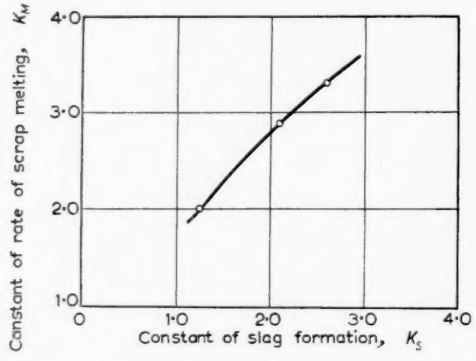

FIG. 4. Relationship between the scrap melting constant and the slag formation constant.
K_M constant of rate of scrap melting.
K_s constant of slag formation.

The appearance of 'limy boiling' and pieces of limestone that float to the surface at the end of the smelting are evidence of the slowness of solution.

In the absence of any preliminary theoretical conditions for estimating the rate of solution of calcium, the same considerations as apply to the kinetics of scrap melting may be used and equation (6) rewritten as

$$(dx/dt) = K_s(100 - x)^{2/3}, \qquad (10)$$

where x is the weight of calcium oxide dissolved in the slag, as a percentage of its overall weight in the non-metallic portion, found in the furnace at the end of the smelting, and K_s is the rate constant of slag formation. The experimental results obtained from the test melts confirm the validity of equation (10).

Fig. 3 shows a curve of solution of calcium oxide in the slag. The curve is typical of saturation processes and its flattening indicates the end of solution of the limestone. The height of the plateau corresponds to 100% solution of calcium oxide. Fig. 3 also shows that the experimental points, plotted as $(100 - x)^{1/3}$ against time, obey a straight line relationship very satisfactorily. The validity of equation (10) is thus confirmed by the data obtained from the test melts.

Fig. 4 shows that there is a regular relationship between K_M and K_s, and thus emphasizes the similarity of the physico-chemical conditions that determine the course of the scrap melting process and the solution of lime.

References

1. OSIPOV A. I., SHVARTSMAN L. A., IUDIN V. E. and SAZONOV M. L., *Conference of the U.S.S.R. Academy of Sciences on the Peaceful Uses of Atomic Energy, Technology Section.* Publ. U.S.S.R. Academy of Sciences, p. 29 (1955).
2. OSIPOV A. I., SHVARTSMAN L. A., IUDIN V. E., SAZONOV M. L. and ALEKSEEV V. I. *Study of mixing processes of high phosphorus iron in steel tanks under reducing conditions.* Publ. TS.N.I.I.CH.M. (1955).

A. I. OSIPOV
L. A. SHVARTSMAN
V. I. ALEKSEEV
V. F. SUROV
M. L. SAZONOV
M. T. BUL'SKII
S. A. TELESOV
A. M. SKREBTSOV
A. M. OFENGENDEN
L. G. GOLDSHTEIN
F. F. SVIRIDENKO

VOL.
4
1958/5

book reviews

M. HAISSINSKY: **La Chimie Nucléaire et ses Applications.** Masson, Paris, 1957. 651 pp. 5,000 fr.

THE scope of nuclear chemistry has never been clearly defined but the subject is often regarded as the use of chemical methods in the study of nuclear physics. Professor HAISSINSKY, however, takes a much wider view in this book and he includes classical radiochemistry, elementary nuclear physics, the radioactive elements, natural and artificial, the effects of radiation on matter, and the use of radioactive materials as indicators in chemical research, with excursions into biochemistry and industrial applications: in fact almost every chemical topic involving radioactive material. He has also included a chapter on geochemistry and astrophysics, as if the list was not long enough. Clearly, the book covers an enormous field of work and consequently it cannot go into great detail in any one subject, but it is difficult to find a subject not included with the exception of the more technological parts of, for example, the processing of nuclear fuels. For those requiring a wide introductory coverage in nuclear and radiation chemistry in one book, *La Chimie Nucléaire et ses Applications* is very suitable indeed, as in addition, copious references are given for further reading.

The book is admirable, produced on high quality paper and contains very few misprints. The chapter headings and contents list and also a list of errors in the text are found at the back of the book.

G. B. COOK

E. H. GRAUL: **Strahlensyndrom-radioaktive Verseuchung** (pathogenetische, klinische, prognostische, genetische und sanitätstaktische Probleme im Atomzeitalter). Gasschutz und Luftschutz, Verlag Dr. Ebeling, Koblenz, 1957. 177 Ss. 19.60 DM.

THIS book is primarily written for people engaged in civil defence work. It deals with the sympomatology, diagnosis and therapy of acute and chronic radiation exposure and describes some of the countermeasures to be taken in cases of small and large scale radiation accidents. Although it must be rather difficult to write a monography in a field which is so rapidly advancing but where, on the other hand, much of the accumulated knowledge is buried in classified reports, this book contains much information, particularly for the layman working in civil defence. It is well written and extensively illustrated; it can be recommended for reading to those who understand German and have no access to the original literature on this subject.

H. VETTER

K. E. HALNAN: **Atomic Energy in Medicine.** Butterworths, London, 1957. 157 pp. 15s.

DR. K. E. HALNAN's book "Atomic Energy in Medicine" in the Atoms for Peace Series (Butterworths Scientific Publications) is a most interesting and valuable introduction to the use of radioactive isotopes, high energy beams and radiation in medical work. It is engagingly written and well-supplied with diagrams and most interesting and clear photographs, which illustrate the text very appropriately.

It starts with a chapter on atomic physics which makes the subject clear even to the layman. The chapter on the principles and use of radioactive isotopes and their measurement, and the chapter on radioisotopes in medical research are of absorbing interest and illustrate well the fundamental principles involved. Radiobiology, the use of radiation and radioisotopes in the treatment of cancer and in the elucidation of fundamental medical problems and in medical diagnosis are all dealt with clearly and in an interesting way. The last two chapters keep the balance of the book: the penultimate chapter deals with the problems and hazards of radiation and, while it does not gloss over any of the dangers, it puts them in perspective, indicating how they can be minimized. The discussion of the future of atomic energy in medicine is imaginative, without being extravagant.

This book is excellent for anyone wishing to have some knowledge of the uses of atomic energy in medicine and would be very useful to any medical student or medical practitioner desiring to have some idea of the subject. In fact, it might be said that no-one's medical education could be complete nowadays without some introduction to the subject, of which this book is one of the best examples.

For any non-medical person, whether of graduate standard or not, it is so clearly written as to be intelligible without much effort, certainly for anyone who has been taught physics and chemistry at school.

It would be a valuable book for people such as physicists, laboratory assistants and students of therapy radiography in addition to medical students and practitioners.

FRANK ELLIS

forthcoming papers

G. V. KURDYUMOV, M. B. NEINAN and G. M. FRANK: The use of radioisotopes in the U.S.S.R.

A. N. MURIN: Soviet radiochemistry.

I. J. GRUVERMAN and P. KRUGER: Cyclotron-produced carrier-free radioisotopes.

J. THIERY: Améliorations dans l'utilisation des radiotraceurs pour l'étude de l'usure des segments de piston. Méthode IFP-RA3-bilan d'usure.

C. LEYMONIE et P. LACOMBE: Méthodes d'étude de l' autodiffusion dans les métaux à l'aide des radioisotopes.

M. C. CORFIELD, S. DILWORTH, J. C. FLETCHER and R. GIBSON: A machine for the automatic chromatography and assay of mixtures of radioactive substances.

E. A. THOMPSON and C. B. MURPHY: Labeling surfaces with radioactive gases.

A. M. BRODSKY, YU. A. KOLBANOVSKY, E. D. FILATOVA and A. S. TCHERNYSHEVA: Radiolysis of normal heptane and its inhibition by dibenzyl sulphide and dibenzyl additions.

G. G. EICHHOLZ, C. M. LAPOINTE and G. E. ALEXANDER: Automatic electronic inspection of manufactured systems using radioactive components.

T. ENGELMANN and B. GRINBERG: Chambre d'ionisation β–γ.

N. B. MIKHEEV: The determination of solubility of difficultly soluble compounds with the aid of non-isotopic radioactive indicators.

K. J. ÖBRINK and H. R. ULFENDAHL: Gamma spectrometry for analysis of mixtures of radioisotopes in biological and medical research.

LOUIS DANGUY et ROBERT QUIVY: Mesure continue d'un flux de neutrons par activation de solutions en circulation.

ROBERT L. BELL: Isotope transfer test in the diagnosis and treatment of hydrocephalus.

ERVIN KAPLAN, JAMES MIREE Jr., EDWIN HIRSCH and THEODORE FIELDS: Autoradiographic localization of P^{32} phosphate in metastatic carcinoma of the breast bone.

W. G. BROWN and J. L. GARNETT: Recoil tritium labeling of deutrated compounds.

G. R. MARTIN and D. G. TUCK: The specific activity of radium.

F. DUTKA and D. GÁL: Investigation of isotope exchange reactions between organic iodides and iodide ions.

PAUL VERCIER et ANDRÉ RAGGENBASS: Détection en continu des rayonnements β dans les solvants aqueux et organiques.

T. H. ODDIE, F. F. RUNDLE and I. MESCHAN: The use of a test-therapy dose of radio-iodine for thyrotoxicosis.

S. H. PINNER: Stress–strain properties of irradiated filled natural rubber.

VOL
4
1958/

Erratum

Int. J. Appl. Rad. Isotopes **3,** 232 (1958).

D. G. GARDNER and W. W. MEINKE:

β-Ray Spectroscopy Using a Hollow Plastic Scintillator.

Line 17, Page 236, right-hand column, line 17 should read:
"the order of $\mu g/cm^2$) for sample mountings."

VOL.
4
58/59